Alma Mater Studiorum – Università di Bologna

DOTTORATO DI RICERCA IN
SCIENZE DELLA TERRA, DELLA VITA E DELL'AMBIENTE

Ciclo XXXI

Settore Concorsuale: 04/A3

Settore Scientifico Disciplinare: GEO/04

SPELEOGENESIS OF SULFURIC ACID CAVES IN SOUTHERN ITALY

Presentata da: Ilenia Maria D'Angeli

Coordinatore Dottorato

Prof. Giulio Viola

Supervisore

Prof. Jo De Waele

Co-supervisore

Prof. Mario Parise

Esame finale anno 2019

to my Father

...Tutto è inutile, se l'ultimo approdo non può essere che la città infernale, ed è là in fondo che, in una spirale sempre più stretta, ci risucchia la corrente.
L'inferno dei viventi non è qualcosa che sarà; se ce n'è uno, è quello che è già quì, l'inferno che abitiamo tutti i giorni, che formiamo stando insieme.
Due modi ci sono per non soffrirne.
Il primo riesce facile a molti: accettare l'inferno e diventarne parte fino al punto di non vederlo più.
Il secondo è rischioso ed esige attenzione e apprendimento continui: cercare e saper riconoscere chi e cosa, in mezzo all'inferno, non è inferno, e farlo durare, e dargli spazio…

...It is all useless, if the last place can only be the infernal city.
The inferno of the living is not something that will be; it is something that is already here, where we live every day, that we create by being together.
There are two ways to escape suffering it.
The first is easy for many: accept the inferno and become such a part of it that you can no longer see it.
The second is risky and demands constant vigilance and apprehension: seek and learn to recognize who and what, in the midst of the inferno, are not inferno, then make them endure, and give them space…

Italo Calvino, Città Invisibili, 1972

SPELEOGENESIS OF SULFURIC ACID CAVES IN SOUTHERN ITALY

ABSTRACT

The main objectives of this research are: a) to investigate the main processes involved in sulfuric acid speleogenesis (SAS) of Italian caves, b) to estimate the dissolution-corrosion rate in several active SAS systems of southern Italy, and c) to contextualize landscape evolution using subhorizontal cave levels in the central-southern Apennine Chain.

SAS caves formed in hypogene conditions (i.e., rising fluids), and are influenced by H_2S-rich waters, which gain their acidity in deep-seated settings. The geological situation of Italy allows it to host ~25% of the worldwide known SAS caves, located along the the Apennine Chain, Apulia, Sicily and Sardinia.

Geomorphological and mineralogical investigations can be used to identify inactive SAS environments, and recognize the conditions in which they originated. The most common geomorphological features refer to unconfined settings, which likely influenced the speleogenesis in the last stages of void formation, and are therefore, well-preserved.

Peculiar suites of secondary byproducts including gypsum, sulfur, alunite, natroalunite, and jarosite strongely contribute to clarify cave speleogenesis. Sulfur stable isotopes may contribute to elucidate the source of H_2S, which in Italy seems to be mainly related to bacterial sulfate reduction of Triassic evaporites interacting with hydrocarbons and/or organic matter. Moreover, gypsum and alunite dating may help to pin down the chronology cave speleogenesis.

Active SAS caves show waters undersaturated with respect to gypsum and calcite and atmosphere composed of degassing hypogene H_2S, CO_2 and CH_4. These special conditions promote the growth of microbial biofilms, composed of extremophile communities of bacteria and archaea able to arrange themselves into special structures. Active SAS caves can be used as laboratories to study the dissolution-corrosion rate, and calculate weight variation over time.

Finally, subhorizontal SAS levels and alunite ages can help in understanding the uplift and erosion rates of the mountain hosting the cave system.

1. INTRODUCTION

1.1. Cave speleogenesis in hypogene conditions

Caves are often defined from an anthropocentric point of view, being "natural voids beneath the land surface that are large enough to admit humans" (White, 1988; Palmer, 2007). This definition has no genetic meaning, and caves can be voids inside a pile of boulders, an open fracture in any kind of solid rock, a lava tube or an underground stream in soluble rock. Most caves are solutional voids, and are also named "karst caves" or "dissolution caves". They are formed by the dissolving and erosive action of underground water as it flows through open spaces in soluble bedrock. Dissolution of the host-rock is a fundamental process, especially in the early phases of cave development, and is at the basis of the formation of karst caves. Nevertheless, chemical processes could be replaced when large sediment grains can be transported in the system and used as erosive agents (Palmer, 2001). Once the openings in the rock are wide enough, generally > 5 mm (the approximative diameter necessary for te undersaturated water to penetrate through the system without approccing 100% of saturation), physical processes overrule the importance of dissolution and allow the underground flowpaths to be enlarged drastically.

Carbonate caves are the most common on Earth, and the limestones and dolostones in which they are hosted dissolve by dissociation, which in pure water is very slow and comparable to the dissolution of quartz. In presence of acidity, however, the dissolution of carbonates increases very rapidly. The most common acid on Earth is carbonic acid, formed by the reaction of carbon dioxide in the water. Carbon dioxide is present in the atmosphere, and in greater quantities into the subsurface, and most acidity of infiltrating waters derives from slow percolation through the first meters of subsurface. Caves whose origin depends on the presence of acids formed at or near the present-day surface are called epigenic (Palmer, 2011, Häuselmann, 2013).

Hypogene speleogenesis is worldwide recognized and is the most important process of karst system development with the classical "epigene" cave formation (Klimchouk, 2007, 2009, 2018). The concept of hypogene speleogenesis has been intensely debated in the last years, and the two main theories established in the past, one strictly geochemical (Palmer, 2000) and the other, more hydrogeological (Klimchouk 2007, 2015), have been recently unified. Hypogene karstification is now defined as *"the formation of solution-enlarged permeability structures by upwelling of fluids that recharge the cavernous zone from hydrostratigraphically lower units, where fluids originate from distant or deep sources, independent of recharge from overlying or immediately adjacent surface"* (Klimchouk, 2017, p.3). The upwelling waters involved in the speleogenesis may have different origins such as juvenile (magmatic), metamorphic, connate, due to deep meteoric and/or marine water

circulation paths or to mixing of different fluids (Mylroie et al.,1995; Hill, 2000; Mylroie and Mylroie, 2018), and their aggressiveness is linked to the interaction with deep-seated sources (Hill, 1990). During rising, these deep fluids undergo several changes in pressure and temperature, which cause a progressive evolution of the solution and precipitation of different mineralogical associations (Klimchouk, 2017) along their (several km long) path. The occurrence of hypogene speleogenesis has been documented in different soluble lithologies such as carbonates, evaporites and lithified deposits with soluble matrix (Klimchouk, 2009). According to the chemical processes involved (Klimchouk, 2017) the different types of hypogene karstification are related to the presence of i) sulfuric acid (Audra, 2008; Palmer, 2013; Jagnow et al., 2000), ii) hydrothermal fluids (Dublyansky, 1980; Bakalowicz et al.,1987), the occurrence of iii) mixing corrosion, and iv) evaporite-dissolution. In general, hypogene caves can originate in both confined or unconfined conditions, but most frequently they develop in confined settings (Klimchouk, 2005, 2009, 2018). Subsequent events such as uplift, exhumation, surficial erosion, and denudation (Klimchouk, 1996) can shift hypogene caves from their native deep settings to shallow environments, where other processes can take over, locally overprinting the original morphologies and deposits. Nevertheless, an interesting research, carried out in four sulfuric acid water table cave systems (De Waele et al., 2016), have shown sulfuric acid speleogenesis (SAS) to occur frequently in unconfined conditions. Thanks to their origin (with recharge coming from below), hypogene caves are climate-indipendent and do not directly rely on seepage from CO_2-enriched surface waters. This explains the apparent paradox that the most famous and longest hypogene caves of the world, such as Carlsbad Caverns and Lechuguilla in the Guadalupe Mountains of New Mexico, USA (Hill, 2000; Jagnow et al., 2000), and Toca da Boa Vista-Toca da Barriguda system in Bahia, Brazil (Auler & Smart, 2003; Klimchouk et al., 2016), do not occur in high rainfall areas, but are located in semi-arid and dry regions. As suggested by several authors (Dublyansky, 1980; Klimchouk, 2007, 2018) the most diagnostic characteristics of inactive hypogene environments are their morphological features and the occurrence of complex sequences of exotic minerals (Polyak and Provencio, 2001). Hypogene caves are characterized by lack of genetic relationship with the external landscape (absence of dolines, sinking streams, and blind valleys, all features typical of epigene karst), thus not showing the typical morphologies of vadose, concentrated and fast water flow. This results in 2 and/or 3D maze networks that mainly follow the fissure systems rather than the bedding planes, most having abrupt endings (Hill, 1995) and well-developed cupola-like morphologies on the ceiling of cave conduits. There is a general lack of fluvial sediments, whereas secondary by-products due to the weathering and replacement of host-rock or primary deposits, calcite (dogtooth spar) and silica coatings are abundant.

Understanding the genesis of a karst system is an important issue for cavers and karst scientists around the world, but it is essential to underline that caves often have a polygenetic history (Hill, 2000; Palmer & Palmer, 2000; Palmer, 2013; Parise et al., 2018), and it is not always possible to recognize all the stages of cave formation and evolution. For this reason, geomorphological, geochemical, mineralogical and hydrogeological observations are necessary to find the most reasonable clues.

1.2. Historical overview

Although the concept of hypogenic caves has mainly been developed over the past 25 years (Klimchouk, 2007, 2009), the role of sulfuric acid in the genesis of some caves has been known for quite a long time in Europe. In fact, rising warm waters with the typical smell of rotten eggs (H_2S) were put in relation with the presence of actively developing karst voids in the thermal spring area of Aix-les-Bains (at the foot of the Bauges massif, Savoie, SE France) at the very beginning of the 19th century (Socquet, 1801), and Martel mentioned the importance of sulfuric acid in speleogenesis (Martel, 1935). In Italy, an underground tunnel for the spa at Triponzo (Southern Umbria) intercepted a small cave in which sulfuric waters actively dissolved the limestone (Principi, 1931). Also in this case the direct relationship between H_2S-rich waters and the active dissolution of the limestone was described accurately. In both cases the direct link between acid waters and speleogenesis was straightforward, since the processes were active and clearly visible. Contrarily, in Kraushöhle (Austria) the process is not active anymore, but the abundant presence of gypsum in the cave led Hauer to hypothesize a link between sulfuric waters, present in a spring located 79 meters below the cave, and the genesis of the cave (Hauer, 1885). Also Kraus, who discovered the cave, was of the idea that limestone was replaced by gypsum in a recent past (Kraus, 1891, 1894). These early ideas were however abandoned quickly in favor of the more simplistic model of modification (infilling) of an already existing cave, or the dissolution of gypsum bodies contained in the carbonate sequences (Trimmel, 1964).

The presence of coatings of gypsum on the walls of some travertine springs in Banff National Park (Alberta, Canada) was reported by Elworthy already in 1918, but only half a century later this mineral and its isotopic signature brought Van Everdingen et al. (1985) to understand the role of H_2S-derived sulfuric acid in the genesis of these small caves in thermal travertines.

However, the first author describing the role of sulfuric acid in cave formation with a certain detail is Morehouse, taking as an example Lower Crevice Cave, in the Tri-State lead-zinc mining district at Dubuque (Iowa, USA) (Morehouse, 1968). Here, sulfuric acid is produced by the oxidation of pyrite, marcasite, and in a minor way, galena, in the Middle Ordovician Galena dolomite. The chemistry of the waters clearly shows sulfate to be produced, in an inorganic way or with the help of iron oxidizing

bacteria (*Crenothrix* and *Gallionella*) abundantly present in the cave streams. Despite the fact that the author recognized some cave morphologies typical of SAS caves (passages pinching out), he stated there are no fundamental morphological differences between caves formed by sulfuric and by carbonic acid. Strangely, the author does not report replacement gypsum in Level Crevice Cave, because the sulfate was entirely carried away in solution.

The breakthrough in the understanding of the sulfuric acid speleogenesis arrived five years later, with the PhD work of Egemeier (1973) on Lower and Upper Kane caves in Wyoming (USA). His findings are based on observations and measurements in these rather small active SAS caves, in which H_2S-rich streams with abundant white microbial filaments can be followed for a little bit over 300 meters (Egemeier, 1981, 1987). In this case the H_2S appears to be produced by the reduction of sulfate beds in petroleum-rich areas of the stratigraphical sequence.

Some years earlier the same Egemeier (1971) was the first to suggest the sulfuric acid origin of the large rooms of Carlsbad Caverns, in the Guadalupe Mts (New Mexico). Also Jagnow, independently and in the same years, proposed the sulfuric acid origin of the caves in the Guadalupe Mts., with the acid deriving from the oxidation of pyrite in the Yates Formation (similar to Morehouse's ideas in Iowa) (Jagnow, 1977, 1978, 1979). This contrasted with the earlier explanation of speleogenesis caves, and in particular of the abundant gypsum deposits, in this cave by Bretz, who believed these cave to have formed in phreatic conditions, followed by vadose periods in which gypsum deposited in large pools (Bretz, 1949). The gypsum, according to Bretz, would have come from the nearby Permian Castile Formation. It is interesting to note that halloysite-10Å (hydrated halloysite or endellite), a mineral typically produced in hydrothermal and highly acid conditions, was already discovered in Carlsbad Caverns many years before (Davies & Moore, 1957) but did not lead to understanding the acid speleogenesis of the cave. The discovery of native sulfur in nearby Cottonwood Cave, on the contrary, brought Davis (1973) to relate the presence of this mineral to the H_2S present in the groundwater and deriving from nearby petroleum deposits. Also Queen (1973), and later Queen et al. (1977) forwarded the idea that gypsum had replaced calcite and dolomite in the Guadalupe caves by a brine mixing model, in which fresh meteoric waters mixed with phreatic waters that ascended from the gypsum and evaporite rich rocks of the Castile Formation in the Delaware Basin. These theories were questioned by Davis some years later, and he was the first to develop the still valid sulfuric acid theory for the formation of the Gualalupe Mts. cave systems (Davis, 1980). His theory was validated by stable isotope measurements on replacement gypsum, which gave negative values compatible with an origin from hydrocarbon deposits, and not related to the evaporites in the Castile Formation (Hill, 1981). From the early 80s, Carlsbad Caverns, the surrounding caves and, later on, Lechuguilla Cave (discovered in 1986) became the main fields of

study regarding the sulfuric acid speleogenesis model. The fundamental work by Hill (1987, 1990) lays down the basis for many other works on SAS caves carried out elsewhere in the world.

In the mid 80s also other North-American caves were recognized as having originated by sulfuric acid interacting with carbonate rocks: some small travertine caves in the Cave-and-Basin springs (Banff National Park, Canada) (Van Everdingen et al., 1985) and Cesspool Cave in Virginia (Hubbard et al., 1986, 1990). Independently, Collignon describes the first African SAS cave, Rhar es Skhoun, in the Azrou Massif in Algeria (Collignon, 1983, 1990).

In Europe, SAS caves began to be recognized mainly in the early 90s. The discovery of Movile Cave in southern Romania sheds new light on very special geoecosystems, in which sulfuric acid is still actively enlarging the cave (Sarbu et al., 1994, 1996; Sarbu & Kane, 1995; Sarbu & Lascu, 1997). This led Galdenzi to understand the genesis of Frasassi Cave in Italy (Galdenzi & Menichetti, 1990), and later on many other caves along the Apennine Chain in Central Italy (Galdenzi & Menichetti, 1995). Today Italy is the richest country in the world regarding both active and inactive SAS caves (De Waele et al., 2014; D'Angeli et al., 2016).

At least 5% of the explored caves in the world were described by Palmer (2007) to have had sulfuric acid speleogenetic origin, and nowadays, an increasingly larger number of SAS caves are known around the world (*Figure 1*), and an overview of these is given in *Table 1*.

Figure 1. Location of the sulfuric acid caves and cave systems of the world.

Table 1. List of the known worldwide caves in which sulfuric acid plays an important role.

Karst area	Location	Age host rock	Caves	References	Active	Pyrite	Size
Canada							
Banff National Park	Alberta	Quaternary	Cave-and-Basin springs	Van Everdingen et al., 1985	x		S
Rocky Mts.	Canada	Middle Cambrian	Castleguard	Yonge & Krouse, 1987		x	G
United States of America							
Crevice Cave, Dubuque	Dubuque, Iowa	Ordovician	Level Crevice Cave	Morehouse, 1968; Lowe et al., 2000; Palmer, 2003	x	x	S
Black Hills	South Dakota	Lower Carboniferous	Jewel, Wind	Bakalowicz et al., 1987; Palmer & Palmer, 1989			G
Bighorn Basin	Wyoming	Lower Carboniferous	Lower and Upper Kane, Hellespont, Salamander, Spence, Big Horn, Mystery	Egemeier, 1973, 1981, 1987; Palmer, 2003; Engel, 2007; Engel et al., 2003, 2004, 2010; Meisinger et al., 2007; Porter & Engel, 2008; Porter et al., 2009; Rossmassler et al., 2012	x		S
Allegheny City	Virginia	Quaternary	Cesspool	Hubbard et al., 1986, 1990; Engel et al., 2001; Porter & Engel, 2008; Porter et al., 2009	x		S
Egan Mts.	Nevada	Cambrian	Whipple	Egemeier, 1981	x		S
Redwall caves	Arizona	Upper Carboniferous	Various caves, Corkscrew	Huntoon, 2000; Palmer, 2003; Onac et al., 2007; Hill & Polyak, 2010			S
Glenwood springs	Colorado	Upper Carboniferous	Fairy, Glenwood	Barton et al., 2004; Barton & Luiszer, 2005; Polyak et al., 2013	x		M
Guadalupe Mts.	New Mexico	Permian	Barancas, Black, Carlsbad, Cottonwood, Endless, Hell Below, Hidden, Lechuguilla, Madonna, Slaughter Canyon, Spider, Virgin, etc.	Davies & Moore, 1957; Davis, 1973; Jagnow, 1977, 1978, 1979, 1986; Queen et al., 1977; Davis, 1980; Egemeier, 1981, 1987; Kirkland, 1982; Davis, 1988; Davis et al., 1990; Spirakis & Cunningham, 1992; Cunningham et al., 1994, 1995; Queen, 1994, 2009; Polyak & Mosch, 1995; Northup et al., 1995; DuChene & Cunningham, 2006; Polyak & Güven, 1996, 2000; Polyak & Provencio, 1998, 2001; Polyak et al., 1998; Jagnow et al., 2000; Lowe et al., 2000; Northup et al., 2000, 2003; Palmer, 2000, 2003; Palmer & Palmer, 2000; Palmer, 2006; Polyak et al., 2006; Barton & Northup, 2007; Burger, 2009; DuChene, 2009; Calaforra			G

				& De Waele, 2011; Palmer & Palmer, 2012; Kirkland, 2014			
McKittrick Hill	New Mexico	Permian	Dry	Allison, 2009			G
Edwards Plateau	Texas	Cretaceous	Sonora, Amazing Maze	Onac et al., 2001; Klimchouk, 2007; Stafford et al., 2008			
Mexico							
Tacotalpa, Tabasco	Mexico	Middle Cretaceous	Cueva de Villa Luz, Luna Azufre, El Susto, La Joya, Sulfur X	Pisarowicz, 1994; Hose & Pisarowicz, 1997, 1999; Taylor, 1999; Hose et al., 2000; Palmer, 2003; Hose & Northup, 2004; Pisarowicz et al., 2005; Hose & Macalady, 2006; Rosales-Lagarde et al., 2008; Gary & Sharp, 2009; Palmer & Palmer, 2012; Jones et al., 2016	x		G
Tamaulipas	NE Mexico	Upper Cretaceous	El Zacaton	Palmer, 2003; Gary & Sharp, 2006, 2009	x		G
Argentina							
Malargue	South Argentina	Jurassic	Las Brujas	Forti et al., 1993; Hill, 2000; Sancho et al., 2004		x	G
Brazil							
Campo Formoso	Eastern Brazil	NeoProterozoic	Toca da Boa Vista, Toca da Barriguda	Auler & Smart, 2003; Klimchouk et al., 2016		x	G
Russian Federation							
Caucasus	S-Russia	Upper Cretaceous	Matsestinsk	Dublyansky, 1980	x		S
Ural	S-Russia	Upper Devonian	Kinderlinsk	Chervyatsova & Potapov, 2014; Chervyatsova et al., 2016		x	M
Abkhazia (Georgia)							
Iverskaya ridge	Georgia	Cretaceous	Novoafonskaya (New Athos)	Dublyansky, 1980; Tintilozov, 1983	x		M
Turkmenistan							
Kopetdagh	Turkmenistan	Upper Jurassic	Bakhardenskaya	Dublyansky, 1980	x		M
Kugitangtau ridge	Turkmenistan	Jurassic	Cupp Coutunn, Fata Morgana, Tush-Jyruck	Maltsev & Malishevsky, 1990; Korshunov & Semikolennyh, 1994; Maltsev & Korshunov, 1998; Bottrell et al., 2001; Semikolenykh & Targulian, 2010			G
Kyrgyzstan							
Tyuya-Muyun massif	Kyrgyzstan	Carboniferous	Fersmana, Surpise, Great Baryte	Dublyansky et al., 1989			S
Iraq							
Ashdakh Mt.	Kurdistan	Tertiary	Tirshawaka	Laumanns et al., 2008	x		M
Bnabawagi and Awa Kurds Mts.	Kurdistan	Lower Cretaceous	Smaquli Krozh	Stevanović et al., 2009	x		S

Sagrma Mt.	Kurdistan	Upper Eocene	Awa Spi	Stevanović et al., 2009	x		S
Jordania							
Bergish Mt.	Jordania	Upper Cretaceous	Al-Daher	Kempe et al., 2006			M
Turkey							
Mali Mt.	SW Turkey	Mesozoic	Kaklik	Gulecal-Pektas & Temel, 2016	x		S
Romania							
Dobrogesa	South Romania	Miocene	Movile	Diaconu & Morar, 1993; Sarbu et al., 1994, 1996; Sarbu & Kane, 1995; Sarbu & Lascu, 1997; Vlasceanu et al., 1997; Galdenzi, 2001; Rohwerder et al., 2003; Hutchens et al., 2004; Porter & Engel, 2008; Porter et al., 2009	x		M
Cerna Valley	SW Romania	Jurassic	Diana, Despicătură, Hercules.	Onac et al., 2009, 2011; Wynn et al., 2010; Onac et al., 2013; Puşcaş et al., 2013	x		S
France							
Barrot dome	Alpes Maritimes	Lower Cretaceous	Grotte du Chat	Audra, 2008; D'Antoni-Nobécourt et al., 2008; De Waele et al., 2016; Audra, 2017			M
Ventoux	Provence	Lower Cretaceous	Baume Galinière	Audra et al., 2015; Audra, 2017		x	S
Donzère	Drome	Upper Cretaceous	Iboussières	Audra & Hofmann, 2004; Audra, 2017		x	S
Pierre St Martin	Pyrenees	Upper Cretaceous	Oilloki	Audra & Hofmann, 2004; Audra, 2017		x	S
Bauges	Savoie	Jurassic	Serpents, Chevalley, Alum	Socquet, 1801; Martel, 1935; Audra & Hobléa, 2007; Audra et al., 2007; Audra, 2017	x		M
Italy							
Faedo-Casaron	Veneto	Eocene-Oligocene	Pisatela-Rana	Tisato et al., 2012		x	G
Frasassi gorge	Marche	Jurassic	Frasassi, Grotte Grande del Vento	Galdenzi & Menichetti, 1995; Galdenzi et al., 1997; Sarbu et al., 2000; Vlasceanu et al., 2000; Galdenzi, 2001; Galdenzi & Maruoka, 2003; Macalady et al., 2006, 2007, 2008; Engel et al., 2007; Galdenzi et al., 2008; Jones et al., 2008, 2012, 2014, 2015, 2016; Menichetti et al., 2008; Porter & Engel, 2008; Dattagupta et al., 2009; Menichetti, 2009; Porter et al., 2009; Galdenzi, 2012; Desai et al., 2013; Harouaka et al., 2016; Zerkle et al., 2016; Galdenzi & Jones, 2017	x		G
Rio Garrafo	Marche	Eocene-Oligocene	Acquasanta Terme	Galdenzi & Menichetti, 1995; Galdenzi, 2001; Menichetti, 2009; Galdenzi et al., 2010; Jones et al., 2010, 2014, 2016; Fusari et al., 2017	x		G
Mt. Cucco	Umbria	Jurassic	La Grotta, Faggeto Tondo, Buca Futura	Forti et al., 1989; Galdenzi & Menichetti, 1995; Galdenzi, 2004; Menichetti et al., 2008; Menichetti, 2009			G

Roccaccia	Umbria	Quaternary travertines	Pozzi della Piana	Lippi Boncambi, 1938; Passeri, 1973; Galdenzi & Menichetti, 1995; Menichetti, 2009, 2011			G
Parrano gorge	Umbria	Cretaceous	Parrano	Lippi Boncambi, 1938; Galdenzi & Menichetti, 1995; Menichetti, 2009, 2011			G
Triponzo	Umbria	Lower Jurassic	Triponzo	Principi, 1931	x		S
Saturnia	Tuscany	Jurassic	Montecchio	Piccini et al., 2015	x		M
Cittàreale	Latium	Cretaceous-Eocene	Cittàreale	Preziosi & Scipioni, 1993; Galdenzi & Menichetti, 1995			G
Cornicolani Mts.	Latium	Lower Jurassic	Pozzo del Merro	Caramanna, 2002; Gary & Sharp, 2009	x		G
Mt. Soratte	Latium	Lower Jurassic	Luk, Sbardy, Santa Lucia	Galdenzi & Menichetti, 1995; Mecchia, 2012			M
Majella Mt.	Abruzzo	Upper Cretaceous-Paleogene	Cavallone-Bove	D'Angeli et al., 201x currently submitted			M
Capo Palinuro	Campania	Lower Jurassic	Cala Fetente, Azzurra, Sulfurea	Forti, 1985; Southward et al., 1996; Stüben et al., 1996; Airoldi et al., 1997; Mattison et al., 1998	x		M
Mt Sellaro	Calabria	Cretaceous-Paleocene	Serra del Gufo, Balze di Cristo, Ninfe	Galdenzi, 1997	x		G
Cassano allo Ionio	Calabria	Triassic	Sant'Angelo, Gigliola, Sette Nani, Sibarite spa caves	Galdenzi, 1997; Catalano et al., 2014;			G
Santa Cesarea	Apulia	Upper Creatceous	Fetida, Gattulla, Sulfurea, Solfatara	D'Angeli et al., 2017	x		S
Sicani Mts.	Sicily	Upper Cretaceous	Acqua Fitusa	Vattano et al., 2013; De Waele et al., 2016; Vattano et al., 2017	x		M
Iglesiente	Sardinia	Cambrian	Santa Barbara, Crovassa Azzurra, Ricchi in Argento, others	De Waele & Forti, 2006; De Waele et al., 2013, 2017; Gazquez et al., 2013			M
Iglesiente	Sardinia	Cambrian quartzite	Corona 'e Sa Craba	Sauro et al., 2014			S
Greece							
Kassandra	N Greece	Upper Jurassic	Aghia Paraskevi	Lazaridis et al., 2011			S
Austria							
Bad Deutsch Altenburg	East Austria	Triassic	Stephanshöhle and others	Plan et al., 2009; De Waele et al., 2016			S
Hochschwab	Austria	Lower Jurassic	Kraushöhle	Hauer, 1885; Kraus, 1891, 1894; Puchelt & Blum, 1989; Plan et al., 2009, 2012; De Waele et al., 2016			M
Republic of Macedonia							
Mariovo Basin	Macedonia	Cambrian	Provalata	Temovski et al., 2013			S

Algeria							
Azrou Massif	Algeria	Upper Cretaceous	Rhar es Skhoun	Collignon, 1983, 1990			M
South Africa							
Nelspruit, Eastern Transvaal	South Africa	Paleoproterozoic	Mbobo Mkulu	Martini et al., 1997		x	M
Namibia							
Otavi	North Namibia	Precambrian	Temple of Doom	Martini & Marais, 1996			M

1.3. Sulfuric acid speleogenesis

1.3.1. Origin and evolution of sulfides

Sulfuric acid speleogenesis (SAS) is deeply influenced by "*deep H_2S-bearing fluids rising toward unconfined carbonate aquifers and water tables*" (Klimchouk, 2017 p.19). The most common H_2S sources are: i) volcanic (Spilde et al., 2004; Aiuppa et al., 2005) and magmatic activities (Cavarretta & Lombardi, 1992); ii) bacterial (BSR) (60-80°C), assimilatory-dissimilatory (ASR-DSR) and thermochemical (TSR) (100-180°C) sulfate reduction (Canfield, 2001; Machel, 2001; Wynn et al., 2010) of deep-seated evaporite rocks and hydrocarbon tiers (Hill, 1990; Hill, 1995; Maggiore & Pagliarulo, 2004); iii) reduction of marine waters involved in deep circulation flows through fissure networks (Santaloia et al., 2016) or buried seawater (Machel, 2001; Wynn et al., 2010).

Other interesting sulfuric acid caves, not related to hypogene processes, might have formed by the oxidation of sulfide ores such as pyrite, marcasite, galena, blenda (Morehouse,1968; Auler & Smart, 2003; Tisato et al., 2012) or through abiotic or microbially-mediated processes (Engel et al., 2004).

In addition, in the surface environment H_2S is produced by the decay of organic matter in an oxygen-depleted environment (e.g. swamps, poorly oxygenated streams), but this source of hydrogen sulfide has a negligible role in speleogenesis.

Reduction of sulfates takes place in presence of organic compounds, hosted in the sedimentary sequences. Independently of which process is occurring (BSR or TSR), the rate of these processes mostly depends on the presence and supply of the main reactants, represented by organic compounds and dissolved sulfate. In comparable geochemical situations, BSR is generally faster than TSR. Distinguishing between BSR and TSR relies on a combination of different geochemical and petrographical criteria, and especially stable isotopes of C, O, and S (Wynn et al., 2010). Both processes, through a series of similar redox-reactions, lead to the formation of the same products, through the following schematic reaction (Machel, 2001):

$HC + SO_4^{2-}$ => altered into HC + solid bitumen + H_2S (HS^-) + HCO_3^- (CO_2) + H_2O + heat ? [1]

in which HC stands for hydrocarbons. Without going into detail, all hydrocarbons go through a maturation stage that can include aerobic biodegradation, anaerobic fermentation, and thermal maturation. These processes, through different reactions, "simplify" the organic molecules to organic acids, alcohols and other compounds (e.g. CH_4), which can then be used by sulfate reducing bacteria during BSR. Thermal maturation of crude oil itself generates small amounts of reagents (up to 3%) through the following reaction (Machel, 2001):

crude oil => light crude oil + H_2S + Polysulfides + CH_4 [2]

The simpler organic compounds produced, which will here be symbolized by CH_4 (being one of the most important end products of the transformation of hydrocarbons by BSR and/or TSR) will then

react with dissolved gypsum (or anhydrite, $CaSO_4$) producing H_2S according to the reaction (Palmer, 2007):

gypsum or anhydrite + HC + H_2O => $H_2S + Ca^{2+} + 2HCO_3^-$ [3]

In general, the H_2S produced migrates as a dissolved gas elsewhere, and limestone precipitates. Some authors talk about a replacement of the original gypsum or anhydrite rocks into bio-epigenetic calcite (Hill, 1995), and the reaction is often written as

$Ca^{2+} + 2SO_4^{2-} + 2CH_4 + 2H^+ => 2H_2S + CaCO_3 + CO_2 + 3H_2O$ [4]

In all cases one of the final products of these redox reactions is hydrogen sulfide, a gas that in normal geological situations of the shallow crust (< 6 km depth) remains in solution in its molecular or dissociated form (H_2S or HS^-). Note that this redox reaction also produces CO_2, which stays in solution at these pressures.

When dissolved H_2S comes in contact with descending oxygenated meteoric waters, elemental sulfur forms following the reaction (Hill, 1995)

$H_2S + ½\ O_2 => {}^xS^0 + H_2O$ [5]

However, generally descending meteoric waters are very poor in dissolved oxygen, and reactions [5] only remove minor parts of the H_2S formed during the earlier stages. Most of the H_2S migrates upward and, entering the adjoining carbonate reef and backreef deposits, this dissolved gas might react with the metal-rich chloride waters in the reducing zone forming the typical Mississippi Valley Type ore deposits according to the following complex redox reaction [6]

$H_2S + CO_2 + MeCl^+ + Mg^{2+} + 2CaCO_3 + H_2O => MeS + Ca^{2+} + CaMg(CO_3)_2 + HCO_3^- + Cl^- + 3H^+$

where Me represents metals such as Pb, Zn, and Fe (Hill, 1995).

If, on the other hand, dissolved hydrogen sulfide comes into the aerated environment, at or close to the potentiometric surface, the oxygen causes its oxidation, with the formation of sulfuric acid involved in SAS.

1.3.2. Sulfuric acid speleogenesis chemistry

The major source of dissolutional aggressivity in SAS caves derives from the oxidation of sulfides, producing sulfuric acid. Hydrogen sulfide (H_2S)-rich ascending fluids that oxidize at or close to the water table are responsible for the vast majority of SAS caves in the world (*Figure 1*).

The importance of the oxidation of hydrogen sulfide (H_2S) into sulfuric acid (H_2SO_4) for the formation of SAS caves was firstly described by Principi (1931) and Egemeier (1981) for the Bighorn basin caves in Wyoming. H_2S oxidation typically occurs in two cave environments (*Figure 2*): 1) where rising fluids enriched in H_2S meet 1a) deep oxidizing waters (it firstly occurs at the lower contact with a O_2-rich aquifer) or 1b) shallow oxidizing waters close to the water table (meteoric or

sea waters, directly exchanging with the external atmosphere), or 2) above the water table, in the oxidizing cave atmosphere (Galdenzi, 1990; Galdenzi and Maruoka, 2003; Audra, 2008).

Some authors, using geomorphological evidences, stated that sulfuric acid dissolution-corrosion occurs mainly below the water table (Davis, 1980; Hill, 1987; Forti et al., 2002).

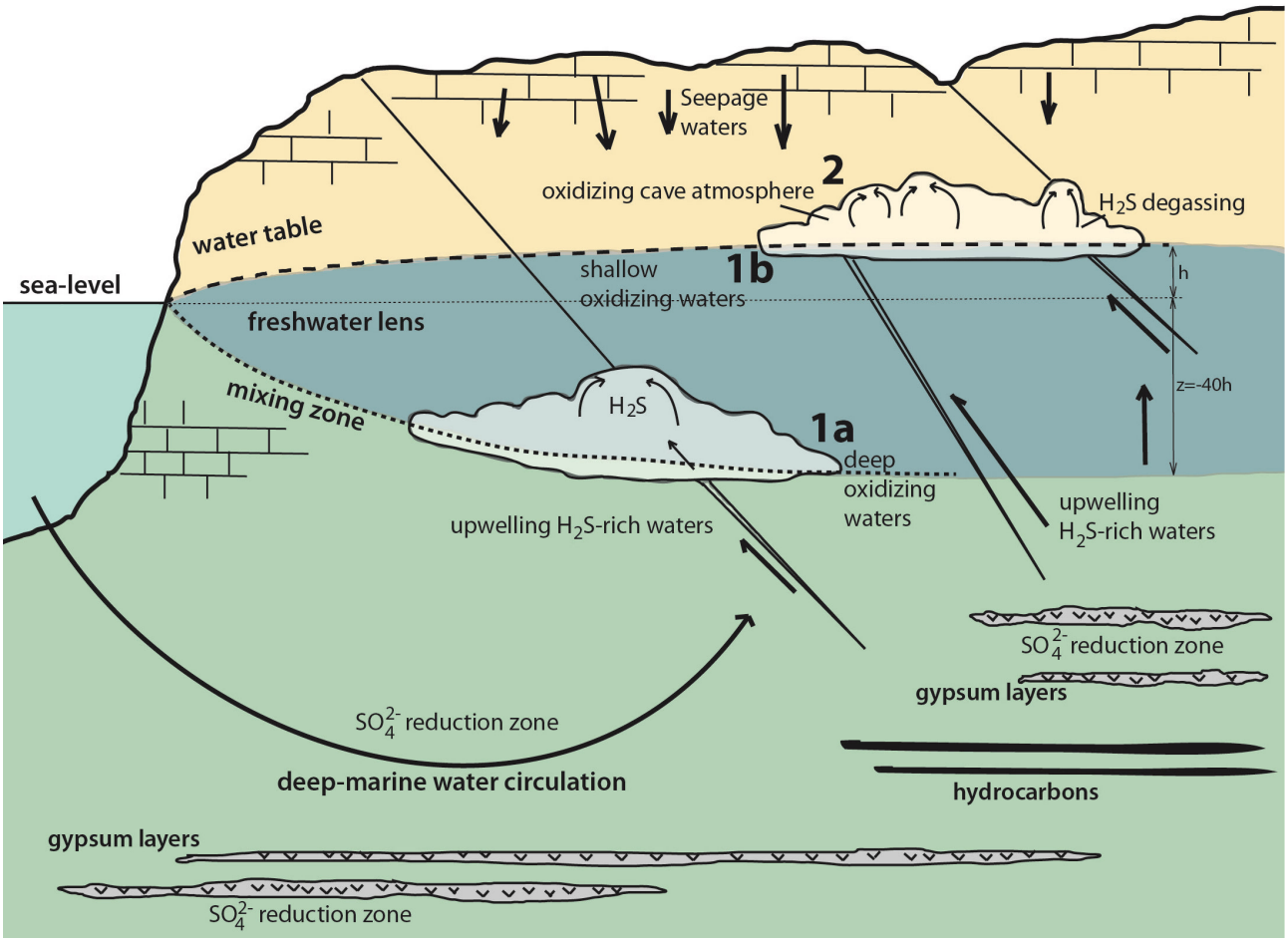

Figure 2. Sketch showing the two typical environments for H_2S oxidation: 1) where rising fluids enriched in H_2S meet 1a) deep oxidizing waters (it firstly occurs at the lower contact with a O_2-rich aquifer) or 1b) shallow oxidizing waters close to the water table (meteoric or sea waters, directly exchanging with the external atmosphere), or 2) above the water table, in the oxidizing cave atmosphere It refers to a special context, Santa Cesarea Terme, Apulia (southern Italy).

The oxidation of H_2S can occur in different ways:

$H_2S + 2O_2 \Rightarrow H_2SO_4$ ($SO_4^{2-} + 2H^+$ in aqueous solution) [7]

$H_2S + ½\ O_2 \Rightarrow S^o + H_2O$ [8]

$2S^o + 3O_2 + 2H_2O \Rightarrow 2SO_4^{2-} + 4H^+$ (in aqueous solution) [9]

The reaction speed is increased if mediation by sulfur-oxidizing bacteria occurs, and reaction [7] takes place bypassing the intermediate phases ([8] and [9]) (Engel et al., 2004; Palmer, 2013).

Since most SAS caves are developed in carbonate environments (Palmer, 2013), these reactions generally occur in this buffering environment at pH close to 7.

Once sulfuric acid (H_2SO_4) comes in contact with the carbonate host rock, it reacts immediately following the reaction

$$CaCO_3 + SO_4^{2-} + 2H^+ + 2H_2O \Rightarrow CaSO_4 \cdot 2H_2O + CO_2 + H_2O \quad [10]$$

The dissolution of limestone ($CaCO_3$) due to sulfuric acid (H_2SO_4) thus produces gypsum ($CaSO_4 \cdot 2H_2O$) and releases CO_2 into the surrounding environment. Already Egemeier (1981) talked about a replacement-solution, in which calcite is replaced by gypsum, whereas dolomite would convert into gypsum and hexahydrate (or epsomite in evaporative conditions). This replacement is often volumetric, and original bedrock textures and fossils are sometimes perfectly preserved (Queen, 1973; Buck et al., 1994; Plan et al., 2012). Gypsum, being more soluble than calcite, can then be taken away in solution by running waters, allowing the voids to enlarge rapidly. Also CO_2 released can contribute in increasing the general acidity of the waters, thus further promoting the dissolution of limestone and other carbonate rocks according to the classical reaction

$$CaCO_3 + CO_2 + H_2O \Rightarrow Ca(HCO_3)_2 \quad [11]$$

Sulfuric acid produced by oxidation of other sulfides, mainly pyrite, but also sphalerite, galena and other common sulfides in Mississippi Valley Type ore deposits, can react following the reaction

$$4FeS_2 + 15O_2 + 14H_2O \Rightarrow 4Fe(OH)_3 + 16H^+ + 8SO_4^{2-} \quad [12]$$

This process is often very localized and creates a scattered porosity. Nevertheless, there are examples in which sulfuric acid produced by oxidation of abundant pyrite has created large cave systems. Generally, pyrite minerals are scattered in the carbonate and their oxidation mainly occurs in saturated conditions, allowing the production of very acidic solution (pH~1) only where there is no contact with carbonates (e.g. on microbial filaments or other non-carbonate surfaces), because the contact with carbonates would prevent the pH from dropping so low. Only in aerated situations can gypsum precipitate as by-product following the reaction [10].

The abundant presence of pyrite in the galena dolomite has made cave formation by sulfide oxidation viable in Level Crevice Cave (Iowa) (Morehouse, 1968). Also the large maze cave systems in Campo Formosa (NE Brazil) are believed to have formed mainly by oxidation of sulfides in the Precambrian host rock (Auler & Smart, 2003). In Transvaal (South Africa) the Mbobo Mkulu Cave has formed between a thick layer of Archean dolostone and an overlying chert breccia overlain by a black shale rich in sulfides. It is the oxidation of these sulfides that is responsible for most of the dissolution in the dolostone (Martini et al., 1997).

However, normally these acid dissolution phenomena are very localized, and can occur in epigenic cave systems such as Pisatela, N-Italy (Tisato et al., 2012). Gypsum also occurs widely in the fossil

levels of Mammoth Cave (Palmer, 1989; Palmer & Palmer, 2009), but in this context sulfuric acid corrosion is only a very minor component in speleogenesis (Metzger et al., 2015). Also gypsum found in Castleguard Cave in Canada derives from the oxidation of pyrite in the surrounding limestones, and has nothing to do with speleogenesis (Yonge & Krouse, 1987). There are however good examples in which localized acid corrosion caused by weathering of pyrite ore bodies give rise to important formation of voids. One good example is the fluted shaft system Queen of the Guadalupes (Jagnow, 1979). Also in Baume Galinière, in the Vaucluse area (France), intense pyrite oxidation has created an almost 200-meter-long maze cave with an exceptional occurrence of SAS-derived cave minerals (Audra et al., 2015).

1.4. Objectives and outline of the thesis

The main objectives of this thesis can be resumed as following:

- Identify geomorphological features and mineralogical by-products, and relate their origin to speleogenesis;
- Describe in detail the microbial population thriving in a peculiar still-active sulfuric acid system evolved along the Adraitic coastline of southern Italy;
- Try to discriminate the main sources of H_2S contributing to the speleogenetic process;
- Understand the main speleogenetic processes (physical, chemical, and biological) involved in the formation of Italian sulfuric acid caves;
- Quantify the effective dissolution-corrosion in sulfuric acid waters, interface zones, and aerated conditions in different localities of southern Italy;
- Reconstruct the speleogenetic history and use cave levels to evaluate landscape evolution.

To achieve these goals, I organized several areas of the field work to visit SAS caves located along the Apeninne Chain, in Apulia, and in the main islands (Sicily and Sardinia), observe geomorphological features and collect mineralogical samples. I focused mainly on the still-active SAS caves of southern Italy, and in particular on Santa Cesarea Terme (Apulia), Cassano allo Ionio, Mt. Sellaro (Calabria), and Acqua Fitusa (Sicily), where, additionally, I collected geochemical and microbiological samples. Moreover, in these active underground environments I created several stations of limestone, marble, and gypsum tables placed in subaqueous, interface, and aerate conditions, with the aim to monitor the diverse dissolution-corrosion rate of these locations.

After the fieldwork, the collected samples were subjected to the following analyses (partly carried out by myself, and by laboratory technicians)

- X-ray diffraction (XRD) for mineralogical recognition (Genoa University);

- Scanning Electron Microscopy and Emission Dispersive spectrum to observe the crystal morphology and gather elemental composition information (Genoa University);
- $\delta^{34}S$ stable isotopes of sulfates and native sulfur deposits to understand the sources of H_2S (ETH Zürich);
- $^{40}Ar/^{39}Ar$ dating of alunite deposits to understand the beginning of sulfuric acid speleogenesis (University of New Mexico, Albuquerque and New Mexico Tech University)
- Major, minor and trace element water chemical analyses (Turin University);
- CO_2, CH_4 concentration and $\delta^{13}C_{CO2\text{-}CH4}$ stable isotopes of the gases dominating the cave atmosphere (Museo Nacional de Ciencas Naturales, Madrid);
- Total and organic C, N, elemental content analyses on microbial substances (Salerno University);
- Molecular biology, cultivation methodologies for microbial substances (IRNAS Seville);
- Field emission scanning electron microscopy to observe microbiological structures (Seville University);
- Next generation sequencing of microbiological samples (Graz University).

Unfortunately, the abundant presence of H_2S, in the still-active SAS caves of southern Italy, induces important errors on the $\delta^{13}C_{CO2}$ and $\delta^{13}C_{CH4}$ isotopic measurements using a Picarro 2201 cavity ring-down spectrometer as demonstrated by Malowany et al., (2015). Nevertheless, the results of this investigation will be shown in the chapter 4.2.

The thesis has been divided into three main sections:

1) Recognize SAS caves using geomorphological (chapter 2), mineralogical (chapter 3), geochemical (chapter 4) and geomicrobiological (chapter 5) signatures;
2) Italian SAS caves described in general (chapter 6) and some detailed examples of southern Italy (chapter 7);
3) Landscape evolution studies carried out through tablet weight loss investigations (chapter 8) and using subhorizontal SAS cave levels as indicator of uplift and erosion rate (chapter 9).

References

Airoldi, L., Southward, A.J., Niccolai, I., Cinelli, F., 1997. Sources and pathways of particulate organic carbon in a submarine cave with sulphur water springs. Water Air Soil Pollution, 99: 353–362.

Aiuppa, A., Inguaggiato, S., McGonigle, A.J.S., O'Dwyer, M., Oppenheimer, C., Padgeit, M.J., Rouwet, D., Valenza, M., 2005. H_2S fluxes from Mt. Etna, Stromboli, and Vulcano (Italy) and implication for the sulfur budjet at volcanoes. Geochimica et Cosmologica Acta, 69(7): 1861-1871.

Allison, S., 2009. Exploration and survey of Dry Cave, McKittrick Hill. In: A.N., Palmer, M.V., Palmer (Eds.), Caves and Karst of the USA. National Speleological Society, Huntsville, AL, 288-289.

Audra, P., 2008. Hypogenic sulfidic speleogenesis. Berliner Höhlenkundliche Berichte, 26: 15-32.

Audra, P., 2017. Hypogene Caves in France. In: A.B., Klimchouk, P., Audra, A.N., Palmer, J., De Waele, A., Auler (Eds.), Hypogene Karst Regions and Caves of the World, Springer, 61-83.

Audra P., Hobléa F., 2007. The first cave occurrence of jurbanite [$Al(OH\ SO_4)\cdot 5H_2O$], associated with alunogen [$Al_2(SO_4)_3\cdot 17H_2O$] and tschermigite [$NH_4Al(SO_4)_2\ \cdot 12H_2O$]: serpents thermal-sulfidic cave, France. Journal of Cave and Karst Studies, 69(2): 243–249.

Audra, P., Hofmann, B.A., 2004. Les cavités hypogènes associées aux dépôts de sulfures métalliques (MVT). Le Grotte d'Italia, 5: 35-56.

Audra, P., Hobléa, F., Bigot, J.-Y., Nobécourt, J.-C., 2007. The role of condensation-corrosion in thermal speleogenesis: study of a hypogenic sulfidic cave in Aix-les-Bains, France. Acta Carsologica, 36: 185-194.

Audra, P., Gázquez, F., Rull, F., Bigot, J.Y., Camus, H., 2015. Hypogene Sulfuric Acid Speleogenesis and rare sulfate minerals in Baume Galinière Cave (Alpes-de-Haute-Provence, France). Record of uplift, correlative cover retreat and valley dissection. Geomorphology, 247: 25-34.

Auler, A.S., Smart, P.L., 2003. The influence of bedrock-derived acidity in the development of surface and underground karst: evidence from the precambrian carbonate of semi-arid northeastern Brazil. Earth Surface Processes and Landforms, 28: 157-168.

Bakalowicz, M.J., Ford, D.C., Miller, T.E., Palmer, A.N., Palmer, M.V., 1987. Thermal genesis of dissolution caves in the Black Hills, South Dakota. Geological Society of America Bulletin, 99: 729-738.

Barton, H.A., Luiszer, F., 2005. Microbial metabolic structure in a sulfidic cave hot spring: Potential mechanisms of biospeleogenesis. Journal of Cave and Karst Studies, 67: 28-38.

Barton, H.A., Taylor, M.R., Pace, N.R., 2004. Molecular phylogenetic analysis of a bacterial

community in an oligotrophic cave environment. Geomicrobiology Journal, 21: 11-20.

Barton, H.A., Northup, D.E., 2007. Geomicrobiology in cave environments: past, current and future prospectives. Journal of Cave and Karts Studies, 69: 163-178.

Bottrell, S.H., Crowley, S., Self, C., 2001. Invasion of a karst aquifer by hydrothermal fluids: evidence from stable isotopic compositions of cave mineralization. Geofluids, 1(2): 103-121.

Bretz, J., 1949. Carlsbad Caverns and other caves of the Guadalupe block, New Mexico. Journal of Geology, 57(7): 447-463.

Buck, M.J., Ford, D.C., Schwarcz, H.P., 1994. Classification of cave gypsum deposits derived from oxidation of H_2S. In: Sasowky, ID, Palmer, MV, (Eds.), Breakthroughs in karst geomicrobiology, Colorado Spring, Colorado, 5-9.

Burger, P., 2009. Structural and facies control of hypogenic karst development in the Guadalupe Mountains, New Mexico, USA. In: K.W., Stafford, L., Land, G., Veni (Eds.), Advances in Hypogene Karst Studies. NCKRI Symposium 1. National Cave and Karst Research Institute, Carlsbad, NM, 60-70.

Calaforra, J.M., De Waele, J., 2011. New peculiar cave ceiling forms from Carlsbad Caverns (New Mexico, USA): zenithal ceiling tube-holes. Geomorphology, 134: 43-48.

Canfield D.E., 2001. Biogechemistry of sulfur isotopes. Reviews in mineralogy and geochemistry, 43: 607-636.

Caramanna, G., 2002. Le porte dell'acqua. Speleologia, 46: 32-39.

Catalano, M., Bloise, A., Miriello, D., Apollaro, C., Critelli, T., Muto, F., Cazzanelli, E., Barrese E., 2014. The mineralogical study of the Grotta Inferiore di Sant'Angelo (southern Italy). Journal of Cave and Karst Studies, 76: 51-61.

Cavarretta, G., Lombardi, G., 1992. Origin of sulphur in minerals and fluids from Latium (Italy): isotopic constraints. European Journal Mineralogy, 4: 1311-1329.

Chervyatsova, O.Y., Potapov, S.S., 2014. Gypsum deposits of the Kinderlinskaya Cave (Southern Urals) as possible indication of sulphuric acid speleogenesis. Speleology & Karstology, 13: 17-30.

Chervyatsova, O.Y., Potapov, S.S., Sadykov, S.A., 2016. Sulfur isotopic composition of sulfur deposits in Ural karst caves. News of the Ural State Mining University, 2: 37-41.

Collignon, B., 1983. Spéléogenése hydrothermale dans les Bibans (Atlas Tellien-Nord de l'Algérie). Karstologia, 2: 45-54.

Collignon, B., 1990. Les karst hydrothermaux d'Algérie. 10^{th} Proceedings of the International Congress of Speleology, Budapest, 758-760.

Cunningham, K.I., DuChene, H.R., Spirakis, C.S., McLean, J.S., 1994. Elemental sulfur in caves of

the Guadalupe Mountains, New Mexico (abs.). In: I.D., Sasowsky, M.V., Palmer (Eds.), Breakthroughs in Karst Geomicrobiology and Redox Chemistry. Karst Waters Institute Special Publication 1: 11-12.

Cunningham, K.I., Northup, D.E, Pollastro, R.M., Wright, W.G., LaRock, E.J., 1995. Bacteria, fungi, and biokarst in Lechuguilla Cave, Carlsbad Caverns National Park, New Mexico. Environmental Geology 25: 2-8.

D'Angeli, I.M., Vattano, M., Parise, M., De Waele, J., 2017. The coastal sulfuric acid cave system of Santa Cesarea Terme (southern Italy). In: A.B., Klimchouk, P., Audra, A.N., Palmer, J., De Waele, A., Auler (Eds.), Hypogene Karst Regions and Caves of the World, Springer, 161-168.

D'Angeli I.M., De Waele J., Galdenzi S., Madonia G., Parise M., Piccini L. & Vattano M., 2016. Sulfuric acid caves of Italy: An Overview. In: Chavez T. & Reehling P. (Eds.). NCKRI Symposium 6, Proceedings "DeepKarst 2016: Origins, Resources, and Management of Hypogene Karst", Carlsbad, New Mexico: 85-88.

D'Angeli Ilenia M., Nagostinis, M., Carbone, C., Bernasconi, S., polyak, V.J., Peters, L., McIntosh, W.C., De Waele, J., 201x. Sulfuric acid speleogenesis in The Majella Massif (abruzzo, Central Apennine, Italy). Geomorphology, xx: xx-xx.

D'Antoni-Nobécourt, J.-C., Audra, P., Bigot, J.-Y., 2008. La spéléogenèse par corrosion sulfurique: l'exemple de la grotte du Chat (Daluis, Alpes-Maritimes). Riviera Scientifique, 91: 53-72.

Dattagupta, S., Schaperdoth, I., Montanari, A., Mariani, S., Kita, N., Valley, J.W., Macalady, J.L., 2009. A novel symbiosis between chemoautotrophic bacteria and a freshwater cave amphipod. ISME Journal, 3: 935-943.

Davies, W.E., Moore, G.W., 1957. Endellite and hydromagnesite from Carlsbad caverns. Bulletin of the National Speleological Society, 19: 24-25.

Davis, D.G., 1973. Sulfur in Cottonwood Cave, Eddy Co., New Mexico. National Speleologiacal Society Bulletin, 35: 89-95.

Davis, D.G., 1980. Cave development in the Guadalupe Mountains: a critical review of recent hypothesis. NSS Bulletin, 42(3): 42-48.

Davis, D.G., 1988. The uniqueness of Lechuguilla Cave. NSS News 46, 426-430.

Davis, D.G., Palmer, M.V., Palmer, A.N., 1990. Extraordinary subaqueous speleothems in Lechuguilla Cave, New Mexico. NSS Bulletin, 52: 70-86.

Desai, M.S., Assig, K., Dattagupta, S., 2013. Nitrogen fixation in distinct microbial niches within a chemoautotrophy-driven cave ecosystem. ISME Journal, 7: 2411-2423.

De Waele, J., Forti, P., 2006. A new hypogean karst form: the oxidation vent. Zeitschrift für Geomorphologie Supplement Issues, 147: 107-127.

De Waele, J., Forti, P., Naseddu, A., 2013. Speleogenesis of an exhumed hydrothermal sulphuric acid karst in Cambrian carbonates (Mount San Giovanni, Sardinia). Earth Surface Processes and Landforms, 38(12): 1369-1379.

De Waele, J., Galdenzi, S., Madonia, G., Menichetti, M., Parise, M., Piccini, L., Sanna, L., Sauro, F., Tognini, P., Vattano, M., Vigna, B., 2014. A review on hypogene caves in Italy. In: A., Klimchouk, I., Sasowsky, J., Mylroie, S.A., Engel, A.S., Engel, (Eds.), Hypogene cave morphologies. Karst Waters Institute Special Publication 18, Leesburg, Virginia, 28-30.

De Waele, J., Audra, P., Madonia, G., Vattano, M., Plan, L., D'Angeli, I.M., Bigot, J.Y., Nobécourt, J.C., 2016. Sulfuric acid speleogenesis (SAS) close to the water table: examples from southern France, Austria and Sicily. Geomorphology, 253: 452-467.

De Waele, J., Gázquez, F., Forti, P., Naseddu, A., 2017. Inactive Hydrothermal Hypogenic Karst in SW Sardinia (Italy). In: a.B., Klimchouk, P., Audra, A.N., Palmer, J., De Waele, A., Auler (Eds.), Hypogene Karst Regions and Caves of the World, Springer, 183-197.

Diaconu, G., Morar, M., 1993. La Grotte de la Movile (Dobroudja, Roumanie). Analyses minéralogiques. Karstologia, 22: 15-20.

Dublyansky, V.N., 1980. Hydrothermal karst in the alpine folded belt of southern parts of U.R.S.S.. Kras i Speleologia, 3(12):18-36.

Dublyansky, V.N., Hevesi, A., Hromas, J., Kraus, S., Machanykova, V., Mikhailov, V., Mucke, D., Sanyakova, V., Szekely, K., Bolner Takacs, K., 1989. Tyuya-Muyun (USSR, Kirghizia – preliminary results of the speleological researches carried out by the International Expedition in 1989). Proceeding of the 10 th International Congress of Speleolology, Budapest, 825-830.

DuChene, H.R., Cunningham, K.I., 2006. Tectonic influences on speleogenesis in the Guadalupe Mountains, New Mexico and Texas. In: New Mexico Geological Society guidebook, 57th field conference, Caves and Karst of Southeastern New Mexico, 211-217.

DuChene, H.R., 2009. The relationship of oil field-derived hydrogen sulfide in the Permian (Guadalupian) Artesia Group to sulfuric acid speleogenesis in the Guadalupe Mountains, New Mexico and Texas. In: K.W., Stafford, L., Land, G., Veni (Eds.), Advances in Hypogene Karst Studies. NCKRI Symposium 1. National Cave and Karst Research Institute, Carlsbad, NM, 111-120.

Egemeier, S.J., 1971. A comparison of two types of solution caves: Unpublished report in the file of Carlsbad Cavern National Park, 7 pp.

Egemeier, S.J., 1973. Cavern Development by thermal waters with a possible bearing on ore deposition. Unpublished Ph.D. dissertation, Standford University, 88 pp.

Egemeier, S.J., 1981. Cavern development by thermal waters. National Speleological Society

Bulletin, 43: 31-51.

Egemeier, S.J., 1987. A theory for the origin of Carlsbad Cavern. NSS Bulletin, 43: 31-51.

Elworthy, R.T., 1918. Mineral springs of Canada. Part II. The chemical character of some Canadian mineral springs. Department of Mines, Mines Branch, Canada, Report 472, Bulletin 20: 173 pp.

Engel, A. S., 2007. Observations on the biodiversity of sulfidic karst habitats. Journal of Cave and Karst Studies, 69: 187-206.

Engel, A.S., Porter, M.L., Kinkle, B.K., Kane, T.C., 2001. Ecological assessment and geological significance of microbial communities from Cesspool Cave, Virginia. Geomicrobiological Journal, 18: 259-274.

Engel, A.S., Lee, N., Porter, M.L., Stern, L.A., Bennett, P.C., Wagner, M., 2003. Filamentous ‘‘Epsilonproteobacteria’’ dominate microbial mats from sulfidic cave springs. Applied and Environmental Microbiology, 69: 5503–5511.

Engel, A.S., Stern, L.A., Bennett, P.C., 2004. Microbial contributions to cave formation: new insights into sulphuric acid speleogenesis. Geology 32(5): 369-372.

Engel, A.S., Meisinger, D.B., Porter, M.L., Payn, R.A., Schmid, M., Stern, L.A., Schleifer, K.H., Lee, N.M., 2010. Linking phylogenetic and functional diversity to nutrient spiraling in microbial mats from Lower Kane Cave (USA). ISME Journal, 4: 98-110.

Forti, P., 1985. Le mineralizzazioni della grotta di Cala Fetente (Salerno, Campania). Mondo Sotterraneo, 41-50.

Forti, P., Menichetti, M., Rossi, A., 1989. Speleothems and speleogenesis of the Faggeto Tondo cave (Umbria, Italy). In: T., Hazslinszky, B.K., Takacsne (Eds.), Proceeding of the 10th International Congress of Speleology, Budapest, 1: 74-76.

Forti, P., Benedetto, C., Costa, G., 1993. Las Brujas cave (Malargue, Argentina): an example of the oil pools control on the speleogenesis. Theoretical and Applied Karst, 6: 87-93.

Forti, P., Galdenzi, S., Sarbu, S.M., 2002. Hypogenic caves: a powerful tool for the study of seeps and their environmental effects. Continental Shelf Reseach, 22: 2373

Fusari, A., Carroll, M. R., Ferraro, S., Giovannetti, R., Giudetti, G., Invernizzi, C., Mussi, M., Pennisi, M., 2017. Circulation path of thermal waters within the Laga foredeep basin inferred from chemical and isotopic ($\delta^{18}O$, δD, ^{3}H, $^{87}Sr/^{86}Sr$) data. Applied Geochemistry, 78: 23-34.

Galdenzi, S., 1997. Initial geologic observations in caves bordering the Sibari Plain (Southern Italy). Journal of Cave and Karst Studies, 59: 81-86.

Galdenzi, S., 2001. L’azione morfogenetica delle acque sulfuree nelle Grotte di Frasassi, Acquasanta Terme (Appennino marchigiano – Italia) e di Movile (Dobrogea – Romania). Le Grotte d’Italia, 5(2): 49-61.

Galdenzi, S., 2004a. I depositi di gesso nella Grotta di Faggeto Tondo: nuovi dati sull'evoluzione geomorfologia dell'area di Monte Cucco (Italia centrale). Studi Geologici Camerti, 2: 71-83.

Galdenzi, S., 2004b. Nuovi dati sui depositi di gesso della Grotta di Faggeto Tondo (Monte Cucco, Italia centrale). Grotte d'Italia, 5: 69-79.

Galdenzi, S., 2012. Corrosion of limestone tablets in sulfidic ground-water: measurements and speleogenetic implications. International Journal of Speleology, 41: 25-35

Galdenzi, S., Jones, D. S., 2017. The Frasassi Caves: A "Classical" Active Hypogenic Cave. In: A.B., Klimchouk, P., Audra, A.N., Palmer, J., De Waele, A., Auler (Eds.), Hypogene Karst Regions and Caves of the World, Springer, 143-159.

Galdenzi, S., Maruoka, T., 2003. Gypsum deposits in the Frasassi Caves, Central Italy. Journal of Cave and Karst Studies, 65: 111-125.

Galdenzi, S., Menichetti, M., 1990. Il carsismo della Gola di Frasassi. Memorie dell'Istituto Italiano di Speleologia, 2(4): 243 pp.

Galdenzi, S., Menichetti, M., 1995. Occurrence of hypogene caves in a karst region: examples from central Italy. Environmental Geology, 26: 39-47.

Galdenzi, S., Cocchioni, M., Morichetti, L., Amici, V., Scuri, S., 2008. Sulfidic ground-water chemistry in the Frasassi Caves, Italy. Journal of Cave and Karst Studies, 70: 94-107.

Galdenzi, S., Cocchioni, F., Filipponi, G., Morichetti, L., Scuri, S., Selvaggio, R., Cocchioni, M., 2010. The sulfidic thermal caves of Acquasanta Terme (central Italy). Journal of Cave and Karst Studies, 72: 43-58.

Gary, M.O., Sharp, J.M., 2006. Volcanogenic karstification of Sistema Zacatón, Mexico. In: Harmon, R.S., Wicks, C.M. (Eds.), Perspectives on Karst Geomorphology, Hydrology, and Geochemistry—A Tribute Volume to Derek C. Ford and William B. White, Geological Society of America Special Papers, 404: 79-89.

Gary, M.O., Sharp, J.M., 2009. Volcanogenic karstification: implications of this hypogene process. In: Stafford, K.W., Land, L., Veni, G. (Eds.), Advances in Hypogene Karst Studies. NCKRI Symposium 1. National Cave and Karst Research Institute, Carlsbad, NM, 27-39.

Gázquez, F., Calaforra, J.M., Fort, P., De Waele, J., Sanna, L., Rull, F., Sanz, A., 2013. Corrosion of calcite crystals by matal-rich mud in caves: Study case in Crovassa Ricchi in Argento Cave (SW Sardinia, Italy). Geomorphology, 198: 138-146.

Ginés, J., Fornós, J.J., Ginés, A., Merino, A., Gràcia, F., 2014. Geologic constraints and speleogenesis of Cova des Pas de Vallgornera, a complex coastal cave from Mallorca Island (Western Mediterranean). Int. J. Speleol. 43 (2), 105–124.

Gulecal-Pektas, Y., Temel, M., 2016. A Window to the Subsurface: Microbial Diversity in Hot Springs of a Sulfidic Cave (Kaklik, Turkey). Geomicrobiology Journal, http://dx.doi.org/10.1080/01490451.2016.1204374, 11 pp.

Harouaka, K., Mansor, M., Macalady, J.L., Fantle, M.S., 2016. Calcium isotopic fractionation in microbially mediated gypsum precipitates. Geochimica et Cosmochimica Acta, 184: 114-131.

Hauer, F., 1885. Die Gypsbildungen in der Krausgrotte bei Gams. Verhandlungen der Geologischen Reichsanstalt, 21-24.

Häuselmann, P., 2013. Large epigenic caves in high-relief areas. In: John F., Shroder (Ed.), Treatise on geomorphology, Academic Press, Karst Geomorphology, 6: 207-219.

Hill, C.A., 1987. Geology of Carlsbad Caverns and other caves in the Guadalupe Montains, New Mexico and Texas. New Mexico Bureau of Miners and Mineral Resources, Bulletin, 117-150.

Hill, C.A., 1990. Sulfuric acid speleogenesis of Carlsbad Cavern and its relationship to hydrocarbon, Delaware Basin, New Mexico and Texas. American Association of Petroleum Geologists Bulletin, 74: 1685-1694.

Hill, C.A., 1995. H_2S-Related Porosity and Sulfuric Acid Oil-Field Karst. In: Budd, D.A., Saller, A.H., Harris, P.M. (Eds.), Unconformities in carbonate strata-Their recognition and the significance of associated porosity, American Association of Petroleum Geologists Memoirs, 61: 301-306.

Hill, C.A., 2000. Sulfuric Acid, hypogene karst in the Guadalupe Mountains of New Mexico and West Texas, USA. In: A.B., Klimchouk, D.C., Ford, A.N., Palmer, W., Dreybrodt, (Eds.), Speleogenesis: Evolution of karst aquifers, 309-318.

Hill, C.A., Polyak, V.J., 2010. Karts hydrology of Grand Canyon, Arizona, USA. Journal of Hydrology, 390: 169-181.

Hose, L.D., Macalady, J.L., 2006. Observations from active sulfidic karst systems: is the present the key to understanding Guadalupe Mountain speleogenesis? In: New Mexico Geological Society guidebook, 57th field conference, Caves and Karst of Southeastern New Mexico,185-194.

Hose, L.D., Northup, D.E., 2004. Biovermiculations: living, vermiculation-like deposits in Cueva de Villa Luz. Journal of Cave and Karst Studies 66(3): 112.

Hose, L.D., Pisarowicz, J.A., 1997. Exploration and mapping of Cueva de Villa Luz (Dueva de la Sardina), Tabasco, Mexico. Journal of Cave and Karst Studies 59: 173.

Hose, L.D., Pisarowicz, J.A.,1999. Cueva de Villa Luz, Tabasco, Mexico: reconnaissance study of an active sulfur spring cave and ecosystem. Journal of Cave and Karst Studies, 61:13-21.

Hose, L.D., Palmer, A.N., Palmer, M.V., Northup, D.E., Boston, P.J., DuChene, H.R., 2000. Microbiology and geochemistry in a hydrogen-sulphide-rich karst environment. Chemical

Geology, 169. 399-423.

Hubbard, D.A. Jr., Herman, J.S., Bell, P.E., 1986. The role of sulfide oxidation in the genesis of Cesspool cave, Virginia, USA. Proceeding of the 9th International Speleological Congress, 255-257.

Hubbard, D.A., Jr., Herman, J.S., Bell, P.E., 1990. Speleogenesis in a travertine scarp: Observations of sulfide oxidation in the subsurface. In: J.S., Herman, D.A., Hubbard, Jr., (Eds.), Travertine-marl: stream deposits in Virginia: Virginia Division of mineral resources publication, 10: 177-184.

Huntoon, P.W., 2000. Karstification associated with groundwater circulation through the Redwall Artesian Aquifer, Grand Canyon, Arizona. In: A.B., Klimchouk, D.C., Ford, A.N., Palmer, W., Dreybrodt (Eds). Speleogenesis. Evolution of Karst Aquifers, National Speleological Society, 287-291.

Hutchens, E., Radajewski, S., Dumont, M.G., McDonald, I. R., Murrell, J.C., 2004. Analysis of methanotrophic bacteria in Movile Cave by stable isotope probing. Environmental Microbiology, 6: 111-120.

Jagnow, D.H., 1977. Geologic factors influencing speleogenesis in the Capitan Reef Complex, New Mexico and Texas. Unpublished MS thesis, University of New Mexico, 197 pp.

Jagnow, D.H., 1978. Geology and speleogenesis of Ogle Cave, New Mexico. NNS bulletin, 40(1): 7-18.

Jagnow, D.H., 1979. Cavern development in the Guadalupe Mountains. Cave Research Foundation, Columbus, Ohio: 55 pp.

Jagnow, D.H., Hill, C.A., Davis, D.G., DuChene, H.R., Cunningham, K.I., Northup, D.E., Queen, J.M., 2000. History of the sulfuric acid theory of speleogenesis in the Guadalupe Mountains, New Mexico. Journal of Cave and Karst Studies, 62(2): 54-59.

Jones, D.S., Lyon, E., Macalady, J., 2008. Geomicrobiology of biovermiculations from the Frasassi cave system, Italy. Journal of Cave and Karst Studies, 70: 78-93.

Jones, D.S., Tobler, D.J., Schaperdoth, I., Mainiero, M., Macalady J.L., 2010. Community structure of subsurface biofilms in the thermal sulfidic caves of Acquasanta Terme, Italy. Applied Environmental Microbiology, 76: 5902-5910.

Jones, D.S., Albrecht, H.L., Dawson, K.S., Schaperdoth, I., Freeman, K.H., Pi, Y., Pearson, A., Macalady, J.L., 2012. Community genomic analysis of an extremely acidophilic sulfur-oxidizing biofilm. ISME Journal, 6: 158-170.

Jones, D.S., Schaperdoth, I., Macalady, J.L., 2014. Metagenomic evidence for sulfide oxidation in extremely acidic cave biofilms. Geomicrobiology Journal, 31: 194-204.

Jones, D.S., Polerecky, L., Galdenzi, S., Dempsey, B.A., Macalady, J.L., 2015. Fate of sulfide in the Frasassi cave system and implications for sulfuric acid speleogenesis. Chemical Geology, 410: 21-27.

Jones, D.S., Schaperdoth, I., Macalady, J.L., 2016. Biogeography of sulfur-oxidizing Acidithiobacillus populations in extremely acidic cave biofilms. ISME Journal, 10: 2879-2891.

Kempe, S., Al-Malabeh, A., Al-Shreideh, A., Henschel, H.V., 2006. Al-Daher Cave (Bergish), Jordan, the first extensive Jordanian limestone cave: A convective Carlsbad-type cave. Journal of Cave and Karst Studies, 68(3): 107-114.

Kirkland, D.W., 1982. Origin of gypsum deposits in Carlsbad Caverns, New Mexico. New Mexico Geology 4: 20-21.

Kirkland, D.W., 2014. Role of hydrogen sulfide in the formation of cave and karst phenomena in the Guadalupe Mountains and western Delaware Basin, New Mexico and Texas. National Cave and Karst Research Institute, Carlsbad, Special Paper Series, 1-77.

Klimchouk, A., 1996. The typology of gypsum karst according to its geological and geomorphological evolution. International Journal of Speleology, 25(3-4): 49-60.

Kilmchouk, A., 2005. Conceptualisation of speleogenesis in multy-storey artesian systems: a model of transverse speleogenesis. International Journal of Speleology, 34(1-2): 45-64.

Klimchouk, A., 2007. Hypogean speleogenesis: hydrogeological and morphometric perspective. Special Paper 1, National Cave and Karst Research Institute, Carlsbad, NM, 106 pp.

Klimchouk, A., 2009. Morphogenesis of hypogenic caves. Geomorphology, 106: 100-117.

Klimchouk, A., 2015. The karst paradigm: changes, trends and prespectives. Acta Carsologica, 44(3): 289-313.

Klimchouk, A., Auler S.A., Bezerra, F.H.R., Cazarin, C.L., Balsamo, F., Dublyansky, Y., 2016. Hypogenic origin, geologic controls and functional organization of a giant cave system in Precambrian carbonates, Brazil. Geomorphology, 253: 385-405.

Klimchouk, A.B., 2017 - Types and settings of hypogene karst. In: Klimchouk, A.B., Palmer, A.N., De Waele, J., Auler, A., Audra, P. (Eds.), Hypogene karst regions and caves of the world. Springer, 1-39. DOI 10.1007/978-3-319-53348-3_1.

Klimchouk, A.B., 2018 - Tafoni and honeycomb structures as indicators of ascending fluid flow and hypogene karstification. In: Parise, M., Gabrovsek, F., Kaufmann, G., Ravbar, N. (Eds.), Advances in Karst Research: Theory, Fieldwork and Applications. Geological Society, London, Special Publications, 466: 79-105.

Korshunov, V., Semikolennyh, A., 1994. A model of speleogenic processes connected with bacterial redox in sulphur cycles in the caves of Kugitangtou Ridge, Turkmenia. In: I.D., Sasowsky, M.V.,

Palmer (Eds.), Breakthroughs in Karst Geomicrobiology and Redox Geochemistry. Karst Waters Institute, Special Publication, 1: 43-44.

Kraus, F., 1891. Höhlenbildung durch Metamorphismus. Die Nature 40: 197-199.

Kraus, F., 1894. Höhlenkunde. Gerold's Sohn, Vienna (reprint 2009, Wiss. Beiheft, Die Höhle, 56, Vienna).

Laumanns, Rasch, A., Audra, P., 2008. Karst and caves of Iraq. Berliner Höhlenkundliche Berichte, 26: 43-45.

Lazaridis, G., Melfos, V., Papadopoulou, L., 2011. The first cave occurrence of orpiment (N. Greece). International Journal of Speleology, 133-139.

Lippi Boncambi, C., 1938. Le Grotte di Parrano. Grotte d'Italia, 2(3):13-27.

Lowe, D.J., Bottrell, S.H., Gunn, J., 2000. Some case studies of speleogenesis by sulfuric acid. In: Klimchouk, A.B., Ford, D.C., Palmer, A.N., Dreybrodt, W. (Eds.), Speleogenesis: Evolution of karst aquifers. Huntsville, National Speleological Society, 304-308.

Macalady, J.L., Lyon, E.H., Koffman, B., Albertson, L.K., Meyer, K., Galdenzi, S., Mariani, S., 2006. Dominant microbial populations in limestone-corroding stream biofilms, Frasassi cave system, Italy. Applied Environmental Microbiology, 72: 5596-5609.

Macalady, J.L., Jones, D. S., Lyon, E. H., 2007. Extremely acidic, pendulous cave wall biofilms from the Frasassi cave system, Italy. Environmental Microbiology, 9: 1402-1414.

Macalady, J.L., Dattagupta, S., Schaperdoth, I., Jones, D.S., Druschel, G.K., Eastman, D., 2008. Niche differentiation among sulfur-oxidizing bacterial populations in cave waters. The ISME Journal, 2(6): 590-601.

Machel, H., 2001. Bacterial and thermochemical sulfates reduction in diagenetic settings – old and new insights. Sedimentary Geology, 140: 143-175.

Maggiore, M., Pagliarulo, P., 2004. Circolazione idrica ed equilibri idrogeologici negli acquiferi della Puglia. Geologi e Territorio, 1: 13-35.

Malowany, K., Stix, J., Van Pelt, A., Lucic, G., 2015. H_2S interference on CO_2 isotopic measurements using a Picarro G1101-I cavity ring-down spectrometer. Atmospheric Measurement Techniques, 8: 4075-4082.

Maltsev, V.A., Malishevsky, D.I., 1990. On hydrothermal phases during later stages of the evolution of Cupp Coutunn Cave System, Turkmenia, USSR. NSS Bulletin, 52: 95-98.

Maltsev, V., Korshunov, V., 1998. Geochemistry of fluorite and related features of the Kugitangtou Ridge caves, Turkmenistan. Journal of Cave and Karst Studies, 60: 151-155.

Martel, E.A., 1935. Contamination, protection et amelioration des sources thermominérales. Congrès International des mines, de la métallurgie et de la géologie appliquéè 7^{e}session, 2: 791-798.

Martini, J.E.J., Marais, J.C.E., 1996. Grottes hydrothermales dans le Nord-Ouest de la Namibie. Karstologia, 28: 13-18.

Martini, J.E.J., Wipplinger, P.E., Moen, F.G., 1997. Mbobo Mkulu Cave, South Africa. In: C.A., Hill, P., Forti (Eds.), Cave Minerals of the World. Huntsville, Alabama, National Speleological Society, 336-339.

Mattison, R.G., Abbiati, M., Dando, P.R., Fitzsimons, M.F., Pratt, S.M., Southward, A.J., and Southward, E.C., 1998. Chemoautotrophic microbial mats in submarine caves with hydrothermal sulphidic springs at Cape Palinuro, Italy. Microbial Ecology, 35: 58-71.

Mecchia, M., 2012. Indizi di speleogenesi ipogenica nelle grotte del Monte Soratte. Notiziario Speleo Club Roma, 16: 58-69.

Meisinger, D.B., Zimmermann, J., Ludwig, W., Schleifer, K.-H., Wanner, G., Schmid, M., Bennett, P.C., Engel, A.S., Lee, N.M., 2007. In situ detection of novel Acidobacteria in microbial mats from a chemolithoautotrophically based cave ecosystem (Lower Kane Cave, WY, USA). Environmental Microbiology, 9: 1523-1534.

Menichetti, M., 2009. Speleogenesis of the hypogenic caves in Central Italy. In: W.B., White (Ed.) Proceding of the 15th International Congress of Speleology, Kerrville, 909-915.

Menichetti, M., 2011. Hypogenic caves in western Umbria (Central Italy). Acta Carsologica, 40: 129-145.

Menichetti, M., Chirenco, M.I., Onac, B., S. Bottrell, 2008. Depositi di gesso nelle grotte del M. Cucco e della Gola di Frasassi, Considerazioni sulla speleogenesi. Memorie dell'Isituto Italiano di Speleologia, 21: 308-325.

Metzger, J.G., Fike, D.A., Osburn, G.R., Guo, C.J., Aadison, A.N., 2015. The source of gypsum in Mammoth Cave, Kentucky. Geology, 43: 187-190.

Morehouse, D.F., 1968. Cave development via the sulfuric acid reaction. National Speleological Society Bulletin, 30(1): 1-10.

Mylroie, J.E., Mylroie, J.R., 2018 – Role of karst denudation on the accurate assessment of glacio-eustasy and tectonic uplift on carbonate coasts. In: M., Parise, F., Gabrovsek, G., Kaufmann, N., Ravbar (Eds.), Advances in Karst Research: Theory, Fieldwork and Applications. Geological Society, London, Special Publications, 466: 171-185.

Mylroie, J.E., Carew, J.L., Vacher, H.R., 1995. Karst development in the Bahamas and Bermuda, Geological Society of America Special Paper, 300: 251-267.

Northup, D.E., Carr, D.L., Crocker, M.T., Hawkins, L.K., Leonard, P., Welbourn, W.C., 1995. Biological investigations in Lechuguilla Cave. NSS Bulletin, 56: 54-63.

Northup D.E., Dahm, C.N., Melim L.A., Spilde M.N., Crossey L.J., Lavoie K.H., Mallory L.M., Boston P.J., Cunningham K.I., Barns S.M., 2000. Evidence for geomicrobiological interactions in Guadalupe caves: Journal of Cave and Karst Studies, 62: 80-90.

Northup, D.E., Barns, S.M., Yu, L.E., Spilde, M.N., Schelble, R.T., Dano, K.E., Crossey, L.J., Connolly, C.A., Boston, P.J., Natvig, D.O., Dahm, C.N., 2003. Diverse microbial communities inhabiting ferromanganese deposits in Lechuguilla and Spider Caves. Environmental Microbiology, 5: 1071-1086.

Onac, B. P., Forti, P., 2011. State of the art and challenges in cave minerals studies. Studia UBB Geologia, 56(1): 33-42.

Onac, B.P., Veni, G., White, W.B., 2001. Depositional environment for metatyuyamunite and related minerals from Caverns of Sonora, TX (USA). European Journal of Mineralogy 13: 135-143.

Onac, B.P., Hess, J.W., White, W.B., 2007. The relationship between the mineral composition of speleothems and mineralization of breccia pipes: evidence from Corkscrew Cave, Arizona, USA. The Canadian Mineralogist 45: 1177-1188.

Onac, B.P., Sumrall, J., Tămaş, T., Povară, I., Kearns, J., Dârmiceanu, V., Veres, D., Lascu, C., 2009. The relationship between cave minerals and H_2S-rich thermal waters along Cerna Valley (SW Romania). Acta Carsologica, 38(1): 27-39.

Onac, B.P., Effenberger, H.S., Wynn, J.G., Povară, I., 2013. Rapidcreekite in the sulfuric acid weathering environment of Diana Cave, Romania. American Mineralogist, 98: 1302-1309.

Palmer, A.N., 1989. Geomorphic history of Mammoth Cave System. In: W.B. White, E.L., White (Eds.), Karst Hydrogeology: Concepts from the Mammoth Cave area: New York, Van Nostrand Reinhold, 317-363.

Palmer, A.N., 2000. Hydrogeologic control on cave patterns. In: Ford, D., Palmer, A., Dreybrodt, W., Klimchouk, A. (Eds.), Evolution of karst Aquifers, National Speleologic Society, Huntsville (AL), Speleogenesis, 77-99.

Palmer, A.N., 2001. Dynamics of cave development by allogenic water. Acta carsologica 30(2), 14-32.

Palmer, A.N., 2003. Sulfuric acid caves of North America. Grotte d'Italia 4, 7-16.

Palmer, A.N., 2006. Support for a sulfuric acid origin for caves in the Guadalupe Mountains, New Mexico. In: New Mexico Geological Society guidebook, 57th field conference, Caves and Karst of Southeastern New Mexico,195-202.

Palmer, A.N., 2007. Cave Geology. Cave Book, Dayton, Ohio, 454 pp.

Palmer, A.N., 2013. Sulfuric acid caves: morphology and evolution. In: Schroder, J, Fromkin, A, (Eds.). Treatise on Geomorphology. Academic Press, Karst Geomorphology, 6: 241-257.

Palmer, A.N., Palmer, M.V., 1989. Geologic history of the Black Hills Caves, South Dakota. NSS Bulletin, 51: 72-99.

Palmer, A.N., Palmer, M.V., 2000. Speleogenesis of the Black Hills Maze Caves, South Dakota, USA. In: A.B., Klimchouck, D.C., Ford, A,N., Palmer, W., Dreybrodt, (Eds.), Speleogenesis: Evolution of karst aquifers, 275-286.

Palmer, A.N., Palmer, M.V. (Eds.), 2009. Caves and karst of the USA: Huntsville, AL, National Speleological Society, 446 pp.

Palmer, A.N., Palmer, M.V., 2012. Petrographic and isotopic evidence for late-stage processes in sulfuric acid caves of the Guadalupe Mountains, New Mexico, USA. International Journal of Speleology, 41: 231-250.

Parise, M., Gabrovsek, F., Kaufmann, G., Ravbar, N., 2018. Recent advances in karts research: from theory to fieldwork and applications. Geological Society of London, 466: 1-24.

Passeri, L., 1973. Canalizzazione sotterranea in regime di fluttuazione freatica nel travertino della Piana (Umbria). Rassegna Speleologica Italiana, 25: 83-97.

Piccini, L., De Waele, J., Galli, E., Polyak, V.J., Bernasconi, S.M., Asmerom, Y., 2015. Sulphuric acid speleogenesis and landscape evolution: Montecchio cave, Albegna river valley (Southern Tuscany, Italy). Geomorphology, 229: 134-143.

Pisarowicz, J.A., 1994. Cueva de Villa Luz - an active case of H_2S speleogenesis. In: I.D., Sasowsky, M.V., Palmer (Eds.), Breakthroughs in Karst Geomicrobiology and Redox Geochemistry. Karst Waters Institute, Special Publication 1: 60–62.

Pisarowicz, J.A., Rykwalder, P., Hose, L.D., Amidon, C., 2005. Return to Tabasco. Association for Mexican Cave Studies Activities Newsletter, 28: 27–57.

Plan, L., Spötl, C., Pavuza, R., Dublyansky, Y., 2009. Hypogene caves in Austria. In: Klimchouk, A.B., Ford, D.C. (Eds.), Hypogene Speleogenesis and Karst Hydrogeology of Artesian Basins. Special Paper, 1. Ukrainian Institute of Speleology and Karstology, Kiev, 121-127

Plan, L., Tschegg, C., De Waele, J., Spötl, C., 2012. Corrosion morphology and cave wall alteration in an alpine sulfuric acid cave (Kraushöhle, Austria). Geomorphology, 169-170: 45-54.

Polyak, V.J., Güven, N., 1996. Alunite, natroalunite and hydrated halloysite in Carlsbad Cavern and Lechuguilla Cave, New Mexico. Clays and Clay Minerals 44: 843-850.

Polyak, V.J., Güven, N., 2000. Clays in caves of the Guadalupe Mountains, New Mexico. J. Cave Karst Stud. 62: 120-126.

Polyak, V.J., Mosch, C.J., 1995. Metatyuyamunite from Spider Cave, Carlsbad Caverns National Park, New Mexico. NSS Bulletin 57: 85-90.

Polyak, V.J., Provencio, P., 1998. Hydrobasaluminite and aluminite in caves of the Guadalupe Mountains, New Mexico. J. Cave Karst Stud. 60: 51-57

Polyak, V.J., Provencio, P., 2001. By-product materials related to H_2S-H_2SO_4 influenced speleogenesis of Carlsbad, Lechuguilla, and other caves of the Guadalupe Mountains, New Mexico. Journal of Cave and Karst Studies, 63(1): 23-32.

Polyak, V.J., McIntosh, W.C., Güven, N., Provencio, P., 1998. Age and origin of Carlsbad Cavern and related caves from $^{40}Ar/^{39}Ar$ of alunite. Science 279: 1919-1922.

Polyak, V.J., DuChene, H.R., Davis, D.G., Palmer, A.N., Palmer, M.V., Asmerom, Y., 2013. Incision history of Glenwood Canyon, Colorado, USA, from the uranium-series analyses of water-table speleothems. International Journal of Speleology, 42: 193-202.

Porter, M.L., Engel, A.S., 2008. Diversity of uncultured Epsilonproteobacteria from terrestrial sulfidic caves and springs. Applied Environmetal Microbiology, 74: 4973-4977.

Porter, M.L., Engel, A.S., Kane, T.C., Kinkle, B.K., 2009. Productivity-diversity relationships from chemolithoautotrophically based sulfidic karst systems. International Journal of Speleology, 38: 27-40.

Preziosi, E., Scipioni, M., 1993. La storia di una grotta. Speleologia, 29: 24-27.

Principi, P., 1931. Fenomeni di idrologia sotterranea nei dintorni di Tripozio. Le Grotte d'Italia, 1: 45-47.

Puchelt, H., Blum, N., 1989. Geochemische Aspekte der Bildung des Gipsvorkommens der Kraushöhle/Steiermark. Oberrheinische Geologische Abhandlungen, 35: 87-99.

Puşcaş, C.M., Onac, B.P., Effenberger, H.S., Povară, I., 2013. Tamarugite-bearing paragenesis formed by sulfate acid alteration in Diana Cave, Romania. European Journal of Mineralogy, 25: 479-486.

Queen, J.M., 1973. Large-scale replacement of carbonate by gypsum in some New Mexico caves (abs). National Speleological Society Convection, Bloomington, Indiana, Abstract, 12.

Queen, J.M., Palmer, A.N., Palmer, M.V., 1977. Speleologenesis in the Guadalupe Mountains, New Mexico: Gypsum replacement of carbonate by brine mixing. Proceedings of the 6th International Speleological Congress, Sheffield, England, 336-339.

Queen, J.M., 1994. Speleogenesis in the Guadalupes: the unsettled question of the role of mixing, phreatic or vadose sulfide oxidation. In: I.D., Sasowsky, M.V., Palmer (Eds.), Breakthroughs in Karst Geomicrobiology and Redox Geochemistry. Special Publication 1. Karst Waters Institute, Charles Town, WV, 64-65.

Queen, J.M., 2009. Geological setting, structure, tectonic hystory and paleokarst as factor in speleogenesis in the Guadalupe Mountains, New Mexico and Texas, USA. Proceeding of the 15th International Congress of Speleology, Kerrville, Texas, 958-963.

Rohwerder, T., Sand, W., Lascu, C., 2003. Preliminary evidence for a sulphur cycling in Movile Cave, Romania. Acta Biotechnologica, 23: 101-107.

Rosales-Lagarde, L., Campbell, A., Boston, P.J., Stafford, K.W., 2008. Groundwater flow-path identification in the Tabasco-Chiapas Mountain Range, Southern Mexico. In: I.D., Sasowsky, C.T., Feazel, J.E., Mylroie, A.N., Palmer, M.V., Palmer (Eds.), Karst from Recent to Reservoirs. Karst Waters Institute, Special Publication, 14: 170-171.

Rossmassler, K., Engel, A.S., Twing, K.I., Hanson, T.E., Campbell, B.J., 2012. Drivers of epsilonproteobacterial community composition in sulfidic caves and springs. FEMS microbiology ecology 79(2): 421-432.

Sancho, C., Peña, J.L., Mikkan, R., Osácar, C., Quinif, Y., 2004. Morphological and speleothemic development in Brujas Cave (Southern Andean range, Argentine): palaeoenvironmental significance. Geomorphology, 57(3): 367-384.

Santaloia, F., Zuffianò, L.E., Palladino, G., Limoni, P.P., Liotta, D., Minissale A., Brogi, A., Polemio, M., 2016. Coastal thermal springs in a foreland setting: The Santa Cesarea Terme system (Italy). Geothermics, 64: 344-361.

Sarbu, S.M., Kane, T.C., 1995. A subterranean chemoautotrophically based ecosystem. NSS Bulletin, 57: 91-98.

Sarbu, S.M., Lascu, C., 1997. Condensation-Corrosion in Movile Cave, Romania. Journal of Cave and Karts Studies, 59(3): 99-102.

Sarbu, S.M., Kane, T.C., Kinkle, B.K., 1996. A chemoautotrophically based groundwater ecosystem. Science, 271: 1953-1955.

Sarbu, S.M., Kinkle, B.K., Vlasceanu, L., Kane, T.C., Popa, R., 1994. Microbiological characterization of a sulfide-rich groundwater ecosystem. Geomicrobiology Journal, 12: 175-182.

Sarbu, S.M., Galdenzi, S., Menichetti, M., Gentile, G., 2000. Geology and biology of Grotte di Frasassi (Frasassi Caves) in Central Italy, an ecological multi-disciplinary study of a hypogenic underground karst system. In: H., Wilkens, D.C., Culver, W., Humphreys (Eds.), Ecosystems of the world, Vol. 30: Subterranean Ecosystems. Oxford, UK: Elsevier Science, 361-381.

Sauro, F., De Waele J., Onac, B.P., Galli, E., Dublyansky, Y., Baldoni, E., Sanna L., 2014. Hypogenic speleogenesis in quartzite: The case of Corona 'e Sa Craba Cave (SW Sardinia, Italy). Geomorphology, 211: 77-88.

Semikolennykh, A. A., Targulian, V. O., 2010. Soil-like bodies of autochemolithotrophic ecosystems in the caves of the Kugitangtau Ridge, eastern Turkmenistan. Eurasian Soil Science, 43: 614-627.

Socquet, J.M., 1801. Analyse des eaux thermales d'Aix (en Savoie), département du Mont-Blanc (Analysis of Thermal Waters at Aix, in Savoy, Mont-Blanc Department). Cleaz, Chambéry, 240 pp.

Southward, A.J., Kennicutt, M.C., Herrera-Alcalà, J., Abbiati, M., Airoldi, L., Cinelli, F., Bianchi, C.N., Morri, C., Southward, E. C., 1996. On the biology of submarine caves with sulphur springs: appraisal of $^{13}C/^{12}C$ ratios as a guide to trophic relations. Journal of the Marine Biological Association of the United Kingdom, 76: 265-285.

Spilde, M.N., Fischer, P.R., Northup, D.E., Turin, H.J., Boston, P.J., 2004. Water, gases, and phylogenetic analyses from sulfur springs in Cueva de Villa Luz, Tabasco, Mexico (abstract). Geological Society of America Abstract Programs, 36(5): 258 pp.

Spirakis, C.S., Cunningham, K.I., 1992. Genesis of sulphur deposits in Lechuguilla Cave, Carlsbad Caverns National Park, New Mexico. In: G., Wessel, B., Wimberley (Eds.), Native Sulphur — Developments in Geology and Exploration. American Institute of Mining, Metallurgical and Petroleum Engineers, Phoenix, AZ, 139-145.

Stafford, K.W., Behnken, F.H., White, J.G., 2008. Hypogene speleogenesis within the Central Basin Platform: karst porosity in the Yates Field, Pecos County, Texas, U.S.A. In: I.D., Sasowsky, C.T., Feazel, J.E., Mylroie, A.N., Palmer, M.V., Palmer (Eds.), Karst from Recent to Reservoirs. Karst Waters Institute, Special Publication 14, 174-178.

Stevanović, Z., Iurkiewicz, A., Maran, A., 2009. New insights into karst and caves of northwestern Zagros (northern Iraq). Acta Carsologica, 38: 83-96.

Stüben D., Sedwick P., Colantoni P., 1996. Geochemistry for submarine warm springs in the limestone cavern of Grotto Azzurra, Capo Palinuro, Italy: Evidence for mixing-zone dolomitization. Chemical Geology, 131: 113-125.

Taylor, M.R., 1999, A trip to lighted house. NSS News, 57: 36-41.

Temovski, M., Audra, P., Mihevc, A., Spangenberg, J.E., Polyak, V., McIntosh, W., Bigot, J.Y., 2013. Hypogenic origin of Provalata Cave, Republic of Macedonia: a distinct case of successive thermal carbonic and sulfuric acid speleogenesis. International Journal of Speleology, 42: 235-246.

Tintilozov, Z.K., 1983. Akhali Atoni cave system. Metsniereba Tiblisi, USSR, 150 pp.

Tisato, N., Sauro, F., Bernasconi, S.M., Brujin R.H.C., De Waele J., 2012. Hypogenic contribution to speleogenesis in a predominant epigenic karst system: A case study from the Venetian Alps, Italy. Geomorphology, 151-152: 156-163.

Trimmel, H., 1964. Die Kraushöhke bei Gams (Steiermark). Höhlenkundliche Mitteilungen Wien und Niederösterreich 20: 70-75.

Van Everdingen, R.O., Shakur, M.A., Krouse, H.R., 1985. Role of corrosion by H_2SO_4 fallout in cave development in a travertine deposit-Evidence from sulfur and oxygen isotopes. Chemical Geology, 49(1-3): 205-211.

Vlasceanu, L., Popa, R., Kinkle, B., 1997. Characterization of *Thiobacillus thioparus* LV43 and its distribution in a chemoautotrophically based groundwater ecosystem. Applied Environmental Microbiology, 63: 3123–3127.

Vlasceanu, L., Sarbu, S.M., Summers Engel, A., Kinkle, B.K., 2000. Acidic Cave-Wall Biofilms Located in the Frasassi Gorge, Italy. Geomicrobiology Journal, 17: 125-139.

White, W.B., 1988. Geomorphology and hydrology of karst terrains. Oxford University Press, New York, 464 pp.

Wynn, J.G., Sumrall, J.B., Onac, B.P., 2010. Sulfur isotopic composition and source of dissolved sulfur species in thermo-mineral springs of the Cerna Valley, Romania. Chemical Geology, 271: 31-43.

Yonge, C.J., Krouse, H.R., 1987. The origin of sulfates in Castleguard cave, Columbia Icefields Canada. Chemical Geology 65, 427-433.

Zerkle, A.L., Jones, D.S., Farquhar, J., Macalady, J.L., 2016. Sulfur isotope values in the sulfidic Frasassi cave system, central Italy: A case study of a chemolithotrophic S-based ecosystem. Geochimica and Cosmochimica Acta, 173: 373-386.

FIRST SECTION: RECOGNITION OF SAS CAVES

2. GEOMORPHOLOGY

2.1. Distinctive geomorphological features

Whereas the identification of active SAS systems is quite straightforward, because of the presence of sulfide-rich waters, inactive SAS caves can be less easy to identify. This is especially true for old caves, in which different epigenic processes, and condensation-corrosion may have masked the original fingerprints of SAS.

Generally, inactive SAS caves can be recognized if searching for peculiar geomorphological features and secondary minerals associations. As shown by Audra (2008) and Palmer (2013) the principal types of hypogene sulfuric acid caves are deep phreatic systems (confined setting) and underground environments developed at or above water table (unconfined setting); their inner morphologies and patterns reflect rising fluid flows and movements. Deep phreatic caves are characterized by slowly flowing fluids giving rise to the formation of 2 and 3D anastomotic network or spongework (Palmer, 2013) mazes galleries (Klimchouk, 2007; Audra, 2008) with circular section, feeders (i.e., vertical and narrow passages through which deep water reaches the cave environment; Klimchouk, 2009), blind chimneys developed close to upwelling points, rising channels and cupola-morphologies, domes created by convective water fluxes triggered by the presence of a thermal gradient (Klimchouk et al., 2016), abrupt dead ends, and imprints of rising gas bubbles along the wall of a submerged pool (Audra et al.,2009c).

Upward developing dendritic and sulfuric water table caves represent typical pattern of hypogene caves formed at or above water table (Audra et al., 2009a). Condensation-corrosion processes related to warmer acidic (H_2SO_4) aerosols condensating on cooler ceiling originate a great variety of forms (Audra, 2008), and in particular, peculiar geomorphic features are (Audra et al., 2009b): niches, ceiling cupolas and spheres (i.e., big convection-rounded morphologies located along walls and on the roof of cave conduits caused by convective air flows), condensation-corrosion channels (due to warm aerosols that tend to raise up following overhanging walls, creating features similar to a half-tube), megacusps (rising warm aerosols create big rounded morphologies on the walls and roof; they were previously defined as “megascallops” (Plan et al., 2012), however, this former term is misleading, because scallops are signs of water turbulence), condensation domes (thermal gradient produces ascending corrosive convection fluxes), vents (they develop in localized points emitting acidic aerosols able to create tubes that sometimes can connect several cave levels), wall partitions (convection aerosol fluxes favor the enlargement of early voids; if the process continues for a long

time the interconnection of voids can occur; Osborne, 2007). Other solutional morphologies are boxworks (the presence of secondary crystalline veins in the micritic host rock can favor the differential dissolution of the micritic matrix), weathered walls (Plan et al., 2012), replacement pockets (hemispherical pockets in which the carbonate rocks is replaced by gypsum, which in turn absorbs sulfuric acid (Audra, 2008) producing a progressive deepening and dissolution of the initial pocket), drip tubes (acidic droplets can create dissolutional tubes in soft rocks below), sulfuric karren (De Waele et al., 2016), sulfuric cups, and corrosion tables (created by sulfuric acid laminar condensation runoff).

The geomorphological observation carried out in several sulfuric acid water table caves and their related figures will be presented in the following paragraph.

2.2. Article 1

Published in Geomorphology, 253: 452-467, http://dx.doi.org/10.1016/j.geomorph.2015.10.019

Sulfuric acid speleogenesis (SAS) close to the water table: example from southern France, Austria, and Sicily.

Jo De Waele (*), Philippe Audra (**), Giuliana Madonia (°), Marco Vattano (°), Lukas Plan (°°), Ilenia Maria D'Angeli (*), Jean-Yves Bigot (**), Jean-Claude Nobécourt (°°°)

(*) Istituto Italiano di Speleologia, University of Bologna, Via Zamboni 67, 40127 Bologna, Italy (jo.dewaele@unibo.it; ilenia.dangeli@alice.it)

(**) University of Nice Sophia-Antipolis, CNRS, IRD, Observatoire de la Cote d'Azur, Geoazur UMR 7329 & Polytech Nice – Sophia, 930 route des Colles, 06903 Sophia-Antipolis, Nice, France, audra@unice.fr

(°) Dipartimento di Scienze della Terra e del Mare, University of Palermo, Via Archirafi 22, 90123 Palermo, Italy (giuliana.madonia@unipa.it; marco.vattano@unipa.it)

(°°) Natural History Museum Vienna, Karst and Cave Working Group, Museumsplatz 1/10, 1070 Vienna, Austria, lukas.plan@nhm-wien.ac.at

(**) Association Française de karstologie (AFK), 21 rue des Hospices, 34090 Montpellier, France (catherine.arnoux@club-internet.fr)

(°°°) Crespe, 06140 Vence, France (jcnobecourt@free.fr)

2.2.2. Abstract

Caves formed by rising sulfuric waters have been described from all over the world in a wide variety of climate settings, from arid regions to mid-latitude and alpine areas. H_2S is generally formed at depth by reduction of sulfates in the presence of hydrocarbons and is transported in solution through the deep aquifers. In tectonically disturbed areas major fractures eventually allow these H_2S-bearing fluids to rise to the surface where oxidation processes can become active producing sulfuric acid. This extremely strong acid reacts with the carbonate bedrock creating caves, some of which are among the largest and most spectacular in the world. Production of sulfuric acid mostly occurs at or close to the water table but also in subaerial conditions in moisture films and droplets in the cave environment. These caves are generated at or immediately above the water table, where condensation-corrosion processes are dominant, creating a set of characteristic meso- and micromorphologies. Due to their close connection to the base level, these caves can also precisely record past hydrological and geomorphological settings. Certain authigenic cave minerals, produced during the sulfuric acid speleogenesis (SAS) phase, allow determination of the exact timing of speleogenesis. This paper

deals with the morphological, geochemical and mineralogical description of four very typical sulfuric acid water table caves in Europe: the Grotte du Chat in the southern French Alps, the Acqua Fitusa Cave in Sicily (Italy), and the Bad Deutsch Altenburg and Kraushöhle caves in Austria.

Keywords: sulfuric acid caves; hypogenic karst; cave morphology; speleogenesis; condensation-corrosion

2.2.3. Introduction

A constantly increasing number of caves are being classified as hypogenic caves since their clear distinction occurred only a few years ago (Klimchouk, 2007, 2009). These caves are typically formed by rising fluids which attain their aggressiveness from deep sources and not from the surface water containing CO_2. Sulfuric acid caves (SAS caves) are the most interesting and best studied among these (e.g. Egemeier, 1981; Hill, 1987; Galdenzi and Menichetti, 1995; Polyak et al., 1998; Hose and Pisarowicz, 1999; Audra, 2008; Palmer, 2013). They have been described for more than a century in Europe (e.g., Socquet, 1801; Hauer, 1885; Principi, 1931; Martel, 1935). Such studies were carried out first in American caves (Morehouse, 1968), while the earliest sulfuric acid speleogenesis (SAS) model was published by Egemeier (1981), relying on observations in Lower Kane Cave in Wyoming (USA).

An increasingly larger number of SAS caves are known around the world, and an overview of these is given in *Table 2*.

Table 2– Examples of the main sulfuric caves in the world

Lower Kane Caves	USA (WY)	Egemeier, 1981; Engel et al., 2004
Carlsbad Caverns, Lechuguilla Cave, etc.	USA (NM) Guadalupe Mts.	Hill, 1987, 1990; Polyak et al., 1998; Palmer and Palmer, 2000; Polyak and Provencio, 2001; Engel et al., 2004, Calaforra and De Waele, 2011; Palmer and Palmer, 2012; Kirkland, 2014
Glenwood Cave	USA (CO)	Barton and Luiszer, 2005; Polyak et al., 2013
Cueva de Villa Luz	Mexico, Tabasco	Hose and Pisarowicz, 1999; Hose et al., 2000
Movile Cave	Romania, Dobrogea	Sarbu et al., 1994, 1996
Frasassi Cave	Italy, Umbria	Galdenzi and Menichetti, 1995; Galdenzi and Maruoka, 2003
Monte Cucco, Faggeto Tondo caves	Italy, Umbria	Galdenzi and Menichetti, 1995; Menichetti, 2011
Acquasanta Terme caves	Italy, Marche	Galdenzi et al., 2000; Jones et al., 2014
Montecchio Cave	Italy, Tuscany	Piccini et al., 2015

Monte Soratte caves	Italy, Latium	Mecchia, 2012
Cala Fetente caves	Italy, Campania	Forti, 1985; Forti et al., 1989
Santa Cesarea Terme caves	Italy, Apulia	De Waele et al., 2014
Grotta di S. Angelo	Italy, Calabria	Galdenzi, 1997
Serra del Gufo-Balze di Cristo	Italy, Calabria	Galdenzi, 1997
Iglesiente mine caves	Italy, Sardinia	De Waele and Forti, 2006; De Waele et al., 2013
Chevalley - Gr. des Serpents	France, Savoie	Audra et al., 2007
Kraushöhle	Austria, Styria	Plan et al., 2012
Bad Deutsch Altenburg caves	Lower Austria	Plan et al., 2009
Diana Cave and Cerna caves	SW Romania	Onac et al., 2009, 2013; Wynn et al., 2010; Puscas et al., 2013
Provalata Cave	Rep. Macedonia	Temovski et al., 2013
Aghia Paraskevi caves	N Greece, Kassandra	Lazarides et al., 2011
Rhar es Skhoun, Azrou massif	Algeria	Collignon, 1983, 1990
Nowi Afon Cave	Georgia, Abkhazia	Dublyansky, 1980
Cupp Coutunn Cave	Turkmenistan	Maltsev and Malishevsky, 1990
Tirshawaka Cave	N Iraq	Stevanovic et al., 2009

The voids in SAS caves are mostly formed above the water table by abiotic and/or biotic oxidation of H_2S deriving from a deep source (Galdenzi and Maruoka, 2003; Jones et al., 2014, 2015). H_2S can derive from volcanic activity, reduction of sulfates, such as gypsum or anhydrite, or hydrocarbons and is brought to the surface through deep tectonic structures. The origin of sulfur and its possible sources can usually be deciphered using the stable isotope signature of sulfur (Onac et al., 2011). Oxidation of H_2S produces sulfuric acid that reacts instantaneously with the carbonate host rock producing replacement gypsum and carbon dioxide. CO_2 can dissolve in water and increase its aggressiveness even more. Also the local oxidation of sulfides such as pyrite, often present in carbonate sequences, can generate sulfuric acid, boosting rock dissolution (Onac, 1991; Auler and Smart, 2003; Filipponi and Jeannin, 2006; Tisato et al., 2012, Audra et al., 2015). Sulfuric acid also reacts with other minerals such as clays and can cause the formation of a typical suite of minerals including the sulfates jarosite, alunite, and basaluminite, and the silicate halloysite. Some of these minerals, especially those containing potassium such as alunite and jarosite, can be dated with radiometric methods (Polyak et al., 1998). Also gypsum can be dated using the U/Th method (Sanna et al., 2010; Piccini et al., 2015). Timing of minerogenesis roughly corresponds to the age of cave formation, certainly when the SAS process was active. Thus, SAS by-products offer a unique

opportunity to date speleogenetic phases, whereas other classical methods relying on dating of the cave filling, only post-date the cave itself.

Sulfuric acid caves are thus often intimately related to the contact zone between the water level, from which H_2S rises, and the air. Enlargement of the voids mainly happens due to condensation-corrosion processes in a highly acidic environment (Audra et al., 2007; Puscas et al., 2013). Condensation is greatly enhanced in the presence of thermal differences between the upwelling waters and the cave walls and atmosphere, even in low thermal environments where the thermal gradient reaches only a few degrees Celsius (Sarbu and Lascu, 1997; Gàzquez et al., 2015). Dissolution of carbonate rock in these conditions is extremely fast compared to normal epigenic caves and can cause the formation of sizeable cavities in probably only a few thousands of years, about 1 or 2 orders of magnitude faster than the time needed to develop a normal meteoric cave. Most cave development occurs close to where sulfidic waters enter the carbonate rocks from below in areas where oxidation gives rise to sulfuric acid. Many SAS caves are water table caves, i.e., they formed along the more or less horizontal plane of the sulfidic groundwater level (Audra et al., 2009a, 2009b). Fluctuations of this level can cause these karst systems to exhibit stacked cave levels, indicating the rise or fall of the groundwater.

This paper deals with the detailed morphological and mineralogical description of four such SAS water table caves, one in France, one in Sicily, and two in Austria, and highlights their importance in the understanding of past hydrological and geomorphological conditions *Figure 3*.

Figure 3. Location of the studied SAS caves: 1) Grotte du Chat; 2) Kraushöhle; 3) Bad Deutsch Altenburg; 4) Acqua Fitusa.

2.2.4. Study areas

2.2.4.1. Grotte du Chat

The Grotte du Chat opens at 940 m a.s.l. in the Southern French Alps at Daluis, Alpes-Maritimes. It is perched about 100 m above the Riou Gorge, a small tributary of the Var River. There are gentle slopes above the cave and the gorge below the cave, with its unstable slopes, probably corresponds to a Quaternary entrenchment.

The cave is developed in an 80 to 100 m-thick Barremian (Lower Cretaceous) limestone sandwiched between thick marl layers belonging to the sedimentary cover of the Argentera-Mercantour basement. This unit is slightly folded but displays in detail complex structures. In the vicinity of the Grotte du Chat, a half-dome is cut by the Rouaine active sinestral fault (*Figure 4*). To the east, the Barremian limestone crops out along the Var Valley slopes, representing the recharge area of the aquifer. To the west, the Barremian limestone strata are confined by the half dome plunge forming a discharge area where limestone is cut by the Riou Gorge and where water can rise from depth along the Rouaine Fault (*Figure 5*). A Triassic gypsum diapir crops out less than 1 km to the south at Daluis village.

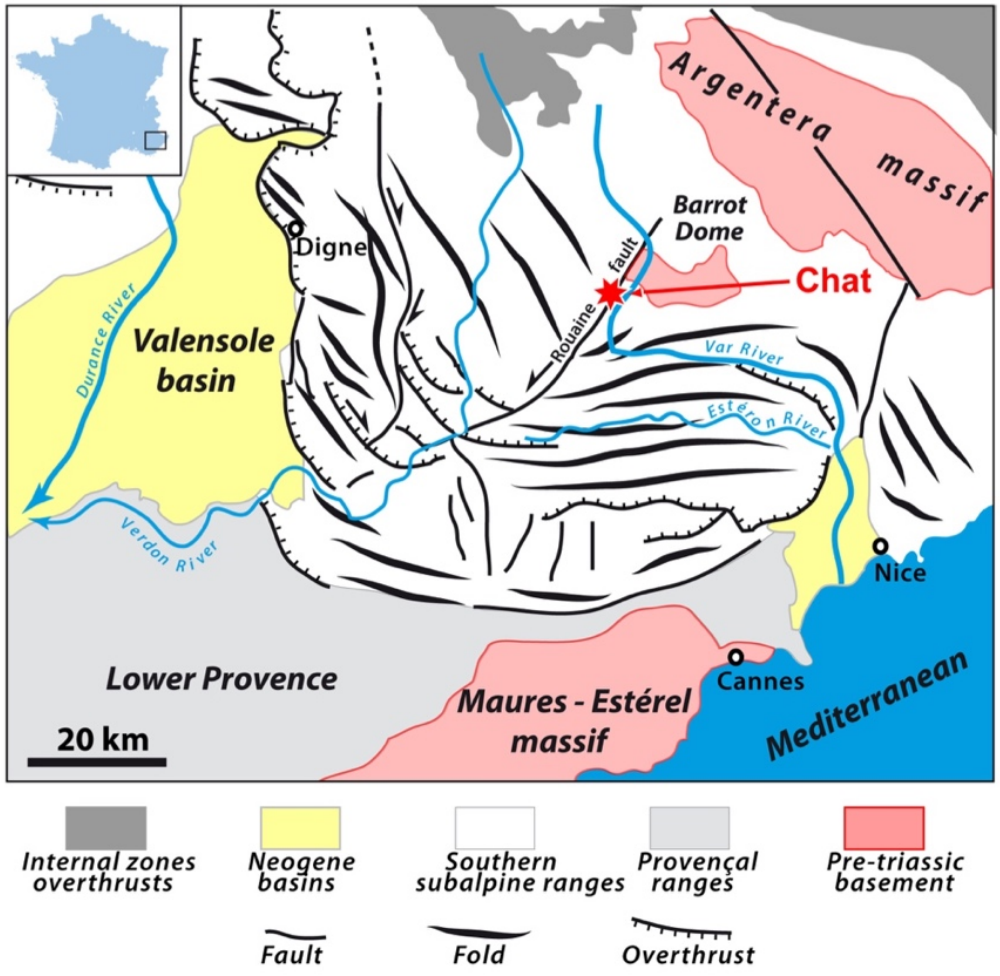

Figure 4. Structural frame of the Castellane Arc in the Southern Alps (after Kerckhove and Roux, 1976). The Grotte du Chat locates along the active Rouaine Fault.

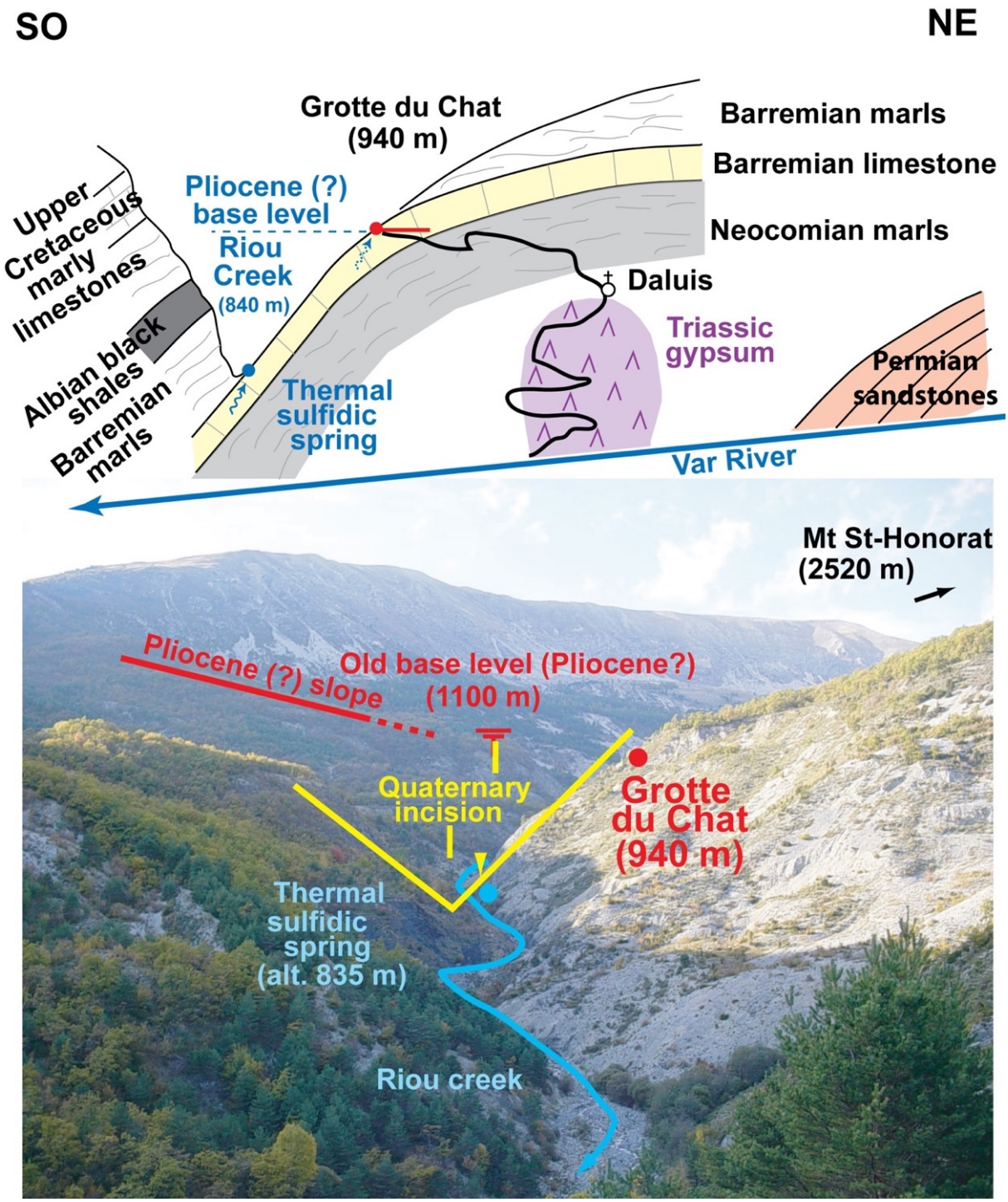

Figure 5. Schematic structural frame of Grotte du Chat, view from Daluis village. The Barremian limestone, sandwiched in between thick marls is confined to the west where the thermal spring discharges along the Rouaine Fault (not visible, parallel to this view). Daluis village is located 1 km in the foreground on a Triassic gypsum diapir. The cave acted as a thermal outlet before the Quaternary entrenchment of the Riou Gorge.

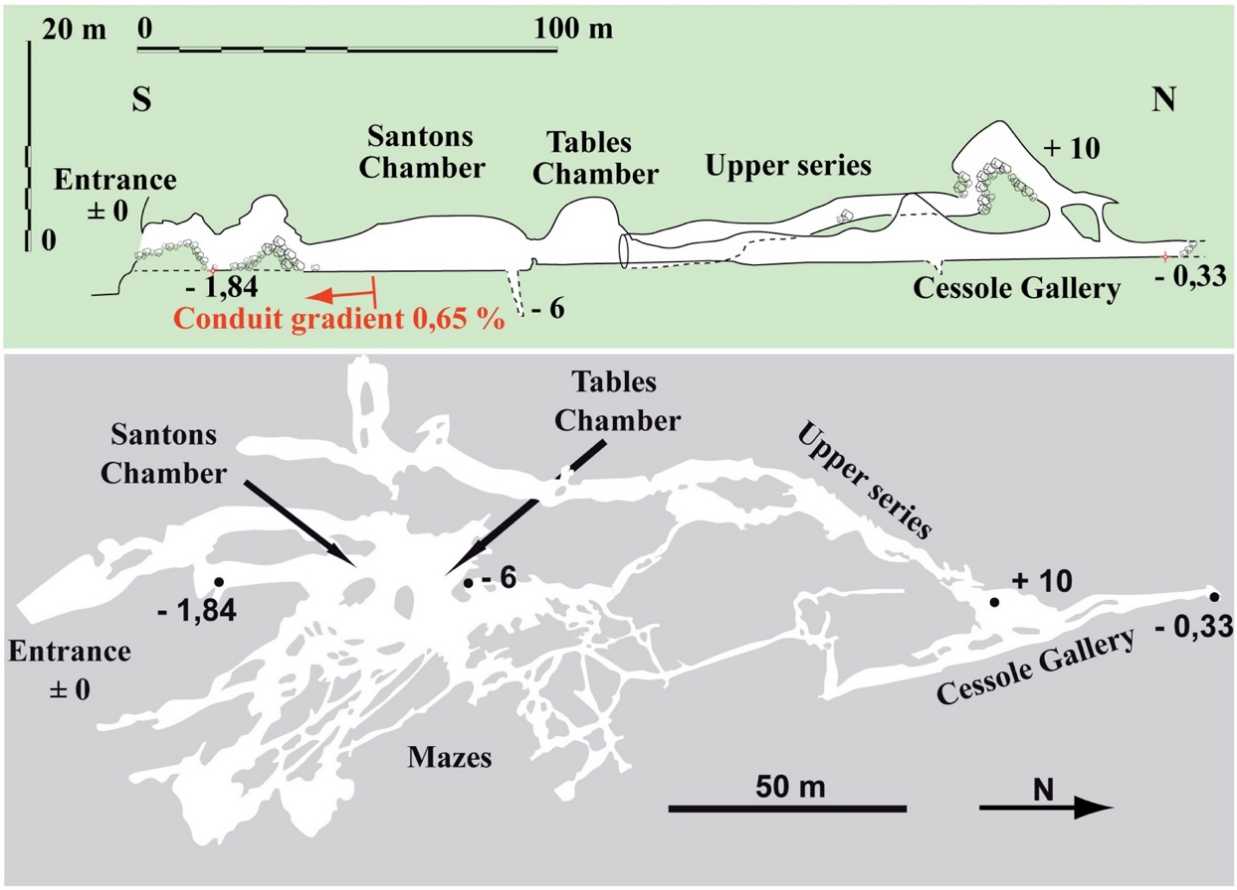

Figure 6. Survey of Grotte du Chat: the typical low gradient profile is visible on the vertical profile (top), while the incipient maze is clear in plan view (below).

In the Riou Gorge at 840 m a.s.l., the thermal spring (18 °C) discharges 2-6 L/s. It is 7 °C above the local mean annual temperature that would correspond to a deep water circulation loop of at least 200 m. Water chemistry is of carbonated-chloride-sulfate type (*Table 3*). Significant hydrogen sulfide content gives a typical rotten-egg smell and sulfur bacterial mats are present.

The cave is well known and was first surveyed at the end of the 19th century. Ducluzaux (1994) observed upward developing morphologies (i.e., cupolas), the absence of connection to a surficial catchment, the presence of a thermal spring in the gorge and suggested a hydrothermal origin. Recent studies (Audra, 2007; D'Antoni-Nobécourt et al., 2008) confirm this origin, showing its SAS origin with a main development by condensation-corrosion producing specific features (i.e., cupola, replacement pockets, corrosion tables).

Grotte du Chat develops as a horizontal maze following the fracture network and extends to the west (*Figure 6*). The Tables Chamber in the center is one of the main cave volumes. In detail, it is organised as tiers, the uppermost ones being upstream and to the west. The cave profile is horizontal with a tiny gradient (0.65%) toward the entrance.

Table 3. Data of the thermal spring of Riou Gorge, Daluis [sampl. 3489, Laboratoire de l'environnement, Ville de Nice, 20/03/06]. (*): corresponding to 1.8 mg/L H_2S

pH	7.6
Temperature (°C)	17.5
Conductivity (µS/cm)	576 – 691
Calcium Ca^{2+}	40.3 mg/L
Magnesium Mg^{2+}	8.7 mg/L
Sodium Na^{+}	51.4 mg/L
Potassium K^{+}	1 mg/L
Chloride Cl^{-}	27 mg/L
Sulfates SO_4^{2-}	36.4 mg/L
Nitrates NO_3^{-}	< 1 mg/L
Sulfides S^{2-} *	1.7 mg/L
Bicarbonates HCO_3^{-}	234.2 mg/L
Fe total	22 µg/L
Cu total	< 10 µg/L

2.2.4.2. Acqua Fitusa Cave

Acqua Fitusa Cave is located in the eastern sector of the Sicani Mountains, in the territory of San Giovanni Gemini (Agrigento province, central Sicily). The cave formed in the breccia member of the Upper Cretaceous Crisanti Formation (part of the basinal Mesozoic Imerese Domain), composed of conglomerates and reworked calcarenites with rudist fragments and benthic foraminifera (Catalano et al., 2013). The main entrance of the cave opens at 417 m a.s.l. on the eastern side of a fault line scarp that cuts a NNE-SSW oriented anticline that forms the La Montagnola Hill; this relief consists of rocks belonging to the Imerese Domain, overthrusting the succession of the Sicanian Domain and the clastic Oligo-Miocene covers (Catalano et al., 2013) (*Figure 7*). At the base of the Imerse and Sicanian Domain Triassic interbedded calcilutites and marls with abundant pyrite and bitumen may occur. A luke-warm sulfuric spring opens at the base of the cliff at 380 m a.s.l., three hundred meters north of the cave entrance. The chlorine-sulfate-alkaline waters have a temperature of around 25 °C (Grassa et al., 2006). From spring to early autumn, the entrance room of the cave hosts a large

breeding colony of bats, including *Myotis myotis* and *Miniopterus schreibersii* (Mucedda pers. comm.), that produce significant amounts of guano. The cave contained numerous lithic fragments, remains of food and burials of Palaeolithic and Chalcolithic periods (Bianchini and Gambassini 1973). The first detailed exploration, description and cave survey was produced by the Gruppo Speleologico Agrigento (Lombardo et al., 2007). According to a more recent survey made in 2011 (Vattano et al., 2013), the cave consists of at least three storeys of sub-horizontal conduits, displaying a total length of 700 m, and a vertical range of 25 m (*Figure 8*). The main passages are generally low and narrow and follow sets of joints oriented in ENE-WSW, E-W and N-S directions, except when they merge producing large volumes such as at the entrance room. Very small passages develop from these galleries forming incipient mazes.

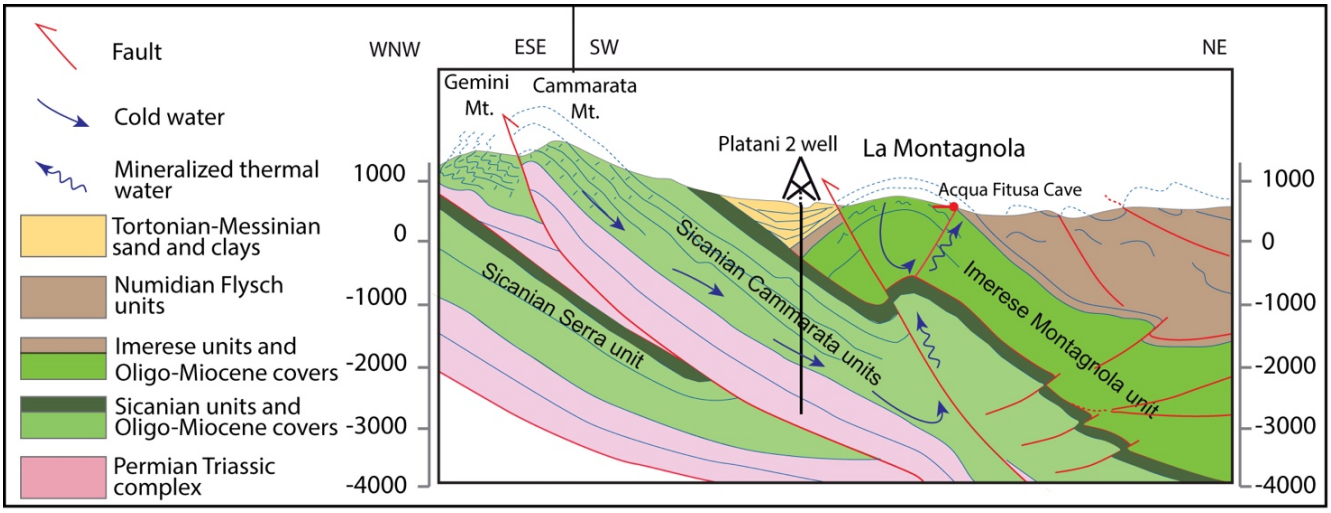

Figure 7. Geological section of the La Montagnola area and location of Acqua Fitusa Cave (modified from Catalano et al., 2013).

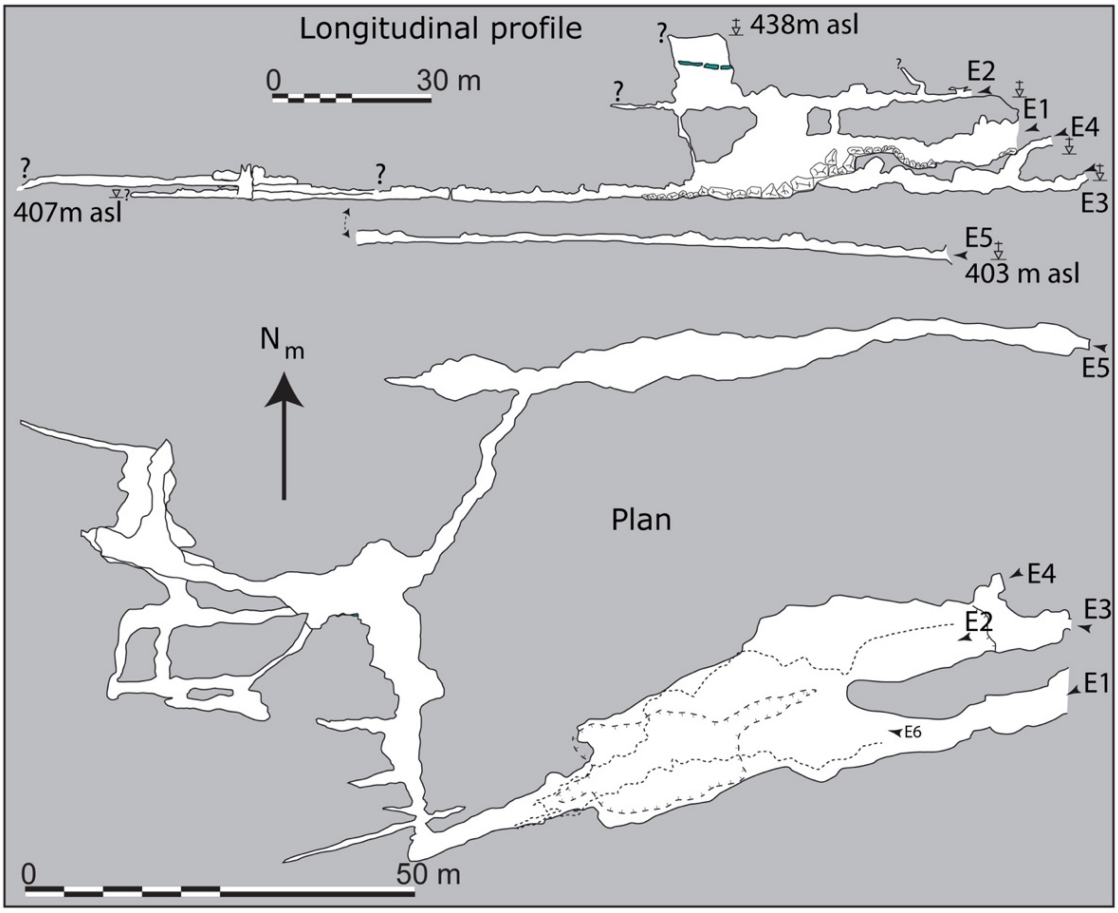

Figure 8. Survey of Acqua Fitusa Cave.

2.2.4.3. Kraushöhle

Kraushöhle opens east of the village Gams bei Hieflau in the north of the Austrian province of Styria (*Figure 9*). It is the only known cave of SAS origin in the Northern Calcareous Alps, which is part of a more than 2 km-thick sequence of Permo-Mesozoic sediments. Middle and Upper Triassic carbonates dominate this sequence, but Kraushöhle developed in a small tectonic wedge of the Lower Jurassic Hierlatz Formation, a limestone that is often developed as a reddish crinoid spar.

The cave opens at 616 m a.s.l. at the end of a narrow gorge of the Gams Brook. A H_2S-rich luke-warm spring emerges 93 m below the cave entrance and 1 m above the brook. A connection of the uprising hydrothermal water to the 400 km-long SEMP-fault system (Salzachtal-Ennstal-Mariazell-Puchberg) with its main strand 5 km to the south, can only be speculated.

Exploration of Kraushöhle started in 1881 and already Hauer (1885) and Kraus (1891) proposed a speleogenetic connection to the sulfur-bearing spring and set up a model for the replacement of limestone by gypsum as a cave forming process. One hundred years later this was confirmed by sulfur isotope studies by Puchelt and Blum (1989). Detailed studies of the cave morphology, mineralogy, cave wall alteration and age dating further confirmed the SAS origin (De Waele et al, 2009; Plan et

al., 2012). They were accompanied by a resurvey of the cave that gave a length of 793 m and a vertical range of 53 m.

The cave consists of two central chambers – the larger one (Main Chamber) measures 50 x 15 m – from which several, partly interconnected, slightly inclined galleries branch off forming a 3D-maze (*Figure 10*). The galleries and several chimneys terminate abruptly and the highest, the so-called Crystal Chimney, reaches 30 m above the Main Chamber (*Figure 10*).

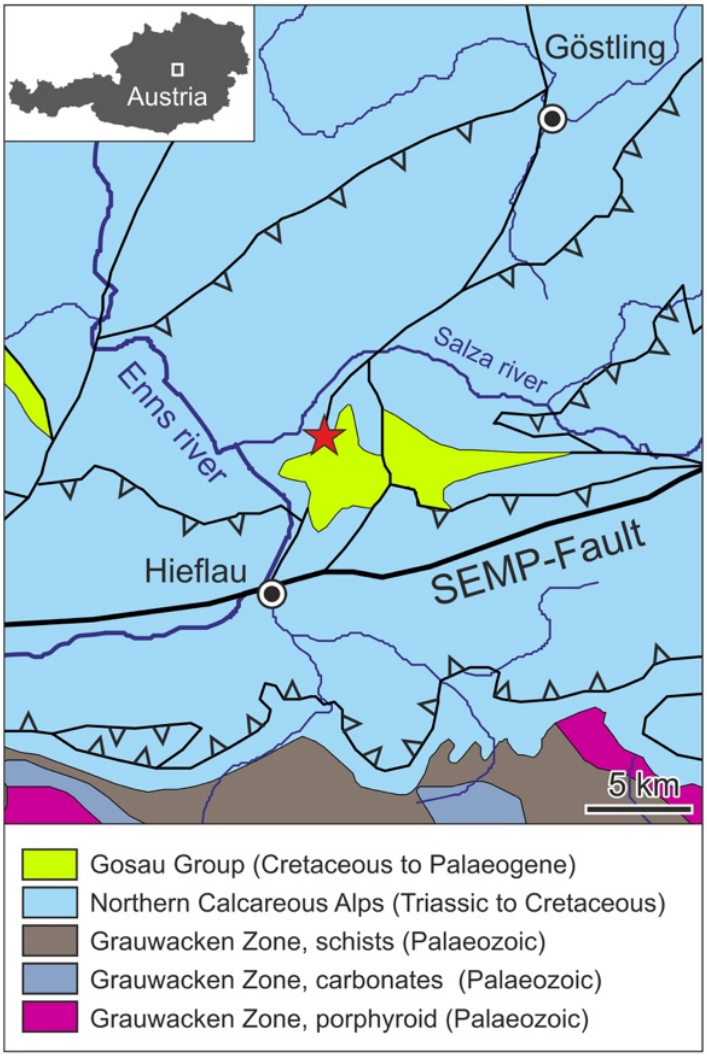

Figure 9. Geological sketch map and location of Kraushöhle (star). Modified after: Schuster et al. (2013).

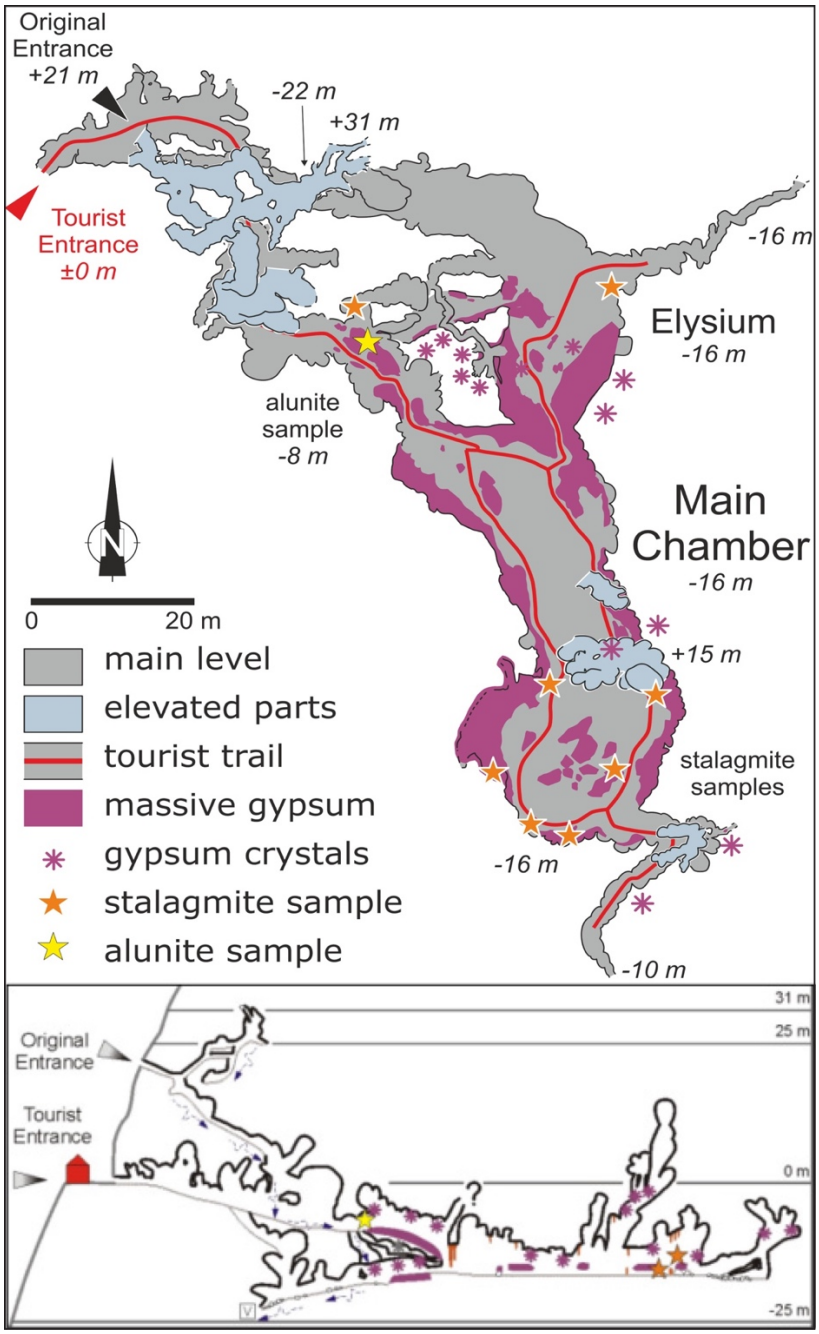

Figure 10. Plan and longitudinal profile of Kraushöhle.

2.2.4.4. Bad Deutsch Altenburg caves

Bad Deutsch Altenburg is a village at the Danube River in the easternmost part of Austria only 15 km west of the Slovak capital Bratislava. It is located at the eastern margin of the Vienna Basin, which is a Miocene pull-apart structure. Along the margins of the southern part of this up to 6 km-deep sedimentary basin, several thermal springs emerge. Since Pre-Roman times the sulfur-bearing thermal water (up to 24.6 °C; 8 L/s) has been used for spas in Bad Deutsch Altenburg. The adjacent Hainburger Berge are part of the Tatricum (a Palaeozoic-Lower Mesozoic crustal thrust sheet of the

Central Western Carpathians) and at Bad Deutsch Altenburg weakly metamorphic Triassic dolomite crops out. The springs emerge at the border of the permeable carbonates and overlying Miocene clays and marls aquiclude. The mineralisation and thermal heating of the water is explained by a circulation system within the carbonates that are underlain by the crystalline basement of the Hainburger Berge (*Figure 11;* Wessely, 1993).

Eight relatively small caves were opened during quarrying, the 121 m-long and 13 m-deep Stephanshöhle being the longest of them. The caves are restricted to a rather small area. Accessible caves are dry but are located only few meters above the high water level of the (regulated) Danube. Unfortunately a 12 m-long cave (Tiefetagenhöhle) that reached into the present ground water of the Danube, was accessible in 1992 for a few months only and was removed by quarrying works before further investigations were possible.

A systematic survey of most caves in this area was conducted in the late 80s (Mayer and Wirth, 1989) and they were attributed to SAS by Plan et al. (2009).

The caves are rather narrow and cross sections are in the order of 1 m². They developed along sets of W(NW)-E(SE) and NNE-SSW trending faults and joints at several sub-horizontal storeys between 142 and 162 m a.s.l. with distinct water table notches (*Figure 12*).

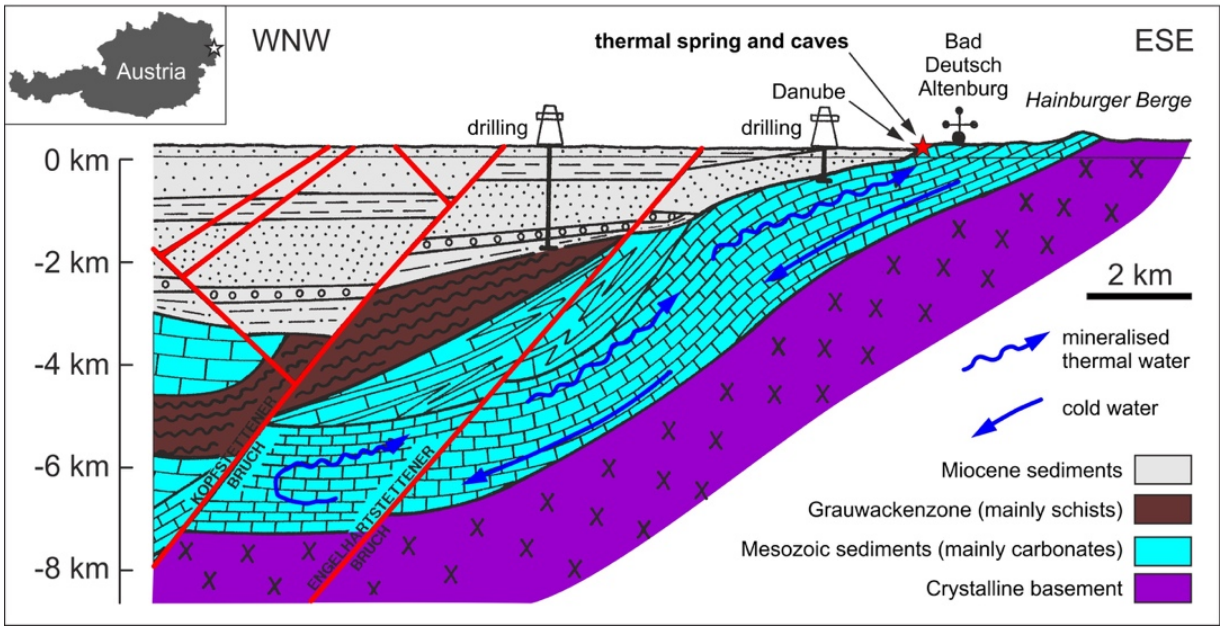

Figure 11. Geological section showing the proposed circulation system of the thermal water of Bad Deutsch Altenberg. Modified after Wessely (1993).

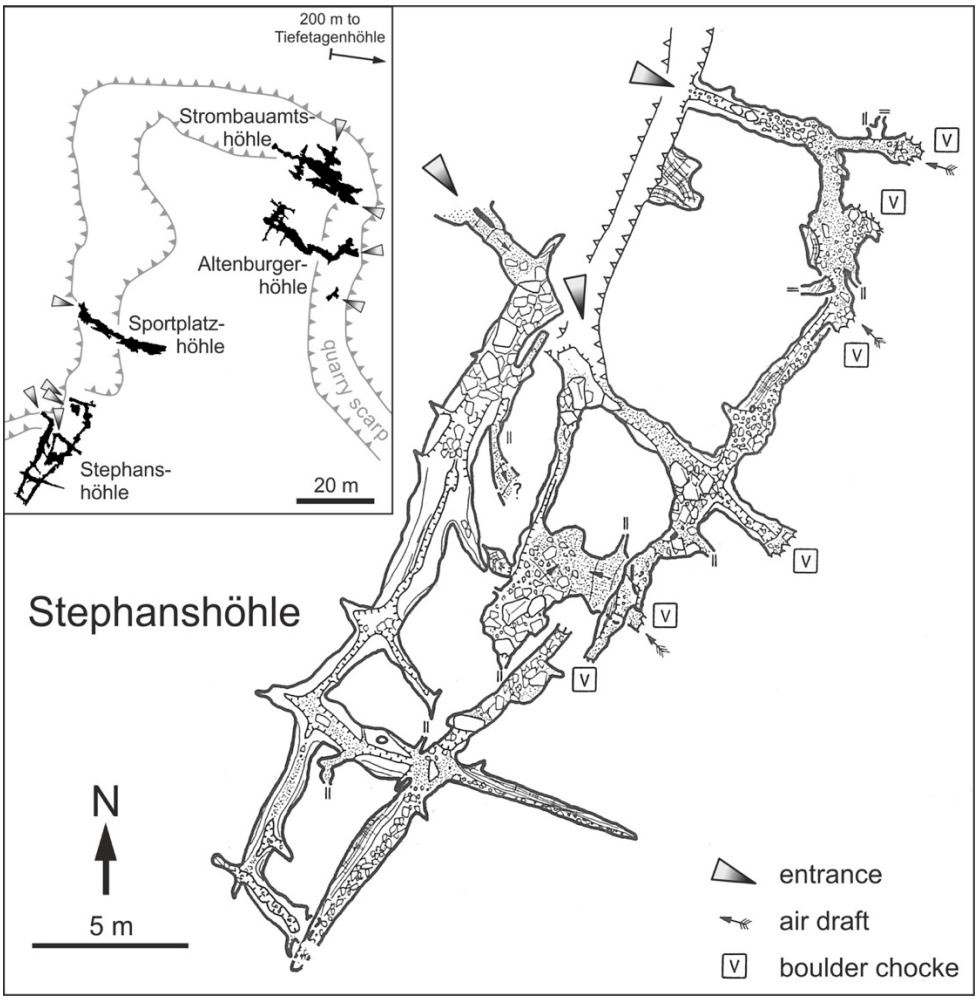

Figure 12. Survey of the Bad Deutsch Altenburg.

2.2.5. Methods

All caves were mapped using traditional caving techniques (compass, clinometer and laser range finder for distances). This delivers cave maps with an accuracy of about 1%. Detailed mapping with a water tube level and laser range finder allowing centimeter accuracy were used for vertical referencing of corrosion notches. Typical meter- to centimeter-sized cave morphologies were mapped and measured, and photographic documentation completed the observations.

Cave minerals and weathering products on the walls were sampled for mineralogical analysis. Samples were analysed using a Philips PW 1050/25 X-ray diffractometer (XRD, 40 kV and 20 mA, CuKα radiation, Ni filter) at the University of Modena and Reggio Emilia, Italy, and on a Philips diffractometer (XRD, 40 kV and 20 mA, CoKα radiation, Graphite filter) at the CEREGE – CNRS, Aix-en-Marseille, France.

Samples of gypsum were analysed for sulfur stable isotopes at the ETH Zurich with a Thermo Fisher Flash-EA 1112 coupled with a Conflo IV, interfaced to a Thermo Fisher Delta V Isotope Ratio Mass Spectrometer (IRMS). Isotope ratios were calibrated with the reference materials NBS 127 ($\delta^{34}S$ =

+21.1 ‰), SO_5 ($\delta^{34}S$= +0.49 ‰) and SO_6 ($\delta^{34}S$ = −34.05 ‰) and are reported in the conventional δ-notation with respect to V-CDT (Vienna Cañon Diablo Troilite) (measurement reproducibility was better than 0.3‰).

Alunite of Kraushöhle was dated using the Ar^{40}/Ar^{39} method similar to that from Polyak et al. (1998) and was previously reported in De Waele et al. (2009).

2.2.6. Results and discussion

2.2.6.1. Cave pattern

The four described caves are characterised by an anastomotic or maze pattern following a network of fractures (*Figure 6, Figure 8, Figure 10, Figure 12*). The caves developed along the fractures through which acidic fluids were discharged, resulting in a more or less elongated anastomotic cave passages with the discharging feeders along its path. In Kraushöhle these feeding fissures are no longer clearly visible, as they are mainly covered by sediments. If the rising fluids were delivered through more fractures a maze cave developed, such as is the case in all caves but Kraushöhle. The larger rooms are located along the major feeding fractures and often at their intersection.

Grotte du Chat, Acqua Fitusa, and the Bad Deutsch Altenburg caves represent typical examples of inactive SAS water table caves (Audra et al., 2009a; 2009b). Kraushöhle, although showing some minimal epigenic overprinting, also has many of the typical characteristics of a SAS water table cave. Despite their relatively small size, all these caves are very interesting for the abundance and variety of morphologies and deposits formed at and above the water table where H_2S degassing and thermal convection produced strong condensation-corrosion processes (*Table 4*).

Table 4. Typical sulfuric acid cave morphologies in the four described caves. Note not all forms are exclusive to SAS caves.

Cave Morphology	Grotte du Chat	Acqua Fitusa Cave	Bad Deutsch Altenburg caves	Kraushöhle
Maze cave	x	x	x	x
Elongated anastomotic passage				x
Feeders	x	x	x	
Sulfuric-acid chimney				x
Sulfuric-acid notches with flat roof		x		x
Wall convection niches	x	x	x	x
Ceiling cupolas	x	x		x
Condensation-corrosion channels	x	x		x
Megascallops	x	x		x

Condensation domes	x	x		x
Boxwork	x	x	x	x
Weathered walls	x	x	x	x
Replacement pockets	x	x	x	x
Sulfuric-acid karren	x	x		x
Ceiling pendant drip holes				x
Sulfuric-acid cups		x		x
Corrosion tables	x	x	x	x
Replacement gypsum crusts	x	x		x
Calcite popcorn	x	x		

2.2.6.2. Feeders and corrosion along standing pools

Where visible, thermo-sulfuric discharge points breach the flat floor of the cave passages and are normally not large enough to allow a person to pass (*Figure 13*A). These feeders tend to pinch out at shallow depth, since most of the corrosion occurs where H_2S can convert into sulfuric acid in an oxidising environment. Only in Acqua Fitusa Cave some of these feeders, located at different levels of the cave, are large enough to be explored to a depth of over 10 m. The walls of one of these feeding fissures are covered with a network of calcite "roots" (*Figure 13*B), which deserve further investigation because their similarity with the morphologies observed by Melim et al., (2016). Upstream of the last discharging fissures, the passage normally comes soon to a dead end since aggressive power of the fluids diminishes with the distance from their injection point into the subaerial part of the cave (*Figure 14*). The largest cave volumes are located above and downstream of the feeders, similar to existing active SAS caves such as Cueva de Villa Luz (Hose and Pisarowicz, 1999) and Lower Kane caves (Egemeier, 1981).

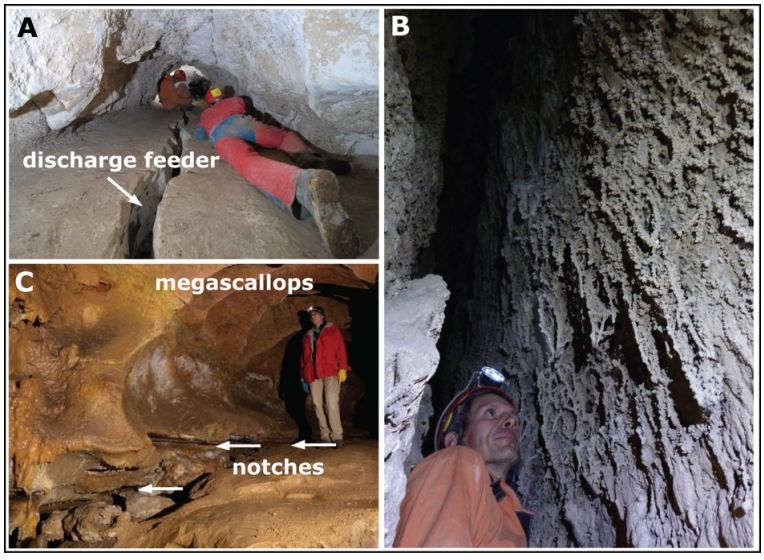

Figure 13. Morphologies in typical SAS watertable caves: A) Thermo-sulfuric feeding fissure cutting planar ground in Acqua Fitusa Cave; B) The curious subaqueous root-like calcite speleothems in

Acqua Fitusa Cave; C) Passage sculpted with megascallops: note the notches with flat roof at the bottom of the passage, Kraushöhle.

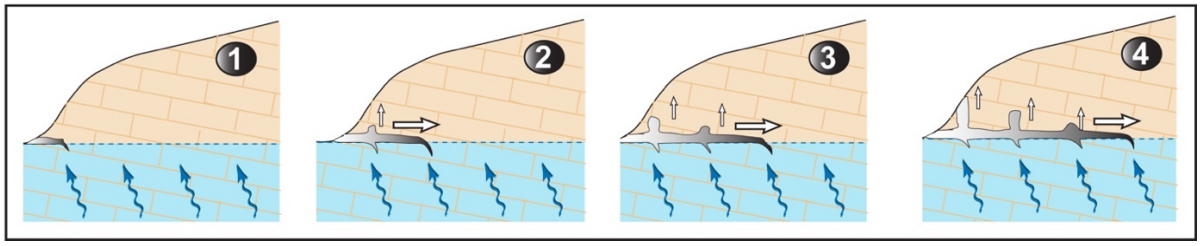

Figure 14. Longitudinal development of a SAS water table cave: regression of the discharge point causes the conduit to retreat ending blindly upstream of the last sulfidic feeder.

When the water level drops these feeding fissures can still act as thermal vents, if warm water is present below the passage. Rising vapours will cause condensation-corrosion processes on the cooler overlying walls and roof, whereas evaporation processes occur only at the edges of the feeders by subsident warming air leading to the deposition of calcite as cave popcorn rims.

When the water level rises to the surface in the enlarged cave, and when the amount of H_2S is significant, the uppermost part of the water column will always be much more aggressive than the deeper one. Also condensation runoff from the walls can continuously feed acidic fluids to the pools. If the water level is stable enough, these pool surface waters will cause lateral corrosion of the limestone bedrock creating notches with a flat roof (*Figure 13*C).

2.2.6.3. Main cave volume developed by condensation-corrosion

While cave enlargement is relatively subdued in phreatic conditions, oxidation of H_2S and formation of sulfuric acid is particularly efficient in the aerated environment, causing extensive corrosion of the cave walls and roof.

The volume of dissolved limestone due to corrosive flowing water in the feeders and the pools is limited compared to that produced by the condensation-corrosion processes that appear to be responsible of most of the volume. Several micro- and macromorphologies generated by condensation-corrosion processes above the water table, can be observed in all SAS caves (Galdenzi, 2001; Audra, 2008). These are particularly well developed above the feeders, but also in Kraushöhle, where the feeders are no longer visible.

Ceiling cupolas and large wall convection niches occur in the largest rooms of both Kraushöhle and Grotte du Chat (*Figure 15*A). This expansion driven by condensation-corrosion may also cause the formation of pendants at junctions of several cupolas or between braided channels. The ascending air flow is responsible for the formation of megascallops, a wave-like corrosional pattern along the roof

and the walls, similar to scallops of phreatic flow origin but at least ten fold larger (*Figure 15*B). Above the main feeding points, especially when rising fluids are warm and rich in H_2S and the thermal gradient is high, condensation-corrosion at the ceiling can be very strong, leading to the development of rounded dome-like chambers. This is clearly visible in Grotte du Chat (*Figure 15*C). Ceiling cupolas and spheres represent convection cells in which condensation is more abundant at the cooler ceiling, heavily increasing their upward development. These ceiling spheres are typical of thermal caves such as those described in Chevalley and Serpents caves in France (Audra et al., 2007) but initially mentioned in Hungary (Szunyogh, 1990) where they have been interpreted as a result of phreatic convections.

When the ceiling of the developing rooms becomes higher, warm air flow will follow the overhanging walls to reach the highest parts. Condensation on the walls will be higher in these places, gradually carving a condensation-corrosion channel. These ceiling channels resemble paragenetic ceiling half-tubes (Renault, 1968; Pasini, 2009) or some shallow bubble trails (Chiesi and Forti, 1987; De Waele and Forti, 2006; Audra et al., 2009c; Ginès et al., 2014) but have a different origin. Condensation-corrosion channels are often sculpted with a set of megascallops that are absent in the last two types of channels. They are also common in thermal caves, and have also been reported in a Mexican cave above guano deposits, where exothermic reactions produce the rising of warm air rich in carbon dioxide (Forti et al., 2006). These convective air flows and related condensation processes can explain the rounded shapes of cross-sections that are easily confused with passages due to phreatic water flow.

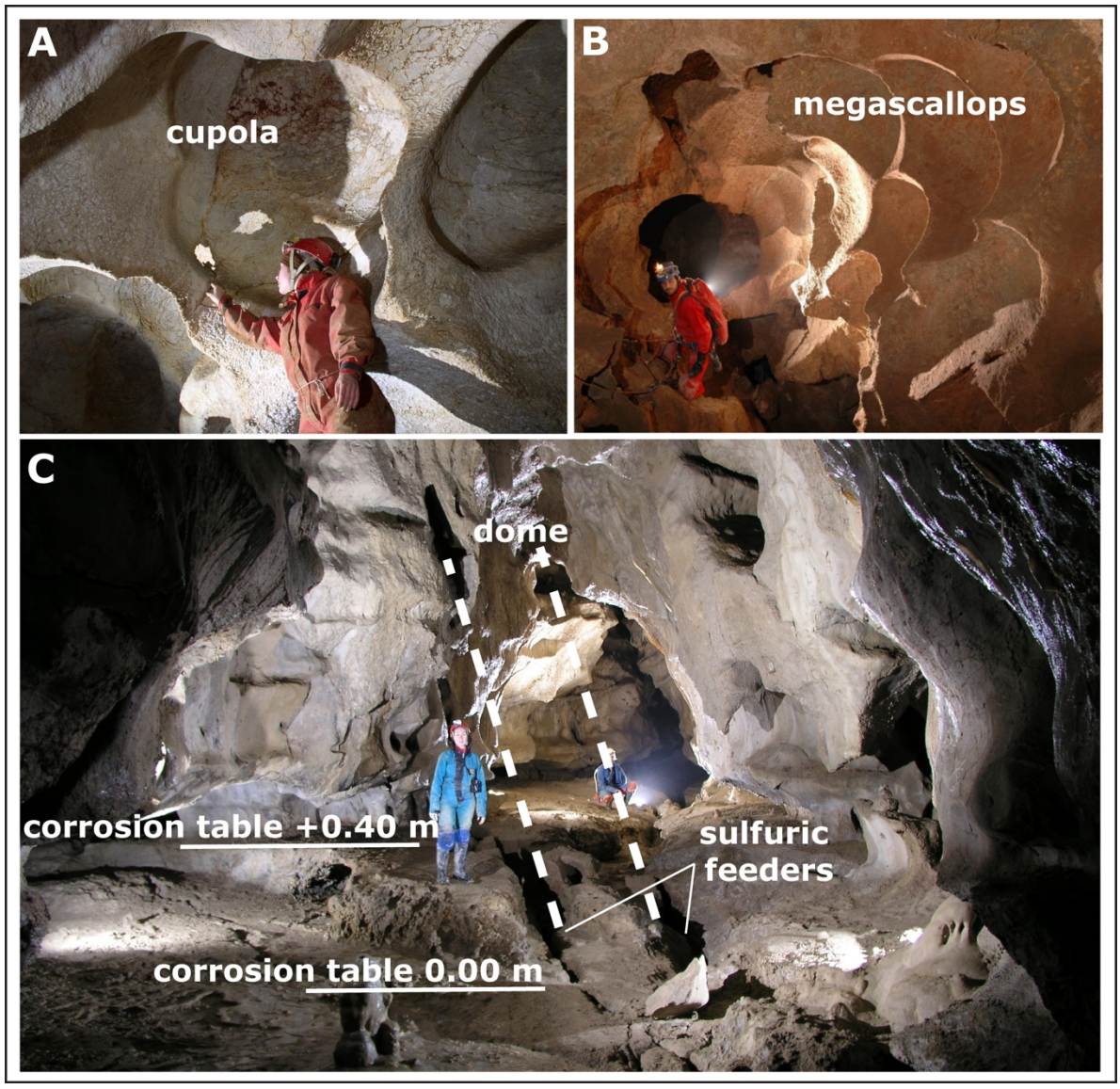

Figure 15. Condensation-corrosion morphologies in SAS water table caves: A) Coalescing ceiling cupola in Kraushöhle; B) Megascallops on the roof of a passage in Kraushöhle; C) Dome-like chamber in Grotte du Chat.

2.2.6.4. Cupolas, domes and chimneys, the upward feedback

Ceilings are the coolest places, being most distant from the thermal source. Consequently, the largest amount of condensation, and thus corrosion, occurs on the ceilings above the feeders, causing a positive feedback in favour of upward expansion of cupolas that evolve in domes or chimneys (*Figure 16*). Condensation waters then flow along walls and concentrate as dripping from pendants that feed a water film smoothing the corrosion table. On the contrary, the lowest roofs remain warm, causing less condensation, thus remaining dryer. Their corresponding floors, also dry, may retain gypsum deposits, as replacement pockets or thick crusts (*Figure 17*A).

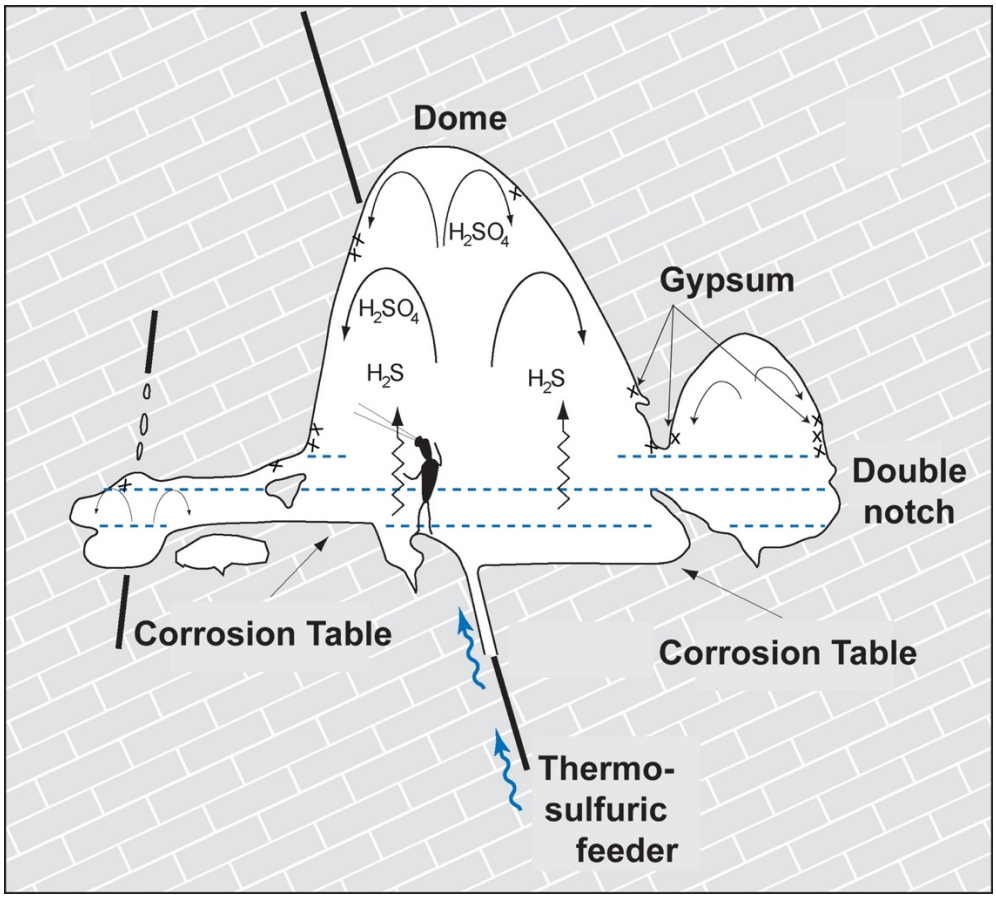

Figure 16. The positive feedback of upward development of the highest ceilings. Dashed lines show variations in the water level. See text for explanation.

2.2.6.5. Medium-scale condensation-corrosion morphologies

Deep and more or less horizontal wall convection niches are present at different heights on the cave walls of many passages. In some places these niches coalesce and align forming notches (*Figure 17*A). These are formed by rising air above a thermal pool, creating convection cells that focus condensation-corrosion processes. Dimensions of these sub-hemispheroidal niches are homogeneous, and they are roughly aligned at the same level.

In general, condensation-corrosion attacks the massive limestone uniformly, slowly weathering (by dissolution) the rock and leaving a powdery residue. In some cases it is possible to scratch the walls because the limestone has become soft. When mineral veins or fossils are present, condensation-corrosion will attack the rock in a differential way, creating boxworks and exposing fossils in relief (*Figure 17*B).

Because condensation is often more abundant in the highest and cooler part of conduits, the differential corrosion is more pronounced on high walls and roofs. If condensation is strong, the water

film will descend by gravity along the walls and increase its flow downward. This allows the sheet of water to wash the median parts of the walls, making them smoother and harder.

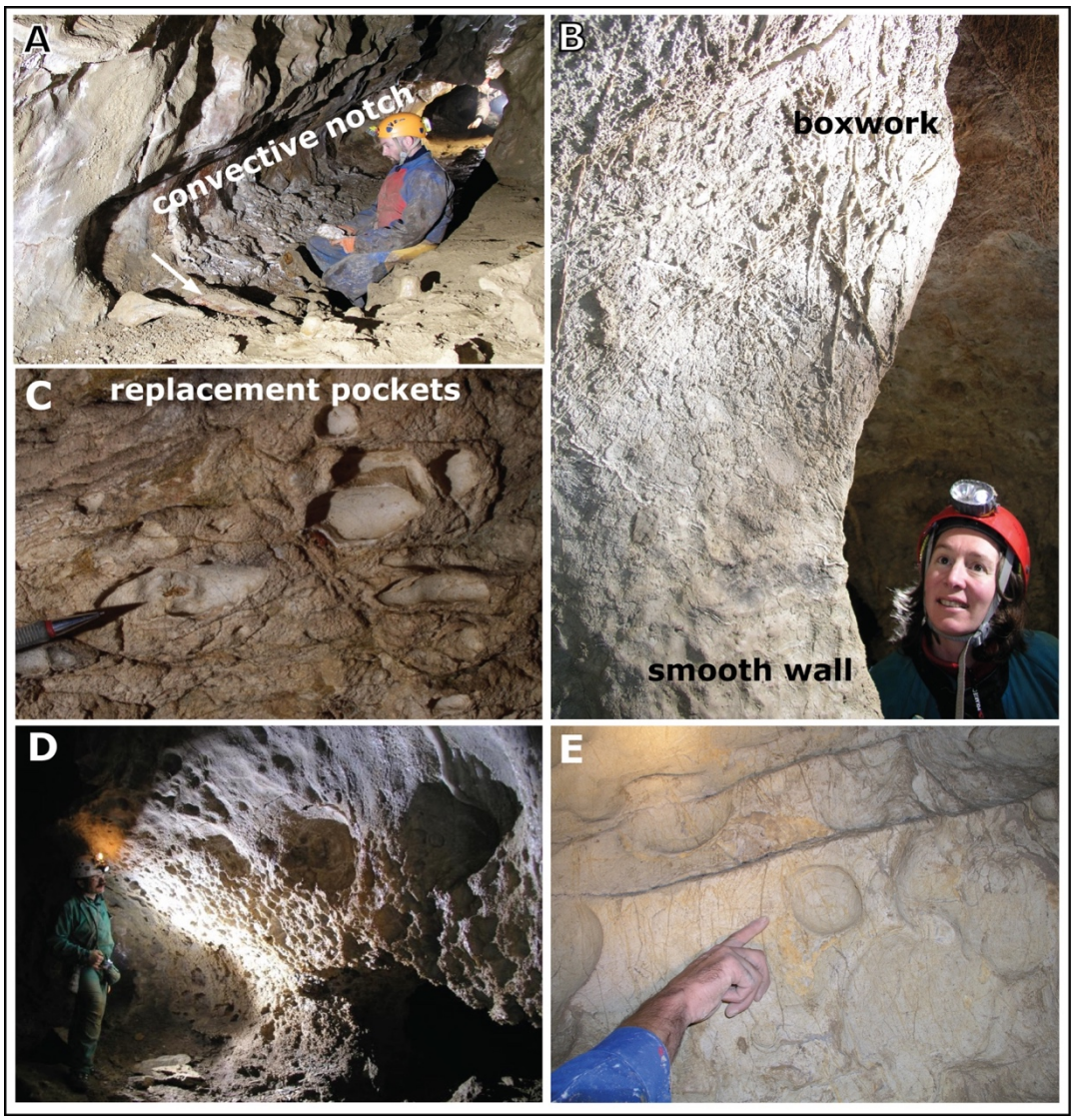

Figure 17. Medium-scale condensation-corrosion morphologies in SAS water table caves: A) Convection-corrosion notches in Grotte du Chat: note the white gypsum piled up at the bottom of the notch; B) Boxwork in Grotte du Chat; C) Typical replacement pockets on the roof above a corrosion table, Stephanshöhle, Bad Deutsch Altenburg; D) Replacement pockets located at half-height on the walls, Grotte du Chat; E) Hemispherical corrosion features.

Replacement pockets due to corrosion-substitution processes are widespread in all caves (*Figure 17*C). These are hemispherical corrosion features (*Figure 17*E) with diameters of some centimeters to more than one decimeter embedded into the wall. They are formed by concentrated sulfuric acid corrosion, with simultaneous replacement of calcite by microcrystalline gypsum (Galdenzi and Maruoka, 2003). These replacement pockets often still contain the original gypsum, except in the Bad

Deutsch Altenburg caves. The fact that gypsum is absent in these caves is due to the subsequent flooding of the passages by the nearby Danube River.

This hygroscopic gypsum retains the sulfuric acid-rich fluids and allows corrosion to proceed, causing the progressive deepening of the pockets. When the gypsum falls off, the pockets become empty, and condensation-corrosion proceeds more slowly. The inner rock surface of the pockets is often very smooth and regular (*Figure 17*D). These pockets are often distributed along a vertical range, becoming smaller and ultimately disappearing in the lower and higher parts of the cave passage. This vertical distribution is related to the geometry of the walls and the possibility of gypsum to remain attached to the carbonate rock without being washed away or fall off. Their density is also higher around the feeders where H_2S degassing occurs.

Replacement pockets are diagnostic features of SAS, since they clearly differ from any other pockets or scallops made by diffuse corrosion of flowing water in epigenic or other hypogenic caves. Replacement pockets have a perfect hemispherical shape, and normally have a smooth inner surface. Only the ones in Bad Deutsch Altenburg caves show a pattern of mm-sized channels or ridges. In general, they are distributed at middle height in the passage, and the walls in between the pockets are rather smooth.

2.2.6.6. Vertical distribution of features and deposits

The process of H_2S degassing and oxidation into sulfuric acid above the feeding point is driven by thermal convection cells. Rising warm air cools on the colder ceiling producing condensation, whereas the corresponding sinking air warms up and produces evaporation, similar to what happens in thermal caves (Sarbu and Lascu, 1997). On the ceiling, condensation moisture strongly corrodes the rock, forming boxwork and causing the upward and lateral development of the passage. Condensation concentrates as downward runoff along walls transporting solutes, both carbonates from limestone wall dissolution and sulfates from replacement. This diffuse runoff along walls gradually increases downward. At middle-height of the passage, discrete areas protected from runoff allow local accumulation of sulfates and the development of replacement pockets. The dnsity of the pockets increases downward following increasing evaporation. In the lower part of the passage, evaporation and high solute concentration allows continuous deposition of gypsum as thick crusts. In a similar way, in areas where evaporation dominates, calcite precipitates as cave popcorn (Caddeo et al., 2015). Finally, the floor displays a perfectly smoothed surface (glacis) resulting from highly corrosive sub-horizontal flow combining the aggressiveness from both the feeder and the dripping condensation. Such convective processes are responsible for the vertical distribution of features and deposits, which is also diagnostic for SAS (*Figure 18*).

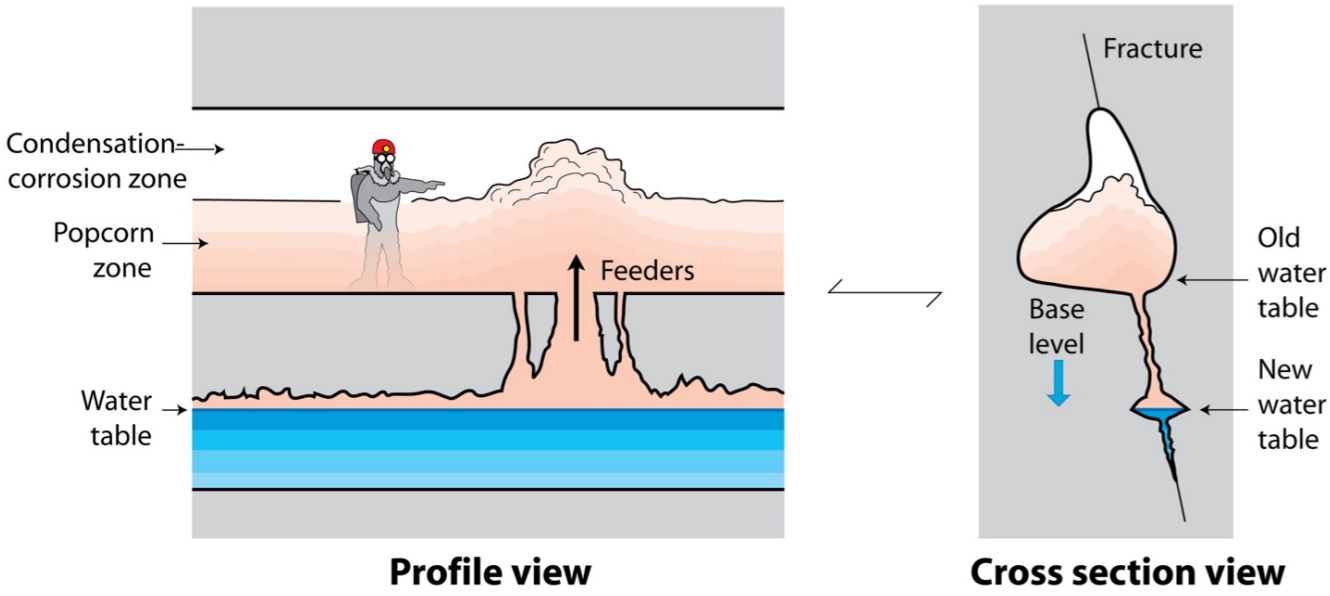

Figure 18. Vertical distribution of wall features and popcorn according to aerial thermal convection loops that produce condensation-corrosion at the top of the passage and evaporation-precipitation in the lower parts. The cross-section (right) is typical of a SAS water table cave.

2.2.6.7. Concentrated sulfuric acid related features

In Grotte du Chat and in Kraushöhle the concentration of sulfuric acid in condensation waters and drip-rate were such to allow acid dripping from the roof, similar to what occurs in active SAS caves such as Cueva de Villa Luz (Hose et al., 2000). In this last cave, droplets are produced at the end of mucolites and in biofilms, or seep through replacement gypsum crusts which prevent, at least to a certain extent, the acid attacking the ceiling carbonate rocks (Hose and Pisarowicz, 1999; Hose et al., 2000). In Grotte du Chat and Acqua Fitusa Cave these extremely acid drops have created a series of morphologies such as sulfuric-acid karren and solution pans (*Figure 19*D); similar features have also been found at the base of the Crystal Chimney in Kraushöhle (Plan et al., 2012) (*Figure 19*A). On the floor of the "Wilczekgang" in this cave, unique 10 to 35 cm-wide bowl-shaped depressions surrounded by walls up to 15 cm high have been found (Plan et al., 2012). Since they are always located 0.8 to 1.7 m below triple junctions of cupolas, forming pendants or lowest points along the ceiling, these have been called "ceiling pendant drip holes", probably also due to acid corrosion (*Figure 19*C). Acidic dripping water can also form drip tubes, half-cylinders carved along walls which originally projected into the rock mass as a full tube with a round bottom. These forms are very rare and have been seen in Kraushöhle.

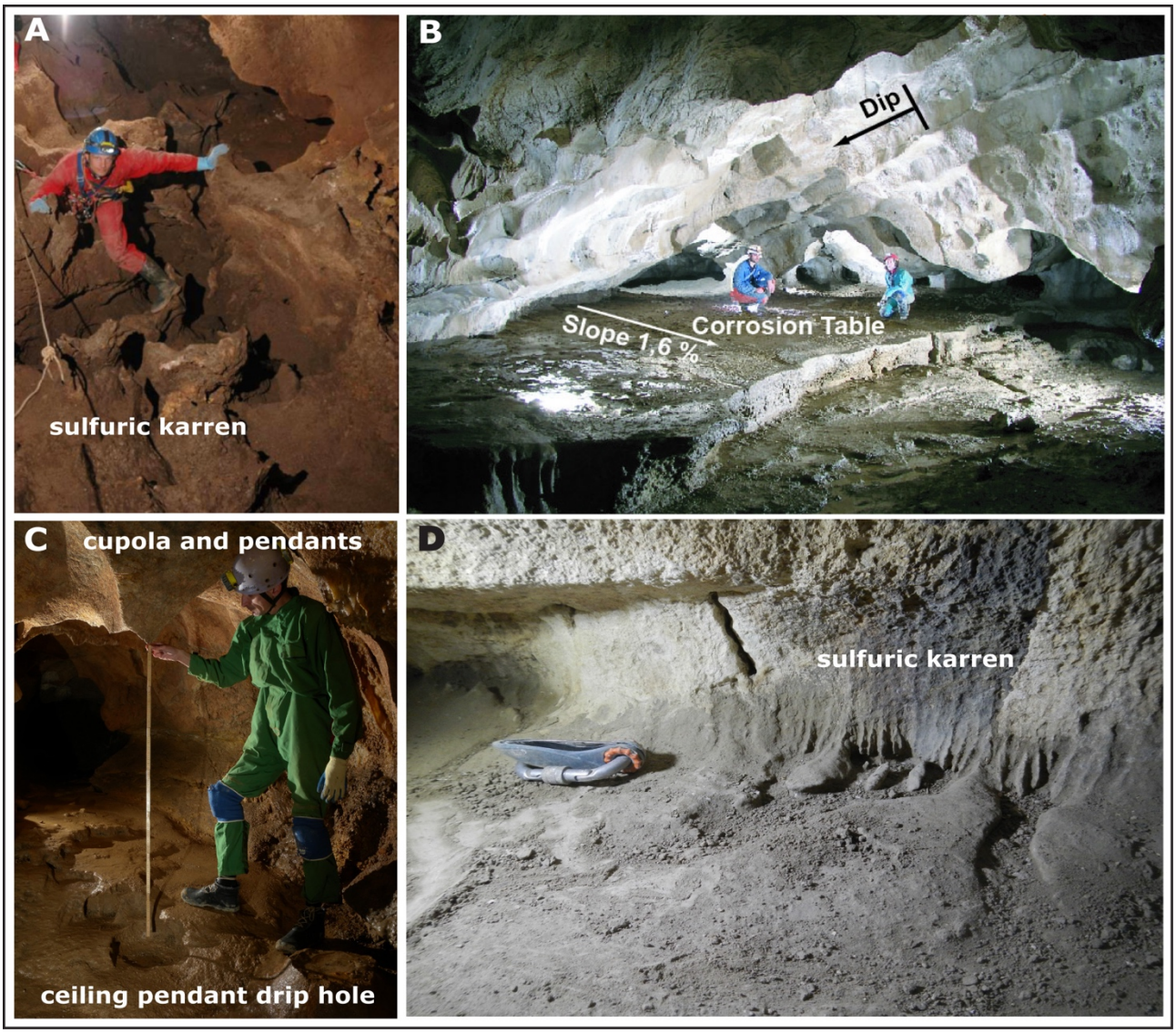

Figure 19. Morphologies related to dripping or flowing acid water A) Sulfuric karren, Kraushöhle; B) Corrosion table in Grotte du Chat cutting the dip of the limestones; C) Ceiling pendant drip holes in Kraushöhle; D) Sulfuric-acid karren and solution pans in Acqua Fitusa Cave (5 cm-long knife for scale).

A very special type of morphology related to the acid condensation waters flowing back to the feeding fissure (or pool) is the corrosion table (*Figure 19*B). These are almost perfectly horizontal surfaces of rock that have been flattened down by corrosion. This planation by sulfuric acid-rich waters creates smooth glacis, in which rocks of different hardness are worn down equally. Corrosion tables can be seen in all investigated caves, but are best developed and preserved in Grotte du Chat. The very small gradient of the corrosion tables both transversely (1.6%) and longitudinally (0.1 to 1.3%) results from a balance between turbulence and oxygenation. Steeper slopes allow water to flow with more turbulence, enhancing oxygenation and thus formation of sulfuric acid by oxidation of dissolved H_2S.

This will eventually lead to higher downwearing rates than in flatter surfaces, leading ultimately to the formation of an equilibrium slope (Egemeier, 1981). The altitude of these corrosion tables adjusts to a position slightly above that of the water level. If the sulfuric water level drops, the corrosion table will be entrenched, starting from the water level. Subsequent drops in water level can leave a set of distinct perched corrosion tables. In Grotte du Chat twelve levels are recorded within only 6 m of elevation (Audra, 2007).

2.2.6.8. Evolution of maze pattern by passage expansion and integration

The widespread and homogeneous dissolution by condensation-corrosion processes leads first to a widening of all open fractures and joints close to or immediately above the discharging H_2S-rich fluids. This creates mazes, similar to the ones formed under epigenic phreatic conditions, but without signs of flowing water like scallops or coarse-grained allochthonous sediments. The evolution proceeds by expansion of volumes around sulfidic feeders while distant passages in the maze are less enlarged. The progressive expansion of neighbouring passages leaves remnants of partings, with typical concave pillars, pendants, blades, projecting corners, arches, and half-tubes originating from integration of lateral tubes that resemble notches (Osborne, 2007). Depending on the distance from the discharging points, the passage sizes are irregular and the entrance into the largest chambers often occurs through narrow or seemingly incidental passages (*Figure 20*).

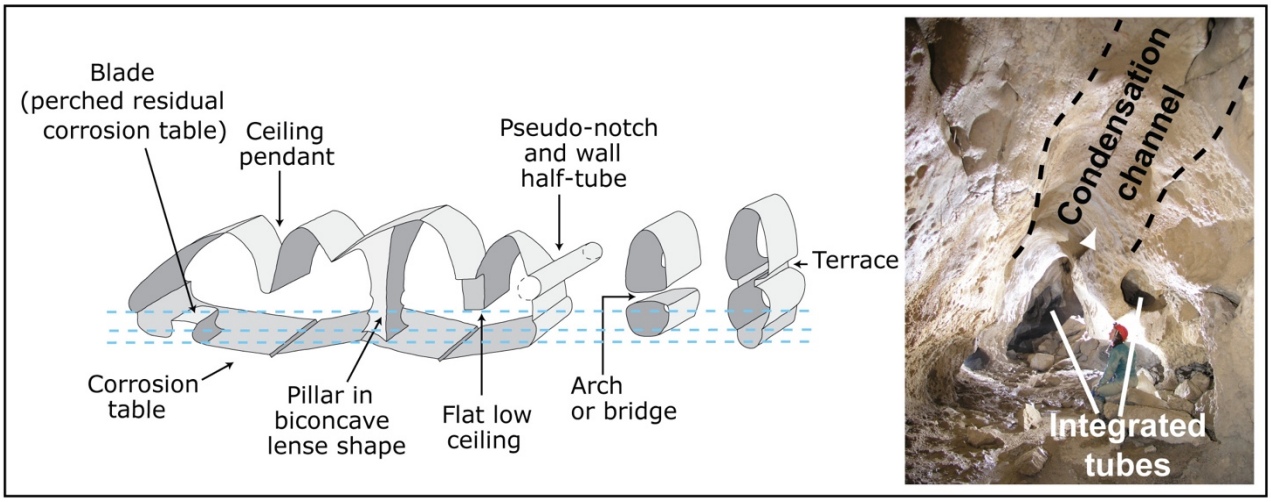

Figure 20. Typical passage configuration of a SAS water table cave with narrows, partings and pillars. The dashed line shows variation in the water level.

2.2.6.9. Sulfate mineral by-products of SAS

The most abundant SAS mineral is gypsum which displays different shapes and colours. Saccharoid replacement gypsum crusts are common in many passages; the gypsum is located in large vertical

fissures along the walls, it can partially cover wall convection notches, or replacement pockets. Large gypsum bodies are found on the floors of the biggest rooms in correspondence of which small ceiling cupolas and pendants are associated on the roof. In Acqua Fitusa Cave centimetric euhedral gypsum crystals have grown inside mud sediments, while in Kraushöhle a chimney rising above the central chamber hosts decimetric yellowish secondary gypsum crystals made by the washing of sulfates by condensation in higher parts followed by crystallization through evaporation in lower parts. Kraushöhle also hosts other sulfates such as alunite, jarosite and met-alunogene, the hydroxide gibbsite, the silicate halloysite, and opal. Grotte du Chat hosts, besides gypsum, jarosite. All these minerals are typical of low-pH conditions typical of SAS caves (Polyak and Provencio, 2001; Plan et al., 2012).

2.2.6.10. Sulfur stable isotopes

Stable sulfur isotopes of all caves (except Bad Deutsch Altenburg) are reported in *Table 5*, with values also for some other well-known SAS caves. Most of these data are consistent with bacterial sulfate reduction or thermochemical sulfate reduction of evaporitic rocks with hydrocarbons (i.e., methane) providing the source of electron donors producing H_2S. Two of the Acqua Fitusa Cave sulfates (both correspond to gypsum sampled in the upper level, while the ones with more negative values come from the lower level) show positive values, and testify to the complexity of sulfur isotopic evolution similar to what has been documented in Cerna Valley (Wynn et al., 2010; Onac et al., 2011). These less negative values can derive from the host rock or from the diminished fractionation during the transformation from sulfate to sulfide. Further stable isotope analyses would be required to better understand the behaviour of the geochemical system.

Table 5. Stable sulfur isotopes of gypsum in the studied SAS caves and comparison with some other cave studies. Isotope ratios are reported in the conventional δ-notation with respect to V-CDT (Vienna Cañon Diablo Troilite).

Cave	**$\delta^{34}S$ (‰)**	**Reference**
Kraushöhle	-23.12 to -15.83	Puchelt and Blum, 1989
Acqua Fitusa Cave	-1.0 to +4.4 and 10.2 to 10.6	this study
Grotte du Chat	-9.4	Audra, 2007
Montecchio Cave	-28.3 to -24.2	Piccini et al., 2015
Lechuguilla Cave	-25 to +5	Hill, 1987
Frasassi Cave	-20 to -8	Galdenzi and Maruoka, 2003
Cueva de Villa Luz	-24.87 to -22.12	Hose et al., 2000
Provalata Cave	-2.3 to -1.9	Temovski et al., 2013

Cerna valley caves	-27.9 to +19.5	Onac et al., 2011

2.2.6.11. Age of caves, cave levels and landscape evolution

SAS water table caves are exceptional recorders of the past position of the water table level. Several meso-morphologies, such as the notches with flat roof and the corrosion tables, are precise indicators of the exact position of the water table at the moment of their formation. Also the overall long-profile development of SAS water table caves, with a very low gradient from the upstream discharging points to the spring, allow precise constraint of the position of the ancient water tables. Horizontal cave passages can be dated in a direct way by constraining chronologically the secondary by-products of the SAS process, which were formed exactly at the time when acid-solutional processes were active. Gypsum, the ubiquitous by-product of SAS, can be dated by U/Th methods (Sanna et al., 2010; Piccini et al., 2015) but the relatively low U content often does not allow precise ages to be determined. Alunite and jarosite, instead, often produced by the reaction of sulfuric acid with clay minerals hosted in the original carbonate sequence, can give useful results with the K/Ar and Ar/Ar methods (Polyak et al., 1998). Alunite has been dated at Kraushöhle and showed this cave, located around 80 m above the present thalweg and active sulfuric spring, to be less than 160 kyr old (Plan et al., 2012). Stalagmites that grew after the cave became vadose were dated by U/Th method and are at least 86 kyr old (Spötl et al., 2014). This testifies to a very rapid (0.5 to 1 m/kyr) entrenchment of the Gams Brook.

The age of the caves in Bad Deutsch Altenburg can only be speculated as they lack speleothems but they must be rather young, since the lowest accessible parts are only a few meters above the level of the Danube River.

2.2.7. Conclusions

Sulfuric acid water table caves are among the most interesting hypogenic caves in limestone and dolostone, from a biological and geological point of view. They have been reported from many regions in the world and typically display a suite of easily recognisable morphological and mineralogical characteristics (*Table 6*). Sulfuric acid produced both by abiotic and biotic oxidation of H_2S is rapidly neutralised by the carbonate host-rock, with the typical replacement of calcite by gypsum. These processes mainly occur in the aerate environment, close to and above the water level, where oxygen levels are high enough to oxidise the degassing H_2S rapidly. Rising waters are often slightly thermal, boosting the condensation of water vapor above the feeding fissures. Some geomorphological features, such as blind ending passages upstream of the discharge points, corrosion tables, replacement pockets, sulfuric cups and karren are unique to these caves. Also the presence of

sulfates, mainly gypsum but also jarosite, alunite and others are diagnostic features of SAS caves. Their speleogenetic evolution is closely related to the water table position and, because of their very fast evolution, they often are very precise records of base level changes. Some of the minerals typically present in these caves are formed during SAS speleogenesis and their dating precisely marks the age of cave formation, and thus of the base level position.

Table 6. Morphological features typical of sulfuric acid water table caves classified according to the dominant process.

HYPOGENIC DOMINANT PROCESS	**FEATURES ALSO PRESENT IN THERMAL HYPOGENIC CAVES WITH HIGH CO_2 CONCENTRATION FROM DEGASSING**	**TYPICAL DIAGNOSTIC FEATURES OF SULFURIC ACID CAVES**
Flowing corrosive water		Discharge points with blind termination upstream
Standing corrosive pools	Notch with flat roof	
Ultra-acidic dripping (mediated by sulfo-oxidant microbial mucolites)	Ceiling pendant drip hole	Sulfuric-acid karren
	Drip tubes / Wall half tubes	Sulfuric-acid cups
Condensation-corrosion	Cupola	Corrosion table
	Dome	
	Chimney	
	Wall convection niche	
	Condensation-corrosion channel	
	Megascallops	
	Vent (feeder)	
	Boxwork/weathered walls/hieroglyphs	
Corrosion under gypsum cover		Replacement pockets
		Massive gypsum deposits
Evaporation of moisture	Calcite popcorn (also present in any epigenic cave where strong evaporation takes place)	

References

Audra, P., 2007. Karst et spéléogenèse épigènes, hypogènes, recherches appliquées et valorisation. Habilitation Thesis, University of Nice Sophia-Antipolis. 278 pp.

Audra, P., 2008. The sulfuric hypogene speleogenesis: processes, cave pattern, and cave features. Berliner Höhlenkundliche Berichte, 26: 5-30.

Audra, P., Hobléa, F., Bigot, J.-Y., Nobécourt, J.-C., 2007. The role of condensation-corrosion in thermal speleogenesis: study of a hypogenic sulfidic cave in Aix-les-Bains, France. Acta Carsologica, 36: 185-194.

Audra, P., Mocochain, L., Bigot, J.-Y., Nobecourt, J.-C., 2009a. Hypogene cave patterns. In: A., Klimchouk, D., Ford (Eds.), Hypogene Speleogenesis and Karst Hydrogeology of Artesian Basins. Special Paper, 1. Ukrainian Institute of Speleology and Karstology, Kiev: 17-22.

Audra, P., Mocochain, L., Bigot, J.-Y., Nobecourt, J.-C., 2009b. Morphological indicators of speleogenesis: hypogenic speleogenesis. In: A., Klimchouk, D., Ford (Eds.), Hypogene Speleogenesis and Karst Hydrogeology of Artesian Basins. Special Paper, 1. Ukrainian Institute of Speleology and Karstology, Kiev: 23-32.

Audra, P., Mocochain, L., Bigot, J.Y., Nobécourt, J.C. 2009c. The association between bubble trails and folia: a morphological and sedimentary indicator of hypogenic speleogenesis by degassing, example from Adaouste Cave (Provence, France). International Journal of Speleology, 38 (2): 93-102.

Audra, P., Gázquez, F., Rull, F., Bigot, J-Y., Camus, H. 2015. Hypogene Sulfuric Acid Speleogenesis and rare sulfate minerals in Baume Galinière Cave (Alpes-de-Haute-Provence, France). Record of uplift, correlative cover retreat and valley dissection. Geomorphology, 247: 25-34.

Auler, A.S., Smart, P.L., 2003. The influence of bedrock-derived acidity in the development of surface and underground karst evidence from the Precambrian carbonates of semi-arid northeastern Brazil. Earth Surface Processes and Landforms, 28:157-168.

Barton, H., Luiszer, F., 2005. Microbial metabolic structure in a sulfidic cave hot spring: Potential mechanisms of biospeleogenesis. Journal of Cave and Karst Studies, 67(1): 28-38.

Bianchini, G., Gambassini, P., 1973. Le Grotte dell'Acqua Fitusa (Agrigento) I - Gli scavi e l'industria litica. Rivista di Scienze Preistoriche, 28 (1): 1-55.

Caddeo, G.A., Railsback, R.A.L., De Waele, J., Frau, F., 2015. Stable isotope data as constraints on models for the origin of coralloid and massive speleothems: The interplay of substrate, water supply, degassing, and evaporation. Sedimentary Geology, 318: 130-141.

Calaforra, J.M., De Waele, J., 2011. New peculiar cave ceiling forms from Carlsbad Caverns (New Mexico, USA): the zenithal ceiling tube-holes. Geomorphology, 134: 43-48

Catalano, R., Agate, M., Albanese, C., Avellone, G., Basilone, L., Gasparo Morticelli, M., Gugliotta, C., Sulli, A., Valenti, V., Gibilaro, C., Pierini S., 2013. Walking along a crustal profile across the Sicily fold and thrust belt. AAPG International Conference & Exhibition, 23-26 October 2011, Milan. Post Conference Field Trip 4, 27-29 October 2011, Palermo. Geological field trips 5(2.3), 213 pp.

Collignon, B., 1983. Spéléogenèse hydrothermale dans les Bibans (Atlas Tellien, Algérie). Karstologia, 2: 45-54.

Collignon, B., 1990. Les karsts hydrothermaux d'Algérie. 10th International Congress of Speleology Budapest 1989, III: 758-760.

Chiesi, M., Forti, P., 1987. Studio morfologico di due nuove cavitá carsiche dell'Iglesiente (Sardegna Sud occidentale). Ipoantropo, 4: 40-45.

D'Antoni-Nobécourt, J.-C., Audra, P., Bigot, J.-Y., 2008**.** La spéléogenèse par corrosion sulfurique: l'exemple de la grotte du Chat (Daluis, Alpes-Maritimes). Riviera Scientifique, 91: 53-72.

De Waele, J., Forti, P., 2006. A new hypogean karst form: the oxidation vent. Zeitschrift für Geomorphologie, 147: 107–127.

De Waele, J., Forti, P., Naseddu, A., 2013. Speleogenesis of a complex example of an exhumed sulphuric acid karst in Cambrian carbonates (Mount San Giovanni, Sardinia). Earth Surface Processes and Landforms. http://dx.doi.org/10.1002/esp.3375.

De Waele, J., Galdenzi, S., Madonia, G., Menichetti, M., Parise, M., Piccini, L., Sanna, L., Sauro, F., Tognini, P., Vattano, M., Vigna, B., 2014. A review on hypogene caves in Italy. In: A., Klimchouk, I., Sasowsky, J., Mylroie, S.A., Engel, A.S., Engel (Eds.), Hypogene Cave Morphologies. Karst Waters Institute Special Publication 18, Leesburg, Virginia: 28-30.

De Waele, J., Plan, L., Audra, P., Rossi, A., Spötl, C., Polyak, V., McIntosh, B., 2009. Kraushöhle (Austria): Morphology and mineralogy of an alpine sulfuric acid cave. In: W.B., White (Ed.), Proceedings of the 15th International Congress on Speleology, Kerrville, 2, 31-37.

De Waele, J., Audra, P., Madonia, G., Vattano, M., Plan, L., D'Angeli, I.M., Bigot, J.Y., Nobécourt, J.C., 2016. Sulfuric acid speleogenesis (SAS)close to the water table: examples from southern France, Austria and Sicily. Geomorphology, 253: 452-467.

Dublyansky, V.N., 1980. Hydrothermal karst in Alpine folded belt of southern part of USSR. Kras i Speleologia, XII: 18-38.

Ducluzaux, B., 1994. Karst et thermalisme. 4e Rencontre d'octobre Pau, Spéléo-club de Paris : 49-52.

Egemeier, S. J., 1981. Cavern development by thermal waters. NSS Bulletin, 43: 31-51.

Engel, A.S., Stern, L.A., Bennet, P.C., 2004. Microbial contributions to cave formation: new insights into sulfuric acid speleogenesis. Geology, 32: 369-372.

Filipponi, M., Jeannin, P.-Y., 2006. Is it possible to predict karstified horizons in tunneling? Austrian Journal of Earth Sciences, 99: 24-30.

Forti, P., 1985. Le mineralizzazioni della grotta di Cala Fetente (Salerno, Campania). Mondo Sotterraneo, 1985(1-2): 41-50.

Forti, P., Menichetti, M., Rossi, A., 1989. Speleothems and speleogenesis of the Faggeto Tondo Cave (Umbria, Italy). In: Hazslinszky, T., Takacsne, B.K. (Eds.), Proceedings of the 10th International Congress of Speleology, Budapest, 1: 74-76.

Forti, P., Galli, E., Rossi, A., 2006. Peculiar minerogenetic cave environments of Mexico: the Cuatro Ciénegas area. Acta Carsologica, 35(1): 79-98.

Galdenzi, S., 1997. Initial geologic observations in caves bordering the Sibari Plain (Southern Italy). Journal of Cave and Karst Studies, 59(2): 81-86.

Galdenzi, S., 2001. L'azione morfogenetica delle acque sulfuree nelle Grotte di Frasassi, Acquasanta Terme (Appennino marchigiano-Italia) e di Movile (Dobrogea-Romania). Le Grotte d'Italia, V(2): 49-61.

Galdenzi, S., Maruoka, T., 2003. Gypsum deposits in the Frasassi caves, Central Italy. Journal of Cave and Karst Studies, 65: 111-125.

Galdenzi, S., Menichetti, M., 1995. Occurrence of hypogenic caves in a karst region: examples from central Italy. Environmental Geology, 26: 39-47.

Galdenzi, S., Cocchioni, F., Filipponi, G., Morichetti, L., Scuri, S., Selvaggio, R., Cocchioni, M., 2000. The sulfidic thermal caves of Acquasanta terme (Central Italy). Journal of Cave and Karst Studies, 72(1): 43-58.

Gàzquez, F., Calaforra, J.-M., Forti, P., De Waele, J., Sanna, L., 2015. The role of condensation in the evolution of dissolutional forms in gypsum caves: Study case in the karst of Sorbas (SE Spain). Geomorphology, 229: 100-111.

Ginés, J., Fornós, J.J., Ginés, A., Merino, A., Gràcia, F., 2014. Geologic constraints and speleogenesis of Cova des Pas de Vallgornera, a complex coastal cave from Mallorca Island (Western Mediterranean). International Journal of Speleology, 43(2): 105-124.

Grassa, F., Capasso, G., Favara, R., Inguaggiato, S., 2006. Chemical and isotopic composition of waters and dissolved gases in some thermal springs of Sicily and adjacent volcanic islands, Italy. Pure and Applied Geophysics, 163: 781-807.

Hauer, F., 1885. Die Gypsbildungen in der Krausgrotte bei Gams. Verhandlungen der Geologischen Reichsanstalt, 1885: 21-24.

Hill, C. A., 1987. Geology of Carlsbad cavern and other caves in the Guadalupe Mountains, New Mexico and Texas. New Mexico Bureau of Mines and Mineral Resources, 117: 1-150.

Hill C.A., 1990. Sulfuric acid speleogenesis of Carlsbad Cavern and its relationship to hydrocarbons, Delaware Basin, New Mexico and Texas. American Association of Petroleum Geologists Bulletin, 74: 1685-1694.

Hose, L.D., Palmer, A.N., Palmer, M.V., Northup, D.E., Boston, P.J., Duchene, H.R., 2000. Microbiology and geochemistry in a hydrogen-sulphide-rich karst environment. Chemical Geology, 169: 399-423.

Hose, L.D., Pisarowicz, J.A., 1999. Cueva de Villa Luz, Tabasco, Mexico: reconnaissance study of an active sulfur spring cave and ecosystem. Journal of Cave and Karst Studies, 61: 13-21.

Jones, D.S., Schaperdoth, I., Macalady, J.L., 2014. Metagenomic Evidence for Sulfide Oxidation in Extremely Acidic Cave Biofilms. Geomicrobiology Journal, 31: 194-204.

Jones, D.S., Polerecky, L., Galdenzi, S., Dempsey, B.A., Macalady, J.L., 2015. Fate of sulfide in the Frasassi cave system and implications for sulfuric acid speleogenesis. Chemical Geology, 410: 21-27.

Kerckhove, C., Roux, M., 1976. Notice de la carte géologique de la France à 1/50 000, 971 Castellane. BRGM, Orléans: 39 pp.

Kirkland, D.W., 2014. Role of hydrogen sulfide in the formation of cave and karst phenomena in the Guadalupe Mountains and western Delaware Basin, New Mexico and Texas. National Cave and Karst Research Institute, Carlsbad, Special Paper Series, 1: 77 p.

Klimchouk, A., 2007. Hypogean speleogenesis: hydrogeological and morphometric perspective. Special Paper 1, National Cave and Karst Research Institute, Carlsbad, NM, 106 pp.

Klimchouk, A., 2009. Morphogenesis of hypogenic caves. Geomorphology, 106: 100-117.

Klimchouk, A., Auler S.A., Bezerra, F.H.R., Cazarin, C.L., Balsamo, F., Dublyansky, Y., 2016. Hypogenic origin, geologic controls and functional organization of a giant cave system in Precambrian carbonates, Brazil. Geomorphology, 253: 385-405.

Kraus, F., 1891. Höhlenbildung durch Metamorphismus. Die Natur, 40: 197-199.

Lazaridis, G., Melfos, V., Papadopoulou, L., 2011. The first cave occurrence of orpiment (As_2S_3) from the sulfuric acid caves of Aghia Paraskevi (Kassandra Peninsula, N. Greece). International Journal of Speleology, 40: 133-139.

Lombardo, G., Sciumè, A., Sollano, G., Vecchio, E., 2007. La Grotta dell'Acqua Fitusa e l'area della Montagnola nel territorio di San Giovanni Gemini (Ag). Speleologia Iblea, 12: 125-132.

Maltsev, V.A., Malishevsky, D.I., 1990. On hydrothermal phases during later stages of the evolution of Cupp Coutunn Cave System, Turkmenia, USSR. National Speleological Society Bulletin, 52: 95-98.

Martel, E.-A., 1935. Contamination, protection et amélioration des sources thermominérales. Congrès international des mines, de la métallurgie et de la géologie appliquée, 2: 791-798.

Mayer, A., Wirth, J., 1989. Höhlen und Stollen in Bad Deutsch Altenburg. Höhlenkundliche Mitteilungen Wien, 45 (11): 230-234.

Mecchia, M., 2012. Indizi di speleogenesi ipogenica nelle grotte del Monte Soratte. Notiziario dello Speleo Club Roma, 16: 58-69.

Melim, L.A., Northup, D.E., Boston, P.J., Spilde, M.N., 2016. Preservation of fossil microbes and biofilm in cave pool carbonates and comparison to microbial carbonate environments. Palaios, 31(4), 177-190.

Menichetti, M., 2011. Hypogenic caves in western Umbria (Central Italy). Acta carsologica, 40(1): 129-145.

Morehouse, D., 1968. Cave development via the sulfuric acid reaction. NSS Bulletin, 30: 1-10.

Onac, B.P., 1991. New data on some gypsum spelothems in the Vântului (Pădurea Craiului mountains) and Răstoci (Somesan plateau) caves. Travaux de l'Institute de Spéologie "Emile Racovitza", 30: 189-193.

Onac, B.P., Sumrall, J., Tămaş, T., Povară, I., Kearns, J., Dărmiceanu, V., Veres, D., Lascu, C., 2009. The relationship between cave minerals and H_2S-rich thermal waters along the Cerna Valley (SW Romania). Acta Carsologica, 38(1): 27-39.

Onac, B.P., Wynn, J.G., Sumrall, J.B., 2011. Tracing the sources of cave sulfates: a unique case from Cerna Valley, Romania. Chemical Geology, 288: 105-114.

Onac, B.P., Effenberger, H.S., Wynn, J.G., Povară, I., 2013. Rapidcreekite in the sulfuric acid weathering environment of Diana Cave, Romania. American Mineralogist, 98: 1302-1309.

Osborne, R.A.L., 2007. Cathedral cave, Wellington Cave, New South Wales, Australia. A multiphase. Non-fluvial cave. Earth Surface Processes and Landforms, 32(14): 2075-2103.

Palmer, A.N., 2013. Sulfuric acid caves: morphology and evolution. In: Schroder, J, Fromkin, A, (Eds.). Treatise on Geomorphology. Academic Press, Karst Geomorphology, 6: 241-257.

Palmer, A.N., Palmer, M.V., 2000. Hydrochemical interpretation of cave patterns in the Guadalupe Mountains, New Mexico. Journal of Cave and Karst Studies, 62: 91-108.

Palmer, A.N., Palmer, M.V., 2012. Petrographic and isotopic evidence for late-stage processes in sulfuric acid caves of the Guadalupe Mountains, New Mexico, USA. International Journal of Speleology, 41(2): 231-250.

Pasini, G., 2009. A terminological matter: paragenesis, antigravitative erosion or antigravitational erosion? International Journal of Speleology, 38: 129-138.

Piccini, L., De Waele, J., Galli, E., Polyak, V.J., Bernasconi, S.M., Asmerom, Y., 2015. Sulphuric acid speleogenesis and landscape evolution: Montecchio cave, Albegna river valley (Southern Tuscany, Italy). Geomorphology, 229: 134-143.

Plan, L., Spötl, C., Pavuza, R., Dublyansky, Y., 2009. Hypogene caves in Austria. - In: Klimchouk, A., Ford, D. (Eds.), Hypogene Speleogenesis and Karst Hydrogeology of Artesian Basins. Special Paper, 1. Ukrainian Institute of Speleology and Karstology, Kiev: 121-127.

Plan, L., Tschegg, C., De Waele, J., Spötl, C., 2012. Corrosion morphology and cave wall alteration in an alpine sulfuric acid cave (Kraushöhle, Austria). Geomorphology, 169-170: 45-54.

Polyak, V.J., Provencio, P., 2001. By-product materials relatied to H_2S-H_2SO_4-influenced speleogenesis of Carlsbad, Lechuguilla, and other caves of the Guadalupe Mountains, New Mexico. Journal of Cave and Karst Studies, 63(1): 23-32.

Polyak, V.J., McIntosh, W.C., Provencio, P., Güven, N., 1998. Age and origin of Carlsbad Caverns and related caves from $^{40}Ar/^{39}Ar$ of alunite. Science, 279: 1919-1922.

Polyak, V.J., DuChene, H.R., Davis, D.G., Palmer, A.N., Palmer, M.V., Asmerom, Y., 2013. Incision history of Glenwood Canyon, Colorado, USA, from the uranium-series analyses of water-table speleothems. International Journal of Speleology, 42 (3): 193-202.

Principi, P., 1931. Fenomeni di idrologia sotterranea nei dintori di Triponzo (Umbria). Le Grotte d'Italia, I (5): 45-47.

Puchelt, H., Blum, N., 1989. Geochemische Aspekte der Bildung des Gipsvorkommens der Kraushöhle/Steiermark. Oberrheinische Geologische Abhandlungen, 35: 87-99.

Puscas, C.M., Onac, B.P., Effenberger, H.S., Povara, I., 2013. Tamarugite-bearing paragenesis formed by sulfate acid alteration in Diana Cave, Romania. European Journal of Mineralogy, 25: 479-486.

Renault, P., 1968. Contribution à l' étude des actions mécaniques et sédimentologiques dans la spéléogenèse. 3e partie: Les facteurs sédimentologiques. Annales de Spéléologie, 23 (3): 529-596.

Sanna, L., Saez, F., Simonsen, S.L., Constantin, S., Calaforra, J.M., Forti, P., Lauritzen, S.-E., 2010. Uranium-series dating of gypsum speleothems: methodology and examples. International Journal of Speleology, 39 (1): 35-46.

Sarbu, S. M., Lascu, C., 1997. Condensation corrosion in Movile cave, Romania. Journal of Cave and Karst Studies, 59(3): 99-102.

Sarbu, S.M., Kinkle, B.K., Vlasceanu, L., Kane, T.C., Popa, R., 1994. Microbiological characterization of a sulfide-rich groundwater ecosystem: Geomicrobiology Journal, 12: 175-182.

Sarbu, S.M., Kane, T.C., Kinkle, B.K., 1996. A chemoautotrophically based cave ecosystem: Science, 272: 1953-1955.

Schuster, R., Daurer A., Krenmayr, H.G., Linner, M., Mandl G., Pestal, G., Reitner, J., 2013. Rocky Austria – Geologie von Österreich kurz und bunt. Geol. Bundesanstalt, Wien: 80 pp.

Socquet, J.-M., 1801. Analyse des eaux thermales d'Aix (en Savoie), département du Mont-Blanc (Analysis of thermal waters at Aix, in Savoy, Mont-Blanc Department), Cleaz, Chambéry : 240 pp.

Spötl, C., Boch, R., Moseley, G., Brandstätter, S., Edwards, R.L., Cheng, H., Mangini, A., Plan, L., 2014. Wann entstanden die Tropfsteine in der Kraushöhle bei Gams (Steiermark)? Die Höhle, 65: 18-24.

Stevanović, Z., Iurkiewicz, A., Maran, A., 2009. New insights into karst and caves of northwestern Zagros (northern Iraq). Acta Carsologica, 38(1): 83-96.

Szunyogh, G., 1990. Theoretical investigation of the developmentvbof spheroidal niches of thermal water origin - second approximation. Proceedings of the 10th International Congress of Speleology, Budapest, 3: 766-768.

Temovski, M., Audra, P., Mihevc, A., Spangenberg, J., Polyak, V., McIntosh, W., Bigot, J.Y., 2013. Hypogenic origin of Provalata Cave, Republic of Macedonia: a distinct case of successive thermal carbonic and sulfuric acid speleogenesis. International Journal of Speleology, 42: 235–246.

Tisato, N., Sauro, F., Bernasconi, S.M., Bruijn, R., De Waele, J., 2012. Hypogenic contribution to speleogenesis in a predominant epigenic karst system: a case study from the Venetian Alps, Italy. Geomorphology, 151-152: 156-163.

Vattano, M., Audra, P., Benvenuto, F., Bigot, J.Y., De Waele, J., Galli, E., Madonia, G. & Nobécourt, J.C., 2013. Hypogenic caves of Sicily (Southern Italy). In: Filippi, M., Bosak, P. (Eds.), Proceedings of the 16th International Congress of Speleology, Brno, 3: 144-149.

Wessely, G., 1993. Bad Deutsch-Altenburg. In: Goldbrunner, J., Zötl, J., (Ed). Die Mineral- und Heilwässer Österreichs. Springer: 268-272.

Wynn, J.G., Sumrall, J.B., Onac, B.P., 2010. Sulfur isotopic composition and the source of dissolved sulfur species in thermo-mineral springs of the Cerna Valley, Romania. Chemical Geology, 271: 31-43.

3. MINERALOGY

3.2. Article 2

Published in the International Journal of Speleology, 47(3): 271-291,
https://doi.org/10.5038/1827-806X.47.3.2175

New insights on secondary minerals from Italian sulfuric acid caves

Ilenia Maria D'Angeli[1*], Cristina Carbone[2], Maria Nagostinis[1], Mario Parise[3], Marco Vattano[4], Giuliana Madonia[4], Jo De Waele[1]

[1] Department of Biological, Geological and Environmental Sciences, University of Bologna, Italy, dangeli.ilenia89@gmail.com; maria.nagostinis@gmail.com; jo.dewaele@unibo.it

[2] DISTAV, Department of Geological, Environmental and Biological Sciences, University of Genoa, Italy, carbone@dipteris.unige.it

[3] Department of Geological and Environmental Sciences, University of Bari Aldo Moro, Italy, mario.parise@uniba.it

[4] Department of Earth and Marine Sciences, University of Palermo, Italy, giuliana.madonia@unipa.it; marco.vattano@unipa.it

[*] Corresponding author

3.2.1. Abstract

Sulfuric acid minerals are important clues to identify the speleogenetic phases of hypogene caves. Italy hosts ~ 25% of the known worldwide sulfuric acid speleogenetic (SAS) systems, including the famous well-studied Frasassi, Monte Cucco, and Acquasanta Terme caves. Nevertheless, other underground environments have been analyzed, and interesting mineralogical assemblages were found associated with peculiar geomorphological features such as cupolas, replacement pockets, feeders, sulfuric notches, and sub-horizontal levels. In this paper, we focused on 15 cave systems located along the Apennine Chain, in Apulia, in Sicily, and in Sardinia, where copious SAS minerals were observed. Some of the studied systems (*e.g.* Porretta Terme, Capo Palinuro, Cassano allo Ionio, Cerchiara di Calabria, Santa Cesarea Terme) are still active, and mainly used as spas for human treatments. The most interesting and diversified mineralogical associations have been documented in Monte Cucco (Umbria) and Cavallone-Bove (Abruzzo) caves, in which the common gypsum is associated with alunite-jarosite minerals, but also with baryte, celestine, fluorite, and authigenic rutile-ilmenite-titanite. In addition, the core of alunite and jarosite, from these two systems, shows enriched with PO_4^{3-}, clearly suggesting hypogene hydrothermal origin.

Santa Cesarea Terme, Capo Palinuro, and Acqua Mintina caves show important native sulfur deposits, which abundantly cover walls, ceilings, and speleothems. Abundant copiapite, pickeringite, tamarugite, hexahydrate assemblages have been observed in the Calabrian systems; their association with pyrite and hematite would suggest they occurred in very acidic conditions with pH ranging between 0 and 4.

Keywords: hypogene, rising waters, Apennine Chain, mineralogy, cave sulfates

3.2.2. Introduction

Italy hosts a wide variety of karstic rocks, such as carbonates (limestone, dolostone, conglomerate), evaporites (gypsum, anhydrite, and halite) and quartzites, in which important epigenic (due to the flow of shallow meteoric waters) or hypogenic (produced by ascending deep-seated waters or by aggressive solutions formed at depth below the surface) cave systems can develop (Palmer, 2007; Palmer, 2011). Recently, the definition of hypogene processes has been rearranged, and cave speleogenesis related to "*the formation of solution-enlarged permeability structures (void-conduit systems) by upwelling fluids that recharge the cavernous zone from hydrostratigraphically lower units, where fluids originate from distant or deep sources, independent of recharge from the overlying or immediately adjacent surface*" (Klimchouk, 2017 p.3).

Upwelling fluids, along the pathway, are normally subjected to changes in pressure and temperature, causing continuous disequilibrium conditions, triggering mineral reactions and formation of macro-porosity. The combination of variable conditions result in diverse genetic types with typical void-conduit patterns (Klimchouk, 2007; 2017). A genetic subdivision has been created in accordance with the dissolutive chemistry involved in cave speleogenesis, and the principal hypogenic karst types are: sulfuric acid (SAS), hydrothermal, mixing-corrosion, and evaporite-dissolution (Klimchouk, 2017).

Here we focus on sulfuric acid speleogenetic (SAS) caves, which represent interesting systems characterized by peculiar geomorphological features due to rising flows (Palmer & Palmer, 2000; Audra, 2008; Klimchouk, 2009; Palmer, 2013; De Waele et al., 2016), secondary mineral deposits (Polyak & Provencio, 2001; Onac et al., 2009; Onac & Forti, 2011; Audra et al., 2015), and peculiar biosignatures such as stream biofilms, vermiculations, moonmilk deposits, and snottites (Summers Engel et al., 2004; Macalady et al., 2006; D'Angeli et al., 2017b). They can evolve both in confined (under pressure) and unconfined settings (Klimchouk, 2005, 2009). Their main features are linked to ascending acidic waters, that gain their aggressiveness from deep-seated sources (Hill, 1990), such as: oxidation of magmatic gases (H_2S and SO_2), assimilatory-dissimilatory (60-80°C) and/or thermochemical (100-180°C) sulfate-reduction (Canfield, 2001; Machel, 2001) of hydrocarbon and

evaporite layers, reduction of marine waters involved in deep circulation flows, and/or reduction of sulfide ore deposits through abiotic and/or microbially-mediated actions (Audra et al., 2015).

The most important mechanism of the sulfuric acid process, firstly demonstrated by Egemeier (1981), is the oxidation of H_2S into H_2SO_4 (1).

1. $H_2S + 2O_2 \rightarrow H_2SO_4$;

This acid immediately reacts with the carbonate host rock (2) producing replacement gypsum deposits and degassing CO_2, further contributing in the dissolution processes.

2. $CaCO_3 + SO_4^{2-} + 2H^+ + 2H_2O \rightarrow CaSO_4 \cdot 2H_2O + CO_2 + H_2O$;

The interaction of H_2SO_4 with the insoluble deposits inside caves produces mineral assemblages belonging to the "speleogenetic by-products" (Polyak & Provencio, 2001), that have been clearly observed in some of the best-documented examples of fossil sulfuric acid caves, such as the case of Guadalupe Mountains (New Mexico, USA) (Hill, 1990; Jagnow et al., 2000; Palmer & Palmer, 2000), which evolved in areas characterized by extremely dry weather conditions, allowing the preservation of original sulfuric acid features also after massif exhumation (Palmer & Palmer, 2000; Klimchouk et al., 2016). The speleogenetic by-products represent a consequence of: a) alteration of insoluble sediments (mostly aluminium phosphates and sulfates), b) replacement or alteration of carbonate rocks, and c) precipitation of dissolved species. They can mainly be divided (Polyak & Provencio, 2001) into "primary" (direct results of H_2SO_4), and "secondary" by-products (due to the alteration of the primary minerals or late-stage remobilization of elements). In addition, aluminium phosphate and sulfate (APS) minerals, containing rare earth elements (REE) or radioactive ones, can constitute economic deposits, and may be used as a guide for meta-bearing ore deposits (Dill, 2001). K-rich APS minerals belonging to the alunite group (alunite, natroalunite, and jarosite) are used to obtain relevant geochronological information, through K/Ar or Ar/Ar dating (Polyak et al., 1998). From an overall point of view, speleogenetic by-products are essential clues to understand the environmental conditions of cave formation.

Italy hosts ~ 25% of the known worldwide sulfuric acid caves (Galdenzi & Menichetti, 1995; De Waele et al., 2014; D'Angeli et al., 2016), located especially along the Apennine Chain, in the southeast Apulian foreland, in Sicily and in Sardinia. Generally, the H_2S source is thought to be related to the deep-seated upper Triassic evaporite unit called "*Anidriti di Burano Formation (Fm.)*" (Martinis & Pieri, 1964; Ciarapica et al., 1986) cropping out in several regions of Italy including Emilia-Romagna, Tuscany, Latium, Umbria, Marche, and Apulia.

The findings of interesting mineralogical assemblages together with the presence of peculiar geomorphological features helped in the recognition of fossil SAS caves, and the aim of this paper is to revise the previous knowledge and put in light new insights into the origin of SAS minerals.

3.2.3. Geological setting

The geological history of Italy is very complex, and characterized by two main orogenic events (Doglioni & Flores, 1997). The Alps were generated by a compression that started during the Eocene caused by the W-NW movement of the Adriatic Plate toward the Eurasian Plate. The Apennines evolved since the upper Eocene because of the slow subduction and movement of the Adriatic Plate toward the West. In Italy, sulfuric acid speleogenetic caves developed mainly along the Apennine Chain (asymmetric arc) divided into northern (E-Liguria, Emilia-Romagna, Tuscany, Marche), central (Latium, Umbria, Abruzzo, Molise), and southern (Campania, Basilicata, Calabria, Sicily), with three main forelands located in the Po Plain, Apulia, and southeastern Sicily. Generally, the stratigraphic succession is characterized by deep Caledonian-Hercynian rocks, constituting the basement, covered by terrigenous clastic and peritidal sediments (upper Carnian), followed by shallow carbonate platforms "Dolomia Principale" (upper Triassic). Subsequently, tectonic movements controlled the geological structures, producing horsts and grabens and creating several sedimentary basins. During the Triassic, red beds called "*Verrucano Fm.*" and evaporites known as the "*Anidriti di Burano Fm.*" were deposited. In the terrains of Basilicata, Calabria, and Sicily deep water conditions allowed the deposition of cherts, limestone, and marls. Due to extensional tectonics, new basins were created during the Jurassic time, in which a series of new sediments were deposited: i) radiolarites and basinal limestones typical of oceanic domain (Liguria, W-Tuscany, southern Apennines), ii) pelagic and hemipelagic carbonates of basinal domain (southern Alps, and Sicily), and iii) shallow marine carbonates (Apulia, Friuli, Latium-Abruzzo, Campania-Lucania, Sicily platforms). The deposition of limestones of the "*Maiolica Fm.*" occurred during the lower Cretaceous, while the "*Scaglia Rossa Fm.*" limestones and Rudistic facies developed during the upper Cretaceous. The above-described terrains were affected by compressive stresses due to the inversion of the relative motion between the Eurasian and Adriatic plates, that saw the later migration of thrust-belts. Paleogene shallow water carbonates (Venetian foothills, Lessini) and Messinian evaporitic rocks "*Gessoso-Solfifera Fm.*" deposited along the Apennine Chain, when the Mediterranean sea-level dropped drastically.

Italy is also characterized by volcanic activities both in the past (Ordovician, upper Carboniferous, lower Permian, Triassic) and in recent times (Vesuvius, Etna, Stromboli, Vulcano and in the Sicily channel). Petroleum and natural gas reserves have been found especially in the Po Plain, in the Adriatic Sea and along the Bradanic trough. Lignitic coals are very abundant (especially in Sardinia) with a sulfur content > 8%, whereas ore deposits are limited, except for the Paleozoic terrains of

Sardinia. Travertines are abundantly present in the central Apennines, both as actively forming and as fossil Quaternary deposits (Taddeucci et al., 1992; Minissale, 2004).

The presence of abundant karstified rocks (*Figure 21*), deep-seated Triassic evaporite deposits (at depths ranging between 600 and 2,500 m) (Martinis & Pieri, 1964), hydrocarbon reservoirs, deep faults and thrust-belts, allows the widespread occurrence of rising acidic waters containing high concentration of H_2S, CO_2 and CH_4, as testified by the presence of still-active and fossil hypogenic cave systems. Several examples of sulfuric acid speleogenetic cave systems are reported in *Figure 21*

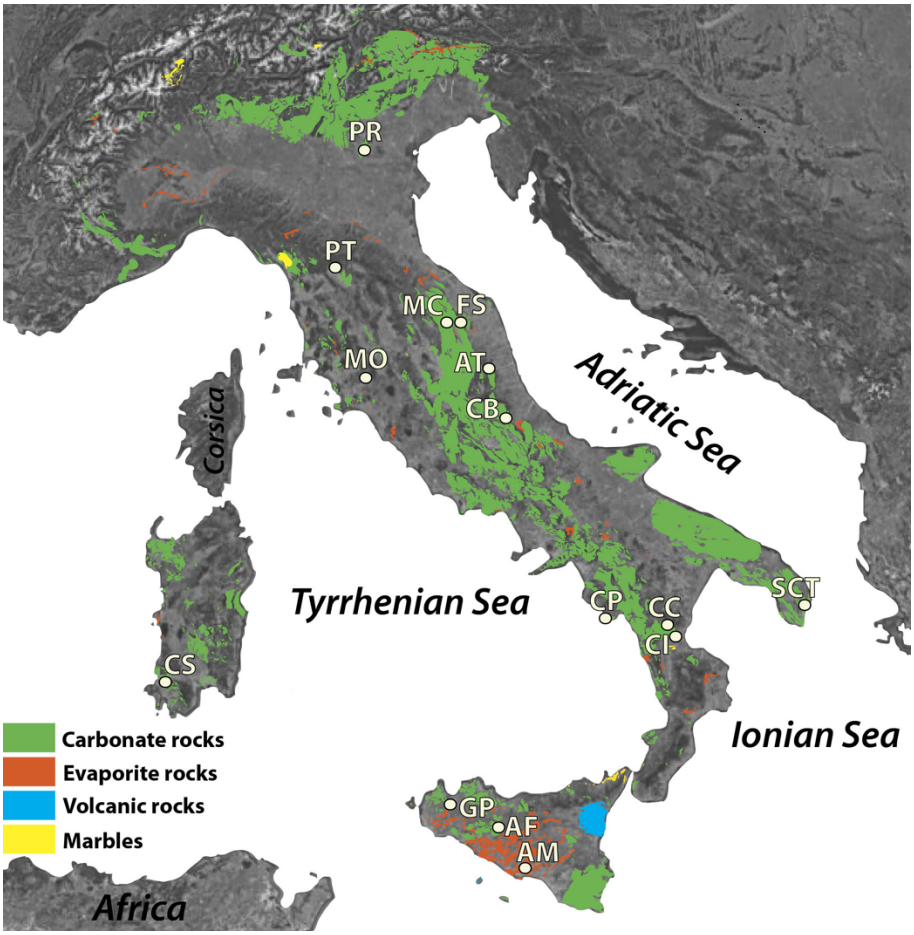

Figure 21. Location of the sulfuric acid speleogenetic (SAS) caves studied: PR (Buso della Pisatela-Rana, Veneto), PT (Porretta Terme spa, Emilia-Romagna), MC (Monte Cucco, Umbria), FS (Frasassi, Marche), AT (Acquasanta Terme, Marche), MO (Montecchio, Tuscany), CB (Cavallone-Bove, Abruzzo), CP (Capo Palinuro, Campania), CC (Cerchiara di Calabria, Calabria), CI (Cassano allo Ionio, Calabria), SCT (Santa Cesarea Terme, Apulia), GP (Grotta che Parla, Sicily), AF (Acqua Fitusa, Sicily), AM (Acqua Mintina, Sicily), CS (Corona'e sa Craba, Sardinia).

Buso della Pisatela-Rana (PR in *Figure 21*) is located in the Venetian foreland, in the Faedo-Casaron Plateau. The area is characterized by shallow water deposits with terrigenous input (calcarenites, marls, claystones) belonging to the "*Priabona Fm.*" (upper Eocene) and Castelgomberto calcarenites

(Oligocene) rich in fossils. The genesis of the cave system is related to a combination of normal epigene speleogenesis and the localized oxidation of pyrite, which induced the subsequently production of H_2SO_4 (Tisato et al., 2012).

Porretta Terme spa (PT in *Figure 21*), in the Tuscan-Emilian Apennines, opens in the "*Arenarie di Suviana*" (Oligocene) belonging to the "*Porretta Terme Fm.*". The artificial tunnels (constructed in the 19th century), similar to cave environments, host several sulfuric thermal springs and secondary mineral deposits.

Monte Cucco (MC in *Figure 21*) and Frasassi (FS in *Figure 21*) caves in the Umbro-Marche Apennines, developed in Jurassic carbonate rocks of the "*Calcare Massiccio Fm.*" (Pialli et al., 1998). They represent the most studied SAS systems of Italy (Galdenzi & Menichetti, 1995). They are huge cave systems (Monte Cucco is fossil, whereas Frasassi is still active) abundantly characterized by secondary minerals related to the interaction of the host rock with H_2SO_4.

Acquasanta Terme caves (AT in *Figure 21*) open in the carbonate rocks belonging to the "*Scaglia Rosata Fm.*" (Jurassic-Eocene), covered by Oligocene-Miocene marls and sandstone of the "*Scaglia Cinerea Fm.*" (Menichetti, 2008). Upwelling sulfuric thermal waters are still flowing through the gorge, and travertine terraces testify to a long-lasting activity. Montecchio Cave (MO in *Figure 21*), situated in southern Tuscany, evolved in massive Jurassic limestone of "*Calcare Massiccio Fm.*", and in cherty limestones of the "*Calcare selcifero di Limano*". It is composed of several sub-horizontal levels, the lower one hosting a still active sulfuric acid pool (Piccini et al., 2015).

Cavallone-Bove cave system (CB in *Figure 21*), is located in the central Apennines, in the Majella Park (Abruzzo), and opens in fossiliferous marine limestones (upper Cretaceous). The two caves (Cavallone and Bove) were part of a larger system partially dismantled by surface erosion through formation of a deep gorge, and present evident signs of sulfuric acid speleogenetic processes, including an interesting association of minerals and typical geomorphological features. The Capo Palinuro (CP in *Figure 21*) massif is located along the coast of Campania region (Tyrrhenian Sea) and is characterized by 32 submarine caves, completely or partially submerged (Canganella et al., 2007), developed in Jurassic marine limestones and dolostones. Only 13 caves show active sulfuric acid springs with elevated concentration of H_2S and temperature up to 25° C (Stüben et al., 1996). The most famous and studied cave is "Grotta Azzurra", in which the innermost part presents upwelling sulfidic waters.

Cerchiara di Calabria (CC in *Figure 21*) and Cassano allo Ionio caves (CI in *Figure 21*) are located in the southern Apennines and developed in upper Miocene biogenic calcarenites of the "*Cerchiara Fm.*" (Selli, 1957) and Triassic dark-grey dolostones (Selli, 1962), respectively. The two areas are composed of well-ramified caves both with sub-horizontal levels, and deep shafts carved by SAS

processes. The lower levels, nowadays used as spa, present a still active flow of rising thermal waters.
Santa Cesarea Terme Caves (SCT in *Figure 21*), situated in the southeastern part of the Apulian foreland, are hosted in micritic limestones and dolostones belonging to the upper Cretaceous "*Calcari d'Altamura Fm.*" (Azzaroli, 1967). The system is composed of four caves of moderate size, developed along the Adriatic coastline at present-day sea level (D'Angeli et al., 2017a). In these environments, the mixing of sulfuric acid and sea waters occurs, producing interesting morphologies due to different dissolution-corrosion processes.
Grotta che Parla Cave (GP in *Figure 21*) opens in the NE sector of Montagna Grande, a relief located close to the Calatafimi village (Western Sicily). It is a small cavity 200 m long and 25 m deep, mainly oriented NW-SE. The cave develops on two levels, which mainly follow the bedding planes with a slope of 25° toward the SE. The passages show cupolas, pillars, pendants, likely related to the sulfuric acid processes. Its entrance opens in an artificial scarp of a still active limestone quarry. The cave evolves in sequences of limestone and dolomitic limestones of *"Inici Fm."* (upper Jurassic). In this Formation a dense network of volcanic dikes filled by Jurassic deposits with Fe-Mn oxides encrustations occurred (Martire et al., 2000; Basilone, 2012).
Acqua Fitusa Cave (AF, in *Figure 21*), is placed in the eastern part of the Sicani Mountains, in San Giovanni in Gemini (Sicily). It opens in the breccia member of "*Crisanti Fm.*" (upper Cretaceous), characterized by conglomerates and calcarenites with rudists and benthic foraminifera (Catalano et al., 2013). It represents a sulfuric water table cave (De Waele et al., 2016), nowadays disconnected from the present-day spring.
Acqua Mintina Cave (AM in *Figure 21*) is situated in the southern Sicily ~7 km NW from Butera village (Caltanissetta province). It opens in the lowest layer of the "*Calcare di base Fm.*" (Miocene) in contact with the underlying Tripoli marls (Lugli et al., 2016; Vattano et al., 2017). Above the "*Calcare di Base Fm.*" there are selenitic layers belonging to the upper Gypsum Unit of the "*Pasquasia Fm.*" (Manzi et al., 2009). Acqua Mintina is a 140 m long fossil cave and the conduit size decreases inland. Its walls are copiously covered by yellowish sulfur deposits, whereas on the floor it is possible to find inactive pools filled with selenitic gypsum crystals.
Corona'e sa Craba Cave (CS in *Figure 21*) is situated in the SW part of Sardinia, develops in quartzites (Sauro et al., 2014) produced by silicification processes that involved Cambrian sediments (Padalino et al., 1973). Corona'e sa Craba is a relative large hydrothermal cave hosting an interesting association of secondary minerals (Sauro et al., 2014). As a matter of fact, the first visitors at the site were mineral collectors, searching for baryte crystals.

3.2.4. Methods

We collected mineralogical samples from Porretta Terme (PT) thermal spa in Emilia-Romagna, Monte Cucco caves (La Grotta and Faggeto Tondo) in Umbria, Cavallone-Bove system in Abruzzo, Cassano allo Ionio and Cerchiara caves in Calabria, Santa Cesarea Terme caves in Apulia, Acqua Fitusa, Acqua Mintina and Grotta che Parla caves in Sicily. The mineralogical data from Buso della Pisatela-Rana (Veneto), Montecchio (Tuscany), Frasassi (Marche), Acquasanta Terme (Marche), Capo Palinuro (Campania) and Corona'e sa Craba (Sardinia) caves came from the literature (*Table 7*). In a few cases, we integrate our results with those reported in previous works (*Table 7*).

Firstly, the samples were ground using agate mortar to obtain ultrafine powders. We analyzed 204 samples using the Philips PW3710 diffractometer (equipped with a Co tube working with the following characteristics: λ=1.78901Å, 20 mA, 40 kV, 3° to 80° 2θ with a step size of 0.02°, analysis time 1 sec per point) and 44 samples, coated with carbon, have been observed using VEGA3-TESCAN type LMU Scanning Electron Microscope provided with a EDS detector (APOLLO XSDD, EDAX) at the University of Genoa.

We recorded 55 different minerals, most strictly related to sulfuric acid processes, and other minerals unrelated to the speleogenetic by-products (such as muscovite, kaolinite, montmorillonite).

Table 7. List of the cave systems for which we used some mineralogical data from the literature

Cave systems	**Location**	**References**	**Symbol**
Buso della Pisatela-Buso della Rana	VI, Veneto	Tisato et al., 2012; Fabiani 1915	a b
Monte Cucco	PG, Umbria	Forti et al., 1989	c
Frasassi	AN, Marche	Caillère & Hénin 1963; Millot 1964; Perna 1973; Bertolani et al., 1976; Galdenzi, 1990	d e f g h
Acquasanta Terme	AP, Marche	Galdenzi & Menichetti, 1995	i
Montecchio	GR, Tuscany	Piccini et al., 2015	j
Capo Palinuro	SA, Campania	Forti & Mocchiutti, 2004	k
Cassano allo Iono	CO, Calabria	Catalano et al., 2014	l
Corona'e Sa craba	CI, Sardinia	Sauro et al., 2014	m

3.2.5. Results

All the caves reported in this paper host peculiar associations of speleogenetic by-products (Polyak & Provencio, 2001). The most common mineral is gypsum [$Ca(SO_4)\cdot 2H_2O$], abundantly present in all the investigated systems (*Table* 8*)*. It can occur in different morphologies (*Figure 22*), displaying

chandelier structures (such as in Faggeto Tondo, Santa Cesarea Terme, and Acqua Mintina caves *Figure 22*A,F,I), microcrystalline deposits (like in Cavallone-Bove and Calabrian caves *Figure 22*B,C,D), stalactites (Santa Cesarea Terme *Figure 22*E), white moonmilk deposits with a creamy appearance, and radial crystals (Santa Cesarea Terme *Figure 22*G,H). In some cases, gypsum is associated with native sulfur [S] deposits (Table 8), developed in small pockets (Faggeto Tondo Cave in *Figure 23*A), on the walls and ceilings (Acquasanta Terme, Santa Cesarea Terme, and Acqua Mintina caves in *Figure 23*B,C,F), and/or covering gypsum speleothems as in Cala Fetente Cave (*Figure 23*D,E), Capo Palinuro (Campania). In Acqua Mintina the external surface of the host rock is deeply weathered and replaced by a mineralogical assemblage of gypsum and celestine [$Sr(SO_4)$], ultimately covered by a thin coating of organic matter with dark tones, visible on the lower part of *Figure 23*F. SEM images show that sulfur deposits (EDX analysis done in the yellow dot in *Figure 24*) of Acqua Mintina Cave result intensely corroded, exhibiting linear weathered structures (*Figure 24*A) and boreholes (*Figure 24*B) on the surface. On the other hand, the sulfur deposits of Santa Cesarea Terme seem to be very porous, showing an overall powdery habit and circular voids.

SEM images (*Figure26*) show these deposits are characterized by tiny crystals, sometimes smaller than 2 μm. EDX analyses allowed us to observe that deposits are not only characterized by pure crystals made of a unique phase, but also by solid solutions of two (*Figure26*A,G) or three (*Figure26*C) mineralogical phases enriched with P (phosphorus). Alunite and jarosite crystals are, mainly, perfect microcrystalline cubes (*Figure26*B,C,E), but sometimes they have defects such as the case occurring in Figure 6 H, showing square voids on the surface of the jarosite cubes. Alunite can also be characterized by bipyramidal crystals (*Figure26*D). Rounded crystals made of solid solutions of jarosite-alunite have been observed, likely related to subsequent weathering processes (*Figure26*G). In a sample coming from Acqua Mintina, we saw tiny jarosite crystals covering quartz (*Figure26*I). Nanostar crystals of ~1 μm, have been noticed on the surface of perfect cubic alunite minerals: they are, likely, composed of gibbsite (*Figure26*E) that formed in a later stage. In the Calabrian cave systems and in Acqua Mintina Cave, we discovered interesting yellowish brown deposits made of quite rare speleogenetic by-products composed of metavoltine, copiapite, pickeringite, hexahydrate [$MgSO_4 \cdot 6H_2O$], and tamarugite (*Figure 27*).

Table 8. List of the minerals found in the SAS systems of Italy; the superscript letters (a-m) refer to the references reported in Table 7. The mineral names and formulas are reported according to the presently accepted IMA list of minerals (http://nrmima.nrm.se//imalist.htm), and sorted following the order: native elements, halides, sulfides, oxides, hydroxides, carbonates, sulfates, phosphates, silicates. Labels for caves as Figure 21.

Names	Formulas	Compounds	PR	PT	MC	FS	AT	MO	CB	CP	CC	CI	SCT	GP	AF	AM	CS
Sulfur	S	Native element	x[a]	x	x		x[i]			x[k]		x	x			x	
Fluorite	CaF_2	Halide			x												
Cinnabar	HgS	Sulfide															x[m]
Pyrite	FeS_2	Sulfide	x[a]									x[l]					
Pyrolusite	MnO_2	Oxide															x[m]
Rutile	TiO_2	Oxide			x				x			x[l]					
Hematite	Fe_2O_3	Oxide	x[a]					x[j]				x[l]					x[m]
Ilmenite	$Fe^{2+}Ti^{4+}O_3$	Oxide							x								
Magnetite	$Fe^{2+}Fe^{3+}{}_2O_4$	Oxide			x				x								
Goethite	FeO(OH)	Hydroxide	x[a]		x			x[j]	x			x[l]					x[m]
Böhmite	AlO(OH)	Hydroxide						x[j]									
Brucite	$Mn(OH)_2$	Hydroxide							x			x					
Gibbsite	$Al(OH)_3$	Hydroxide			x				x								
Todorokite	$(Na,Ca,K,Ba,Sr)_{1-n}(Mn,Mg,Al)_6O_{12}\cdot 3\text{-}4H_2O$	Hydroxide															x[m]
Calcite	$Ca(CO_3)$	Carbonates	x[a,b]		x		x[i]	x[j]	x		x	x		x	x	x	x[m]
Aragonite	$Ca(CO_3)$	Carbonates					x[i]										x[m]
Magnesite	$Mg(CO_3)$	Carbonates										x[l]					
Dolomite	$CaMg(CO_3)_2$	Carbonates	x[a,b]									x	x	x			x[m]
Thénardite	$Na_2(SO_4)$	Sulfate													x		
Celestine	$Sr(SO_4)$	Sulfate	x[a]		x[c]											x	
Baryte	$Ba(SO_4)$	Sulfate			x	x[f]						x[l]					x[m]
Hexahydrite	$Mg(SO_4)\cdot 6H_2O$	Sulfate										x				x	
Epsomite	$Mg(SO_4)\cdot 7H_2O$	Sulfate										x				x	
Gypsum	$Ca(SO_4)\cdot 2H_2O$	Sulfate	x[a]	x	x	x[h]	x[1]	x[j]	x	x	x	x	x	x	x	x	x[m]
Felsőbányaite	$Al_4(SO_4)(OH)_{10}\cdot 4H_2O$	Sulfate															x[m]
Tamarugite	$NaAl(SO_4)_2\cdot 6H_2O$	Sulfate										x					
Alum-(K)	$KAl(SO_4)_2\cdot 12H_2O$	Sulfate														x	
Pickeringite	$MgAl_2(SO_4)_4\cdot 22H_2O$	Sulfate										x					
Natroalunite	$NaAl_3(SO_4)_2(OH)_6$	Sulfate							x								x[m]
Alunite	$KAl_3(SO_4)_2(OH)_6$	Sulfate			x			x[j]	x							x	x[m]
Walthierite	$Ba_{0.5}Al_3(SO_4)_2(OH)_6$	Sulfate															x[m]
Tschermigite	$(NH_4)Al(SO_4)_2\cdot 12H_2O$	Sulfate									x					x	
Eugsterite	$Na_4Ca(SO_4)_3\cdot 2H_2O$	Sulfate													x		
Metavoltine	$K_2Na_6Fe^{2+}Fe^{3+}{}_6O_2(SO_4)_{12}\cdot 18H_2O$	Sulfate														x	
Jarosite	$KFe^{3+}{}_3(SO_4)_2(OH)_6$	Sulfate		x	x	x[d,e,g]		x[j]	x			x	x			x	
Copiapite	$Fe^{2+}Fe^{3+}{}_4(SO_4)_6(OH)_2\cdot 20H_2O$	Sulfate									x						
Berlinite?	$Al(PO_4)$	Phosphate															x[m]
Fluorapatite	$Ca_5(PO_4)_3F$	Phosphate			x												
Hydroxylapatite	$Ca_5(PO_4)_3(OH)$	Phosphate			x				x								x[m]
Leucophosphite	$KFe^{3+}{}_2(PO_4)_2(OH)\cdot 2H_2O$	Phosphate			x												
Vashegyite	$Al_{11}(PO_4)_9(OH)_6\cdot 38H_2O$	Phosphate															x[m]
Robertsite	$Ca_2Mn^{3+}{}_3O_2(PO_4)_3\cdot 3H_2O$	Phosphate															x[m]
Spheniscidite	$(NH_4)Fe^{3+}{}_2(PO_4)_2(OH)\cdot 2H_2O$	Phosphate															x[m]
Taranakite	$K_3Al_5(PO_3OH)_6(PO_4)_2\cdot 18H_2O$	Phosphate															x[m]
Goyazite	$SrAl_3(PO_4)(PO_3OH)(OH)_6$	Phosphate			x												
Quartz	SiO_2	Silicate		x	x			x[j]	x		x	x	x		x	x	x[m]
Opal	$SiO_2\cdot nH_2O$	Silicate				x[d,e,g]											
Titanite	$CaTi(SiO_4)O$	Silicate			x												
Muscovite	$KAl_2(Si_3Al)O_{10}(OH)_2$	Silicate		x					x			x					
Kaolinite	$Al_2Si_2O_5(OH)_4$	Silicate			x			x[j]	x								
Greenalite	$(Fe^{2+},Fe^{3+})_{2\text{-}3}Si_2O_5(OH)_4$	Silicate												x			
Lizardite	$Mg_3Si_2O_5(OH)_4$	Silicate															x[m]
Montmorillonite	$(Na,Ca)_{0.33}(Al,Mg)_2Si_4O_{10}(OH)_2\cdot nH_2O$	Silicate										x					
Halloysite-10Å	$Al_2Si_2O_5(OH)_4\cdot 2H_2O$	Silicate			x[c]	x[d,e,g]			x								x[m]

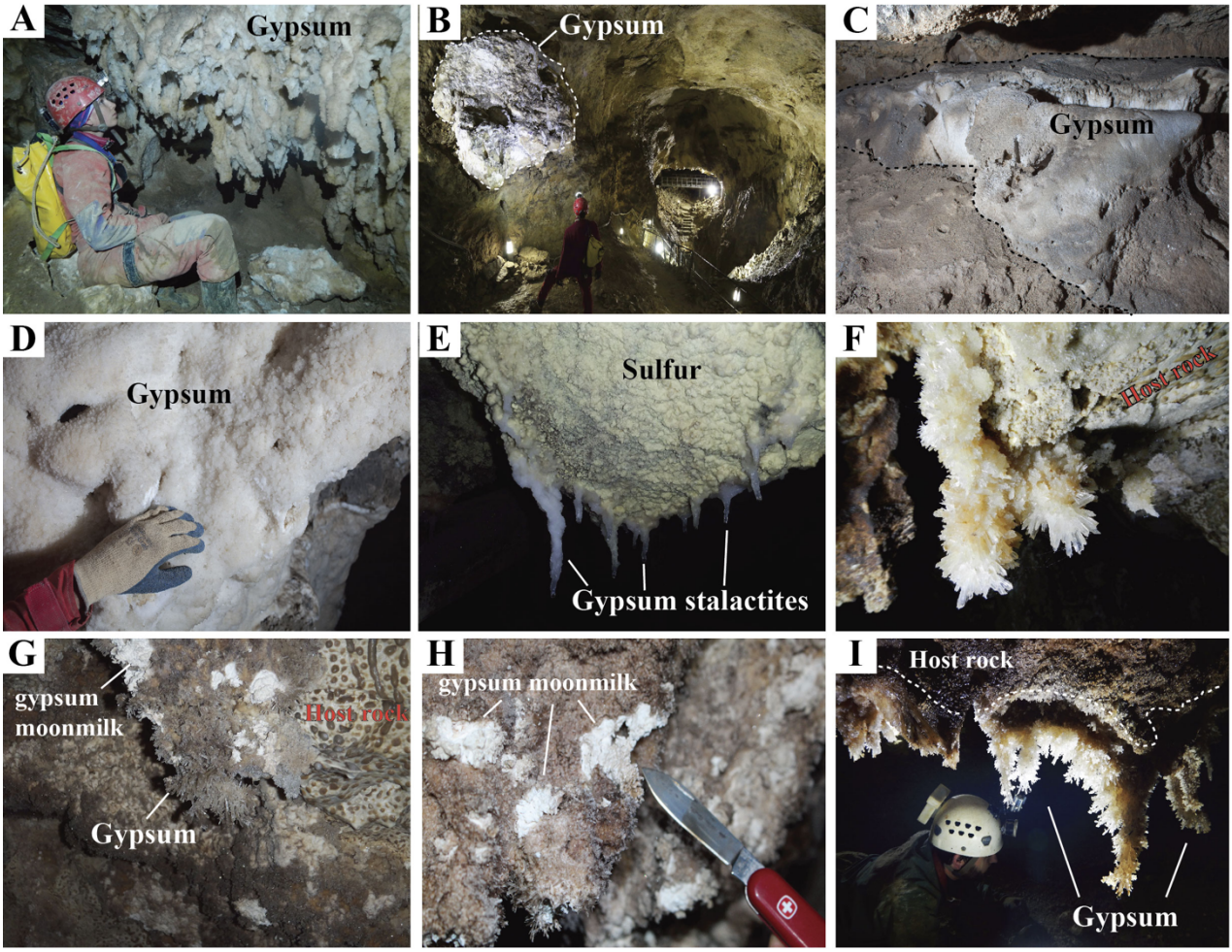

Figure 22. Gypsum deposits from several SAS caves of Italy; A) Gypsum chandeliers of Faggeto Tondo Cave, Monte Cucco, Umbria (photo J. De Waele); B) Gypsum deposits of Cavallone Cave in Abruzzo (photo G. Antonini); C) Gypsum deposits along a water table level of Gigliola Cave, Cassano allo Ionio, Calabria (photo O. Lacarbonara); D) Gypsum deposits in the lower part of Sant'Angelo Cave in Cassano allo Ionio, Calabria (photo O. Lacarbonara); E) Sulfur deposits and gypsum stalactites growing on walls and the ceiling of Gattulla Cave, in Santa Cesarea Terme, Apulia (photo M. Parise); F) Gypsum crystals growing on the host rock of Solfatara Cave, in Santa Cesarea Terme, Apulia (photo M. Vattano); G) Gypsum crystals and gypsum moonmilk growing of walls and roof of Fetida Cave, in Santa Cesarea Terme, Apulia (photo M. Parise); H) Gypsum moonmilk on the wall of Fetida Cave, Santa Cesarea Terme, Apulia (photo I.M. D'Angeli); I) Gypsum deposits growing on the ceiling of a small cave close to Acqua Mintina (photo M. Vattano).

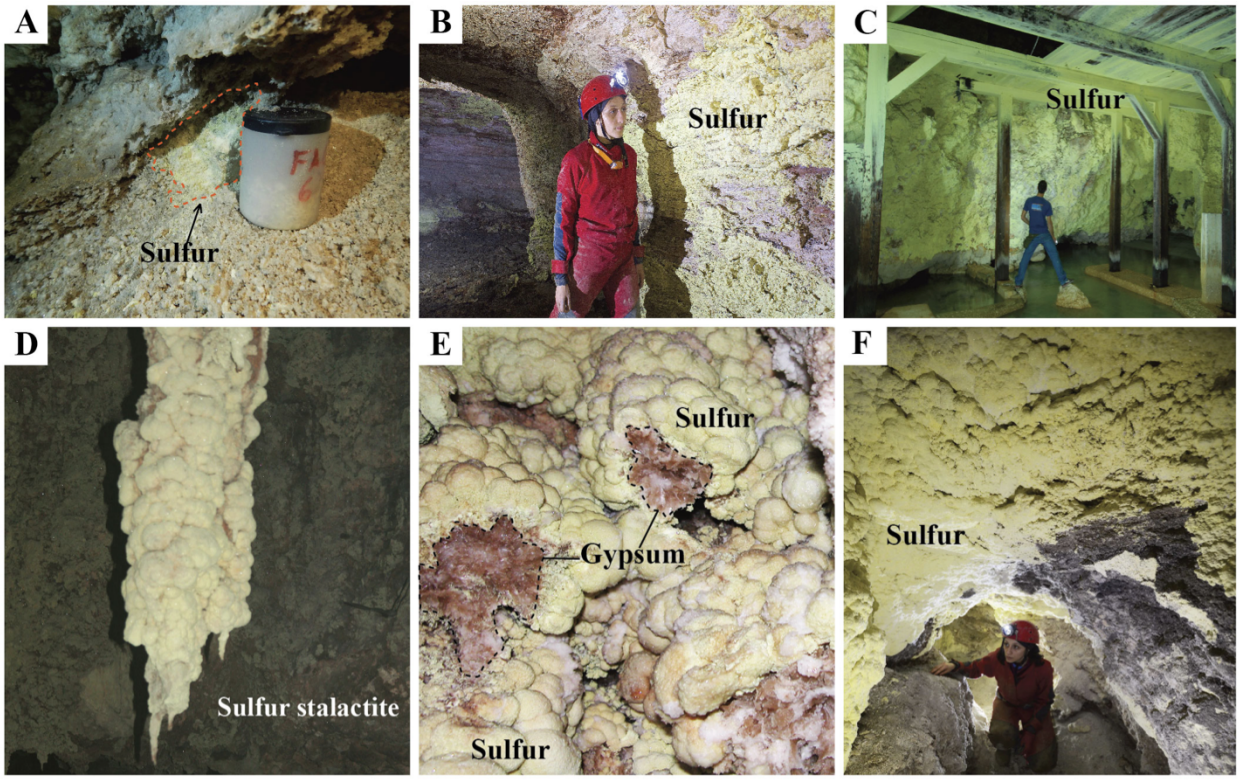

Figure 23. Sulfur deposits from several SAS caves in Italy; A) Sulfur deposited in little pockets in Faggeto Tondo Cave located in Monte Cucco (photo M. Nagostinis); B) Sulfur deposits on the walls in the lower part of Grotta Nuova, Acquasanta Terme (photo R. Simonetti); C) Sulfur covering walls and ceiling in Gattulla Cave in Santa Cesarea Terme (photo M. Vattano), D) The biggest sulfur stalactite (1.5 m long) of Cala Fetente Cave in Capo Palinuro (photo P. Forti); E) Bothryoidal sulfur deposits covering gypsum speleothems of Cala Fetente Cave in Capo Palinuro (photo P. Forti); F) Sulfur deposited on walls and ceiling of Acqua Mintina Cave (Sicily), and coating a thin layer of organic matter characterized by dark color in the lower part of the picture (photo M. Vattano).

SEM analyses allowed us to elucidate their crystal habits. Metavoltine (*Figure 27*A,D) exhibits tabular crystal with hexagonal outlines (EDX analysis carried out in the yellow dot), and developed in association with Mg sulfates (such as epsomite [$Mg(SO_4)\cdot 7H_2O$] and hexahydrate). Copiapite minerals *(Figure 27*E) are tabular with a perfect hexagonal shape and can occur together with gypsum and jarosite deposits (*Figure 24*E) or with elongated crystals of pickeringite (*Figure 27*E,F) and tabular rhombohedral hexahydrate (*Figure 27*F) (EDX analyses are shown, respectively, in the light blue and orange dot). Rutile [TiO_2], ilmenite [$Fe^{2+}Ti^{4+}O_3$], and titanite [$CaTi(SiO_4)O$] have been found, especially, in Monte Cucco and Cavallone-Bove systems (*Figure 28*A,B) and EDX analyses are shown in *Figure 29* (yellow-light blue-orange dots). SEM images (*Figure 29*A,B,C,D) point out their morphology: needle (*Figure 29*A) and rhombohedral (*Figure 29*D) crystals of rutile, and

spherical (*Figure 29*C) and rounded (*Figure 29*B) crystals of titanite have been observed. We found them in association with solid solutions of alunite-jarosite-natroalunite (*Figure 29*C), muscovite [$KAl_2(Si_3Al)O_{10}(OH)_2$] (*Figure 29*A), goyazite [$SrAl_3(PO_4)(PO_3OH)(OH)_6$] (*Figure 29*B), or baryte [$Ba(SO_4)$] (*Figure 29*D-E). The fossil branches of several systems such as La Grotta (in Monte Cucco), Frasassi, Sant'Angelo (Cassano allo Ionio), and Corona'e sa Craba caves host important baryte deposits (*Figure 28*C,D), whilst Faggeto Tondo Cave (in Monte Cucco) accommodates significant fluorite [CaF_2] deposits (*Figure 28*E,F,G,H,I). The spectrum of baryte from La Grotta (*Figure 29*, blue dot) points out the presence of Sr, likely related to a solid solution between baryte and celestine. Celestine was found also in other SAS systems like Buso della Pisatela-Rana (where it is related to allogenic volcanic sediments brought into the cave), and Acqua Mintina (*Figure 29*F), where it is authigenic. Hydroxides such as gibbsite [$Al(OH)_3$] and goethite [$FeO(OH)$] (*Figure 29*I, *Figure 30*D,E,F) together with phosphates (PO_4) have been observed and sometimes they occur on the surface of fluorites (*Figure 29*G,H,I). Interesting solid solutions of goyazite-alunite-jarosite (*Figure 30*A), hydroxylapatite-goyazite (*Figure 30*C), and nanocrystals of leucophosphite [$KFe^{3+}_2(PO_4)_2(OH)\cdot 2H_2O$] (*Figure 30*C) are common in the fossil middle branches of La Grotta (Monte Cucco system), whereas hydroxylapatite [$Ca_5(PO_4)_3(OH)$], vashegyite [$Al_{11}(PO_4)_9(OH)_6\cdot 38H_2O$], robertsite [$Ca_2Mn^{3+}_3O_2(PO_4)_3\cdot 3H_2O$], spheniscidite [$(NH_4)Fe^{3+}_2(PO_4)_2(OH)\cdot 2H_2O$], berlinite [$Al(PO_4)$], and taranakite [$K_3Al_5(PO_3OH)_6(PO_4)_2\cdot 18H_2O$] have been detected only in Corona'e Sa Craba Cave, where they are related to bat guano.

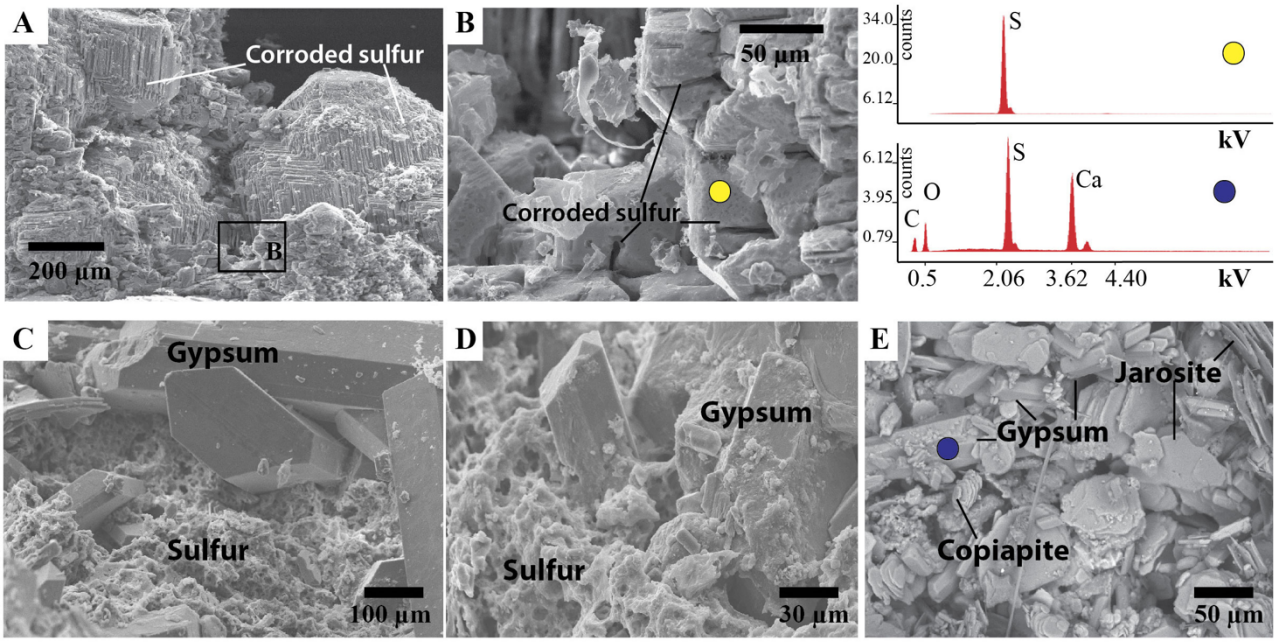

Figure 24. Sulfur and gypsum deposits observed with Scanning Electron Microscope and EDX analyses; A) Sulfur deposits from Acqua Mintina Cave (Sicily). The crystal faces are deeply corroded.

B) A higher magnification allowed us to see both lines of corrosion and interesting etching structures with rounded shapes; C) and D) The sulfur deposits of Gattulla Cave in Santa Cesarea Terme (Apulia) have a very porous structure (with circular holes). They are always associated with gypsum crystals. E) Gypsum deposits found in Ninfe Cave (Cerchiara di Calabria) are associated with laminae of jarosite and hexagonal crystals of copiapite.

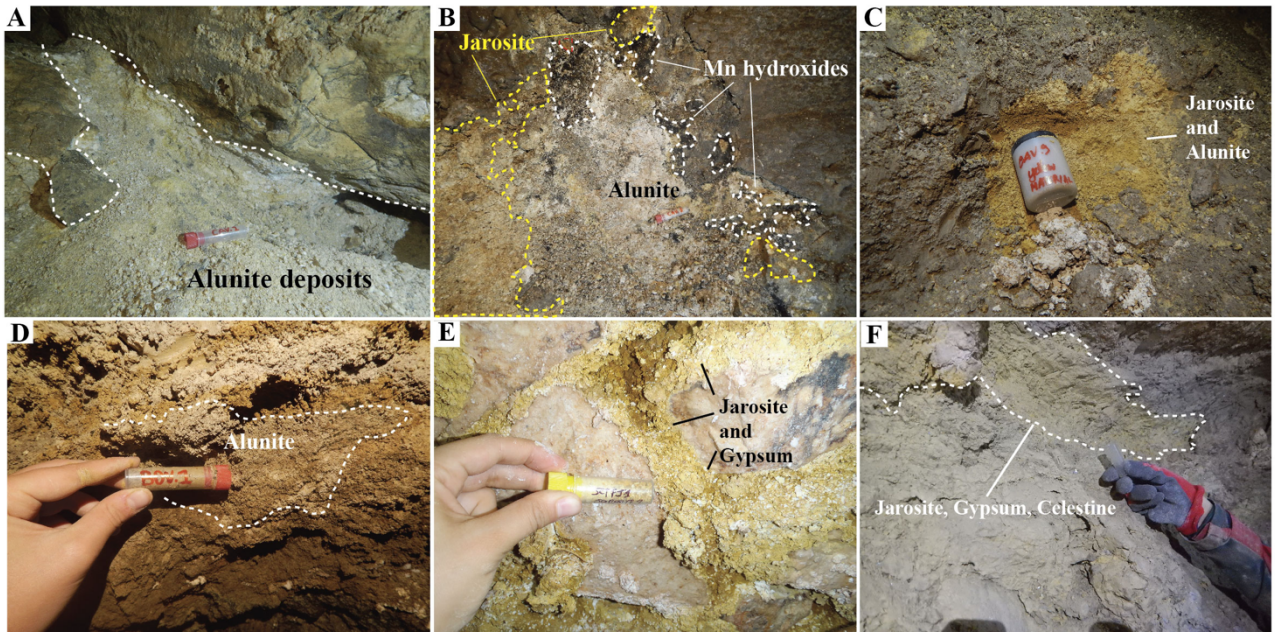

Figure 25. Appearance of alunite and jarosite deposits; A) Whitish deposits located in Cavallone Cave, Abruzzo. They are dominated by alunite minerals, with a minor amount of jarosite, brucite and quartz minerals (photo M. Nagostinis); B) Deposits with different colors in the innermost part of Cavallone Cave, Abruzzo. The dark materials are made of Mn hydroxide, silicates and alunite, the brownish sediments of alunite and jarosite, while the greyish ones are characterized by alunite and natroalunite minerals (photo M. Nagostinis); C) Brownish deposits in Cavallone Cave, Abruzzo. They are composed of jarosite, alunite and 10% of muscovite minerals (photo M. Nagostinis); D) Light brown deposits in Bove Cave, Abruzzo, made of alunite, quartz, muscovite and magnesite minerals (photo M. Nagostinis); E) Jarosite and gypsum deposits found in Fetida Cave, Santa Cesarea Terme, Apulia (photo I.M. D'Angeli); F) Grey-yellowish deposits located in Acqua Mintina Cave, Sicily. They are characterized by jarosite, gypsum, celestine and quartz minerals (photo M. Vattano).

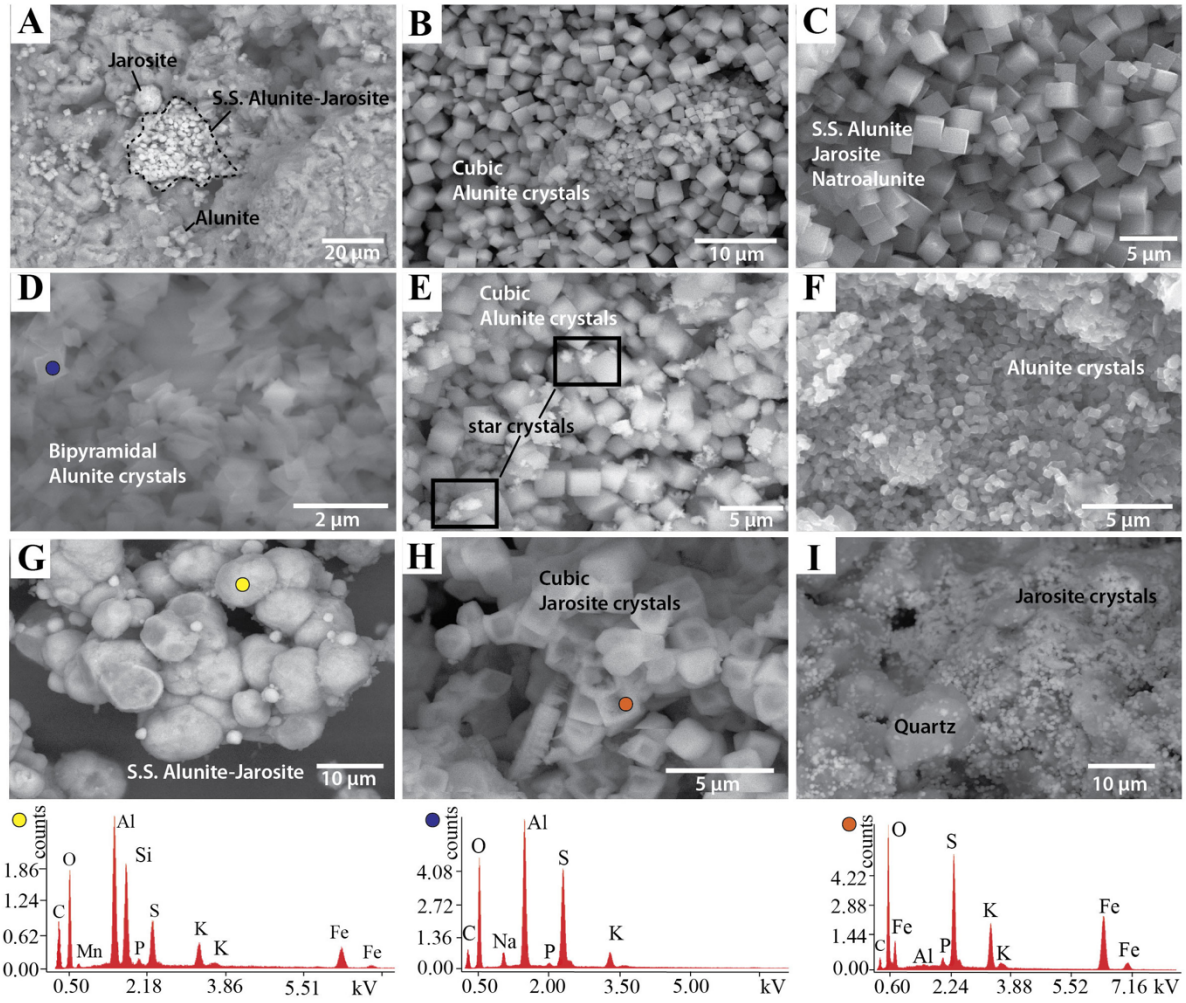

Figure 26. Alunite and jarosite deposits observed with SEM and some EDX analyses; A) Cubic alunite minerals are found together with pure jarosite crystals and solid solution (S.S.) of alunite-jarosite, Cavallone Cave, Abruzzo; B) Pure alunite crystals with a perfect cubic shape have been observed in Cavallone Cave, Abruzzo; C) Cubic crystals, characterized by a solid solution of alunite-jarosite-natroalunite, have been observed in Bove Cave, Abruzzo; D) Bipyramidal crystals of alunite are present in Cavallone Cave, Abruzzo. The blue dot represents the site of EDX analysis shown in the lower part of the figure; E) Sometimes, the cubic crystals of alunite are covered by star-shaped crystals (dark squares), probably made of gibbsite; F) Small crystals of alunite in Cavallone Cave, Abruzzo; G) Rounded and degraded crystals composed of a solid solution (S.S.) of alunite-jarosite, likely related to secondary weathering processes, found in Cavallone Cave, Abruzzo. The EDX analysis of the yellow dot shows the presence of an important amount of Si, likely related to clay minerals; H) Cubic crystals of jarosite, showing a peculiar defect of crystallization, Bove Cave, Abruzzo. The EDX analysis in the orange dot shows an almost pure jarosite composition; I) Small crystal of jarosite covering quartz minerals, Acqua Mintina Cave, Sicily. The carbon peak is related to the coating used to analyzed the samples under SEM microscope.

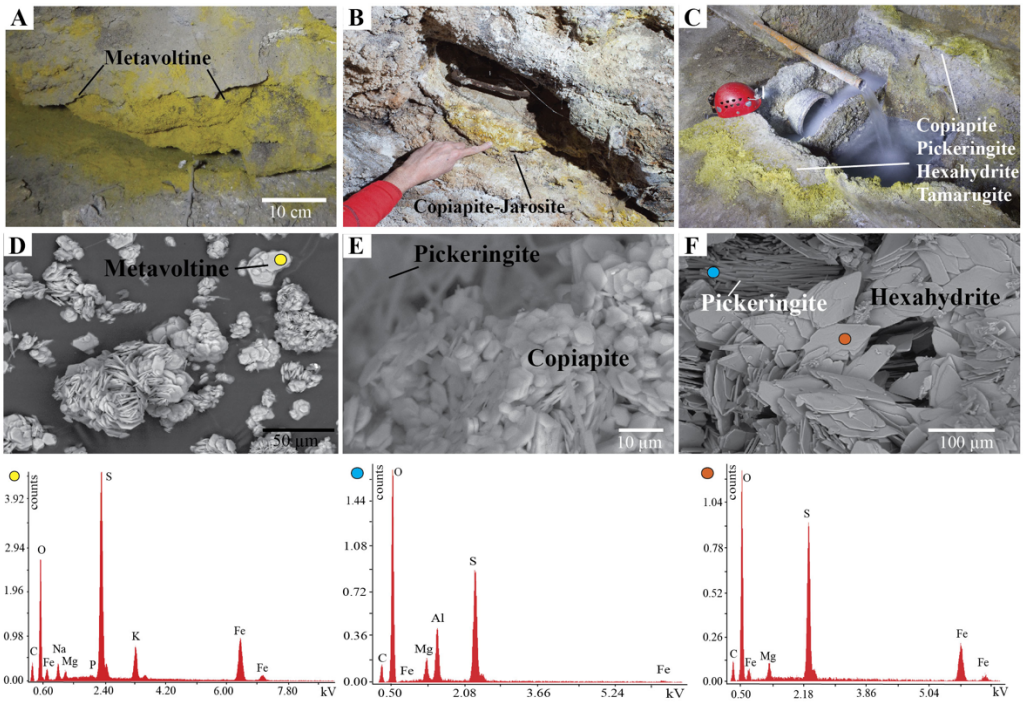

Figure 27. Yellowish deposits found in some SAS cave of Italy and SEM-EDX analysis; A) Metavoltine-hexahydrite deposits, in Acqua Mintina Cave, Sicily (photo I.M. D'Angeli); B) Copiapite-jarosite deposits found in the spring of Ninfe Cave, Cerchiara di Calabria (photo O. Lacarbonara); C) Copiapite-pickeringite-hexahydrite-tamarugite deposits observed in Terme Sibaryte Spring, Cassano allo Ionio, Calabria (photo O. Lacarbonara); D) Laminae of metavoltine minerals (the yellow dot represents the site of EDX analysis); E) Hexagonal laminae of copiapite, in the background it is possible to see elongated crystals of pickeringite; F) Pickeringite crystals (site of EDX analysis in the light blue dot), and hexahydrate minerals (EDX analysis in the orange dot). The carbon peak is related to the coating used to analyzed the samples under SEM microscope.

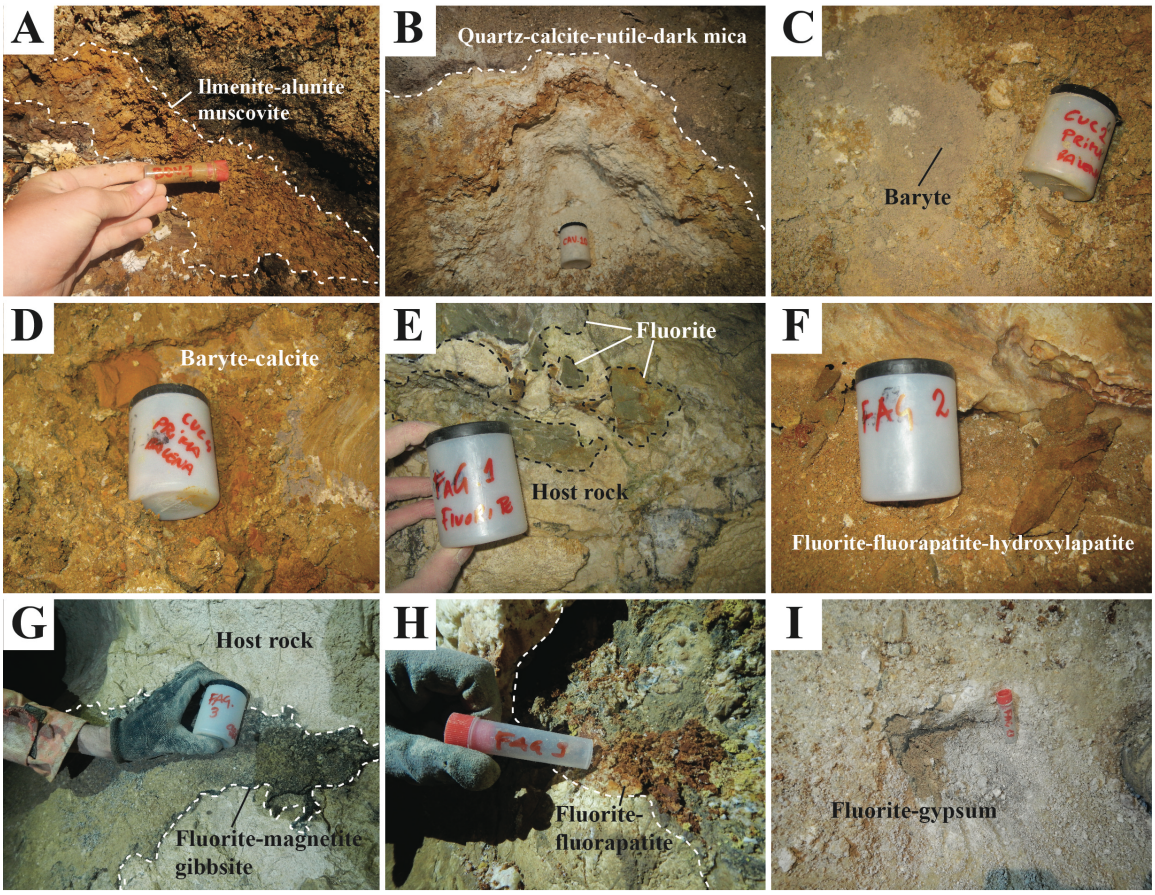

Figure 28. Appearance of deposits containing ilmenite, rutile, baryte, fluorite, flourapatite minerals. A) Reddish-brown deposit characterized by ilmenite, alunite and muscovite, located in Cavallone-Bove system (photo M. Nagostinis); B) Grey-browinsh deposit containing rutile minerals, in Cavallone-Bove system (photo M. Nagostinis); C) Greyish deposits of baryte, in the deepest part of La Grotta, Monte Cucco (photo J. De Waele); D) Orange-yellowish deposits characterized by baryte and calcite, in the deepest part of La Grotta, Monte Cucco (photo J. De Waele); E) Green-greyish fluorite deposits in contact with the carbonate host rock, in the upper part of Faggeto Tondo, Monte Cucco system (photo J. De Waele); F) Orange-brownish deposits made of fluorite-flourapatite and hydroxylapatite, in Faggeto Tondo, Umbria (photo J. De Waele); G) Weathered fluorite, gibbsite and magnetite deposits in contact with the host rock (limestones), in Faggeto Tondo Cave, Umbria (photo M. Nagostinis); H) Brownish deposits made of fluorite and flourapatite, in the middle part of Faggeto Tondo, Umbria (photo M. Nagostinis); I) Whitish fluorite and gypsum, in the middle-lower part of Faggeto Tondo, Umbria (photo M. Nagostinis).

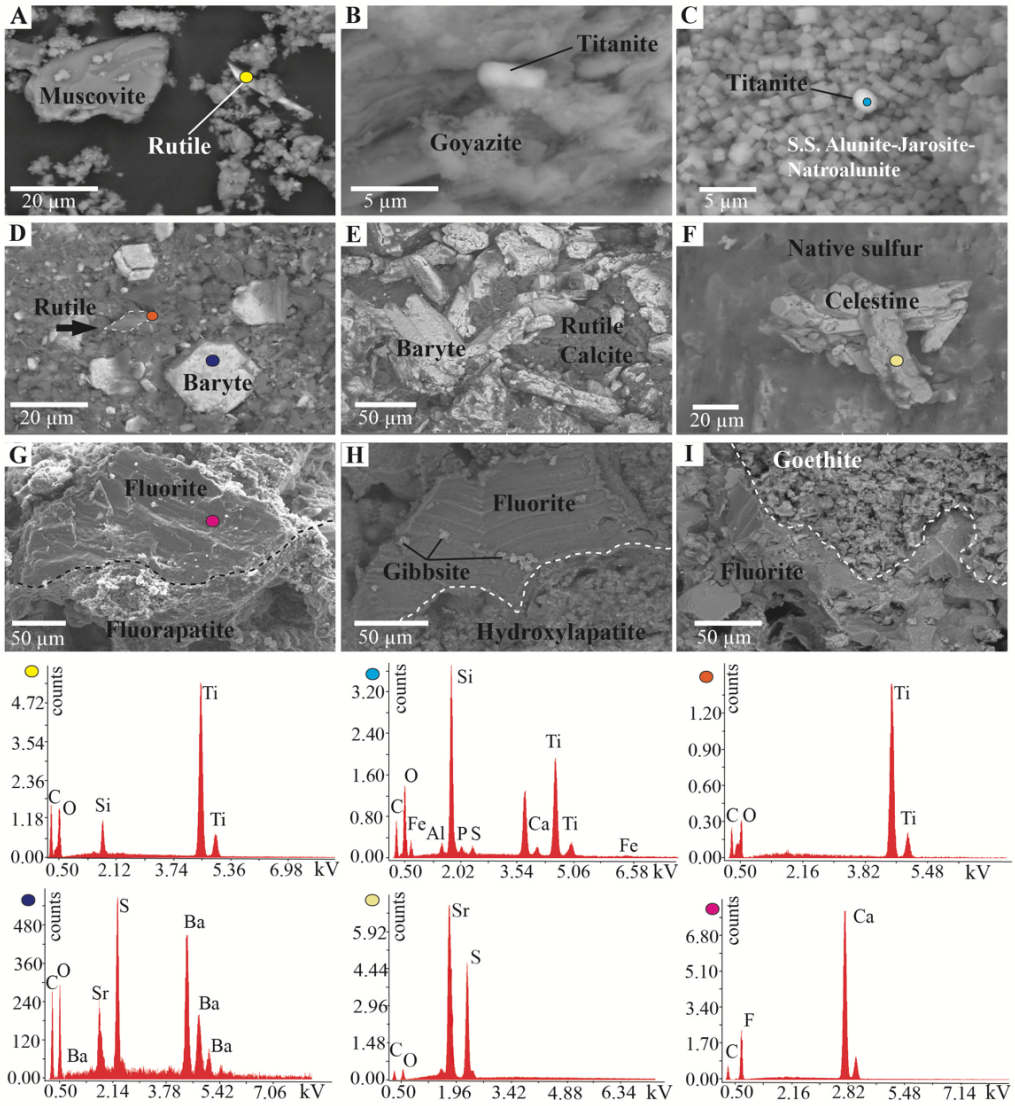

Figure 29. SEM and EDX analyses of the deposits reported in Fig. 8 A) The SEM image shows an elongated rutile crystal found in Cavallone-Bove system, Abruzzo (EDX analysis in the yellow dot); B) Rounded crystal of titanite found in the middle branches of La Grotta, Monte Cucco, Umbria; C) Sphere of titanite, while the background is dominated by a solid solution of alunite-jarosite, La Grotta, Monte Cucco, Umbria (EDX analysis in the light blue dot); D) The image shows an assemblage of rhombohedral rutile and baryte crystals found in the lower branches of La Grotta, Monte Cucco, Umbria (EDX analysis of rutile and baryte in the orange and blue dots); E) Baryte deposits associated with dark micas, found in the lower branches of La Grotta, Monte Cucco, Umbria; F) Celestine found in Acqua Mintina Cave, Sicily (EDX analysis in the beige dot); G) Cubic fluorite surrounded by flourapatite and hydroxylapatite microcrystalline deposits due to weathering, in the upper part of Faggeto Tondo Cave, Monte Cucco, Umbria (EDX analysis in the magenta dot); H) Fluorite covered by hydroxylapatite and gibbsite, due to weathering processes, Faggeto Tondo Cave, Umbria; I) Fluorite in association with goethite, found in the lower branches of Faggeto Tondo

Cave, Umbria. The carbon peak is related to the coating used to analyzed the samples under SEM microscope.

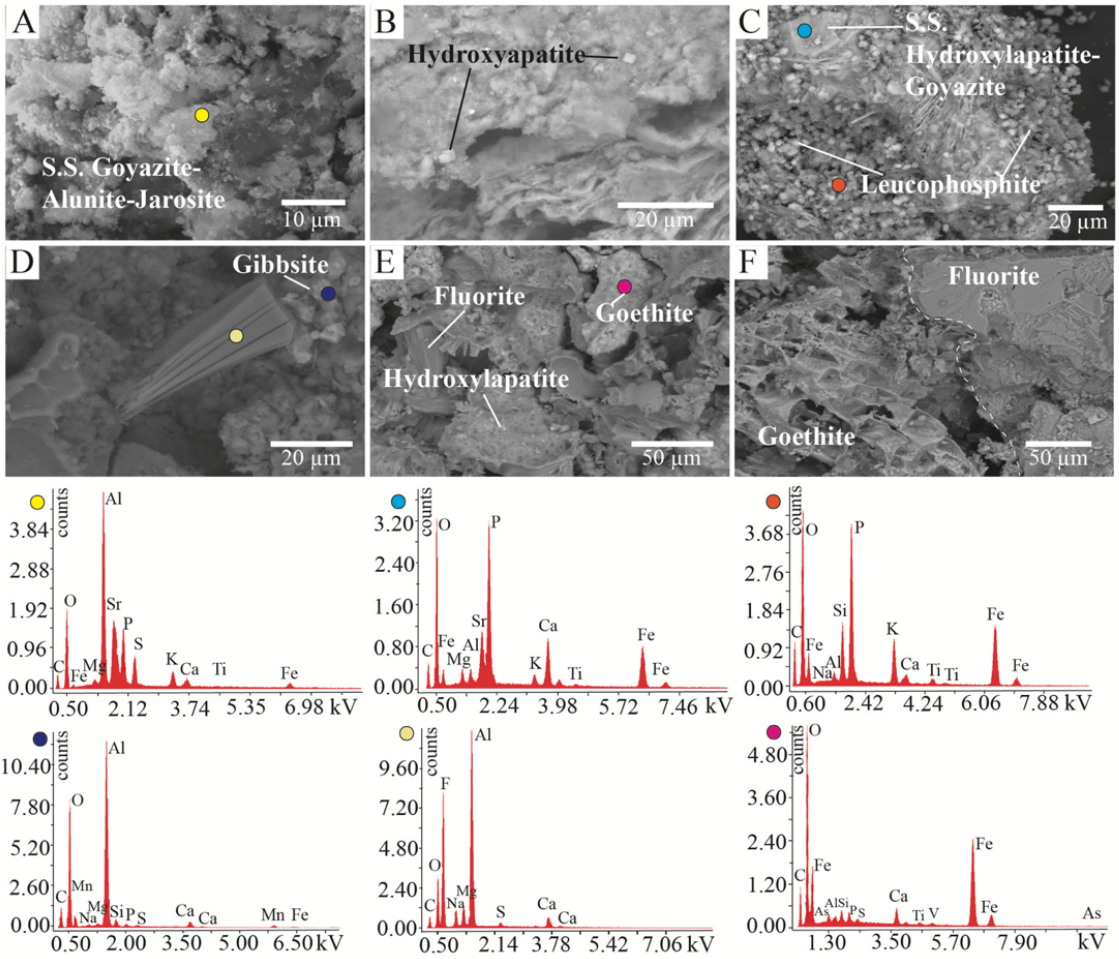

Figure 30. SEM and EDX analyses of phosphates, aluminum-phosphates and hydroxides of Al and Fe. A) It is possible to see the appearance of a solid solution of goyazite-alunite-jarosite, found in the middle galleries of La Grotta, Umbria (EDX analysis is reported in the yellow dot); B) Cubic hydroxylapatite crystals found in association with goyazite and alunite-jarosite, La Grotta, Monte Cucco; C) The picture shows an assemblage of hydroxylapatite-goyazite solid solution (light blue dot) and leucophosphite (orange dot), La Grotta, Umbria; D) Gibbsite associated with fluorite (EDX in the dark blue dot). A laminated mineral made of Al, F and O, is visible (EDX in the beige dot); E) Goethite (EDX in magenta dot) is also present in association with hydroxylapatite and fluorite crystals in La Grotta, Monte Cucco, Umbria. From the EDX of goethite it is possible to observe elements such as As, V, Ti; F) The picture shows the association of fluorite and goethite in more detail. The carbon peak is related to the coating used to analyzed the samples under SEM microscope.

3.2.6. Discussion

As observed in all the Italian sulfuric acid caves, gypsum is the most common secondary mineral, derived from the immediate reaction between H_2SO_4 and the carbonate host rock (see reaction 2), a process well-explained by Egemeier (1981). Abundant gypsum deposits have been found in several famous sulfuric acid caves including Carlsbad Cavern and Lechuguilla in New Mexico (Hill, 1995), Cueva de Villa Luz in Tabasco, Mexico (Hose et al., 2000), Grotte du Chat in France (Audra, 2007; De Waele et al., 2016), Kraushöhle in Austria (Plan et al., 2012), and Movile and Cerna Valley in Romania (Sarbu et al., 1994; Galdenzi, 2001; Onac et al., 2011). Several modes of gypsum precipitation have been described causing, for instance, different structures of cave gypsum deposits, depending on the genetic environment. Buck et al. (1994) classified them in: 1) subaqueous replacement crusts, 2) subaqueous sediments, 3) subaerial replacement crusts, 4) subaerial replacement crust breccias, and 5) evaporitic crusts. In *Figure 22*A,E,F,I we observed several examples of evaporitic speleothems formed in sub-aerial environments and similar to the ones described by Davis (2000). In *Figure 22*E gypsum-like-stalactites that lack the central feeding channels are presented, whilst the speleothems in *Figure 22*A,F,I seem to be tiny chandelier stalactites. Their formation is related to airflow convection that leads to several condensation/evaporation cycles (Davis, 2000), inducing the dissolution-corrosion of carbonate rock and, subsequently, its replacement by gypsum materials.

In *Figure 22*B and C it is possible to observe subaqueous replacement crusts located in inactive SAS caves, as Cavallone Cave (*Figure 22*B) in Abruzzo, and Gigliola Cave (*Figure 22*C) in Calabria. They developed parallel to ceilings and walls, but they are currently occurring as collapsed blocks with well-altered external surface characterized by vertical holes caused by active dripping. In *Figure 22*D, there are sub-aerial replacement crusts in the fossil SAS cave called Sant'Angelo (Calabria), and nowadays they are subjected to secondary sub-aerial weathering. *Figure 22*G,H display sub-aerial gypsum deposits made of creamy moonmilk with a microcrystalline structure and macrocrystalline euhedral needles growing in a still active cave in Apulia (Fetida cave at Santa Cesarea Terme). The genesis of such gypsum moonmilk deposits seems to be related to interesting acidophilic communities of archaea and bacteria, and deserves further studies. They thrive only in the innermost part of the Fetida Cave, where H_2S contained in the upwelling waters, reaching the atmosphere, degasses and produces intense condensation-corrosion processes, inducing the dissolution of the carbonate host rock and precipitation of newly formed gypsum minerals.

Gypsum moonmilk deposits have been described in other SAS systems around the world, and especially, in wet environments or where the aggressivity of H_2SO_4 is strong enough, such as in Lower Kane Cave in Wyoming (Egemeier, 1981), Guadalupe Mountains in New Mexico (Buck et

al., 1994), Cocalière Cave in France, but also in Faggeto Tondo and Fiume-Vento Caves in Central Italy (Cucchi & Forti, 1988; Forti et al., 1989), and recently in Grotta Bella and Ramo Sulfureo in Frasassi Cave (Mansor et al., 2018).

Sulfur deposits have been found in several locations (*Table 8*), but they are, really, abundant only in a few Italian cave systems such as: Capo Palinuro (CP), Santa Cesarea Terme (SCT), and Acqua Mintina (AM). They occur in the areas where the sulfuric waters reach the surface producing intense H_2S exhalations. As demonstrated by Forti & Mocchiutti (2004), the sulfur cannot deposit directly on carbonate rock (because of its buffering capacity). In Cala Fetente (*Figure 23*D,E), it has been observed that sulfur starts to grow on gypsum minerals only when the concentration of H_2SO_4 rapidly increases, whilst Ca^{2+} (related to carbonate dissolution) decreases (Forti & Mocchiutti, 2004). In Santa Cesarea Terme (*Figure 23*C), as in Cala Fetente, sulfur developed on top of gypsum, completely covering cave walls and man-made wooden structures. Otherwise, in Acqua Mintina Cave (Sicily), sulfur grows (*Figure 23*F) on a dark material characterized by organic matter, at the external weathered rock-surface characterized by gypsum and celestine, as a result of carbonate replacement. Generally, the observed sulfur deposits are more than 1 cm thick and present a fine lamination as in the case of Santa Cesarea Terme (D'Angeli et al., 2017a). Well-developed sulfur folia have been described by Lugli et al. (2016) in Acqua Mintina Cave.

As shown in *Figure 24*, sulfur minerals exhibit linear corrosive structures (*Figure 24*A,B), microscopic boreholes (*Figure 24*C), porous and powdery habits (*Figure 24*C,D). Sometimes it is possible to see filaments, likely related to biological activity (D'Angeli et al., 2017a). As a matter of fact, in Santa Cesarea Terme, a still active sulfuric acid system, we found and collected interesting biological substances including creamy white moonmilk deposits, vermiculations, and white substances floating on the water surface close to the spots where fluids are upwelling (D'Angeli et al., 2017b). The role of sulfur-oxidizing and sulfur-reducing microorganisms has been demonstrated to be important in the sulfur cycle (Hill, 1992, 1995; Canfield, 2001, Mansor et al., 2018). It is well known that "purple sulfur bacteria" such as Chromatiales (Chromatiaceae and Ectothiorhodospiraceae) can use sulfide as sole electron donor and precipitate elemental sulfur inside or outside the cells, during oxidation (Imhoff, 2006). Intracellular storage of elemental sulfur (Angert et al., 1998) allows their endogenous respiration under dark and oxidative conditions (cave environment), whilst it can be used as an electron acceptor during endogenous fermentation of carbohydrates (Imhoff, 2006 and references therein) in dark anoxic (deep-seated) environments.

Significant baryte deposits have been described in Monte Cucco (Forti et al., 1989), Frasassi (Perna, 1973), Cassano allo Ionio (Catalano et al., 2014), and Corona'e Sa Craba (Sauro et al., 2014).

In Monte Cucco cave system baryte occurs in association with fluorite. This paragenesis might invoke Mississippi Valley-type ore deposition, formed during large-scale orogenic events (Hanor, 2000). As demonstrated by Barbieri et al. (1982) the interaction between Ba-bearing (>7,000 ppm) deep fluids in contact with phyllites of the basement (Ba exists in solid solutions with K in minerals like K-feldspar and K-micas) and deep-seated Triassic evaporites allowed the deposition of baryte minerals in Tuscany.

Barium can precipitate only in limited conditions, such as >10 ppm of Ba content, high salinity ranges (10,000-30,000 ppm), <200 ppm of sulfates, otherwise the Ca-sulfate precipitation is favored (Hanor, 2000 and references therein). In SO_4-rich environments, Ba can be mobilized, as barium chloride, only in highly reducing conditions, when sulfates are completely reduced (Hanor, 2000; Sauro et al., 2014). Instead, celestine might be deposited when fluids with an extremely high Sr/Ba content (in condition of high salinity, high SO_4^{2-}, and low Ba^{2+} concentration) reacted with evaporite-carbonate rocks. The most famous occurrence of celestine deposits in cave, as described by Wright (1898) and reported in Hill & Forti (1997), occurs in Crystal Cave (Put-in-Bay, Ohio), but other celestine deposits associated with gypsum have been described in Cumberland Caverns (Tennessee), Flint-Mammoth Caves (Kentucky) and Carlsbad Cavern (New Mexico) (Hill, 1981; Hill 1987).

Celestine, in the Italian SAS caves, has been observed, especially, in the Buso della Pisatela-Rana (Tisato et al., 2012) as inclusion in volcanic allogenic pebbles, in Acqua Mintina strictly associated with carbonate host rock and gypsum deposits, and in Monte Cucco system (Forti et al., 1989) in assemblage with baryte deposits. In Acqua Mintina, celestine likely deposited when SO_4 and Sr-rich fluids, related to sulfuric acid processes, interacted with the host rock, inducing the precipitation of $SrSO_4$ and gypsum as replacement of carbonate. SEM observations on some samples of baryte from La Grotta (Monte Cucco) show minerals with perfect crystalline habits (*Figure 29*D), indicating that they formed in situ. In fact, baryte is highly resistant in oxidizing environments, and the interaction with sulfuric acid waters, enhancing dissolution-corrosion of carbonate rocks, aids in stabilizing its crystallization. Nevertheless, as visible from EDX analysis (in the blue dot of *Figure 29*), baryte is enriched in Sr, indicating a solid solution between baryte-celestine. Complete solid solutions between $Ba(SO_4)$ and $Sr(SO_4)$ occur due to the similarity of their ionic radii (1.16 and 1.36 Å for Sr and Ba, respectively); moreover, the incorporation of Sr^{2+} into baryte is facilitated at room temperature (Hanor, 2000). This occurrence would suggest the replacement of early baryte with Sr-rich baryte might have happened when the temperature of the mother-solution was close to room temperature, and the concentration of sulfate was too low to precipitate $Ca(SO_4)\cdot 2H_2O$. The rising acidic waters, involved in the sulfuric acid speleogenesis are normally aggressive toward carbonates, and the dissolution of the host rock, due to sulfuric acid, might have increased the concentration of Sr^{2+} (stable

in saline and high SO_4^{2-} habitat) and the possibility of a secondary substitution of Ba^{2+} (in baryte) with Sr^{2+}. In addition, baryte (*Figure 28*C,D) and fluorite (*Figure 28*E,F,G,H,I) deposits of Monte Cucco systems exhibit an altered appearance with rusty colors. Fluorite (*Figure 29*G) sometimes occurs as perfect cubes with weathered surfaces covered by flourapatite [$Ca_5(PO_4)_3F$]-hydroxylapatite [$Ca_5(PO_4)_3(OH)$] (*Figure 29*G), gibbsite (*Figure 29*H) and/or goethite (*Figure 29*I). The spectrum of goethite, grown in contact with fluorite (*Figure 30* dot in magenta color), is enriched with peculiar trace elements such as As and V.

Baryte and fluorite deposits have been observed in Luceram Cave (French Alps), and its association with vanadium and uranium materials has been found in Khaidarkan and Ferghana caves (Kirghizistan) and in some thermal springs in Hungary (Hill & Forti, 1997). They are thought to be deposited from hydrothermal fluids with temperature >150-180°C.

As suggested by Williams-Jones et al. (2000) fluorite can form when hydrothermal fluids (400°C characterized by sulfate-rich NaCl-KCl brines) meet CO_2-bearing and sulfate-poor NaCl brines of external origin. The mixing between REE-fluoride-bearing fluids and Ca-carbonate-bearing fluids (or the interaction with carbonate rocks) is an important control of REE-fluorocarbon mineral deposition (Williams-Jones et al., 2000).

Monte Cucco cave system also hosts magnetite [$Fe^{2+}Fe^{3+}{}_2O_4$]. The stability of baryte-magnetite occurs in limited conditions characterized by pH ranging between 10-12 and log f_{O2} -57, suggesting that magnetite, probably, precipitated in deep-seated conditions and reached the cave environment through the ascending flows.

Interesting is the association of baryte, pyrite [FeS_2], and hematite [Fe_2O_3] observed in Sant'Angelo Cave (Cassano allo Ionio) typical of pH ranging between 0 and 4 and highly oxidizing conditions (log f_{O2} between -52 and -47) (Hanor, 2000 and references therein), whereas in Corona'e sa Craba the study of fluid inclusions found in baryte suggests their deposition at a temperature lower than 50°C, only when the rising reducing fluid became more oxidative (Sauro et al., 2014).

Of significant interest are the assemblages of titanite-rutile crystals in Monte Cucco and rutile-ilmenite in Cavallone-Bove caves, shown in *Table 8*. The solubility of titanium is very low, and if transported by water flows, it occurs as a solid phase. Nevertheless, Ti can be found in the ionic form due to highly exothermic reactions linked to acid digestion (HNO_3 and/or H_2SO_4) (Westerhoff et al., 2011). The important role of sulfur in some replacement reactions has also been described by Tracy & Robinson (1988) and Henry & Guidotti (2002). The breakdown of muscovite flakes releases Fe, Si, Al, and K necessary to the growth of dark micas [$K(Mg,Fe^{2+})_3\ AlSi_3(OH,F)_2$] within ilmenite deposits (Carswell & O'Brien, 1993; Angiboust & Harlov, 2017). Titanium ions can precipitate as: 1) spheres of TiO_2, 2) aluminosilicates with a flaky appearance (with absorbed surface iron and/or in

association with kaolinite deposits), and 3) mixed environmental silicates without aluminum. In *Figure 29*, several crystalline morphologies for rutile (*Figure 29*A,D) and titanite (*Figure 29*B,C) have been pointed out, suggesting that titanium was in solution and not only transported as particles by the slowly rising fluid. Rutile shows needle crystals (*Figure 29*A) and perfect rhombohedral structure (*Figure 29*D), whereas titanite has rounded (*Figure 29*B) to spherical appearances.

Rising waters, enriched in H_2S, can also produce an extensive suite of insoluble pH/Eh-dependent hydroxysulfates and oxyhydroxides (Carbone et al., 2013) and APS materials of significant value for extractive and environmental geology (Dill, 2001). Fe-rich waters precipitate yellow-to red-to brown materials, whereas Al-rich fluids form milky-white precipitates (Bigham & Nordstrom, 2000; Carbone et al., 2013). Acidity (pH) is one of the most significant limiting factors in sulfuric-acid solutions, being Fe and Al pH-dependent (Tombácz et al., 2000). Generally, Al^{3+} is stable in quite acid conditions (pH <5), and the conservative solute transport values for Fe^{3+} are limited in comparison to the species Fe^{2+}. In fact, Fe^{3+} is stable at very low pH (< 1) and Eh ranging between 0.8 and 1.8, while Fe^{2+}, depending on the potential values (-0.4 to 0.8), starts to precipitate from very acidic (pH <1) to neutral (pH =7) conditions. In non-sulfuric-acid conditions Fe and Al oxides, hydroxides, and oxyhydroxides typically occur at pH ranging between 5 and 9 (Stumm, 1992). The presence of dissolved SO_4^{2-} in water changes the conservative solute transport threshold, inducing a drop of pH value (<4.5) and decreasing the areas of stability for Al^{3+}, Fe^{3+} and Fe^{2+}. In this circumstance, Al^{3+} can stay in solution at pH <4.5, whilst the solubility of Fe species is controlled by jarosite and goethite precipitation (Bigham & Nordstrom, 2000).

Commonly, Al-rich sulfates precipitate separately from Fe-rich ones. Even if present in the same deposits, alunite and jarosite rarely belong to the same event (Rye et al., 1993; Stoffregen, 1993). Minerals belonging to the jarosite group normally form at pH <2.5, alunite precipitates at pH values of 3-4, and ferrihydrite [$(Fe^{3+}_{10}O_{14}(OH)_2$] (Kulp et al., 2009) with microcrystalline gibbsite at pH ranging from 6-8. (Bigham & Nordstrom, 2000).

Alunite, natroalunite, and jarosite deposits have been described in several famous SAS systems around the world (Palmer & Palmer, 1992; Polyak & Güven, 2000; Polyak & Provencio, 2001). Table 2 shows that the most abundant hydroxysulfate, in Italian SAS systems, is jarosite. Jarosite formation, generally, requires more extreme acidity and oxidizing conditions compared to those of alunite. In contrast to alunite (easily attributed to hypogene processes), jarosite is commonly considered a product of supergene weathering (Dill, 2001), and can replace alunite when the fluids become more acidic and oxidizing (Stoffregen et al., 2000). The occurrence of jarosite deposits has also been documented during dry summer seasons in sea caves along the coast in the central part of California

(Rogers 1988; Hill & Forti, 1997). However, jarosite can also form in highly oxidizing fluids at temperature ranging between 150-200°C, and rich in sulfuric-acid.

As reported by Dutrizac & Jambor (2000) and Stoffregen et al. (2000) jarosite, in surficial conditions, typically alters to goethite, whereas in low-temperature metamorphic environments the destruction of jarosite produces goethite and hematite. Changes in pH (due to the addition of a buffering agent such as carbonate rocks) can induce the precipitation of dissolved Fe (in low concentration), and the deposition of goethite (Dutrizac & Jambor, 2000 and references therein). Jarosite abundance increases with decreasing pH, whereas goethite is stable at pH 3.3-3.6 (Bigham & Nordstrom, 2000). The source of iron can be related to the sedimentary deposition of iron-rich formations along margins of cratons or continental platforms over extended periods of time (Gross, 1983).

Aluminum in natural environments is related to the weathering of various aluminosilicates including K-feldspar [$KAlSi_3O_8$], muscovite, and kaolinite [$Al_2Si_2O_5(OH)_4$] (Bigham & Nordstrom, 2000). Alunite can also be due to the interaction between H_2SO_4 and illite-series at pH 3-4 (Goldbery, 1980). The studied alunite deposits (*Figure 26*) present fine-grained structures, occurring like pseudo-cubic to bipyramidal grains (0.7-2.5 μm), deposited as bedded sediments. Jarosite has been observed both with a pseudo-cubic (*Figure 26*H) or laminar structure (*Figure 24*E). The pseudo-cubic crystals (*Figure 26*H) found in Cavallone-Bove system present evident defects, probably linked to a complete substitution of previous alunite deposits. As suggested by Stoffregen et al. (2000), fine-grained alunite usually forms at quite low temperature. Bighman & Nordstrom (2000) observed precipitation of alunite crystals after the mixing of acid mine waters with carbonate-rich warm (>20°C) fluids with elevated concentration of chloride (700-800 ppm). Microcrystalline alunite also forms in evaporative conditions together with silica speleothems in Australian caves at room temperature (Wray, 2011). Sulfate in this case derives from pyrite oxidation, and reaches high concentrations because of intense evaporation. Copious solid solutions (*Figure 26* and *Figure 30*A) have been found in the studied samples, especially those from Cavallone-Bove and Monte Cucco systems. The most common solid solution series are alunite-natroalunite, jarosite-natrojarosite, alunite-jarosite, but interesting are the coupled substitutions of sulfate (SO_4^{2-}) with phosphate (PO_4^{3-}) or arsenate (AsO_4^{3-}). Hydroxylapatite replacements can occur in zones of "advanced argillitic" alteration (Stoffregen et al., 2000), defined by the assemblage of kaolinite, alunite, smectite (Shanks III, 2012) typical of environments with pH lower than 4 and well-described in different hydrothermal ore deposits (Meyer & Hemley, 1967). Minerals belonging to the alunite supergroup can have hypogene hydrothermal, hypogene steam-heated and supergene origin (Dill, 2001). Hypogene hydrothermal alunite is commonly enriched in PO_4^{3-}, and cations such as Ca^{2+}, Sr^{2+}, Ba^{2+} whereas steam-heated alunites lack a complex core and are characterized by a limited range of alunite-natroalunite solid solutions (Aoki et al., 1993). P- and

Sr-content in alunite deposits reflects the source of the parent solution (accessory hydroxylapatite, monazite, xenotime, and alkali feldspar).

We discovered abundant phosphates (i.e., goyazite and leucophosphite) and solid solutions between phosphates and sulfates in Monte Cucco systems *(Figure 30*A), and Corona'e sa Craba (vashegyite, berlinite, taranakite), but also flourapatite-hydroxylapatite minerals associated with gibbsite, likely related to subsequent events that induce weathering of primary-acidic deposits.

Hydroxylapatite is stable at pH close to 6, whilst gibbsite (the final product of phosphate alteration) occurs at pH >5 (Dill, 2001 and references therein). In all the studied cases, we have never observed andalusite [Al_2SiO_5] as an alteration product; this means that the temperature never exceeded 400°C and the widespread presence of jarosite suggests the temperature was always below 200°C (Barth-Wirshing et al., 1990). In acidic sulfate waters kaolinite and gibbsite (the last products of aluminosilicate weathering) are not the most stable phases. Other minerals such as pickeringite and aluminocopiapite may form (Bigham & Nordstrom, 2000). Pickeringite and copiapite have been previously described in cave environments, and in association with tamarugite (Forti et al., 1995; 1996), in the Alum volcanic cave (Vulcano Island, Sicily) and with römerite [$Fe^{2+}Fe^{3+}{}_2(SO_4)_4 \cdot 14H_2O$] and coquimbite [$Fe^{3+}{}_2(SO_4)_3 \cdot 9H_2O$] in Carlsbad Cavern (Mosch & Polyak, 1996). Pickeringite, metavoltine and tamarugite have been seen in the volcanic-fumarole related environment of Grotta dello Zolfo (Naples, Italy) (Franco, 1961), pickeringite and tamarugite have been encountered in thermal caves such as the case of Diana in Romania (Diaconu & Medesan, 1973; Pușcaș et al., 2013). The sources of Na^+, inducing the precipitation of tamarugite and metavoltine, can be linked to the upwelling waters, whilst Mg^{2+} (pickeringite) to the dissolution of dolostone (Triassic Dolomia Principale): this would also explain why we found pickeringite only in the Calabrian systems.

Bellini (1901) and Lacroix (1907) firstly documented metavoltine deposits, showing them to be characterized by yellowish small rosettes with hexagonal crystals, as those found in Acqua Mintina (*Figure 27*D). Hexahydrite is a stable species in caves; in fact, it has been recorded in several natural underground environments worldwide (Freeman et al., 1973; Shopov, 1990; Martini, 1993; Forti et al., 1995). We found it in association with pickeringite-copiapite-tamarugite-epsomite-tschermigite in Calabrian thermal spas and with metavoltine-epsomite in Acqua Mintina Cave. Tschermigite deposits are explained by Hill & Forti (1997) by a combined presence of pyrite, fresh bat guano, and clay minerals, which supply all the elements needed for its growth (Martini, 1983). Tschermigite has also been observed in the thermal sulfidic Serpents cave in France where it occurs together with alunogen [$Al_2(SO_4)_3(H_2O)_{12} \cdot 5H_2O$] and jurbanite [$Al(SO_4)(OH) \cdot 5H_2O$] (Audra & Hobléa, 2007). In the Calabrian thermal spas (Terme Sibaryte at Cassano allo Ionio and Ninfe Cave at Cerchiara di

Calabria), we also found copiapite deposits associated with gypsum, jarosite and/or pickeringite, tamarugite, hexahydrate. A feasible explanation for the presence of copiapite deposits can be linked to the partial oxidation of effluorescent Fe-sulfate minerals (melanterite [$Fe(SO_4)\cdot 7H_2O$], rozenite [$Fe^{2+}(SO_4)\cdot 4H_2O$], and szomolnokite [$Fe(SO_4)\cdot H_2O$]), forming when a solution, after the precipitation of soluble iron-sulfate minerals, becomes progressively more concentrated in iron (Bigham & Nordstrom, 2000). An upwelling K-poor and Fe^{3+}-rich acidic fluid can deposit copiapite (Bigham & Nordstrom, 2000).

At pH higher than 5, aluminum is insoluble, and if an Al-rich solution mixes with a fluid with pH higher than 5, felsőbányaite will precipitate. Felsőbányaite (Martini, 1993; Shopov, 1993; Hill & Forti, 1997) can form because of the dissolution of Al-rich shales in sulfuric acid environments. In Corona'e sa Craba, felsőbányaite is associated with alunite, jarosite, and halloysite 10 Å [$Al_2Si_2O_5(OH)_4\cdot 2H_2O$], thought to have developed in sub-aerial conditions, when H_2SO_4 reacted with the host rock and Al-Fe-Mg residues were released during silicification of dolomite (Sauro et al., 2014). As a matter of fact, even after the drop of the sulfuric water table, convective H_2S-rich air flow induced by the thermal gradient could encounter the O_2-rich atmosphere (Ritchie, 1994) and interfere with insoluble deposits producing aluminum sulfates and silicates.

The presence of halloysite 10 Å deposits in Monte Cucco caves can also be due to the alteration of smectite clays following the reaction (3);

3) 6 smectite + $12H^+$ + $2H_4SiO_4$ + $2Al(OH)_4$ => 12 Halloysite + Ca^{2+}.

The free Ca^{2+} ions, together with Ti, were able to produce titanite.

Finally, greenalite [$(Fe^{2+}, Fe^{3+})_{2-3}Si_2O_5(OH)_4$] characterized by green to reddish colors has been found in Grotta che Parla, in Sicily, together with gypsum, calcite, and dolomite deposits. Greenalite is considered a part of the kaolinite-serpentine mineral group, and can be associated with pyrite and with "Mantos" or stratabound type ore deposits, in the mineralogical assemblage constituted by greenalite-magnetite-sulfide-carbonate-silica (López-García et al., 2011). Greenalite minerals could be linked to the presence of volcanic intrusive dikes and Fe-Mn encrustations. In addition, Montagna Grande represents part of a huge thrust-belt system overlapping terrigenous deposits containing pyrite.

3.2.7. Conclusions

The mineralogical associations described in this paper reveal new insights into sulfuric acid speleogenesis of Italy. Cave environments are preferential sites able to yield clues that are no longer present at the surface because of erosion, preserving important information about the geological processes and landscape evolution. We focused on 15 cave systems showing that each of them

contains peculiar mineral assemblages typical of sulfuric acid speleogenesis. XRD and SEM results allowed us to understand how geomorphological features (cupolas, replacement pockets, feeders, sulfuric notches, sub-horizontal cave levels, etc.) fit well with the observed mineralogy, suggesting sulfuric acid occurrences also for systems never studied in detail such as Cavallone-Bove, Santa Cesarea Terme, Acqua Mintina, and Grotta che Parla. Nevertheless, further investigations (*i.e.,* stable isotopes, trace elements, dating of alunite-jarosite deposits) deserve to be done to better elucidate the condition of their genesis. Gypsum is the most common mineral, as already explained by Hill & Forti (1997), due to its capacity to immediately replace carbonate in H_2SO_4-rich environments. Native sulfur deposits have been observed in almost all the studied systems, but they are very abundant only in a few caves such as Santa Cesarea Terme, Cala Fetente, and Acqua Mintina, where they entirely cover walls, ceilings and speleothems. Such occurrences would suggest these systems have had important H_2S degassing at that time. A biogenic or microbially-induced precipitation of S should be further investigated. Of great interest are the mineralogical associations found in the Monte Cucco caves characterized by baryte-fluorite deposits, likely formed during large orogenic events (Barbieri et al, 1982; Hanor, 2000). Their subsequent interaction with H_2SO_4 allowed the formation of solid solution between baryte and celestine and alteration of fluorite in a series of minerals going from flourapatite to gibbsite. The presence of rutile needles and spheres of titanite would testify to their authigenic origin, which means that the titanium was in solution and not transported as particles by the upwelling flow. In Monte Cucco caves alunite is in assemblage with peculiar phosphates like goyazite and leucophosphite. Other relevant results have been obtained from Cavallone-Bove caves, where pure white alunite, yellowish jarosite deposits and bountiful alunite-natroalunite-jarosite solid solutions are also PO_4-rich. The abundant presence of PO_4, in the core of alunite-jarosite deposits strongly suggests hypogene hydrothermal origin of fluids involved in the formation of aluminium phosphates and sulfates (Dill, 2001).

Corona'e sa Craba Cave is the only hypogene system, described here, to have developed in quartzite rocks. As well explained by Sauro et al. (2014), the several stages of rising fluids have been characterized by a clear evolution of pH, from alkaline-reductive solutions (allowing silicification of dolomite rocks, mobilization of Ba ions and deposition of felsőbányaite and cinnabar [HgS] minerals) to more acidic-oxidative conditions (inducing the deposition of typical sulfates and silicates such as alunite-jarosite-halloysite 10Å).

The Buso della Pisatela-Rana (Tisato et al., 2012) and Grotta che Parla represent sulfuric acid systems that gain their acidity from the oxidation of pyrite minerals contained in the host rock, as suggested by both the lack of diagnostic suites of sulfates and the presence of greenalite, described (López-García et al., 2011) in association with ore materials and pyrite.

Finally, yellowish deposits of copiapite-pickeringite-tamarugite-hexahydrite have been observed above the present sulfuric water-level in Calabrian caves, whereas deposits of metavoltine (a quite rare SAS mineral) in the entrance hall of Acqua Mintina Cave, demonstrating H_2SO_4 degassing to produce a peculiar sulfuric acid association of minerals, have already been documented in other famous SAS system around the world.

References

Angert, E.R., Northup, D.E., Reysenbach, A.-L., Peek, A.S., Goebel, B.M., Pace, N.R., 1998. Molecular phylogenetic analysis of a bacterial community in Sulphur River, Parker Cave, Kentucky. American Mineralogist, 83, 1583-1592.

Angiboust, S., Harlov, D., 2017. Ilmenite breakdown and rutile-titanite stability in metagranitoids: natural observations and experiment results. American Mineralogist. DOI: http//dx.doi.org/10.2138/am-2017-6064

Aoki, M., Comsti, E.C., Lazo, F.B., 1993. Advanced argillic alteration and geochemistry of alunite in an evolving hydrothermal system at Baguio, Northern Luzon, Philippines. Resource Geology, 43: 155-164.

Audra, P., 2007. Karst et spéléogenèse épigènes, hypogènes, recherches appliquées et valorisation (Habilitation Thesis). University of Nice Sophia-Antipolis, 278 pp.

Audra, P., 2008. Hypogenic sulfidic speleogenesis. Berliner Höhlenkundliche Berichte, 26: 15-32.

Audra, P., Hobléa, F., 2007. The first cave occurrence of Jurbanite [Al(OH SO_4)•$5H_2O$], associated with alunogen [$Al_2(SO_4)_3$•$17H_2O$] and Tschermigite [$Al_2(SO_4)_2$•$12H_2O$]: thermal sulfidic serpents cave, France. Journal of Cave and Karst studies, 68(2): 243-249.

Audra, P., Gázquez, F., Rull, F., Bigot, J.Y., Camus, H., 2015. Hypogene Sulfuric Acid Speleogenesis and rare sulfate minerals in Baume Galinière Cave (Alpes-de-Haute-Provence, France). Record of uplift, correlative cover retreat and valley dissection. Geomorphology, 247: 25-34.

Azzaroli, A., 1967. Calcare di Altamura. Note illustrative della Carta Geologica d'Italia. Formazioni Geologiche, 1: 151-156.

Barbieri, M., Masi, U., Tolomeo, L., 1982. Strontium geochemistry in the epithermal baryte deposits from the Apuan Alps (Northern Tuscany, Italy). Chemical Geology, 35: 351-356.

Barth-Wirsching U., Ehn R., Höller H., Klammer D. & Sitte W., 1990 – Studies of hydrothermal alteration by acid solution dominated by SO_4^{2-}: formation of the alteration products of the Gleichenberg latitic rock (Styria, Austria). Experimental evidence. Mineralogy and Petrology, 41: 81-103.

Basilone, L., 2012. Unità carbonatiche Mesozoico-Paleogeniche. Litostratigrafia delle Sicilia, 24-64.

Bellini, R., 1901. La Grotta dello Zolfo nei Campi Flegrei. Bollettino della Società Geologica Italiana, 20: 470-475.

Bertolani, M., Garuti, G., Rossi, A., Bertolani Marchetti, D., 1976. Motivi di interesse mineralogico-petrografico nel complesso carsico Grotta Grande del Vento-Grotta del Fiume (Genga, Ancona). Le Grotte d'Italia, IV(6): 109-144.

Bigham, J.M., Nordstrom, D.K., 2000. Iron and Aluminium Hydroxysulfates from acid sulfate waters. Reviews in Mineralogy and Geochemistry, 40: 351-403.

Buck, M.J., Ford, D.C., Schwarcz, H.P., 1994. Classification of cave gypsum deposits derived from oxidation of H_2S. In: I., Sasowsky, M.V., Palmer (Eds.), Breakthroughs in karst geomicrobiology and redox geochemistry. Karst Water Institute, Special publication, 1: 5- 9.

Callière, S., Hénin, S., 1963. Minéralogie des argiles. Masson et C.ie, (Ed.), Paris, 356 pp.

Canfield, D.E., 2001. Biogechemistry of sulfur isotopes. Reviews in mineralogy and geochemistry, 43: 607-636.

Canganella, F., Bianconi, G., Kato, C., Gonzales, J., 2007. Microbial ecology of submerged marine caves and holes characterised by high levels of hydrogen sulphide. Review in Environmental Science and Bio/Technology, 6: 61-70. http://doi.org/10.1007/s11157-006-9103-2.

Carbone, C., Dinelli, E., Marescotti, P., Gasparotto, G., Lucchetti, G., 2013. The role of AMD secondary minerals in controlling environmental pollution: indications from bulk leaching tests. Journal of Geochemical Exploration 132: 188-200.

Carswell, D.A., O'Brien, P.J., 1993. Thermobarometry and geotectonic significance of high-pressure granulites: examples from the Moldanubian Zone of the Bohemian Massif in Lower Austria. Journal of Petrology, 34(3): 427-459.

Catalano, R., Agate, M., Albanese, C., Avellone, G., Basilone, L., Gasparo, M., Gugliotta, C., Sulli, A., Valenti, V., Gibilaro, C., Pierini, S., 2013. Walking along a crustal profile across the Sicily fold and thrust belt. American Association of Petroleum Geologists. Post Conference Field Trip 4, Palermo. Geological field trips, 5(2-3): 213 pp.

Catalano, M., Bloise, A., Miriello, D., Apollaro, C., Critelli, T., Muto, F., Cazzanelli, E., Barrese, E., 2014. The mineralogical study of the Grotta Inferiore di Sant'Angelo (southern Italy). Journal of Cave and Karst Studies, 76(1): 51-61.

Ciarapica, G., Cirilli, S., Passeri, L., Trincardi, E., Zaninetti, L., 1986. "Anidriti di Burano" et "Formation du Monte Cetona" (nouvelle formation), biostratigraphie de duex series-types du Trias supérieur dans l'Apennin septentrional. Revue de paléobiologie, 6(2): 341-409.

Cucchi, F., Forti P., 1988, Speleogenetic evolution of Fiume-Vento karst system (San Vittore Genga-Marche). International Symposium of Physics, Chemistry and Hydrology Reservoir of Karst, Kosice: 193-199.

D'Angeli, I.M., De Waele, J., Galdenzi, S., Madonia, G., Parise, M., Piccini, L., Vattano, M., 2016. Sulfuric acid caves of Italy: an Overview. In: T., Chavez, P., Reehling (Eds.), NCKRI Symposium 6, Proceedings of DeepKarst 2016: Origins, Resources, and Management of Hypogene Karst, Carlsbad, New Mexico: 85-88.

D'Angeli, I.M., Vattano, M., Parise, M., De Waele, J., 2017a. The coastal sulfuric acid cave system of Santa Cesarea Terme (southern Italy). In: Klimchouk A.B., Palmer A.N., De Waele J., Auler A. & Audra P., (Eds.), Hypogene karst regions and caves of the world. Springer: 161-168. http://doi.org/10.1007/978-3-319-53348-3.

D'Angeli, I.M., De Waele, J., Ieva, M.G., Leuko, S., Cappelletti, M., Parise, M., Jurado, V., Miller, A.Z., Saiz-Jimenez, C., 2017b. Next-Generation Sequencing for microbial characterization of biovermiculations from a sulfuric acid cave in Apulia (Italy). Proceedings of the XVIIth International Congress of Speleology, Sydney, 377-380.

Davis, D.G., 2000. Extraordinary features of Lechuguilla cave, Guadalupe Mountains, New Mexico. Journal of Cave and Karst Studies, 62(2): 147-157.

De Waele, J., Galdenzi, S., Madonia, G., Menichetti, M., Parise, M., Piccini, L., Sanna, S., Sauro, F., Tognini, P., Vattano, M., Vigna, B., 2014. A review on hypogene caves in Italy. In: A.B., Klimchouk, I., Sasowsky J., Myrloie S., Engel S.A., Engel A. (Eds.), Hypogene cave morphologies. Karst Water Institute, Special Publication, 18: 28-30.

De Waele, J., Audra, P., Madonia, G., Vattano, M., Plan, L., D'Angeli, I.M., Bigot, J.-Y., Nobécourt, J.-C., 2016. Sulfuric acid speleogenesis (SAS) close to the water table: examples from southern France, Austria, and Sicily. Geomorphology, 253: 452-467. http://doi.org/10.1016/j.geomorph.2015.10.19.

Dill, H.G., 2001. The geology of aluminium phosphates and sulphates of alunite group minerals: a review. Earth-Science Reviews, 53: 35-93.

Diaconu, G., Medesan, A., 1973. Sur la presence du pickeringite dans la grotte Diana (Băile Herculane Roumanie). Travaux de l'Institut Spélogique "Em. Racovita", 14: 149-156.

Doglioni, C., Flores, G., 1997. An introduction to the Italian geology. Lamisco, Potenza, 98 pp.

Dutrizac, J.E., Jambor, J.L., 2000. Jarosite and their application in hydrometallurgy. Reviews in Mineralogy and Geochemistry, 40: 405-452.

Egemeier, S.J., 1981. Cavern development by thermal waters. National Speleological Society Bulletin, 43: 31-51.

Fabiani, R., 1915. Il paleogene del Veneto. Memorie dell'Istituto di Geologia della Regia Università di Padova, 3: 1-336.

Forti, P. Mocchiutti, A., 2004. Le condizioni ambientali che permettono l'evoluzione di speleotemi di zolfo in cavità ipogeniche: nuovi dati dalle grotte di Capo Palinuro (Salerno, Italia). Le Grotte d'Italia, V(4): 39-48.

Forti, P., Menichetti, M., Rossi, A., 1989. Speleothems and speleogenesis of the Faggeto Tondo cave (Umbria-Italy). Proceedings of the X International Speleological Congress, Budapest, 1: 74-76.

Forti, P., Panzicala Manna, M., Rossi A., 1995. Il particolare ambiente della Grotta dell'Allume (Vulcano, Sicilia). Atti del secondo Convegno Regionale di Speleologia, Catania, 37(348): 251-272.

Forti, P., Panzicala Manna, M., Rossi, A., 1996. The peculiar mineralogic site of the Alumn Cave (Vulcano, Sicily). 7° International Symposium Vulcanospeleological, Canary Islands, 15-17.

Franco, E., 1961. Su alcuni minerali della Grotta dello Zolfo (Miseno). Bollettino della Società dei Naturalisti Napoli, 70: 156-160.

Freeman, J.P., Smith, G.P., Poulson, T.L., Watson, P.J., White, W.B., 1973. Lee Cave, Mammoth Cave National Park, Kentucky. National Speleological Society Bullettin, 35(4): 109-126.

Galdenzi, S., 1990. Un modello genetico per la Grotta Grande del Vento. Memorie dell'Istituto Italiano di Speleologia, II(4): 123-142.

Galdenzi, S., 2001. L'azione morfogenica delle acque sulfuree nelle grotte di Frasassi, Acquasanta Terme (Appennino-Umbro-Marchigiano, Italia) e di Movile (Dobrogea, Romania). Le Grotte d'Italia, V(2): 49-61.

Galdenzi, S. Menichetti, M., 1995. Occurrence of hypogene caves in a karst region: example from central Italy. Environmental Geology, 26: 39-47.

Goldbery, R., 1980. Early diagenetic, Na-alunites in Miocene algal mat intertidal facies, Ras Sudar, Sinai. Sedimentology, 27:189-198.

Gross, G.A., 1983. Tectonic systems and the deposition of iron-formation. Precambrian Research, 20: 171-187.

Hanor, J.S., 2000. Baryte-Celestine geochemistry and environment of formation. Reviews in Mineralogy and Geochemistry, 40: 193-275.

Henry, D.J., Guidotti, C.V., 2002. Titanium in biotite from metapelitic rocks: temperature effects, crystal-chemical controls, and petrologic application. American Mineralogist, 87: 375-382.

Hill, C.A., 1981. Celestine growing in Floyd Collins Crystal Cave. Cave Research Foundation, Annual Report, 23: 9.

Hill, C.A., 1987. Celestine in Carlsbad Caverns. Cave Research Foundation, Annual Report, 29: 15.

Hill, C.A., 1990. Sulfuric acid speleogenesis of Carlsbad Cavern and its relationship to hydrocarbons, Delaware Basin, New Mexico and Texas. American Association of Petroleum Geologists Bullettin, 74: 1685-1694.

Hill, C.A., 1992. Isotopic values of native sulfur, baryte, celestite, and calcite: their relationship to sulfur deposits and to the evolution of the Delaware basin (preliminary results). In G.R. Wessell, B.H., Wimberly (Eds.), Native sulfur-development in geology and exploration. Phoenix, AZ: Society of Mining, Metallurgy and Exploration: 147-157.

Hill, C.A., 1995. Sulfur redox reactions: hydrocarbon, native sulfur, Mississippi Valley-type deposits, and sulfuric acid karst in the Delaware Basin, New Mexico and Texas. Environmental Geology, 25: 16-23.

Hill, C.A., Forti, P., 1997. Cave Minerals of the World. National Speleological Society, Second Edition, 463 pp.

Hose, L.D., Palmer, A.N., Palmer, M.V., Northup, D.E., Boston, P.J., DuChene, H.R., 2000. Microbiology and geochemistry in hydrogen-sulfide-rich karst environment. Chemical Geology, 169: 399-423.

Imhoff, J.F., 2006. The Chromatiaceae. Prokaryotes, 6: 846-873. DOI: 10.1007/0-387-30746-x_31.

Jagnow, D.H., Hill, C.A., Davis, D.G., DuChene, H.R., Cunningham, K.I., Northup, D.E., Queen, J.M., 2000. History of the sulfuric acid theory of speleogenesis in the Guadalupe Mountains, New Mexico. Journal of Cave and Karst Studies, 62(2): 54-59.

Klimchouk, A.B., 2005. Conceptualization of speleogenesis in multy-storey artesian systems: a model of transverse spelegenesis. International Journal of Speleology, 34(1-2): 45-64.

Klimchouk, A.B., 2007. Hypogene speleogenesis: hydrogeological and morphogenetic perspective. National Cave and Karst Research Institute Special Paper 1, Carlsbad.

Klimchouk, A.B., 2009. Morphogenesis of hypogenic caves. Geomorphology, 106: 100-117.

Klimchouk, A.B., 2017. Types and settings of hypogene karst. In: Klimchouk, A.B., Palmer, A.N., De Waele, J., Auler, A., Audra, P., (Eds.), Hypogene karst regions and caves of the world. Springer, 1-39. DOI 10.1007/978-3-319-53348-3.

Klimchouk, A.B., Auler, A., Bezerra, F.H.R., Cazarin, C.L., Balsamo, F. Dublyansky, Y., 2016. Hypogenic origin, geologic controls and functional organization of a giant cave system in Precambrian carbonates, Brazil. Geomorphology, 253: 385-405.

Kulp, E.A., Kothari, H.M., Limmer, S.J., Yang, J., Gudavarthy, R.V., Bohannan, E.W., Switzer, J.A., 2009. Electrodeposition of epitaxal magnetite films and ferrihydrite nanoribbons on single-crystal

gold. Chemistry Materials, 21(21): 5022-5031.

Lacroix, A., 1907. Sur deux gisements nouveaux de metavoltine. Bulletin Française de Minéralogie et de Cristallographie, 30: 30.

López-García, J.A., Oyarzun, R., López Andrés, S. Manteca Martínez, J.I., 2011. Scientific, educational, and environmental considerations regarding mine sites and geoheritage: A perspective from SE Spain. Geoheritage, 3(4): 267-275.

Lugli, S., Ruggieri, R., Orsini, R., Sammito, G., 2016. Grotta dell'Acqua Mintina, a peculiar geosite with the smell of sulfur. Proceeding of the 4th International Symposium on karst in the South Mediterranean area. Karst Geosites: 65-71.

Macalady, J.L., Lyon, E.H., Koffman, B., Albertson, L.K., Meyer, K., Galdenzi, S. Mariani, S., 2006. Dominant microbial population in limestone-corroding stream biofilms, Frasassi cave system, Italy. Applied Environmental Microbiology, 72(8): 5596-5609.

Machel, H., 2001. Bacterial and thermochemical sulfates reduction in diagenetic settings – old and new insights. Sedimentary Geology, 140: 143-175.

Mansor, M., Harouaka, K., Gonzales, M.S., Macalady, J.L., Fantle, M.S., 2018. Transport-induced spatial patterns of sulfur isotopes ($\delta^{34}S$) as biosignature. Astrobiology, 18(1): 1-14. DOI: 10.1089/ast.2017.1650.

Manzi, V., Lugli, S., Roveri, M., Schreiber, B.C., 2009. A new facies model for the Upper Gypsum (Sicily, Italy): chronological and paleoenvironmental constraints for the Messinian salinity crisis in the Mediterranean. Sedimentology, 56: 1937-1960.

Martini, J.E., 1983. Lonecreenite, sabietite, and clairite, a new secondary ammonium ferric-iron sulphate from Lone Creek Fall Cave, near Sabie, eastern Transvaal. Bullettin Geological Survey of South Africa, 17: 29-34.

Martini, J.E., 1993. A concise review of the cave mineralogy of Southern Africa. Proceeding 11th International Speleological Congress, Beijing, 72-75.

Martinis, B., Pieri, M., 1964. Alcune notizie sulla formazione evaporitica del Triassico superiore nell'Italia centrale e meridionale. Memorie della Società Geologica Italiana, 4(1): 649-678.

Martire, L., Pavia, G., Pochettino, M., Cecca, F., 2000. The Middle-Upper Jurassic of Montagna Grande (Trapani): Age, Facies, and Depositional Geometries. Memorie della Società Geologica Italiana, 55:219-225.

Menichetti, M., 2008. Assetto strutturale del sistema geotermico di Acquasanta Terme (Ascoli Piceno). Rendiconti online della Società Geologica Italiana, 1: 118-122.

Meyer, C., Hemley, J.J., 1967. Wall rock alteration. In: H.L., Barnes (Ed.), Geochemistry of hydrothermal ore deposits. John Wiley & Sons, Hoboken: 166-235.

Millot, G., 1964. Géologie des argiles. Masson at C.ie (Ed.), Paris, 499 pp.

Minissale, A., 2004. Origin, transport and discharge of CO_2 in central Italy. Earth-Science Reviews, 66: 89-141.

Mosch, C., Polyak, V.J., 1996. Canary yellow-cave precipitates: late stages of hydrated uranyl-vanadate, uranyl silicate, and iron sulfate minerals (abs.). National Speleological Society, Salida, Colorado, August 5-9: 51.

Onac, B.P., Forti, P., 2011. Minerogenic mechanisms occurring in the cave environment: an overview. International Journal of Speleology, 40(2): 79-98.

Onac, B.P., Sumrall, J., Tămaş, T., Povară, I., Kearns, J., Dârmiceanu, V., Veres, D., Lascu, C., 2009. The relationship between cave minerals and H_2S-rich thermal waters along the Cerna Valley (SW Romania). Acta Carsologica, 38(1): 27-39.

Onac, B.P., Wynn, J.G., Sumral, J.B., 2011. Tracing the sources of cave sulfates: a unique case from Cerna Valley, Romania. Chemical Geology, 288(3-4): 105-114.

Padalino, G., Pretti, S., Tamburrini, D., Tocco, S., Uras, I., Violo, M., Zuffardi, P., 1973. Ore deposition in karst formations with examples from Sardinia. In: G.C., Amstutz, C., Bernard (Eds.), Ores in sediments. Springer Verlag, Berlin: 209-220.

Palmer, A.N., 2007. Cave geology. Cave Books, Dayton, 454 pp.

Palmer, A.N., 2011. Distinction between epigenic and hypogenic maze caves. Geomorphology, 134: 9-22.

Palmer, A.N., 2013. Sulfuric acid caves: Morphology and Evolution. In: A., Frumkin, J., Shroder (Eds.), Treatise on Geomorphology. Elsevier, 241-257.

Palmer, A.N., Palmer, M.V., 1992. Geochemical and petrological observations in Lechuguilla cave, New Mexico (abs.). In: A.E., Ogden (Ed.), Friends of Karst Meeting, Proceedings of the Tennessee Tech University, Cooksville, Tennessee: 25-26.

Palmer, A.N., Palmer, M.V., 2000. Hydrochemical interpretation of cave patterns in the Guadalupe Mountains, New Mexico. Journal of Cave and Karst Studies, 62(2): 91-108.

Perna, G., 1973. Fenomeni carsici e giacimenti minerari. Le Grotte d'Italia, IV(3): 5-44.

Pialli, G., Barchi, M., Minelli, G., 1998. Results of the CROP 03 deep seismic reflection profile. Memorie della Società Geologica Italiana, 57: 1-657.

Piccini, L., De Waele, J., Galli, E., Polyak, V.J., Bernasconi, S.M., Asmerom, Y., 2015. Sulfuric acid speleogenesis and landscape evolution: Montecchio cave, Albegna river valley (southern Tuscany, Italy). Geomorphology, 229: 134-143.

Plan, L., Tschegg, C., De Waele, J., Spötl C., 2012. Corrosion morphology and cave wall alteration in Alpine sulfuric acid cave (Kraushöhle, Austria). Geomorphology, 169(170): 45-54.

Polyak, V.J., Güven, N., 2000. Clay in the caves of Guadalupe Mountains, New Mexico. Journal of Cave and Karst Studies, 62(2): 120-126.

Polyak, V.J., Provencio, P., 2001. By-product materials related to H_2S-H_2SO_4 influenced speleogenesisi of Carlsbad, Lechuguilla, and other caves of the Guadalupe Mountains, New Mexico. Journal of Cave and Karst Studies, 63(1): 23-32.

Polyak, V.J., McIntosh, W.C., Güven, N., Provencio P., 1998. Age and origin of Carlsbad Caverns and related caves from $^{40}Ar/^{39}Ar$ of alunite. Science, 279: 1919-1922.

Pușcaș, C.M., Onac, B.P., Effenberger, H.S., Povara, I., 2013. Tamarugite-bearing paragenesis formed by sulphate acid alteration in Diana cave, Romania. European Journal of Mineralogy, 25(3): 479-486. http://dx.doi.org/10.1127/0935-1221/2013/0025-2294.

Ritchie, A.I.M., 1994. The waste rock environment. In: Jambor J.L. & Blowes D.W. (Eds), The Environmental Geochemistry of Sulfide Mine-Wastes. Mineral Association Canada Short Course, 22: 131-161.

Rogers, W.B., 1988. Noncarbonate minerals in California caves (abs.). National Speleological Society Conference, Hot Spring (South Dakota), 1-4.

Rye, R.O., Bethke, P.M., Lanphere, M.A., Steven, T.A., 1993. Age and stable isotope systematics of supergene alunite and jarosite from the Creede mining district, Colorado: implications for supergene processes and Neogene geomorphic evolution and climate of the southern Rocky Mountains (abs). Geological Society of America Abstract with programs 25, A-274.

Sarbu, S.M., Kinkle, B.K., Vlasceanu, L., Kane, T.C., Popa, R., 1994. Microbiological characterization of a sulfide-rich groundwater ecosystem. Geomicrobiological Journal, 12: 175-182.

Sauro, F., De Waele, J., Onac, B.P., Galli, E., Dublyansky, Y., Baldoni, E. & Sanna, L., 2014. Hypogenic speleogenesis in quartize: the case of Corona'e sa Craba cave (SW Sardinia, Italy). Geomorphology, 211: 77-88. http://dx.doi.org/10.1016/j.geomorph.2013.12.031.

Selli, R., 1957. Sulla trasgressione del Miocene dell'Italia meridionale. Giornale di Geologia, 26: 1-54.

Selli, R., 1962. Il Paleogene nel quadro della geologia dell'Italia centro-meridionale. Memorie della Società Geologica Italiana, 3: 737-789.

Shanks III, W.C.P., 2012. Hydrothemal alteration in volcanogenic massive sulfide occurrence model. U.S. Geological Survey Scientific Investigations Report, 11: 12 pp.

Shopov, Y.Y., 1990. Development of Bulgarian Cave Mineralogy (1923-1986). Bulgarian Speleology, 2: 21-32.

Shopov, Y.Y., 1993. Genetic Classification of cave minerals. Procceding 10th International Congress

of Speleology, Beijing (1993-1994), 101-105.

Stoffregen, R.E., 1993. Stability relations of jarosite and natroalunite at 100-250°C. Geochimica et Cosmochimica Acta, 58: 903-916.

Stoffregen, R.E., Alpers C.N. & Jambor J.L., 2000 – Alunite-jarosite crystallography, thermodynamics, and geochronology. Reviews in Mineralogy and Geochemistry, 40: 453-479.

Stüben, D., Sedwick, P., Colantoni, P., 1996. Geochemistry of submarine warm springs in the limestone cavern of Grotta Azzurra, Capo Palinuro, Italy: evidence for mixing-zone dolomitisation. Chemical Geology, 131: 113-125.

Stumm, W., 1992. Chemistry of the Solid-Water Interface: Process at the Mineral-Water and Particle-Water Interface in Natural system. John Wiley, New York, 428 pp.

Summers Engel, A., Stern, L.A., Bennett, P.C., 2004. Microbial contributions to cave formation: new insights into sulphuric acid speleogenesis. Geology, 32(5): 369-372.

Taddeucci, A., Tuccimei, P., Voltaggio M., 1992. Studio geocronologico del complesso carsico "Grotta del Fiume-Grotta Grande del Vento" (Gola di Frasassi, AN) e indicazioni paleoambientali. Il Quaternario, 5: 213-222.

Tisato, N., Sauro, F., Bernasconi, S.M., Bruijn, R.H.C., De Waele, J., 2012. Hypogene contribution to speleogenesis in a predominant epigenic karst system: a case study from the Venetian Alps, Italy. Geomorphology, 151-152: 156-163.

Tombácz, E., Dobos, Á., Szekeres, M., Narres, H.D., Klumpp, E., Dékány, I., 2000. Effect of pH and ionic strength on the interaction of humic acid with aluminium oxide. Colloid and Polymer Science, 278(4): 337-345.

Tracy, R.J., Robinson, P., 1988. Silicate-sulfide-oxide fluid reactions in granulite politic rocks, central Massachusetts. American Journal of Science, 288: 45-74.

Vattano, M., Madonia, G., Audra, P., D'Angeli, I.M., Galli, E., Bigot, J.-Y., Nobécourt, J.-C., De Waele J., 2017. An overview of the hypogene caves of Sicily. In: A.B., Klimchouk A.N., Palmer J., De Waele J., A., Auler, P., Audra (Eds.), Hypogene karst regions and caves of the world. Springer: 199-210.

Westerhoff, P., Song, G., Hristovski, K., Kiser, M.A., 2011. Occurrence and removal of titanium at full scale wastewater treatment plants: implications for TiO_2 nanomaterials. Journal of Environmental Monitoring, 13: 1195-1203.

Williams-Jones, A.E., Samson, I.M., Olivo, G.R., 2000. The genesis of hydrothermal fluorite-REE deposits in Gallinas Mountains, New Mexico. Economic Geology, 95(2): 327-341.

Wray, R.A.L., 2011. Alunite formation within silica stalactites from the Sydney Region, South-eastern Australia. International Journal of Speleology, 40(2): 109-116.

Wright, G.F., 1898. A recently discovered cave of Celestine crystals at Put-in-Bay, Ohio. Science, 8(198): 502-503.

4. GEOCHEMISTRY

4.1. Sulfur stable isotopes

Chemical signatures of SAS in inactive-fossil caves are mainly preserved in the stable isotopes of sulfur, which can give important information regarding both the source of H_2S and the reactions (see paragraph 1.3.2) involved in the sulfur cycles, and in addition, stable isotopes of carbon and oxygen can give further constraints on the origin (meteoric or deep upwelling) of the feeding sulfuric waters. In addition, the thermality of the rising waters can also be ascertained by fluid inclusion studies, especially in the case of baryte, fluorite, and dogtooth spar samples (Decker et al., 2015; 2016).

In general, $\delta^{34}S$ stable isotope investigations, of gypsum and sulfur found as by-products in underground SAS environments, represent the most robust evidence of both active and past SAS processes. Sulfur has four stable isotopes in nature (^{32}S, ^{33}S, ^{34}S and ^{36}S), but only ^{32}S (95%) and ^{34}S (4.2%) have mostly been used, mainly because the other two isotopes account for less than 1% (Eckardt, 2001; Canfield, 2001). Nevertheless, some authors proved ^{33}S to represent a valuable tool in unravelling complex biogeochemical sulfur cycling (Canfield et al., 2010; Zerkle et al., 2010).

In general, the isotopic composition of geological samples is expressed in $\delta^{34}S$, the ratio of ^{34}S and ^{32}S in ‰, normalized to the universal standard (Cañon Diablo Troilite: CDT), and the average values of $\delta^{34}S$ observed, vary significantly from -50 to +35 ‰.

One of the most striking chemical signatures of SAS is the often very negative value of $\delta^{34}S$ (down to -25‰) of gypsum attributable to the BSR (bacterial sulfate reduction) or DSR (dissimilatory sulfate reduction). These low $\delta^{34}S$ values were the first compelling evidence for the implication of hydrocarbons for the origin of sulfides in the Guadalupe Mountains in New Mexico (Hill, 1981). Here, the hydrocarbons of the Delaware Basin provided the electrons for the bacterial sulfate reduction of the Castile Formation evaporites, demonstrated by a $\delta^{34}S$ shift of around +10‰ of these Permian gypsum deposits to around −20‰ for the H_2S (Hill, 1987, 1990; Spirakis & Cunningham, 1992). The low reaction rate, limited by the supply of hydrocarbons from the deep petroleum reservoirs to the Castile Formation evaporites, causes this fractionation to be around -30‰.

Studies on S isotope fractionation during S oxidation have shown that $\delta^{34}S$ shift can be very small, producing no fractionation at high T (Ohmoto and Rye, 1979) or small fractionation at low T (Fry et al., 1988). This means that the $\delta^{34}S$ values of SAS minerals (e.g., gypsum, Al-Fe-sulfates) due to TSR (thermal sulfate reduction) are more or less similar to that of the original source of reduced sulfur (Yonge and Krouse, 1987; Bottrell, 1991; Bottrell et al., 2001). Nevertheless, as the case of Cerna valley, the wide range of $\delta^{34}S$ values have been proven to derive from thermal sulfate reduction (TSR) of sedimentary sulfates and their reaction with methane, produced by bacterial decay of nearby coal

deposits (Onac et al., 2011). These reactions are limited by methane and or sulfate during reduction, and by oxygen during their oxidation, and lead to this wide gamma of $\delta^{34}S$ values.

On the contrary, sulfate reducing bacteria are able to use ^{32}S for their metabolic reactions and produce ^{34}S-depleted H_2S (Strauss, 1997). In this case, bacterial reduction of sulfate (BSR) causes $\delta^{34}S$ values to shift by as much as -30‰, and sulfides resulting from this process have an average $\delta^{34}S$ value of -12‰ (Seal, 2006). Furthermore, dissimilatory sulfate reduction (DSR) can produce sulfides depleted in ^{34}S by more than -40‰ (Zerkle et al., 2016); also, the biological disproportion of intermediate compounds, such as ($S_2O_3^-$), sulfite (SO_3^-), and elemental sulfur (S^0), can induce large isotope differences, with H_2S depleted in ^{34}S (+5 to +7‰) with respect to SO_4^{2-}, which values range between +17 to +21‰ (Canfield & Thamdrup, 1994).

In general, the final $\delta^{34}S$ value obviously depends on the initial isotopic signature of the sulfate, which may have four main sources in carbonate karst: oxidation of sulfides, redeposition of marine evaporites, degradation of bat guano, and rising of volcanic fluids. Sulfur deriving from a magmatic source is commonly slightly lower than CDT (+22.22‰). Rye (2005) summarized the $\delta^{34}S$ values in A) *Supergene Steam-Heated* (H_2S-pyrite oxidation), and B) *Magmatic Steam Steam-Heated* and C) *Magmatic Hydrothermal* (SO_2 disproportion) conditions. In A $\delta^{34}S$ (‰) values of sulfur, sulfates and sulfides range from -3 to +3.9, in B from +4 to +11.5, and in C from +12 to +18‰.

Similar to the Guadalupe Mountains (Spirakis & Cunningham, 1992), low sulfur isotopic compositions of gypsum have been found in Villa Luz Cave (Mexico) where H_2S most probably derives from bacterial reduction of evaporite sediments using electrons of hydrocarbons coming from the nearby oil fields (Hose et al., 2000). Also $\delta^{34}S$ values of gypsum in Kraushöhle are very low (Puchelt & Blum, 1989; Plan et al., 2012), deriving from the fractionation of Triassic evaporites (gypsum layers in the Werfen Formation) by bacterial reduction, and successive oxidation in the Hirlatz Limestones. The very negative values encountered also in the Montecchio gypsum derive from bacterial reduction of Triassic gypsum layers of the Burano Formation (+15 to +23.0‰) or, alternatively, from sedimentary pyrite (-15 to +4‰) hosted in the Triassic carbonates or sulfide ore bodies hosted at the contact between the Permian basement rocks and the Triassic sediments (Cortecci et al., 1983, 2002; Cinti et al., 2011; Piccini et al., 2015).

Kinderlinsk Cave also shows very negative $\delta^{34}S$ values of gypsum (Chervyatsova et al., 2016). The sulfur in this cave probably derives from bacterially reduced sulfates present in the bituminous limestones.

Recently, interesting investigations regarding sulfur isotopes have been carried out in some Italian SAS systems such as Frasassi caves (Zerkle et al., 2016) and Calabrian caves, located in Cassano allo Ionio, Cerchiara di Calabria and Terme Luigiane (Cosenza) (Galdenzi & Maruoka, 2019). Especially

in Frasassi, both waters, biofilms, and sediments were analyzed, providing valuable insights into sulfur cycling in still-active SAS environments. In general, they found sulfide $\delta^{34}S$ values ranging between -21 and -13‰, whilst sulfate $\delta^{34}S$ ranged between +16 and +23‰, demonstating the deep-seated Triassic evaporites of the "Burano Fm." to play an important role as dominant source of sulfate (Galdenzi & Menichetti, 1995). In addition, they observed sulfate reduction to be concentrated in the stream sediments, being fuelled by organic C input from the overlying biofilms; differently the dominant process in biofilms is chemolithotrophic sulfide oxidation (Zerkle et al., 2016).
Comparably, the water samples collected in the Calabria region, show a wide range of sulfide $\delta^{34}S$ values ranged between -25 and +8.85‰, whilst sulfate $\delta^{34}S$ varies from +14.73 to +19.92‰, and testifies the most important process to be the sulfate reduction of Triassic evaporites, likely involving sulfur-reduces and oxidizers microorganisms (Galdenzi & Maruoka, 2019).

Table 9. Stable sulfur isotopes of gypsum deposits in the studied hypogene SAS caves and comparison with some caves related to pyrite oxidation (Isotope ratios are reported in the conventional δ-notation with respect to V-CDT (Vienna Cañon Diablo Troilite).

State	Cave	$\delta^{34}S$ (‰)	Reference
SAS caves			
Austria	Kraushöhle	-23.12 to -15.83	Puchelt & Blum, 1989
France	Grotte du Chat	-9.4	Audra, 2007
Italy	Acqua Fitusa Cave	-1.0 to +4.4 and 10.2 to 10.6	De Waele et al., 2016
Italy	Montecchio Cave	-28.3 to -24.2	Piccini et al., 2015
Italy	Frasassi Cave	-24.24 to -7.53	Galdenzi & Maruoka, 2003
Italy	Mt. Sellaro caves	-10.44 to 0.882	Galdenzi & Maruoka, 2019
Italy	Cassano Caves	-28.75 to -21.04	Galdenzi & Maruoka, 2019
Italy	Terme Luigiane	-3.37 to 24.30	Galdenzi & Maruoka, 2019
Romania	Cerna valley caves	-27.9 to +19.2	Onac et al., 2011
Romania	Movile Cave	3.5 to 4.2	Sarbu & Kane, 1995
Macedonia	Provalata Cave	-2.3 to -1.9	Temovski et al., 2013
Russia	Kinderlinsk Cave	-23.51 to -13.85	Chervyatsova et al., 2016
Turkmenia	Cupp Coutunn Cave	9.0 to 15.6	Bottrell et al., 2001
New Mexico	Lechuguilla Cave	-25 to +5	Spirakis & Cunningham, 1992
New Mexico	Carlsbad Caverns	-19.3 to -15.00	Kirkland, 1982 and Hill, 1987
Arizona	Corkscrew Cave	-10.2 to -8.1	Onac et al., 2007
Mexico	Cueva de Villa Luz	-24.87 to -22.12; -11.7 (H_2S)	Pisarowicz, 1994; Hose et al., 2000
	Pyrite oxidation		
Wales	Cave Ogof Daren Cilau	-33.3 to -26.3	Bottrell, 1991
Italy	Buso della Rana-Pisatela	-33.2 to -29.5	Tisato et al., 2012
Alberta	Castleguard Cave	+14.2 to 22.6	Yonge & Krouse, 1987
Argentina	Las Brujas Cave	+5.4 to +9.6	Sancho et al., 2004

In addition, further sulfur stable isotopic analyses of mineralogical samples (sulfur, gypsum, and Al-Fe-sulfates) collected in several SAS systems of Italy (*Figure 21*) show peculiar distributions likely

induced by the interaction of hydrocarbon-related substances and deep-seated evaporites, comparable with the values of Triassic and Messinian evaporites, and bitumen deposits (*Figure 31*). The most negative values of sulfur have been detected in Santa Cesarea Terme (-32.3 to – 22.0 ‰), and are likely due to the BSR or DSR involving more hydrocarbon tiers respect to Triassic evaporites. Monte Cucco and Cassano allo Ionio caves present a wide range of sulfur stable isotopes. As demonstrated by D'Angeli et al. (2018), Monte Cucco showed phases of hypogene hydrothermal processes that probably influenced thermally the reduction of sulfates, in the same way as at Cerna Valley (Onac et al., 2011). The samples collected in Cassano allo Ionio caves showed more or less the same distribution as those described by Galdenzi & Maruoka, 2018, and can be thought to be related to Triassic evaporite reduction. Only one sample of gypsum collected in a recently (January 2016) discovered cave (called "Terme Sibarite Cave") located close to the present sulfuric water table recorded a positive value of 15.8‰.

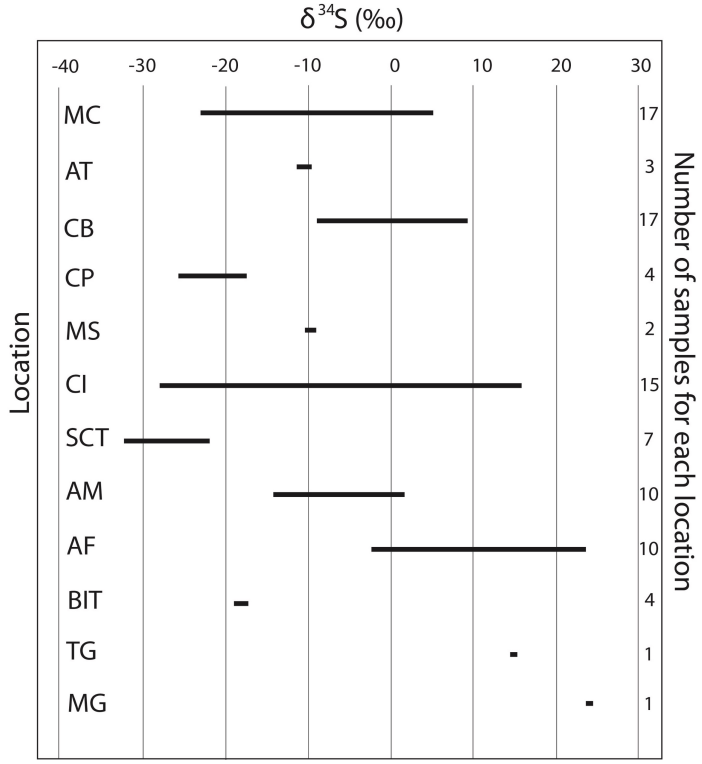

Figure 31. $\delta^{34}S$ values recorded in sulfur, gypsum and Al-Fe-sulfate deposits collected in several SAS systems of Italy (see Figure 21 for the location of cave systems). MC represents Monte Cucco caves (Umbria), AT Acquasanta Terme caves (Marche), CB Cavallone-Bove system (Abruzzo), CP Capo Palinuro (Campania), MS Monte Sellaro (Calabria), CI Cassano allo Ionio caves (Calabria), SCT Santa Cesarea Terme system (Apulia), AM Acqua Mintina Cave (Sicily), AF Acqua Fitusa Cave (Sicily), BIT represents deposits of bitumen collected in the Majella Massif area (Abruzzo), TG is the Triassic Gypsum from Pietre Nere in Apulia, and MG Messinian Gypsum from Sicily. The numbers on the right represent the number of samples analyzed for each location.

4.2. CO_2 and CH_4 concentration and carbon stable isotopes

As explained in paragraph 1.3 (reactions [1] and [2]), the production of H_2S can be associated with the presence of CO_2 and CH_4, which both are important greenhouse gases, able to control some reactions including the ones related to sulfuric acid speleogenesis. These two gases can have atmospheric or deep origin, and $\delta^{13}C$ isotopic investigations can aid to identify their sources and the mechanisms that influence their concentration in the environment. Fernández-Cortès et al. (2015), compared several epigene cave systems of Spain, and observed their subterranean atmosphere to behave as methane sinks. In contrast, Webster et al. (2017) tested the importance of hydrocarbon and methane in sulfuric acid speleogenesis, analyzing the concentration of CH_4, H_2S, and CO_2 (and also stable isotopes), in a special sulfuric cave, Cueva de Villa Luz. They observed very negative isotope signatures, estimated the values of feeding springs ($\delta^{13}C_{CH4}$ of -24±3‰ and $\delta^{2}H_{CH4}$ of -40±50‰) and the potential $\delta^{13}C_{CO2}$ end members of CO_2 by use of Keeling plots (Thom et al., 1993; Rey et al., 2012). Rising fluids enriched with hypogene CH_4 and CO_2 may contribute to enhance the concentration of greenhouse gases in the atmosphere, and for this reason the study of CH_4, CO_2 and H_2S content in sulfuric acid caves deserves further investigation, especially because geological carbon sources may complicate the measurement of the Earth's carbon balance (Rey et al., 2012).
As a matter of fact, only a few SAS caves have been studied in detail including Movile Cave (Sarbu et al., 1996; Hutchens et al., 2004), Frasassi caves (Jones et al., 2012), Cueva del Villa Luz (Webster et al., 2017), and Sulfur Cave (Sarbu et al., 2018). Gas/air samples can be collected employing in-situ techniques in which 1 L Tedlar bags are filled with air samples, and analyzed in laboratory using gas chromatography able to reveal the concentration of gas phases, and an isotope-ratio mass spectrometer (IRMS) to measure stable isotopes. Nevertheless, a new method has been developed to monitor greenhouse gases and measuring a variety of other isotopes: the cavity ring-down spectroscopy (O'Keefe & Deacon, 1998; Malowany et al., 2015).

For this study, cave atmosphere was monitored with a MSA Altair4x multigas detector (0-30±0.1 vol % for O_2, 0-100±1% LEL for CH_4, 0-20±0.1 ppm for SO_2, and 0-200±1 ppm for H_2S) (*Figure 32*A), to check for the presence of H_2S in three still-active SAS systems located in the southern Italy, in particular, Santa Cesarea Terme (Apulia) (*Figure 33*A), Cassano allo Ionio (*Figure 33B*) and Mt. Sellaro (Cerchiara di Calabria) (*Figure 33C*).
Several gas/air samples have been collected, with a portable pump and 1 LTedlar bags (*Figure 32B*), and then analyzed in the laboratory of the Museo Nacional de Ciencas Naturales, in Madrid, using a cavity ring-down spectroscopy Picarro 2201 able to measure CH_4 and CO_2 concentration and their respective stable isotopes.

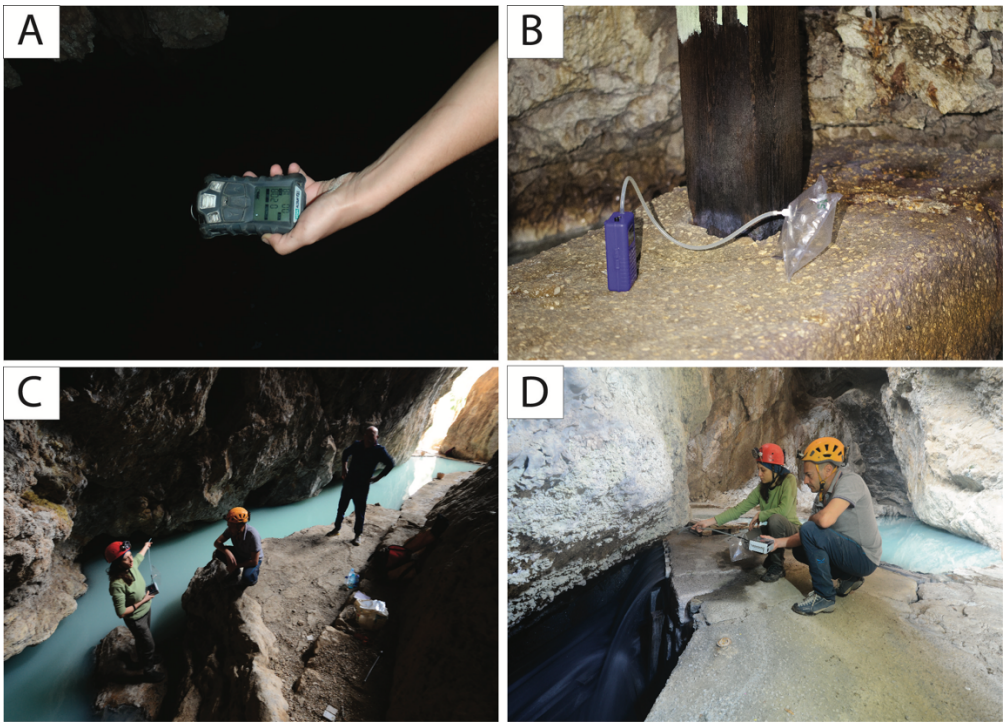

Figure 32. Gas/air sampling; A) MSA Altair4x multigas detector (photo of M. Parise); B) portable pump and 1L Tedlar bag (photo of O. Lacarbonara); C) and D) gas/air sampling of cave atmosphere in Ninfe Cave (Mt. Sellaro, Cerchiara di Calabria) (photos of M. Vattano).

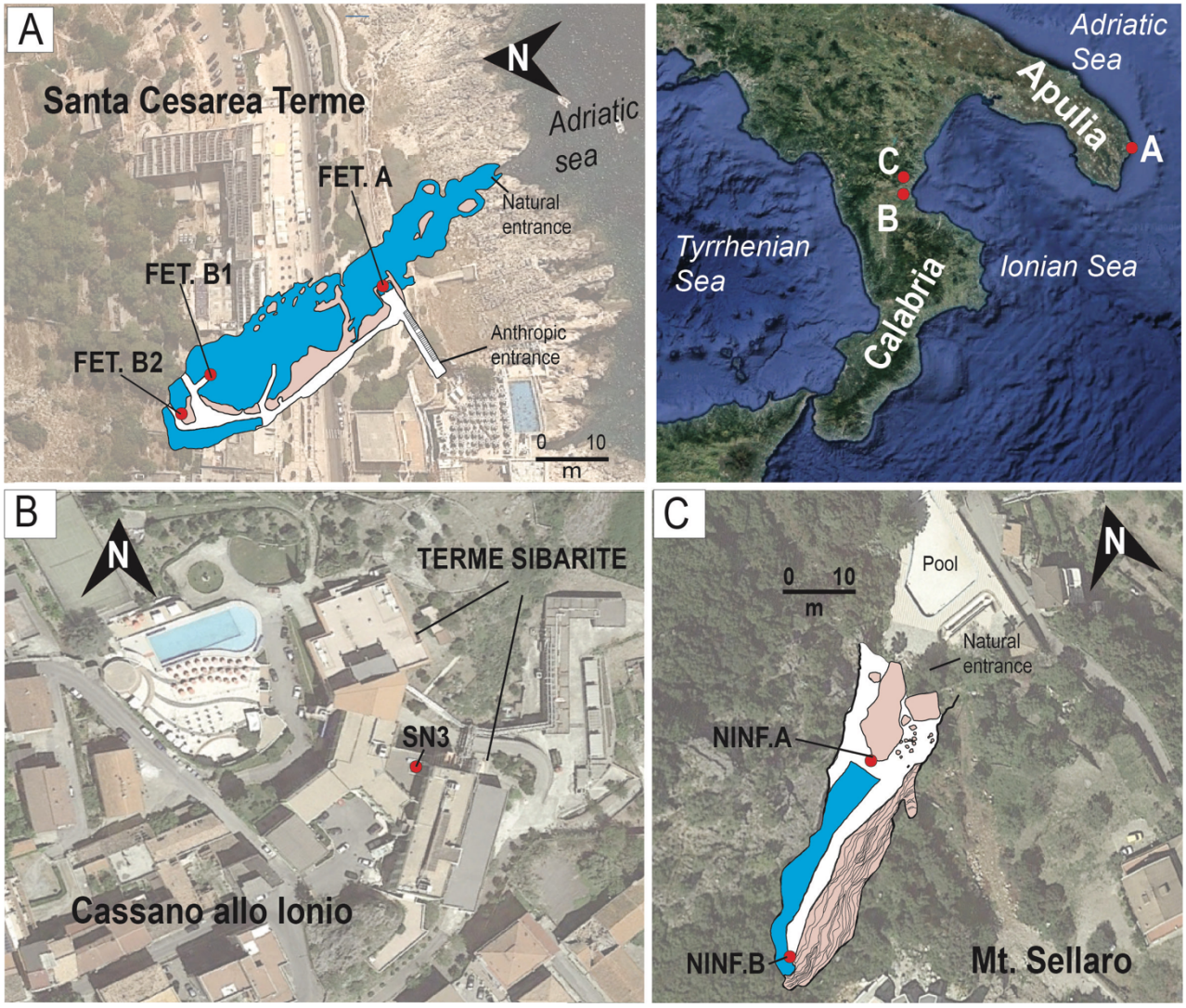

Figure 33. Setting of the gas/air sampling sites. A) Fetida Cave in Santa Cesarea Terme; B) Spring number 3 of Terme Sibarite, in Cassano allo Ionio; C) Ninfe Cave in Monte. Sellaro (Cerchiara di Calabria). The red points represent the sampling sites of gas/air monitoring.

MSA Altair4x multigas detector showed the concentration of O_2 to be 20.8 % during the whole monitoring, whereas H_2S and SO_2 are quite variable (*Table 10*). The concentration of CH_4 and CO_2 and their isotopic composition is reported in *Table 11*, and is compared with the values obtained from soil and external atmosphere.

In general, the H_2S ranges between 0.28 and 43.80 ppm. In Fetida Cave (Santa Cesarea Terme), the most interesting sampling site is FET.B1, where sulfidic rising waters are clearly observed. As a matter of fact, the H_2S concentration, here, is higher with respect to both FET.B2 (innermost portion of the cave) and FET.A (nearer to the entrances). The spring number 3, in Cassano allo Ionio also showed high H_2S values (10.9-12.8 ppm). Differently from Fetida Cave, in the Ninfe Cave, the H_2S degassing in the cave atmosphere is higher near to the natural entrance in NINF.A, because of the

presence of a waterfall, created to deviate the sulfidic water in the pool outside for human treatment, being these place a thermal spa.

Table 10. Concentration of SO_2 and H_2S in three still active SAS systems of southern Italy (Santa Cesarea Terme, Cassano allo Ionio, Monte Sellaro in Cerchiara di Calabria) during two different periods of monitoring. The sampling sites refer to Figure 33.

Santa Cesarea Terme						
	25/05/17			**08/06/17**		
FET. A	**SO_2 (ppm)**	**H_2S (ppm)**	**T(°C)**	**SO_2 (ppm)**	**H_2S (ppm)**	**T(°C)**
min	0.00	1.60	25.00	0.00	0.00	28.00
max	0.10	5.90	29.00	0.10	1.40	31.00
mean	0.02	3.32	27.74	0.05	0.28	29.36
median	0.00	2.90	29.00	0.00	0.10	29.00
FET. B1	**SO_2 (ppm)**	**H_2S (ppm)**	**T(°C)**	**SO_2 (ppm)**	**H_2S (ppm)**	**T(°C)**
min	0.00	2.30	28.00	0.00	0.60	30.00
max	0.10	15.40	28.00	0.10	6.90	30.00
mean	0.02	4.98	28.00	0.05	2.17	30.00
median	0.00	4.00	28.00	0.00	1.70	30.00
FET. B2	**SO_2 (ppm)**	**H_2S (ppm)**	**T(°C)**	**SO_2 (ppm)**	**H_2S (ppm)**	**T(°C)**
min	0.00	1.30	25.00	0.00	1.00	30.00
max	0.10	6.40	28.00	0.10	3.30	34.00
mean	0.01	2.85	27.88	0.06	2.32	32.61
median	0.00	2.40	28.00	0.10	2.30	32.00
Cassano allo Ionio						
	09/06/17			**05/05/18**		
SN3	**SO_2 (ppm)**	**H_2S (ppm)**	**T(°C)**	**SO_2 (ppm)**	**H_2S (ppm)**	**T(°C)**
min	0.00	0.00	29.00	0.1	1.8	25
max	0.20	12.80	33.00	0.2	10.9	26
mean	0.06	4.12	31.53	0.10	3.25	25.5
med	0.10	4.60	31.00	0.1	2.5	25.5
Cerchiara di Calabria (Mt. Sellaro)						
	09/06/17			**06/05/18**		
NINF.A	**SO_2 (ppm)**	**H_2S (ppm)**	**T(°C)**	**SO_2 (ppm)**	**H_2S (ppm)**	**T(°C)**
min	0.00	0.20	30.00	0.10	0.10	23.00
max	0.10	14.90	30.00	1.40	43.80	31.00
mean	0.06	4.56	30.00	0.20	8.80	26.77
median	0.10	4.70	30.00	0.10	2.80	28.00
NINF.B	**SO_2 (ppm)**	**H_2S (ppm)**	**T(°C)**	**SO_2 (ppm)**	**H_2S (ppm)**	**T(°C)**
min	0.00	0.00	30.00	0.10	0.90	23.00
max	0.20	15.20	37.00	0.10	32.70	24.00
mean	0.06	1.16	33.08	0.10	3.84	23.39
median	0.10	1.10	32.00	0.10	3.30	23.00

Table 11. Average values of concentration of CO_2 and CH_4 and their respective $\delta^{13}C$ from the sampling sites located in Santa Cesarea Terme (Apulia), and Cassano allo Ionio and Mt. Sellaro in Cerchiara di Calabria (Calabria). Tha gas/air sampling have been carried out both in cave atmosphere (FET.A, FET.B1, FET.B2, SN3, NINF.A, NINF.B) and at the external surface (atmosphere and soil) for comparison.

Apulia-Santa Cesarea Terme								
	08/06/17				07/05/18			
	CO_2 ppm	**$\delta\ ^{13}C_{CO2}$ (‰)**	**CH_4 ppm**	**$\delta\ ^{13}C_{CH4}$ (‰)**	**CO_2 ppm**	**$\delta\ ^{13}C_{CO2}$ (‰)**	**CH_4 ppm**	**$\delta\ ^{13}C_{CH4}$ (‰)**
External soil	5867.09	-20.48	0.70	-44.25	1415.44	-18.98	1.94	-49.16
External atmosphere	446.63	-10.97	2.01	-48.17	423.55	-93.75	1.98	-49.02
FET.A	478.89	-148.79	2.19	-46.26	464.07	-833.90	2.12	-46.85
FET.B1	536.80	-191.18	2.13	-45.39	503.86	-1197.00	2.10	-46.04
FET.B2	647.64	-82.91	2.06	-45.16	521.20	-803.25	2.16	-46.68
Calabria-Cassano allo Ionio and Cerchiara di Calabria (Mt. Sellaro)								
	09/06/17				05-06/05/2018			
	CO_2 ppm	**$\delta\ ^{13}C_{CO2}$ (‰)**	**CH_4 ppm**	**$\delta\ ^{13}C_{CH4}$ (‰)**	**CO_2 ppm**	**$\delta\ ^{13}C_{CO2}$ (‰)**	**CH_4 ppm**	**$\delta\ ^{13}C_{CH4}$ (‰)**
External soil	1903.91	-21.41	1.37	-43.46	2684.17	-48.75	1.36	-48.01
External atmosphere	440.61	-23.57	2.02	-47.20	446.99	-177.34	2.01	-49.25
SN3	729.98	-160.38	2.55	-41.95	658.93	-289.80	2.82	-28.63
NINF.A	973.33	-2005.89	16.82	-38.57	850.90	-2266.00	13.12	-32.73
NINF.B	535.83	-365.57	2.78	-43.57	512.65	-618.30	3.06	-41.74

In all these still-active stystems it is evident that the concentration of CO_2 and CH_4 is far greater in the underground environment than at the surface. The source of CO_2, as demonstrated by the very negative $\delta^{13}C_{CO2}$ isotopic values, clearly differs from the external surface (soil and atmosphere). CH_4 displays $\delta^{13}C_{CH4}$ isotopic values that are slightly more positive with respect to the surface.

Similarly to Cueva de Villa Luz (Webster et al., 2017), these isotopic values confirm that CH_4 and CO_2 are escaping from the rising sulfidic waters.

However, the values of $\delta^{13}C_{CO2}$ are extremely depleted with respect to ^{13}C, reaching -22.66‰ in NINF.A, during the monitoring occurred in May 2018. As described before, these gas/air samples have been analyzed using cavity ring-down spectroscopy (CRDS). Malowany et al. (2015), demonstrated this instrument to reveal some limitations and interferences in the near-infrared spectrum during the measurement of gas concentration and isotopes, especially in H_2S-rich

environments, e.g. in active volcanic habitats. In particular, H_2S interferes with CO_2 resulting in erroneous ^{13}C measurements, not only in volcanic centers, but also in sulfuric acid underground environments. H_2S provokes an increase in $^{12}C_{CO2}$ and resulting in evident depletetion of $\delta^{13}C_{CO2}$ values (Malowany et al., 2015).

For this reason, together with the team of Sergio Sanchez-Moral (Museo Nacional de Ciencas Naturales) studies in these three still-active systems will continue in order to perform further gas/air sampling. This time, the CRDS will be provided with a copper tube and copper fillings (see Malowany et al., 2015 *Figure 1*) able to immediately react with the H_2S, removing it from the gaseous phase, allowing the measurement of pure CO_2 and CH_4. Malowany et al., (2015) observed that a small content of H_2S (20 ppb) can cause a change in $\delta^{13}C_{CO2}$ of -0.5‰, and that H_2S interference is inversely proportional to the CO_2 concentration in the sample. In addition, they argued that there is no interference of H_2S with other common gaseous species such as H_2O, CH_4, or NH_3 at the atmospheric concentration, using a CRDS Picarro G1101-i.

Despite that, at high CH_4 concentrations (e.g. Fetida Cave, Spring number 3, and Ninfe Cave) likely a depletion of $^{13}C_{CH4}$ (in the same way of $^{13}C_{CO2}$) appears to exist, and consequently the $\delta^{13}C_{CH4}$ would be also slightly affected.

References

Audra, P., 2007. Karst et spéléologenèse épigènes, hypogenes, recherches appliquéès et valorization (Epigene and hypogene karst and speleogenesis. Operative research and valorization): Habilitation Thesis, University of Nice Sophia-Antipolis, 278 pp.

Bottrell, S.H., 1991. Sulphur isotope evidence for the origin of cave evaporites in Ogof v. Daren Cilau, South Wales. Mineralogical Magazine, 55(2); 209-210.

Bottrell, S.H., Crowley, S., Self, C., 2001. Invasion of a karst aquifer by hydrothermal fluids: evidence from stable isotopic compositions of cave mineralization. Geofluids, 1(2): 103-121.

Canfield, D.E., 2001. Biogeochemistry of Sulfur isotopes. Reviews in Mineralogy and Geochemistry, 43; 607–636.

Canfield, D.E., Thamdrup, B., 1994. The production of ^{34}S-depleted sulfide during bacterial disproportion of elemental sulfur. Science, 266: 1973-1975.

Canfield, D.E., Farquhar, J., Zerkle, A.L., 2010. High isotope fractionations during sulfate reduction in a low sulfate euxinic ocean analog. Geology, 38: 415-418.

Chervyatsova, O.Y., Potapov, S.S., Sadykov, S.A., 2016. Sulfur isotopic composition of sulfur deposits in Ural karst caves. News of the Ural State Mining University, 2: 37-41.

Cinti, D., Procesi, M., Tassi, F. Montegrossi, G., Sciarra, A., Vaselli, O., Quattrocchi, F., 2011. Fluid geochemistry and geothermometry in the western sector of the Sabatini Volcanic District and the Tolfa Mountains (Central Italy). Chemical Geology, 284: 160-181.

Cortecci, G., Klemm, D.D., Lattanzi, P., Tanelli, G., Wagner, J., 1983. A sulphur isotope study on pyrite deposits of southern Tuscany. Mineralogical Deposita, 18: 285-297.

Cortecci, G., Dinelli, E., Bencini, A., Adorni-Braccesi, A., La Ruffa, G., 2002. Natural and anthropogenic SO_4 sources in the Arno river catchment, northern Tuscany, Italy: a chemical and isotopic reconnaissance. Applied Geochemistry, 17: 79-92.

D'Angeli, I.M., Carbone, C., Nagostinis M., Parise M., Vattano M., Madonia G., De Waele, J., 2018. New insights on secondary minerals from Italina sulfuric acid caves. International Journal of Speleology, 47(3): 271-291.

De Waele, J., Audra, P., Madonia, G., Vattano, M., Plan, L., D'Angeli, I.M., Bigot, J.-Y., Nobécourt, J.-C., 2016. Sulfuric acid speleogenesis (SAS) close to the water table: Examples from southern France, Austria, and Sicily. Geomorphology, 253: 452-467.

Decker, D.D., Polyak, V.J., Asmerom, Y., 2015. Depth and timing of calcite spar and "spar cave" genesis: Implication for landscape evolution studies. Geological Society of America, GSA Special Publication, 516, Cave and Karst Acrossthe Time.

Decker, D.D., Polyak, V.J., Asmerom, Y., 2016. A supercritical CO_2 hypogene speleogenesis model: the origin of spar caves and cave spar in the Guadalupe Mountains, USA. National Cave and Karts Research Institute Deep Karts Symposium Proceedings, Carlsbad, New Mexico, USA.

Eckardt, F., 2001. The origin of sulphates: an example of sulphur isotopic applications. Progress in Physical Geography, 25(4): 512-519.

Fernandez-Cortes, A., Cuezva, S., Alvarez-Gallego, M., Garcia-Anton, E., Pla, C., Benavente, D., Jurado, V., Saiz-Jimenez, C., Sanchez-Moral, S., 2015. Subterrranean atmosphere may acta s daily methane sinks. Nature Communication, 6:7003. DOI: 10.1038/ncomms8003.

Fry, B., Ruf, W., Gest, H., Hayes, J.M., 1988. Sulfur isotope effects associated with oxidation of sulfide by O2 in aqueous solution. Chemical Geology, 73: 205-210.

Galdenzi, S., Menichetti, M., 1995. Occurrence of hypogenic caves in a karst region: examples from central Italy. Environmental Geology, 26: 39-47.

Galdenzi, S., Maruoka, T., 2003. Gypsum deposits in the Frasassi Caves, Central Italy. Journal of Cave and Karst Studies, 65: 111-125.

Galdenzi, S., Maruoka, T., 2019. Sulfuric acid caves in Calabria (South Italy): Cave morphology and sulfate deposits. Geomorphology, 328: 211-221.

Hill, C.A., 1981. Speleogenesis of Carlsbad Caverns and other caves in the Guadalupe Mountains. In: Beck, B.F. (Ed.), Proceedings of 8th International Congress of Speleology, Bowling Green, Kentucky, 1: 143-144.

Hill, C.A., 1987. Geology of Carlsbad Caverns and other caves in the Guadalupe Mountains, New Mexico and Texas. New Mexico Bureau of Mines and Mineral Resources Bulletin, 117: 1-150.

Hill, C.A., 1990. Sulfuric acid speleogenesis of Carlsbad Cavern and its relationship to hydrocarbons, Delaware Basin, New Mexico and Texas. American Association of Petroleum Geologists Bulletin, 74: 1685-1694.

Hose, L.D., Palmer, A.N., Palmer, M.V., Northup, D.E., Boston, P.J., DuChene, H.R., 2000. Microbiology and geochemistry in a hydrogen-sulphide-rich karst environment. Chemical Geology 169, 399-423.

Hutchens, E., Radajewski, S., Dumont, M.G., McDonald, I.R., Murrell, J.C., 2004. Analysis of methanotrophic bacteria in Movile Cave by stable isotope probing. Environmental Microbiology, 6(2): 111-120.

Jones, D.S., Albrecht, H.L., Dawson, K.S., Schaperdoth, I., Freeman, K.H., Pi, Yundan, Pearson, A., Macalady, J.L., 2012. Community genomic analysis of an extremely acidophiclic sulfur oxidizing biofilm. The ISME Journal, 6:158-170.

Kirkland, D.W., 1982. Origin of gypsum deposits in Carlsbad Caverns, New Mexico. New Mexico Geology, 4: 20-21.

Malowany, K., Stix, J., Van Pelt, A., Lucic, G., 2015. H_2S interference on CO_2 isotopic measurement using a Picarro G1101-I cavity ring –down spectrometer. Atmospheric Measurement Techniques, 8: 4075-4082.

O'Keefe, A., Deacon, D.A.G., 1998. Cavity ring-down optical spectrometer for absorpition measurements using plse laser sources. Review of Scientific Instruments, 59: 2544-2551. DOI:10.1063/1.1139895.

Ohmoto, H., Rye, R.O., 1979. Isotopes of sulfur and carbon, In: H.L., Barnes (Ed.), Geochemistry of Hydrothermal Ore Deposits, second ed. JohnWiley & Sons, 509–567.

Onac, B.P., Hess, J.W., White, W.B., 2007. The relationship between the mineral composition of speleothems and mineralization of breccia pipes: evidence from Corkscrew Cave, Arizona, USA. The Canadian Mineralogist, 45: 1177-1188.

Onac, B.P., Wynn, J.G., Sumrall, J.B., 2011. Tracing the source of cave sulfates: a unique case from Cerna Valley, Romania. Chemical Geology, 288: 105-114.

Piccini, L., De Waele, J., Galli, E., Polyak, V.J., Bernasconi, S.M., Asmerom, Y., 2015. Sulphuric acid speleogenesis and landscape evolution: Montecchio cave, Albegna river valley (Southern Tuscany, Italy). Geomorphology, 229: 134-143.

Pisarowicz, J.A., 1994. Cueva de Villa Luz - an active case of H_2S speleogenesis. In: I.D., Sasowsky, M.V., Palmer (Eds.), Breakthroughs in Karst Geomicrobiology and Redox Geochemistry. Karst Waters Institute, Special Publication ,1: 60–62.

Plan, L., Tschegg, C., De Waele, J., Spötl, C., 2012. Corrosion morphology and cave wall alteration in an Alpine sulfuric acid cave (Kraushöhle, Austria). Geomorphology, 169-170: 45-54.

Puchelt, H., Blum, N., 1989. Geochemische Aspekte der Bildung des Gipsvorkommens der Kraushöhle/Steiermark. Oberrheinische Geologische Abhandlungen 35, 87-99.

Sancho, C., Peña, J.L., Mikkan, R., Osácar, C., Quinif, Y., 2004. Morphological and speleothemic development in Brujas Cave (Southern Andean range, Argentine): palaeoenvironmental significance. Geomorphology, 57(3): 367-384.

Rye, R.O., 2005. A review of the stable-isotope geochemistry of sulfate minerals in selected igneous environments and related hydrothermal system. Chemical Geology, 215, 5-36.

Rey, A., Etiope, G., Belelli-Marchesini, L., Papale, D., Valentini, R., 2012. Geological carbon sources may confound ecosystem carbon balance estimates. Evidence from a semi-arid steppe in southern of Spain. Journal of Geophysical Research Biogesciences, 117(G03034).

Sarbu, S.M., Kane, T.C., 1995. A subterranean chemoautotrophically based ecosystem. NSS Bulletin, 57: 91-98.

Sarbu, S.M., Kane, T.C., Kinkle, B.K., 1996. A chemoautotrophically based cave ecosystem. Science, 272 (5270): 1953-1955.

Sarbu, S.M., Aerts, J.W., Flot, J.-F., Van Spanning, R.J.M., Baciu, C., Ionescu, A., Kis, B.M., Incze, R., Siko-Barabasi, S., Para, Z., Hegyeli, B., Atudorei, N._V., Barr, C., Nealson, K.H., Forray, F.L., Lascu, C., Fleming, E.J., Bitter, W., Popa, R., 2018. Sulfur Cave (Romania), an extreme environment with microbial mats in a CO_2-H_2S/O_2 gas chemocline dominated by mycobacteria. International Journal of Speleology, 47(2): 173-187.

Seal, R.R., 2006. Sulfur isotope geochemistry of sulfide minerals. Reviews in Mineralogy and Geochemistry, 61(1): 633-677.

Spirakis, C.S., Cunningham, K.I., 1992. Genesis of sulphur deposits in Lechuguilla Cave, Carlsbad Caverns National Park, New Mexico. In: Wessel, G., Wimberley, B. (Eds.), Native Sulphur - Developments in Geology and Exploration. American Institute of Mining, Metallurgical and Petroleum Engineers, Phoenix, AZ, 139-145.

Strauss, H., 1997. The isotopic composition of sedimentary sulfur through time. Palaeo, 132: 97-118.

Temovski, M., Audra, P., Mihevc, A., Spangenberg, J.E., Polyak, V., McIntosh, W., Bigot, J.Y., 2013. Hypogenic origin of Provalata Cave, Republic of Macedonia: a distinct case of successive thermal carbonic and sulfuric acid speleogenesis. International Journal of Speleology, 42: 235-246.

Thom, M., Bösinger, R., Schmidt, M., Lavin, I., 1993. The regional budget of atmospheric methane of a highly populated area. Chemosphere, 26: 143-160.

Tisato, N., Sauro, F., Bernasconi, S. M., Bruijn, R. H., De Waele, J., 2012. Hypogenic contribution to speleogenesis in a predominant epigenic karst system: a case study from the Venetian Alps, Italy. Geomorphology, 151: 156-163.

Yonge, C.J., Krouse, H.R., 1987. The origin of sulfates in Castleguard cave, Columbia Icefields Canada. Chemical Geology, 65: 427-433.

Zerkle, A.L., Jones, D.S., Farquhar, J., Macalady, J.L., 2016. Sulfur isotope values in sulfidic Frasassi cave system, central Italy: A case of a chemolithotropic S-based ecosystem.

Zerkle, A.L., Kamyshny, A., Kump, L.R., Farquhar, J., Oduro, H., Arthur, M.A., 2010. Sulfur cycling in a stratified euxinic lake with moderately high sulfate: constraints from quadruple S isotopes. Geochimica and Cosmochimica Acta, 74: 4953-4970.

Webster, K.D., Lagarde, L.R., Sauer, P.E., Schimmelmann, A., Lennon, J.T., Boston, P.J., 2017. Isotopic evidence for the migration of themogenic methane into a sulfidic cave, Cueva de Villa

Luz, Tabasco, Mexico. Journal of Cave and Karst Studies, 79(1): 24-24. DOI:10.4311/2016ES0125.

5. GEOMICROBIOLOGY

5.1. Sulfuric acid signature in active environments

From an overall point of view, the fluids interacting in SAS caves are, at least in part, derived from a deep (hypogenic) source. As explained in the earlier chapters, these fluids are enriched with H_2S that interacts with oxygenated water in the surficial parts of the karst systems (1 in *Figure 2),* leading to the formation of sulfuric acid that reacts with the carbonate host rock. If the origin of these rising waters is deep enough, these fluids will also be thermal, as documented in many active SAS caves (e.g. Aquasanta Terme, Italy, Galdenzi et al., 2010; Fusari et al., 2017; Montecchio Cave, Tuscany, Italy, Piccini et al., 2015; Chevalley Aven and Serpents Cave, France, Audra et al., 2007; Cerna Valley caves, Romania, Wynn et al., 2010, Onac et al., 2011), but this is not necessarily the case (e.g. Frasassi cave, Italy, Galdenzi et al., 2008; Galdenzi, 2012). Often, this thermality is rather weak, such as at Movile Cave (Romania), where waters are only 8°C warmer than the mean annual temperature (Sarbu & Kane, 1995), or Cueva de Villa Luz where they are only 5°C warmer (Hose et al., 2000).

In general, the active SAS systems are characterized by circumneutral pH (~7, due to the buffering effect of carbonate host rock) and Ca-Cl-SO_4 or Na-Cl-SO_4 waters (Hose & Pisarowicz, 1999; Hose et al., 2000; Grassa et al., 2006; Vespasiano et al., 2016; Santaloia et al., 2016; D'Angeli et al., 2017b) with variable contents of dissolved H_2S. Waters rich in H_2S have a typical rotten-egg smell and milky appearance (due to elemental sulfur) (*Figure 32C*). Commonly, they are abundantly colonized by white biofilms (Engel et al., 2004; Imhoff, 2006; Hamilton et al., 2015) dominated by chemolithoautotrophic sulfide-oxidizing microorganisms (Hose et al., 2000; Macalady et al., 2008), which demonstrated their important role in sulfide oxidation, it being an essential energetic source for their metabolism (Zerkle et al., 2016). If the concentration of $H_2S(g)$ is high enough, its degassing in cave atmosphere produces the formation of peculiar vermiculation deposits exhibiting a widespread range of colors and shapes (Hose & Northup, 2004; Jones et al., 2008; D'Angeli et al., 2017a), white pastry materials (i.e., moonmilk), mucolites and snottites as well (Galdenzi et al., 1999b; Hose et al., 2000; Galdenzi and Maruoka, 2003, Macalady et al., 2007) can abundantly colonize walls and ceilings.

5.2. Article 3

Submitted to PLoS one

Geochemistry and geomicrobiology of a seawater-influenced active sulfuric acid cave in Santa Cesarea Terme.

Ilenia M. D'Angeli[a*], Daniele Ghezzi[b*], Stefan Leuko[c], Mario Parise[d], Adriano Fiorucci[e], Bartolomeo Vigna[e], Rosangela Addesso[f], Daniela Baldantoni [f], Cristina Carbone[g], Ana Zelia Miller[h], Valme Jurado[h], Cesareo Saiz-Jimenez[h], Andrea Firrinceli[i], Jo De Waele[a§], Martina Cappelletti[b*§]

[a]Department of Biological, Geological and Environmental Sciences, University of Bologna, Italy, dangeli.ilenia89@gmail.com; jo.dewaele@unibo.it;

[b]Department of Pharmacy and Biotechnology, University of Bologna, Italy, daniele.ghezzi11@gmail.com; martina.cappelletti2@unibo.it;

[c]DLR Deutsches Zentrum für Luft- und Raumfahrt Institute of Aerospace Medicin Radiation Biology, Köln, Germany, stefan.leuko@dlr.de;

[d]Department of Geological and Environmental Sciences, University of Bari Aldo Moro, Italy, mario.parise@uniba.it;

[e] Department of Territorial Engineering, of the Environment and of Geotechnologies, Politechnical University of Turin, Corso Duca degli Abruzzi 24, 10129 Torino, Italy, adriano.fiorucci@polito.it, bartolomeo.vigna@polito.it;

[f] Department of Chemistry and Biology "Adolfo Zambelli", University of Salerno, Via Giovanni Paolo II, 132, 84084 Fisciano (SA), Italy, addros04@gmail.com; dbaldantoni@unisa.it

[g] DISTAV, Department of Geological, Environmental and Biological Sciences, University of Genoa, Italy, carbone@dipteris.unige.it

[h] Instituto de Recursos Naturales y Agrobiología, IRNAS-CSIC, 41012 Sevilla, Spain, anamiller@irnas.csic.es; vjurado@irnase.csic.es; saiz@irnase.csic.es;

[i] Department for Innovation in Biological, Agro-food and Forest systems, University of Tuscia, Via S. Camillo de Lellis snc, 01100 Viterbo, Italy, e-mail: andres.firrincieli@gmail.com;

[*] Corresponding authors

[§] Both authors share senior status

5.2.1. Abstract

Fetida Cave is a still-active sulfuric acid cave influenced by seawater hydrodynamics, showing abundant microbial communities that organize themselves in collective structures within three

types of microbial-rich deposits, white filaments (-WF/SF), vermiculations (-V) and moonmilk (-M). Moonmilk deposits are composed of gypsum and show extremely acidic pH (0-1), whereas vermiculations present a widespread range of colors influenced by mineralogy and elemental contents. White filaments abundantly colonize water pools of the whole cave. The Illumina sequencing analysis revealed that the microbial communities of these three types of deposits to be highly diversified. White filaments are generally composed of members of *Gamma-*, *Delta-*, *Alphaproteobacteria* and *Bacteroidetes, but also Epsilonproteobacteria* (mainly *Campylobacterales*) and *Chloroflexi* are abundant. Vermiculations showed highly diverse microbial communities composed of *Alpha-*, *Beta-*, *Delta-, Gammaproteobacteria*, *Planctomycetes, Acidobacteria*, and *Chloroflexi,* many of them being possibly associated to chemolithotrophic and biomineralization activities. In contrast, moonmilk shows low microbial diversity and dominance of archeal sequences related to the *Euryarchaeota Thermoplasma* genus.

This work describes for the first time the microbial communities hosted in Fetida Cave and point outs the importance of seawater hydrodynamics in geochemical and microbiological cycles within a still-active sulphuric acid cave.

Keywords: sulfuric acid cave; sulfide-rich waters; marine cave habitat; vermiculation; moonmilk; streamer biofilm

5.2.2. Introduction

Caves provide a unique portal into the deep subsurface habitat, which is typically characterized by relatively stable environmental conditions, absence of light and low nutrient supply (Tomczyk-Żak and Zielenkiewicz, 2015; Leuko et al., 2017). Several studies indicated that microbes sustain cave ecosystems by dominating primary production and fueling biogeochemical cyclings (Lavoie et al., 2010). Chemolithotrophic microbial activities, which support chemosynthetic primary production in deep isolated caves, involve the oxidation of methane, manganese, iron, inorganic hydrogen, nitrogen, and sulfide (Northup and Lavoie, 2001; Lavoie et al., 2010; Jones and Macalady, 2016). Additionally, microbial cave life can also depend on small inputs of organic carbon, transported into the underground through percolating waters, air circulation and fauna. To survive in these nutrient-poor environments, microorganisms have been shown to organize themselves into collective structures, offering cooperation and mutualistic relationships and producing, as results of their interaction, biosignatures (Boston et al., 2001). In this context, underground environments have attracted wide attention because of the peculiar metabolic processes, the interesting mutual interactions,

and the relationship between microorganisms and minerals (Whitman et al., 1998; Boston et al., 2001; Lavoie et al., 2010; Riquelme et al., 2015; Tisato et al., 2015). Several studies have demonstrated the strong influence of mineralogy and elemetal composition on subsurface microbial diversity (Miller et al., 2018), but also microbial activity has been shown to have an impact on the mineral formations and cave speleogenesis (Engel et al., 2004; Jones et al., 2010; Miller et al., 2012).

Hypogene underground karst systems, because of their limited interaction with infiltrating surface waters (Forti et al., 2002; Klimchouk, 2017), are extremely interesting locations to search for microbial life (Mansor et al., 2018), and in particular, caves that have been formed by sulfuric acid speleogenesis (SAS) have been shown to host novel and unusual biosignatures (Hose et al., 2000; Boston et al., 2001; Jones and Macalady, 2016). SAS caves (Klimchouk, 2017; D'Angeli et al., 2018) are related to the upwelling of acidic sulfide-rich waters that oxidize, producing sulfuric acid (H_2SO_4) (see reaction 1) (Egemeier, 1981; Hill, 2000; Galdenzi, 1990; Jagnow et al., 2000). The hydrogen sulfide (H_2S) oxidation can occur: i) where deep and shallow water mix, or ii) where sulfidic water reaches the cave environment (Galdenzi, 1990; Engel et al., 2004; De Waele et al., 2016). SAS caves are very abundant in carbonates, mainly because the dissolution of CO_3^{2-} caused by sulfuric acid (see reaction 2) is rapid, and immediately induces the replacement of the host rock by gypsum and the release of carbonic acid in the atmosphere.

1. $H_2S + 2O_2 \Leftrightarrow H_2SO_4$ ($SO_4^{2-} + 2H^+$ in aqueous solution)
2. $CaCO_3 + SO_4^{2-} + 2H^+ + 2H_2O \Rightarrow CaSO_4 \cdot 2H_2O + CO_2 + H_2O$

The oxidation of H_2S provides an important energy source for sulfur oxidizing microorganisms, and their chemosynthetic activity can contribute to heterotrophic organism growth (Jones et al., 2008, 2010). The biological oxidation of H_2S also generates local acidity able to contribute to the dissolution of carbonate rocks, favoring speleogenesis (Engel et al., 2004).

Extensive microbiological studies have been carried out in Frasassi and Acquasanta Terme caves (Galdenzi, 1990; Galdenzi and Menichetti, 1995; Galdenzi et al., 2000; Galdenzi 2004a,b), because they have been shown to typically host conspicuous water streamers, and viscous snottites, ragu-like deposits, and vermiculations (Jones and Macalady, 2016) covering walls and ceilings. Among these, the microbial diversity of the water streamers has been the most extensively studied through molecular methods (16S rRNA clone library) and microscopy and culture-based experiments (Hose and Pisarowicz, 1999; Hose et al., 2000, Engel et al., 2004; Hamilton et al., 2015). *Gamma*-, *Beta*- and *Epsilonproteobacteria*-related sulfur-oxidizing microorganisms were generally shown to dominate the water streamers (Macalady et

al., 2006). Snottites (Pisarowicz, 1994) are extremely acidic biofilms growing on hanging gypsum walls and hosting low microbial diversity composed of a few species of acidophilic bacteria and archaea (Vlasceanu et al., 2000; Macalady et al., 2007). The snottites and vermiculations documented in Frasassi caves showed high abundance of sulfur-oxidizers (Macalady et al., 2007; Jones et al., 2008). The study of Jones et al. (2008) regarding the geomicrobiology of vermiculations reported a wide biodiversity including members of *Betaproteobacteria*, *Gammaproteobacteria*, *Acidobacteria*, *Nitrospirae* and *Planctomycetes*.
The purpose of this work is to describe for the first time the microbial population thriving in Fetida Cave, a still-active SAS cave (D'Angeli et al., 2017; Zuffianò et al., 2018), influenced by seawater hydrodynamics, and located in southeastern Salento (Apulia region, S-Italy), in the municipality of Santa Cesarea Terme (Italy) (Fig.1). Fetida Cave hosts water streamers floating (-WF) or accumulated on the water stream bed (-SF), and brown and grey vermiculations (-Vb, -Vg) and moonmilk deposits (-M).

5.2.2.1. Geographical and geological setting

Fetida is a 150-meter-long cave, partially submerged, and entirely carved in the "Calcari di Altamura Fm." (Pieri et al., 1997; Amato et al., 2014) following a NW-SE regional lineament. It consists of a main stream characterized by a mixture of seawater and H_2S-rich upwelling fluids; moving from the entrances (Site A) to the inner portion (Site B), the marine influence decreases and the effect of rising acidic H_2S waters increases (*Figure 34*). Both sites (A and B) are affected by tidal fluctuations (±0.7 m), deeply controlling the behavior of upwelling fluids and, consequently, the concentration of H_2S in the cave atmosphere and water. Additionally, site B has been divided into two portions: B1 (middle-inner zone) and B2 (innermost zone); in B1 we have localized a spring of H_2S-rich rising fluids (*Figure 34*). At the present-day, seawater and rising fluids never reach walls and ceilings, whose are wetted only by degassing vapor enriched with H_2S. The source of the H_2S-rich fluids has not yet been identified, but is thought to derive from the reduction of either: 1) deep-seated Triassic evaporites (Galdenzi, 1990; 2004a), 2) hydrocarbons (Maggiore and Pagliarulo, 2004; Velaj, 2015), 3) organic matter in the carbonate rocks (Calò and Tinelli, 1995), 4) reduction of sulfate contained in seawater, or 5) complex interactions between heated seawater and deep-seated evaporite rocks (Santaloia et al., 2016).

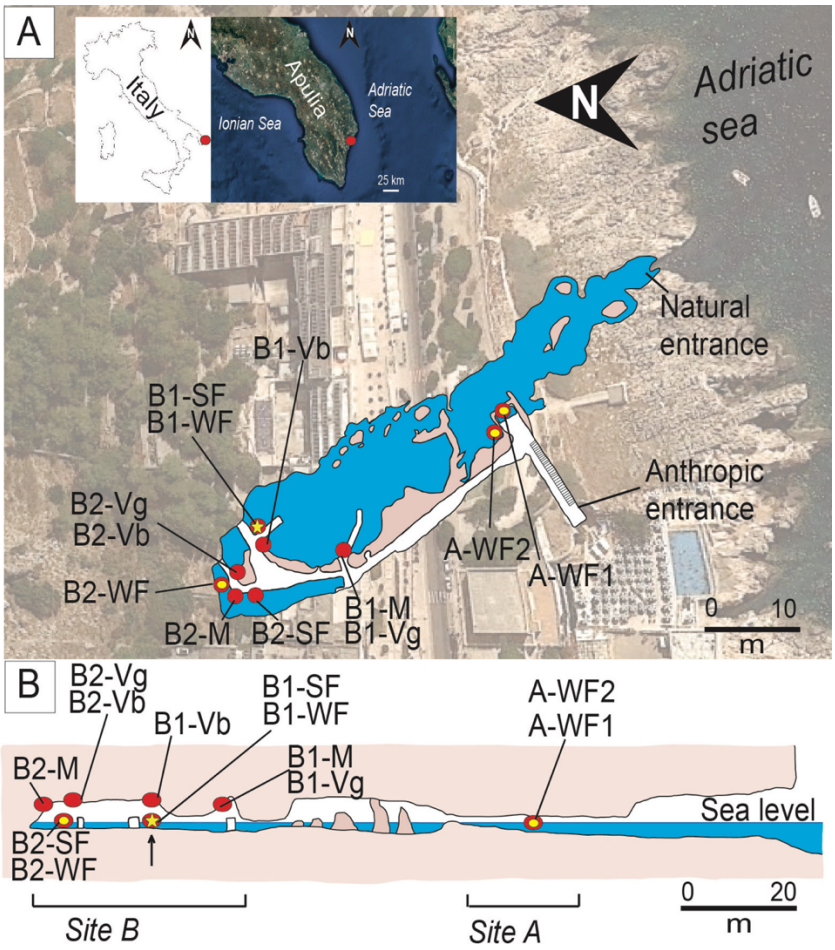

Figure 34. A) Location of Fetida Cave in Santa Cesarea Terme, Salento (SE Italy) and planimetry of the cave. The cave opens along the Adriatic coastline following a NW-SE direction. The sampling points are highlighted along the cave planimetry; B) Cross-section of Fetida Cave and samples collected in the two sites A (mainly influenced by seawater) and B (dominated by rising acidic waters). The survey has been provided thanks to the Vigor Project.

5.2.3. Material and methods

5.2.3.1. Sample description and collection

Three types of microbial-rich deposits were visible in Fetida Cave and some representative samples were collected to characterize the microbial diversity (site A is colonized exclusively by water streamers). Twelve samples (sampling spots displayed in *Figure 34* and described in *Table 12*) were collected aseptically for DNA-based analyses and transferred into falcon tubes filled with 5 ml of RNAlater during two sampling campaigns (October 2015 and December 2017) to preserve them and stored 5-6 hs at room temperature, 24hs at -20°C, and at -80°C until the DNA extraction. The aim was the understanding of microbial diversity and population to clarify their respective relationship with mineralogical and geochemical content.

In particular, i) four samples of water streamers floating and/or rock-attached to submerged rocks (A-WF1, A-WF2, B1-WF, B2-WF) were collected during periods of low tide (*Figure 35*A,B), ii) two samples of water streamers accumulated on the water stream floor up to 1 m from the water table during low tide (B1-SF, B2-SF) (*Figure 35*C), iii) two samples of white pasty moonmilk deposits (B1-M, B2-M) (*Figure 35*D), iv) two samples of greyish vermiculations (B1-Vg, B2-Vg) (*Figure 35*E), v) two brownish vermiculations (B1-Vb, B2-Vb) (*Figure 35*F).

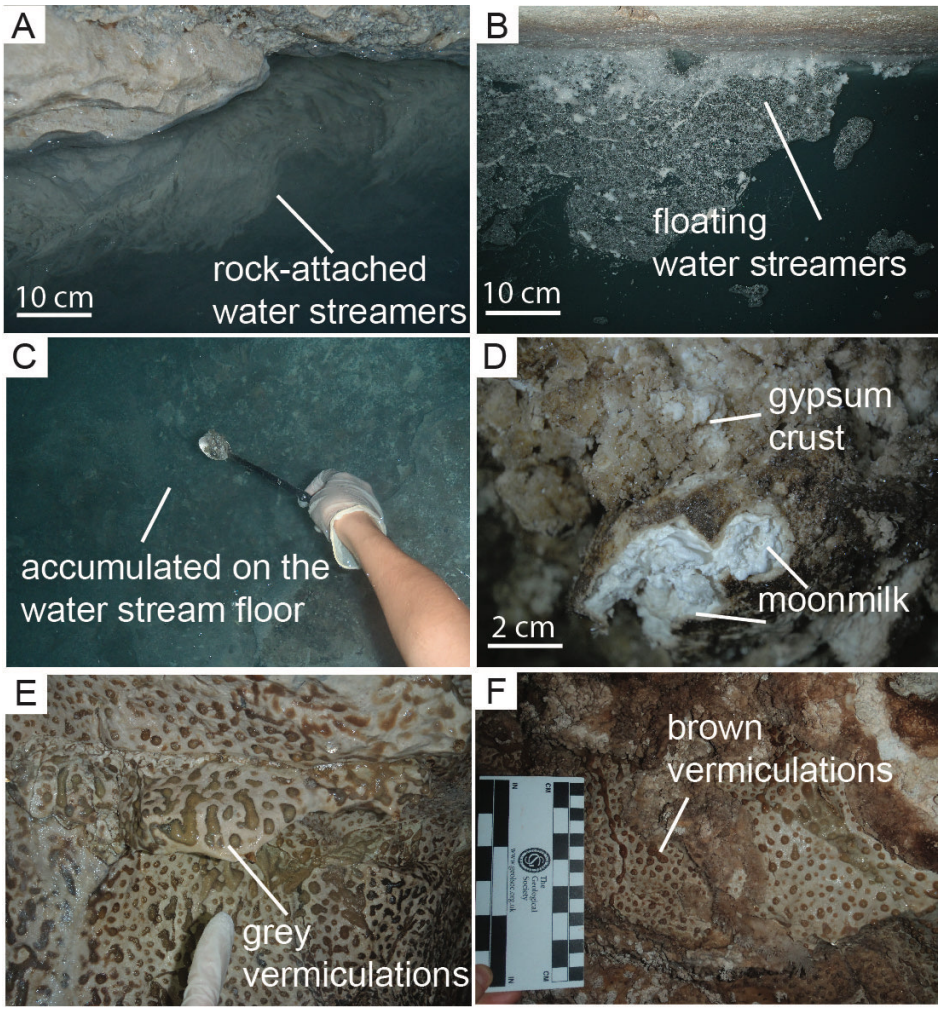

Figure 35. Field pictures of the most representative biofilms observed in Fetida Cave. A) White filaments attached to the submerged rocks (A-WF1, A-WF2); B) White filaments floating in the water (B1-WF, B2-WF); C) filaments accumulated on the water stream floor (B1-SF, B2-SF); D) White pasty moonmilk (B1-M, B2-M), surrounded by hard whitish gypsum crusts; E-F) Greyish (B1-Vg, B2-Vg) and brownish (B1-Vb, B2-Vb) vermiculations thriving on walls and ceiling.

Table 12. List of the description and the cave site of the samples collected for microbiological analysis.

Sample name	Cave Site	Description

A-WF1	A	White slimy filaments collected from a squared water pool located at the end of the anthropic staircase
A-WF2	A	White slimy filaments in the water stream behind an anthropic window
B1-WF	B	White slimy filaments floating on water close to the point of evident rising sulfidic fluids in the middle-inner zone
B1-SF	B	Sedimented white filaments at the bottom of the water stream in the middle-inner zone
B2-WF	B	White slimy filaments floating on water in the innermost zone
B2-SF	B	Sedimented white filaments at the bottom of the water stream in the innermost zone
B1-Vb	B	Brown vermiculation taken from the wall at 1.60 m height from the boardwalk in the middle-inner zone
B1-Vg	B	Grey vermiculation deposit collected on the wall at 1.90 m height from the boardwalk in the middle-inner zone
B2-Vb	B	Brown vermiculation taken from the wall at 1.50 m height from the boardwalk in the innermost zone
B2-Vg	B	Grey vermiculation taken from the wall at 1.70 m height in the innermost zone of the cave
B1-M	B	Moonmilk deposit sampled on the wall at 1.70 m height from the boardwalk in the middle-inner zone
B2-M	B	Moonmilk deposit sampled from the wall at 1.70 m height from the boardwalk in the innermost zone

5.2.3.2. Geochemistry

Microbiological samples were collected also for elemental analyses carried out at the University of Salerno (Italy). Each sample was oven-dried at 75°C until constant weight was obtained, and was then manually ground with a porcelain mortar and pestle. Total and organic C and N content were determined on triplicate samples with a CHSN-O Gas Chromatography Flash EA 1112 (Thermo Fisher Scientific Inc. Waltham, MA, USA). Organic C was measured removing carbonates using 37% HCl and distilled water (1:1= v:v). Moreover, the concentration of Ca, Co, Cu, Fe, K, Mg, Mn, Na, P, and Zn was determined in triplicate with a PerkinElmer Optima 7000 DV ICP-OES. Prior to the determination of trace elements, samples (125 mg) were subjected to microwave mineralization in a Milestone Microwave Laboratory Systems (mls 1200, Shelton, CT, USA) by a combination of 50% HF and 65% HNO_3 (1:2 = v:v), and addition of deionized water after sample digestion. Standard Reference Material (Mackey et al., 2004) was used to evaluate the analytical accuracy. The pH values of the three type samples were measured in situ with litmus papers (range 0-14).

5.2.3.3. Morphology and Mineralogy

Water streamers (-WF), vermiculation (-V) and moonmilk (-M) deposits were examined by Field Emission Scanning Electron Microscopy (FESEM) combined with Energy Dispersive X-ray spectroscopy (EDX) for assessing crystal morphology, surface topography, elemental composition and detection of microbial structures. Previously, samples were fixed with 2.5% glutaraldehyde in 0.1 M cacodylate-buffer (pH 7.4) at 4 °C for 2 h and washed in cacodylate-buffer. Subsequently, they were postfixed in 1% osmium tetroxide for 1 h at 4 °C and dehydrated by subsequent dilution series in ethanol and acetone finishing with 100% acetone before drying. The samples were then dried in a critical point drying device (Leica EM 300) at 34.5 °C. Finally, the fixed samples were observed

using a FEI TENEO microscope equipped with an Ametek EDAX detector at the University of Seville. The mineralogical composition of moonmilk and vermiculations was determined in the laboratories of the University of Genoa (Italy) using a Philips PW3710 diffractometer (current 20mA, voltage 40 kV, range 2θ 5-80°, step size 0.002° 2θ, time per step 2 sec) equipped with a Co-anode and interfaced with a Philips High Score software package for data acquisition and processing.

5.2.3.4. DNA extraction and Illumina sequencing data analysis

Total DNA was extracted from the deposits shown in *Figure 34* using the PowerSoil extraction kit (MoBIO) according to the manufacturer's protocol. Briefly, 0.3 g of sample was employed and DNA was extracted using a combination of bead-beading and lysis buffer. DNA was eluted into a final volume of 50 µL of C6 eluted buffer. The extracted DNA (ranging from 22.7 to 54.33 ng/µl) was used as template for PCR amplification targeting the V4 region of the 16S rRNA gene using the primers 515F (5'GTGCCAGCMG-CCGCGGTAA'3) and 806R (5' GGACTACHVGGGTWTCTAAT'3) (Caporaso et al., 2010) modified with an Illumina adaptor sequence at the 5' end. Samples were submitted to Illumina MiSeq next-generation sequencing platform for indexing and pair-end sequencing (2x250 bp; reagent kit, v2) at the University of Graz. Reads were analyzed using the DADA2 package version 1.5.0 and workflow (35) in R version 3.1.2 (http://www.R-project.org). Taxonomic assignment has been performed by querying the sequence reads against a SILVA SSU 128 reference database (Quast et al., 2013). Diversity indices, richness estimations and Unifrac PCoA were analyzed using core-matrix-phylogenetic plugins on QIIME2 software. Clustering and nMDS analyses were performed using Primer-E v7 based on Bray-Curtis Distance Matrix. Sequenced data were deposited in NCBI Sequence Read Archive (SRA) with the submission number PRJNA494546.

5.2.3.5. Prediction of metagenomic content in white filaments, vermiculations, and moonmilk

Sequence variance (SV) abundance table and the corresponding SV representative sequences were used for metagenomics content prediction in Piphillin with default parameters (Iwai et al., 2016). Differentially abundant KEGG Orthologue (KO) between white filaments, vermiculations, and moonmilk were determined using linear discriminant analysis (LDA) effect size (LEfSe) (Segata et al., 2011) according to LDA score of ≥ 2.0 and P-value < 0.05.

5.2.4. Results and discussion

5.2.4.1. Morphology, geochemistry and mineralogy of the biofilm samples

Elemental analyses have been carried out on nine of the twelve microbiological samples. They exhibit very characteristic contents in N, C (*Table 13*) and Na, K, Ca, Mg, Fe, Mn, P, Co, Cu, and Zn (*Table 14*).

Table 13. Mean values of the three replicates for total N, C, and organic and inorganic C (% dry weight) in white filaments, vermiculations, and moonmilk.

Sample	N tot (%d.w.)	C org (%d.w.)	C inorg (%d.w.)	C tot (%d.w.)
A-WF1	0.05±0.03	1.19±0.07	0.23±0.14	1.42±0.13
A-WF2	0.86±0.03	4.81±0.17	0.2±0.06	5.01±0.11
B1-WF	2.07±0.10	11.05±3.34	0.84±0.34	11.89±0.40
B1-SF	0.51±0.03	3.75±0.40	5.57±0.14	9.32±0.31
B2-WF	2.1±0.15	11.38±0.54	0.8±0.10	12.18±0.60
B1-Vb	0.97±0.02	7.21±0.42	0.00	7.12±0.18
B2-Vb	0.97±0.04	7.39±1.05	0.00	7.36±0.44
B2-Vg	0.31±0.04	2.34±0.19	0.00	2.32±0.13
B2-M	0.00	0.14±0.05	0.04±0.38	0.19±0.01

Table 14. Mean values of the three replicates for total Na, K, Ca, Mg, Mn, Fe, P, Co, Cu, and Zn (µg/g) in the white filaments, vermiculations, and moonmilk.

Sample	Na	K	Ca	Mg	Fe	Mn	P	Co	Cu	Zn
A-WF1	231.41±19.32	43.87±0.89	1.79±0.20	5.48±0.54	0.04±0.01	0.00	0.27±0.09	0.07±0.02	1.37±0.22	0.00
A-WF2	192.31±10.87	37.25±3.95	2.91±0.38	5.63±0.41	0.29±0.05	0.01±0.00	0.86±0.08	0.26±0.01	18.99±1.41	0.33±0.03
B1-WF	93.15±7.57	41.40±3.44	8.40±0.28	4.31±0.12	3.44±0.22	0.11±0.01	3.31±0.38	2.51±0.22	26.74±2.60	0.04
B2-WF	101.37±5.16	28.63±1.55	6.59±0.43	2.26±0.67	2.88±0.17	0.10	2.52±0.12	1.93±0.10	36.55±3.06	0.03
B1-SF	60.42±7.09	28.13±5.09	25.04±1.42	2.26±0.67	2.14±0.18	0.12±0.01	1.23±0.15	2.05±0.32	30.63±4.92	0.10±0.02
B1-Vb	2.13±0.47	14.85±1.64	41.28±1.11	15.71±0.55	36.97±2.16	1.37±0.12	8.73±1.08	19.61±1.71	58.89±8.45	0.14±0.01
B2-Vb	1.81±0.41	10.53±0.04	51.13±4.77	7.49±0.73	19.14±0.10	0.84±0.06	9.24±0.93	9.50±0.48	51.42±4.04	0.09±0.01
B2-Vg	2.80±0.03	52.28±9.72	6.97±1.13	4.00±0.60	9.72±1.90	0.19±0.03	1.74±0.38	6.87±1.33	25.72±2.92	0.07±0.01
B2-M	0.05±0.04	0.08±0.06	1.56±0.05	0.03±0.00	0.01±0.01	0.00	0.04±0.04	0.00	0.63±0.26	0.00

The water streamers in site A show significant geochemical differences than the ones in site B. The B1-WF and B2-WF samples display the most abundant values of N, organic C, Ca, Fe, Mn, P, Co, Cu, whilst A-WF1 and A-WF2 are dominated especially by Na, Mg and Zn, likely due to seawater influence. The streamers accumulated on the water floor (B1-SF) present high concentrations in inorganic C, Ca, and Cu. Their pH ranges between 6.9 and 7.5 (depending on water-pH). Interesting is also the difference between brownish (B1-Vb, B2-Vb) and greyish (B2-Vg) vermiculations, and moonmilk (B2-M) deposits. Moonmilk totally lacks N, and is poor in almost all the elements.

Water streamers in site B, and vermiculation deposits present comparable contents of C, N, and P (only for vermiculations) to those previously described for similar deposits collected from Grotta Sulfurea in the Frasassi cave system (i.e., stream biofilms GS06-15, and vermiculations GS04-58, GS06-31, respectively) by Jones et al. (2008). This elemental analysis adds information on the similarities between the two sulfuric acid cave systems (Santa Cesarea Terme and Frasassi), in spite of the different geological and geographical locations.

Mineralogical investigations carried out on moonmilk and vermiculation deposits (*Table 15*), demonstrated their mineral content strongly influence their appearences (*Figure 35*D,E,F).

Table 15. Mineralogical composition and pH of samples.

Sample	Deposit	Color	Mineralogy	pH
A/B-WF/SF	Water streamers	White	-	6.9-7.5
B-Vg	Vermiculation	Grey	Quartz, calcite, muscovite, gypsum	5-5.5
B-Vb	Vermiculation	Brown	Quartz, diopside, hematite	5-5.5
B-M	Moonmilk	White	Gypsum	0-1

Greyish vermiculations are dominated by quartz [SiO_2], calcite [$Ca(CO_3)$], muscovite [$KAl_2(AlSi_3O_{10})(OH)_2$], and gypsum [$Ca(SO_4)\cdot 2H_2O$], whereas the brownish ones are characterized by quartz, diopside [$CaMg(Si_2O_6)$] and hematite [Fe_2O_3]. The white pasty moonmilk is exclusively composed of gypsum (*Figure 36*D). Grey and brown vermiculations show slightly acidic pH, with pH values ranging between 5 and 5.5, while gypsum moonmilk has an extremely acidic pH (0-1) (*Table 15*). FESEM images of the white slimy filaments from A and B showed clear differences (*Figure 36*A,B,C). In A, it is possible to see sulfur crystals surrounded by pristine filaments (*Figure 36*A,B) whereas, in B, filaments are thinner and coccoid cell-like structures appear totally damaged and corroded (*Figure 36*C). As a matter of fact, water streamers at site B were collected where rising sulfidic waters and H_2S degassing were evident. The moonmilk deposits are dominated by microscopic gypsum crystals (*Figure 36*D) as previously documented by Onac and Lauritzen (1995), likely of biogenic origin, whereas vermiculations (both brown and grey) show a tangled network of thin filaments (*Figure 36*E) and prosthecate bacteria (*Figure 36*F), the latter frequently being observed in oligotrophic cave environments (Staley, 1964; Barton et al., 2004). Additionally, mineral particles can be easily observed (*Figure 36*E). Such complex arrangement would aid in trapping and binding particles coming from the surrounding environment or subaerially transported, which would also explain the extraordinary presence of diopside (*Table 15*), a mineral generally absent in carbonate rocks, and likely transported by waves into Fetida Cave.

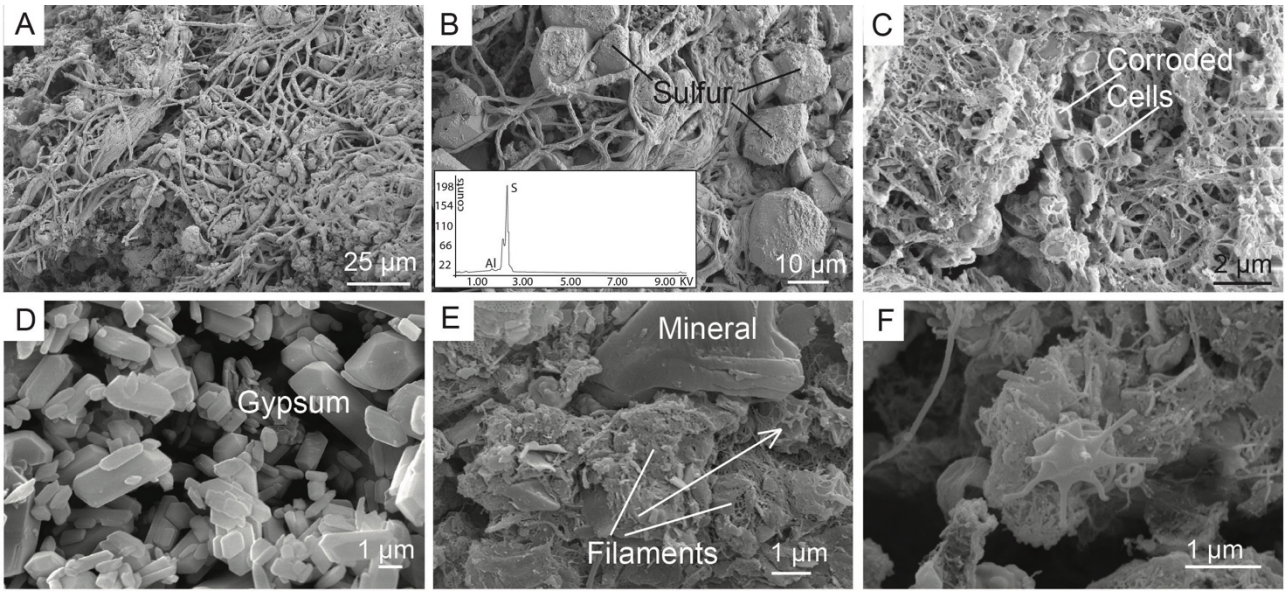

Figure 36. Appearance of the microbiological biofilms collected from Fetida Cave. A) Water streamers sampled at site A. It is possible to see elongated filaments and particles characterized by sulfur crystals; B) The sulfur crystals (EDS spectrum) are surrounded by filaments; C) Water streamers taken at site B. They appear more corroded than the ones observed in A; D) The moonmilk deposits are dominated by tiny gypsum crystals; E) General view of brown vermiculation deposit composed of a network of thin filaments likely trapping and binding minerals; F) Prosthecate bacterium observed in greyish vermiculations.

5.2.4.2. Bacterial diversity within the different deposits collected from Fetida Cave

As a result of the processing of the demultiplexed fastq files with DADA2 package, 154,536 reads were obtained with an average length of 290 bp; they were clustered into a total of 2,969 sequence variances (SVs) (*Table 16*).

Table 16. Summary of Illumina MiSeq sequencing and calculated diversity indices for each sample (using QIIME2 on rarefied sequencing data). Observed SVs and diversity indeces calculations for each sample were based upon randomly subsampling down to the lowest reads number (i.e., 3,729) to avoid bias associated with library size (Gihring et al., 2012; Wu et al., 2015).

Sample	Observed SVs	Chao1	Shannon (H')	Simpson (1-D)	Pielou
A-WF1	272	279.5	7.7127	0.9944	0.9944
A-WF2	338	340.25	8.1016	0.9957	0.9957
B1-WF	219	222.0	7.2897	0.9912	0.9912
B2-WF	274	278.87	7.7236	0.9944	0.9944
B1-SF	347	365.05	8.0531	0.9952	0.9952
B2-SF	398	409.45	8.1145	0.9943	0.9378
B1-Vb	216	216.11	7.4809	0.9936	0.9655

B2-Vb	298	315.0	7.8810	0.9948	0.9585
B1-Vg	324	333.0	7.7190	0.9908	0.9272
B2-Vg	218	223.25	7.3493	0.9920	0.9450
B1-M	57	67.0	3.4603	0.7900	0.6002
B2-M	51	51.0	4.1952	0.8744	0.7396

Variability in SV richness (observed SVs) among the samples has been observed, and is mainly depenedent on sample type and location throughout the cave (*Table 16*). The moonmilk (-M) samples show the lowest SV richness. The calculation of Shannon and Inverse Simpson indices further confirmed the significantly limited diversity pattern of moonmilk compared to vermiculations and white filaments (*Table 16*). This is most probably due to the extremely low pH values (comprised between 0-1) detected within moonmilk deposits. Indeed, extreme acidophilic conditions are known to strongly select the biodiversity (Macalady et al., 2007; Jones and Macalady, 2016). On the other hand, the wide diversity pattern detected in Fetida Cave's vermiculations is in line with the previous geomicrobiological work carried out on vermiculations from Frasassi caves (Jones et al., 2008). Vermiculations were described to host one of the most diverse microbial communities in Frasassi Cave. Pairwise Bray-Curtis distance between samples is calculated based on SV abundance (*Figure 37*A) and based on SV taxonomy classification in SILVA (*Figure 37*B), and shows two major groups depending on substrates: 1) "water" for the streamers (-WF and -SF) and 2) "cave wall" for moonmilk and vermiculation deposits (-M, -Vg, and -Vb). On the basis of SV abundance (*Figure 37*A), vermiculations clustered independently from the color (grey or brown), whereas on the basis of SV taxonomy, brown (or grey) vermiculations grouped together (*Figure 37*B).

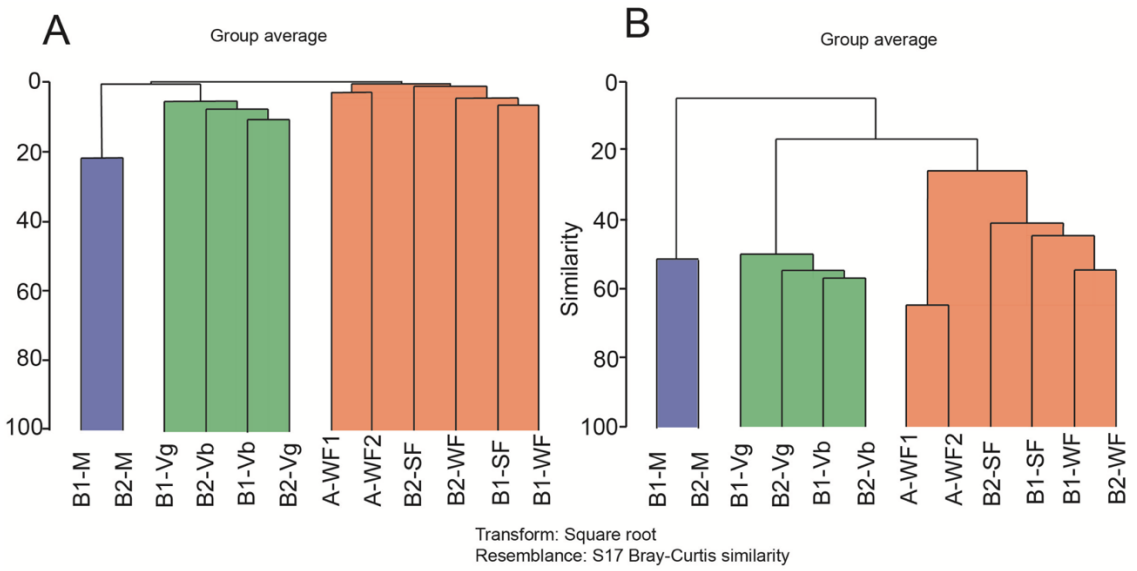

Figure 37. Clusters calculated using the Bray-Curtis distance between samples based on A) SV presence/absence and abundance; B) SV taxonomy classification in SILVA. White filaments are represented in orange, moonmilk in blue, and vermiculation deposits in green.

A non-multidimensional scaling (nMDS) analysis was conducted to determine the correlation of physical and chemical parameters with the microbial communities present in each type of deposit (*Figure 38*).

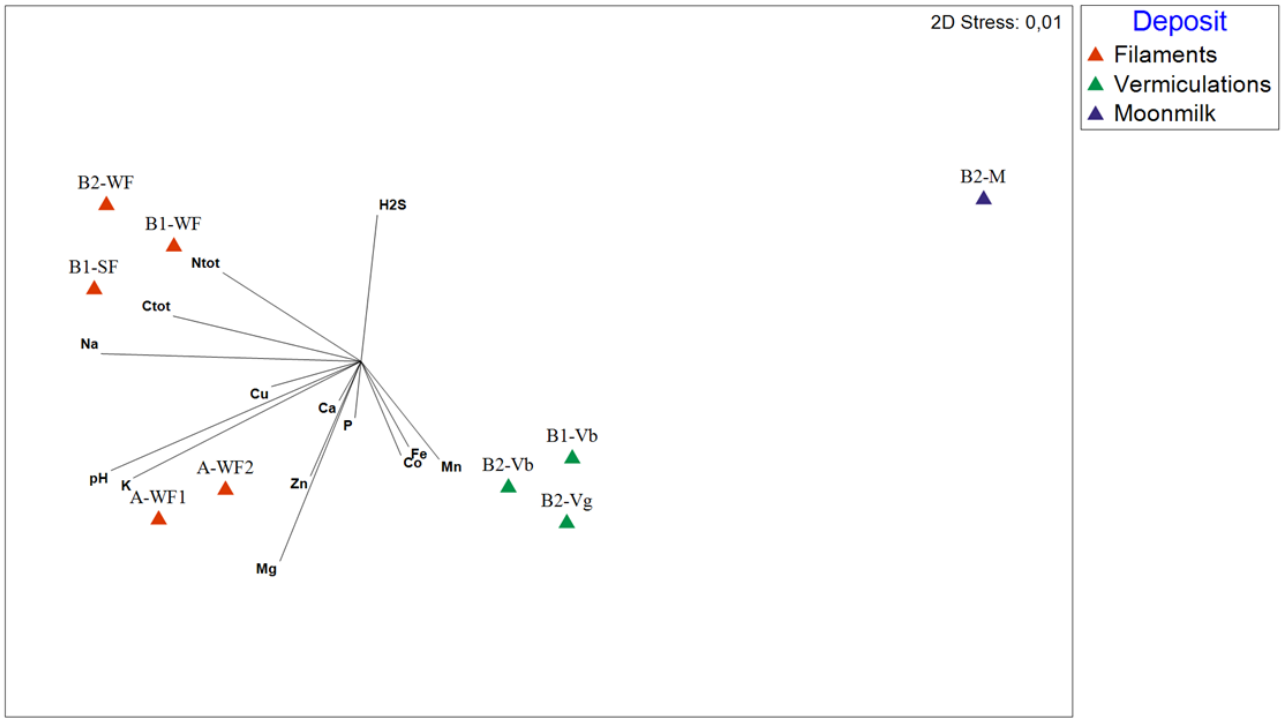

Figure 38. Non-metric multidimensional analysis showing correlation between physical and chemical factors and samples. Samples cluster in the plot according to their microbial community composition.

Among a selection of physical chemical parameters examined in this work (i.e., pH, H_2S, N_{tot}, C_{tot}, and the elements in *Table 14; Table 15*), those that most affected (Pearson Correlation >0.8) the microbial diversity were pH and Na. The concentration of K, Fe, Co, Mg and H_2S concentration also affected the microbial diversity although with a lower Pearson correlation (p>0.4). These results can be associated to the extremely acidic pH of moonmilk compared to the neutral and slightly acidic pH of WF/SF and V, respectively, and to the higher abundance of seawater-associated elements (i.e., Na, K) in WF/SF-samples compared to the wall-related deposits. In general values >0.7 mean there is a strong correlation between environmental parameters and microbial community composition.

5.2.4.3. Microbial community composition of the Fetida Cave biofilms

A total of 49 bacterial phyla (of which 23 with abundance >0.1% in at least one sample) and 10 archeal phyla (of which 3 with abundance >0.1% in at least one sample) are identified from all the microbial samples under analysis, with varying dominant phyla depending on deposits and locations

(*Figure 39*). Differently, the sequences unclassified at phylum level are <7% (maximum value in B2-M). Moving to higher taxonomy levels, the abundance of unclassified sequences increases reaching, at genus level, the maximum values of 55-60% and 47-63% in samples -WF and in –V, respectively.

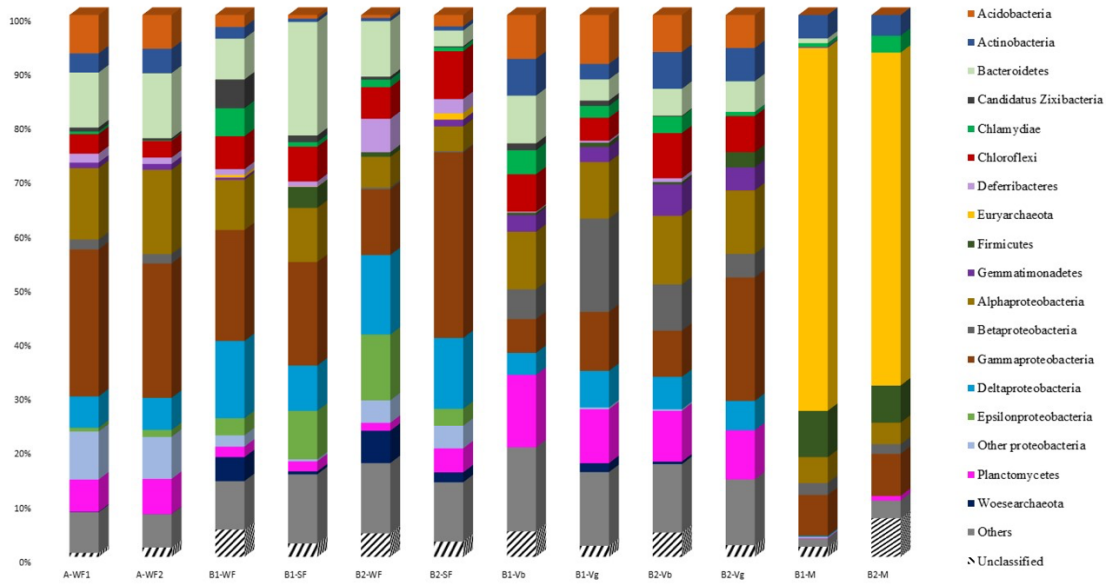

Figure 39. Microbial community composition at phylum/proteobacteria class level of Fetida samples. Phyla and proteobacteria classes with abundances <5% are included in "Others" and in "Other proteobacteria", respectively. "Others" refers to Aenigmarchaeota, Altiarcheales, Diapherotrites, Lokiarchaeota, Thaumarchaeota, AC1, Acetothermia, Aminicenantes, Armatimonadetes, BRC1, Caldiserica, Chlorobi, Cyanobacteria, Deinococcus-Thermus, Elusimocrobia, Fibrobacteres, Fusobacteria, GAL 15, Gracilibacteria, Hydrogenedentes, Ignavibacteriae, KSB3, Latescibacteria, Lentisphaerae, Marinimicrobia, Microgenomates, Nitrospinae, Nitrospirae, Omnitrophica, Parcubacteria, PAUC34f, Peregrinibacteria, Saccharibacteria, SBR1093, Spirochaetae, SR1, Tectomicrobia, Tenericutes, Thermotogae, TM6, WS1. "Other proteobacteria" refers to Milano-WF1B-44, SPOTSOCT00m83, pltb-vmat-80, Proteobacteria Incertae Sedis, unclassified Proteobacteria.

5.2.4.3.1. Water streamers*

The taxonomic analysis of SVs indicated the dominance of *Bacteria* domain within all the water streamers. Archeal sequences constituted <1.5% of total microbial communities in A-WF samples and B1-SF, whereas they ranged between 3.8 and 6.0% in B1-WF, B2-WF, and B2-SF. In B-WF samples, Archeal sequences were mainly affiliated with *Woesearchaeota* phylum, unclassified at lower taxonomy levels (*Figure 39*). The phylum *Proteobacteria* was the most abundant in all the water streamers accounting for 47-60% of the *Bacteria* domain. In both A-WF samples, the class

Gammaproteobacteria was dominant (24-27% of each total community) followed by *Alphaproteobacteria* (13-15%, almost exclusively of *Rhodospirillales* order and *Rhodospirillaceae* family) (*Figure 39*).

In these samples, classified gammaproteobacterial sequences were mainly affiliated to *Thiotrichales* order of *Thiotricaceae* family (4.2-6.2%), *Chromatiales* (2.7-3.0%) and *Oceanospirillales* (2.5-3.0%). At genus level, these sequences mainly belonged to *Granulosicoccus*, *Thiohalophilus*, *Marinobacterium*, *Cocleimonas* and *Candidatus* Thiobios, which are genera typically associated with marine and halophilic water habitats, featured by chemolithotrophic activities related to sulfur and sulfidic compounds oxidation, and nitrogen metabolism (Hirano, 2003; Sorokin et al., 2007; Tanaka et al., 2011; Kang et al., 2018). The class *Deltaproteobacteria* accounted for 5.7-5.9% of the total sequences from A-WF samples, showing the predominance of the orders *Desulfobacterales* (of the genus Sva0081 sediment group) and the '*Candidatus* NB1-J' (*Figure 39).*

Both these bacterial groups have been previously associated with sulfur-reducing activity occurring in marine waters and sediments (Giovannelli et al., 2016; Dyksma et al., 2018). Other abundant phyla (>5%) in A-WF samples were *Bacteroidetes* (10-12%) (major orders *Cytophagales* and *Flavobacteriales*), *Planctomycetes* (6-6.5%) and *Acidobacteria* (6.2-7.1%) (major order Subgroup 10) *(Figure 39*). Members of all these bacterial taxa have been described to possibly contribute to carbon recycling and sulfur transformation in oligotrophic and poorly oxygenated marine environments (Fernández-Gómez et al., 2013; Kielak et al., 2016; Wasmund et al., 2017). Lower abundant bacterial phyla were *Actinobacteria* (3.5-4.5%) and *Chloroflexi* (3.1-3.6%).

The WF-samples collected from site B were more differentiated in terms of microbial community than A-WF samples (*Figure 39*). *Gammaproteobacteria* was the predominant group in B1-WF (20.5%) and B2-SF (34.3%), and the second most abundant in B1-SF (19.1%) and B2-WF (12.1%). Within *Gammaproteobacteria*, the '*Candidatus* Thiopilula*'* genus of *Thiotrichaceae* family and *Thiotricales* order was highly abundant in B2-SF (12.5%), whereas, in B1-WF and B1-SF, sequences related to *Arenicellaceae* family, of Arenicellales order and unclassified at genus level, dominated (13.4% and 6.5%, respectively). The order *Chromatiales* was <1.7% in all the B samples with the highest abundance in B2-WF, where they were mainly composed of sulfur-oxidizing *Halothiobacillus* genus. *Deltaproteobacteria* covered 8.4-14.7 % of the biodiversity in B samples and represented the most abundant bacterial group in B2-WF (*Figure 39*), being mainly composed of *Desulfobacterales* (~9.5% in B2 samples) and *Desulfuromonadales* orders (maximum abundance of 2.3% in B2-WF). *Desulfobacterales*-related sequences are unclassified at higher taxonomy level in B1 samples, in B2 samples, they were affiliated to the sulfate-reducing genera *Desulfobulbus*, *Desulfocapsa* and MSBL7. *Epsilonproteobacteria* accounted for 12.1% of the total communities in

B2-WF, 9.0% in B1-SF, 3.1% in B1-WF and B2-SF. Epsilonproteobacterial sequences were exclusively related to *Helicobacteraceae* and *Campylobacteraceae* families, both of *Campylobacterales* order. The most represented genera were *Sulfurimonas*, *Arcobacter*, *Campylobacter*, *Sulfurovum*, widely described for their sulfur- and sulfide-oxidizing activities in different environments with high temperatures, mainly hydrothermal marine habitats and oil fields (Wirsen et al., 2002; Han and Perner, 2015). *Alphaproteobacteria* were 4-6% in B2 samples and 9-10% in B1 samples (*Figure 39)* and were mainly represented by sequences related to the orders *Rhizobiales* and *Rhodospirillales*. In all B-samples, *Chloroflexi* phylum ranged between 6% and 9% and was represented by members of *Anaerolineaceae* family and unclassified genera. *Bacteroidetes*-related sequences were the most abundant in B1-SF (21%), mainly belonging to *Flavobacteriales* (6.9%), *Bacteroidales* (3.9%), and *Sphingobacteriales* (2.1%) orders and unclassified at higher taxonomy levels. Sequences affiliated to *Caldithrix* genus of *Deferribacteres* phylum were also abundant in B2 samples with the highest presence observed in B2-WF (6.2%) (*Figure 39)*. Most *Caldithrix* sequences have been recovered from hydrothermal sulfide-rich marine niches, but they have also been recovered from previously described sulfidic caves (Macalady et al., 2006; Hamilton et al., 2015).

Based on SVs analysis, A-WF, B-WF and B-SF samples are clustered and displayed similar phylum diversity profiles compared to vermiculation (-V) and moonmilk (-M) samples (*Figure 37*; *Figure 39)*. The phylogenetic tree and showed high similarity (97-99%) with sequences of uncultivated strains retrieved from cold seeps and sulfidic sediments (Loescher et al., 2014; Grünke et al., 2012) and associated with sulfur metabolism (*Figure 40*). On the other hand, the similarity of these SVs was <90% with gammaproteobacterial sequences retrieved from Frasassi Cave water filaments affiliated to *Beggiatoa* genus.

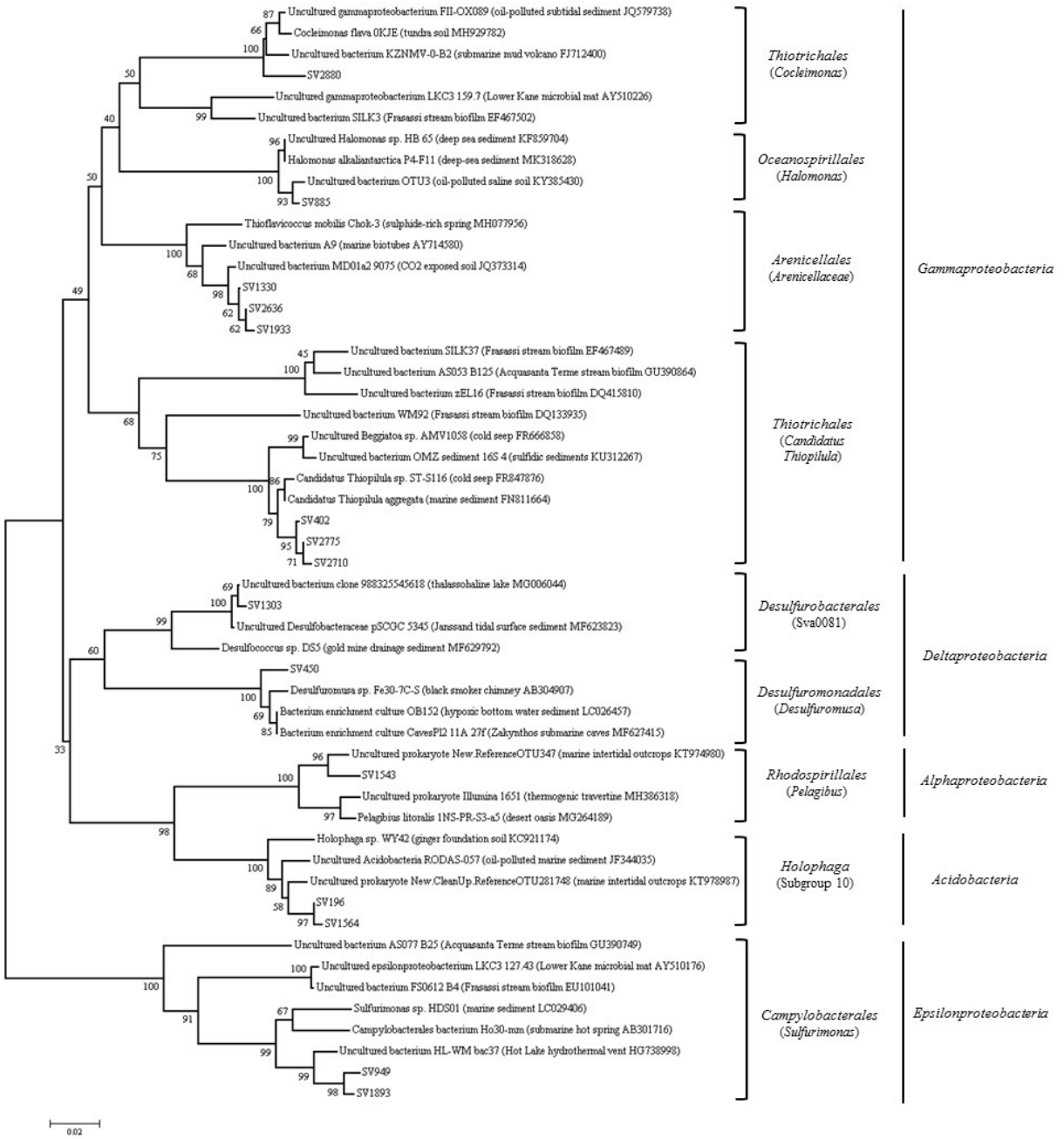

Figure 40. Phylogenetic tree for water streamers both floating (A-WF1, A-WF2, B1-WF, B2-WF) and accumulated on the water stream floor (B1-SF, B2-SF).

Among the most abundant SVs in the other B-WF samples, SVs affiliated with *Sulfurimonas* genus and *Arenicellaceae* and *Desulfuromonadaceae* families were detected. In the phylogenetic tree, these SVs were related to reference sequences detected from hydrothermal deep vents, submarine caves and tidal marshes exposed to elevated CO_2 concentration (*Figure 40*). The most abundant SVs in A-WF samples were found to be similar to *Acidobacteria*, *Alpha*- and *Deltaproteobacteria* sequences retrieved from tidal surface sediments and hypersaline lakes (*Figure 40*). Taken together, the sequencing analyses showed the presence, in WFs collected from both A and B sites, of members of bacterial groups involved in sulfur metabolism, but also typically associated with marine habitats

(e.g. *Marinobacterium, Thiohalophilus, Arcobacter, Sulfurimonas, Sulfurovum, Halothiobacillus*) (Wang et al., 2017). This is due to the peculiar nature of the cave water that results from the mixing of rising sulfide-rich fluids with the seawaters entering the cave. Different dominant gammaproteobacterial groups were found in A-WF and B-WF samples, i.e., *Thiotrichales* and *Arenicellaceae*, respectively, that were also affiliated with gammaproteobacterial sequences retrieved in other previously described sulfidic caves (Macalady et al., 2006; Jones et al., 2010). Interestingly, the gammaproteobacterial sulfur-oxidizing *Candidatus* Thiopilula was specifically found as predominant in B2-SF and still needs further metabolic and taxonomical classification (being previously categorized in the *Beggiatoaceae* family and recently included within *Thiotrichaceae*) (Jones et al., 2015). Further, compared to A-WF samples, B-WF/SFs generally showed higher abundance of the sulfur-reducing *Deltaproteobacteria* and sulfur-oxidizing *Epsilonproteobacteria*, being the latter found in traces (<1.3%) in A-WFs. The previously described biofilms collected from the sulfidic Parker and Cesspool Caves, did not contain significant amounts of *Deltaproteobacteria* (Engel et al., 2001, 2007), likely due to the use of clone library which didn't contain those information at that time. On the other hand, 20-22% and 5-6% of all the sequences retrieved from stream biofilms collected from caves from Frasassi and Acquasanta Terme caves, respectively, were affiliated with *Deltaproteobacteria* of unrelated higher taxonomy levels. The physical association between sulfur-oxidizing bacteria and *Deltaproteobacteria*, which have been frequently observed in microbial mats developing on marine and lacustrine sediments, optimizes the sulfur cycling over reduced and oxidized forms having strong implications on the ecology and geochemistry of the cave (Macalady et al., 2006). The differences found in the *Epsilonproteobacteria* population between B-WF/SF and A-WF samples in terms of abundance and taxonomy might be related to the physical-chemical parameters depending on the location and degree of sea-deepwater mixing. Indeed, Epsilonproteobacteria have been described as the most abundant group in sulfuric acid cave microbial biofilms (Engel et al., 2004; Macalady et al., 2008) that have high sulfide concentration, observed in the innermost portion (site B) of Fetida Cave. Further, the distribution of specific Epsilonbacteria in other sulfidic environments was reported to be influenced by pH, temperature, bicarbonate and salinity (Rossmassler et al., 2011). In Fetida Cave, Epsilonproteobacteria have been found to be associated with other highly abundant bacterial groups (e.g. *Alphaproteobacteria*, *Bacteroidetes*, *Chloroflexi*) that are thought to actively contribute to the microbial community structure and metabolism in the different -WF/SF retrieved from the cave.

5.2.4.3.2. Vermiculations*

Sequencing analysis indicated the dominance of *Bacteria* in all the vermiculations (*Figure 39*). Archeal sequences constituted <4.3% of the total sequences, and were mainly composed of *Thaumarchaeota* phylum (included in "Others" in *Figure 39*).

Proteobacteria was the most abundant bacterial phylum accounting for 44-46% of the total sequences in B-Vg samples, 36% in B2-Vb and 26% in B1-Vb. *Alphaproteobacteria* and *Deltaproteobacteria* showed a quite uniform abundance in vermiculations, ranging between 10 and 13% and between 4 and 7%, respectively (*Figure 39*). Alphaproteobacterial sequences in all V samples were mainly affiliated to members of *Rhizobiales* and *Rhodospirillales* orders, unclassified at higher taxonomic levels. Around half of the deltaproteobacterial sequences were affiliated to *Desulfurellaceae* family of *Desulfurellales* order, mainly belonging to *Candidatus* H16 genus. Sequences of this genus were previously retrieved from cool hydrothermal sediments (Zinke et al., 2018). Conversely, *Betaproteobacteria* and *Gammaproteobacteria* showed more variation among vermiculations, representing the largest taxonomic groups in B1-Vg (17%), and B2-Vg (23%), respectively (*Figure 39*). Most of betaproteobacterial sequences belonged to unclassified taxa, except for those in B1-Vg that were mainly affiliated to the sulfur-oxidizing *Sulfuriferula* genus of *Hydrogenophilaceae* family. Members of this genus were highly abundant in microbial consortia responsible for the weathering of sulfide minerals occurring under acidic conditions (Jones et al., 2017). Considering Gammaproteobacteria, in all the vermiculation samples, almost half of the sequences belonging to this class were affiliated to *Sulfurifustis* genus of *Acidiferrobacteraceae* family and *Acidiferrobacterales* order. Sequences affiliated to *Pseudomonas* genus reached a high abundance (17% of the entire microbial community) only in the B2-Vg sample. Other abundant phyla were *Planctomycetes* (9-13%, predominant sequences were affiliated to *Planctomycetaceae* family), *Acidobacteria* (6-9%, with Subgroup 4 as the most abundant classified family), *Chloroflexi* (4-9%), *Bacteroidetes* (4-9%, with *Cytophagaceae* family being >1% in all V samples) and *Actinobacteria* (3-7%, with *Gaiella* genus of *Gaiellaceae* family present in all samples and accounting >3% in the two Vb samples). Although present at a lower abundance, *Gemmatimonadetes*, *Verrucomicrobia*, *Nitrospirae*, and *Chlorobi* were >1% in all the samples.

In line with taxonomic analysis, the most abundant SVs in B1-Vg were affiliated to *Sulfuriferula* and *Sulfurifustis* genera, in B2-Vg were related to *Pseudomonas* genus, and in B2-Vb were affiliated to taxonomically undefined members of *Betaproteobacteria*. In B1-Vb, several SVs belonging to different bacterial taxa (e.g. *Verrucomicrobia* (*Opitutus*), *Actinobacteria Mycobacterium* and *Pseudonocardia*) were present at ~1% without showing a clear dominance. Generally, the most abundant SVs are specific to each single V sample; only in few cases, the most abundant SVs were

also shared among all the vermiculations, e.g. *Betaproteobacteria*-related. In the phylogenetic tree in *Figure 41*, an uncultured *Comamonadaceae* clone was identified from a sewage sludge capable of autotrophic nitrogen removal (Yue et al., 2018). *Sulfuriferula*-related SVs clustered together with *Betaproteobacteria* clones sequenced from a biofilm streamer from Pozzo dei Cristalli (PC) in Frasassi cave system and from a sulfidic mine (Korehi et al., 2014; Hamilton et al., 2015). *Sulfuriferula* is still a scarcely studied genus, with some members being associated with weathered mine tailings and with possible chemolitothrophic activities including sulfide compounds oxidation, nitrogen-oxidation and nitrate-reducing activities (Watanabe et al. 2015; Jones et al., 2017). *Sulfurifustis*-affiliated SVs showed high similarity (99%) with gammaproteobacterial sequences retrieved from different Frasassi cave deposits (stream biofilms and vermiculations), and also clustered with sequences identified in metal rich sediments and microbial-induced concrete corrosion of wastewater with high concentration of hydrogen sulfide (*Figure 41*). In particular, the Frasassi cave sequences were classified as *Acidithiobacillus*, in the case of vermiculations, and *Sulfurovum*-like, in the case of biofilm streamers, and were hypothesized to be involved in biomineralization processes (Jones et al., 2008). In the present work, these SVs are classified as *Sulfurifustis* which recently have been described as sulfur-oxidizers belonging to the same family of the iron- and sulfur-oxidizer *Acidiferrobacter* i.e., *Acidiferrobacteracea* (Umezawa et al., 2016). The *Pseudomonas*-related SVs grouped with affiliated clones detected in cave waters and in PAHs contaminated soils (*Figure 41*).

Richness and diversity indeces were comparable to those calculated for the Fetida's water streamers (*Table 16*). Although the microbial communities differed among the V samples under analysis, the general microbial composition of Fetida's -V samples was similar to that described for the same type of deposit collected from other sulfidic caves, i.e., the high abundance of *Betaproteobacteria, Gammaproteobacteria, Acidobacteria, Planctomyces* and *Actinobacteria* (Hose and Northup, 2004; Jones et al., 2008). In particular, representative sequences related to sulfur-oxidizing bacteria could be identified in Fetida vermiculations, which were affiliated to those found in other sulfidic cave vermiculations or biofilm streamers (e.g. *Sulfuriferula, Sulfurifustis*) (*Figure 41*). Possible iron-oxidizing activities can also be associated with these bacterial genera, in line with the high concentration of Fe ions and hematite minerals detected in some vermiculations, and mainly in the brownish (-Vb) samples (*Table 14*). Like in Frasassi vermiculations, *Nitrospira* were also found in Fetida V samples having possible oxidizing activities towards reduced nitrogen compounds (Jones et al., 2008). Further, some Fetida vermiculation SVs were found to be affiliated with sequences retrieved from extreme environments (e.g. desert, drylands, high CO_2 exposed soil), mine tailings and metal rich sediments (*Figure 41*), possibly the first being related with the harsh conditions of the cave

wall as growth substrate and the second with the high concentration of microelements featuring this type of deposit.

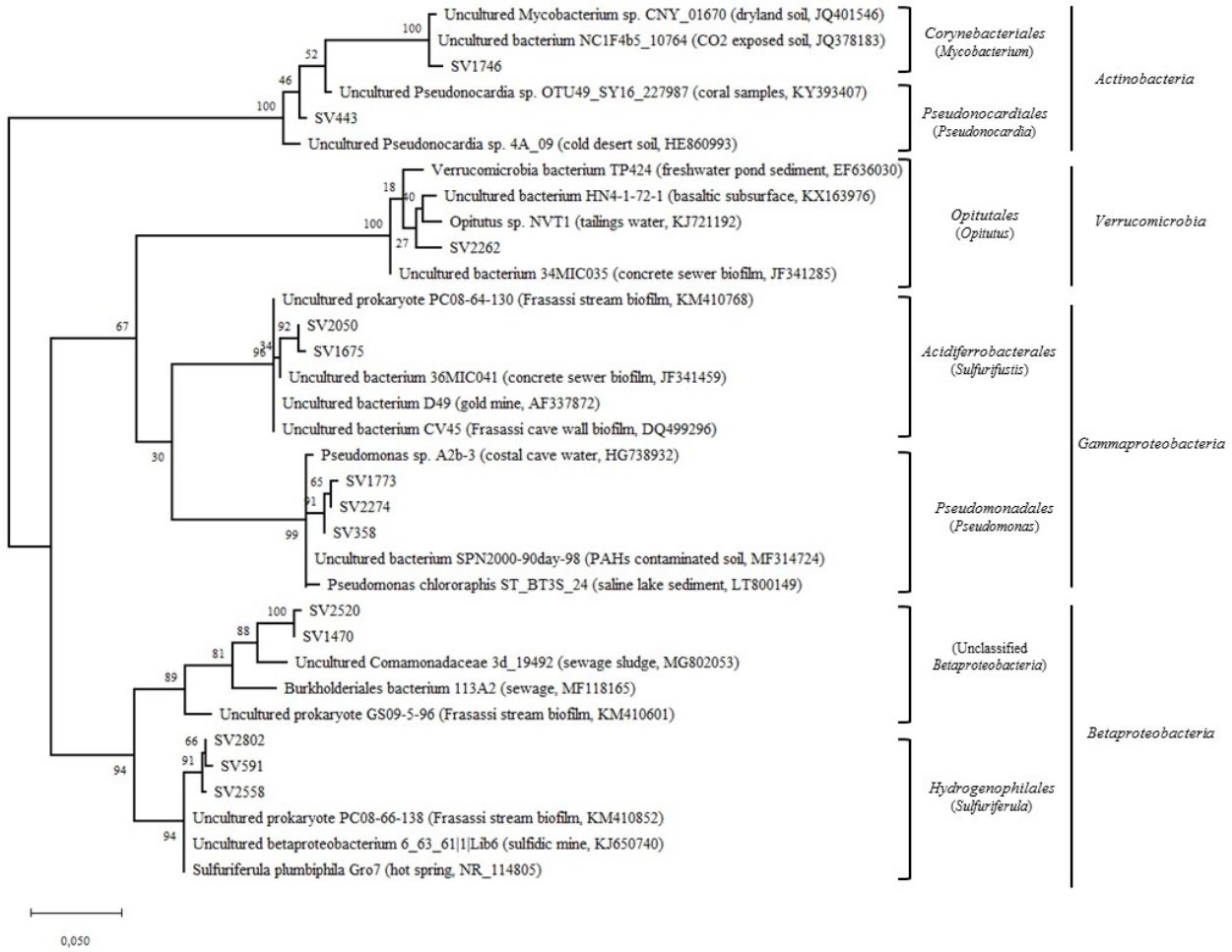

Figure 41. Phylogenetic tree for the greyish (B1-Vg, B2-Vg) and brownish vermiculations (B1-Vb, B2-Vb).

5.2.4.3.3. Moonmilk*

Taxonomic analysis of the two -M samples revealed the presence of only 3 phyla in B2-M and 4 phyla in B1-M with abundance >5% (*Figure 39*). Moonmilk was dominated by *Archaea*-related sequences (61% in B2-M and 67% in B1-M) exclusively belonging to the *Thermoplasmatales* order of *Euryarchaeota* phylum (*Figure 39*). In B1-M, they were only represented by *Thermoplasma* genus of *Thermoplasmataceae* family, whereas in B2-M, in addition to *Thermoplasma* (57.1%), some *Thermoplasmatales*-related sequences were also affiliated to *Ferroplasma* (2.3%) of *Ferroplasmaceae* family. Among the sequences related to the *Bacteria* domain, *Gammaproteobacteria* and *Firmicutes* accounted for 7-8% and 7-8.5%, respectively, for each -M sample (*Figure 39*). At genus level, *Acidithiobacillus* was the most representative genus of *Gammaproteobacteria* in both -M samples, whereas, in the only B2-M, *Metallibacterium* was also highly abundant but only in B2-M. Within *Firmicutes*, which almost exclusively included members

of *Bacillales* order, sequences were mostly affiliated with the genera *Acidibacillus* of *Bacillales* order (in B1-M and B2-M), *Sulfobacillus* of *Clostridiales* order (in B1-M and B2-M) and *Paenibacillus* of *Bacillales* order (in B2-M only) genera. At a lower abundance, *Rhodospirillales*, *Rickettsiales* and *Chlamydiales* were present in both –M samples, as well as *Actinobacteria* affiliated to *Acidimicrobiales* order of unclassified family and to *Mycobacterium* of *Corynebacteriales* order.

The phylogenetic analysis showed their taxonomic affiliation with the sequences related to *Thermoplasmatales* order retrieved from acidic cave biofilms (snottites) described in Ramo Sulfureo (RS) from the Frasassi cave system and other acidic environmental sites such as mine drainage waters (*Figure 42*). Members of *Thermoplasma* and *Ferroplasma* genera have been described to be acidophilic; although most of them grow under heterotrophic conditions, few strains have shown chemolithotrophic activities such as ferrous iron oxidation, carbon fixation and anaerobic sulfur respiration (Segerer et al., 1988; Golyshina et al., 2000; Golyshina et al., 2017). Additional abundant SVs from moonmilk were specific to only one of the two samples under analysis, i.e., *Acidithiobacillus* in B1-M, and *Metallibacterium* in B2-M.

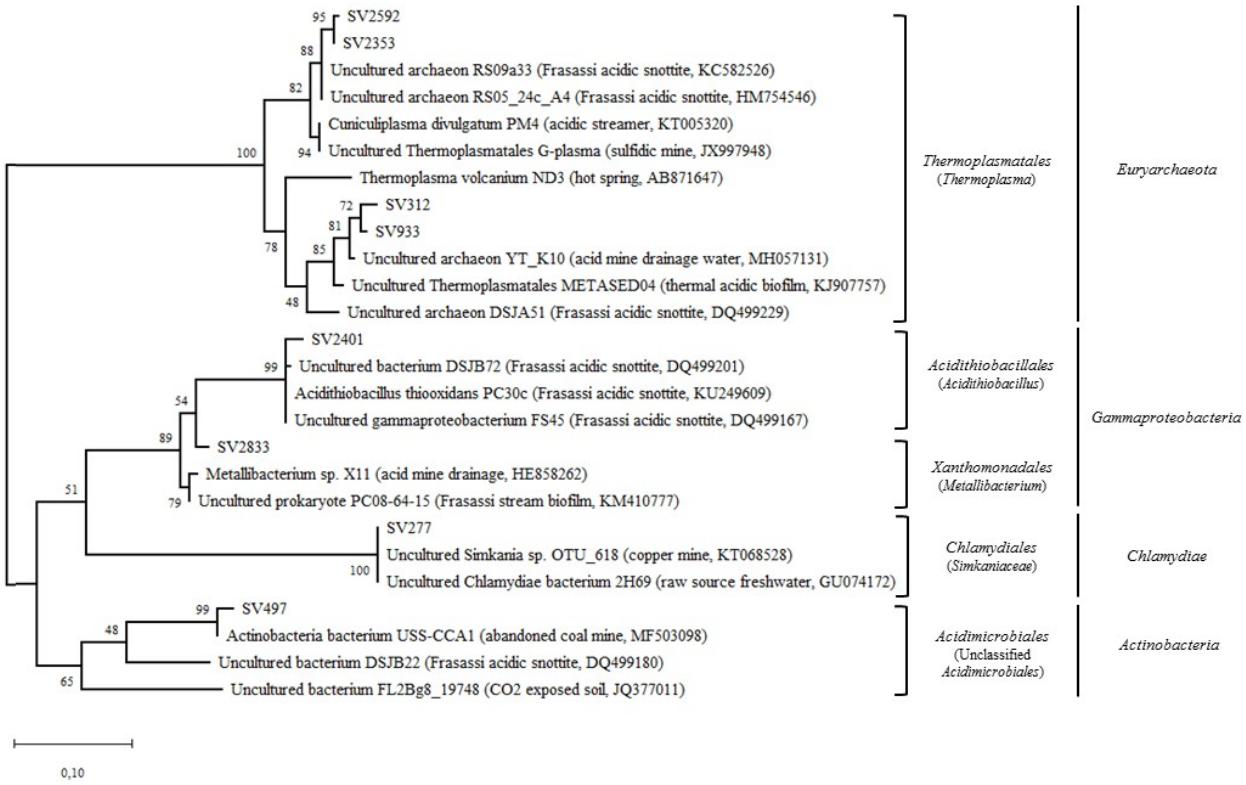

Figure 42. Phylogenetic tree for the white creamy moonmilk (B1-M, B2-M)

In particular, *Acidithiobacillus*-related SV2401 shared 99% of sequence identity with *Acidithiobacillus thiooxidans* isolated from snottites in PC of the Frassassi cave system (Jones et al., 2016). In particular, all the clones or most of the clones of the libraries constructed using three snottites from PC and RS in Frasassi cave system were affiliated with *Acidithiobacillus* (Macalady et

al., 2007). The same study reported the presence of *Sulfobacillus*, *Acidimicrobium* and *Thermoplasmata*, although at a much lower abundance. In line with this work, in the present study, we have also found high abundance of an *Acidimicrobiales*-related SV (SV497), which showed the highest similarity (99%) with a clone sequence identified in an abandoned coalmine (*Figure 42*). SV497 showed 87% of similarity with one clone sequence identified in the Ramo Sulfureo snottite from Frasassi cave system described by Macalady et al. (2007). Moreover, in Fetida's moonmilk *Sulfobacillus* was the third most abundant genus detected. *Sulfobacillus* species are able to grow heterotrophically but also autotrophically or mixotrophically on elemental sulfur (Norris et al., 1996). The *Metallibacterium*-related SV2833 shared maximal identity of 97% with reference sequences retrieved from biofilm streamers in PC from Frasassi Cave and from biofilms causing pipeline corrosion due to sulfur-oxidizing activities (*Figure 42*). Different members of *Metallibacterium* genus have been described to be acidophilic, heterotrophic, also capable of lithotrophic metabolism, using Fe (II) and reduced sulfur species, as well as anaerobic Fe(III) respiration (Brantner et al., 2014). The *Simkaniaceae*-affiliated SV277 shared 100% identity with an uncultured clone sequence retrieved from a bacterial community involved in sulfur and iron cycling in a copper mine (*Figure 42*). Although generally associated to anthropic activity, because of the presence of affiliated sequences in other caves, including Frasassi (Jones et al., 2012), a possible role of *Simkaniaceae* members in biogeochemical cycles in Fetida Cave snottites cannot be excluded.

Moonmilk is usually composed of secondary carbonates (95%), but also of sulfate, silicate and phosphate (5%) minerals (Chirienco, 2004; Miller et al., 2018). In previous studies, the microbial community composition of different carbonate moonmilk deposits was described and was found to be highly diversified, and their biogenic origin was discussed in detail (Gradzinski et al., 1997; Northup et al., 1997, 2000; Maciejewska et al., 2017; Miller et al., 2018). On the other hand, gypsum moonmilk deposits have been previously observed in SAS systems, without being microbiologically characterized (Onac and Ghergari, 1993, Galdenzi and Maruoka, 2003; Galdenzi, 2004b). Fetida's moonmilk resulted to be associated to low diverse microbial communities dominated by one archeal genus and few other bacterial taxa adapted to extremely acidic pH. The microbial composition of Fetida's moonmilk showed high similarities with the biodiversity described in acidic pendulous biofilms (snottites) collected from other SAS caves, i.e., Frasassi Cave system and Lower Kane Cave (Vlasceanu et al., 2000; Macalady et al., 2007; Jones et al., 2016), and greatly differed from that described for other moonmilk deposits collected from carbonatic, but not sulfidic, caves. In line with previous studies (Jones et al., 2008), the main driver of the limited microbial diversity observed in Fetida Cave moonmilk is the acidic pH. Indeed, SAS moonmilk and snottites have in common extremely acidic pH (0-1), mineralogy, and cave location; however, they also present relevant

differences in morphology and arrangement. In fact, moonmilk is a pasty and creamy white deposit composed of gypsum, which is found on the walls and ceiling of Fetida Cave from 1 m above the water table, whereas snottites are pendulous structures, developed on gypsum substrate, thriving from 0.5 to 4 m above the water stream. The different morphology and arrangement of these two deposits might be associated with the stability of geochemical parameters and environmental conditions featuring the hosting caves (e.g. degassing H_2S and O_2 content as a function of hydrodynamic conditions). These differences also be related with the difference found in the dominance of specific bacterial taxa in the Fetida's moonmilk, dominated by *Thermoplasma*, compared to Frasassi's snottite, dominated by *Acidithiobacillus* (Macalady et al., 2007). Probably, the extreme acidophilic community, which is colonizing the moonmilk deposits of Fetida Cave, contributes to the precipitation of gypsum crystals, but further investigations are required to confirm this theory.

5.2.4.4. Prediction of metagenomic content in water streamers, vermiculations, and moonmilk*

The genetic potential of the microbial communities associated to all the water streamers floating/accumulated at the stream bottom (-WF/SF), vermiculations (-V), and moonmilk deposits (-M) under analysis, was predicted by generating a catalogue of kegg orthologs (KO) using Piphillin (Iwai et al., 2016). In total, the 7925 KO were identified. Within the energy metabolism, in all the deposits, 78 KO were associated with the 'Sulfur metabolism', among these the complete set of KO involved in three modules were identified, i.e., the 'assimilatory sulfate reduction', 'dissimilatory sulfate reduction and oxidation', 'thiosulfate oxidation by SOX complex'.

Similarly, among the 47 KO found in all deposits which map against the 'Nitrogen metabolism', the complete set of KO required for 'Nitrogen fixation', 'Assimilatory nitrate reduction', 'Dissimilatory nitrate reduction', 'Denitrification', and 'Nitrification' were detected. The N cycle is completed and composed of denitrification (NO_3>N_2), nitrogen fixaction (N_2>NH_4), and nitrification (NH_4>NO_3). In addition, processes of ammonification, due to 1) organic nitrogen degradation in aerobic and/or anaerobic conditions, or 2) dissimilatory/assimilatory reduction of nitrogen in ammonium (NO_3>NO_2>NH_4). The nitrification seems to be exclusive of water filaments (-WF), in fact, the *Hydroxylamine dehydrogenase* (KO10535) has been predicted only in water streamers. Nevertheless, any taxon, in the water streamers SV, is clearly correlated to nitrification at the family level.

In the moonmilk deposits have been predicted KO involved in the nitrogen fixaction, denitrification, and dissimilatory reduction of nitrate. Denitrification is carried out by *Pseudomonadaceae* and *Clostridiales* (the most abundant SV in the –M samples), whereas the *Acithiobacillaceae* are nitrogen

fixing taxa. *Acidithiobacillaceae* are also involved in ammonification processes through the dissimilatory reduction of nitrogen.

Finally, the 'Carbon fixation metabolism' was represented by 79 unique KO which completed the following pathway modules, i.e., 'Reductive pentose phosphate cycle', the 'Reductive citrate cycle', and the 'Phosphate acetyltransferase-acetate kinase pathway'.

We performed a linear discriminant analysis (LDA) effect size (LefSe) to detect differentially abundant functional features (KO) that might support the differences in microbial community composition observed in -WF/SF, -V and -M samples. From a catalogue of 7925 KO, 1188 functional features were identified as differentially abundant (DA), and interesting relationship between DA genes and taxonomic composition of the microbial community were detected for -WF/SF and -M samples. Specifically, 452 KO were significantly more abundant in white filaments compared to the other deposits, whereas 279, and 459 functional features were significantly enriched in the microbial communities associated to vermiculations and moonmilk, respectively. Among the DA KO, the bifunctional enzyme CysN/CysC (K00860) and the sulfate adenylyltransferase (K00958) were more abundant in the -WF/SF microbial communities compared to the other deposits. These two enzymes are included within the 'assimilatory sulfate reduction' and 'dissimilatory sulfate reduction and oxidation', respectively; this difference being probably related to the higher presence of bacterial taxa involved in sulfur metabolism in -WF/SF. On the other hand, within the KO more abundant in moonmilk samples, KO linked to the adaptation to extremely acidic ecological niches were observed. These DA KO were represented by K00054 (hydroxymethylglutaryl-CoA reductase), K01597 (diphosphomevalonate decarboxylase), K06981 (isopentenyl phosphate kinase), K17942 (phosphomevalonate decarboxylase) which code for mevalonate pathway enzymes required for the synthesis of isoprenoid in Archaea adapted to extreme acidic conditions (Vinokur et al., 2016). This last aspect can be related to the dominance in -M samples of archeal *Thermoplasma* genus, whose members have been commonly identified in extreme environmental conditions, and recently characterized in their capability to carry out isoprenoid biosynthesis under extreme acidic conditions (Vinokur et al., 2016).

(Further details are available if Revisors will require them).*

5.2.5. Conclusions

Fetida Cave represents a unique system in which rising sulfidic fluids mix with sea and meteoric waters. This peculiar subterranean environment presents a variety of ecological niches that host different microbial-rich deposits floating or accumulated on the water stream floor (whater

streamers) or growing on the walls (vermiculation and moonmilk). Geochemical, mineralogical and microscopic studies and 16S rRNA sequencing with the recently developed DADA2 software analysis showed the morphological, elemental and pH composition determine differences in the microbial communities. In particular, these three deposits were dominated by diverse bacterial and archeal members involved in sulphur metabolism or chemolithotrophic activities. Specifically, classified and unclassified members belonging to *Proteobacteria* and *Euryarchaeota* phyla (e.g. *Gammaproteobacteria* of undefined lineage, *Candidatus* Thiopilula and *Epsilonproteobacteria Campylobacterales* in whater streamers; *Betaproteobacteria* of undefined lineage and *Sulfuriferula* and *Gammaproteobacteria Sulfurifustis* in vermiculations; *Archaea Thermoplasma*, and *Gammaproteobacteria Acidithiobacillus* and *Metallibacterium* in moonmilk), characterized each type of microbial-rich deposit, being associated to biomineralization processes and sulfur-oxidizing activity, both possibly contributing to the cave speleogenesis. Therefore, the present work provides valuable insights into the geomicrobiology population of a SAS marine-dominated cave, demonstrating that, in spite of the influence of seawater hydrodynamics is important (and clearly visible in the water streamer communities), the sulfuric acid component is more efficient and stronger. Further work will attempt to clarify the role of the microbial populations in each type of deposit in the processes of dissolution and precipitation of secondary minerals (e.g. gypsum and sulfur), trapping and binding activities (presence of pyroxene, diopside, transported by seawater into the cave), and corrosion of rocks.

References

Alcalá, F.J., Custodio, E., 2008. Using the Cl/Br ratio as tracer to identify the origin of salinity in aquifers in Spain and Portugal. Journal of Hydrology, 359: 189-207.

Amato, A., Bianchi, I., Piana Agostinetti, N., 2014. Apulian crust: Top to bottom. Journal of Geodynamics, 82: 125-137.

Audra, P., Hobléa, F., Bigot, J.-Y., Nobécourt, J.-C., 2007. The role of condensation-corrosion in thermal speleogenesis: study of a hypogenic sulfidic cave in Aix-les-Bains, France. Acta Carsologica, 36: 185-194.

Barton, H.A., Northup, D.E., 2007. Geomicrobiology in cave environments: past, current and future perspectives. Journal of Cave and Karst Studies, 69: 163-178.

Barton, H.A., Taylor, M.R., Pace, N.R., 2004. Molecular Phylogenetic Analysis of a Bacterial Community in an Oligotrophic Cave Environment. Geomicrobiology Journal, 21: 11-20.

Bigham, J.M., Nordstrom D.K., 2000. Iron and Aluminium hydroxysulfates from acid sulfate waters. Review of Mineralogy and Geochemistry, 40: 351-403.

Boston, P.J., Spilde M.N., Northup, D.E., Melim, L.A., Soroka, D.G., Kleina, L.G., Lavoie, K.H., Hose, L.D., Mallory, L.M., Dahm, C.N., Crossey, L.J., Schelble, R.T., 2001. Cave Biosignature Suites: Microbes, minerals, and Mars. Astrobiology, 1(1): 25-55.

Brantner, J.S., Haake, Z.J., Burwick, J.E., Menge, C.M., Hotchkiss, S.T., Senko, J.M., 2014. Depth-dependent geochemical and microbiological gradients in Fe(III) deposits resulting from coal mine-derived acid mine drainage. Frontiers in Microbiology, 5: 215. doi: 10.3389/fmicb.2014.00215.

Burlet, C., Vanbrabant, Y., Piessens, K., Welkenhuysen, K., Verheyden, S., 2015. Niphargus: A silicon band-gap sensor temperature logger for high-precision environmental monitoring. Computers & Geosciences, 74: 50-59.

Calò, G.C., Tinelli, R., 1995. Systematic hydrogeological study of a hypothermal spring (S. Cesarea Terme Apulia), Italy. Journal of Hydrology, 165: 185-205.

Caporaso, J.G., Lauber, C.L., Walters, W.A., Berg-Lyons, D., Lozupone, C.A., Turnbaugh, P.J., Fierer, N., Knight, R., 2010. Global patterns of 16S rRNA diversity at a depth of millions of sequences per sample. Proceedings of the National Academy of Sciences, 108: 4516-4522. https://doi.org/10.1073/pnas.1000080107

Carbone, C., Dinelli, E., Marescotti, P., Gasparotto, G., Lucchetti, G., 2013. The role of the AMD secondary minerals in controlling environmental pollution: indications from bulk leaching tests. Journal of Geochemical Exploration, 132: 188-200.

Chirienco, M., 2004. The crystalline phase of the carbonate moonmilk: a terminology approach. Acta Carsologica, 17: 257-264.

Da Cunha, A. R., 2015. Evaluation of measurement errors of temperature and relative humidity from HOBO data logger under different conditions of exposure to solar radiation. Environmental Monitoring and Assessment, 187(5): 236.

D'Angeli I.M., De Waele J., Ieva M.G., Leuko S., Cappelletti M., Parise M., Jurado V., Miller A.Z. & Saiz-Jimenez C., 2017a - Next-Generation Sequencing for microbial characterization of biovermicuations from a sulfuric acid cave in Apulia (Italy). Proceedings 17th International Congress of Speleology, Sydney: 377-380.

D'Angeli I.M., Vattano M., Parise M. & De Waele J., 2017b – The coastal sulfuric acid cave system of Santa Cesarea Terme (southern Italy). In: A.B., Klimchouk A.N, Palmer, J., De Waele A., Auler, P., Audra (Eds.), Hypogene karst regions and caves of the world. Springer: 161-168. http://doi.org/10.1007/978-3-319-53348-3_9.

D'Angeli, I.M., Carbone, C., Nagostinis, M., Parise, M., Vattano, M., Madonia, G., De Waele, J., 2018. New insights on secondary minerals from Italian sulfuric acid caves. International Journal of Speleology, 47(3): 271-291.

De Waele, J., Audra, P., Madonia, G., Vattano, M., Plan, L., D'Angeli, I.M., Bigot, J.Y., Nobécourt, J.C., 2016. Sulfuric acid speleogenesis (SAS) close to the water table: examples from southern France, Austria and Sicily. Geomorphology, 253: 452-467.

Dublyansky, Y.V., 1995. Speleogenetic history of the Hungarian hydrothermal karst. Environmental Geology, 25: 24-35.

Dyksma, S., Pjevac, P., Ovanesov, K., Mussmann, M., 2018. Evidence for H_2 consumption by uncultured Desulfobacterales in coastal sediments. Environmental Microbiology, 20(2): 450-461. Doi: 10.1111/1462-2920.13880.

Egemeier, S.J., 1981. Cavern development by thermal waters. National Speleological Society Bulletin, 43: 31-51.

Engel, A. S., 2007. Observations on the biodiversity of sulfidic karst habitats. Journal of Cave and Karst Studies, 69: 187-206.

Engel, A.S., Porter, M.L., Kinkle, B.K., Kane, T.C., 2001. Ecological assessment and geological significance of microbial communities from Cesspool Cave, Virginia. Geomicobiology Journal, 18: 259-274.

Engel, A.S., Stern, L.A., Bennett, P.C., 2004. Microbial contributions to cave formation: new insights into sulphuric acid speleogenesis. Geology, 32(5): 369-372.

Fernández-Gómez, B., Richter, M., Schüler, M., Pinhassi, J., Acinas, S.G., González, J.M., Pedrós-Alió, C., 2013. Ecology of marine Bacteroidetes: a comparative genomics approach. ISME Journal, 7(5):1026-37. doi: 10.1038/ismej.2012.169.

Forti, P., Galdenzi, S., Sarbu, S.M., 2002. Hypogenic caves: a powerful tool for the study of seeps and their environmental effects. Continental Shelf Research, 22: 2373-2386.

Freeman, J.T., 2007. The use of bromide and chloride mass rations to differentiate salt-dissolution and formation brines in shallow groundwater of the Western Canadian Sedimentary Basin. Hydrogeology Journal, 15(7): 1377-1385.

Fusari, A., Carroll, M. R., Ferraro, S., Giovannetti, R., Giudetti, G., Invernizzi, C., Mussi, M., Pennisi, M., 2017. Circulation path of thermal waters within the Laga foredeep basin inferred from chemical and isotopic ($\delta^{18}O$, δD, ^{3}H, $^{87}Sr/^{86}Sr$) data. Applied Geochemistry, 78: 23-34.

Galdenzi, S., 1990. Un modello genetico per la Grotta Grande del Vento. Memorie dell'Istituto Italiano di Speleologia, II(4): 123-142.

Galdenzi, S., 2004a. I depositi di gesso nella Grotta di Faggeto Tondo: nuovi dati sull'evoluzione geomorfologica dell'area di Monte Cucco (Italia centrale). Studi Geologici Camerti 2, 71-83.

Galdenzi, S., 2004b. L'azione morfogenetica delle acque sulfuree nella Grotta di Fiume Coperto (Latina). Le Grotte d'Italia, V(4): 17-27.

Galdenzi, S., 2012. Corrosion of limestone tablets in sulfidic ground-water: measurements and speleogenetic implications. International Journal of Speleology, 41: 25-35

Galdenzi, S., Maruoka, T., 2003. Gypsum deposits in the Frasassi caves, central Italy. Journal of Cave Karst Studies, 65(2): 111-125.

Galdenzi, S., Menichetti, M., 1995. Occurrence of hypogene caves in a karst region: examples from central Italy. Environmental Geology, 26: 39-47.

Galdenzi, S., Menichetti, M., Sarbu, S., Rossi, A., 1999b. Frasassi Cave: a biogenic hypogene karst system?. Karst 99, etudes de Géographie physique, travaux, suppl. 28 CAGEP, Université de Provence : 101-106.

Galdenzi, S., Cocchioni, F., Filipponi, G., Morichetti, L., Scuri, S., Selvaggio, R., Cocchioni, M., 2000. The sulfidic thermal caves of Acquasanta terme (Central Italy). Journal of Cave and Karst Studies, 72(1): 43-58.

Galdenzi, S., Cocchioni, M., Morichetti, L., Amici, V., Scuri, S., 2008. Sulfidic ground-water chemistry in the Frasassi Caves, Italy. Journal of Cave Karst and Studies, 70: 94-107.

Galdenzi, S., Cocchioni, F., Filipponi, G., Morichetti, L., Scuri, S., Selvaggio, R., Cocchioni, M., 2010. The sulfidic thermal caves of Acquasanta Terme (central Italy). Journal of Cave and Karst Studies, 72: 43-58.

Giovannelli, D., d'Errico, G., Fiorentino, F., Fattorini, D., Regoli, F., Angeletti, L., Bakran-Petricioli, T., Vetriani, C., Yücel, M., Taviani, M., Manini, E., 2016. Diversity and Distribution of Prokaryotes within a Shallow-Water Pockmark Field. Frontiers in Microbiology, 7: 941. doi:

10.3389/fmicb.2016.00941.

Golyshina, O.V., Pivovarova, T.A., Karavaiko, G.I., Kondratéva, T.F., Moore, E.R., Abraham, W.R., Lünsdorf, H., Timmis, K.N., Yakimov, M.M., Golyshin, P.N., 2000. Ferroplasma acidiphilum gen. nov., sp. nov., an acidophilic, autotrophic, ferrous-iron-oxidizing, cell-wall-lacking, mesophilic member of the Ferroplasmaceae fam. nov., comprising a distinct lineage of the Archaea. International Journal of Systematic and Evolutionary Microbiology, 50 Pt 3:997-1006.

Golyshina, O.V., Tran, Hai, Reva, O.N., Lemak, S., Yakunin, A.F., Goesmann, A., Nechitaylo, T.Y., LaCono, V., Smedile, F., Slesarev, A., Rojo, D., Barbas, C., Ferre, M., Yakimov, M.M., Golyshin, P.N., 2017. Metabolic and evolutionary patterns in the extremely acidophilic archaeon *Ferroplama acidiphilum* Y^T. Scientific Report, 7, Article number 3682.

Gradzinski, M., Szulc, J., Smyk, B., 1997. Microbial agents of moonmilk calcification. 12th International Congress of Speleology, Neuchatel 1, 275-278.

Grassa, F., Capasso, G., Favara, R., Inguaggiato, S., 2006. Chemical and isotopic composition of waters and dissolved gases in some thermal springs of Sicily and adjacent volcanic islands, Italy. Pure and Applied Geophysics, 163: 781–807.

Grotenhuis, J.T., Smit, M., Plugge, C.M., Xu, Y.S., Van Lammer, A.A., Stams, A.J., Zehnder, A.J., 1991. Bacteriological composition and structure of granular sludge adapted to different substrates. Applied Environmental Microbiology, 57: 1942-1949.

Grünke, S., Lichtschlag, A., De Beer, D., Felden, J., Salman, V., Ramette, A., Schulz-Vogt, H.N., Boetius, A., 2012. Mats of psychrophilic thiotrophic bacteria associated with cold seeps of the Barents Sea. Biogeosciences, 9: 2947-2960.

Hamilton, T.L., Jones, D.S., Schaperdoth, I., Macalady, J.L., 2015. Metagenomic insight into S80) precipitation in a terrestrial subsurface lithoautotrophic ecosystem. Frontiers of Microbiology, 5(756):1-16.

Han, Y., Perner, M., 2015. The globally widespread genus Sulfurimonas: versatile energy metabolisms and adaptations to redox clines. Frontiers in Microbiology, 6: 989. doi: 10.3389/fmicb.2015.00989.

Hanor J.S., 2000. Barite-celestine geochemistry and environment of formation. Review in Mineralogy and Geochemistry, 40: 193-275.

Hill, C. A., 1987. Geology of Carlsbad cavern and other caves in the Guadalupe Mountains, New Mexico and Texas. New Mexico Bureau of Mines and Mineral Resources, 117: 1-150.

Hill, C.A., 1990. Sulfuric acid speleogenesis of Carlsbad Cavern and its relationship to hydrocarbons, Delaware Basin, New Mexico and Texas. American Association of Petroleum Geologists Bulletin, 74: 1685-1694.

Hill, C.A., 2000. Sulfuric Acid, hypogene karst in the Guadalupe Mountains of New Mexico and West Texas, USA. In: A.B., Klimchouk, D.C., Ford, A.N., Palmer, W., Dreybrodt (Eds.), Speleogenesis: Evolution of karst aquifers, National Speleological Society, Huntsville, 309-318.

Hirano, H., Yoshida, T., Fuse, H., Endo, T., Habe, H., Nojiri, H., Omori, T., 2003. Marinobacterium sp. strain DMS-S1 uses dimethyl sulphide as a sulphur source after light-dependent transformation by excreted flavins. Environmental Microbiology, 5(6): 503-509.

Hose, L.D., Pisarowicz, J.A., 1999. Cueva de Villa Luz, Tabasco, Mexico: reconnaissance study of an active sulphuric spring cave and ecosystem. Journal of Cave and Karst Studies 61(1): 13-21.

Hose, L.D., Northup, D.E., 2004. Biovermiculations: Living vermiculation-like deposits in Cueva de Villa Luz, Mexico. Proceedings of the Society: selected abstract, National Speleological Society Convention. Journal of Cave Karst Studies 66: 112.

Hose, L.D., Palmer, A.N., Palmer, M.V., Northup, D.E., Boston, P.J., DuChene, H.R., 2000. Microbiology and geochemistry in a hydrogen-sulphide-rich karst environment. Chemical Geology 169: 399-423.

Imhoff J.F., 2006. The Chromatiaceae. Prokaryotes, **6**: 846-873. DOI: 10.1007/0-387-30746-x_31.

Iwai, S., Weinmaier, T., Schmidt, B.L., Albertson, D.G., Poloso, N.J., Dabbagh, K., DeSantis, T.Z., 2016. Piphillin: improved prediction of metagenomic content by direct inference from human microbiomes. PLoS One 11(11), e0166104.

Jagnow, D.H., Hill, C.A., Davis, D.G., DuChene, H.R., Cunningham, K.I., Northup, D.E., Queen, J.M., 2000. History of the sulfuric acid theory of speleogenesis in the Guadalupe Mountains, New Mexico. Journal of Cave and Karst Studies, 62(2): 54-59.

Jones, D.S., Macalady, J.L., 2016. The snotty and stringy: energy for subsurface life in caves. In: C.J. Hurst (Ed.), Their World: A diversity of Microbial Environments, Advances in Environmental Microbiology 1, Springer, chapter 5, 203-224. DOI.10.1007/978-3-319-28071-4_5.

Jones, D.S., Lyon, E.H., Macalady, J.L., 2008. Geomicrobiology of biovemiculations from the Frasassi cave systems, Italy. Journal of Cave and Karst Studies, 70(2): 78-93.

Jones, D.S., Tobler, D.J., Schaperdoth, I., Maniero, M., Macalady, J.L., 2010. Community structure of subsurface biofilms in the thermal sulfidic caves of Acquasanta Terme, Italy. Applied and Environmental Microbiology, 76(17): 5902-5910.

Jones, D.S., Albrecht, H.L., Dawson, K.S., Schaperdoth, I., Freeman, K.H., Pi, Y., Pearson, A., Macalady, J.L., 2012. Community genomic analysis of an extremely acidophilic sulfur-oxidizing biofilm. ISME Journal, 6(1): 158-70. Doi: 10.1038/ismej.2011.75.

Jones, D.S., Schaperdoth, I., Macalady, J.L., 2014. Metagenomic evidence for sulfide oxidation in extremely acidic cave biofilms. Geomicrobiology Journal, 31: 194–204.

Jones, D.S., Schaperdoth, I., Macalady, J.L., 2016. Biogeography of sulfur-oxidizing *Acidithiobacillus* populations in extremely acidic cave biofilms. ISME Journal, 10(12): 2879–2891.

Jones, D.S., Flood, B.E., Bailey, J.V., 2015. Metatranscriptomic analysis of diminutive Thiomargarita-like bacteria ("Candidatus Thiopilula" spp.) from abyssal cold seeps of the Barbados Accretionary Prism. Appl Environmental Microbiology, 81(9): 3142-3156. doi: 10.1128/AEM.00039-15.

Jones, D.S., Roepke, E.W., An Hua, A., Flood, B.E., Bailey, J.V., 2017. Complete Genome Sequence of Sulfuriferula sp. Strain AH1, a Sulfur-Oxidizing Autotroph Isolated from Weathered Mine Tailings from the Duluth Complex in Minnesota. Genome Announcements, 5(32): e00673-17. doi: 10.1128/genomeA.00673-17.

Kabata-Pendias, A., 2010. Trace elements in soils and plants. CRC Press, Boca Raton, FL (fourth edition).

Kang, I., Lim, Y., Cho, J.C., 2018. Complete genome sequence of Granulosicoccus antarcticus type strain IMCC3135T, a marine gammaproteobacterium with a putative dimethylsulfoniopropionate demethylase gene. Mar Genomics, 37:176-181. doi: 10.1016/j.margen.2017.11.005.

Kielak, A.M., Barreto, C.C., Kowalchuk, G.A., van Veen, J.A., Kuramae, E.E., 2016. The Ecology of Acidobacteria: Moving beyond Genes and Genomes. Frontiers in Microbiology, 31;7:744. doi: 10.3389/fmicb.2016.00744.

Klimchouk, A.B., 2017. Types and settings of hypogene karst. In: A.B., Klimchouk, A.N., Palmer, A.N., J. De Waele, A., Auler, P., Audra, (Eds.), Hypogene karst regions and caves of the world. Springer: 1-39. DOI 10.1007/978-3-319-53348-3_1.

Korehi, H., Blöthe, M., Schippers, A., 2014. Microbial diversity at the moderate acidic stage in three different sulfidic mine tailings dumps generating acid mine drainage. Research in Microbiology, 165(9): 713-718. Doi: 10.1016/j.resmic.2014.08.007.

Lavoie, K.H., Northup, D.E., Barton, H.A., 2010. Microbe-Mineral interactions: cave geomicrobiology. In: Jain, S.K., Khan, A.A., Rai, M.K (Eds.), Geomicrobiology, CRC Press, New York: 1-45.

Leuko, S., Koskinen, K., Sanna, L., D'Angeli, I.M., De Waele, J., Marcia, P., Moissl-Eichinger, C., Rettberg, P., 2017. The influence of human exploration on the microbial community structure and ammonia oxidizing potential of the Su Bentu limestone cave in Sardinia, Italy. PLoS ONE, 12(7): e0180700. https://doi.org/10.1371/journal.pone.0180700

Loescher, C.R., Großkopf, T., Desai, F.D., Gill, D., Schunck, H., Croot, P.L., Schlosser, C., Neulinger, S.C., Pinnow N., Lavik G., Kuypers M.M.M., LaRoche J., Schmitz R.A., 2014. Facets

of diazotrophy in the oxygen minimum zone waters off Peru. ISME Journal, 8(11): 2180-2192

Macalady, J.L., Lyon, E.H., Koffman, B., Albertson, L.K., Meyer, K., Galdenzi, S., Mariani, S., 2006. Dominant microbial population in limestone-corroding stream biofilms, Frasassi cave system, Italy. Applied Environmental Microbiology, 72(8): 5596-5609.

Macalady, J.L., Jones, D.S., Lyon, E.H., 2007. Extremely acidic, pendulous cave wall biofilms from the Frasassi cave system, Italy. Environmental Microbiology, 9(6): 1402-1414.

Macalady, J.L., Dattagupta, S., Schaperdoth, I., Jones, D.S., Druschel, G.K., Eastman, D., 2008. Niche differentiation among sulfur-oxidizing bacterial populations in cave waters. The ISME Journal, 2(6): 590-601.

Maciejewska, M., Adam, D., Naômé, A., Martinet, L., Tenconi, E., Calusińska, M., Delfosse, P., Hanikenne, M., Baurain, D., Compère, P., Carnol, M., Barton H.A., Rigali, S., 2017. Assessment of the potential role of the *Streptomyces* in cave moonmilk formation. Frontiers in Microbiology, 8: article 1181. Doi: 10.3389/fmicb.2017.01181.

Mackey, E.A., Becker, D.A., Spatz, R.O., Paul, R.L., Greenberg, R.R., Lindstrom, R.M., Yu, L.L., Wood, L.J., Long, S.E., Kelly, W.R., Mann, J.L., MacDonald, B.S., Wilson, S.A., Brown, Z.A., Briggs, P.H., Budhan, J., 2004. Certification of NIST Standard Reference Material 1575a pine needles and results of an international laboratory comparison. NIST Special Publication: 260-156.

Maggiore, M., Pagliarulo, P., 2004. Circolazione idrica ed equilibri idrogeologici negli acquiferi della Puglia. Geologi e Territorio, 1: 13-35.

Mansor, M., Harouaka, K., Gonzales, M.S., Macalady, J.L., Fantle, M.S., 2018. Transport-Induced Spatial Patterns of Sulfur Isotopes (δ^{34} S) as Biosignatures. Astrobiology, 18(1): 59-72.

Miller, A.Z., Dionísio, A., Sequeira Braga, M.A., Hernández-Mariné, M., Afonso, M.J., Muralha, V.S.F., Herrera, L.K., Raabe, J., Fernández-Cortès, A., Cuezva, S., Hermosin, B., Sanchez-Moral, S., Chaminé, H., Saiz-Jimenez, C., 2012. Biogenic Mn oxide minerals coating in a subsurface granite environment. Chemical Geology, 322-323: 181-191.

Miller, A.Z., Pereira, M.F.C., Calaforra, J.M., Forti, P., Dionísio, A., Saiz-Jimenez, C., 2014. Siliceous speleothems and associated microbe-mineral interactions from Ana Heva lava tube in Easter Island (Chile). Geomicrobiology Journal, 31: 236–245.

Miller, A.Z., Garcia-Sanchez, A.M., Martin-Sanchez, P.M., Costa Pereira, M.F., Spangenberg, J.E., Jurado, V., Dionísio A., Afonso, M.J., Iglésias Chaminé, H.I., Hermosin, B., Saiz-Jimenez, C., 2018. Origin of abundant moonmilk deposits in a subsurface granitic environment. Sedimentology, 65(5): 1482-1503.

Norris, P.R., Clark, D.A., Owen, J.P., Waterhouse, S., 1996. Characteristics of Sulfobacillus acidophilus sp. nov. and other moderately thermophilic mineral-sulphide-oxidizing bacteria. Microbiology, 142 (Pt 4):775-83.

Northup, D.E., Lavoie, K.H., 2001. Geomicrobiology of caves: a review. Geomicrobiology Journal, 18: 199-222.

Northup, D.E., Reysenbach, A-L., Pace, M.N., 1997. Microorganisms and speleothems. In: C.A., Hill, P., Forti (Eds.), Cave minerals of the world, National Speleological Society, Huntsville: 261-266.

Northup, D.E., Dahn, C.N., Melim, A., Spilde, M.N., Crossey, L.J., Lavoie, K.H., Mallory, L.M., Boston, P.J., Cunningham, K.I., Barns, S.M., 2000. Evidence for geomicrobiological interactions in Guadalupe caves. Journal of Cave and Karst Studies, 62(2): 80-90.

Onac, B.P., Ghergari, L., 1993. Moonmilch mineralogy in some Romanian and Norwegian Caves. Cave Science, 20: 107-111.

Onac, B.P., Lauritzen, S-E., 1995. On some cave minerals from northern Norway. International Journal of Speleology, 1(4): 67-75.

Onac, B.P., Wynn, J.G., Sumrall, J.B., 2011. Tracing the source of cave sulfates: a unique case from Cerna Valley, Romania. Chemical Geology, 288: 105-114.

Pieri, P., Festa, V., Moretti, M., Tropeano, M., 1997. Quaternary activity of the Murge area (Apulian foreland-Southern Italy). Annals of Geophysics, 40(5): 1395-1404.

Pisarowicz, J.A., 1994. Cueva de Villa Luz - an active case of H_2S speleogenesis. In: I.D., Sasowsky, M.V., Palmer (Eds.), Breakthroughs in Karst Geomicrobiology and Redox Geochemistry. Karst Waters Institute, Special Publication 1: 60–62.

Quast, C., Pruesse, E., Yilmaz, P., Gerken, J., Schweer, T., Yarza, P., Peplies, J., Glockner, F.O., 2013. The SILVA ribosomal RNA gene database project: improved data processing and web-based tools. Nucleic Acids Research, 41 (D1): D590-D596.

Riquelme, C., Hathaway, J.J.M., Dapkevicius, M.D.L.E., Miller, A.Z., Kooser, A., Northup, D.E., Jurado, V., Fernandez, O., Saiz-Jimenez, C., Cheeptham, N., 2015. Actinobacterial diversity in volcanic caves and associated geomicrobiological interactions. Frontiers in Microbiology, 6: 1342.

Rossmassler, K., Engel, A.S., Twing, K.I., Hanson, T.E., Campbell, B.J., 2012. Drivers of epsilonproteobacterial community composition in sulfidic caves and springs. FEMS Microbiology Ecology, 79(2): 421-32. doi: 10.1111/j.1574-6941.2011.01231.x.

Santaloia, F., Zuffianò, L.E., Palladino, G., Limoni, P.P., Liotta, D., Minissale A., Brogi, A., Polemio, M., 2016. Coastal thermal springs in a foreland setting: The Santa Cesarea Terme system (Italy). Geothermics, 64: 344-361.

Segata, N., Izard, J., Waldron, L., Gevers, D., Miropolsky, L., Garrett, W.S., Huttenhower, C., 2011. Metagenomic biomarker discovery and explanation. Genome Biology, 12(6): R60.

Segerer, A., Langworthy, T.A., Stetter, K.O., 1988. Thermoplasma acidophilum and Thermoplasma volcanium sp. nov. from Solfatara Fields. Systematic and Applied Microbiology, 10:161-171.

Sorokin, D.Y., Tourova, T.P., Braker,G., Muyzer,G., 2007. Thiohalomonas denitrificans gen.nov., sp.nov. and Thiohalomonas nitratireducens sp. nov., novel obligately chemolithoautotrophic, moderately halophilic, thiodenitrifying Gammaproteobacteria from hypersaline habitats. International Journal of Systematic Evolutionary Microbiolbiology, 57: 1582–1589. doi:10.1099/ijs.0.65112-0

Spilde, M. N., Northup, D. E., Boston, P. J., Schelble, R. T., Dano, K. E., Crossey, L. J., Dahm, C. N., 2005. Geomicrobiology of cave ferromanganese deposits: a field and laboratory investigation. Geomicrobiology Journal, 22(3-4): 99-116.

Staley, J.T. 1968. *Prosthecomicrobium* and *Ancalomicrobium*: New prosthecate freshwater bacteria. Journal of Bacteriology, 95: 1921-1942.

Stumm, W., 1992. Chemistry of Solid-Water Interface: Process at the Mineral-Water and Particle-Water Interface in Natural system. John Wiley, New York.

Tanaka, N., Romanenko, L.A., Iino, T., Frolova, G.M., Mikhailov, V.V., 2011. Cocleimonas flava gen. nov., sp. nov., a gammaproteobacterium isolated from sand snail (Umbonium costatum). International Journal of Systematic Evolutionary Microbiology, 61(Pt 2):412-6. doi: 10.1099/ijs.0.020263-0

Tisato, N., Torriani, S., Monteaux, S., Sauro, F., De Waele, J., Tavagna, M.L., D'Angeli, I.M., Chailloux, D., Renda, M., Eglinton, T.I., Bontognali, T.R.R, 2015. Microbial mediation of complex subterranean mineral structures. Scientific Report, 5(15525). DOI: 10.1038/srep15525.

Tombácz, E., Dobos, Á., Szekeres, M., Narres, H.D., Klumpp, E., Dékány, I., 2000. Effect of pH and ionic strength on the interaction of humic acid with aluminium oxide. Colloid and Polymer Science, 278(4): 337-345.

Tomczyk-Żak, K., Zielenkiewicz, U., 2015. Microbial diversity in caves. Geomicrobiology Journal, 33(1), 20-38.

Umezawa, K., Watanabe, T., Miura, A., Kojima, H., Fukui, M., 2016. The complete genome sequences of sulfur-oxidizing Gammaproteobacteria Sulfurifustis variabilis skN76T and Sulfuricaulis limicola HA5T. Standards in Genomic Sciences, 11: 71. doi: 10.1186/s40793-016-0196-0.

Velaj, T., 2015. New ideas on the tectonic of the Kurveleshi anticlinal belt in Albania, and the perspective for exploration in its subthrust. Petroleum, 1: 269-288.

Vespasiano, G., Apollaro, C., Muto, F., De Rosa, R., Dotsika, E., Marini, L., 2016. Preliminary geochemical characterization of the thermal waters of the Grotta delle Ninfe near Cerchiara di Calabria (South Italy). Società Geologica Italiana, 39: 130-133. DOI: 103301/ROL.2015.130.

Vinokur J.M., Cummins, M.C., Korman, T.P., Bowie, J.U., 2016. An adaptation to life in acid through a novel mevalonate pathway. Scientific Reports, 6: 39737.

Vlasceanu, L., Sarbu, S.M., Engel, A.S., Kinkle, B.K., 2000. Acidic cave wall biofilms located in the Frasassi Gorge, Italy. Geomicrobiology Journal, 17: 125-139.

Wang, C., Guo, G., Huang, Y., Hao, H., Wang, H., 2017. Salt adaptation and evolutionary implication of a Nah-related PAHs dioxygenase cloned from a halophilic phenanthrene degrading consortium. Scientific Reports, 7: 12525. DOI:10.1038/s41598-017-12979-z.

Wasmund, K., Mußmann, M., Loy, A., 2017. The life sulfuric: microbial ecology of sulfur cycling in marine sediments. Environmental Microbiology Reports, 9(4): 323-344. doi: 10.1111/1758-2229.12538.

Watanabe, T., Kojima, H., Fukui, M., 2015. Sulfuriferula multivorans gen. nov., sp. nov., isolated from a freshwater lake, reclassification of 'Thiobacillus plumbophilus' as Sulfuriferula plumbophilus sp. nov., and description of Sulfuricellaceae fam. nov. and Sulfuricellales ord. nov. International Journal of Systematic Evolutionary Microbiology, 65(Pt 5): 1504-8. doi: 10.1099/ijs.0.000129.

Whitman, W.B., Coleman, D.C.., Wieble, W.J., 1998. Prokaryotes: The unseen majority. Proceedings of the National Academy of Sciences, 95: 6578-6583.

Wirsen, C.O., Sievert, S.M., Cavanaugh, C.M., Molyneaux, S.J., Ahmad, A., Taylor, L.T., DeLong, E.F., Taylor, C.D., 2002. Characterization of an autotrophic sulfide-oxidizing marine Arcobacter sp. that produces filamentous sulfur. Applied Environmental Microbiology, 68(1): 316-325.

Wynn, J.G., Sumrall, J.B., Onac, B.P., 2010. Sulfur isotopic composition and the source of dissolved sulfur species in thermo-mineral springs of the Cerna Valley, Romania. Chemical Geoleology, 271: 31-43.

Yue, X., Yu, G., Lui, Z., Lu, Y., Li, Q., 2018. Start-up of the completely autotrophic nitrogen removal over nitrite process with a submerged aerated biological filter and the effect of inorganic carbon nitrogen removal and microbial activity. Bioresource Technology, 254: 347-352.

Zerkle, A.L., Kamyshny, A., Kump, L.R., Farquhar, J., Oduro, H., Arthur, M.A., 2010. Sulfur cycling in a stratified euxinic lake with moderately high sulfate: constraints from quadruple S isotopes. Geochimica and Cosmochimica Acta, 74: 4953-4970.

Zinke, L.A., Kiel Reese, B.K., McManus, J., Wheat, C.G., Orcutt, B.N., Amend, J.P., 2018. Sediment Microbial Communities Influenced by Cool Hydrothermal Fluid Migration. Frontiers Microbiology, 9:1249 doi: 10.3389/fmicb.2018.01249.

Zuffianò, L.E., Polemio, M., Laviano, R., De Giorgi, G., Pallara, M., Limoni, P.P., Santaloia, F., 2018. Sulfuric acid geofluid contribution on thermal carbonate coastal springs (Italy). Environmental Earth Sciences, 77(13): 517. DOI: 10.1007/s12665-018-7688-8.

SECOND SECTION: ITALIAN SAS CAVES

6. ITALIAN SAS CAVES

6.1. Article 4

Accepted from Geomorphology

Sulfuric acid caves of Italy: A review.

Ilenia M. D'Angeli[1*], Mario Parise[2], Marco Vattano[3], Giuliana Madonia[3], Sandro Galdenzi[4], Jo De Waele[1]

[1]Department of Biological, Geological and Environmental Sciences, University of Bologna, Via Zamboni 67, 40126 Bologna, Italy, dangeli.ilenia89@gmail.com; jo.dewaele@unibo.it

[2]Department of Geological and Environmental Sciences, University of Bari Aldo Moro, Via E. Orabona 4, 70125 Bari, Italy, mario.parise@uniba.it

[3]Department of Earth and Marine Sciences, University of Palermo, Via Archirafi n. 20, 90123 Palermo, Italy, marco.vattano@unipa.it; giuliana.madonia@unipa.it;

[4]Jesi, Italy, galdenzi.sandro@tiscali.it;

[*] Corresponding author

6.1.1. Abstract

In Italy, especially along the Apennine Chain, numerous active and inactive sulfuric acid speleogenetic (SAS) caves have been documented in the last two decades. Here we present an overview of these peculiar hypogene systems, illustrating their main geomorphological and mineralogical features, and the microbial signatures observed in the active underground environment. SAS caves are abundantly diffuse in the northern and central Apennines, whereas they are less copious in the southern Apennines, in the Apulian foreland, in Sicily and in Sardinia. Their location is significantly influenced by lithological and structural rock properties, as they occur in carbonate areas where acidic fluids, deriving from the interactions with deep-seated sulfates and/or sulfides, rise through deeply rooted geological structures.

Geomorphological observations demonstrated sub-horizontal maze networks to be common arrangements for SAS caves, whereas gypsum, sulfur and alunite supergroup minerals are the most abundant sulfuric acid by-products. The δ^{34} S results demonstrated the deep-seated H_2S sources to be mainly related to the interaction between Triassic evaporites and bitumen.

Keywords: hypogene caves, speleogenesis, karst, cave sulfates, stream biofilms

6.1.2. Introduction

Hypogene speleogenesis is worldwide recognized and is the most important process of karst system development together with the classical "epigene" cave formation (Klimchouk, 2007, 2009, 2018). The concept of hypogene speleogenesis has been intensely debated in the last years, and the two main theories established in the past, one strictly geochemical (Palmer, 2000) and the other, more hydrogeological (Klimchouk 2007, 2015), have been recently unified. Hypogene karstification is now defined as *"the formation of solution-enlarged permeability structures by upwelling of fluids that recharge the cavernous zone from hydrostratigraphically lower units, where fluids originate from distant or deep sources, independent of recharge from overlying or immediately adjacent surface"* (Klimchouk, 2017, p.3). The upwelling waters involved in speleogenesis may have different origins such as juvenile (magmatic), metamorphic, connate, due to deep meteoric and/or marine water circulation paths or to mixing of different fluids (Mylroie et al., 1995; Hill, 2000; Mylroie and Mylroie, 2018), and their aggressiveness is linked to interaction with deep-seated sources (Hill, 1987; 1990). During rising, these deep fluids undergo changes in pressure and temperature, which cause a progressive evolution of the solution and precipitation of different mineralogical associations (Klimchouk, 2017) along their (often several km long) path. The occurrence of hypogene speleogenesis has been documented in several karstified lithologies such as carbonates, evaporites and quartzites (Klimchouk, 2009; Sauro et al., 2014), and according to the chemical processes involved (Klimchouk, 2017) the different types of karstification are related to the presence of sulfuric acid (Jagnow et al., 2000; Audra, 2008; Palmer, 2013), hydrothermal fluids (Dublyansky, 1980; Bakalowicz et al., 1987), mixing corrosion, and evaporite-dissolution. In general, hypogene caves can originate in both confined or unconfined conditions, but frequently they develop in confined settings (Klimchouk, 2005, 2009, 2018). Subsequent events such as uplift, exhumation, surficial erosion, and denudation (Klimchouk, 1996) can shift hypogene caves from their native deep settings to shallow environments, where other processes can take over, locally overprinting the original morphologies and deposits.

Nevertheless, a recent research, carried out in four sulfuric acid water table cave systems (De Waele et al., 2016), has shown sulfuric acid speleogenesis (SAS) to occur frequently in unconfined conditions. Thanks to their origin (with recharge coming from below), hypogene caves are climate-independent and do not directly rely on seepage from CO_2-enriched surface waters. This explains the apparent paradox that the most famous and longest hypogene caves of the world, such as Carlsbad Caverns and Lechuguilla in the Guadalupe Mountains of New Mexico, USA (Hill, 2000; Jagnow et al., 2000), and Toca da Boa Vista-Toca da Barriguda system in Bahia, Brazil (Auler and Smart, 2003;

Klimchouk et al., 2016), do not occur in high rainfall areas, but are located in semi-arid and dry regions.

As suggested by several authors (Dublyansky, 1980; Klimchouk, 2007, 2018) the most diagnostic characteristics of inactive hypogene environments are their morphological features and the occurrence of complex sequences of exotic minerals (Polyak and Provencio, 2001). Hypogene caves are characterized by the lack of genetic relationship with the external landscape (absence of dolines, sinking streams, and blind valleys, all features typical of epigene karst), thus not showing the typical morphologies of vadose, concentrated and fast water flow. This results in 2 and/or 3D maze networks that mainly follow the fissure systems rather than the bedding planes, most having abrupt endings (Hill, 1995) and well-developed cupola-like morphologies on the ceilings of cave conduits. There is a general lack of fluvial sediments, whereas secondary by-products due to the weathering and replacement of host rock or primary deposits, calcite (dogtooth spar) and silica coatings are abundant.

Understanding the genesis of a karst system is an important issue for cavers and karst scientists around the world. Nevetheless, caves often have a polygenetic history (Hill, 2000; Palmer and Palmer, 2000; Palmer, 2013; Parise et al., 2018), and it is not always possible to recognize all the stages of cave formation and evolution. For this reason, geomorphological, geochemical, mineralogical and hydrogeological observations and analyses are necessary to find the most reasonable clues.

Sulfuric acid speleogenesis (SAS) is caused by "*deep H_2S-bearing fluids rising toward unconfined carbonate aquifers and water tables*" (Klimchouk, 2017 p.19). The most common H_2S sources are: i) volcanic (Aiuppa et al., 2005) and magmatic activities (Cavarretta and Lombardi, 1992); ii) assimilatory-dissimilatory (60-80°C) and thermochemical (100-180°C) sulfate reduction (Canfield, 2001; Machel, 2001; Wynn et al., 2010) of deep-seated evaporite rocks and hydrocarbon tiers (Hill, 1995; Maggiore and Pagliarulo, 2004); iii) reduction of marine waters involved in deep circulation flows through fissure networks (Santaloia et al., 2016) or buried seawater (Machel, 2001; Wynn et al., 2010).

Other interesting sulfuric acid caves, not related to hypogene processes, might form due to the oxidation of sulfide ores such as pyrite, marcasite, galena, blenda (Morehouse, 1968; Auler and Smart, 2003; Tisato et al., 2012) in supergene conditions through abiotic or microbially-mediated processes (Engel et al., 2004).

In addition, the presence of SAS caves may be the evidence of "H_2S-related porosity" and/or "sulfuric acid oil-field karst" (Hill, 1995).

The production of H_2S due to sulfate reduction takes place in deep-seated environments when natural gases interact with evaporite rocks that are, subsequently, replaced by bio-epigenetic calcite (reaction 1)

1. $Ca^{2+} + 2SO_4^{2-} + 2H_2O + 2CH_4 + 2H^+ => 2H_2S + CaCO_3 + CO_2 + 5H_2O$

The most important reaction for SAS, firstly demonstrated by Principi (1931) and Egemeier (1981), is the oxidation of hydrogen sulfide (H_2S) into sulfuric acid (H_2SO_4), which immediately reacts with the surrounding rocks (Palmer, 2013). H_2S oxidation can occur in two environments (*Figure 2*): 1) where rising fluids enriched in H_2S meet 1a) deep oxidizing waters (it firstly occurs at the lower contact with a O_2-rich aquifer) or 1b) shallow oxidizing waters close to the water table (meteoric or sea waters, directly exchanging with the external atmosphere), or 2) above the water table, in the oxidizing cave atmosphere (Galdenzi, 1990; Galdenzi and Maruoka, 2003; Audra, 2008).

The oxidation of H_2S can be direct (reaction 2) or characterized by intermediate steps with the production of native sulfur (reactions 3 and 4). Sulfur-oxidizing bacteria mediation can enhance the reaction speed bypassing the intermediate phases (Engel et al., 2004; Imhoff, 2006; Palmer, 2013).

2. $H_2S + 2O_2 \Leftrightarrow H_2SO_4$ ($SO_4^{2-} + 2H^+$ in aqueous solution)
3. $H_2S + O_2 => 2S^0 + H_2O$
4. $2S^0 + 3O_2 + 2H_2O => 2SO_4^{2-} + 2H^+$ (in aqueous solution)

Once sulfuric acid (H_2SO_4) comes in contact with the host rock, it starts immediately to dissolve large amounts of carbonate, possibly creating large karst chambers (Hill, 1995), following the reaction below (reaction 5)

5. $CaCO_3 + SO_4^{2-} + 2H^+ + 2H_2O => CaSO_4 \cdot 2H_2O + CO_2 + H_2O$.

Limestone ($CaCO_3$) is replaced by gypsum ($CaSO_4 \cdot 2H_2O$) and the CO_2 is released into the cave atmosphere, which in turn contributes to increase the general acidity of the water film, and to enhance dissolution of further limestone (reaction 6)

6. $CaCO_3 + CO_2 + H_2O => Ca^{2+} + 2HCO_3^-$.

Geomorphological observation of cave features, and mineralogical sampling together with geochemical (in active environments) investigations may help to understand the stages of cave formation and landscape evolution (Palmer, 2013).

6.1.2.1. Sulfuric acid signature in active environments

Generally, the active SAS systems are characterized by Ca-Cl-SO_4 or Na-Cl-SO_4 waters (Hose and Pisarowicz, 1999; Hose et al., 2000; Grassa et al., 2006; Santaloia et al., 2016; Vespasiano et al., 2016; D'Angeli et al., 2017b) with variable contents of dissolved H_2S. Waters rich in H_2S have a typical rotten-egg smell, and are often, but not always, thermal. Commonly, in these peculiar settings, waters have a milky appearance (due to elemental sulfur) and are abundantly colonized by white biofilms (*Figure 43*A) (Engel et al., 2004; Imhoff, 2006; Hamilton et al., 2015). If $H_2S_{(g)}$ degasses in the cave atmosphere in high concentrations, vermiculation deposits (*Figure 43*B) (Hose & Northup,

2004; Jones et al., 2008; D'Angeli et al., 2017a), white pastry materials such as moonmilk (*Figure 43*C), and mucolites and snottites as well (Galdenzi et al., 1999b; Hose et al., 2000; Galdenzi and Maruoka, 2003, Macalady et al., 2007) can abundantly thrive on walls and ceilings.

6.1.2.2. Geomorphological features

Differently from the active environments, inactive SAS caves can be recognized if searching for diagnostic geomorphological features (*Table 18*) However, these forms are not exclusively of SAS processes, but they concern general rising movements and can occur in all kind of hypogene environment.

As shown by Audra (2008) and Palmer (2013), hypogene SAS caves can be deep phreatic systems (confined setting) and/or underground environments developed at or the above water table (unconfined setting). Nevetheless, it is difficult to discriminate the morphologies based on setting/environment, especially because the same form might occur in different conditions (phreatic and/or vadose). Here, we provide a list of all the morphologies that commonly might be observed in SAS systems. Generally, slow rising fluids create 2D and 3D anastomotic networks or spongeworks (Palmer, 2013), feeders (i.e. vertical and often narrow passages through which deep water ascended intospacious caves, and where the dissolution reactions take mainly place; Klimchouk, 2009), and blind chimneys. Rising channels (and/or rising half tubes) might form when ascending fluids (water and/or aerosols) develop along overhanging walls, cupola-morphologies create along walls and ceilings close to feeders (*Figure 43*E). Domes are due to convective underwater/aerosol flows triggered by thermal gradient towards the ceilings of cave condits (Klimchouk et al., 2016). Bubble trails represent the corrosive imprints of rising gas bubbles along the wall of standing water bodies (Audra et al*.,* 2009c). Mazes with circular cross-section (Klimchouk, 2007; Audra, 2008) (*Figure 43*D) might occur, but they are often comprised of rift-type passages. Abrupt dead ends form far away from the source of acidity, and are indicative of a weaker dissolutional power of the involved solution. Other specific features are (Audra, 2008; Audra et al., 2009b; De Waele et al., 2016) niches and spheres located along walls and ceilings of the cave conduits and due to convective flow movements. Rising warm fluids can also create big rounded morphologies on the walls and ceilings defined as "megascallops" (Plan et al*.,* 2012). Nevertheless, this term is misleading being scallops indicative signs of water turbulence. In this work, we propose to replace "megascallops" with "megacusps" (V. Polyak personal comment). Vents might develop only in localized points emitting acidic fluids able to create tubes that, sometimes, can connect several cave levels. Instead, wall partitions are favored by convection fluxes able to enlarge former voids; if the process continues for a long time the interconnection of voids can occur (Osborne, 2007). Boxworks are similar to honeycombs, and were

recently suggested to indicate pre-exposure interactions of rising conduit- and pore-waters in the surrounding wallrock, resulting in the formation of structured heterogeneity (Klimchouk, 2018). Thus, the presence of secondary crystalline veins in the micritic host rock can favor the differential dissolution of the micritic matrix. The general acidity of hypogene settings produces weathered walls (Plan et al., 2012), but also drip tubes (acidic droplets can create dissolutional tubes in soft rocks below).

In sulfuric acid conditions, sulfuric-acid karren (De Waele et al., 2016), sulfuric-acid cups, and sulfuric-acid laminar condensation runoff might happen. Replacement pockets form exclusively in aerate conditions where the warm acid vapors (enriched with H_2SO_4) condensate on the carbonate rocks, corroding and replacing them with gypsum. The gypsum, behaving as hygroscopic materials, is able to attrack further condensation of acidic vapor (Audra, 2008), producing a progressive deepening and of the initial pocket.

6.1.2.3. Mineralogical and geochemical features

SAS caves may contain peculiar secondary mineral deposits (Onac et al., 2009; Audra et al., 2015) well-known as "speleogenetic by-products" (Polyak and Provencio, 2001), considered important indicators of cave formation, inasmuch, related to the interaction between H_2SO_4 and bedrock. They can be the product of dissolution and subsequent replacement of the host rock (generally carbonates), weathering of insoluble minerals and sediments (clay minerals), and precipitation of ions present in the solution (Temovski, 2017; Onac and Drăguşin, 2017).

The most abundant speleogenetic by-products are gypsum (*Figure 43*D,E,G) and native sulfur (*Figure 43*H), alunite group minerals (*Figure 43*I), felsöbányaite, hydrous manganese oxides, aluminite, uranyl vanadates and others less common minerals (Onac et al., 1995, 2009; Polyak and Provencio, 2001; Feier, 2003; Sauro et al., 2014; D'Angeli et al., 2018).

Furthermore, interesting information about the water table position can be inferred from the arrangement of gypsum deposits (Buck et al.,1994), whereas fluid acidity can be obtained using alunite supergroup minerals (Polyak et al.,1998; Polyak and Provencio, 2001; D'Angeli et al., 2018). The investigation of stable sulfur isotopes can give important information about the source of H_2S. Table 3 provides a list with the sulfur $\delta^{34}S$ results obtained analyzing gypsum deposits collected in the caves object of this work. Generally, the samples exhibit several domains, which likely related to different degrees of interaction between Triassic (δ^{34} S +15 to +17.2‰) or Messinian (δ^{34} S +20 to +23.7‰) evaporites (Lugli et al., 2007; Boschetti et al., 2011; Natalicchio et al., 2014) and bitumen (δ^{34} S -18.9 to -13.5‰; values observed in bitumen deposits collected in the *Majella* Massif, Abruzzo), and deserve further investigations.

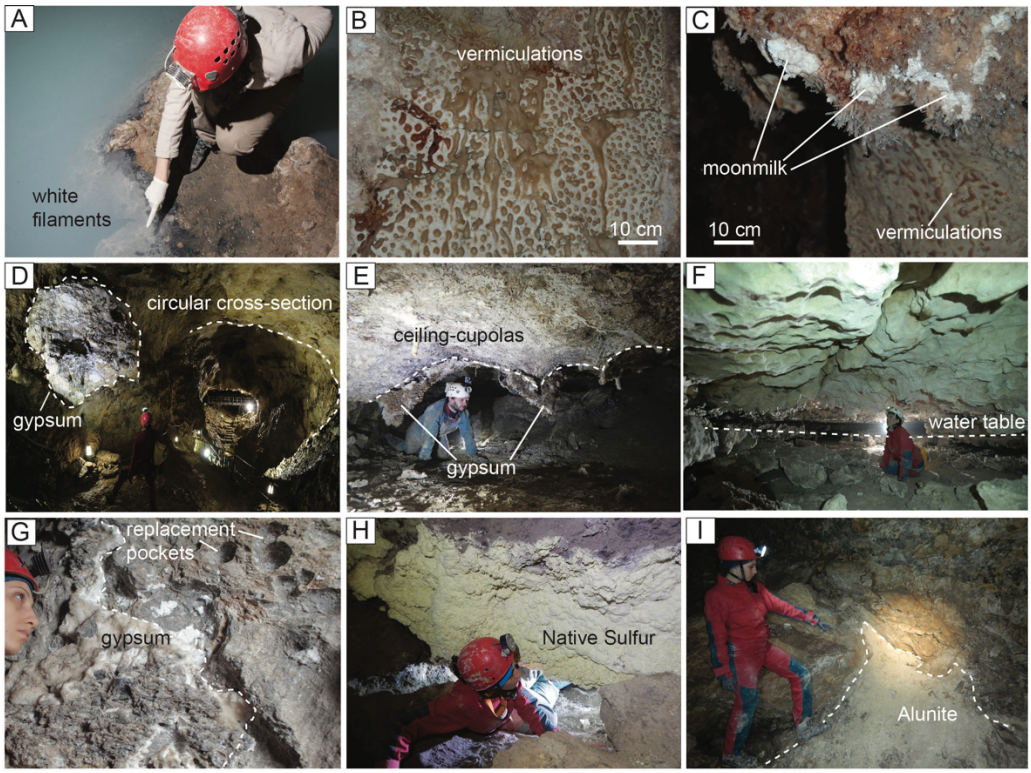

Figure 43. Pictures showing some of the most peculiar signatures of SAS caves, both in active and inactive conditions. A) White biofilms growing in the milky sulfidic waters of Ninfe Cave, Cerchiara di Calabria (photo O. Lacarbonara); B) Vermiculation deposits totally covering walls and ceilings of Fetida Cave, Santa Cesarea Terme, Apulia (photo M. Parise); C) Whitish moonmilk deposits growing on the walls in the same environmental conditions of vermiculations (photo M. Parise); D) Circular cross-section of the main gallery of Cavallone Cave, Abruzzo. A metric gypsum deposit can be observed on the left (photo G. Antonini); E) Ceiling cupolas in a small cavity close to Acqua Mintina Cave, Sicily. The condensation-corrosion processes, producing the dissolution of carbonate rocks, immediately induce the precipitation of gypsum deposits as chandelier structures (photo M. Vattano); F) The picture clearly displays the evidence of a fossil water table, in Acqua Fitusa Cave, Sicily (photo M. Vattano); G) Circular replacement pockets and gypsum deposits on the walls of the lower Sant'Angelo Cave, Calabria (photo O. Lacarbonara); H) Native sulfur growing on the walls of Acqua Mintina Cave, Sicily. The limestone is partially replaced by gypsum and celestine, and covered by a thin layer of organic matter characterized by dark colors (photo M. Vattano); I) Whitish alunite deposits in the innermost zone of Cavallone Cave, Abruzzo (photo M. Nagostinis).

6.1.3. Why are SAS caves so abundant in Italy?

Italy hosts about 25% of the worldwide known SAS cave systems. To the present-day knowledges, excluding Italy, the SAS processes are well developed in USA, having ~30 systems. Nevertheless,

also France (~7), Mexico (~6), Turkimenistan (~5), Austria, Kyrgyztan, Romania (~4 main systems), Iraq (~3), Canada, Russia (~2), Algeria, Argentina, Brazil, Georgia, Greece Jordania, Macedonia, Namibia, Turkey, and, South Africa (only 1) host exceptional examples.

In Italy most of the SAS systems are still active, and located especially along the Apennine Chain (Galdenzi and Menichetti, 1995; Galdenzi et al., 2008; Galdenzi, 2012, 2015), in Apulia, Sicily and Sardinia (De Waele et al., 2014; D'Angeli et al., 2016) (*Table 17*).

Italy is characterized by diversified terrains, indicating a very complex geological evolution derived from a still active dynamic interaction between the Eurasia and Adria plates (Doglioni and Flores, 1997). Generally, along the Apennine Chain, the geological units consist of 1) Paleozoic crystalline basement covered by 2) Triassic limestone, dolostone and evaporite sequences enriched with organic matter, 3) Jurassic-Oligocene carbonate rocks, 4) middle Cenozoic arenaceous clayey sediments, and 5) upper Cenozoic silico-clastic foredeep deposits, intensely deformed by fold and thrust-belts. The principal detachments occurred in correspondence of the contact between the Triassic evaporites and the Hercynian basement, during the first stages of the Apennine mountain belt formation. Synsedimentary normal faults affected the sedimentary pile during Jurassic times and also later, during the opening of the Tyrrhenian basin (Bally et al., 1988).

In such conditions, deep faults would behave as direct connection between the more surficial carbonates and the deep-seated sulfate-rich layers (*Figure 44*), thus allowing the upwelling of acidic fluids, and consequently the formation of hypogene sulfuric acid caves. The sulfate reduction of deep-seated Triassic evaporites is probably the main source of H_2S in the Italian SAS caves located especially along the northern-central Appennines (Galdenzi and Menichetti, 1995); nevertheless, also Messinian evaporites, volcanic and magmatic activities, hydrocarbon, and locally pyrite oxidation (Auler and Smart, 2003; Tisato et al., 2012) may have contributed, in various amounts, to the formation of sulfuric acid caves.

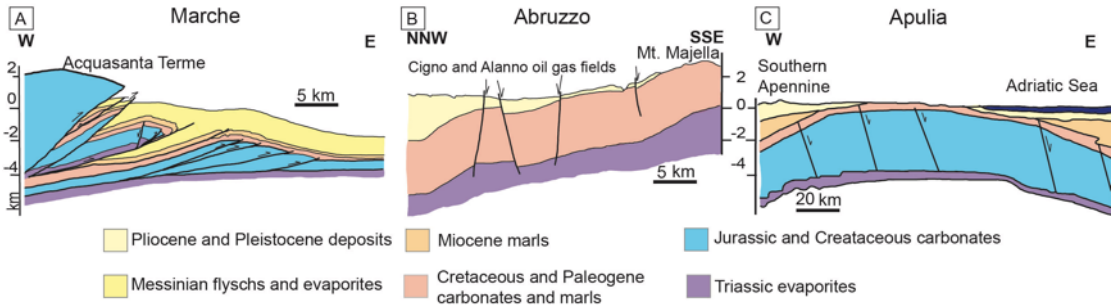

Figure 44. General sketches of three different portions of Italy. A) The Marche Apennine is characterized by fold and thrust belt, in which deep faults are well-connected with Triassic evaporites (modified from Ghisetti and Vezzani, 2000); B) Cross section along the Majella anticline (Abruzzo) showing horst and graben structures connected with Triassic evaporites (modified from Ghisetti and

Vezzani, 2002); C) Apulian foreland exhibiting a distensive domain (modified from Velaj, 2015). The location of each cross section is reported (A, B, and C) in Figure 50.

6.1.4. Sulfuric acid cave systems in Italy

Sulfuric acid karst systems and caves showing only some hypothetical features of SAS process, have been described from 12 Italian regions, mainly located along the Apennine Chain (*Table 17*). Most of these systems are well-known, and have been studied for decades, others are known but not yet investigated, whereas four have been mentioned in literature and await to be confirmed as SAS. Interesting examples of pyrite oxidation contained in the host rock have also been documented in Veneto (Tisato et al., 2012). In addition, a case of hydrothermal hypogene cave located in Sardinia, such as *Corona'e Sa Craba* evolved in quartzite rocks, has been documented to contain a peculiar suite of SAS minerals (Sauro et al., 2014).

Table 17. List of SAS systems of Italy and their respective location, and present-day condition. Key to the last columns: S = studied; K = known; P = presumed. The present-day conditions have been described as a function of the cave position on the sulfuric water table: inactive (no trace of recent sulfuric waters, the sulfuric acid waters are far below the lowest levels of the caves), active (the process is still in action and caves open at/or close to the sulfuric water table), active/inactive (the sulfuric water table abandoned main cave galleries, but it is still close to the lowest cave passages).

Cave system	Location	Present-day condition	S	K	P
1. Pisatela-Rana	Veneto	Inactive	x		
2. Porretta Terme	Emilia-Romagna	Active	x		
3. Triponzo	Umbria	Active	x		
4. Monte Cucco	Umbria	Inactive	x		
5. Frasassi	Marche	Active	x		
6. Acquasanta Terme	Marche	Active	x		
7. Parrano	Umbria	Active-Inactive	x		
8. Pozzi della Piana	Umbria	Inactive		x	
9. Montecchio	Tuscany	Active	x		
10. Cittareale	Latium	Inactive		x	
11. Monti della Tolfa	Latium	Active-Inactive		x	
12. Monte Soratte	Latium	Inactive			x
13. Buco del Pretaro	Latium	Inactive			x
14. Subiaco	Latium	Inactive			x
15. Grotta di Fiume Coperto	Latium	Active	x		
16. Cavallone-Bove	Abruzzo	Inactive	x		
17. Monti Lattari	Campania	Active			x
18. Capo Palinuro	Campania	Active	x		
19. Monte Sellaro	Calabria	Active-Inactive	x		
20. Cassano allo Ionio	Calabria	Active-Inactive	x		
21. Terme Luigiane	Calabria	Inactive	x		
22. Santa Cesarea Terme	Apulia	Active	x		
23. Acqua Mintina	Sicily	Inactive	x		
24. Acqua Fitusa	Sicily	Active-Inactive	x		
25. Corona'e Sa Craba	Sardinia	Inactive	x		
26. Iglesiente-Sulcis mine caves	Sardinia	Inactive	x		

Figure 45 shows the cross-sections of the most representative SAS caves, whereas *Figure* 46 the their planimetries. *Table 18* describes the main geomorphological features, whereas *Table 19* reports the available mineralogical results and δ^{34} S isotope data of gypsum deposits. The microbiological substances occurring in the still active caves are summarized in *Table 20*.

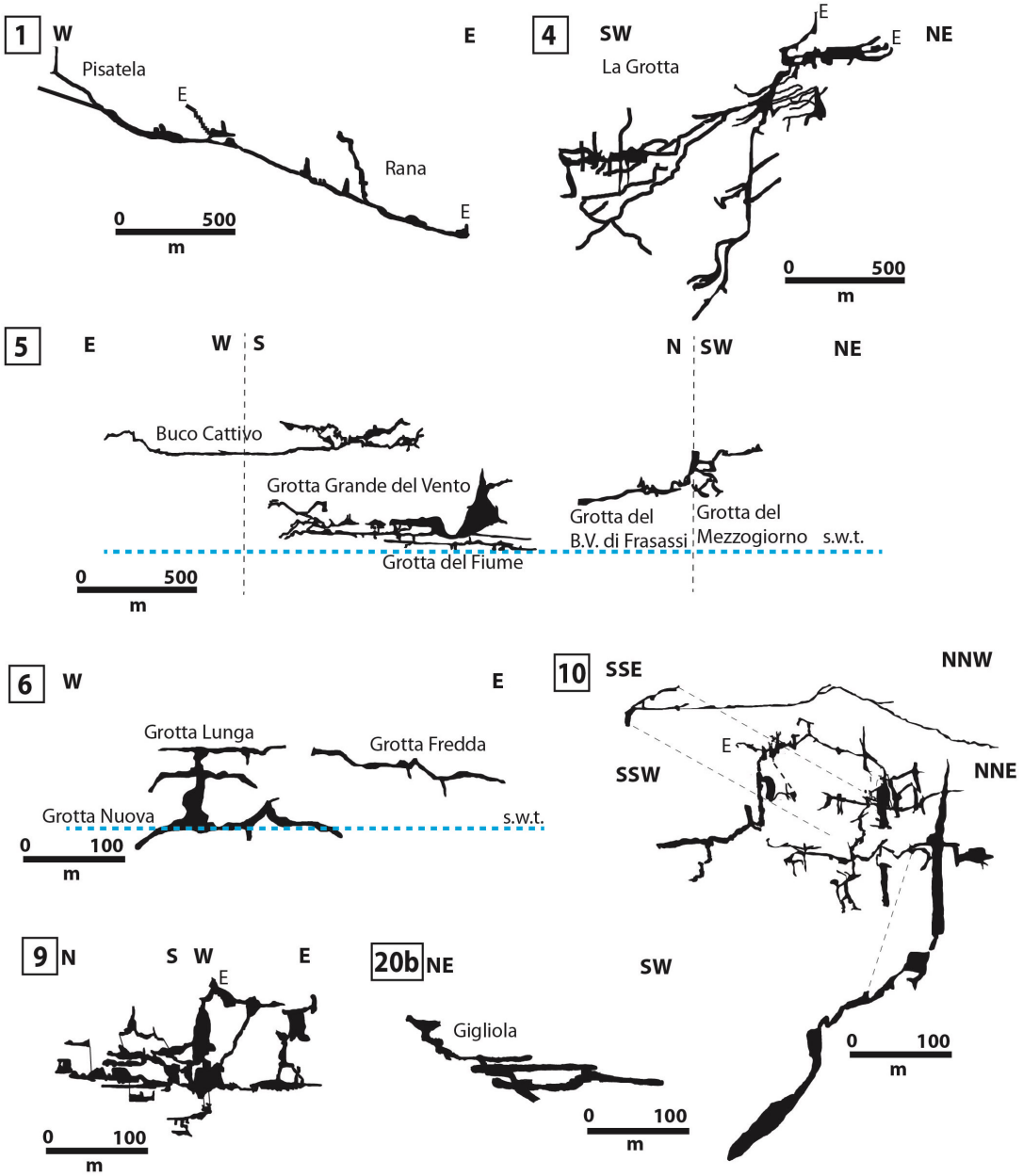

Figure 45 The most representative SAS cave profiles. 1. Pisatela-Rana caves, 4. La Grotta*, 5. Frasassi caves, 6. Acquasanta Terme caves, 9. Montecchio Cave, 10. Cittareale Cave, 20b. Gigliola Cave.*

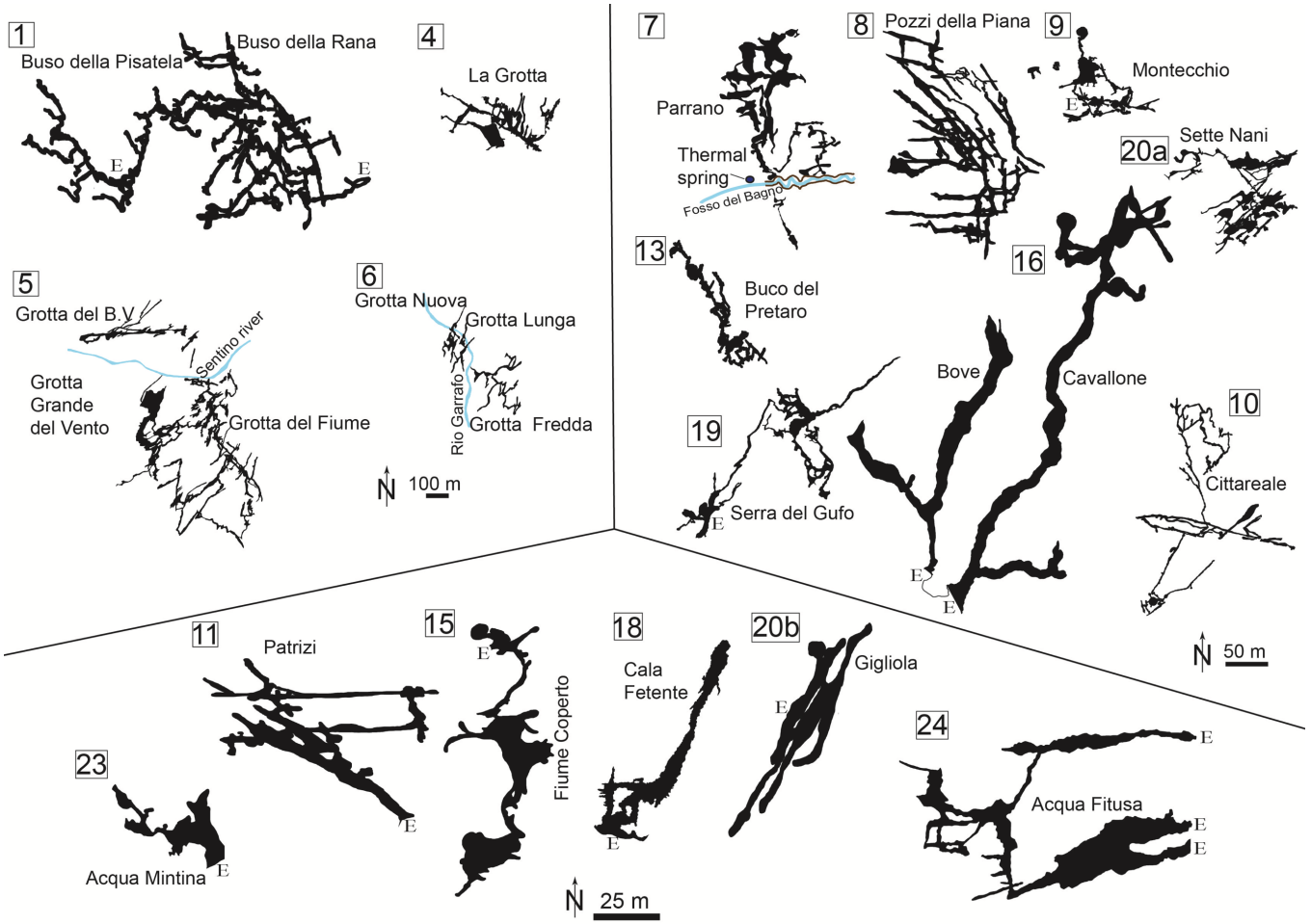

1

2 *Figure 46. Principal SAS systems of Italy (with available and suitable survey). They have been divided into three main group in function of their*

3 *size. The biggest caves are on the top left (i.e.: 1. Pisatela-Rana caves, 4. La Grotta, 5. Frasassi caves, 6. Acquasanta Terme caves), the mid-size*

on the top right (i.e.: 7. Parrano caves, 8. Pozzi della Piana Cave, 9. Montecchio Cave, 10. Cittareale Cave, 13. Buco del Pretaro, 16. Cavallone-Bove caves, 19 Serra del Gufo, 20a. Sette Nani Cave), and the smallest in the lower part of the image (i.e.: 11. Grotta Patrizi, 15. Grotta del Fiume coperto, 18. Grotta di Cala Fetente, 20b. Gigliola Cave, 23. Acqua Mintina, 24. Acqua Fitusa).

Table 18. Geomorphological features. The numbers represent the cave systems listed in Table 1. Note that not all morphologies are exclusive to SAS caves.

Geomorphology	**1**	**3**	**4**	**5**	**6**	**7**	**8**	**9**	**10**	**11**	**12**	**13**	**15**	**16**	**18**	**19**	**20**	**21**	**22**	**23**	**24**	**25**	**26**
Maze networks	x		x	x			x	x	x	x		x				x	x				x		
Elongated anastomotic networks				x	x												x	x					
Spongeworks				x								x				x				x			
Circular galleries			x	x	x		x	x	x			x		x		x							
Feeders		x		x	x	x					x			x	x	x	x		x		x		
Blind chimneys							x		x				x	x		x					x		
Rising channels		x		x	x						x		x	x		x			x				
Domes		x	x	x		x				x	x	x		x		x					x		
Pendants				x										x			x				x		
Convection niches																					x		
Abrupt endings				x								x	x	x		x	x		x	x	x*	x	
Bubble trails				x				x															x
Notches with flat roofs				x												x	x				x		
Sulfuric-acid notches													x			x	x				x		
Sub-horizontal galleries		x	x		x	x	x	x	x			x	x	x	x		x		x	x	x		
Cupolas-morphologies	x		x	x	x	x	x	x		x		x		x	x	x	x		x	x	x		x
Megacusps														x		x			x		x		x
Vents																							x
Boxworks				x												x					x	x	
Weathered walls	x	x			x							x					x		x	x	x		
Drip tubes			x											x			x				x		
Sulfuric-acid karren													x								x		
Replacement pockets			x					x						x		x	x				x		
Sulfuric cups																					x		

Table 19. Mineralogical and isotopic ($\delta^{34}S$) composition of the speleogenetic by-products found in each cave system. The minerals are listed according to the recently accepted IMA list of minerals (http://nrmima.nrm.se//imalist.htm).

Cave system	Secondary Minerals	δ^{34} S Gypsum (‰) V-CDT	References
1	Sulfur, Pyrite, Hematite, Goethite, Celestine, Gypsum	-29.5 to +27.1	Tisato et al., 2012
2	Sulfur, Gypsum, Jarosite		D'Angeli et al., 2018
3	Gypsum	-24 to -19	Principi, 1931 Galdenzi and Maruoka, 2003 Mansor et al., 2018
4	Sulfur, Fluorite, Rutile, Magnetite, Goethite, Gibbsite, Celestine, Baryte, Gypsum, Alunite, Jarosite, Hydrotalcite, Fluoroapatite, Leucophosphite, Goyazite, Titanite, Halloysite 10Å	-22.7 to -9.2	Forti et al., 1989 Galdenzi, 2004b D'Angeli et al., 2018
5	Baryte, Gypsum, Jarosite, Opal, Halloysite 10Å	-24.2 to -7.5	Bertolani et al., 1976 Galdenzi and Sarbu, 2000 Galdenzi and Maruoka, 2003
6	Sulfur, Gypsum		Galdenzi, 2001 Galdenzi, 2017
7	Gypsum		Galdenzi and Menichetti, 1995
8	Gypsum		Galdenzi and Menichetti, 1995
9	Hematite, Goethite, Calcite rafts, Gypsum, Alunite, Jarosite	-28.3 to -25.6	Piccini et al., 2015
10	Gypsum		Antonini, 2001 Mecchia et al., 2003
11	Fluorite, Baryte, Gypsum		Mecchia et al., 2003
12	Gypsum		Mecchia et al., 2003
13	Gypsum		Mecchia et al., 2003
15	Gypsum	-9.5 to -6.6	Galdenzi, 2004a
16	Rutile, Ilmenite, Magnetite, Goethite, Brucite, Gibbsite, Gypsum, Natroalunite, Alunite, Jarosite, Apatite, Halloysite 10Å	-8.9 to 9.3	D'Angeli et al., 2018; D'Angeli et al., 2019
18	Sulfur, Mn-oxydes, Gypsum		Colantoni et al., 1994; Forti and Mocchiutti, 2004
19	Gypsum, Tschermigite, Copiapite	-10.4 to 0.9	D'Angeli et al., 2018 Galdenzi and Maruoka, 2019
20	Sulfur, Pyrite, Rutile, Hematite, Goetithe, Brucite, Baryte, Hexahydrite, Epsomite, Gypsum, Tamarugite, Pickeringite, Jarosite.	-28.8 to -21.0	Catalano et al., 2014; D'Angeli et al., 2018 Galdenzi and Maruoka, 2019
21	Fluorite, Baryte, Gypsum.	-3.4 to 24.3	Galdenzi and Maruoka, 2019
22	Sulfur, Gypsum, Jarosite		Forti and Mocchiutti, 2004; D'Angeli et al., 2017b; D'Angeli et al., 2018;
23	Sulfur, Celestine, Hexahydrite, Epsomite, Gypsum, Alunite, Tschermigite, Metavoltine, Jarosite,		D'Angeli et al., 2018
24	Thenardite, Gypsum, Eugsterite	-1.0 to 10.6	De Waele et al., 2016; D'Angeli et al., 2018
25	Cinnabar, Hematite, Pyrolusite, Goethite, Todorokite, Baryte, Gypsum, Felsöbányaite, Natroalunite,, Alunite,Walthierite, Lizardite, Halloysite 10Å	20.5	Sauro et al., 2014; D'Angeli et al., 2018;
26	Galena, Sphalerite, Cinnabar, Fe-Mn oxy-hydroxides, Baryte, Anglesite, Bianchite, Epsomite, Brochantite		De Waele and Forti, 2006; De Waele et al., 2013; De Waele et al., 2017

Table 20. Microbiological materials found in still active SAS caves of Italy

	Cave system	**Microbiological materials**	**References**
5	Frasassi	Whitish stream biofilms, brownish vermiculations, mucus-like snottites, whitish moonmilk	Sarbu et al., 2000; Galdenzi and Maruoka, 2003; Macalady et al., 2006; 2008
6	Acquasanta Terme	Whitish stream biofilms, brown vermiculations, mucus-like snottites,	Jones et al., 2010; Hamilton et al., 2015
15	*Grotta di Fiume Coperto*	Brownish vermiculation, whitish moonmilk wall biofilm	Galdenzi, 2004a
18	Capo Palinuro	Whitish stream biofilms	Mattison et al., 1998; Canganella et al., 2007
19	Monte Sellaro	Whitish stream biofilms	Present paper
20	Cassano allo Ionio	Whitish stream biofilms	Present paper
22	Santa Cesarea Terme	Whitish stream biofilms, brown to grey vermiculations, whitish moonmilk deposits	D'Angeli et al., 2017a
24	*Acqua Fitusa*	Purple stream biofilms	Present paper

Here we report 1) well-known sulfuric acid systems, 2) a system showing supergene pyrite oxidation, 3) a case of hydrothermal hypogene hosting peculiar SAS minerals, 4) acidic mine caves, 5) some examples that await to be confirmed, pointing out their respective geological setting.
SAS caves occur in the following six main domains:

- Venetian Forealps;
- Northern and Central Apennine;
- Southern Apennine;
- Apulian Foreland;
- Sicily;
- Sardinia.

6.1.4.1. Venetian Forealps

Pisatela-Rana cave system (Vicenza, Veneto) (no. 1 in *Figure 45,Figure 46,Figure 50*) is 37 km long and contrarily to the other systems, is clearly connected to surface morphologies such as sinking streams and dolines (Tisato et al., 2012). The caves develop in Eocene calcarenites, marls and claystones typical of shallow water, following the main faults with WSW-ENE and NNW-SSE directions, and have general epigenic origin. One part of the cave (*Pisatela*), however, has striking SAS morphologies such as cupola-morphologies, walls and ceilings abundantly covered by gypsum

crusts. Sulfuric acid is produced in vadose and supergene conditions by the oxidation of abundant pyrite hosted in some beds of the limestone sequence.

6.1.4.2. Northern and Central Apennines

The most famous and studied SAS systems, both still-active (e.g. Frasassi, Acquasanta Terme, Triponzo) and inactive (e.g. Monte Cucco caves and Pozzi della Piana), are located in the northern-central Apennines (Galdenzi and Menichetti, 1995), and mainly evolved in Jurassic and Cretaceous-Eocene carbonates.

The most famous and studied SAS systems, both still active (e.g. Frasassi, Acquasanta Terme, Triponzo) and inactive (e.g. Monte Cucco and Pozzi della Piana), are located in the northern-central Apennines (Galdenzi and Menichetti, 1995) (Tab. 1), and mainly evolved in Jurassic and Cretaceous-Eocene carbonates.

Porretta Terme (Bologna, Emilia-Romagna) is located in the Tuscan-Emilian Apennines (no. 2 in *Figure 50*). It is characterized by artificial galleries excavated in Oligocene arenites. Some small natural caves have formed close to sulfuric springs in these tunnels, with some arenites cemented by calcite. Native sulfur, gypsum and jarosite deposits (D'Angeli et al., 2018) have been found close to the sulfidic springs.

Triponzo (Perugia, Umbria) (no. 3 in *Figure 50*) is a small active water table cavity discovered during the excavation of the Grogale gallery, located 100 m north of the Triponzo spa. The cave is not accessible at present. It was described by Principi (1931), which explained it as a product of SAS in subaerial conditions. It develops in Jurassic limestones following a NW-SE lineament, and is characterized by a triangular planimetry, lacking any external connection, and with sulfidic water rising from a series of feeders. As described by Principi (1931), the chamber presents rounded ceiling with a dome structure, feeders, rising channels in sub-horizontal arrangement, likely controlled by the water level position. Walls and ceiling are deeply weathered and covered by whitish gypsum crystals and crusts. The water temperature at the spring ranged from 29 to 30°C (Principi, 1931; Galdenzi and Maruoka, 2003). In the early theory of cave formation, described by Principi (1931), the pyrite ores scattered in the host rock likely contributed to the sulfuric acid speleogenesis. Nevertheless, nowadays, the source of H_2S is thought to be mostly related to deep-seated evaporite rocks.

Monte Cucco (Perugia, Umbria) is one of the most famous and studied inactive SAS cave systems (Menichetti, 1987; Forti et al., 1989; Galdenzi, 2004b), composed of three main separated caves: *La Grotta*, *Buca di Faggeto Tondo* and *Buca Futura* (no. 4 in *Figure 50*) evolved in Jurassic carbonates. The caves consist of large, relict passages of phreatic origin, developed towards the SSW in zones

with high syngenetic porosity along bedding planes, inclined 20-25° SW (Passeri, 1972). *La Grotta* (no. 4 in *Figure 45, Figure 46)* is a huge cave, 25 km-long, in which a sequence of wide, deep shafts reach the maximum depth (~900 m deep), *Buca di Faggeto Tondo* is characterized by 3 km of inclined passages, and *Buca Futura* presents small maze galleries, 1 km long, partially filled with clay and gypsum deposits (Menichetti et al*.,* 2008). In the *Buca di Faggeto Tondo*, abundantly finely-grained whitish gypsum deposits (Fig. 6B-C) can be observed on the walls (thickness ~25 cm) and on the floor, in the form of large meters-thick gypsum glaciers sometimes affected by drip tubes (Forti et al*.*, 1989). They were deposited above the sulfuric water table, as confirmed by the widespread replacement pockets and $\delta^{34}S$ of the gypsum (Galdenzi, 2004b). Other interesting minerals such as fluorite, baryte, celestine, and halloysite 10Å have been described by Forti et al. (1989) and D'Angeli et al. (2018), and would suggest events of low thermalism (~25°C). In *La Grotta* the gypsum deposits are less impressive and mainly located on the floor of Barbari gallery-Saracco hall (at 1200 m a.s.l.), in the Infernaccio-Regione Italiana (at 1050 m a.s.l.) galleries, and also in some upper levels. From a geomorphological standpoint, in these caves it is possible to observe rounded galleries guided by bedding planes (Forti et al*.*, 1989), domes (*Figure 47*A), and ceiling cupolas, blind rising channels, 2 and 3D mazes (e.g. Canin Hall and Infernaccio in *La Grotta*), corkscrew solutional patterns (Menichetti, 2009), sub-horizontal galleries, drip tubes affecting gypsum deposits, whereas high-velocity flow morphologies such as scallops are absent (except in the recent vadose entrenching passages such as shafts and canyons). The main galleries of *La Grotta* and *Buca di Faggeto Tondo* mostly follow the bedding planes (Forti et al*.*, 1989; Galdenzi and Menichetti, 1995), and developed at the top of the karstified limestone, below a thin and poorly permeable limestone unit, which contributes to preserve the gypsum deposits from solution due to seepage waters.

Three stages of speleogenesis in Monte Cucco Massif have been hypothesized by Galdenzi (2004b): 1) the cave would have formed under sulfuric acid deep-seated conditions during the Upper Pliocene and the Lower Pleistocene. Then 2) the lowering of the sulfuric water table caused by surface erosion, likely, occurred during the late Pleistocene, produced the dewatering of the cave, and promoted subaerial corrosion and the deposition of replacement gypsum. Nowadays, 3) Monte Cucco karst area is no longer influenced by rising sulfidic water, and currently, meteoric water, vadose incision and gravitative processes are the dominant processes (Passeri, 1972).

Frasassi (Ancona, Marche) is the best documented still active SAS system (no. 5 in *Figure 50*) of Italy (Galdenzi and Menichetti, 1995; Galdenzi, 2009), evolved in an area dominated by Mesozoic rocks. Here deep-seated Triassic evaporites belonging to the Anidriti di Burano Fm. (Martinis and Pieri, 1964) are covered by pure Jurassic limestones of the Calcare Massiccio Fm., cherty limestone of the Maiolica Fm. (Jurassic-Cretaceous), marls, and marly limestones belonging to the Scaglia Fm.

(Cretaceous-Paleocene), which together with structural factors intensely influence the hydrodynamics involved in the speleogenetic processes. The cave system mainly develops on the southern flank of the Frasassi gorge (Galdenzi and Menichetti, 1990) in the Calcare Massiccio Fm. and consists of more than 100 caves. Nevertheless, only *Grotta del Fiume*, *Grotta Grande del Vento*, *Grotta di Mezzogiorno-Frasassi* and *Buco Cattivo* reach remarkable lengths (no. 5 in Figure 45, *Figure 46*). Their sub-horizontal maze galleries are located on seven main levels (~25 km long), testifying to several stages of formation related to a lowering base level (Galdenzi and Sarbu, 2000). The galleries evolved following the typical lineaments of the northern-central Apennines (NE-SW, NW-SE, E-W) (Mariani et al., 2007). In general, the level of sulfidic water table is controlled by the position of the Sentino River, behaving as a local base level. The rising non-thermal sulfidic waters (~13°C) have a salinity up to 2 g/L and contain abundant quantities of H_2S (18 ppm) (Galdenzi et al., 2008; Galdenzi, 2012), and flow only in the lower galleries (*Grotta del Fiume*), seasonally mix with Ca-Mg-HCO_3 meteoric waters (Galdenzi *et al.*, 1999a, 2008; Galdenzi, 2001). As described by Singhinolfi (1990), the rising sulfidic waters clearly interact with the deep-seated Triassic evaporites, and produce typical geochemical signatures (Jones et al., 2015). They are abundantly colonized by whitish stream biofilms (Galdenzi and Sarbu, 2000; Galdenzi and Maruoka, 2003; Hamilton et al., 2015). On walls and ceilings, it is possible to observe vermiculations (Jones et al., 2008), mucus-like snottites (Galdenzi et al., 1999b; Vlasceanu et al., 2000; Galdenzi and Maruoka, 2003) and gypsum moonmilk deposits (Galdenzi, 1990), especially close to the sulfidic springs.

The sub-horizontal galleries present phreatic and vadose features evolved throughout the sulfidic water table lowering, but also due to condensation-corrosion processes (Galdenzi, 1990, 2001). The most common geomorphological features are 2D rectilinear mazes, spongeworks, anastomotic forms, abrupt ending of cave passages, wide rooms connected with narrow conduits, sulfuric-acid notches, feeders, rising channels, ceiling cupolas, domes, pendants, boxworks, and bubble trails.

The upper inactive branches host a huge amount of gypsum deposits (~5 m thick and 1000 m^3) such as replacement crusts, large floor deposits and macroscopic crystals inside clay layers, but other interesting SAS by-product, such as jarosite, halloysite 10Å, opal, and baryte (Procaccini Ricci, 1809; Bertolani et al., 1976). Tazioli et al. (1990), analyzing stable isotopes of sulfates, suggested rising sulfidic waters to have a meteoric origin and a relative brief residence time. In general, the most significant theory proposes the earlier rooms (the highest of the whole system) to have likely formed 1.4 Ma ago, when the Sentino River was 200-300 m higher than today. In this condition, and especially during interglacial phases, the water rapidly carved the limestones and produced the lowering of the riverbed, creating vertical conduits and narrow rooms. On the contrary, sub-horizontal levels formed when the gorge was filled with detritus during glacial periods (Mariani et al. 2007). In

addition, some experiments have been carried out in the active galleries of *Grotta del Fiume* (Galdenzi et al., 1997; Galdenzi, 2012) to quantify the rate of dissolution-corrosion and limestone weight loss both in the groundwater and in the cave atmosphere, using limestone tablets, and demonstrated that the highest values (68-119 mm ka^{-1}) of dissolution-corrosion occurred where the flow of sulfidic waters was quite fast. These measurements, in agreement with the previous theories, confirmed that the *Fiume-Vento* system originated during the Middle-Upper Pleistocene (Bocchini and Coltorti, 1990; Taddeucci et al., 1992).

Acquasanta Terme (Ascoli Piceno, Marche) opens on the eastern side of the Apennine Chain, at only 40 km from the Adraitic Sea. It represents a still active SAS system (no. 6 in *Figure 50*), formed in a wide anticline characterized by Miocene marls, sandstone and mudstone (Galdenzi et al., 2010). Terraced travertines, formed because of the rising of sulfidic thermal water (Boni and Colacicchi, 1966), represent the most significant unit of the area (Galdenzi et al., 2010). The historical Acquasanta Cave is ~300 m long and opens at the base of these travertine bodies, in contact with the underlying Oligocene marls. Here, the water temperature reaches 30°C (Galdenzi and Menichetti, 1995) and in the past, it was used for human treatments. Nevertheless, the main SAS system, composed of *Grotta Fredda*, *Grotta Lunga* and *Grotta Nuova* are carved just below the Rio Garrafo gorge (no. 6 in *Figure 45*, *Figure 46*) in Jurassic-Eocene cherty limestone belonging to the Scaglia Fm. (Menichetti, 2008; Galdenzi, 2017). *Grotta Fredda* (1.5 km long) presents a ramified pattern composed of sub-horizontal galleries following bedding planes, dominated by phreatic morphologies. On the contrary, *Grotta Lunga* and *Grotta Nuova* (1.2 km long) developed along regional lineaments (NE-SW, NW-SE), alternating vertical shafts and circular sub-horizontal tubes (*Figure 47*D). The lower levels of both caves reach the sulfidic thermal water table (Galdenzi and Menichetti, 1995; Galdenzi et al., 2010; Hamilton et al., 2015; Galdenzi, 2017) with temperature ranging between 36-45°C, salinity of 7 g/L and high H_2S content. On the contrary, the higher branches are less warm and influenced by seasonal changes (mean 10±2°C). Such huge temperature difference allows turbulent convective air flows and condensation-corrosion processes to be very efficient (Galdenzi, 2001; 2017). Ascending features such as rising channels, feeders, corroded ceilings and walls (*Figure 47*E), suggest upwelling fluid movements (Galdenzi, 2001, 2017). Gypsum deposits are widespread in all the cave passages, whereas native sulfur *Figure 47*E) crusts are abundant, especially in environments close to the sulfidic water table. Microbial mats colonize the sulfidic water (Jones et al., 2010; Hamilton et al., 2015), and extremely acidic (pH 0-1) mucus-like snottites and vermiculations can be observed in the zone of active condensation phenomena (Galdenzi et al., 2010).

Parrano (Terni, Umbria) cave system (no. 7 in *Figure 50*) develops along the Fosso del Bagno canyon in a small outcrop of Cretaceous cherty limestone (Lippi-Boncambi, 1938), covered by low

permeability marls and sandstones (Oligocene-Miocene). The thermal sulfidic water (~26°C) intersects the surface flowing through a normal fault zone with a NW-SE direction (Galdenzi and Menichetti, 1995), and springs out in the thermal baths of Parrano (no. 7 in *Figure 46*). The original temperature in the deep reservoir is thought to be 120-130°C (Chiodini et al., 1982). In the Parrano area, more than eight caves have been recognized and called *Tane del Diavolo*. The longest ones open on the northern side of the Fosso del Bagno gorge and show sub-horizontal galleries located at different levels, likely influenced by base-level lowering (Lippi-Boncambi, 1938). The inner morphologies are dominated by features such as feeders, cupolas and domes. White-powdery gypsum, gypsum rosettes (Galdenzi and Menichetti, 1995) and moonmilk deposits can easily be seen. In addition, no fluvial sediments have been observed (Lippi-Boncambi, 1938).

The **Pozzi della Piana** (Perugia, Umbria) system (no. 8 in *Figure 50*) is located in Gola del Forello, close to the town of Titignano (west of Todi), and is crossed by the Tevere River. It opens in a 30 m thick travertine deposits related to Pleistocene volcanic activity (Passeri, 1965; Manfra et al., 1976; Galdenzi and Menichetti, 1995). The conduits (3.5 km long) follow N-S, E-W and NW-SE directions and present sub-horizontal 2D rectilinear mazes (no. 8 in *Figure 46*). They have rounded morphologies typical of phreatic passages, cupola-like morphologies, blind chimneys, and fissure networks (Galdenzi and Menichetti, 1995). The development of two levels of sub-horizontal galleries should be related to a base-level lowering, and the exposure of their entrances linked to processes of surface erosion along the gorge. Gypsum deposits have been reported (Galdenzi and Menichetti, 1995).

Montecchio Cave (Grosseto, Tuscany) (no. 9 in *Figure 50*) opens in a 0.5 km^2 outcrop of Jurassic carbonates (Bonazzi et al., 1992), cut by the Albegna River valley. The area hosts thermal springs and travertine terraces (Piccini et al., 2015). The cave system reaches a length 1.7 km following N-S, E-W, NE-SW and NW-SE lineaments (no. 9 in *Figure 45*, *Figure 46*). It is an active SAS system in which the sulfidic water table (31-36°C), located 100 m below the entrance (Telolli and Bartolini, 2007), is linked to the Amiata Mt. and Vulsini volcanic activities (Piccini et al., 2015). It is characterized by several sub-horizontal levels, corresponding to past thermal sulfuric water levels, with typical 3D maze pattern, rounded galleries, ceiling cupolas, replacement pockets and bubble trails. Deposits of alunite, jarosite, gypsum, calcite rafts, kaolinite, goethite, and hematite have been documented. Gypsum samples have been dated following the method described in Asmerom et al. (2010), and the obtained results gave Pleistocene and Holocene ages (Piccini et al., 2015).

Cittareale (Rieti, Latium) Cave (no. 10 in *Figure 45*, *Figure 46*, and *Figure 50*) is located in the southern part of Sibillini Mountains at 1420 m a.s.l., close to the town of Cittareale. It is an inactive SAS cave, ~3 km long and 450 m deep (Mecchia et al., 2003). It develops in marly and cherty

limestone of Cretaceous-Eocene age belonging to the Scaglia Fm.. Limestone rocks dip eastward with direction with slope of 20-30° in the upper part, and 50° in the lower part of the cave. Several sub-horizontal levels connected by shafts with a typical 3D maze arrangement with circular morphologies and rising blind chimneys have been documented (Antonini, 2001). The upper levels are thought to have originated ~0.7-0.8 Ma ago (Mecchia et al., 2003), whilst the lower ones intercept the present water table and are infilled with gravel deposits. Only rare speleothems can be found. Abundant gypsum deposits have been observed in the upper sub-horizontal galleries.

Monti della Tolfa (Rome, Latium) are located 15 km eastward of Civitavecchia city (no. 11 in *Figure 50*). They are three small outcrops (1 km^2) characterized by cherty limestones of Jurassic age (Mecchia et al., 2003). In the bigger outcrop, called Monte delle Fate, several caves with some features of hypogene sulfuric acid evidences have been observed. The first, *Grotta Patrizi* (no. 11 in *Figure 46*) is 260 m long and 47 m deep. The galleries follow faults and fractures, but also bedding planes, dipping 30-35°. The galleries host important amounts of fluorite, baryte, calcite dogtooth crystals, mammillary calcite, and gypsum flowers. The mean temperature inside the cave is 20°, but cyclic plumes of rising warm (26-31°C) aerosols have been monitored (Agostini et al., 1981), likely coming from the sulfidic warm (45°C) spring located just 1.4 km away from the cave, and showing abundant concentration H_2S and CO_2 (Camponeschi and Nolasco, 1978).

Monte Soratte (Rome, Latium) is a NW-SE massif, 6 km long and 1.5 km wide (no. 12 in *Figure 50*) made of Jurassic carbonates. The surface lacks of normal epigene features such as dolines, sinkholes, poljes, and karren. Nevertheless, this area hosts several well-developed karst systems, some of which might have SAS hypogene origin (Mecchia et al., 2003). Several caves are known *Andrea Innocenzi, Santa Lucia, Abisso Erebus, Mero del Soratte* (Mecchia et al., 2003). Recently, *Grotta Luk*, has been discovered (Forconi and Russo, 2015). It is 200 m deep and characterized by narrow galleries and wide halls alternated with shafts. Cupola-like morphologies and gypsum deposits have been observed. In addition, the cave lacks evident connections with the external surface. As the case of Frasassi system, vertical shafts might be related to a fast water table lowering, and cupolas and gypsum likely formed due aerosol exhalations.

Buco del Pretaro (Rieti, Latium) Cave is located in Monte Cosce, and carved in Jurassic carbonates (no. 13 in *Figure 50*). Its planimetry (13 in *Figure 46*) is characterized by maze networks with circular section following bedding planes (30-65° WSW-ENE) and NE-SW and NW-SE discontinuities. Narrow passages alternate with wide rooms dominated by ceiling cupolas, and spongework morphologies. Locally the walls are deeply weathered (Mecchia et al., 2003). Sub-horizontal galleries with ceiling cupolas, condensation domes, and gypsum deposits have been observed. No natural connections with the surface have been documented.

Subiaco (Rome, Latium) opens in the Simbruini Mountains (no. 14 in *Figure 50*), made of Miocene carbonates. Here, *Fossa di Agosta, Catino di Cervara* and *Chiavica di Arsoli*, three small but 100 m deep caves (likely related to water table lowering), have been documented (Mecchia et al., 2003). At the present-days, sulfidic springs have been observed in Campo Orella, 4 km SSW from *Chiavica di Arsoli*. The waters have opalescent colors with temperature of 15-16°C, and are enriched in H_2S and CO_2. Moreover, in Ruffi Mt. along the left hydrographical side of the Aniene gorge, other sulfidic springs such as Marano Equo have been documented.

Grotta di Fiume Coperto (Latina, Latium) opens at the foot of Acquapuzza Mt. (literally meaning stinking waters mountain) in the Lepini massif (no. 15 in *Figure 50*), and is a small 170 m long cave (Mecchia et al., 2003; Galdenzi 2004a), developed in fossiliferous shallow water limestones (Jurassic-Cretaceous). The sulfidic waters, which influenced its speleogenesis, come to the surface in several points. The most famous is located close to a restaurant, having a mean discharge of 500 L/s (Piro, 2000). The cave evolves, mainly, following a NE-SW direction parallel to the massif. It is characterized by sub-horizontal galleries close to the sulfidic water table, and by wide rooms alternating with narrow passages (no. 15 in *Figure 46*). Blind chimneys, rising channels, sulfuric karren, and notches have been observed (Galdenzi, 2004a). The walls are covered by gypsum crusts and needles. A large stalagmite (likely created when the sulfidic water table was lower than today) shows intense corrosive features and replacement of calcite with gypsum. The walls are also covered by biofilms (Galdenzi, 2004a), especially brownish vermiculations and whitish creamy moonmilk with acidic pH (~1-1.5).

Cavallone-Bove (Chieti, Abruzzo) is an inactive SAS system placed in the external part of the central Apennine Chain (no. 16 in *Figure 50*), in the Majella Park, and opens at about 1470 m a.s.l., along the *Taranta Peligna* gorge. The karst system is carved in limestone sequences of deep and shallow marine waters (Cretaceous-Miocene) deposited upon Triassic evaporites. These sequences have been faulted during several stages of the Apennine mountain formation, and the main regional structures follow NNE-SSW, NE-SW and NW-SE directions. As shown in the survey (no. 16 in *Figure 46*), both the caves are clearly developed along the main fault domains. Cavallone Cave is characterized by a main sub-horizontal passage, 1 km long, with a circular cross-section (*Figure 43*D), and which in the innermost part divides into two smaller conduits. Speleothems are abundant in the area close to the entrance, and tend to be less present in the deeper sectors. Instead, Bove Cave presents two galleries with a descendent arrangement from the entrance towards the innermost portion. Differently from the first one, it is much less decorated by speleothems, and for this reason, shows evident faulted zones and rockfalls. The main geomorphological evidences for SAS origin are rising channels, megacusps (*Figure 47*G), feeders (*Figure 47*F), replacement pockets and cupolas (*Figure 47*F).

Abundant deposits of SAS by-products have been sampled and interesting mineralogical associations were discovered. Deposits of natroalunite, alunite (Figure 43I), jarosite (*Figure 47*I), Fe-Mn oxides, rutile, ilmenite, gibbsite, and halloysite 10Å are abundant in the innermost galleries (D'Angeli et al., 2018; 2019), whereas metric gypsum blocks (*Figure 47*H) can be observed only in the middle part of the main branch of Cavallone Cave.

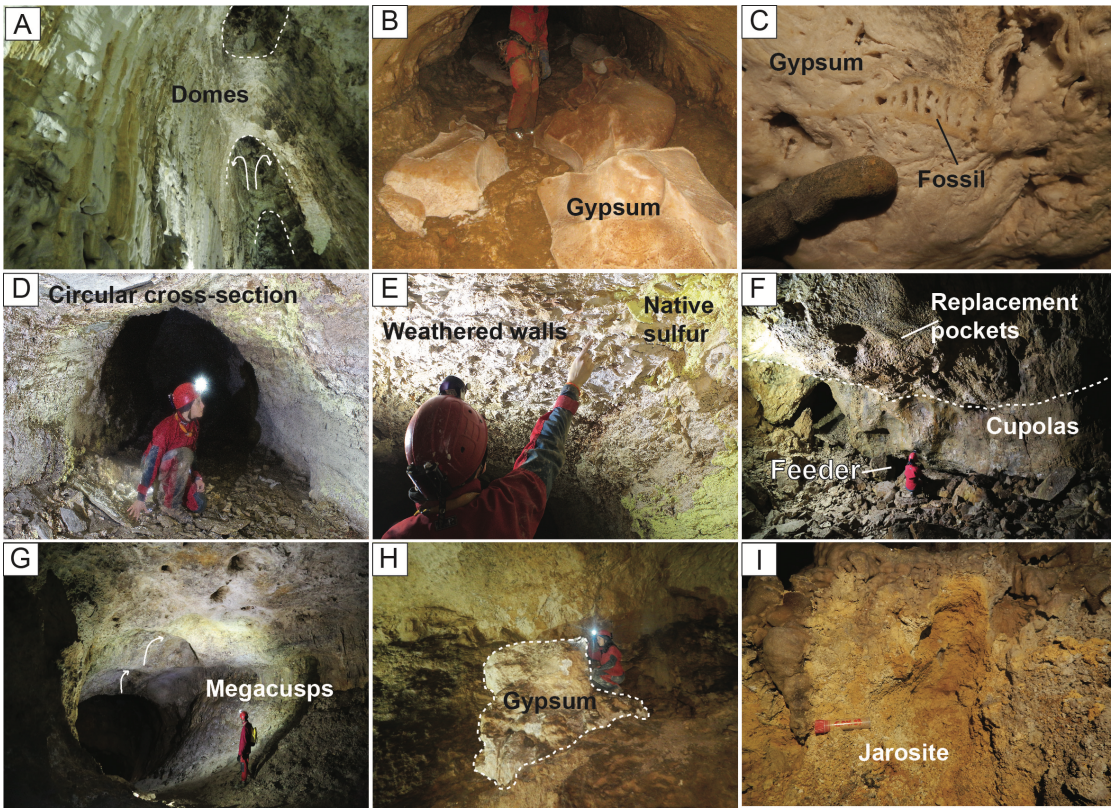

Figure 47. A) Dome structures observed in the tourist branches of La Grotta*, in* Monte Cucco *(photo M. Nagostinis); B) Metric gypsum deposits, in the lower branches of* La Grotta*,* Monte Cucco *(photo G. Antonini); C) The host rock has been totally (including fossils) replaced by gypsum,* Buca di Faggeto Tondo Cave*, Umbria (photo M. Nagostinis); D) Weathered wall in the lower galleries of* Grotta Nuova, Acquasanta Terme*, Marche (photo R. Simonetti); E) Weathered walls characterized by replacement gypsum and sulfur deposits, along the lower galleries of* Grotta Nuova, Acquasanta Terme*, Marche (photo R. Simonetti); F) Feeder, cupolas, and replacement pockets in the innermost part of* Cavallone *Cave, Abruzzo (photo G. Antonini); G) Megacusps on the ceiling of the innermost branch of* Cavallone *Cave, Abruzzo (photo G. Antonini); H) Metric gypsum deposit in Cavallone Cave, Abruzzo (photo M. Nagostinis); I) Orange-brownish jarosite deposits observed in the innermost zone of* Cavallone *Cave, Abruzzo (photo M. Nagostinis). The size of the containers is 6 cm.*

6.1.4.3. Southern Apennines

In the **Monti Lattari** area (Naples, Campania) (no. 17 in *Figure 50*), characterized by intensely faulted Triassic-Cretaceous carbonates (main domains are NE-SW and NW-SE), Faito Mt. is known to host rising of sulfidic waters, interfering with the surface in Castellammare di Stabia and Scrajo, in the Sorrento Peninsula (Corniello et al., 2013). The speleogenesis of *Jala*, *San Francesco*, *Sperlonga*, *Pozzano 1* and *2* caves (Cozzolino et al., 2007; Iannace et al., 2015) might be linked to the presence of these sulfuric acid waters. Corniello et al. (2013) has described the existence in Scrajo, of a marine cave along the Tyrrhenian coastline, characterized by sulfidic springs with a constant temperature of 17°C.

Capo Palinuro (Salerno, Campania) (no. 18 in *Figure 50*), which opens along the Tyrrhenian coastline of Campania region (Alvisi et al., 1994; Canganella et al., 2007), hosts more than 32 submarine caves, with 13 of them being still active sulfuric acid systems, including *Grotta Azzurra, Grotta delle Colonnine, Grotta Viola, Grotta Sulfurea*, and *Grotta di Cala Fetente*. Their waters have temperatures of 18-25°C and pH of 7.22-8.15, and are colonized by stream biofilms (Mattison et al., 1998; Canganella et al., 2007). *Grotta a Ovest di Cala Fetente*, and *Grotta di Punta Galena* show fossil signatures of sulfuric acid activities (Forti and Mocchiutti, 2004). In the *Grotta Azzurra*, a wide hall is connected with small lateral passages, and is mainly characterized by ceiling cupolas (Colantoni et al., 1994) and feeders, through which the sulfidic waters reach the cave atmosphere. In addition, rare sulfur speleothems, found in *Grotta di Cala Fetente* (no. 18 in *Figure 46*) have been studied in detail by Forti and Mocchiutti (2004). They can be observed only in the innermost part of the cave close to sulfidic springs, where H_2S degasses into the cave atmosphere.

Monte Sellaro (Cosenza, Calabria) (no. 19 in *Figure 50*) is characterized by a faulted monocline of Cretaceous limestones, covered by low-permeable Miocene calcarenites, claystones and rocks belonging to the Liguride Complex (Galdenzi and Maruoka, 2019). It is located in the Sibari Plain, North Calabria. SAS cave systems have been described by Larocca (1991), and some of them are still active environments fed by thermal H_2S-rich springs. *Voragine delle Balze di Cristo* (Or San Marco Cave), is a 100 m-deep cave in which the lower level reaches the sulfidic water table with a temperature ranging between 28 and 40°C. This sulficic water flows towards Ninfe Cave (Galdenzi, 1997; Vespasiano et al., 2016) (*Figure 48*A), the first natural emergence of the described SAS system, and then reaches a small cave, *Grotta Scura*. These waters present pH values ranging between 7.01 and 7.21, redox potential -0.069 and 0.045, temperature of ~29°C (Vespasiano et al., 2016), and are abundantly colonized by whitish stream biofilms. Their walls are covered by replacement pockets, gypsum deposits, and rare yellowish to white sulfates such as tschermigite and copiapite (*Figure 48*B) (D'Angeli et al., 2018). An interesting inactive SAS cave is *Serra del Gufo*, ~2 km-long (no. 19 in

Figure 46), which conduits are controlled by bedding planes and evolved towards N-S, NE-SW, NNW-SSE directions. The general morphologies are maze networks, phreatic rounded tubes, blind chimneys, feeders and dome structures, rising channels, ceiling cupolas, megacusps and replacement pockets. Wall notches have been documented by Galdenzi and Maruoka (2019) and represent the past sulfidic water table. Gypsum deposits have been abundantly observed and documented. *Grotta Damale* is another inactive SAS cave, 300 m-long, and characterized by feeders, domes, blind chimneys, ceiling cupolas, megacusps, pendants, and boxwork. In general, the lower portion of the cave is quite narrow and shows weathered walls and spongework arrangements.

Cassano allo Ionio (Cosenza, Calabria) (no. 20 in *Figure 50*) is also located in the Sibari Plain, North Calabria. The most famous and touristic cave system is Sant'Angelo, located in San Marco Mt. (Galdenzi, 1997), on the western edge of the town, and developed in Triassic dolostones. It represents a complex SAS system, more than 2 km-long and 40 m-deep, and is composed of 16 caves characterized by sub-horizontal levels, likely related to the lowering of the sulfuric water table now flowing more or less 200 m lower, in the Cassano allo Ionio municipality. Wide halls are connected with narrow passages, in which abundant gypsum deposits and replacement pockets (Figure 43G) can easily be observed. Recently, Gigliola Cave (no. 20b in *Figure 45*, *Figure 46*) and Sette Nani Cave (no. 20a in *Figure 46*) have been discovered in the Muraglione area, whereas a small cave called *Grotta delle Terme* has been found immediately below the Terme Sibarite spa. All these caves are characterized by several sub-horizontal levels, in which sulfuric notches (*Figure 48*C,D,E), feeders (*Figure 48*C,D), cupolas (*Figure 48*D), altered walls, and drip tubes are clearly visible. Maze alternate with elongated anastomotic networks and tend to end abruptly. Inside these underground environments interesting gypsum deposits, but also rare yellowish cave sulfates such as tamarugite, pickeringite, and jarosite have been described by D'Angeli et al. (2018) (*Figure 48*G). The sulfidic waters surfacing in the Terme Sibarite spa are colonized by white stream biofilms (*Figure 48*F).

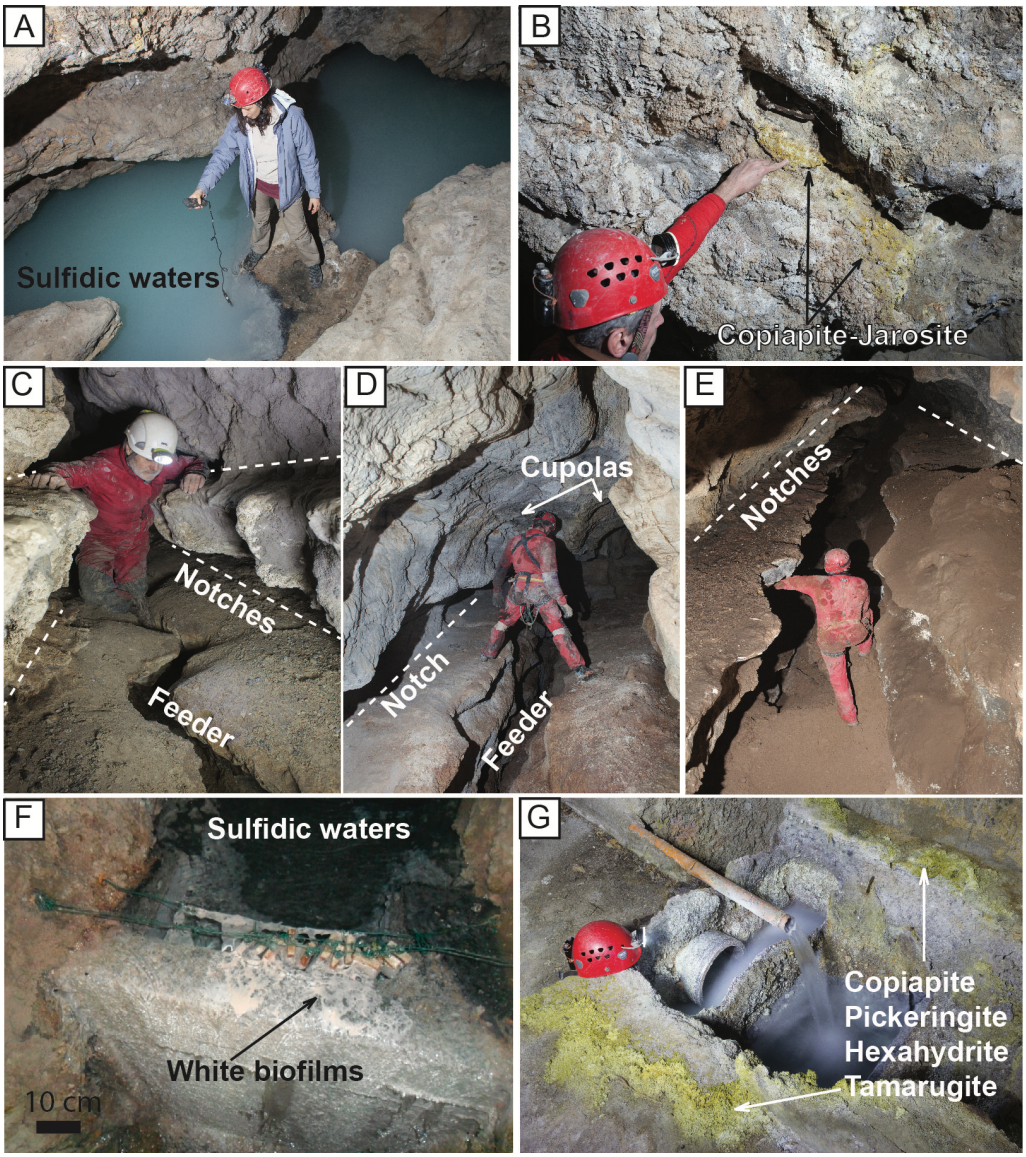

Figure 48. A) Sulfidic waters flowing in Ninfe Cave, Monte Sellaro in Cerchiara di Calabria (photo O. Lacarbonara); B) Yellowish deposits of copiapite and jarosite sampled in the Ninfe Cave, Mt. Sellaro in Cerchiara di Calabria (photo O. Lacarbonara); C) Sulfuric-acid notches and feeder observed in Sant'Angelo cave system, Cassano allo Ionio (photo O. Lacarbonara); D) Sulfuric-acid notch, feeder, and cupolas in Sette Nani Cave, Cassano allo Ionio (photo O. Lacarbonara); E) Sulfuric notches observed in the lower part of Gigliola Cave, Cassano allo Ionio (photo O. Lacarbonara); F) Sulfidic waters and white biofilms in Terme Sibarite spa (photo I. D'Angeli); G) Yellowish deposits made of copiapite, pickeringite, hexahydrite, and tamarugite, precipitated close to the spring in Terme Sibarite spa (photo O. Lacarbonara).

Terme Luigiane (Cosenza, Calabria) (no. 21 in *Figure 50*) are located in the Bagni River on the Tyrrhenian side of Calabria Region. The area is characterized by Jurassic weakly-metamorphosed cherty limestones and dolostones belonging to the Verbicaro Unit (Dietrich, 1976). In this territory two SAS caves, (*Grotta Pieru Porcaru* and *Milogno*) are known. The most important is *Grotta Milogno*, 0.5 km long, and is characterized by sub-parallel slightly inclined phreatic passages rising

towards the valley. Vertical shafts evolved following discontinuities. Gypsum crusts are commonly observed. *Grotta Pieru Porcaru* presents small rooms, located close to the surface, and on the walls, it is possible to find baryte and fluorite crystals (Galdenzi and Maruoka, 2019).

6.1.4.4. Apulian Foreland

Santa Cesarea Terme (Lecce, Apulia) (no. 22 in *Figure 50*) is located in the southern part of the Apulia region, and in this area, Amato et al. (2014) described 1 km of Plio-Pleistocene wackestone-packstone carbonates, 2 km of microcrystalline Cretaceous limestones, and ~8 km of Triassic evaporites covering the basement rocks. At the surface, a variety of karst features characterize the landscape, with sinkholes and dry valleys of different sizes and typologies (Pepe and Parise, 2012). Along the coastline, four sub-horizontal caves, *Fetida, Sulfurea, Gattulla,* and *Solfatara*, carved in the Cretaceous units have been documented (D'Angeli et al., 2017b). Inside the caves, it is possible to observe cupolas, rising channels, megacusps, submerged feeders, weathered walls, replacement pockets, and important deposits of gypsum. Sulfur is very abundant in *Gattulla* (D'Angeli et al., 2017b). Generally, these caves present quite big halls and galleries that end abruptly. The caves host interesting biosignatures, such as whitish streamers floating in the sulfidic waters or accumulated on the pool floors, vermiculation deposits (*Figure 43*B) and moonmilk (*Figure 43*C) diffusely covering walls and ceilings (D'Angeli et al., 2017a).

6.1.4.5. Sicily

Acqua Mintina (Caltanisetta, Sicily) Cave (no. 23 in *Figure 50*) is placed in southern Sicily, about 7 km NW from the village of Butera, and entirely develops in Messinian limestones (Lugli et al., 2016; Vattano et al., 2017), for an overall length of 140 m (no. 23 in *Figure 46*). It is an inactive SAS cave, in which conduit size decreases inward ending abruptly. The walls result replaced by gypsum and celestine minerals, covered by a thin layer of dark organic matter, upon which copious yellowish sulfur crusts deposited (*Figure 43*H), sometimes creating folia speleothems (Lugli et al., 2016). In the big room close to the entrance, yellow deposits of rare metavoltine (*Figure 49*A) have been observed (D'Angeli et al., 2018). The ceilings are dominated by cupola- morphologies (*Figure 43*E).
Acqua Fitusa (Agrigento, Sicily) Cave (no. 24 in *Figure 50*) is a typical example of SAS water table cave. It evolved in Upper Cretaceous carbonate breccias of the Imerese basin (Catalano et al., 2013a,b; De Waele et al., 2016) in the eastern portion of the Sicani Mountains, in San Giovanni Gemini territory. The cave (no. 24 in *Figure 46*) has several entrances and develops on many sub-horizontal levels, separated from the current active level (*Figure 49*B), dominated by sulfidic springs with abundant floating microbial substances (white and purple filaments; *Figure 49*C). From the

geomorphological standpoint, the maze networks are dominated by condensation-corrosion features such as ceiling cupolas and convection niches, but also by sulfuric-acid notches, and replacement pockets (Figure 43F, *Figure 49*D), formed close to feeder morphologies (*Figure 49*D). Sulfuric-acid karren (*Figure 49*E) and cups can be found along sulfuric-acid notches (Vattano et al., 2012, 2017; De Waele et al., 2016). Gypsum, thenardite, and eugsterite deposits have been collected especially in the active level (D'Angeli et al., 2018).

Figure 49 A) Yellowish metavoltine deposits sampled in the hall close to the entrance of Acqua Mintina Cave, Butera (photo I. D'Angeli); B) Lower part of Acqua Fitusa cave system (Sicily) where the sulfidic water comes to the surface (photo M. Vattano); C) Purple filaments are clearly visible in the sulfidic spring of Acqua Fitusa cave system. These substances have been collected and are currently undergoing microbiological investigations. They are likely characterized by purple sulfur bacteria (photo M. Vattano); D) Sulfuric notch and feeder in Acqua Fitusa Cave (photo M. Vattano); E) Sulfuric karren developed along the sulfuric notch reported in D (photo M. Vattano).

6.1.4.6. Sardinia

Corona'e Sa Craba (Carbonia-Iglesias) (no. 25 in *Figure 50*) is a a hydrothermal hypogene cave 250 m-long developed in dark grey to brownish Ordovician quartzite rocks, following SE-NW lineaments. It is characterized by a large passage with wide rooms, following an evident fracture. On walls and ceilings, it is possible to observe boxworks. The biggest hall, during spring and summer seasons, hosts a bat colony producing abundant guano, thus inducing the precipitation of phosphate minerals. However, beside the presence of hydrothermal evident features, Corona'e Sa Craba hosts an interesting suite of sulfuric acid minerals (Sauro et al., 2014) such as beautiful bluish baryte crystals, gypsum, alunite, natroalunite, basaluminite, and Fe-Mn oxy-hydroxides (Sauro et al., 2014).
The **Iglesiente-Sulcis mine caves** (Carbonia-Iglesias) (no. 26 in *Figure 50*), including *San Giovanni*, *Santa Barbara*, *Crovassa Ricchi in Argento*, *Grotta Pisani*, *Grotta Quarziti*, the Phaff caves and many others, represent inactive hypogene systems in which sulfuric acid contributed in producing peculiar morphologies and minerals (De Waele et al., 2017). More than 50 karst voids (4 km-long) lacking any natural connection with the surface have been encountered by the *San Giovanni*; among these, the *Santa Barbara*, the most famous hypogene cave of Sardinia, shows clear geomorphic features (De Waele and Forti, 2006; Pagliara et al., 2010; De Waele et al., 2013) such as megacusps, cupolas, and the rare oxidation vents.
Bell-shaped rooms entirely covered with calcite dogtooth spar, baryte and gypsum characterize the Phaff caves (Forti and Perna, 1982). From an overall standpoint, Iglesiente-Sulcis mine caves present typical hypogene morphologies including bubble trails, cupolas, megacusps, and replacement pockets. Sulfides (galena, sphalerite, cinnabar) and sulfate minerals (baryte, anglesite, bianchite, epsomite, brochantite) are abundant (De Waele et al., 2017, and references therein), but most secondary sulfate minerals of SAS origin have disappeared, likely because such processes occurred a long time ago (De Waele et al., 2013).

6.1.5. Conclusions

Sulfuric acid caves are widespread in Italy (26 main areas in which SAS caves have been documented) (*Figure 50*; *Table 17*), and are particularly abundant especially in the northern-central Apennines, where deep faults act as connection between the deep-seated sulfates and the outcropping carbonate rocks. SAS caves can evolve both in confined (deep-seated) and unconfined settings, and in inactive conditions they can be recognized especially using geomorphological and mineralogical features.

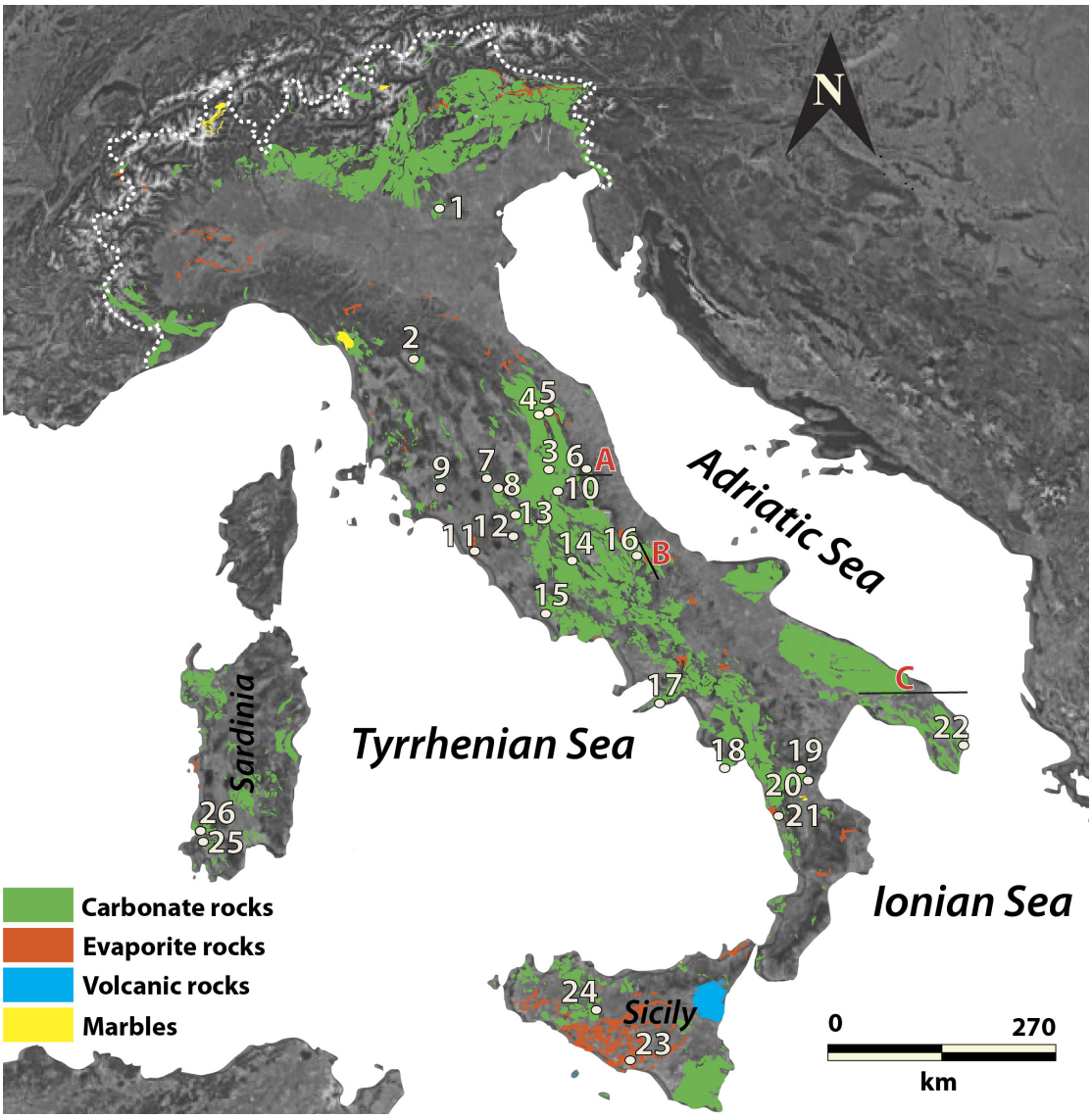

Figure 50 Italian karst areas and SAS cave systems (numbers as in Table 1 and in the text): 1 Pisatela-Rana (Vicenza); 2 Porretta Terme (Bologna); 3 Triponzo (Perugia); 4 Monte Cucco (Perugia); 5 Frasassi (Ancona); 6 Acquasanta Terme (Ascoli Piceno); 7 Parrano (Terni); 8 Pozzi della Piana (Perugia); 9 Montecchio (Grosseto); 10 Cittareale (Rieti); 11 Monti della Tolfa (Roma); 12 Monte Soratte (Roma); 13 Buco del Pretaro (Rieti); 14 Subiaco (Roma); 15 Grotta di Fiume Coperto (Latina); 16 Cavallone-Bove (Chieti); 17 Monti Lattari (Napoli); 18 Capo Palinuro (Salerno); 19 Monte Sellaro (Cosenza); 20 Cassano allo Ionio (Cosenza); 21 Terme Luigiane (Cosenza); 22 Santa Cesarea Terme (Lecce); 23 Acqua Mintina Cave (Caltanissetta); 24 Acqua Fitusa Cave (Agrigento); 25 Corona'e Sa Craba (Carbonia-Iglesias); 26 Iglesiente mine caves (Carbonia-Iglesias). (Modified from D'Angeli et al., 2018). The red letters refer to location of the cross section presented in Figure 44.

All the described systems clearly show typical sulfuric acid features, both in active and inactive conditions. The active systems, such as Porretta Terme, Triponzo, Frasassi, Acquasanta Terme, Montecchio, *Grotta del Fiume Coperto,* Monti Lattari, Capo Palinuro, Monte Sellaro, Cassano allo

Ionio, Santa Cesarea Terme, and *Acqua Fitusa* are fed by warm rising sulfidic Ca-Cl-SO_4 and Na-Cl-SO_4 waters enriched with H_2S, having temperatures ranging between 13 and 45°C. Among these, Capo Palinuro and Santa Cesarea Terme represent very interesting SAS systems developing along the Tyrrhenian and Adriatic coastline, and are partially influenced by mixing between rising thermal fluids and marine waters. From the overall point of view, Italian SAS caves represent mid-size systems, and rarely reach the length of the large epigene cave systems (*Figure 45*, *Figure 46*). Nevertheless, there are large voids, as in the case of the Frasassi cave system, in which the Abisso Ancona represents an impressive wide room.

The biggest SAS systems, excluding Pisatela-Rana (an epigene system partially influenced by supergene pyrite oxidation), are located in the Umbria-Marche regions (Monte Cucco, Frasassi and Acquasanta Terme), whereas the smallest ones are those in Latium (Monti della Tolfa) and Apulia (Santa Cesarea Terme).

Geomorphological observations and mineralogical sampling allowed to recognize inactive SAS systems such as Monte Cucco, Pozzi della Piana, Cittareale, Cavallone-Bove, Monte Sellaro, Cassano allo Ionio, and several mine caves in the Iglesiente-Sulcis area of Sardinia.

In addition, this study has shown the development of sub-horizontal maze networks to be one of the most favorite arrangements for SAS caves. Generally, the circular conduits are more abundant than sulfuric-acid notches, likely suggesting phreatic conditions are more common than the vadose ones. Feeders are common structures, and also ceiling cupola morphologies are abundant. Deep shafts might occur especially very the sulfuric water table lowering was fast, whereas in slow conditions sub-horizontal galleries are favorited.

Gypsum is the most typical secondary mineral in SAS underground environments, produced by the interaction between H_2SO_4 and $CaCO_3$, whereas native sulfur requires very special boundary conditions (i.e., growth on acidic surfaces such as gypsum and organic matter and very high concentration of degassing H_2S), and is abundant only in a few caves including *Grotta di Cala Fetente* (Capo Palinuro), *Gattulla* (Santa Cesarea Terme), and *Acqua Mintina* (Butera). Significant are the mineralogical associations found in Monte Cucco, *Corona'e Sa Craba* and several of the Iglesiente-Sulcis mine caves, testifying stages of intense hydrothermal hypogene phenomena. Differently, Pisatela-Rana system is an epigene cave, partially influenced by sulfuric acid due to the supergene oxidation of pyrite minerals contained in the host rock (Auler and Smart, 2003; Tisato et al., 2012).

Active sulfuric acid caves host biofilms floating in the waters, moonmilk and vermiculations, and extremophiles able to thrive in the acidic conditions with high concentration of H_2S-SO_2, and CO_2, often high temperature and humidity. SAS caves should prove to be interesting places to look for

microbiological substances both of medical and astrobiological interest, as already demonstrated in Frasassi caves (Vlasceanu et al., 2010; Mansor et al., 2018).

References

Agostini, S., Terragni, F., Zapparoli, M., 1981. La Grotta Patrizi (la 183) nel comune di Cerveteri. Notiziario del Circolo Speleologico Romano, anno XXIV, 1-2: 3-20.

Aiuppa, A., Inguaggiato, S., McGonigle, A.J.S., O'Dwyer, M., Oppenheimer, C., Padgeit, M.J., Rouwet, D., Valenza, M., 2005. H_2S fluxes from Mt. Etna, Stromboli, and Vulcano (Italy) and implication for the sulfur budjet at volcanoes. Geochimica et Cosmologica Acta, 69(7): 1861-1871.

Alvisi, M., Barbieri, F., Colantoni, P., 1994. Le Grotte Marine di Capo Palinuro. Memorie dell'Istituto Italiano di Speleologia, 6(II): 143-181.

Amato, A., Bianchi, I., Piana Agostinetti, N., 2014. Apulian crust: Top to bottom. Journal of Geodynamics, 82: 125-137.

Antonini, G., 2001. Nuovo importante ramo in salita all'Abisso di Cittareale (RI). Speleologia, 44: 85.

Asmerom, Y., Polyak, V.J., Burn, S.J., 2010. Variable winter moisture in the south-western United States linked to rapid glacial climate shift. Nature Geosciences, 3: 114-117.

Audra, P., 2008. Hypogenic sulfidic speleogenesis. Berliner Höhlenkundliche Berichte, 26: 15-32.

Audra, P., Mocochain, L., Bigot, J.Y., Nobécourt, J.C., 2009a. Hypogene cave patterns. In: Klimchouk A, Ford DC (Eds) Hypogene speleogenesis and karst hydrogeology of artesian basins. Ukrainian Institute of Speleology and Karstology, Special Paper 1: 17–22.

Audra, P., Mocochain, L., Bigot, J.Y., Nobécourt, J.C., 2009b. Morpholgical indicator of speleogenesis: Hypogenic speleogenesis. In: A.B., Klimchouk, D.C., Ford (Eds.), Hypogene speleogenesis and karst hydrogeology of artesian basins. Ukrainian Institute of Speleology and Karstology, Special Paper 1: 23-32.

Audra, P., Mocochain, L., Bigot, J.Y., Nobécourt, J.C., 2009c. The association between bubble trails and folia: a morphological and sedimentary indicator of hypogene speleogenesis by degassing from Adaouste cave (Provence, France). International Journal of Speleology, 38: 93-102.

Audra, P., Gázquez, F., Rull, F., Bigot, J.Y., Camus, H., 2015. Hypogene Sulfuric Acid Speleogenesisand rare sulfate minerals in Baume Galinière Cave (Alpes-de-Haute-Provence, France). Record of uplift, correlative cover retreat and valley dissection. Geomorphology, 247: 25-34.

Auler, A.S., Smart, P.L., 2003. The influence of bedrock-derived acidity in the development of surface and underground karst: evidence from the precambrian carbonate of semi-arid northeastern Brazil. Earth Surface Processes and Landforms, 28: 157-168.

Bakalowicz, M.J., Ford, D.C., Miller, T.E., Palmer, A.N., Palmer, M.V., 1987. Thermal genesis of

dissolution caves in the Black Hills, South Dakota. Geological Society of America Bulletin, 99: 729-738.

Bally, A., Burgi, W.L., Cooper, C., Ghelardoni, R., 1988. Balanced sections and seismic reflection profiles across the Central Apennines. Memorie della Società Geologica Italiana, 35, 257-310.

Bertolani, M., Garuti, G., Rossi, A., Bertolani Marchetti, D., 1976. Motivi di interesse mineralogico-petrografico nel complesso carsico Grotta Grande del Vento-Grotta del Fiume (Genga, Ancona). Le Grotte d'Italia, IV(6): 109-144.

Bocchini, A., Coltorti, M., 1990. Il complesso carsico grotta del Fiume Grotta Grande del Vento e l'evoluzione geomorfologica della Gola di Frasassi. Memorie dell'Istituto Italiano di Speleologia, II(4):155-180.

Bonazzi, U., Fazzini, P., Gasperi, G., 1992. Note alla carta geologica del bacino del fiume Albegna. Bollettino della Società Geologica Italiana, 111: 341-354.

Boni, C., Colacicchi, R., 1966. I travertini della valle del Tronto. Memorie Società Geologica Italiana, V: 315-339.

Boschetti, T., Cortecci, G., Toscani, L., Iacumin, P., 2011. Sulfur and oxygen isotope compositions of Upper Triassic sulfates from northern Apennines (Italy): paleogeographic and hydrogeochemical implications. Geologica Acta, 9(2): 129-147.

Buck, M.J., Ford, D.C., Schwarcz, H.P., 1994. Classification of cave gypsum deposits derived from oxidation of H_2S. In: I.D., Sasowky, M.V, Palmer, (Eds.), Breakthroughs in karst geomicrobiology, Colorado Spring, Colorado: 5-9.

Camponeschi, B., Nolasco, F., 1978. Le risorse naturali della Regione Lazio. Monti della Tolfa e Ceriti. Regione Lazio, 3: 157 pp.

Canfield D.E., 2001. Biogechemistry of sulfur isotopes. Reviews in mineralogy and geochemistry, 43: 607-636.

Canganella, F., Bianconi, G., Kato, C., Gonzales, J., 2007. Microbialecology of submerged marine caves and holes characterized by high levels of hydrogen sulphide. Review in Environmental Science and Bio/Technology, 6: 61-70. https://doi.org/10.1007/S11157-006-9103-2.

Catalano, M., Bloise, A., Miriello, D., Apollaro, C., Critelli, T., Muto, F., Cazzanelli, E., Barrese, E., 2014. The mineralogical study of the Grotta Inferiore di Sant'Angelo (southern Italy). Journal of Cave and Karst Studies, 76(1): 51-61.

Catalano, R., Agate, M., Albanese, C., Avallone, G., Basilone, L., Gasparo Morticelli, M., Gugliotta, C., Sulli, A., Valenti, V., Gibilaro, C., Pierini, S., 2013a. Walking along the crustal profile acrocc the Sicily fold and thrust belt. AAPG International Conference & Exhibition,

23-26 October 2011, Milan. Post Conference Fieltrip, Palermo. Geological fieldtrip, 5(2.3): 213 pp.

Catalano, R., Valenti, V., Albanese, C., Accaino, F., Sulli, A., Tinivella, U., Gasparo Morticelli, M., Zanolla, C., Giustiniani, M., 2013b. Sicily's fold-thrust belt and slab rollback: The SI.RI.PRO. seismic crustal transect. Journal of the Geological Society, 170: 451-464.

Cavarretta, G., Lombardi, G., 1992. Origin of sulphur in minerals and fluids from Latium (Italy): isotopic constraints. European Journal Mineralogy, 4: 1311-1329.

Chiodini, G., Giaquinto, S., Zanzari, A.R., 1982. Caratteri idrochimici e analisi della distribuzione degli indicatori geotermici nelle acque del bacino del Fiume Paglia. CNR PFE RF, 16: 56-90.

Colantoni, P., Franchi, R., Ferretti, E., 1994. Nota preliminare sulle caratteristiche mineralogiche e petrografiche dei sedimenti di alcune grotte sommerse di Capo Palinuro (Salerno). Memorie descrittive della carta geologica d'Italia, LII: 33-40.

Corniello, A., Trifuoggi, M., Ruggieri, G., 2013. The mineral springs of the Scrajo spa (Sorrento Peninsula, Italy): a case of "natural seawater" intrusion. Environmental Earth Sciences, DOI 10.1007/s12665-013-2942-6.

Cozzolino, L., Pianese, N., Santangelo, N., Di Crescenzo, G., 2007. Sinkholes di origine carsica nell'area dei Monti Lattari. Proceedings I Regional Congress of Speleology "Campania Speleologica", June 2007, Oliveto Citra (SA): 85-101.

D'Angeli, I.M., De Waele, J., Galdenzi, S., Madonia, G., Parise, M., Piccini, L., Vattano, M., 2016. Sulfuric acid caves of Italy: an Overview. In: T., Chavez, P., Reehling (Eds.), NCKRI Symposium 6, Proceedings "DeepKarst 2016", Origins, Resources, and Management of Hypogene Karst", Carlsbad, New Mexico: 85-88.

D'Angeli, I.M., De Waele J., Ieva M.G., Leuko S., Cappelletti M., Parise M., Jurado V., Miller A.Z. & Saiz-Jimenez C., 2017a. Next-Generation Sequencing for microbial characterization of biovermicuations from a sulfuric acid cave in Apulia (Italy). Proceedings XVIIth International Congress of Speleology, Sydney: 377-380.

D'Angeli, I.M., Vattano M., Parise M. & De Waele J., 2017b. The coastal sulfuric acid cave system of Santa Cesarea Terme (southern Italy). In: A.B., Klimchouk A.N., Palmer J., De Waele A., Auler P., Audra P., (Eds.), Hypogene karst regions and caves of the world. Springer: 161-168. http://doi.org/10.1007/978-3-319-53348-3_9.

D'Angeli, I.M., Carbone, C., Nagostinis, M., Parise, M., Vattano, M., Madonia, G., De Waele, J., 2018. New insights on secondary minerals from Italian sulfuric acid caves. International Journal of Speleology, 47(3): 271-291.

D'Angeli, I.M., Nagostinis, M., Carbone, C., Bernasconi, S.M., Polyak, V.J., Peters, L.,

McIntosh, W.C., De Waele, J., 2019. Sulfuric acid speleogenesis in the Majella Massif (Abruzzo, Central Apennines, Italy). Geomorphology, in press.

De Waele, J., Forti, P., 2006. A new hypogene karst form: the oxidation vent. Zeitschrift fur Geomorphol N.F. Supplementband, 147: 107-127.

De Waele, J., Forti, P., Naseddu, A., 2013. Speleogenesis of an exhumed hydrothermal sulphuric acid karst in Cambrian carbonates (Mount San Giovanni, Sardinia). Earth Surface Processes and Landforms, 38(12): 1369-1379.

De Waele, J., Galdenzi, S., Madonia, G., Menichetti, M., Parise, M., Piccini, L., Sanna, L., Sauro, F., Tognini, P., Vattano, M., Vigna, B., 2014. A review on hypogene caves in Italy. In: A., Klimchouk, I., Sasowsky, J., Mylroie, S.A., Engel, A.S., Engel (Eds.), Hypogene cave morphologies. Karst Waters Institute Special Publication 18, Leesburg, Virginia: 28-30.

De Waele, J., Audra, P., Madonia, G., Vattano, M., Plan, L., D'Angeli, I.M., Bigot, J.Y., Nobécourt, J.C., 2016. Sulfuric acid speleogenesis (SAS) close to the water table: examples from southern France, Austria and Sicily. Geomorphology, 253: 452-467.

De Waele, J., Gázquez, F., Forti, P., Naseddu, A., 2017. Inactive Hydrothemal Hypogene Karts in SW Sardinia (Italy). In: A.B., Klimchouk A.N., Palmer J., De Waele A., Auler, P., Audra (Eds.), Hypogene karst regions and caves of the world. Springer: 183-197. http://doi.org/10.1007/978-3-319-53348-3_11.

Dietrich, D., 1976. La geologia della catena Costiera Calabra tra Cetraro e guardia piemontese. Memorie della società Geologica Italiana, 17: 61-121.

Doglioni, C., Flores, G., 1997. An Introduction to the Italian Geology. Lamisco, 98 pp.

Dublyansky, V.N., 1980. Hydrothermal karst in the alpine folded belt of southern parts of U.R.S.S.. Kras i Speleologia, 3(12): 18-36.

Egemeier, S.J., 1981. Cavern development by thermal waters. National Speleological Society Bulletin, 43: 31-51.

Engel, A., Stern, L.A., Bennett, P.C., 2004. Microbial contributions to cave formation: New insights into sulfuric acid speleogenesis. Geology, 5: 369-372.

Frank, E.D., Mylroie, J., Troester, J., Alexander Jr., E.C., Carew, J.L., 1998. Karst development and speleogenesis, Isla de Mona, Puerto Rico. Journal of Cave and Karst Studies, 60(2): 73-83.

Feier, N., 2003. New data on the mineralogy of Valea Rea Cave, Bihor Mountains. Ecocarst, 4: 22-24.

Forconi, P., Russo, L., 2015. Grotta Luk. Elder Graphics: 45pp.

Forti, P., Perna, G., 1982. Le cavità naturali dell'Iglesiente. Memoria dell'Istituto Italiano di Speleologia, 2(1): 1-229.

Forti, P., Mocchiutti, A., 2004. Le condizioni ambientali che permettono l'evoluzione di speleotemi di zolfo in cavità ipogeniche: nuovi dati dalle grotte di Capo Palinuro (Salerno, Italia). Le Grotte d'Italia, V(4): 39-48.

Forti, P., Menichetti, M., Rossi A., 1989. Speleothems and Speleogenesis of the Faggeto Tondo Cave (Umbria-Italy). Proceedings X International Speleological Congress, Budapest, 1: 74-76.

Galdenzi, S., 1990. Un modello genetico per la Grotta Grande del Vento. Memorie dell'Istituto Italiano di Speleologia, II(4): 123-142.

Galdenzi, S., 1997. Initial Geologic observation in caves bordering the Sibari Plain (Southern Italy). Journal of Cave and Karst Studies, 59(2): 81-86.

Galdenzi, S., 2001. L'azione morfogenetica delle acque sulfuree nelle grotte di Frasassi, Acquasanta Terme (Appennino Marchigiano-Italia) e di Movile (Dobrogea-Romania). Le Grotte d'Italia, V(2): 49-61.

Galdenzi, S., 2004a. L'azione morfogenetica delle acque sulfuree nella Grotta di Fiume Coperto (Latina). Le Grotte d'Italia, V(4): 17-27.

Galdenzi, S., 2004b. I depositi di gesso nella Grotta di Faggeto Tondo: nuovi dati sull'evoluzione geomorfologica dell'area di Monte Cucco (Italia centrale). Studi Geologici Camerti 2: 71-83.

Galdenzi, S., 2009. Hypogene caves in the Apennines (Italy). In: A.B., Klimchouk, D.C., Ford (Eds), Hypogene speleogenesis and karst hydrogeology of artesian basins. Ukrainian Institute of Speleology and Karstology, Speial Publication, 1: 101-115.

Galdenzi, S. 2012. Corrosion of limestone tablets in sulfidic ground-water: measurements and speleogenetic implications. International Journal of Speleology, 41(3):149-159.

Galdenzi, S., 2015. Acque sotterranee e grotte nell'Alta Valle del Potenza. In: L., Carestia (Ed.), Alta Valle di Potenza. Ricerche di idrologia e carsismo. Tipografia Cingolati, Potenza Picena (MC): 34-113.

Galdenzi, S., 2017. The termal hypogenic caves of Acquasanta Terme (Central Italy). In: A.B., Klimchouk, A.N., Palmer, J., De Waele, A., Auler, P., Audra (Eds.), Hypogene karst regions and caves of the world. Springer: 169-182. DOI 10.1007/978-3-319-53348-3

Galdenzi, S., Maruoka, T., 2003. Gypsum deposits in the Frasassi Caves, Central Italy. Journal of Cave and Karst Studies, 65(2): 111-125.

Galdenzi, S., Maruoka, T., 2019. Sulfuric acid caves in Calabria (South Italy): Cave morphology and sulfate deposits. Geomorphology, 328, 211-221.

Galdenzi, S., Menichetti, M., 1990. Il carsismo della Gola di Frasassi. Memorie dell'Istituto Italiano di Speleologia, II(4): 243 pp.

Galdenzi, S., Menichetti, M., 1995. Occurrence of hypogene caves in a karst region: examples from

central Italy. Environmental Geology, 26: 39-47.

Galdenzi, S., Sarbu, S.M., 2000. Chemiosintesi e speleogenesi in un ecosistema ipogeo: i rami sulfurei delle Grotte di Frasassi (Italia centrale). Le Grotte d'Italia, V(1): 3-18.

Galdenzi, S., Menichetti, M., Forti, P., 1997. La corrosione di placchette calcaree ad opera di acque sulfuree: dati sperimentali in ambiente ipogeo. In: P.Y., Jeannin (Ed), Proceedings of the12th International Congress of Speleology, La Chaux-de-Fonds, 1: 187-190

Galdenzi, S., Forti, P., Menichetti, M., 1999a. L'acquifero sulfureo di Frasassi: aspetti idrogeologici e naturalistici. Proceedings National Congress on Pollution of Caves and Karst Aquifers, Ponte di Brenta (PD): 181-193.

Galdenzi, S., Menichetti, M., Sarbu, S., Rossi, A., 1999b. Frasassi Cave: a biogenic hypogene karst system?. Karst 99, etudes de Géographie physique, travaux, suppl. 28 CAGEP, Université de Provence : 101-106.

Galdenzi, S., Cocchioni, M., Morichetti, L., Amici, V., Scuri, S., 2008. Sulfuric ground-water in the Frasassi Caves, Italy. Journal of Cave and Karst Studies, 70(2): 94-107.

Galdenzi, S., Cocchioni, F., Filipponi, G., Morichetti, L., Scuri, S., Selvaggio, R., Cocchioni, M., 2010. The sulfidic thermal caves of Acquasanta Terme (Central Italy). Journal of Cave and Karst Studies, 72(1): 43-58.

Ghisetti, F., Vezzani, L., 2000. Detachments and normal faulting in the Marche fold-and thrust belt (central Apennines, Italy): inferences on fluid migration paths. Journal of Geodynamics, 29: 345-369.

Ghisetti, F., Vezzani, L., 2002. Normal faulting and uplift in the outer thrust belt of the central Apennines (Italy): role of the Caramanica fault. Basi Research, 14: 225-236.

Grassa, F., Capasso, G., Favara, R., Inguaggiato, S., 2006. Chemical and isotopic composition of waters and dissolved gases in some thermal springs of Sicily and adjacent volcanic islands, Italy. Pure and Applied Geophysics, 163: 781–807.

Hamilton, T.L., Jones, D.S., Schaperdoth, I., Macalady, J.L., 2015. Metagenomic insight into S80) precipitation in a terrestrial subsurface lithoautotrophic ecosystem. Frontiers of Microbiology, 5(756): 1-16.

Hill, C.A., 1987. Geology of Carlsbad Caverns and other caves in the Guadalupe Montains, New Mexico and Texas. New Mexico Bureau of Miners and Mineral Resources, Bulletin: 117-150.

Hill, C.A., 1990. Sulfuric acid speleogenesis of Carlsbad Cavern and its relationship to hydrocarbon, Delaware Basin, New Mexico and Texas. American Association of Petroleum Geologists Bulletin, 74: 1685-1694.

Hill, C.A., 1995. H_2S-Related Porosity and Sulfuric Acid Oil-Field Karst. In: D.A., Budd, A.H.,

Saller, P.M., Harris (Eds.), Unconformities in carbonate strata-Their recognition and the significance of associated porosity, American Association of Petroleum Geologists Memoirs, 61: 301-306.

Hill, C.A., 2000. Sulfuric Acid, hypogene karst in the Guadalupe Mountains of New Mexico and West Texas, USA. In: A.B., Klimchouk, D.C., Ford, A.N., Palmer, W., Dreybrodt (Eds.), Speleogenesis: Evolution of karst aquifers: 309-318.

Hose, L.D., Pisarowicz, J.A., 1999. Cueva de Villa Luz, Tabasco, Mexico: reconnaissance study of an active sulphuric spring cave and ecosystem. Journal of Cave and Karst Studies 61(1): 13-21.

Hose, L.D., Northup, D.E., 2004. Biovermiculations: Living vermiculation-like deposits in Cueva de Villa Luz, Mexico. Proceedings of the Society: selected abstract, National Speleological Society Convention. Journal of Cave Karst Studies, 66: 112.

Hose, L.D., Palmer, A.N., Palmer, M.V., Northup, D.E., Boston, P.J., DuChene, H.R., 2000. Microbiology and geochemistry in a hydrogen-sulphide-rich karst environment. Chemical Geology, 169: 399-423.

Iannace, A., Merola, D., Perrone, V., Amato, A., Cinque, A., Santacroce, R., Sbrana, A., Sulpizio, R., Zanchetta, G., Budillon, F., Conforti, A., D'Argenio, B., 2015. Fogli 466-485 Sorrento-Termini. Note Illustrative della carta geologica d'Italia.

Imhoff J.F., 2006. The Chromatiaceae. Prokaryotes, 6: 846-873. DOI: 10.1007/0-387-30746-x_31

Jagnow, D.H., Hill, C.A., Davis, D.G., DuChene, H.R., Cunningham, K.I., Northup, D.E., Queen, J.M., 2000. History of the sulfuric acid theory of speleogenesis in the Guadalupe Mountains, New Mexico. Journal of Cave and Karst Studies, 62(2): 54-59.

Jones, D.S., Lyon, E.H., Macalady, J.L., 2008. Geomicrobioly of biovermiculations from the Frasassi cave system, Italy. Journal of Cave and Karst studies, 70(2): 78-93.

Jones, D.S., Tobler, D.J., Schaperdoth, I., Maniero, M., Macalady, J.L., 2010. Community structure of subsurface biofilm in the thermal sulfidic caves of Acquasanta Terme, Italy. Applied and Environmental Microbiology, 76(17): 5902-5910.

Jones, D.S., Polerecky, L., Galdenzi, S., Dempsey, B.A., Macalady, J.L. 2015. Fate of sulfide in the Frasassi cave system and implications for sulfuric acid speleogenesis. Chemical Geology, 410: 21-27

Klimchouk, A., 1996. The typology of gypsum karst according to its geological and geomorphological evolution. International Journal of Speleology, 25(3-4): 49-60.

Klimchouk, A., 2005. Conceptualisation of speleogenesis in multy-storey artesian systems: a model of transverse speleogenesis. International Journal of Speleology, 34(1-2): 45-64.

Klimchouk, A., 2007. Hypogean speleogenesis: hydrogeological and morphometric perspective.

Special Paper 1, National Cave and Karst Research Institute, Carlsbad, NM: 106 pp.

Klimchouk, A., 2009. Morphogenesis of hypogenic caves. Geomorphology, 106: 100-117.

Klimchouk, A., 2015. The karst paradigm: changes, trends and prespectives. Acta Carsologica, 44(3): 289-313.

Klimchouk, A.B., 2017. Types and settings of hypogene karst. In: A.B., Klimchouk, A.N., Palmer, J., De Waele, A., Auler, P., Audra (Eds.), Hypogene karst regions and caves of the world. Springer: 1-39. DOI 10.1007/978-3-319-53348-3_1.

Klimchouk, A.B., 2018. Tafoni and honeycomb structures as indicators of ascending fluid flow and hypogene karstification. In: M., Parise, F., Gabrovsek, G., Kaufmann, N., Ravbar (Eds.), Advances in Karst Research: Theory, Fieldwork and Applications. Geological Society, London, Special Publications, 466: 79-105.

Klimchouk, A., Auler S.A., Bezerra, F.H.R., Cazarin, C.L., Balsamo, F., Dublyansky, Y., 2016. Hypogenic origin, geologic controls and functional organization of a giant cave system in Precambrian carbonates, Brazil. Geomorphology, 253: 385-405.

Larocca, F., 1991. Le Grotte della Calabria. Nuova Editrice Apulia, Martina Franca: 224 pp.

Lippi-Boncambi, C., 1938. Le Grotte di Parrano (Umbria). Le Grotte d'Italia, II(3): 101-118.

Lugli, S., Bassetti, M.A., Manzi, V., Barbieri, M., Longinelli, A., Roveri, M., 2007. The Messinian "Vena del Gesso" evaporites revisited: characterization of isotopic composition and organic matter. The Geological Society of London, 285: 179-190. DOI: 10.1144/SP285.11.

Lugli, S., Ruggieri, R., Orsini, R., Sammito, G., 2016. Grotta dell'Acqua Mintina, a peculiar geosite with the smell of sulfur. Proceeding 4th International Symposium on karst in the South Mediterranean area. Karst Geosites: 65-71.

Macalady, J.L., Lyon, E.H., Koffman, B., Albertson, L.K., Meyer, K., Galdenzi, S., Mariani, S., 2006. Dominant microbial population in limestone-corroding stream biofilms, Frasassi cave system, Italy. Applied Environmental Microbiology, 72(8): 5596-5609.

Macalady, J.L., Jones, D.S., Lyon, E.H., 2007. Extremely acidic, pendulous cave wall biofilms from the Frasassi cave system, Italy. Environmental Microbiology, 9(6): 1402-1414.

Macalady, J.L., Dattagupta, S., Schaperdoth, I., Jones, D.S., Druschel, G.K., Eastman, D., 2008. Niche differentiation among sulfur-oxidizing bacterial populations in cave waters. The ISME Journal, 2(6): 590-601.

Machel, H., 2001. Bacterial and thermochemical sulfates reduction in diagenetic settings – old and new insights. Sedimentary Geology, 140: 143-175.

Maggiore, M., Pagliarulo, P., 2004. Circolazione idrica ed equilibri idrogeologici negli acquiferi della Puglia. Geologi e Territorio, 1: 13-35.

Manfra, L., Masi, U., Turi, U., 1976. La composizione isotopica dei travertini del Lazio. Geologica Romana, 15: 127-174.

Mansor, M., Harouaka, K., Gonzales, M.S., Macalady, J.L., Fantle, M.S., 2018. Transport-Induced Spatial Patterns of Sulfur Isotopes (δ^{34} S) as Biosignatures. Astrobiology, 18(1): 59-72.

Mariani, S., Mainiero, M., Barchi, M., van der Borg, K., Vonhof, H., Montanari, A., 2007. Use of the speleogenetic data to evaluate Holocene uplifting and tilting: an example from the Frasassi anticline (northeastern Apennines, Italy). Earth Planetary Science Letters, 257(1-2): 313-328.

Martinis, B., Pieri, M., 1964. Alcune notizie sulla formazione evaporitica del Triassico Superiore nell'Italia centrale e meridionale. Memorie della Società Geologica Italiana, 4 (1): 649-678.

Mattison, R.G., Abbiati, M., Dando, P.R., Fitzsimons, M.F., Pratt, S.M., Southward, A.J., Southward, E.C., 1998. Chemoautotrophic microbial mats in submarine caves with hydrothermal sulphidic springs at Cape Palinuro, Italy. Microbial Ecology, 35: 58-71.

Mecchia, G., Mecchia, M., Piro, M., Barbati, M., 2003. Le grotte del Lazio. Collana Verde dei Parchi, serie Toscana, Lazio, Roma.

Menichetti, M., 1987. Evoluzione spaziale e temporale del sistema carsico di Monte Cucco nell'Appennino Umbro Marchigiano. Proceedings XI National Congress of Speleology, Castellana Grotte: 731-762.

Menichetti, M., 2008. Assetto strutturale del sistema geotermico di Acquasanta Terme (Ascoli Piceno). Rendiconti online Italian Geological Society: 118-122.

Menichetti, M., 2009. Speleogenesis of the hypogenic caves in Central Italy. Proceedings XV International Speleological Congress, Kerrville, 2: 909-915.

Menichetti, M., Chirenco, M.I., Onac, B., Bottrell, S., 2008. Depositi di gesso nelle grotte del Monte Cucco e della Gola di Frasassi - Considerazioni sulla speleogenesi. Memorie dell'Istituto Italiano di Speleologia, II(21): 308-325.

Morehouse, D.F., 1968. Cave development via the sulfuric acid reaction. National Speleological Society Bulletin, 30(1): 1-10.

Mylroie, J.E., Mylroie, J.R., 2018. Role of karst denudation on the accurate assessment of glacio-eustasy and tectonic uplift on carbonate coasts. In: M., Parise, F., Gabrovsek, G., Kaufmann, N., Ravbar (Eds.), Advances in Karst Research: Theory, Fieldwork and Applications. Geological Society, London, Special Publications, 466: 171-185.

Mylroie, J.E., Carew, J.L., Vacher, H.R., 1995. Karst development in the Bahamas and Bermuda, Geological Society of America Special Paper, 300: 251-267.

Natalicchio, M., Dela Pierre, F., Lugli, S., Lowenstein, T.K., Feiner, S.J., Ferrando, S., Manzi, V., Roveri, M., Clari, P., 2014. Did the Late Miocene (Messinian) gypsum precipitate from evaporited

marine brines? Insights from the Piedmont Basin (Italy). Geology, 42(3): 179-182.

Onac, B.P., Drăguşin, V., 2017. Hypogene Caves of Romania.In: Klimchouk, A.B., Palmer, A.N., De Waele, J., Auler, A., Audra, P. (Eds.), Hypogene karst regions and caves of the world. Springer: 1-39. DOI 10.1007/978-3-319-53348-3_16.

Onac, B.P., Bengeanu, M., Botez, M., Zih, J., 1995. Preliminary report on the mineralogy of Peştera din Valea Rea (Bihor Mountains, Romania). Theoretical and Applied Karstology, 8: 75-79.

Onac, B.P., Sumrall, J., Tămaş, T., Povară, I., Kearns, J., Dârmiceanu, V., Veres, D., Lascu, C., 2009.The relationship between cave minerals and H_2S-rich thermal waters along the Cerna Valley (SW Romania). Acta Carsologica, 38(1): 27-39.

Osborne, R.A.L., 2007. Cathedral cave, Wellington Cave, New South Wales, Australia. A multiphase. Non-fluvial cave. Earth Surface Processes and Landforms, 32(14): 2075-2103.

Pagliara, A., De Waele. J., Forti, P., Galli, E., Rossi, A., 2010. Speleothems and speleogenesis of the hypogenic Santa Barbara cave system (South-West Sardinia, Italy). Acta Carsologica 39(3): 551-564.

Palmer, A.N., 2000. Hydrogeologic control on cave patterns. In: Ford, D., Palmer, A., Dreybrodt, W., Klimchouk, A. (Eds.), Evolution of karst Aquifers, National Speleologic Society, Huntsville (AL), Speleogenesis: 77-99.

Palmer, A.N., 2013. Sulfuric acid caves: morphology and evolution. In: Schroder, J, Fromkin, A, (Eds.). Treatise on Geomorphology. Academic Press, Karst Geomorphology, 6: 241-257.

Palmer, A.N., Palmer, M.V., 2000. Speleogenesis of the Black Hills Maze Caves, South Dakota, USA. In: Klimchouck, AB, Ford, DC, Palmer, AN, Dreybrodt, W, (Eds.), Speleogenesis: Evolution of karst aquifers: 275-286.

Parise, M., Gabrovsek, F., Kaufmann, G., Ravbar, N., 2018 – Recent advances in karst research: from theory to fieldwork and applications. In: M., Parise, F., Gabrovsek, G., Kaufmann, N., Ravbar (Eds.), Advances in Karst Research: Theory, Fieldwork and Applications. Geological Society, London, Special Publications, 466: 1-24.

Passeri, L., 1965. Il Pozzo della Piana I nei travertini di Titignano. Proceedings VI Congress of Speleology: 170-175.

Passeri, L., 1972. Ricerche sulla porosità delle rocce carbonatiche nella zona di Monte Cucco (Appennino Umbro Marchigiano) in relazione alla genesi della canalizzazione interna. Le Grotte d'Italia, IV(3): 5-44.

Pepe P. & Parise M., 2012. Integration of geomorphological and speleological datasets in karst terrains. Rendiconti Online Società Geologica Italiana, 21 (1): 629-631.

Plan, L., Tschegg, C., De Waele, J., Spötl, C., 2012. Corrosion morphology and cave wall alteration

in an alpine sulfuric acid cave (Kraushöhle, Austria). Geomorphology, 169-170: 45-54.

Piccini, L., De Waele, J., Galli, E., Polyak, V.J., Bernasconi, S.M., Asmerom, Y., 2015. Sulphuric acid speleogenesis and landscape evolution: Montacchio cave, Albegna river valley (southern Tuscany, Italy). Geomorphology, 229: 134-143.

Piro, M., 2000. Grotta di Fiume Coperto. Speleologia del Lazio, 1:17-20.

Polyak, V.J., McIntosh, W.C., Güven, N., Provencio, P., 1998. Age and origin of Carlsbad Cavern and related caves from $^{40}Ar/^{39}Ar$ of alunite. Science, 279:1919-1922.

Polyak, V.J., Provencio, P., 2001. By-product materials related to H_2S-H_2SO_4 influenced speleogenesis of Carlsbad, Lechuguilla, and other caves of the Guadalupe Mountains, New Mexico. Journal of Cave and Karst Studies, 63(1): 23-32.

Principi, P., 1931. Fenomeni di idrologia sotterranea nei dintorni di Tripozio. Le Grotte d'Italia, 1: 45-47.

Procaccini Ricci, V., 1809. Memoria sulla Grotta di Frasassi nei contorni di Fabriano. Tip. Lazzarini, Senigallia.

Santaloia, F., Zuffianò, L.E., Palladino, G., Limoni, P.P., Liotta, D., Minissale A., Brogi, A., Polemio, M., 2016. Coastal thermal springs in a foreland setting: The Santa Cesarea Terme system (Italy). Geothermics, 64: 344-361.

Sarbu, S.M., Galdenzi, S., Menichetti, M., Gentile, G., 2000. Geology and Biology of the Frasassi Caves in Central Italy, an ecological multidisciplinary study of a hypogene underground ecosystem. In: Wilkens, H., Culver, D.C., Humphreys, W.F., (Eds.), Ecosystems of the World, Subterranean ecosystems, New York, Elsevier: 359-378.

Sauro, F., De Waele, J., Onac, B.P., Galli, E., Dublyansky, Y., Baldoni, E., Sanna, L., 2014.Hypogenic speleogenesis in quartize: the case of Corona'e sa Craba cave (SW Sardinia, Italy). Geomorphology, 211: 77-88. http://dx.doi.org/10.1016/j.geomorph.2013.12.031.

Segre, A.G., 1948. I fenomeni carsici e la speleologia nel Lazio. Pubblicazioni dell'Istituto di Geografia dell'Università di Roma: 239 pp.

Singhinolfi, G.P., 1990. Studio chimico delle acque del complesso "Grotta di Frasassi (Ancona)". Implicazioni Speleogenetiche e ambientali. Memorie dell'Istituto Italiano di Speleologia, II(4): 109-122.

Taddeucci, A., Tuccimei, P., Voltaggio, M., 1992. Studio geocronologico del complesso carsico "Grotta del Fiume-Grotta Grande del Vento" (Gola di Frasassi, AN) e indicazioni paleoambientali. Il Quaternario, 5: 213-222.

Tazioli, G.S., Cocchioni, M., Coltorti, M., Dramis, F., Mariani, M., 1990. Circolazione idrica e chimismo delle acque sotterranee dell'area carsica di Frasassi nelle Marche. In: Galdenzi, S,

Menichetti, M, (Eds), Il carsismo nella Gola di Frasassi. Memorie dell'Istituto Italiano di Speleologia, II(4): 93-108.

Telolli, D., Bartolini, P., 2007. La Grotta di Montecchio, ultimo aggiornamento: il ramo dei Dannati. Talp 34: 6-9.

Temovski, M., 2017. Hypogene karst of Macedonia. In: A.B., Klimchouk, A.N., Palmer, J., De Waele, A., Auler, P., Audra (Eds.), Hypogene karst regions and caves of the world. Springer: 241-256. DOI 10.1007/978-3-319-53348-3_15.

Tisato, N., Sauro, F., Bernasconi, S.M., Brujin R.H.C., De Waele J., 2012. Hypogenic contribution to speleogenesis in a predominant epigenic karst system: A case study from the Venetian Alps, Italy. Geomorphology, 151-152: 156-163.

Vattano, M., Audra, P., Bigot, J.-Y., De Waele, J., Madonia, G., Nobécourt, J.-C, 2012. Acqua Fitusa Cave: an example of inactive water-table sulphuric acid cave in Central Sicily. Rendicontazione Online della Società Geologica Italiana, 21: 637-639

Vattano, M., Madonia, G., Audra, P., D'Angeli, I.M., Galli, E., Bigot, J.-Y., Nobécourt, J.-C., De Waele, J., 2017. An overview of the hypogene caves of Sicily. In: A.B., Klimchouk, A.N., Palmer, J., De Waele, A., Auler, P., Audra (Eds.), Hypogene karst regions and caves of the world. Springer: 199-210. http://doi.org/10.1007/978-3-319-53348-3_12.

Velaj, T., 2015. New ideas on the tectonic of the Kurveleshi anticline belt in Albania, and the perpective for the exploration in its subthrust. Petroleum, 1, 269-288.

Vespasiano, G., Apollaro, C., Muto, F., De Rosa, R., Dotsika, E., Marini, L., 2016. Preliminary geochemical characterization of the thermal waters of the Grotta delle Ninfe near Cerchiara di Calabria (South Italy). Società Geologica Italiana, 39: 130-133. DOI: 103301/ROL.2015.130

Vlasceanu, L., Sarbu, S.M., Summers Engel, A., Kinkle, B.K., 2000. Acidic, cave-wall biofilms located in the Frasassi gorge. Italy. Geomicrobiological Journal, 17: 1-15.

Vlasceanu, L., Sarbu, S.M., Engel, A.S., Kinkle, B.K., 2010. Acidic Cave-Wall Biofilms located in the Frasassi Gorge, Italy. 17(2): 125-139.

Wynn, J.G., Sumrall, J.B., Onac, B.P., 2010. Sulfur isotopic composition and source of dissolved sulfur species in thermo-mineral springs of the Cerna Valley, Romania. Chemical Geology, 271: 31-43.

7. SOME EXAMPLES OF SAS CAVES IN SOUTHERN ITALY

7.1. Article 5

Published in Hypogene Karst Regions and Caves of the World, Springer, 161-168. http://doi.org/10.1007/978-3-319-53348-3_9.

The coastal sulfuric acid cave system of Santa Cesarea Terme (southern Italy)

D'Angeli Ilenia M. [1], Vattano Marco [2], Parise Mario [3], De Waele Jo [1]

[1] Italian Institute of Speleology, Department of Biological, Geological and Environmental Sciences, University of Bologna. Via Zamboni, 67, 40126 Bologna (Italy)

[2] Department of Earth and Marine Sciences, University of Palermo (Italy)

[3] National Research Council, IRPI, Bari (Italy)

7.1.1. Abstract

Santa Cesarea Terme in Salento is the only area in which hypogenic caves have been recognized in the Apulia region. In this spa area the rising of sulfidic thermal waters that mix with both recent fresh infiltration waters and coastal salt water has formed four active sulfuric acid speleogenesis (SAS) caves. These caves are characterized by the typical set of sulfuric acid meso-and micro-morphologies, and also by the presence of both gypsum and native sulfur. In all caves biofilms are visible in the sulfidic thermal waters and on the cave walls.

Keywords: Thermal water; Spa; Speleogenesis; Hypogenic cave

7.1.2. Introduction

Apulia (southeastern Italy) is one of the Italian sectors most affected by karst processes, due to the widespread presence of carbonate rocks. The configuration of the region as an elongated peninsula makes the Apulian coastlines extensively carved by karst caves and coastal karst landforms (Palmentola, 2002; Inguscio et al., 2007; Parise, 2008; De Waele et al., 2011; Parise et al., 2013), including sinkhole features both along the low-lying coasts (Bruno et al., 2008; Margiotta et al., 2012; Basso et al., 2013) and offshore (Taviani et al., 2012). Salento, the southernmost part of the peninsula, is particularly rich in remarkable karst caves along the coast, with sites of great paleontological and archeological importance (Grotta Romanelli, Porto Badisco) (Margiotta and Sansò, 2014), together with sites opened to public (Zinzulusa show cave; Parise, 2011; D'Agostino et al., 2015) and the many caves visited during the summer season by tourists.

In such scenario, Santa Cesarea Terme stands as an important spa area, known since the XIX century, with many sites of emergence of thermal waters. In this paper, after describing the main geological and morphological features of the area, we summarize the hydrogeology of the Santa Cesarea Terme aquifer and the morphological and mineralogical characteristics of the caves.

7.1.3. Geology and karst geomorphology

The sulfur springs of Santa Cesarea Terme (*Figure 51*) flow out along a coastal sector of the Salento peninsula, part of the Apulian carbonate platform (Ricchetti et al., 1988; Bosellini et al., 1999; Bossio et al., 2005). The carbonate succession, consisting of over 5 km-thick Jurassic and Cretaceous limestone and dolostone, rests above Late Triassic evaporites, and is unconformably overlain by Cenozoic calcareous successions.

Figure 51. A view of the Santa Cesarea Terme spa area: the milky color in the sea (yellow arrows) is due to plumes of sulfur-rich waters coming out of the thermal sulfuric acid speleogenesis (SAS) caves. Photo Mario Parise.

Starting from the Early Triassic, the area was part of the Apulian carbonate platform, characterized by shallow-water carbonate sedimentation (Mostardini and Merlini, 1986). Since Cretaceous times, it experienced a number of transgression-regression phases, giving rise to a succession constituted by multiple unconformities. Eventually, during the Middle Pleistocene, the area underwent a severe regional uplift (Doglioni et al., 1994).

As concerns the main geological structures, the Santa Cesarea Terme area shows extensional and trans-tensional structures, with related pull-apart features. The NW-SE faults are the most diffuse, with subordinate presence of SW-NE, E-W and N-S fault systems. In particular, the NW-SE trans-

tensional faults appear to be the youngest (Zuffianò et al., 2013), also controlling the development of the main karst landforms in the area. The thermal springs are located, as the village of Santa Cesarea Terme, on a structural high, with the caves distributed along the NW-SE fault zones.

The study area hosts a variety of karst surface landforms, mostly represented by dolines and by typical karst valleys, locally termed *lame* (Parise et al., 2003). Apart from a number of inland caves (mostly with development limited to a few tens of meters, and maximum depth around 40 m), the most relevant karst features are distributed along the coast (*Figure 52*), and correspond to the three caves within the spa area (PU105 Grotta Gattulla, PU102 Grotta Fetida, and PU103 Grotta Sulfurea), and an additional one further south (PU914 Grotta Solfatara).

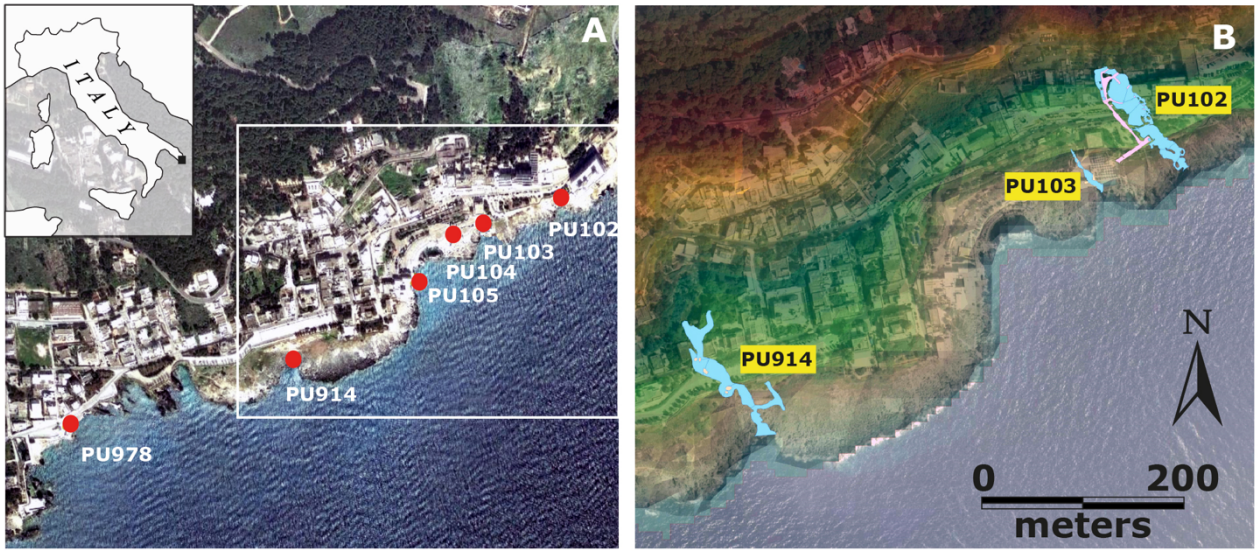

Figure 52. A) Google Earth image showing the distribution of caves along the Santa Cesarea Terme coastline. PU 102 = Grotta Fetida; PU 103 = Grotta Sulfurea; PU 104 = Grotta Bagno Marino; PU 105 = Grotta Gattulla; PU914 = Grotta Sulfurara; PU 978 = Riparo Gli Archi. B) Sketch showing the map of Grotta Fetida, Grotta Sulfurea, and Grotta Solfatara. Surveys Apulian Speleological Federation (FSP).

7.1.4. The Santa Cesarea Terme caves

Known and described by several scholars since 1800 (Mauget, 1875; De Giorgi, 1882), and used starting from the 1930s as spa (Corti, 1992), the set of caves at Santa Cesarea Terme represents a significant tourist attraction in this coastline stretch of southern Apulia. Apart from the touristic and therapeutic interests (Dell'Oca, 1962), the caves are of great scientific importance, being, nowadays in Apulia, the only caves of hypogenic origin sensu Klimchouk (2007) and De Waele et al. (2014).

All caves are clearly developed along N30°E fractures running perpendicular to the coast and developing up to a little over 100 m landward. In their innermost parts sulfur-rich thermal waters

enter the caves from below. The cave passages are up to ten meters wide, but generally rather low (on average 3-4 m, never exceeding 10 m) and show no signs of former water levels. The walls and roofs are intensely corroded, with dissolution enlarging every possible fracture, forming a network of enlarged joints and less corroded pendants (*Figure 53*A). At a centimeter scale replacement pockets can be seen in many places (*Figure 53*B), with gypsum crusts covering the walls of the fractures and the inner parts of the pockets. All caves have their floor flooded by the sea on which the thermal milky-colored sulfuric water flows (*Figure 53*C,D).

Gypsum occurs as solid crusts, but covers the walls also with fine and delicate crystals from which biofilms pend (*Figure 53*E). The microbial mats are also present in the form of very nicely drawn patterns of vermiculations of brownish-yellowish color (*Figure 53*F) and white moonmilk materials with low pH close to 3.

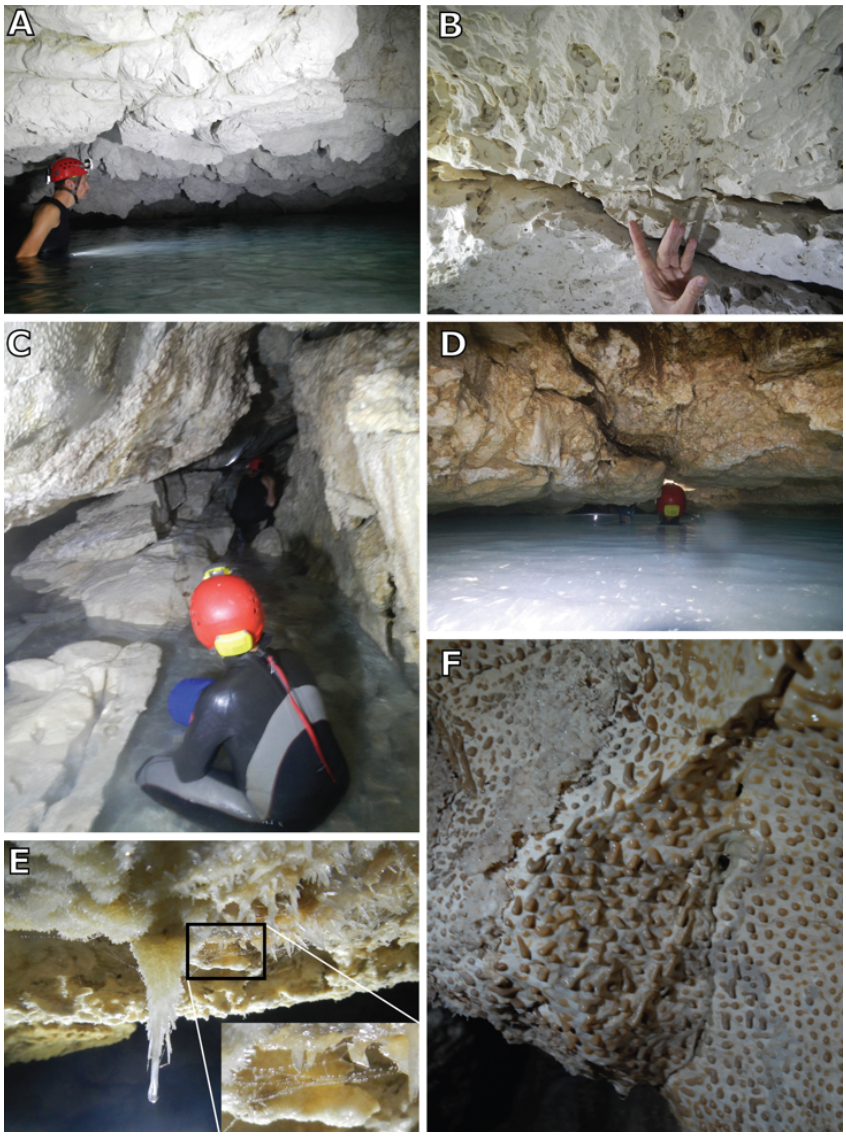

Figure 53. Morphologies of the sulfuric acid caves: A) Corroded cave roof in fossiliferous limestones, Grotta Sulfurea; B) Replacement pockets, Grotta Sulfurea; C) The main fracture from which sulfuric waters rise (note the milky color of the water), Grotta Sulfurara; D) Swimming in the milky sulfuric

water, Grotta Sulfurara; E) Gypsum crystals with biofilms, mainly visible on the roof: the crystals are 2 cm long (Grotta Sulfurara); F) Vermiculations in Grotta Fetida, field of view is half a meter wide. Photos Marco Vattano.

The replacement gypsum occurs in different forms: as toothpaste-like, not yet consolidated, material (*Figure 54*A), as prismatic crystals (*Figure 54*B), or as hard crusts (*Figure 54*C) or powders-crusts inside the replacement pockets (*Figure 54*D). As observed in an Austrian sulfuric acid cave (Plan et al., 2012) gypsum is pseudomorphic, replacing the mineralogy of original fine sedimentary structures of the replaced limestone, including fossils (*Figure 54*A). In one of the caves, Grotta Gattulla, the walls are covered with an over 1 cm thick coating of vivid yellow native sulfur (*Figure 54*C,E) that formed above the present water level. In Grotta Fetida fine crystalline gypsum crusts covering the limestone walls occur alongside the vermiculations (*Figure 54*F).

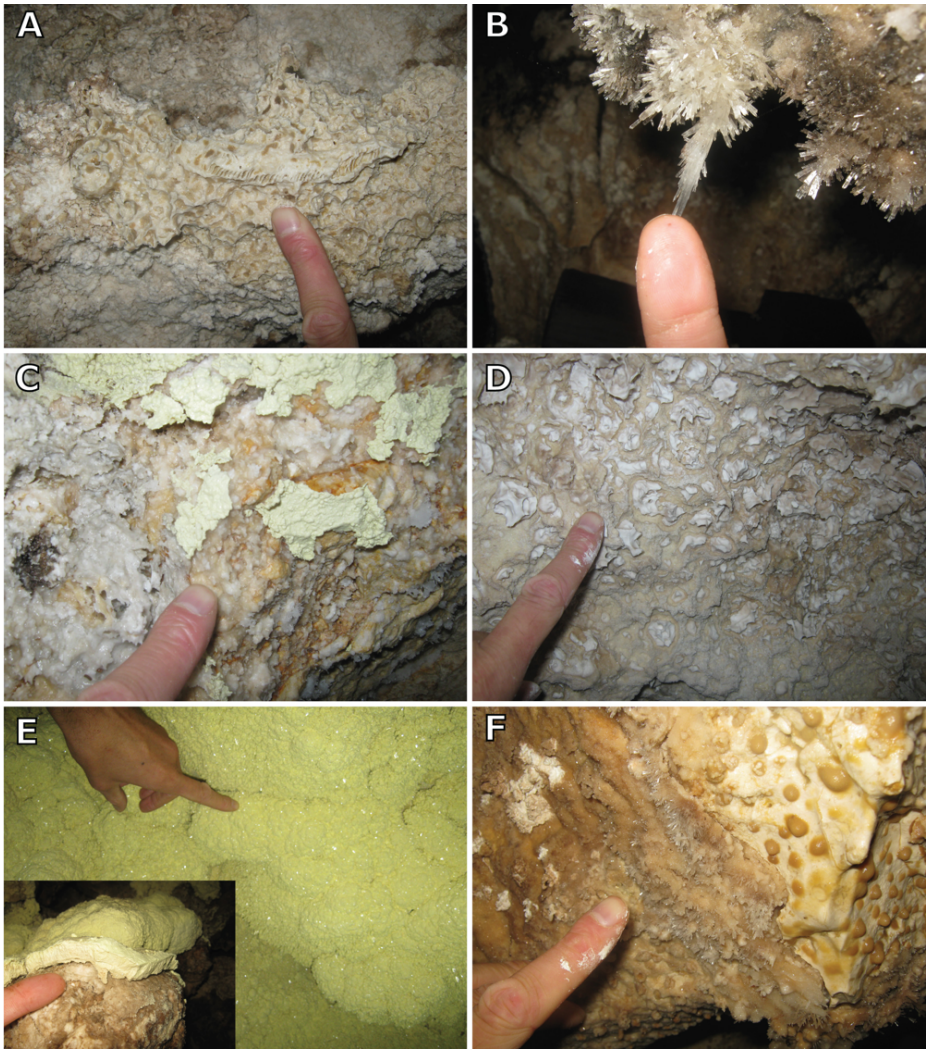

Figure 54. A) Pseudomorphic replacement gypsum still showing the fossils of the original limestone, Grotta Fetida; B) Needle crystals of gypsum, Grotta Gattulla; C) Gypsum and sulfur crusts in Grotta Gattulla; D) Sugar-like gypsum still present in replacement pockets, Grotta Gattulla; E) Thick native

sulfur crusts, Grotta Gattulla; F) Gypsum crust and vermiculations in Grotta Fetida. Photos Jo De Waele.

In Grotta Sulfurea some common calcite speleothems (stalactites, flowstones and stalagmites) decorate the cave. Stalagmites and columns are now submerged by the sea and occur up to 2 m below sea level (*Figure 55*). These appear to be slightly corroded and have developed when sea level was at least several meters lower than today. The rather fresh appearance of these speleothems seem to demonstrate that dissolution in these sulfidic waters is not very active, or has started rather recently, or that dissolution/corrosion processes occur mainly on the surficial water layer (i.e., at the water-air interface) where H_2S can oxidize becoming H_2SO_4.

Figure 55. Vadose speleothems in Grotta Sulfurea occur below present sea level. Photos Marco Vattano

It is obvious that cave enlargement occurred downstream of the sulfur springs, where the oxidation of hydrogen sulfide produces sulfuric acid that immediately reacts with the host rock replacing calcite with gypsum. This process appears to be active essentially above the water level, on the wet walls and ceiling.

Different hypotheses about the springs have been presented in the literature, but there is no accordance so far on their origin (Zezza, 1980; Calò et al., 1983; Calò and Tinelli, 1995), and several uncertainties still exist.

The caves are distributed along a 500 m-long coastline stretch at sea level, at the base of the carbonate coastal cliff. As concerns water types, the overall system seems to be due to three components, in all creating a mixing solution undersaturated with respect to calcite: i) the fresh water deriving from meteoric infiltration in the carbonate rocks, ii) the brackish water due to seawater intrusion, and iii) a sulfur-rich thermal saline fluid.

The thermal waters coming from the caves are distributed in the Na-Cl-SO_4 quadrant of *Ludwig-Langelier* diagram, and their pH ranges from 7.2 to 7.8 from the ones dominated by deep water to that ones mainly influenced by water mixing (seawater-deep water). As pointed out by previous studies, their spring waters show variable chemical-physical properties, essentially as a function of the tides. For example, changes in the content of ion chloride, hydrogen and temperature have been observed between low and high tide (Visintin, 1945; Polemio et al., 2012).

The cave development is certainly controlled by the main geological-structural elements in the area. This can be deduced from the cave entrances, from their N30°E development, as well as at many sites within the cave systems. The spring waters are well recognizable due to milky white plumes of warm floating sulfur-rich waters flowing out of the caves, visible only in particularly calm sea and wind conditions (*Figure 51*).

The Santa Cesarea Terme caves, thanks to their interesting location, show very typical inner morphologies and a mineralogy associated with sulfuric acid speleogenesis. These evidences, together with the geochemical analysis, can shed some new insights on the mixing of thermal sulfur-enriched water with salt and freshwater and their interaction with carbonate rocks, and elucidate the velocity and the main processes of cave formation in this unique geochemical and geological setting.

From the hydrogeological point of view meteoric waters can penetrate at depth through the high porosity and permeability of the calcareous rocks, or flow directly into the sea due to the presence of Quaternary impermeable deposits (Zuffianò et al., 2013). Saltwater strongly interacts with the freshwater not only along the halocline, but also inland, thus creating salt water intrusion problems due to intense water withdrawal for agriculture and human settlements (Tadolini and Bruno, 1993).

Shallow waters can occasionally interfere with deep water bodies flowing in calcareous and calcareous-dolomitic Cretaceous rocks of the Salento peninsula (Tadolini and Bruno, 1993). The deep water presents a very high salt concentration (58 g/L) and temperature of 22-33°C (several degrees higher than the waters coming from shallow resources, showing temperatures of 18-19°C; Zuffianò et al., 2013). Such values are probably due to the exothermic reaction of sulfate contained in the

seawater interacting with organic matter in the Miocene calcarenite layers (Zezza, 1980; Calò et al., 1983).

Geochemical studies (Santaloia et al., 2016) revealed that these waters are undersaturated with respect to calcite, dolomite and seem to be undersaturated with respect to gypsum, too. The high Lithium (Zuffianò et al., 2013) and the low Tritium concentration (Santaloia et al., 2016) is a clear indicator of residence time of groundwater in the aquifer (Edmunds and Smedley, 2000). This evidence, together with stable isotope analyses of $\delta^{18}O$ (between -3.5 and +2 ‰) and δ D (between -23 and +5 ‰) suggest that the thermal springs appear to be at least partially fed by groundwater with a long residence time (greater than 55 years) connected to a deep circulation system (Zuffianò et al., 2013).

7.1.5. Conclusions

Santa Cesarea Terme caves represent the only hypogenic system in Apulia, but have never been so far object of dedicated projects aimed at defining the processes acting within the cave systems, and their origin. The research described in this paper brought us to identify a number of peculiar morphologies (replacements pockets, cupola-like morphologies), and of minerals such as huge amounts of gypsum deposits, sulfur native coatings and jarosite minerals, which characterize the caves, and allow to define them as a SAS system. From the geochemical standpoint the waters are enriched with Na-Cl-SO_4 and colonized by white soft floating filaments. On the ceiling and roof, brown and yellowish bio-vermiculations and white toothpaste materials (moonmilk) can be observed, especially at those sites where H_2S degassing is important. In submerged environments mixing between sulfidic rising fluids and seawater seems to have an important role on dissolution processes. These latter, with particular regard to the dissolution rates, are being monitored since October 2015 following the method by Galdenzi (2012), in order to understand which is the dominant phenomenon/process (H_2S degassing vs. water mixing) in submerged environments and cave atmosphere. Limestone and gypsum tablets have been located in three environments: water, interface and air in several cave sections moving from a site dominated by sea water to the deep part of the cave, dominated by rising H_2S-rich fluids. We observed that dissolution at the water-air interface is faster in the middle section (where mixing between sea and deep water occurs, while dissolution in air is higher in the deep section where H_2S degassing is more abundant.

At the same time, a further issue under investigation is the role of microbial substances on the speleogenesis of Santa Cesarea Terme caves, in particular the role of sulfo-oxidizing and sulfo-reducing bacteria (Jones et al., 2011) involved in secondary mineral precipitation and rock dissolution.

References

Basso, A., Bruno, E., Parise, M., Pepe, M., 2013. Morphometric analysis of sinkholes in a karst coastal area of southern Apulia (Italy). Environmental Earth Sciences, 70(6): 2545-2559.

Bosellini, A., Bosellini, F.R., Colalongo, M.L., Parente, M., Russo, A., Vescogni, A., 1999. Stratigraphic architecture of the Salento coast from Capo d'Otranto to Santa Maria di Leuca (Apulia, southern Italy). Rivista Italiana di Paleontologia e Stratigrafia, 105 (3): 397-416.

Bossio, A., Mazzei, R., Monteforti, B., Salvatorini, G., 2005. Stratigrafia del Neogene e Quaternario del Salento sud-orientale (con rilevamento geologico alla scala 1:25.000). Geologica Romana, 38: 31-60.

Bruno, E., Calcaterra, D., Parise, M., 2008. Development and morphometry of sinkholes in coastal plains of Apulia, southern Italy. Preliminary sinkhole susceptibility assessment. Engineering Geology, 99:198-209.

Calò GC, Tinelli R (1995) Systematic hydrogeological study of a hypothermal spring (S. Cesarea Terme, Apulia), Italy. Journal of Hydrology 165:185-205

Calò, G.C., Spizzico, M., Tinelli, R., Zezza, F., 1983. Hydrogeological investigations on the area surrounding Santa Cesarea Terme springs (southern Apulia). Geologia Applicata e Idrogeologia, 18(2):129-144

Corti, E., 1992. Relazione sul Convegno Nazionale di Speleologia di Castro, 14-15-16 settembre 1936. Itinerari Speleologici, 6: 89-97

D'Agostino, D., Beccarisi, L., Camassa, M., Febbroriello, P. 2015. Microclimate and microbial characterization in the Zinzulusa show cave (South Italy) after switching to led lighting. Journal of Cave and Karst Studies, 77(3):133-144.

De Giorgi, C., 1882. I bagni solfurei di Santa Cesarea in Terra d'Otranto. Rivista Idrologica e Climatica Medica, 4:8

Dell'Oca, S., 1962. Note di speleologia economica. Rassegna Speleologica Italiana, 1:76-109

De Waele, J., Lauritzen, S.E., Parise, M., 2011. On the formation of dissolution pipes in Quaternary coastal calcareous arenites in Mediterranean settings. Earth Surface Processes and Landforms, 36(2):143-157.

De Waele, J., Galdenzi, S., Madonia, G., Menichetti, M., Parise, M., Piccini, L., Sanna, L., Sauro, F., Tognini, P., Vattano, M., Vigna, B., 2014. A review on hypogene caves in Italy. In: A., Klimchouk, I.D., Sasowski, J., Mylroie, S.A., Engel, A., Summers Engel (Eds), Hypogene cave morphologies. Karst Water Institute, special publication, 18: 28-30.

Doglioni, C., Mongelli, F., Pieri, P., 1994. The Puglia uplift (SE-Italy): an anomaly in the foreland of the Apenninic subduction due to buckling of a thick continental lithosphere. Tectonics,

13(5):1309-1321.

Edmunds, W.M., Smedley, P.L., 2000. Residence time indicators in groundwater: the East Midlands Triassic sandstone aquifer. Applied Geochemistry, 15:737-752

Galdenzi, S., 2012. Corrosion of limestone tablets in sulfidic ground-water: measurements and speleogenetic implications. International Journal of Speleology, 41(2):149-159.

Inguscio, S., Lorusso, D., Pascali, V., Ragone, G., Savino, G., (Eds), 2007. Grotte e carsismo in Puglia. Regione Puglia: 200.

Jones, A.A., 2011. Microbe-mineral affinity in sulfuric acid karst systems. Thesis, University of Austin.

Jones, D.S., Polerecky, L., Galdenzi, S., Dempsey, B.A., Macalady, J.L., 2015. Fate of sulfide in the Frasassi cave system and implications for sulfuric acid speleogenesis. Chemical Geology, 410: 21-27.

Klimchouk, A.B., 2007. Hypogene speleogenesis: hydrogeological and morphogenetic perspective. Natl. Cave Karst Res. Inst., Carlsbad.

Margiotta, S., Sansò, P., 2014. The Geological Heritage of Otranto–Leuca Coast (Salento, Italy). Geoheritage, 6(4): 305-316

Margiotta, S., Negri, S., Parise, M., Valloni, R., 2012. Mapping the susceptibility to sinkholes in coastal areas, based on stratigraphy, geomorphology and geophysics. Natural Hazards, 62 (2): 657-676.

Mauget, A., 1875. Note geologiche sulla Provincia di Lecce. Lecce.

Mostardini, F., Merlini, S., 1986. Appennino centro meridionale. Sezioni geologiche e proposta di modello strutturale. Memorie della Società Geologica Italiana, 35: 177-202.

Palmentola, G., 2002. Il paesaggio carsico della Puglia. Grotte e dintorni, 4: 203-220.

Parise, M., 2008. Elementi di geomorfologia carsica della Puglia. In: M., Parise, S., Inguscio, A., Marangella (Eds), Atti del 45° Corso CNSS-SSI di III livello di "Geomorfologia Carsica, Grottaglie, 2-3 febbraio 2008: 93-118.

Parise, M., 2011. Some considerations on show cave management issues in Southern Italy. In: P.E., Van Beynen (Ed) Karst management. Springer, Dordrecht, 159-167.

Parise, M., Federico, A., Delle Rose, M., Sammarco, M., 2003. Karst terminology in Apulia (southern Italy). Acta Carsologica, 32(2): 65-82

Parise, M., De Pasquale, P., Martimucci, V., Meuli, V., Pentimone, N., Pepe, P., 2013. Grotta della Rondinella a Polignano a Mare: un progetto di ricerca della Federazione Speleologica Pugliese. In: F., Cucchi, P., Guidi (Eds), Proceedings of the 21th National Congress of Speleology "Diffusione delle Conoscenze", Trieste, 2-5 giugno 2011, Ed. Università di Trieste: 437-448.

Plan, L., Tschegg, C., De Waele, J., Spötl, C., 2012. Corrosion morphology and cave wall alteration in an Alpine sulfuric acid cave (Kraushöhle, Austria). Geomorphology, 169: 45-54.

Polemio, M., Limoni, P.P., Zuffianò, L.E., Santaloia, F., 2012. Santa Cesarea thermal springs (Southern Italy). In: M., Thangarajan, C., Mayilswami, P.S., Kulkarni V.P., Singh (Eds), 5th International Groundwater Conference (IGWC), Assessment and management of groundwater resources in hard rock systems with special reference to basaltic terrain, 15: 737-752.

Ricchetti, G., Ciaranfi, N., Luperto Sinni, E., Mongelli, F., Pieri, P., 1988. Geodinamica ed evoluzione sedimentaria e tettonica dell'Avampaese Apulo. Memorie della Società Geologica Italiana, 41: 57-82.

Santaloia, F., Zuffianò, L.E., Palladino, G., Limoni, P.P., Liotta, D., Minissale, A., 2016. Coastal thermal springs in a foreland setting: the Santa Cesarea Terme system (Italy). Geothermics, 64: 344-361.

Tadolini, T., Bruno, G., 1993. The influence of geostructural setting upon water thermo-mineralization in certain areas of Apulia (Southern Italy). Proceedings of the Antalya Symposium and Field Seminar, October 1990, IAHS, 207: 75-83.

Taviani, M., Angeletti, L., Campiani, E., Ceregato, A., Foglini, F., Maselli, V., Morsilli, M., Parise, M., Trincardi, F., 2012. Drowned karst landscapes offshore the Apulian Margin (Southern Adriatic Sea, Italy). Journal of Cave and Karst Studies, 74(2):197-212.

Visintin, B., 1945. Studio sull'acqua della Grotta Gattulla delle Terme demaniali di S. Cesarea. Annali di Chimica Applicata, 35 (6-7): 97-111.

Zezza, F., 1980. Le sorgenti ipotermali solfuree di Santa Cesarea Terme. Azienda di cura e soggiorno e turismo Santa Cesarea Terme. Salentum: 1–2.

Zuffianò, L.E., Palladino, G., Santaloia, F., Polemio, M., Liotta, D., Limoni, P.P., Parise, M., Pepe, M., Casarano, D., Rizzo, E., Minissale, A., De Franco, R., 2013. Geothermal resource in a foreland environment: the Santa Cesarea Terme thermal springs (Southern Italy). European Geothermal Congress 2013, Pisa, 3-7 June 2013: 6.

7.2. Article 6

Published in Hypogene Karst Regions and Caves of the World, Springer,

An overview of the hypogene caves of Sicily

Marco Vattano[1], Giuliana Madonia[1], Philippe Audra[2], Ilenia M. D'Angeli[3], Ermanno Galli[4], Jean-Yves Bigot[5], Jean-Claude Nobécourt[6], Jo De Waele[3]

[1]Dipartimento di Scienze della Terra e del Mare, University of Palermo, Via Archirafi 22, 90123 Palermo, Italy.

[2]University of Nice Sophia-Antipolis, Innovative City URE 005 & Polytech Nice – Sophia, 930 route des Colles, 06903 Sophia-Antipolis, Nice, France.

[3]Istituto Italiano di Speleologia, University of Bologna, Via Zamboni 67, 40127 Bologna, Italy

[4]Dipartimento di Scienze della Terra, University of Modena and Reggio Emilia, Largo S. Eufemia 19, 41121 Modena, Italy.

[5]Association française de karstologie (AFK), 21 rue des Hospices, 34090 Montpellier, France.

[6]CRESPE, Avenue des Poilus, 06140 Vence, France.

7.2.1. Abstract

Karst in Sicily develops in both Messinian gypsum and Mesozoic or Tertiary limestone rocks. Caves are also found in the basalts of Mount Etna. Except for some rare cases, until recently most caves developed in limestone were considered to be of epigenic origin. The discovery of gypsum in some of these caves, and especially detailed morphological studies, have allowed defining a hypogenic origin for a dozen of caves up to now. In some of these the hypogenic evidences are very clear, while other remain in doubt because of the widespread presence of well-developed condensation-corrosion morphologies not necessarily related to hydrothermal fluids. This paper reports the present knowledge of hypogenic caves in the Sicilian Island.

Keywords: Hypogenic caves, Sicily, Sulfuric acid speleogenesis, Condensation-corrosion, Wall sculpturing

7.2.2. Introduction

In recent years, knowledge on hypogene karst increased significantly in many aspects. Studies on hypogenic caves in Sicily are quite recent. Except for some investigations carried out at Monte Inici and Monte Kronio (Messana, 1994; Perotti, 1994 and references therein), systematic research only began in 2010. These investigations have allowed identifying several hypogenic karst systems, previously thought to be epigenic caves fed by meteoric water. The analysis of pattern, large and mid-

scale morphologies, mineral deposits and the presence of warm springs in areas close to the cavities in fact suggest that the genesis of these caves is linked to hypogenic processes (Vattano et al., 2012, 2013, 2015; De Waele et al., 2016).

New explorations allowed inferring the hypogenic origin of other caves based on the presence of peculiar morphologies and deposits. In most cases speleogenetic, geomorphological, mineralogical and biological studies are still in progress (*Table 21*).

In this paper, we illustrate the main morphological, mineralogical, and speleogenetic features of the hypogenic caves investigated up to now.

Table 21. List of the Sicilian hypogene cave systems.

Cave system	Studied	Under investigation	Lenght	Depth
1 Abisso dei Cocci - Grotta dell'Eremita	x		2 km 2.9 km	-61 m; -300 m; -306 m
2 Grotta dei Personaggi	x		1.7 km	+15 m; -32 m
3 Grotta dei Personaggini		x	110 m	-16 m
4 Grotta Barone		x	85 m	-14 m
5 Monte Kronio	x			
6 Grotta dell'Acqua Fitusa	x		700 m	+10 m / -16 m
7 Abisso del Vento		x	2 km	-210 m
8 Grotta dell'Acqua Mintina		x	not available	not available
9 Grotta Palombara		x	800 m	-80 m
10 Grotta Scrivilleri		x	2 km	not available
11 Grotta Monello		x	200 m	-32 m
12 Grotta Chiusazza		x	190 m	0 m

7.2.3. Geology

Sicily is a segment of the Alpine collisional belt that develops along the Africa-Europe plate boundary and links the Southern Apennine and the Calabrian Arc to the Tellian and Atlas systems of Northeastern Africa. The collisional complex of Sicily consists of several stratigraphic and tectonic elements (Catalano et al., 2013b and references therein; Avellone et al., 2010; Gasparo Morticelli et al., 2015, *Figure 56*): a) the Hyblean foreland (Hyblean Plateau) outcropping in southeastern Sicily, made up of Triassic-Liassic platform and scarp-basin carbonates overlain by Jurassic-Eocene pelagic carbonates and Oligocene-Quaternary open shelf carbonates; b) a NW-dipping foredeep located north of the foreland, consisting of Plio-Pleistocene pelagic marly limestones, silty mudstones and sandy clays overlying Messinian evaporites; c) a complex composed of an E- to SE-vergent fold and thrust belt consisting of: an "European" element (Peloritani-Calabrian Units), exposed in NE Sicily,

composed of allochthonous Paleozoic igneous and metamorphic rocks overlain by remnants of a mostly carbonate Mesozoic–Cenozoic sedimentary cover; a "Tethian" element, characterized by repeated imbricated units deriving from the deformation of Sicilidi Units, made of uppermost Jurassic–Oligocene deep-water carbonates and sandy mudstones and covered by Upper Oligocene–Lower Miocene flysch deposit nappes; an "African" element (Sicilian Units) composed of several thrust systems involving the deformation of Permian–Miocene deep-water carbonates and bedded cherts (Imerese and Sicanian basins), and Mesozoic–Cenozoic shelf-to-pelagic carbonates (Panormide, Trapanese, Saccense and Iblean–Pelagian carbonate platform or seamount facies domain); a thrust wedge (Gela Thrust System) consisting of Miocene-Pleistocene coeval foreland, wedge-top and foredeep basin sediments (terrigenous, evaporitic and clastic carbonate rocks).

The fold and thrust belt of Sicily resulted from a progressive accretion of thrust sheets and duplex formation combined with the clockwise rotation of allochthonous blocks started in the Middle Miocene and continued up to Middle-Late Pleistocene (Gasparo Morticelli et al., 2015). Plio-Pleistocene high-angle extensional faults affect the northern coastal sectors of Sicily and the foreland area (Catalano et al., 2013a).

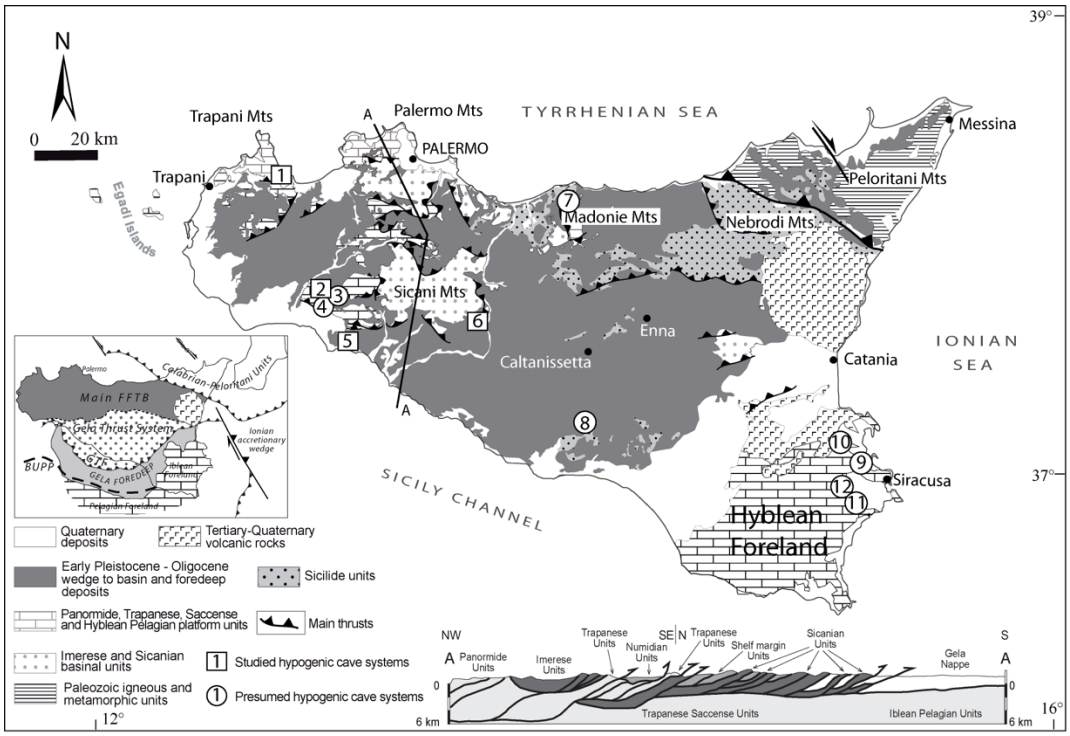

Figure 56. Geological map of Sicily (from Catalano et al. 2000; 2013) and location of hypogenic cave systems. 1. Monte Inici caves; 2. Grotta dei Personaggi; 3. Grotta dei Personaggini; 4. Grotta Barone; 5. Monte Kronio caves; 6. Grotta dell'Acqua Fitusa; 7. Abisso del Vento; 8. Grotta dell'Acqua Mintina; 9. Grotta Palombara; 10. Grotta Scrivilleri; 11. Grotta Monello; 12. Grotta Chiusazza. Inset map shows the main elements of the collisional complex of Sicily (FFTB, Fold and Thrust Belt; BUPP, Boundary of Undeformed Hyblean-Pelagian carbonate Platform).

7.2.4. Hypogene caves

In Sicily hypogene caves developed in carbonate rocks and are located in different sectors of the Sicilian collisional complex; presumed hypogenic caves also occur in the foreland area in the southeastern corner (Hyblean Plateau) (*Figure 56*).

Most of these are inactive sulfuric acid speleogenesis (SAS) caves mainly formed by corrosion processes of carbonate rock by H_2S-rich thermal water rising along important faults. Thermal waters, some of which used for therapeutic and recreational purposes, often spring out close to the caves (Grassa et al., 2006 and references therein).

These active and inactive SAS caves are among the most developed systems of the Island, reaching lengths of almost 3 km and depth of 300 m. A clear example of inactive SAS water table cave is represented by the "Grotta dell'Acqua Fitusa", which despite its small dimensions, shows many diagnostic features of this type of caves (Vattano et al., 2012; Plan et al., 2012; De Waele et al., 2016).

Hypogenic caves with dendritic pattern of stacked spheres seem to be linked mainly to condensation-corrosion processes by airflow rich in CO_2 (i.e., Grotta dei Personaggi).

All the caves have developed along structures such as bedding, fracture or fault planes; an important role in enlarging voids is played by processes of condensation-corrosion caused by thermal convective airflow in the cave atmosphere.

7.2.4.1. The Monte Inici cave system

The Monte Inici cave system is located in NW Sicily (*Figure 56*), along the SE side of Mt. Inici, a gently westward – dipping monoclinal relief affected by NW-SE, NE-SW and NNW-SSE high angle faults. It is composed of two caves, Grotta dell'Eremita and Abisso dei Cocci, formed in Lower Jurassic platform limestones and dolomitic limestones (Inici Fm.), and Upper-Middle Jurassic pelagic reddish-gray limestones with ammonites (Buccheri Fm.) of the Trapanese Domain. Thermal springs with temperature between 44.2 and 49.6 °C and chloride-sulfate alkaline-earth waters (Grassa et al. 2006) are located eastward and at lower altitude with respect to the cave system (*Figure 57*A).

Grotta dell'Eremita and Abisso dei Cocci are 3D inactive phreatic maze caves characterized by large subhorizontal galleries and chambers connected by deep shafts, which reach respectively a total length of more than 2 km and a depth of about 300 m (*Figure 57*B,C). Some galleries are inclined and follow the dip of bedding planes, whereas the shafts correspond to vertical fissures or fault planes. Passages display subcircular cross-sections, or vadose entrenchments (*Figure 57*D,E). In some galleries of the Grotta dell'Eremita several small conduits filled by well-cemented fine reddish

sediment of continental nature occur at the bedding plane along which the passage develops (*Figure 57*F).

Morphologies due to condensation-corrosion processes are widespread in both caves. The walls and ceiling of several passages are tapered by convection wall niches, mega-scallops, ceiling cupolas (*Figure 57*D) and spheres, spongework-like forms, while in some cases passages are divided by partitions.

Both caves lack alluvial sediments. Chemical deposits consist mainly of calcite occurring in powder, thin crusts, frostwork, popcorn or reddish laminae (Grotta dell'Eremita), and gypsum in the form of crusts, and small acicular, fibrous or tabular crystals along the lower parts of the walls of several passages. The caves are rich in phosphate minerals (i.e., hydroxylapatite, taranakite, crandallite, carbonate-apatite, montgomeryite) derived from the transformation of large fossil bat guano deposits. Beside powders or crusts, apatite often occurs as small stalactites and stalagmites (Messana 1994; Vattano et al. 2013).

Patterns and cross-sections of the main passages of the Abisso dei Cocci and Grotta dell'Eremita suggest that the early speleogenetic phases took place under phreatic conditions by rising thermal water. In the Grotta dell'Eremita, phreatic conditions are recorded also by the several sediment filled anastomosed protoconduits visible at the bedding plane, along which the passages develop. After switching from phreatic to vadose conditions, as a consequence of the uplift phases of this sector of the Sicilian chain, entrenchment of passages and development of 3D maze caves occurred. In addition widening of subterranean voids was connected to significant condensation-corrosion processes by airflow rich in H_2S that also favored the deposition of gypsum deposits in the lower parts of the passages.

In the Abisso dei Cocci a more recent epigenic phase is recorded by important calcite speleothems (i.e., flowstones, stalactites, stalagmites) fed by dripping meteoric water.

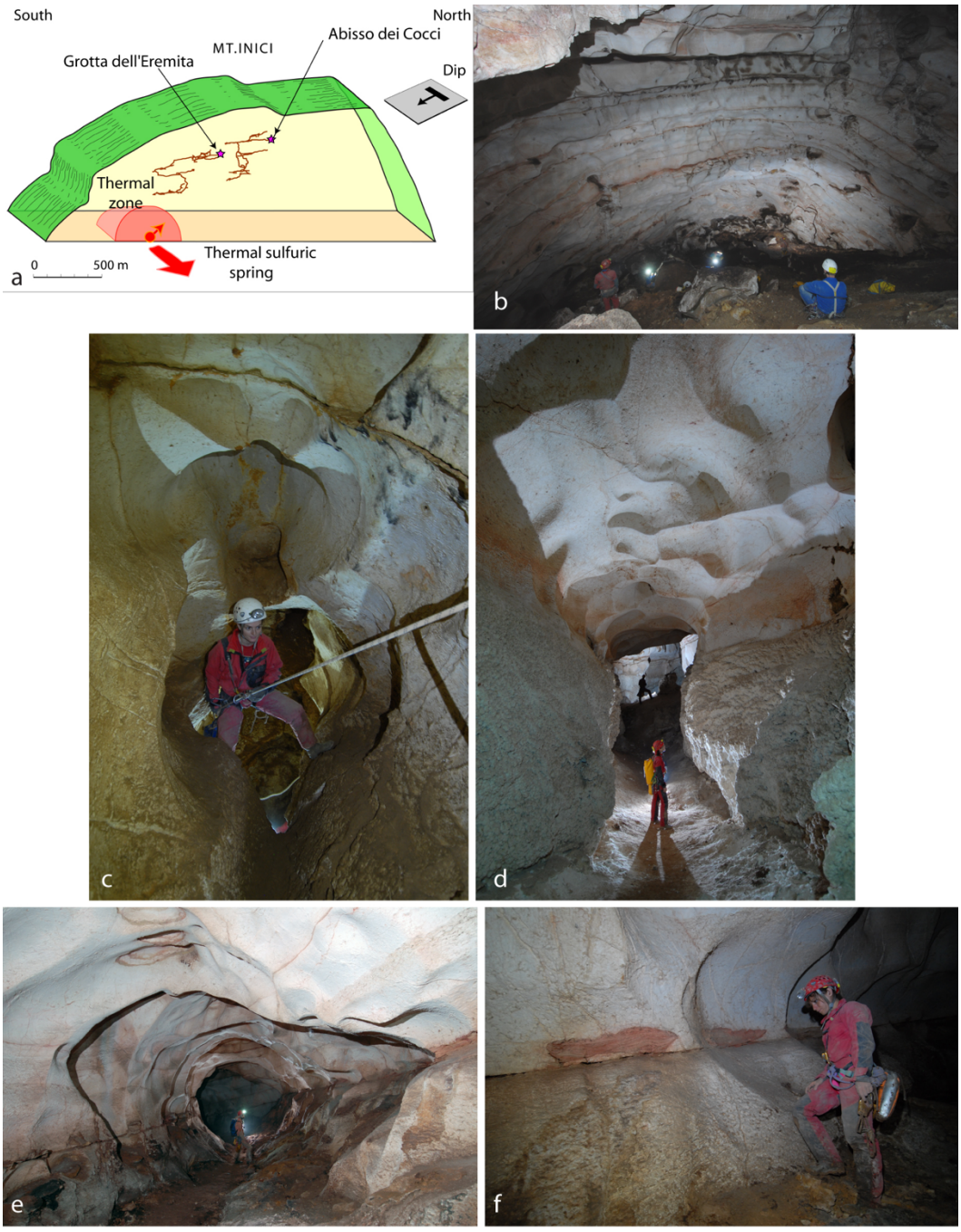

Figure 57. Monte Inici cave system. A) Sketch of Monte Inici and its caves and location of the thermal zone (from Vattano et al. 2013); B) Big chamber enlarged by condensation-corrosion processes caused by huge guano deposits (Grotta dell'Eremita); C) Vertical passage with rounded walls and cupolas on the roof (Abisso dei Cocci); D) Entrenched phreatic passage characterized by cupolas, and calcite/aragonite and gypsum deposits in the lower parts (Abisso dei Cocci); E) Inclined passage along a bedding plane with large convection wall niches and ceiling cupolas (Grotta dell'Eremita); F) Close view of protoconduits filled by continental silt along the gallery shown in E.

7.2.4.2. The Monte Kronio cave system

The active hypogenic Monte Kronio cave system is unique in Sicily and probably in the world. It is characterized by the rising of hot moist air linked to a deep thermal aquifer, lying below the explored caves. Although this system was visited by man since the end of the Mesolithic for shelter, place of worship, necropolis, and from the I century BC for thermal purposes, yet little is known about its real development and speleogenetic mechanisms due to the harsh environmental conditions with temperatures of about 38°C and humidity of 100%, that makes exploration extremely difficult. The first attempts to explore the caves date back to the end of the XVII century; since the 1940s several exploration campaigns organized by the Commission Grotte "E. Boegan" of Trieste identified and surveyed the cave system discovering an extended maze of passages up to 200 m deep (Perotti 1994). The cave system opens NE of Sciacca town (South Sicily), in the southern scarp of Mt. Kronio or Mt. San Calogero. Mt. Kronio consists of a complex structure linked to ENE-striking, closely spaced imbricate thrust sheets, involving Triassic to Miocene platform and pelagic platform carbonate deposits (Monaco et al. 1996). It is made up of a series of caves, whose origin is probably linked to Na-CL waters some of which rich in H_2S (Dongarrà and Hauser 1982), with temperature ranging between 32 and 55 °C (Grassa et al. 2006 and references therein) emerging along the southern slope of Mt. Kronio at lower altitude with respect to the cave entrances.

The caves are located at different altitudes and consist of subhorizontal passages (*Figure 58*A) connected by deep shafts or steep passages. The passages connecting the different branches of this cave system are not always big enough to allow a person to pass (*Figure 58*B). Some galleries breach the southern scarp of Mt. Kronio through small openings some of which emit hot air, while other ones let cold air in from outside. Walls and ceiling of the caves are weathered, characterized by condensation-corrosion forms, and powdery and/or crusty gypsum deposits are present (*Figure 58*C,D; Vattano et al. 2013). Multidisciplinary studies are currently in progress to improve our knowledge on the extent, speleogenesis and the evolution of this important cave system.

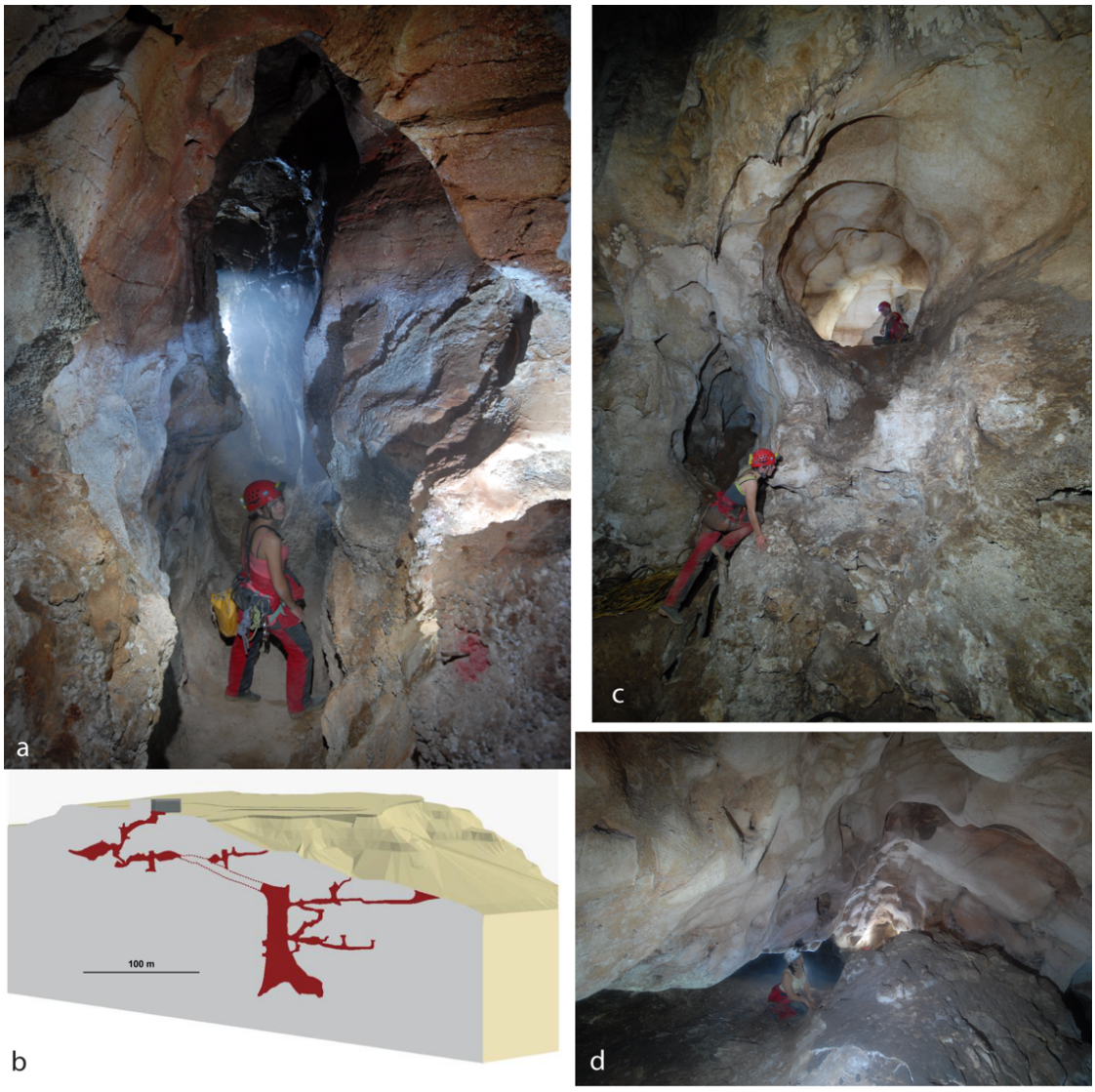

Figure 58. Monte Kronio cave system. A) Gallery where the condensation level of the airflow is visible on the walls. Above the caver it is possible to see fog linked to different air temperature: hot in the upper part, cold at the bottom; B) 3D sketch of the karst system (after www.boegan.it); C) Passages with forms due to condensation-corrosion processes, separated by partitions; D) Gypsum deposits in the form of crusts, below cupolas in the hot part of the cave system.

7.2.4.3. Grotta dell'Acqua Fitusa

The *Grotta dell'Acqua Fitusa* represents a good example of inactive water-table sulfuric acid cave (De Waele et al., 2016). The cave is located in central Sicily (*Figure 56*), along the north-eastern fault scarp of a N-S oriented westward vergent anticline forming the Mt. La Montagnola. This relief consists of rocks belonging to the basinal Imerese Domain, overthrusting the succession of the Sicanian Domain and the clastic Oligo-Miocene covers (Catalano et al., 2013a). Triassic interbedded calcilutites and marls with abundant pyrite and bitumen may occur at the base of the basinal Imerese

and Sicanian Domain. The cave formed in the Upper Cretaceous rudist breccias member of the Crisanti Fm. (Imerese Domain), composed of conglomerates and reworked calcarenites with rudist fragments and benthic foraminifera. Chloride-sulfate alkaline-earth waters with temperature of 25.2 °C (Grassa et al., 2006) still emerge 300 m north and at a lower altitude than the cave.

The cave consists of at least three stories of subhorizontal conduits (*Figure 59*A), arranged in a maze pattern following sets of joints oriented in ENE–WSW, E–W and N–S directions, forming large rooms on their intersections. The cave reaches a total length of 700 m and a vertical range of 25 m.

The passages developed at the former level of the piezometric surface and are characterized by a very low gradient from the upstream discharging points to the spring. They all show a flat floor breached by discharging feeders up to 10 m deep along their path, and notches with flat roof along the walls indicate lateral corrosion processes by the sulfuric thermal water (*Figure 59*B). Blind-ending passages develop upstream of the discharge points.

The cave is rich in different small and large morphological features generated by condensation-corrosion processes above the water table, due to H_2S degassing in the cave atmosphere, oxidation of sulfides and thermal convection of the acid air flows (Audra et al., 2010 and references therein). Ceiling cupolas and large wall convection niches occur in the largest rooms of the cave (*Figure 59*C); deep wall convection niches, in places forming notches, incise cave walls at different heights (*Figure 59*B); condensation-corrosion channels similar to ceiling-half tubes carve the roof of some passages; boxworks, and replacements pockets due to condensation-corrosion processes are widespread (*Figure 59*D). In some places the condensation waters with a high degree of acidity have produced sulfuric karren, such as rills and solution pans (*Figure 59*E).

Beside calcite speleothems due to recent dripping water, gypsum is the most abundant mineral in the cave. Replacement gypsum crusts fill large vertical fissures along the walls, cover wall convection notches or replacement pockets, and totally coat narrow blind passages. A deposit of about 50 cm of thickness occurs on the floor of the biggest room in correspondence of which small ceiling cupolas and pendants are associated on the roof (*Figure 59*F). Finally, centimeter-sized euhedral gypsum crystals grew inside mud sediments.

Since the genesis of the cave is closely related to the piezometric surface position, the different stories of passages record past stages of stability of the water table, in relation to changes of the base-level (*Figure 59*A; Audra et al., 2010 and references therein).

Further research on dissolution rates, according to Galdenzi (2012), are being performed.

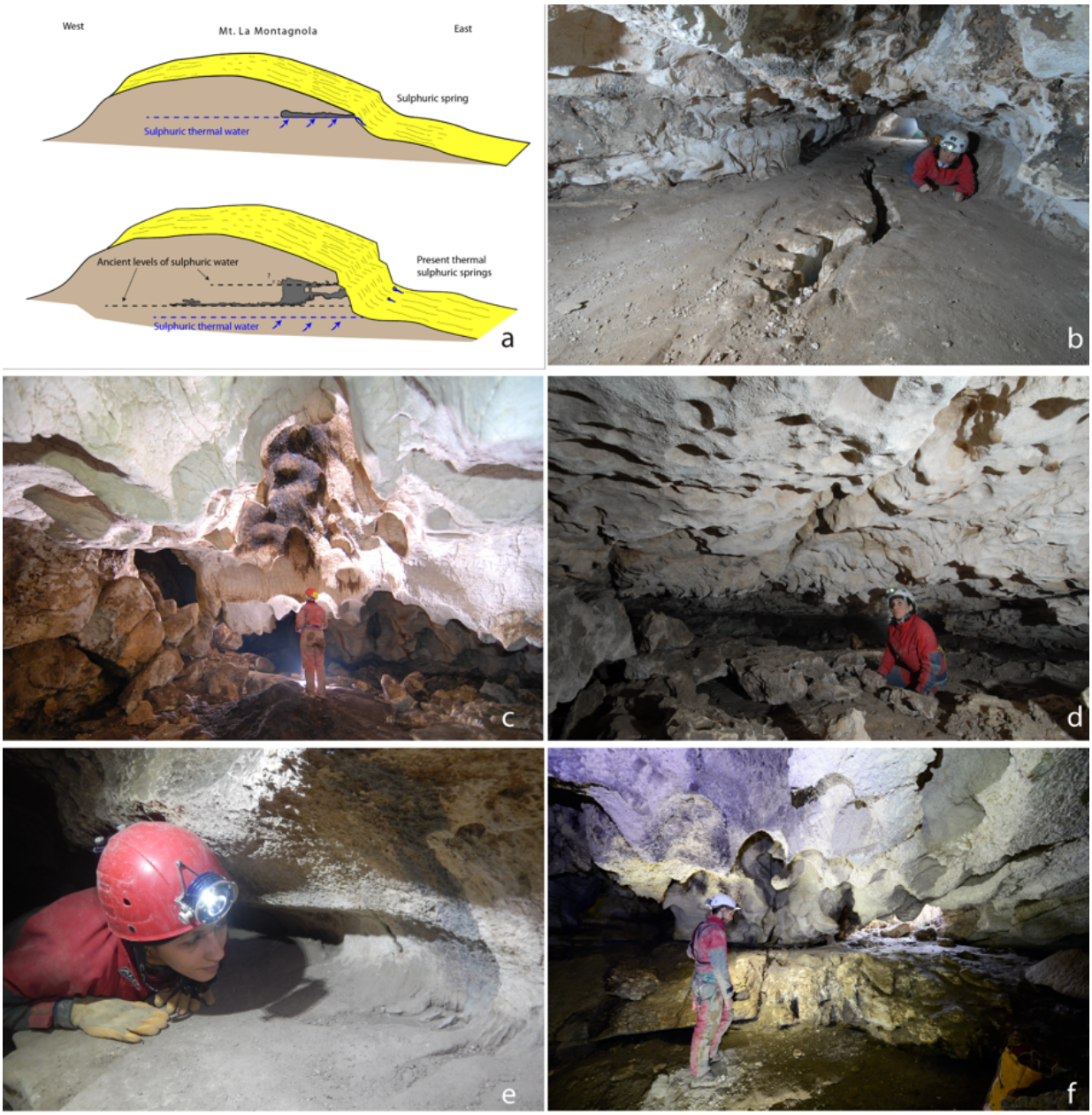

Figure 59. Grotta dell'Acqua Fitusa. A) Sketch of the cave and its evolution due to different stages of base-level lowering; B) Passage with discharge feeder at the floor and different levels of wall convection niches; C) Convection ceiling cupolas in the largest chamber of the cave; D) Room characterized by replacement pockets on the roof; E) Sulfuric karren formed by condensation water film; F) Massive gypsum deposit below cupolas.

7.2.4.4. Grotta dei Personaggi

The Grotta dei Personaggi is located in SW Sicily, south of the Montevago village. The cave is known since the early 1900s and is famous for the archeological findings inside, but it was never surveyed and studied in detail from a geological point of view. The cave opens along a fault scarp in the NW sector of the Magaggiaro Mount and developed in well-bedded white platform limestones (Inici Fm.,

Lower Jurassic) and in nodular or massive reddish to brown pelagic limestones with ammonites (Buccheri Fm., Upper-Lower Jurassic) of the Saccense Domain (Di Stefano et al., 2013). Thermal springs, characterized by chloride-sulfate alkaline-earth waters with an average temperature of 39.2°C (Grassa et al., 2006) are located about 3 km NW of the cavity.

The cave consists of sub-horizontal passages that follow bedding and fault planes oriented in the NNE-SSW, NE-SW and NW-SE directions forming a maze pattern. In many sectors of the cave cupolas develop upward in a dendritic pattern of stacked spheres. The cave shows a total length of roughly 1.7 km, a highest point at +15 m and a depth of - 32 m. It is characterized by morphologies linked mainly to condensation-corrosion processes by convective airflow. Deep feeders guided by the main joints and fault planes (*Figure 60*A), and vents connecting levels of galleries occur in several sectors of the cave. Megascallops and cupolas (*Figure 60*B) are found in all the passages; big cupolas develop mainly on the pelagic limestone where they sometimes stack upward forming vertical passages. Condensation-corrosion channels often associated with cupolas are widespread. Pillars, blades and thin partitions preserved from condensation-corrosion separate different passages located at different levels or along the same level (*Figure 60*B,C). Limestone on the walls and roof is weathered, whereas boxwork occur on the upper portions of the walls.

In many cases calcite rims and popcorn due to evaporation of condensation waters are located in the lower sides of the corrosion forms such as cupolas, channels, vents, etc. (*Figure 60*C).

The Grotta dei Personaggi hosts a large bat colony (Vattano et al., 2015) responsible for an extensive amount of guano, which influences the cave morphology in several places through condensation-corrosion processes or by chemical corrosion at the guano-rock contact.

The cavity lacks alluvial deposits; on the other hand mineral deposits rich in phosphates, iron, manganese and silica are present (*Figure 60*D). The speleogenetic evolution of the cave after a first phase under phreatic conditions seems to be linked mainly to intensive convective thermal condensation-corrosion processes by acid airflow. Calcite speleothems linked to seepage water are related to a more recent epigenic evolution of the cave.

Figure 60. Grotta dei Personaggi. A) Deep feeder along a fault plane enlarged by condensation-corrosion processes; B) Passage with cupolas interpenetrating upward and partitions in the lower parts; C) Cupolas due to condensation-corrosion and calcite popcorns in their lower part linked to evaporation processes; D) Gallery characterized by megascallop-like forms partially covered by phosphate crusts.

7.2.4.5. Grotta dell'Acqua Mintina

The Grotta dell'Acqua Mintina is located in south-central Sicily and was described by Lugli et al. (2014). It opens in the Messinian Calcare di Base of the Gruppo Gessoso-Solfifero in the brecciated and laminated clastic limestone facies (*Figure 61*A; cf. Manzi et al., 2011), along a valley slope cut by a small stream fed by a sulfur spring.

It is a small horizontal cave in which carbonate walls and ceilings are extensively covered by native sulfur and gypsum. Sulfur occurs as centimeter-thick laminated and microcrystalline speleothems, crystals up to 1 cm long, clouds and popcorn-like speleothems (*Figure 61*B), and dusty crusts covering acicular gypsum crystals. Fibrous and prismatic crystals of gypsum have been recognized (*Figure 61*C; Lugli et al., 2016); they formed in small pools on the floor of the room close to the entrance.

Some morphologies such as wall convection niches due to condensation-corrosion and the large amount of gypsum and native sulfur deposits suggest that the cave is linked to sulfuric acid dissolution of limestone in an oxidizing environment.

Figure 61 Grotta dell'Acqua Mintina. A) Entrance of the cave associated with laminated limestone. B) Native sulfur covering almost completely roof and walls; C) Prismatic gypsum crystals.

7.2.5. Conclusions

The new surveys carried out in several karst systems highlighted that hypogenic caves are very common on the Sicilian Island and that several caves previously considered to be of epigenic origin, are instead connected to the rising of deep thermal water. All the hypogenic caves are developed in carbonate rocks. Most of them are SAS caves and their speleogenetic evolution is strongly influenced by the structural features of the rocks, changes of the water table position, and by significant thermal convective condensation-corrosion processes in aerated environment.

Recently detailed studies started to better understand their morphologies, deposits, environmental features, and their evolution in relation also to the geomorphological evolution of the area in which they develop. New studies are planned to improve knowledge about the origin and characteristics of rising deep fluids and the residence time of deep water in the caves.

Multidisciplinary researches are in progress in the newly presumed hypogenic caves to establish their origin and speleogenetic evolution.

References

Audra, P., D'Antoni-Nobécourt, J.C., Bigot, J.-Y., 2010. Hypogenic caves in France. Speleogenesis and morphology of the cave systems. Bulletin de la Société Géologique de France, 181(4): 327-335.

Avellone, G., Barchi, M.R., Catalano, R., Gasparo Morticelli, M, Sulli, A., 2010. Interference between shallow and deep-seated structures in the Sicilian fold and thrust belt, Italy. Journal of the Geological Society, 167(1):109-126.

Catalano, R., Franchino, A., Merlini, S., Sulli, A., 2000. Central Western Sicily structural setting interpreted from seismic reflection profiles. Memorie della Società Geologica Italiana, 55: 5-16.

Catalano, R., Agate, M., Albanese, C., Avallone, G., Basilone, L., Morticelli, M.G., Gugliotta, G., Sulli, A., Valenti, V., Gibilaro, C., Pierini, S., 2013a. Walking along a crustal profile across the Sicily Fold and Thrust Belt. AAPG International Conference and Exhibition. Post Conference Field Trip Guide. Geological Field Trips, 5 (2.3): 213.

Catalano, R., Valenti, V., Albanese, C., Accaino, F., Sulli, A., Tinivella, U., Gasparo Morticelli, M., Zanolla, C., Giustiniani, M., (2013b) Sicily's fold-thrust belt and slab rollback: The SI.RI.PRO. seismic crustal transect. J Geol Soc 170(3):451-464

De Waele, J., Audra, P., Madonia, G., Vattano, M., Plan, L., D'Angeli, I.M., Bigot, J.Y., Nobécourt, J.C., 2016. Sulfuric acid speleogenesis (SAS)close to the water table: examples from southern France, Austria and Sicily. Geomorphology, 253: 452-467.

Di Stefano, P., Renda, P., Zarcone, G., Nigro, F., Cacciatore, M.S., 2013. Carta geologica d'Italia alla scala 1:50.000 e note illustrative del Foglio 619, Santa Margherita di Belice. Roma: ISPRA, Servizio Geologico d'Italia.

Dongarrà, G., Hauser, S., 1982. Isotopic composition of dissolved sulphate and hydrogen sulphide from some thermal springs of Sicily. Geothermics, 11(3): 193-200.

Galdenzi, S., 2012. Corrosion of limestone tablets in sulfidic ground-water: measurements and speleogenetic implications. International Journal of Speleology, 41(2): 149-159.

Gasparo Morticelli, M., Valenti, V., Catalano, R., Sulli, A., Agate, M., Avallone, G., Albanese, C., Basilone, L., Gugliotta, C., 2015. Deep controls on foreland basin system evolution along the Sicilian fold and thrust belt. Bulletin de la Société Géologique de France, 186: 273-290.

Grassa, F., Capasso, G., Favara, R., Inguaggiato, S., 2006. Chemical and isotopic composition of waters and dissolved gases in some thermal springs of Sicily and adjacent volcanic islands, Italy. Pure Applied Geophysics, 163: 781-807.

Lugli, S., Ruggieri, R., Orsini, R., Smmito, G., 2016. The Acqua Mintina cave: a rare geosite with a sulfur smell. 4th International Symposium on karst in the South Mediterranea area. Karst Geosites, 65-71.

Manzi, V., Lugli, S., Roveri, M., Schreiber, B.C., Gennari, R., 2011. The Messinian "Calcare di Base" (Sicily, Italy) revisited. Geological Society of American Bulletin, 123(1-2): 347-370.

Messana, E., 1994. Il sistema carsico del gruppo montuoso di M. Inici (Castellammare del Golfo, TP). Bollettino delle sedute dell'Accademia Gioenia di Scienze Naturali, 27(348): 547-562.

Monaco, C., Mazzoli, S., Tortorici, L., 1996. Active thrust tectonics in western Sicily (southern Italy): the 1968 Belice earthquake sequence. Terra Nova, 8: 372-381.

Perotti, G., 1994. Kronio - Le stufe di San Calogero e il loro flusso vaporoso. Bollettino delle sedute dell'Accademia Gioenia di Scienze Naturali, 27(348): 435-475.

Plan, L., Tschegg, C., De Waele, J., Spötl, C., 2012. Corrosion morphology and cave wall alteration in an alpine sulfuric acid cave (Kraushöhle, Austria). Geomorphology, 169-170: 45-54.

Vattano, M., Audra, P., Bigot, J.-Y., De Waele, J., Madonia, G., Nobécourt, J.-C, 2012. Acqua Fitusa Cave: an example of inactive water-table sulphuric acid cave in Central Sicily. Rendicontazione Online della Società Geologica Italiana, 21: 637-639.

Vattano, M., Audra, P., Benvenuto, F., Bigot, J.-Y., De Waele, J., Galli, E., Madonia, G., Nobécourt, J.-C., 2013. Hypogenic Caves of Sicily (Southern Italy). In: M., Filippi P., Bosak (Eds.), Proceedings of the 16th International Congress of Speleology, Brno 19-27 July 2013, 3:144-149.

Vattano, M., Scopelliti, G., Fulco, A., Presti, R., Sausa, L., Valenti, P., Di Maggio, C., Lo Valvo, M., Madonia, G., 2015. La Grotta dei Personaggi di Montevago (AG), una nuova segnalazione di cavità ipogenica in Sicilia. In: De Nitto L, Maurano F, Parise M (Eds), Atti del XXII Congresso Nazionale di Speleologia, Pertosa-Auletta (SA), 30/05-02/06/2015. Memorie dell'Istituto Italiano di Speleologia, II(29): 295-300.

THIRD SECTION: LANDSCAPE EVOLUTION

8. TABLETS WEIGHT LOSS

8.1. Introduction

In the 2006, Gabrovšek and Peric state that a basic process as the case of dissolution/corrosion is the core of the geomorphic activity, and the key for the understanding of karst speleogenesis and evolution. In cave, geomorphological changes are slow, invisible (being the rock trasformed into solution) but observable (Prelovšek, 2012).

But, is it really possible to relate present-day morphology and present-day processes with a long evolutionary history? (Prelovšek, 2012).

Present-day dissolution can be measured using three main methodologies: 1) micrometer also known as micro-erosion meter (MEM) (High and Hanna, 1970; Mihevc, 2001) or traversing micro-erosion meter (TMEM) (Furlani et al., 2009), 2) limestone tablets (Gams, 1959; Sweeting, 1979), and 3) hydrochemical method (using solute load and discharge; Pulina and Sauro, 1993; Ford and Williams, 2007). Micrometer measurements have been carried out to evaluate the chemical denudation. The errors related to the methodology strictly depend on temperature changes, materials of the MEM, rock softness, number and care of measurements. Very often the measurement error exceeds the dissolution rate (Spate et al., 1985). Limestone tablet dissolution rate is based on the weight-loss and/or gain during the exposure in cave. The weight loss is calculated using a balance, and it results more precise that micrometer. If the reaction surface is known, it is possible to transform weight loss into metric unit. On the other hands, the hydrogeological method is based on differences of soulte load between input (surface) and output (spring) (Prelovšec, 2012).

As explained in the previous chapters, in sulfuric acid environments the oxidation of H_2S is the most important process inducing speleogenesis. The exposed surface of carbonate rocks, in both aerate and subaqueous conditions, is actively corroded by sulfuric acid (H_2SO_4). In addition, in aerate settings, $CaCO_3$ can be easily replaced by $CaSO_4 \cdot 2H_2O$, the most common SAS by-product, which produces an initial weight gain. The understanding of dissolution-corrosion rate in active SAS environments is a very important issue that can help in evaluating the speleogenetic stages of a cave, and in correlating them with landscape evolution, as demonstrated by previous studies (Galdenzi et al., 1997; Mariani et al., 2007; Galdenzi, 2012) carried out in the Grotta del Fiume at Frasassi.

Italy hosts 25% of the known worldwide SAS caves, and some of them are still-active (*Table 17*). In some of these, especially in those located in southern Italy, dissolution-corrosion rate studies started

at the end of the 2015-beginning of 2016, and will continue for at least other two years (for a total of five whole years), to have a better distribution of weight loss-gain rates.

The SAS environments under investigation are Ninfe Cave (Monte Sellaro in Calabria no.19), Sibarite spa (Cassano allo Ionio in Calabria no. 20), Fetida Cave (Santa Cesarea Terme in Apulia no. 22), and Acqua Fitusa Cave (San Giovanni Gemini in Sicily no.24) (*Figure 50*).

8.2. Materials and methods

Carbonate (limestone and marble) and gypsum tablets, 7x4x1 cm, with a mean initial weight of 74 g, have been realized and placed in the cave atmosphere, underwater (between 10 and 20 cm below the water table), and at the interface zone (*Figure 62*). Two tablets for each lithology, 1) selenitic gypsum (-G), 2) "Istria" limestones (-I), 3) "Carrara" marble (-M), and in the case of Fetida and Acqua Fitusa caves also 4) "Calcare di Altamura Fm." (-C) or "Crisanti Fm." (-B) host rock, were placed in different locations to check their behavior in peculiar dissolution-corrosion conditions (i.e., subaqueous indicated with "w", interface "i", and aerate with "a").

In Fetida Cave, two tablet sections have been arranged in the innermost portion (B1 and B2; in *Figure 33;* in B1, the presence of an active feeder discharging sulfidic waters was observed) of the cavity, where the H_2S degassing is higher with respect to the zone close to the entrances, whereas in *Acqua Fitusa* (*Figure 49*B), Spring no. 3 of Terme Sibarite spa, and Ninfe Cave (*Figure 33*), they have been arranged in a single section of monitoring. In Acqua Fitusa Cave tablets were put in the lower still-active level where the sulfidic water table is currently located (*Figure 62*E). In Terme Sibarite spa, the sulfidic spring has been diverted into a small pool (*Figure 62*B) where it has been possible to set the tablets, and in Ninfe Cave the station has been placed in the innermost zone of the cave (*Figure 62*A). In addition, in the section B2 of Fetida Cave, several tablets in aerate conditions have been arranged horizontally to check for differences in dissolution-corrosion rate as a function of rock orientation in space (horizontale vs. vertical).

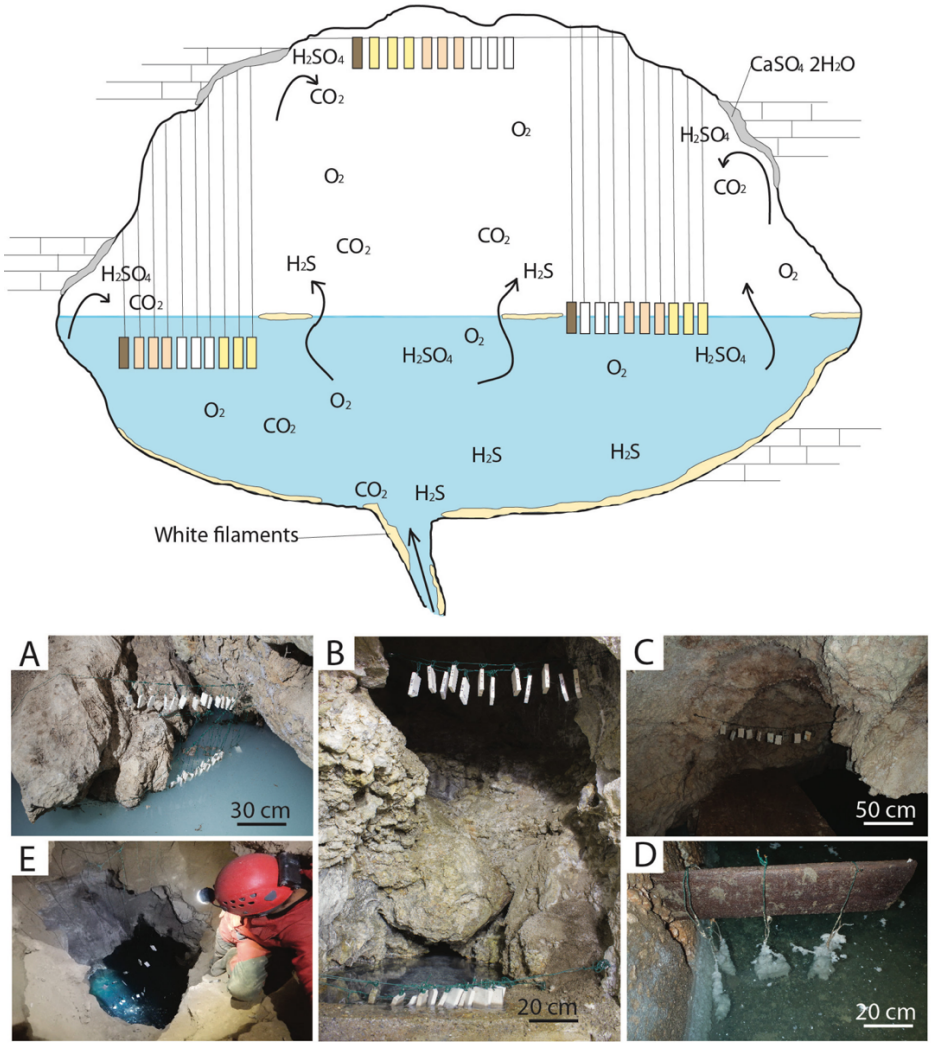

Figure 62. Sketch showing the location of dissolution-corrosion rate measurements. A) Ninfe Cave (Monte Sellaro, Cerchiara di Calabria); B) Spring no. 3, Sibarite spa (Cassano allo Ionio, Calabria), C) Tablets in aerate conditions in Fetida Cave (Santa Cesarea Terme, Apulia); D) Tablets underwater in Fetida Cave (Santa Cesarea Terme, Apulia). The tablets are totally surrounded by water streamers (well-described in chapter 5); E) Tablets in Acqua Fitusa Cave (San Giovanni Gemini, Sicily).

In addition, in these settings both water and air samples have been collected to check for their environmental parameters (water and air). Water parameters (pH, T, EC) were monitored with a Hanna HI991001 instrumentation, and for each section two water samples (250 ml) were collected (one of them was acidified with 65% HNO_3). Water samples were analyzed at the Polytechnic University of Turin, where Na^+, K^+, Mg^{2+} and Ca^{2+} were measured by Atomic Absorption Spectrophotometry (AA-6800 Shimadzu), SO_4^{2-}, Cl^-, F^-, Br^-, PO_4^{3-}, NO_2^-, and NO_3^- with Ionic Chromatography (883 IC Plus Metrohm with high-performance separating column Metrosep A Supp. 5-250), NH_4^+ by Spectrophotometric determination using Indophenol Method (UV-VIS Recording

Spectrophotometer UV-2501 PC Shimadzu), and alkalinity (HCO_3^-) through titration with H_2SO_4 0.5N with automatic control of pH (809 Titrando Metrohm).

Calcite, dolomite, and gypsum saturation indices (SI) were measured using the ratio between ion activity product (K_{IAP}) and solubility products (K_{sp}). Each K_{IAP} has been calculated using the Debye-Hückel equation to determine the ion activity coefficient. SI values close to 1 are indicative of saturated solution at equilibrium, whereas SI values <1 are indicative of undersaturation (i.e., corrosive-dissolutive conditions).

As described in *chapter 4.2*, air monitoring of cave atmosphere, in Apulia and Calabria, was carried out using a MSA Altair4x multigas detector, able to control O_2 (%), CH_4 (%), SO_2 (ppm), and H_2S (ppm). Their resolution is respectively, 0-30 ± 0.1 vol% for O_2, 0-100 ± 1% LEL for CH_4, 0-20 ± 0.1 ppm for SO_2, and 0-200 ± 1 ppm for H_2S (*Table 10*).

In addition, a preliminar experiment has been conducted to observe microscopic features of dissolution-corrosion on the surface of carbonate tablets in underwater conditions. In particular, limestone tablets of "Calcare di Altamura" put in B1 and B2 sections of Fetida Cave for three months, were examined by Field Emission Scanning Electron Microscopy (FESEM). To compare dissolution-corrosion structures a negative control (piece of rock that never was in sulfuric acid environment) has been analyzed. Previously, tablets were washed with ethanol to remove organic matter for morphological evaluation. Finally, the tablets were observed using a FEI TENEO microscope equipped with an Ametek EDAX detector at the University of Seville.

8.3. Results

8.3.1. Environmental parameters

Ludwig-Langelier diagrams showed these SAS underground environments to be dominated by Na-Cl-SO_4 fluids, as the case of Fetida and Acqua Fitusa Cave (*Figure 63*A,B), whereas Calabrian systems (Spring no 3 and Ninfe Cave) have Ca-Cl_2-SO_4 waters (*Figure 63*C,D).

In Fetida Cave the mean recorded pH is 7.13 and temperature 23.7°C, in Acqua Fitusa 7.8 and 21°C, in the spring no. 3 of Terme Sibarite spa the respective values are 7.41 and 23°C, in Ninfe Cave 7.14 and 27.4°C.

Saturation indices demonstrated these waters to be understaurated with respect to gypsum, whereas they show peculiar distribution regarding calcite and dolomite saturation (*Figure 64*). The Na-Cl-SO_4 waters seem to be slightly oversaturated with respect to dolomite, whereas the ones from Ninfe Cave are highly oversaturated with respect to calcite.

In general, the concentration of H_2S results (*Table 10*) variable during the time, depending on rising inputs, likely controlled by surface water head (sea and fresh waters). In Fetida Cave (B1 and B2) the

recorded H_2S concentration ranges between 0.60 to 15.40 ppm, in Terme Sibarite spa (SN3) between 0 and 12.8 ppm, and in Ninfe Cave (B) from 0.90 to 32.70 ppm.

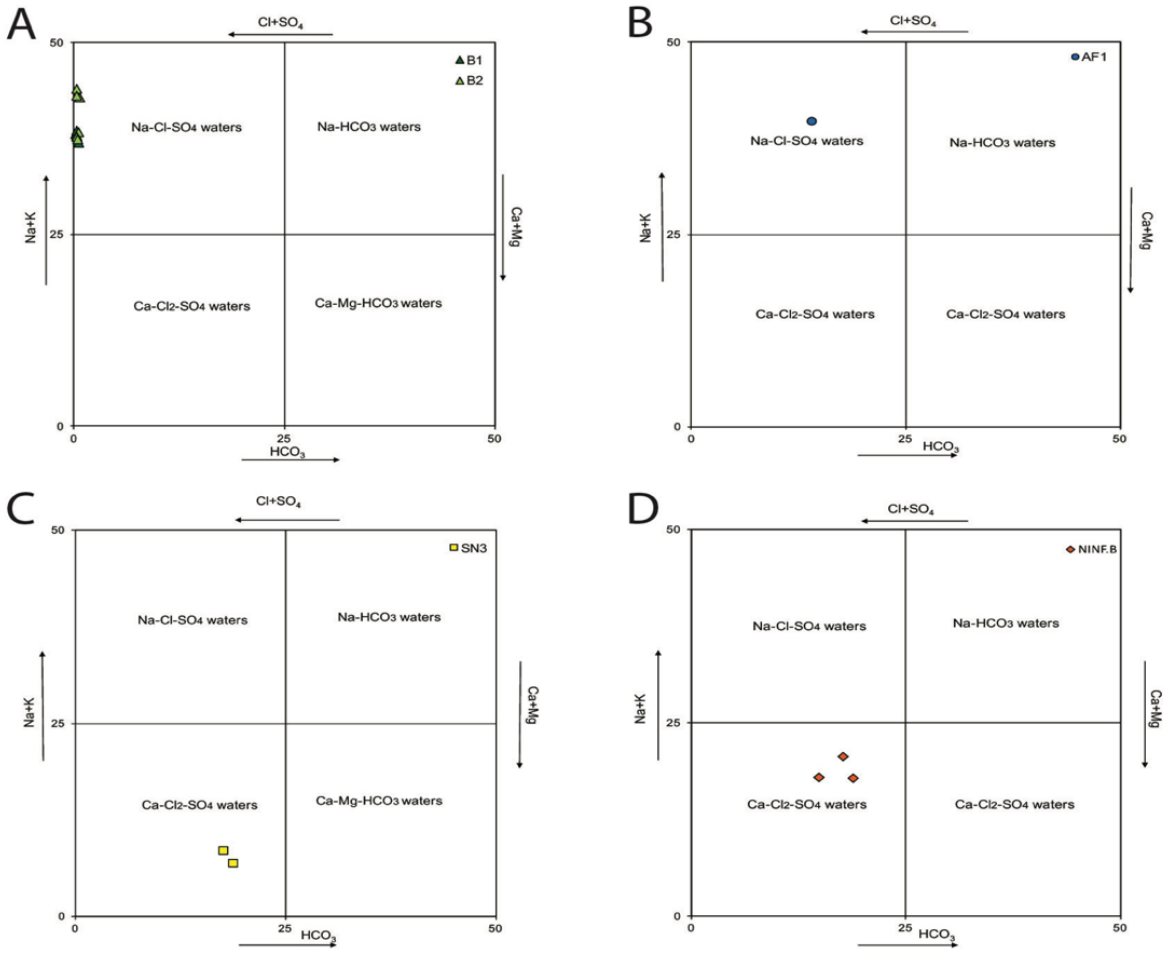

Figure 63. Ludwig-Langelier diagrams for the waters collected in A) Fetida Cave (B1, B2, see Figure 33); B) Acqua Fitusa (AF1); C) Spring no 3 of Terme Sibarite spa (SN3 see Figure 33); D) Ninfe Cave, Mt. Sellaro (NINF.B see Figure 33).

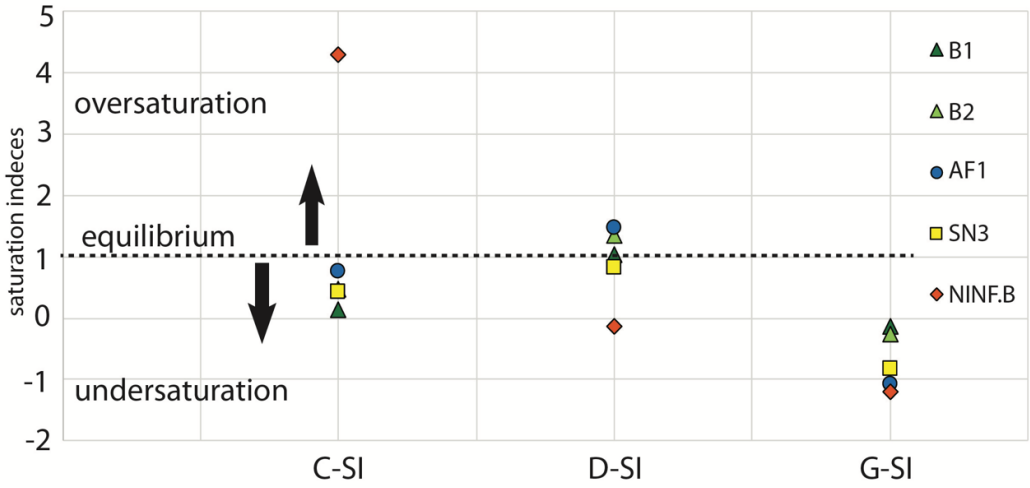

Figure 64. Mean values of calcite (C-SI), dolomite (D-SI), gypsum (G-SI) saturation indices represent the mean values for each sampling site (B1, B2 in Fetida Cave, AF1 in Acqua Fitusa Cave, SN3 in

Terme Sibarite spa, NINF.B in Ninfe Cave). Dashed line is the equilibrium state, the points above indicate oversaturated waters, whereas the ones below are undersaturated. Generally, waters result clearly undersaturated with respect to gypsum (G-SI) and calcite (C-SI), except for NINF.B, which value is close to 4 (oversaturated). Na-Cl-SO_4 waters (B1, B2, and AF1) are slightly oversaturated with respect to dolomite (D-SI).

8.3.2. Weight variation measurements

Gypsum tablets exhibit different dissolution rates as a function of their locations (i.e., subaqueous, interface, aerate conditions). In Fetida Cave (B1-B2) the gypsum placed underwater meanly lost 92% of its initial weight in 33 days, and in the same period 60% at the interface zone. In aerate conditions the dissolution was much slower, in 601 days the mean recorded weight loss was 0.49%.

In the Spring no. 3 (SN3), inside Terme Sibarite spa in 2 days mean values of 59 and 35% were observed, respectively in underwater and interface conditions, whereas in Ninfe Cave (NINF.B) in 10 days the weight loss underwater and at interface zone was 36 and 5%. In the lower spring of *Acqua Fitusa* (AF1) the gypsum tablets underwater were totally dissolved in 40 days; values of 72% and 0.9% of weight loss were monitored at the interface zone and in aerate conditions.

Interesting is the weight variation of carbonates observed in Fetida Cave (*Figure 65*). The dissolution-corrosion in B1 presents higher values with respect to B2, reaching almost 7% of weight loss in 837 days. In B1 dissolution-corrosion underwater is higher in the first period of the monitoring, wherears there is a moment (in the last part of the graph) in which the weight loss at the interface zone seems to proceed faster (especially after 582 days of permanence in cave). In aerate conditions the initial small weight loss rate is followed by weight gain. In B2 the higher values of dissolution-corrosion can be observed at the interface zone, whereas dissolution occurring underwater is quite stable over time. In aerate conditions, the tablets arranged horizontally (Ch) present an initial important weight loss, which is subsequently followed by a weight gain. The general tendency of Ch tablets is similar to Ca, Ma, Ia tablets (where “a” means in aerate conditions), but with a noteworthy contribution of weight loss.

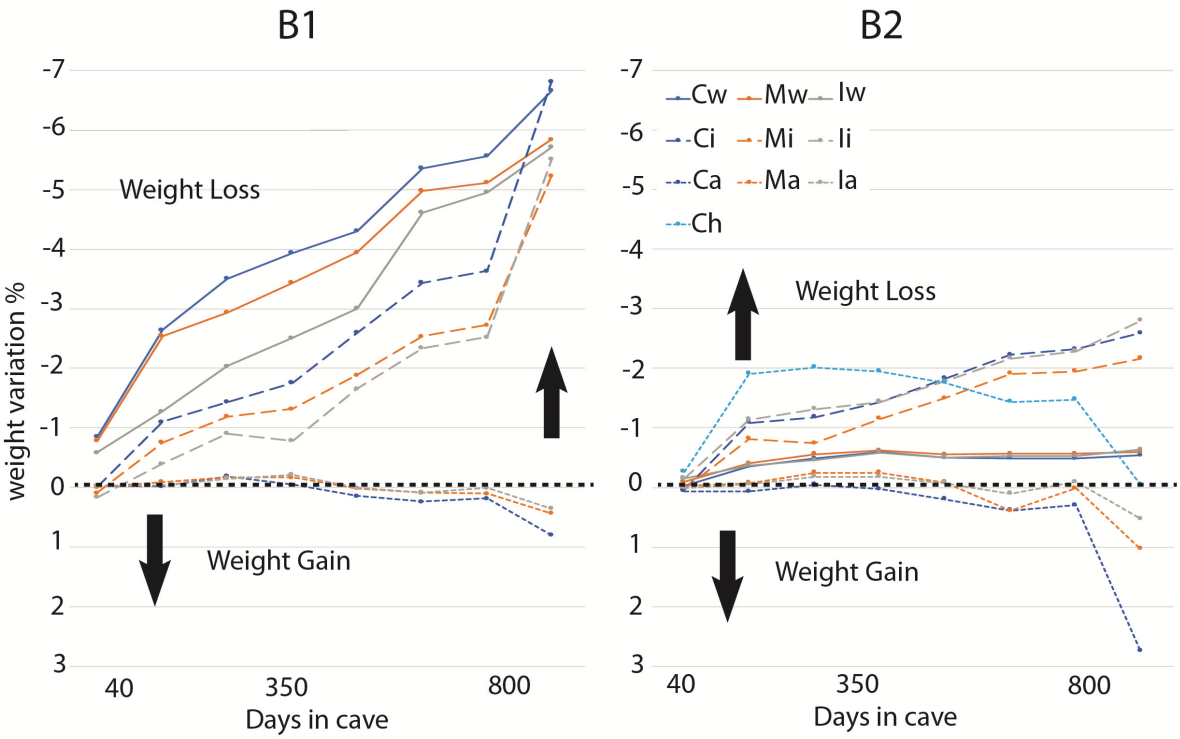

Figure 65. Weight variation (%) of carbonate rocks over time in the two sections of Fetida Cave (B1 and B2). B1 located close to a submerged feeder behaving as a source of rising sulfidic waters, whereas B2 is placed in the innermost zone of the cave. C means "Calcare di Altamura" limestones (host rock), M "Carrara" marble, and I "Istria" limestone, whereas "w" means underwater, "i" means at the interface, and "a" in aerate conditions, and "h" horizontally arranged tablets (it is represented in light blue). Colors and line types helped discriminating different lithologies (blue, orange, grey) and dissolution-corrosion conditions (solid line means underwater, long dashed at the interface zone, dashed in aerate locations).

The weight variation observed in the Spring no. 3 of Terme Sibarite (SN3) demonstrated the higher values of dissolution-corrosion to occur underwater. In Ninfe Cave (NINF.B) the dissolution of "Carrara" marble is higher with respect to "Istria" limestone both underwater and at the interface zone. In *Acqua Fitusa* the "Carrara" marble is the sole lithology able to show a certain degree of dissolution-corrosion, which occurs exclusively at the interface zone (*Figure 66*).

In all these systems, it was difficult to observe weight variation (%) in aerate conditions.

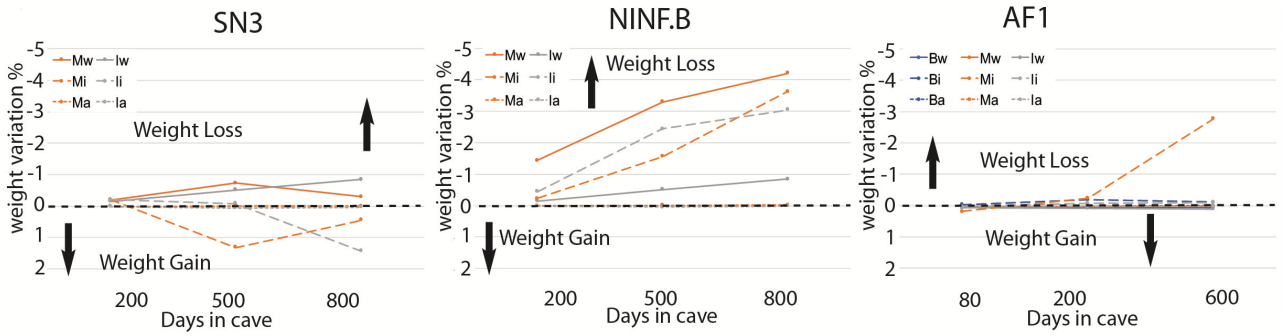

Figure 66. Weight variation (%) of carbonates over time in the Spring no. 3 (SN3) of Terme Sibarite, Ninfe Cave (NINF.B), and Acqua Fitusa Cave (AF1). B means "Crisanti" brecciated limestones (host rock), M "Carrara" marble, and I "Istria" limestone, whereas "w" means underwater, "i" means at the interface, and "a" in aerate conditions. Colors and line types helped discriminating different lithologies (blue, orange, grey) and dissolution-corrosion conditions (solid line means underwater, long dashed at the interface zone, dashed in aerate locations).

8.3.3. Morphological observations

Differently from the negative control (*Figure 67*A), the stone pieces placed in B1 (*Figure 67*B) and B2 exhibit typical dissolution-corrosion features, that in B2 (*Figure 67*C,D,E,F) are magnified. The rock shows a clear decayed surface, likely corroded by the pure interaction between limestone and sulfuric acid or enhanced by the presence of microbial organisms in the form of water streamers (*Figure 62*D).

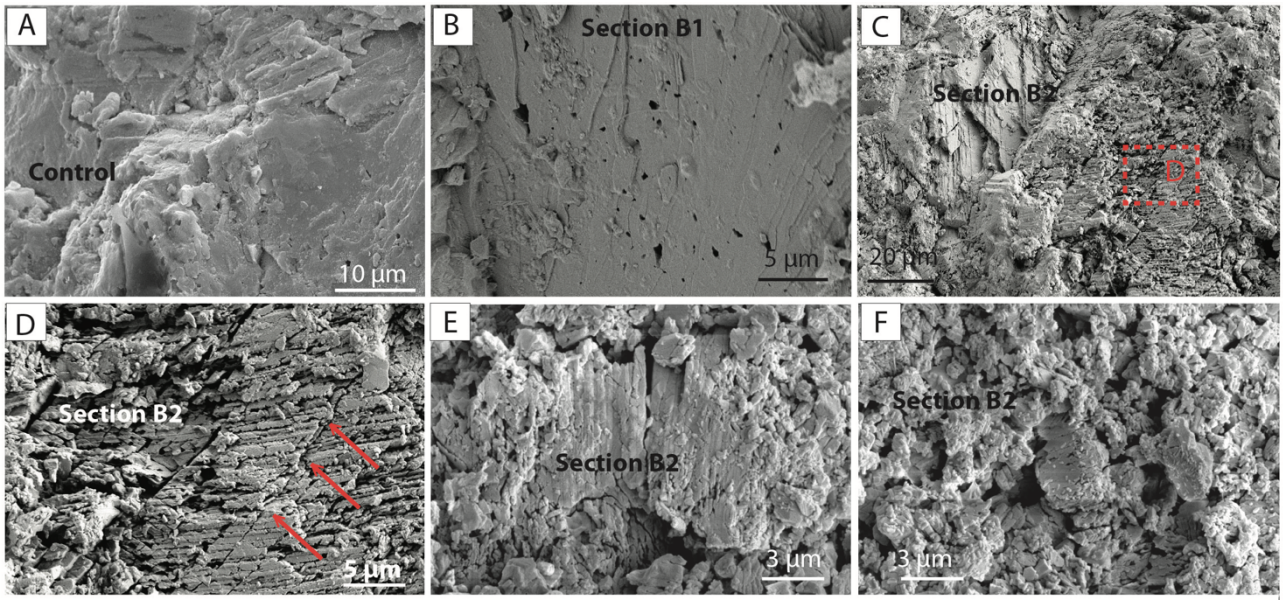

Figure 67. Dissolution-corrosion features observed on "Calcare di Altamura" limestone tablets put underwater in Fetida Cave. A) Limestone control used for comparison with tabltes that were in sulfidic waters; B) Tablets that was in B1; C, D, E, F) Tablets that were in B2, where it is possible to see clear structures of dissolution-corrosion. The rock surface seems to be intensely corroded.

8.4. Discussion and conclusions

Dissolution-corrosion measurements showed interesting results, and demonstrated environmental parameters to be essential controls in weight loss/gain rate. In general, gypsum tablets in underwater and interface conditions are easily dissolved, essentially due to the undersaturation of these fluids with respect to gypsum. As a matter of fact, the weight loss for gypsum tablets in aerate conditions is abundantly lower.

At the Calabrian and Sicilian sites, the dissolution-corrosion rate seems to be controlled by lithologies, in fact, in all these locations weight loss is favored in marble tablets. In the Spring no. 3 of Terme Sibarite and Ninfe Cave, the dissolution-corrosion is fastest at underwater conditions, whereas in Acqua Fitusa caves dissolution is faster in the interface zone.

Detailed studies have been carried out in Fetida Cave and demonstrate the dissolution-corrosion to behave differently being a function of the vicinity to rising sulfidic waters. Here, weight loss reached a mean value of 7% close to the zone of active rising sulfidic waters (B1). At the beginning the dissolution-corrosion was faster in underwater conditions, whereas during the last period of monitoring (after 582 days of permanence in cave) the dissolution at the interface zone increased, sometimes even greater than the rate observed in subaqueous conditions (*Figure 65*). Differently in B2, the innermost portion of Fetida Cave, the major dissolution-corrosion rate has been found at the interface zone. FESEM investigations, carried out on tablets that were placed underwater for three months in B1 and B2 display different degrees of dissolution-corrosion dominated by decayed structures, likely influenced by the behavior observed during weight loss monitoring.

In general, in aerate conditions is possible to observe an initial weight loss subsequently followed by weight increase. This behavior is due to the reaction of the external surface of tablets with degassing H_2S, which immediately oxidizes and transforms into sulfuric acid (H_2SO_4), producing weight loss. The subsequent replacement of $CaCO_3$ (on the tablet surface) with $CaSO_4 \cdot 2H_2O$ induces an increase in the weight. Interesting is the amount of weight loss observed on the horizontally arranged tablets. The weight loss rate in this case is quite high, and has been amplified by the fall of acidic (pH 0-1) moonmilk deposits on their upper surface. After removing moonmilk, their weight variation followed the same tendency of the other tablets in aerate conditions.

Galdenzi et al. (1997) tried to estimate the weight loss of limestone tablets placed in subaqueous conditions in Frasassi caves. The values proposed ranged between -15 to -20 mg/cm^2 per year. In *Table 22* it is possible to observe the mean values of weight loss calculated on a surface of 7x4 cm^2 during a whole year in Fetida, Acqua Fitusa, Spring no. 3, and Ninfe Cave. The highest values of dissolution-corrosion (weight loss) occurred in subaqueous and interface conditions in the proximity of the feeder (B1). The marble tablets placed in Ninfe Cave showed comparable results. On the

contrary, the higher values of weight gain due to the precipitation of secondary gypsum has been documented in aerate condition along the section B2 (*Table 22*) where the deposition of secondary gypsum is very fast.

Table 22. Values of weight loss/gain calculated on the surface (7x4 cm) in a year, in the two sections (B1 and B2) of Fetida Cave, in Acqua Fitusa Cave (AF1), in the Spring no. 3 (SN3) of Terme Sibarite, and in Ninfe Cave (NINF.B). Negative values indicate weight loss, whereas positive weight gain.

Locations	Lithologies	Underwater	Interface	Air
		mg/cm^2 per year	mg/cm^2 per year	mg/cm^2 per year
B2	C	-6.49	-26.89	+28.62
	M	-6.95	-23.71	+11.33
	I	-6.04	-33.31	+6.49
B1	C	-84.10	-79.27	+8.88
	M	-64.01	-63.31	+4.75
	I	-75.77	-72.03	+4.28
AF1	B	+1.11	-1.56	+0.11
	M	+0.56	-44.79	+0.22
	I	+2.12	-1.45	+0.22
SN3	M	-4.62	+7.03	0
	I	-13.16	+22.46	+0.68
NINF.B	M	-66.01	-56.77	-0.22
	I	-9.05	-47.65	+0.20

An interesting test study with limestone tablets has been performed in Slovenian epigene caves. Here, tablets were attached to cave walls and exposed to low and high water level. As documented by Prelovšek (2009), the prevailing process was dissolution. The mean dissolution rate was estimated to be 7.4 μm/a (calculated using the equation $D = \frac{\Delta m}{\rho A t}$ where D is the dissolution rate, Δm change in weight, density of limestone, A exposed surface, t time).

Using the same equation, I observed higher values of dissolution-corrosion rate. As a matter of fact, taking in account the case of Fetida Cave, the dissolution rate, in underwater conditions, ranges from 25.8 to 90.3 mm/a in B2 (depending on lithologies; i.e. 25.8 mm/a for Calcare di Altamura, 26.2 mm/a for marble, 90.3 mm/a for Istria limestone), and from 234.1 to 293.1 mm/a in B1 (293.1 mm/a Calcare di Altamura, 234.1 marble, and 279.3 Istria limestone).

These results are significant, and demonstrate hypogene sulfuric acid to produce rapid dissolution-corrosion signatures, in comparison to epigene settings, and evident weight loss also in less than three years. Nevertheless, five years of monitoring are necessary to better understand the behavior of these interesting systems and to estimate how fast has been/will be the speleogenesis of these cave systems and compare them with the other well studied SAS caves of the world.

References

Ford, D., Williams, P., 2007. Karst Hydrogeology and Geomorphology. John Wiley & Sons: 562 pp.

Furlani, S., Cucchi, F., Forti, F., Rossi, A., 2009. Comparison between coastal and inland karst limestone lowering rates in the northeastern Adraitic Region (Italy and Croatia). Geomorphology, 104: 73-81.

Gabrovšek, F., Peric, B., 2006. Monitoring the flood pulses in the epiphreatic zone of karst aquifers. Acta Carsologica, 35(1): 35-45.

Galdenzi, S. 2012. Corrosion of limestone tablets in sulfidic ground-water: measurements and speleogenetic implications. International Journal of Speleology, 41(3):149-159.

Galdenzi, S., Menichetti, M., Forti, P., 1997. La corrosione di placchette calcaree ad opera di acque sulfuree: dati sperimentali in ambiente ipogeo. In: P.Y., Jeannin (Ed), Proceedings of the12th International Congress of Speleology, La Chaux-de-Fonds, 1: 187-190.

Gam, 1959. Poskus s ploščicami v Podpeški jami. Naše jame, 1(2): 76-77.

High, C.J., Hanna, K., 1970. A method for the sirect measurement of erosion on rock surfaces. British Geomorphological Research Group, Technical Bulletin 5.

Mariani, S., Mainiero, M., Barchi, M., van der Borg, K., Vonhof, H., Montanari, A., 2007. Use of the speleogenetic data to evaluate Holocene uplifting and tilting: an example from the Frasassi anticline (northeastern Apennines, Italy). Earth Planetary Science Letters, 257(1-2): 313-328.

Mihevc, A., 2001. Speleogeneza Divaškega krasa (The speleogenesis of the Divača karst). Zalozba ZRC, Ljubljana: 148 pp.

Pulina, M. Sauro, U., 1993. Modello dell'erosione chimica potenziale di rocce carbonatiche in Italia. Memorie della Società Geologica Italiana: 313-323.

Prelovšek, M., 2009. Present-day Speleogenetic Processes, Factors and Features in the Epiphreatic Zone. PhD Thesis, University of Nova Gorica: 297.

Prelovšek, M., 2012. The dynamics of the present-day speleogenetic processes in the stream caves of Slovenia. Carsologia, 15: 152 pp.

Spate, A.P., Jannings, J.N., Smith, D.I., Greenaway, M.A., 1985. The micro-erosion meter, British Geomorphological Research Group, Technical Bulletin 29: 3-17.

Sweeting, M.M., 1979. Solution and erosion in the karst of the Melinau limestone in Gunung Mulu national park, Sarawak, Borneo. In: Proceedings of the 4th International Congress of Speleology in Yugoslavia. Lubljana: 227-232.

9. SUBHORIZONTAL SAS CAVE LEVELS AS INDICATOR OF UPLIFT AND EROSION RATE

9.1. Article 7

Accepted in Geomorphology

Sulfuric acid speleogenesis in the Majella Massif (Abruzzo, Central Apennines, Italy)

Ilenia M. D'Angeli[1*], Maria Nagostinis[1], Cristina Carbone[2], Stefano M. Bernasconi[3], Victor J. Polyak[4], Lisa Peters[5], William C. McIntosh[5], Jo De Waele[1]

[1] Department of Biological, Geological and Environmental Sciences, University of Bologna, Italy, dangeli.ilenia89@gmail.com; maria.nagostinis@gmail.com; jo.dewaele@unibo.it

[2] Department of Geological, Environmental and Biological Sciences, University of Genoa, Italy, carbone@dipteris.unige.it

[3] ETH Zurich, Geological Institute, Soneggstrasse 5, 8092 Zurich, Switzerland, stefano.bernasconi@erdw.ethz.ch

[4] Department of Earth & Planetary Sciences, University of New Mexico, Albuquerque, New Mexico 87131, USA, polyak@unm.edu

[5]Department of Earth and Environmental Science, New Mexico Institute of Mining and Mineral Resources, Socorro, New Mexico 87801, lisa.peters@nmt.edu; william.mcintosh@nmt.edu

[*]Corrisponding author

9.1.1. Abstract

Many active and inactive hypogene sulfuric acid cave systems are known along the Apennines, Italy. The Cavallone-Bove cave system is located in the external part of the central Apennine Chain, in the Majella Massif, and opens at 1470 m asl along the Taranta Gorge (South of Chieti). The presence in these caves of peculiar geomorphological features, such as feeders, rising channels, megacusps, cupolas, and replacement pockets, offers evidence of rising acidic fluids. The secondary mineral deposits, including meter-size white gypsum deposits, alunite, jarosite, black layers of iron-manganese oxides and hydroxides, along with a rare association of authigenic rutile-ilmenite minerals indicate a sulfuric acid origin. Stable isotope analyses of sulfates further confirm a sulfuric acid speleogenetic (SAS) origin of these minerals and, in general, of the whole cave system, with H_2S coming from the bacterial sulfate reduction of deep-seated Triassic evaporites interacting with hydrocarbons. Alunite dating demonstrates this water table SAS cave to have been active at least until 1.52±0.28 Ma. All the evidence suggests that Cavallone-Bove is an ancient sulfuric acid karst system

that was uplifted <1 km above pre-existing base level. The age of speleogenesis further suggests that tectonic uplift of this area was as high as 670 m My^{-1} over the last 1.5 Ma.

Keywords: Rising waters, hypogene karst, alunite dating, mountain uplift, valley incision rate

9.1.2. Introduction

Since the first description of the role of sulfuric acid in the genesis of caves in the thermal spring area of Aix-les-Bains (SE France) by Socquet (1801), many years passed before researchers realized the importance of this strong acid in the formation of certain caves. In central Italy, during the construction of an artificial tunnel for the exploitation of thermal waters at Triponzo (southern Umbria), a small cave in which sulfuric waters actively dissolved the limestone was intercepted (Principi, 1931). Morehouse (1968), describing Lower Crevice Cave (Iowa, USA) is the first modern karstologist highlighting the importance of sulfide oxidation, and subsequent formation of sulfuric acid, in cave development. This appeared to be a very localized phenomenon, but the PhD work of his student Egemeier (1973) in Lower and Upper Kane caves in Wyoming (USA) showed these caves to exist also in absence of sulfide ores. These small caves are the first active sulfuric acid speleogenesis (SAS) caves to be studied in great detail (Egemeier, 1981, 1987), and the presence of H_2S appears to be explained by the reduction of sulfate beds in petroleum-rich areas in the stratigraphic sequence. Egemeier (1971) was also among the first along with Jagnow (1977, 1978, 1979, 1986), to suggest the sulfuric acid origin of the large rooms of Carlsbad Caverns, and many other caves in the Guadalupe Mountains (New Mexico, USA). The sulfuric acid theory for the formation of the Guadalupe Mountains cave systems, based on the reduction of sulfates of the Castile Formation interacting with rising hydrocarbon fluids, was validated by stable isotope measurements (very negative $\delta^{34}S$ values) on replacement gypsum (Davis, 1980; Hill, 1981; Kirkland, 1982). The Guadalupe Mountain caves became the basis for the general sulfuric acid speleogenesis model, which was developed in many studies (Hill, 1987, 1990, 2000; Jagnow et al., 2000; DuChene, 2000; Kirkland, 2014; DuChene et al., 2017).

Today, many active sulfuric acid caves are known, the most important and well-known of which are Cueva de Villa Luz and neighboring caves in Tabasco, Mexico (Hose and Pisarowicz, 1999; Hose et al., 2000; Hose and Rosales-Lagarde, 2017), Movile Cave in Romania (Sârbu and Kane, 1995; Sârbu et al., 1996), Chevalley Aven and Serpents Cave in southern France (Audra et al., 2007), Rhar es Skhoun and other caves in the Biban area in Algeria (Collignon, 1983), several caves in the Cerna Valley in Romania (Wynn et al., 2010, Onac et al., 2009, 2011; Onac and Drăguşin, 2017), and several karst systems in Italy (Galdenzi and Menichetti, 1995; De Waele et al., 2014) such as Frasassi caves (Galdenzi et al., 2008; Galdenzi, 2012; Galdenzi and Jones, 2017), Acquasanta Terme in the Marche

(Galdenzi et al., 2010; Galdenzi, 2017), Montecchio Cave in Tuscany (Piccini et al., 2015), different caves in Calabria (Galdenzi, 1997; Galdenzi and Maruoka, 2019) and Santa Cesarea Terme in Apulia (D'Angeli et al., 2017, 2018).

Whereas the identification of active SAS systems is quite straightforward, because of the presence of sulfide-rich waters, inactive SAS caves can be less easy to identify. This is especially true for old caves, in which different epigenic and condensation-corrosion processes have masked or erased the original fingerprints of SAS. However, SAS caves have preserved some unique morphological and mineralogical characteristics that can allow speleologists to identify this type of speleogenesis. In this way, over the last decades, many cave systems previously thought to be of normal meteoric origin have been identified as sulfuric acid caves: good examples are Kraushöhle in Austria (Plan et al., 2012), Al-Daher Cave in Jordan (Kempe et al., 2006) and Provalata Cave in Macedonia (Temovski et al., 2013, 2018; Temovski, 2017) just to name a few. Especially in the Italian Apennines such caves have been recognized since the mid 1990s, including famous cave systems such as La Grotta and Faggeto Tondo in Monte Cucco (Galdenzi and Menichetti, 1995, 2017; Galdenzi, 2004). More recently several sulfuric acid caves have also been found in Sicily (Vattano et al., 2017), such as the Acqua Fitusa (De Waele et al., 2016) and Acqua Mintina Cave (D'Angeli et al., 2018).

In this paper, we describe an inactive SAS system located in the Majella Massif, that includes two adjacent cavities: the Cavallone and Bove caves. The aim of our paper was to clearly demonstrate the sulfuric acid origin of these caves based on the discovery of typical weathering products derived from the interaction of sulfuric acid with the host rock, the few morphological evidences still preserved on the cave walls, and the geochemical fingerprints of SAS such as stable isotopes. Our geomorphological, mineralogical and geochemical evidence clearly point to their origin at the former water table by rising sulfidic fluids. Dating of speleogenetic alunite in Cavallone Cave constrains the age of speleogenesis, and allows some conclusions to be drawn regarding the evolution of the Cavallone-Bove cave system in this rapidly uplifting mountain area.

9.1.3. Geographical and Geological setting

Cavallone-Bove cave system opens along the central-southern Apennine Chain, in the Majella Massif (Abruzzo) (*Figure 68*), south of Chieti. The Majella Mt. is bordered to the northeast by the Pescara River valley, and to the south by the Sangro River valley. The central part of this mountain hosts several peaks of over 2000 m asl. Cavallone and Bove entrances are located respectively at 1475 m and 1460 m asl on the hydrographic left side of the Taranta Gorge, an important NW–SE-trending steeply walled canyon developed along the southeast flank of Majella (*Figure 69*), perpendicular to the Aventino Gorge (NE-SW). Both caves are shared between the municipalities of Taranta Peligna

and Lama dei Peligni, located in the hydrographic basin of the Aventino River, which currently flows at around 450 m asl in Taranta Peligna village (*Figure 68*).

The Cavallone Cave is open to public since 1894, and from the late 1930s visitors were brought close to the entrance (and back down) from the villages below using wooden sleighs pulled by the guides (Cerruti et al., 1946). From here (and from the end of the cable car line) a small, gently rising path, followed by 300 stairs carved in the rock, allow access to the entrance of Cavallone Cave. Since 1978 tourists can get to the cave using a cableway (with open cabs) located at 767 m asl to overcome the 1000 meters of elevation difference between the Taranta Peligna village and the Cavallone Cave entrance.

From a geological point of view, the Majella Massif is the most external (eastern) portion of the central-southern Apennine Chain. It was formed during the Middle Pliocene-Lower Pleistocene and represents an asymmetric gentle anticline with a NW-SE oriented axis in its northern part, becoming N-S in its central portion, and NE-SW in the south (*Figure 68*). It is cut to the W by the Caramanico Fault, which dips to the W and is directed N-S/NW-SE (Pizzi, 2003; Brandano et al., 2012). The origin of this anticline can be explained by the formation of a frontal thrust, covered by Mio-Pliocene deposits (Scisciani et al., 2002; Patacca and Scandone, 2007). The whole area was affected by two important uplift and erosional phases, the first occurred during the Lower-Upper Pliocene, during which the overthrusting and folding took place, the second was a general uplift with a rate 0.3-1.0 mm y^{-1} (Pizzi, 2003).

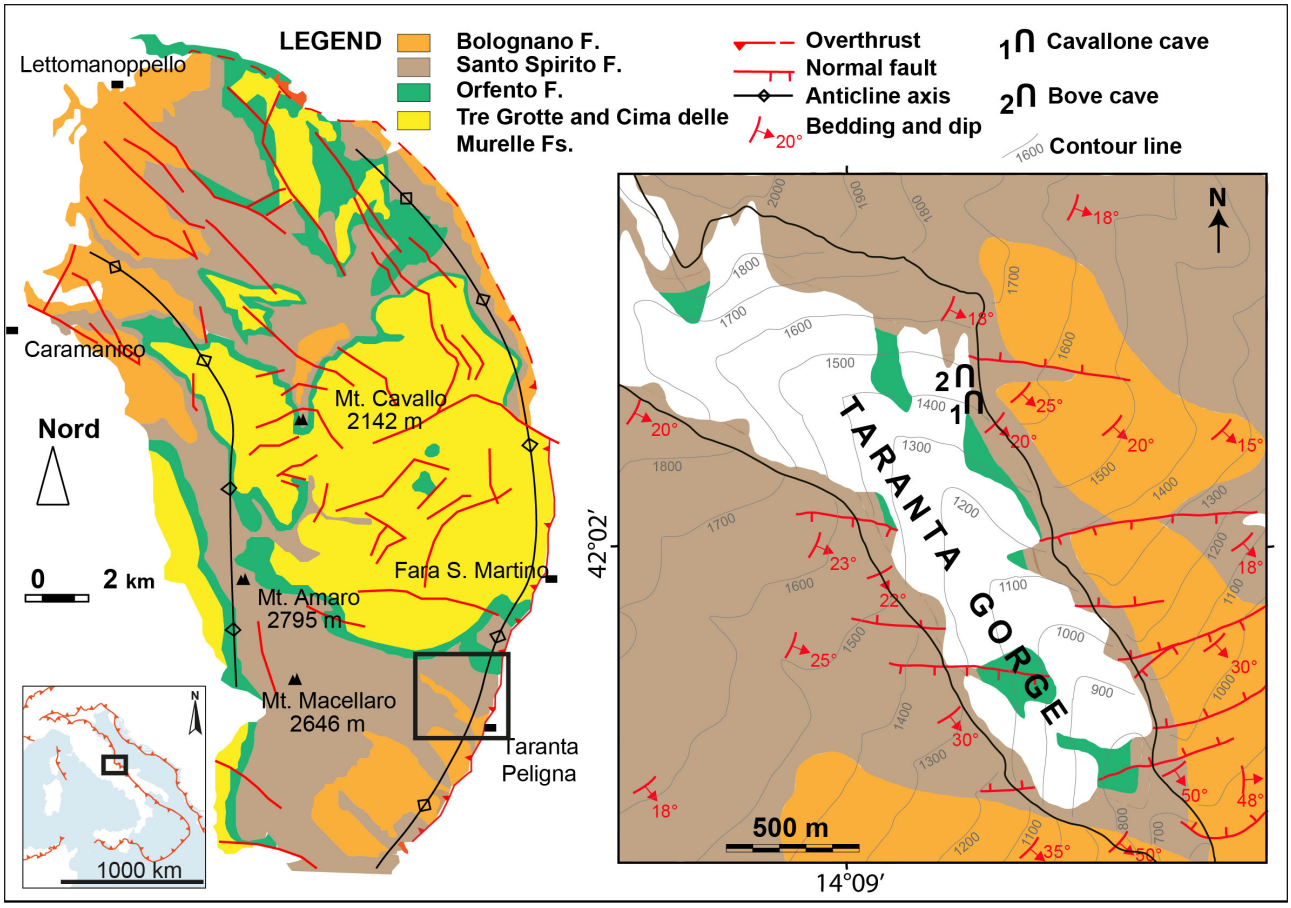

Figure 68. Geographical and geological setting of the study area. Left: general geological scheme of the Majella Massif (modified from Aydin et al., 2010); Right: Detailed simplified geological map of the Taranta Gorge (modified from Festa et al., 2014).

The Majella Massif is characterized by carbonate rocks of deep and shallow waters of Cretaceous to Miocene age. These represent the entire geodynamic evolution of the Apennines, from the final rift phases of the Tethys during the Lower Cretaceous, over the inversion of the stress field preceding the closure of the Alpine Tethys (Upper Cretaceous-Tertiary), up to the final formation of the Central Apennines during the Plio-Pleistocene (Brandano et al., 2012, 2016). This sedimentary sequence overlies Triassic evaporites and dolostones (Burano Formation) and is intersected by the typical Apennine and anti-Apennine faults, with N-S, NE-SW, and NW-SE directions.

Along the Taranta Gorge carbonate rocks of Upper Cretaceous–upper Miocene are exposed and are affected by E–W pre-thrusting conjugate normal fault systems (Festa et al., 2014) (*Figure 68*). The limestone beds dip 20° to the southeast close to the entrance of Cavallone Cave, and become steeper going southeastwards (up to 30°). The following formations (from the oldest to the youngest) crop out along the northeastern flank of Taranta Gorge (where both caves are located) (Festa et al., 2014): Orfento Formation (Maastrichtian), composed of massively bedded biocalcarenites and whitish

calcirudites with rudists; Alveolina limestones (Middle Paleocene-Middle Eocene), a chert-containing whitish calcilutite with some calcareous turbidite levels; Santo Spirito Formation nummulitic limestones (Upper Eocene-Lower Oligocene), a porous whitish-yellowish calcarenite with chert; Bryozoan limestones and *Orbulina* marls (Burdigalian-Tortonian), a calcarenite grading into a marly limestone in its uppermost parts; and Bolognano Formation limestones with *Lithothamnium* grading into more marly horizons at the top (Tortonian-Lower Messinian).

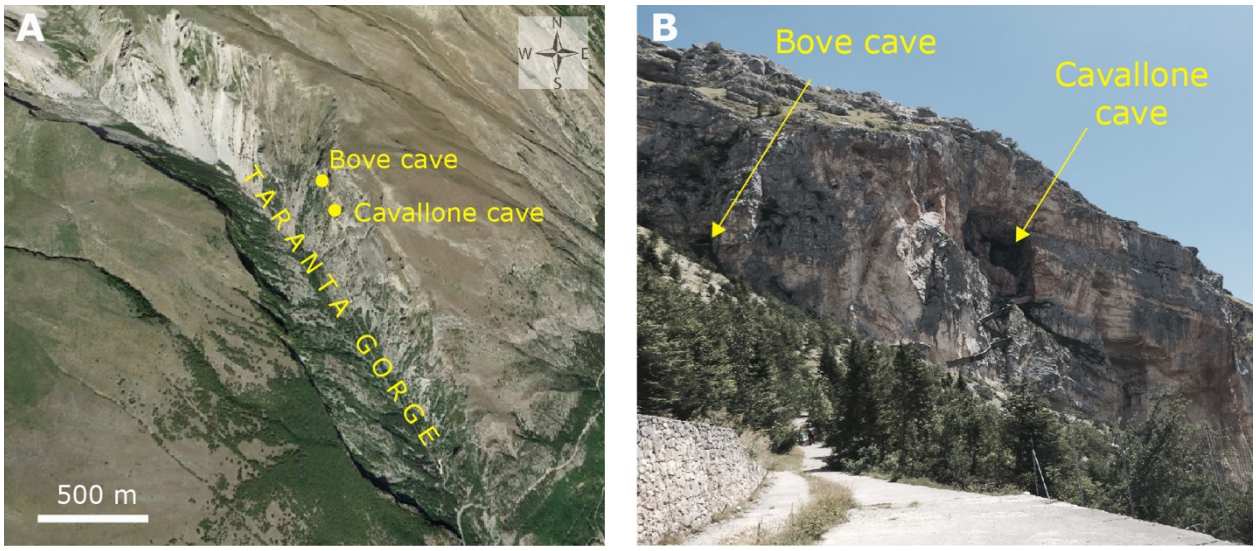

Figure 69. Location of the Cavallone and Bove caves. A) the Taranta Gorge (from Google Earth); B) View of the eastern flank of the gorge with the two cave entrances.

9.1.4. Methods

9.1.4.1. Field surveys and sampling

The morphology of Cavallone and Bove caves was investigated in order to recognize dissolution-corrosion features due to SAS and to precisely locate the secondary mineral deposits. Visits took place using speleological equipment and a geological compass, whereas sampling was carried out using hammer and chisel, and a 10x handheld lens. Each sampling site and each sample were documented with photographs using flashes and Scurion© headlamps. Sampling sites were accurately reported on cave maps, based on speleological surveys by Speleo Club Chieti.

We collected 38 mineralogical samples in the underground system (21 in Cavallone and 17 in Bove). To understand the possible origin of sulfur in the caves 7 samples of bitumen and secondary gypsum were taken in three abandoned mines in the W-Majella Massif (*Table 23*), whereas 2 gypsum bedrock samples were also taken, representing Messinian (from Sicily), and Triassic evaporites (from the Pietre Nere locality, near Gargano, 95 km East of our study area).

9.1.4.2. Mineralogy

Samples were dried and then ground and reduced to an ultrafine powder using an agate mortar. All the 47 samples were analyzed using a Philips PW3710 diffractometer (Co tube: λ=1.78901Å, 20 mA, 40 kV, 3° to 80° 2θ with a step size of 0.02°, analysis time 1 sec per point), and 21 of these, coated with graphite, have been observed using a VEGA3-TESCAN type LMU Scanning Electron Microscope (SEM) provided with an Energy Dispersive X-ray Analysis (EDS) detector (APOLLO XSDD, EDAX) at the University of Genoa. Results are reported in Table 1. A sample of relatively pure alunite was sent to the University of New Mexico, Albuquerque (USA), where it was processed for dating.

9.1.4.3. Stable isotopes

Twenty-six samples of sulfates (17 from the Cavallone and Bove caves, 2 gypsum bedrocks, 7 from the abandoned mines in the W-Majella Massif) were analyzed for sulfur stable isotopes at the ETH Zurich (*Table 23*). The samples were wrapped in tin capsules with V_2O_5 and converted into SO_2 in a Thermo Fisher Flash-EA 1112 coupled with a Conflo IV, interfaced to a Thermo Fisher Delta V Isotope Ratio Mass Spectrometer (IRMS). Isotope ratios are reported in the conventional δ-notation with respect to V-CDT (Vienna Cañon Diablo Troilite), where

$$\delta^{34}S\text{sample-CDT} = [(^{34}S/^{32}S)\text{sample} / (^{34}S/^{32}S)\text{CDT} -1]\ 1000‰.$$

The method was calibrated with the reference materials NBS 127 ($\delta^{34}S$ = +21.1‰), IAEA SO-5 ($\delta^{34}S$ = +0.5‰) and IAEA SO-6 ($\delta^{34}S$ = -34.1‰). Measurement reproducibility based on the repeated analysis of an internal standard was better than 0.3‰.

9.1.4.4. Radiometric dating of alunite

One sample of alunite (CAV2) was treated with HF (to recover pure alunite) and analyzed using the $^{40}Ar/^{39}Ar$ method at the New Mexico Tech Argon Geochronology Laboratory. Minerals were separated with a standard heavy liquid, Franz Magnetic and hand-picking techniques. The provided sample was loaded into aluminum discs and irradiated for 8 hours at the USGS TRIGA reactor in Denver Colorado, and then, it was exposed to neutron flux monitor (Fish Canyon Tuff sanidine, with an assigned age of 28.201 Ma, Kuiper et al., 2008). Total fusion analyses were performed on a Argus VI mass spectrometer on line with automated all-metal extraction system. In addition, alunite was step-heated on a Helix MCPlus mass spectrometer and was exposed to flux monitors fused with a Photon Machines CO_2 laser. Decay constants and isotopic abundances follow Min et al. (2000) theory. Results are shown in *Table 24*.

9.1.5. Results

9.1.5.1. Geomorphology

The two caves show a general sub-horizontal trend following the main regional faults (NW-SE and NE-SW), but also bedding planes (having a slope of 20-25° SE). Both Cavallone and Bove caves mainly develop in the Santo Spirito limestones, and have a general NE-SW direction. They evolve almost parallel, coming as close as 60 meters from each other (*Figure 70*).

Cavallone Cave has a very large entrance (*Figure 69*), and is characterized by a spacious main passage, developing for almost a kilometer northeastward into the mountain. It has a more or less horizontal profile, with up and down moving passages with altitude differences of less than 50 meters (*Figure 70*). Although no clear signs such as notches are visible, two levels can be distinguished: the upper one developing at around 1470 m asl, comprising the portion close to the entrance and the conduit between *Bolgia Dantesca* and *Sala delle Sette Note*. This level corresponds to the mouth of the feeder (point E in *Figure 70*), and is located just below the altitude of the gypsum blocks found in this area (point F in *Figure 70*). A second lower level can be drawn at around 1440 m asl, corresponding to some lower passages before reaching *Bolgia Dantesca* and some of the farthest parts in the cave. Its total development is around 2 kilometers, with 1360 meters being open to tourists. It has four main side passages, one close to the entrance (*Galleria della Devastazione*), developing eastward for 130 meters, the other three separating from the main gallery 600 meters deep into the cave. Normal epigene speleothems such as stalactites, stalagmites and columns (Di Domenica and Pizzi, 2017) are mainly located close to the entrance, associated to slope decompression fractures; much less speleothems are present in the innermost zone of the cave, demonstrating the scarcity of surficial connection and meteoric seepage here.

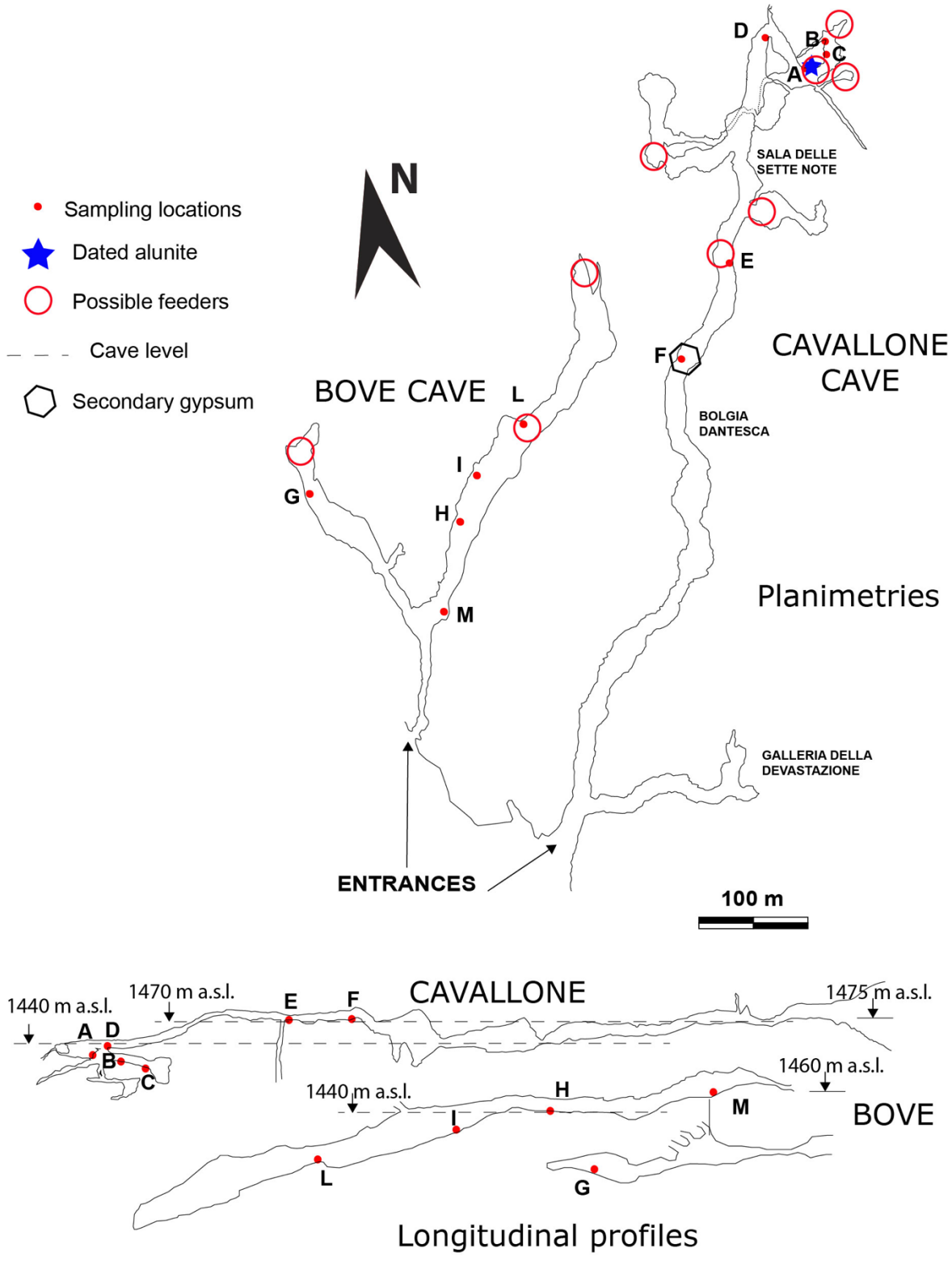

Figure 70. Plan and profile of the caves, with sampling sites and some prominent features (surveys from Speleo Club Chieti).

The Bove Cave has a small entrance, and around 100 meters into the cave it divides into two main conduits (*Figure 70*). The most important one develops toward the NE for 350 meters ca., and ends in a rockfall. The secondary branch, 200 meters long, is directed to the NW. This cave has a distinct downward profile reaching a depth of around 50 meters from the entrance. The side branch and the intermediate part of the main branch (point H in *Figure 70*) are more or less horizontal, and are located at the same altitude of the lower level in Cavallone Cave (1440 m asl). There are no important dripstone/flowstone speleothems in this cave. The main passages in both caves have impressive dimensions, around 10x10 meters, reaching up to 50 meters in height.

Both caves are characterized by a suite of unusual morphologies, visible mainly where the normal calcite speleothems and deposits are lacking (especially in the deeper part of Cavallone Cave, and most of Bove Cave), and/or where frost shattering or breakdown has not occurred. In several parts of Cavallone Cave (sites A and C in *Figure 70*) rising channels have been observed, and are characterized by smooth and rounded roofs, called megacusps (Frank et al., 1998) (a name preferred to the former megascallops; Plan et al., 2012, that recalls the scallops, formed by turbulent water flow instead), which grade into cupola and/or blind chimneys in their higher parts (*Figure 71*A,B). The shafts and low areas near the back of the caves may have been the main inputs of upwelling H_2S- and CO_2-bearing solutions.

The ceiling profile, in both caves, has a wavy shape, with upward stacking concave morphologies only visible in the first part of the main branch in Bove Cave (*Figure 72*). This original morphology is heavily modified by rockfall and faulting, and the original dissolutional ceiling is visible only at places. Replacement pockets (small concavities; Galdenzi and Maruoka, 2003; Audra et al., 2009; De Waele et al., 2016) are visible on the roof of the rising channel in point C in Cavallone Cave (*Figure 71*C,D), and also cover the walls and roof in "*Sala delle Sette Note*" (the final room where the cave splits into two branches) (*Figure 71*E). These replacement pockets are from 1 to 5 cm wide, semicircular, and up to 1.5 cm deep. Roof and wall portions etched with solutional cavities and replacement pockets (similar to the bedrock pockets of Polyak and Güven, 1996) are visible in different areas, and are often cut by pre-existing sub-vertical faults (*Figure 72*A,B).

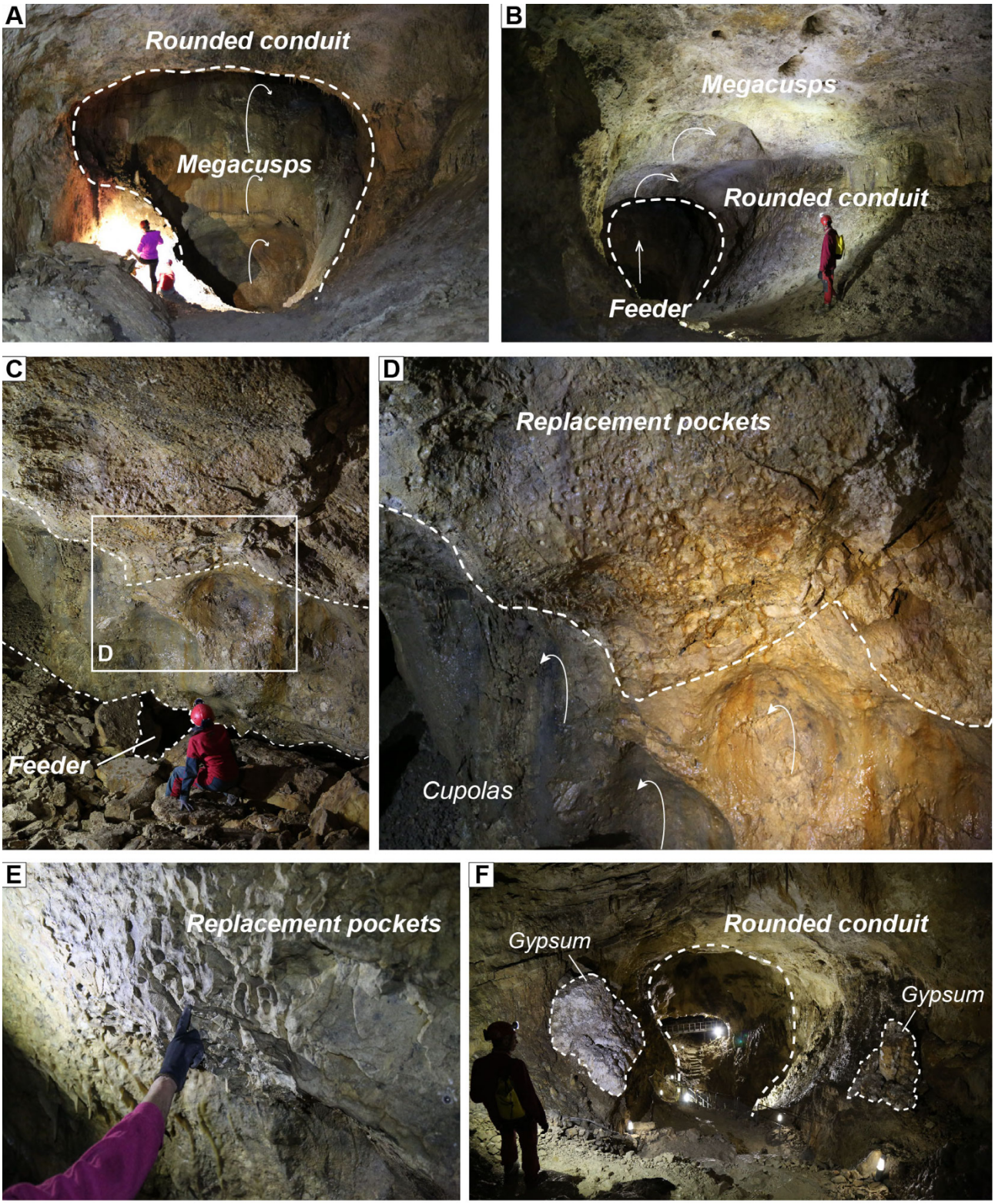

Figure 71. Main morphological features of Cavallone Cave: A-B) Rising channels with megacusps in the innermost part of the cave, close to the point A in Figure 70, where the dated alunite sample has been taken; C) One of the possible feeders of Cavallone Cave, halfway between points A and C in Figure 70; D) Detail of the roof above the feeder with replacement pockets and megacusps-cupola; E) Replacement pockets on the roof in the Sala delle Sette Note*; F) The two large microcrystalline gypsum blocks (point F in Figure 70).*

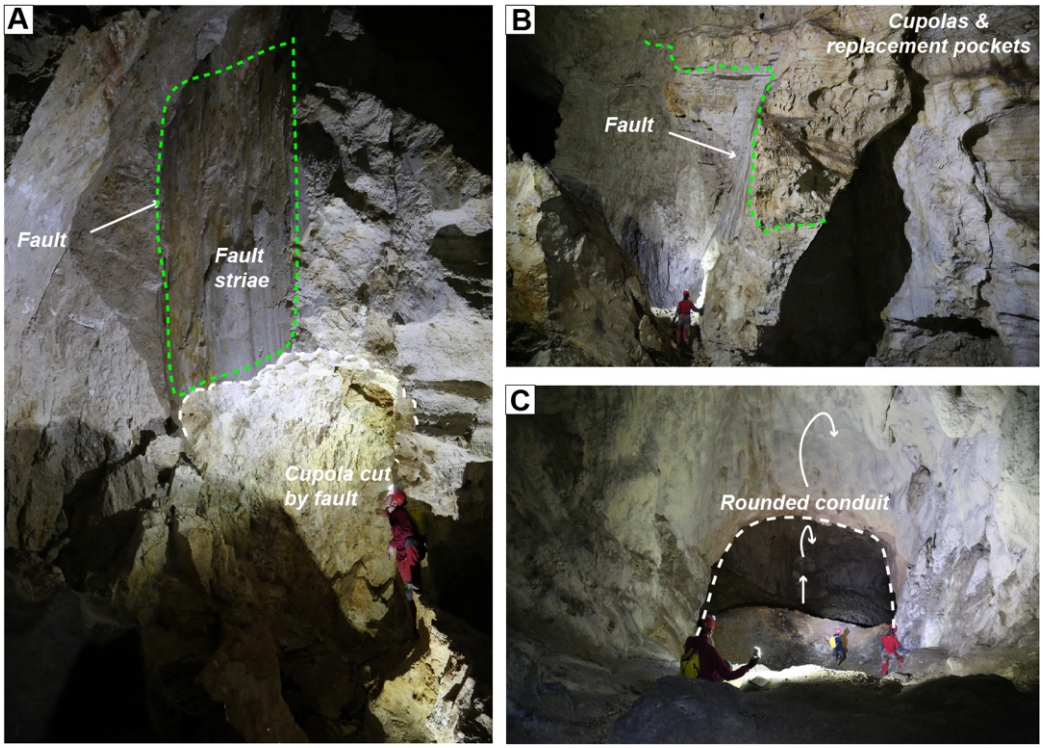

Figure 72. Main morphological features of Bove Cave: A-B) Fault with evident striae cutting a ceiling covered with rounded morphologies resembling solutional cavities, and in particular replacement pockets and cupola in the main passage of Bove Cave; C) Rising channel.

The cave conduits lack scallops or erosional notches, and their general morphology (when visible) is smoothly rounded, sometimes elongated vertically along the faults, but with no clear vadose entrenchment (*Figure 71*B and F, *Figure 72*C). Also no trace has been seen of coarse fluvial sediments, or any type of allogenic cave sediment brought in by running waters. Worth noting, in Cavallone Cave, is a deep and narrow shaft (presently closed by material due to the construction of the pathway) known as "*Pozzo senza fine*" (i.e., "Endless well"), a feeder which was descended only once and appears to be at least 50 meters deep (point E in *Figure 70*).

9.1.5.2. Mineralogy

The geomorphological features in both caves are associated with abundant secondary deposits not related to the well-known calcite-CO_2 equilibrium reaction (producing classical calcite speleothems). First of all, between the "*Bolgia Dantesca*" and the "*Sala dell'Alabastro*" (point F in *Figure 70*), adjacent to the tourist path at 500 meters from the entrance, two large blocks of saccharide white gypsum of 1 m^3 each are what remains of an undoubtedly much larger sulfate deposit (*Figure 71*F).

These blocks are located in the highest point reached by the cave and represent the substitution of the limestone cave wall with gypsum ($CaSO_4 \cdot 2H_2O$). Original structures are still preserved in the gypsum, demonstrating replacement to have occurred in a close system (where CO_2 released during the acid reaction was not lost) (Palmer and Palmer, 2012). This shows that the cave was not yet connected to the surface while this replacement reaction took place (i.e., the cave was still well below the surface, and there were still no entrances allowing strong airflow in cave). Going deeper into the cave the floor and walls are covered with layered deposits, with colors ranging from white to grey, beige, yellowish, and orange, mainly composed of alunite, natroalunite, jarosite, but also gibbsite. These layered mineral deposits have been sampled in five locations in Cavallone Cave (from A to E) (*Figure 73*A,D).

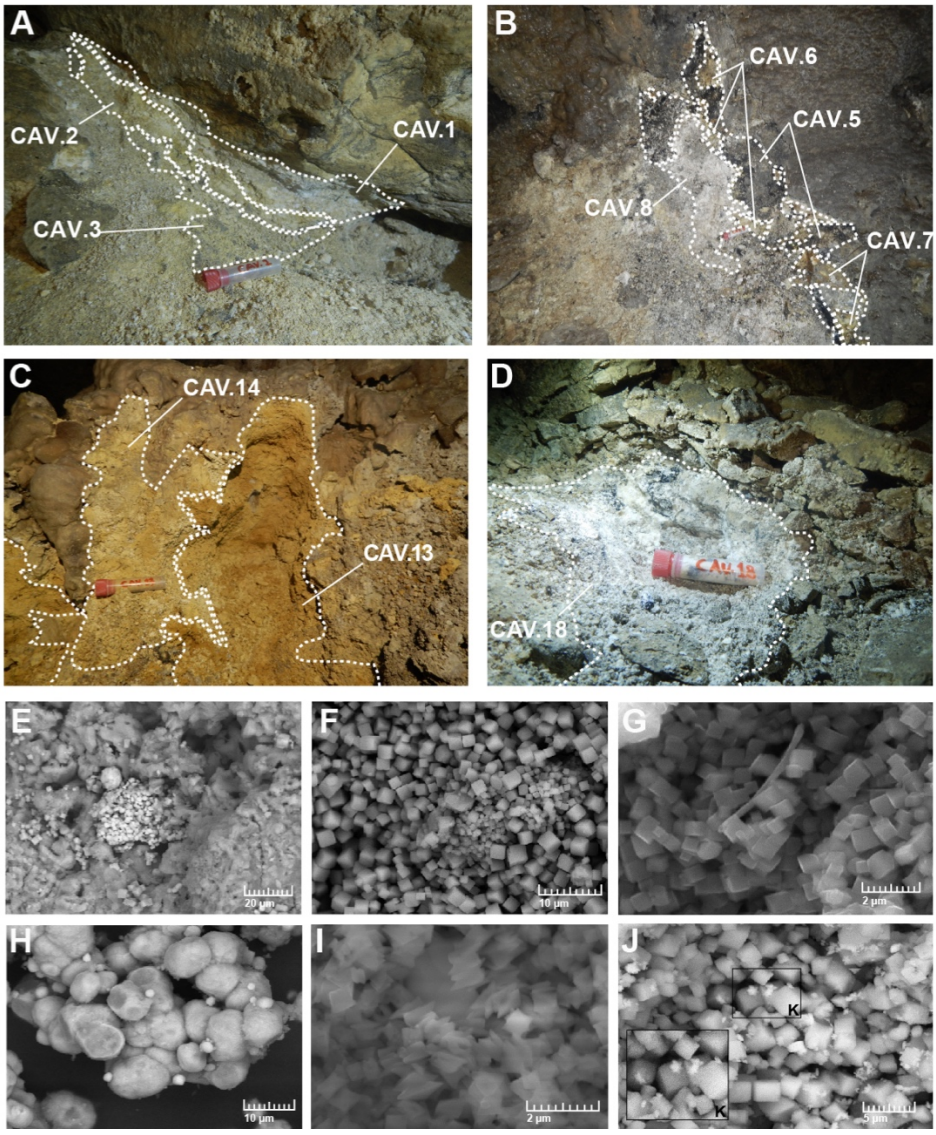

Figure 73. Mineralogy of Cavallone Cave. A. The appearance of sampling sites (in order A, C, D, and E see also Figure 70) are reported in the panels from A to D whereas the SEM images are reported from E to J. In E) it is possible micro-aggregates or crystals of intimately associated jarosite and alunite in sample CAV1; F) Pseudo-cubic crystals of relatively pure alunite in CAV2; G) Pseudo-

cubic crystals of alunite with some minor minerals in CAV3; H) Rounded form of crystals and jarosite crystals in CAV6; I) Rhombohedral crystals of alunite and jarosite in CAV8; J) Pseudo-cubic alunite-jarosite crystals in CAV 11; K) Star-like aggregates of gibbsite in CAV11. (Figure modified from D'Angeli et al., 2018).

Bove Cave also hosts these colored and layered secondary mineral deposits, but completely lacks gypsum. Five sites (mostly from the floor and one inside a solution cavity on the wall) have been extensively sampled (points G-M in *Figure 70*) (*Figure 74*A,C)

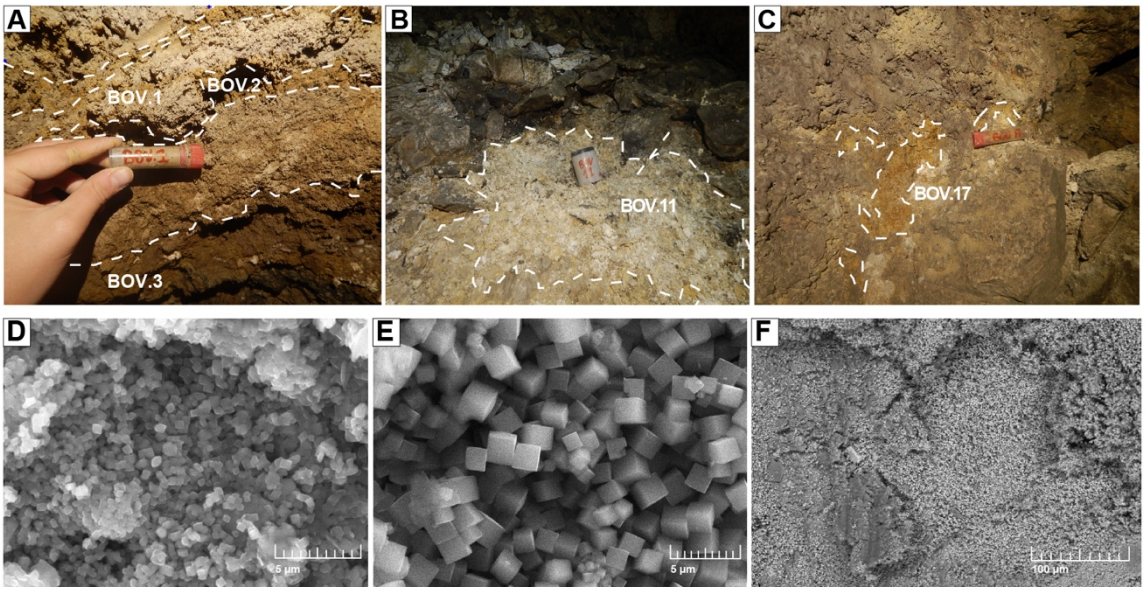

Figure 74. Mineralogy of Bove Cave: A) Sampling site G; B) Alunite, natroalunite and gibbsite sample in site (BOV11); C) Alunite, jarosite and mica in sampling site M (BOV17); D) Alunite crystals associated with quartz, magnetite, and muscovite in BOV1; E) Alunite-natroalunite microcrystalline aggregates of perfect cubic crystals (BOV11); F) Quartz, muscovite, halloysite, and Fe-oxides in sample BOV3 (Figure modified from D'Angeli et al., 2018).

The results of the mineralogical analyses are reported in *Table 23*. Most samples are composed of sulfates of the alunite supergroup (alunite, natroalunite, jarosite, natrojarosite) (*Figure 73*E,J and *Figure 74*D,F). In general, alunite and jarosite deposits present fine-grained structures (0.7-2.5 μm) and show a regular habit dominated by pseudo-cubic (*Figure 75*A) or rhombohedral (*Figure 75*B) crystals, and only rarely they appear rounded (*Figure 73*H). Sometimes, as the case of the sample CAV9, pseudo-cubic crystals (*Figure 75*A) present evident defects, probably linked to a complete substitution of previous alunite deposits with jarosite.

Quartz is abundant especially in Bove Cave, being present in 7 of the 17 samples, whereas in Cavallone Cave it occurs only 3 times. Quartz is often associated with mica group minerals, also copiously present, 8 times in Bove and 6 times in Cavallone Cave. Fe-Mn-Al-hydroxides and oxides have been observed. Star-like morphologies of crystalline aggregates of gibbsite were documented in association with alunite-jarosite (CAV11).

Other interesting minerals, likely of authigenic origin (given their perfect shape), are rutile and ilmenite, the first has been identified in a single place in Cavallone Cave (site C), whereas the second occurs in two places in Bove Cave (in G and L). Rutile crystals are elongated (*Figure 75*) and have been found associated with laminar muscovite particles. Magnetite crystals, likely of detrital origin, were exclusively noticed in Bove Cave.

Table 23. Sample list with mineralogical results and $\delta^{34}S$ data (in ‰ V-CDT). The sampling sites are reported in Figure 70. The depositional settings are reported as floor deposits (F.D.), bedrock (B.), solutional cavities (S.C.), and wall residue (W.R.) as described by Polyak and Güven (1996)

Sample	Description	Site	Depositional setting	$\delta^{34}S$‰
	Bove Cave			
BOV1	Alunite, quartz, magnetite, muscovite	G	F.D.	1.4
BOV2	Alunite, quartz, goethite, jarosite, muscovite, magnetite	G	F.D.	0.5
BOV3	Quartz, muscovite, halloysite 10Å, Fe-oxides	G	F.D.	
BOV4	Quartz, magnetite	G	F.D.	
BOV5	Quartz, mica, Fe-oxides	G	F.D.	
BOV6	Quartz, mica	G	F.D.	
BOV7	Muscovite, alunite, ilmenite	G	F.D.	4.7
BOV8	Quartz, muscovite	G	F.D.	
BOV9	Chert nodule	G	B.	
BOV10	Jarosite	H	F.D.	3.6
BOV11	Alunite, natroalunite, gibbsite	I	F.D.	4.2
BOV12	Calcite, alunite, quartz, gibbsite	L	S.C.	
BOV13	Alunite, jarosite, quartz, ilmenite, jarosite	L	S.C.	-1.4
BOV14	Alunite, calcite, quartz	L	S.C.	
BOV15	Calcite	L	S.C.	
BOV16	Jarosite, quartz	M	F.D.	-8.9
BOV17	Alunite, jarosite, muscovite	M	F.D.	-6.0
	Cavallone cave			
CAV1	Alunite, jarosite	A	F.D.	
CAV2	Alunite	A	F.D.	8.5
CAV3	Alunite, quartz, jarosite, Fe-hydroxides	A	F.D.	9.1
CAV4	Mica	A	F.D.	
CAV5	Alunite, Mn-hydroxides	B	F.D.	
CAV6	Alunite, jarosite	B	F.D.	8.7
CAV7	Calcite, alunite	B	F.D.	
CAV8	Alunite, natroalunite	B	F.D.	9.3
CAV9	Alunite, jarosite, muscovite	B	F.D.	6.2

CAV10	Mica	C	F.D.	
CAV11	Alunite, jarosite	C	F.D.	8.7
CAV12	Quartz, calcite, rutile, biotite, apatite, muscovite	C	F.D.	
CAV13	Jarosite	D	F.D.	8.2
CAV14	Jarosite	D	F.D.	8.1
CAV15	Quartz, goethite, jarosite, kaolinite, apatite	D	F.D.	
CAV16	Mica	D	F.D.	
CAV17	Calcite	D	F.D.	
CAV18	Gibbsite	E	W.R.	
CAV19	Gibbsite	E	W.R.	
CAV20	Gibbsite	E	W.R.	
CAV21	Gypsum	F	W.R.	8.9
	Gypsum bedrock			
G1	Messinian gypsum	Sicily		23.6
PN1	Triassic gypsum, Pietre Nere	Gargano		15.1
	Other S containing deposits			
P1	Bitumen, Pilone Mine	Majella		-17.2
P2	Secondary Gypsum, Pilone Mine	Majella		-7,4
P3	Bitumen, Pilone Mine	Majella		-17.8
PM1	Bitumen, Piana dei Monaci Mine	Majella		-17.5
SL1	Bitumen, Santa Liberata Mine	Majella		-18.9
SL2	Gypsum/Bitumen, Santa Liberata Mine	Majella		-14.3
SL3	Gypsum/Bitumen, Santa Liberata Mine	Majella		-13.5

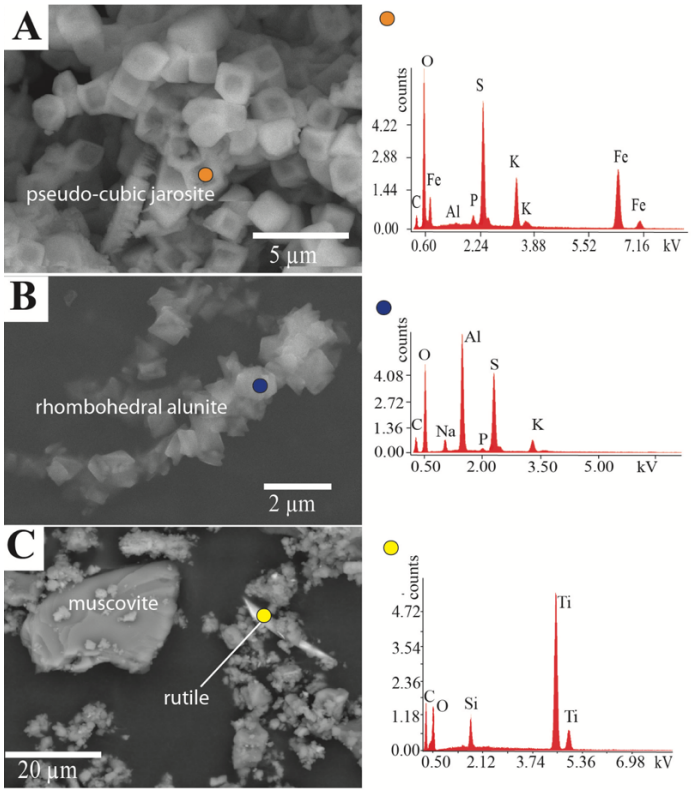

Figure 75. A) Pseudo-cubic jarosite crystals with clear defects (CAV9); B) Rhombohedral alunite (CAV8); C) Elongated rutile crystal associated with muscovite (CAV12). (Figure modified from D'Angeli et al., 2018). The graphs on the right report the EDAX analyses of the indicated spots.

9.1.5.3. Stable isotopes

Sulfur isotopes were measured on alunite, natroalunite, jarosite, gypsum, and bitumen (*Figure 76*). Eight samples were from Bove Cave, nine from Cavallone, two of Messinian and Triassic evaporites respectively, whereas seven samples came from abandoned bitumen mines (four of which were mainly composed of bitumen, three also contained gypsum).

$\delta^{34}S$ values of bitumen samples range between -18.9 and -17.2‰, whereas the samples with gypsum showed slightly more positive values (-14.3 and -13.5‰) up to -7.4‰ for the sample predominantly composed of secondary gypsum. The $\delta^{34}S$ values for the Messinian and Triassic gypsum bedrocks, obtained in this study are positive, +23.6 and +15.1‰ respectively.

The $\delta^{34}S$ values observed in Cavallone and Bove caves are clearly fall between bitumen and gypsum bedrock values. Cavallone Cave samples are very homogeneous, with $\delta^{34}S$ values ranging between +6.2 and +9.3‰ (mean 8.4‰), whereas Bove samples are much more heterogeneous, ranging from negative values (-8.9‰) to rather positive ones (+4.7‰), and a mean of +0.2‰.

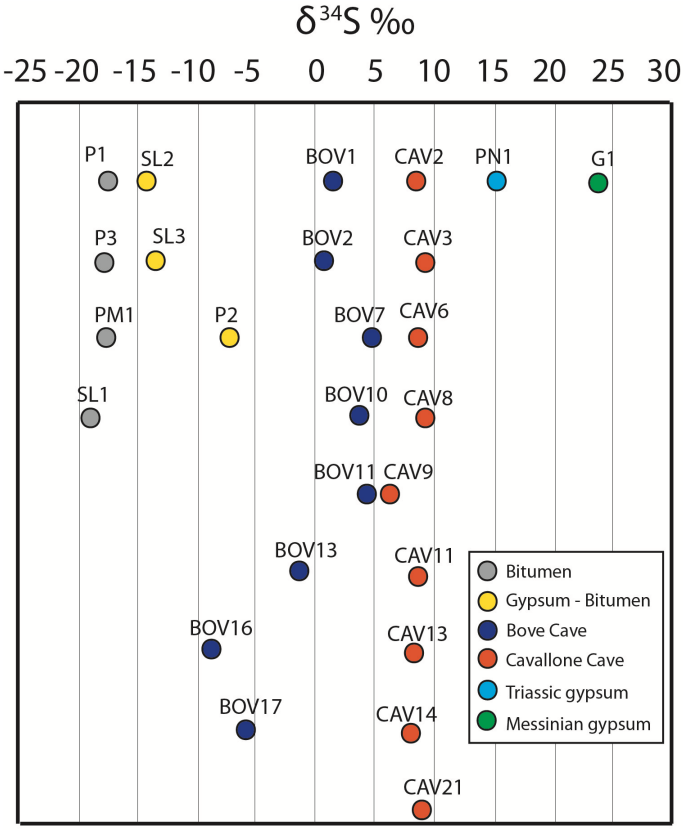

Figure 76. $\delta^{34}S$ values (in ‰) for the analyzed samples, including sulfates from Bove and Cavallone caves, gypsum and bitumen collected in abandoned mines, Triassic and Messinian gypsum bedrocks.

9.1.5.4. $^{40}Ar/^{39}Ar$ Alunite age

One sample of relatively pure alunite (CAV2) collected in location A in Cavallone Cave (*Figure 73*A) yielded an $^{40}Ar/^{39}Ar$ age (*Table 24*) of 1.52±0.28 Ma. The rather high error in age is due to the relatively low radiogenic yield. Polyak et al., (1998) interpretated the age of cave alunite to represent the timing of sulfuric acid speleogenesis in Carlsbad Caverns, Lechuguilla Cave, and other caves in the Guadalupe Mountains. Similarly, this alunite age represents the timing of speleogenesis of Cavallone and Bove cave caves.

Table 24. $^{40}Ar/^{39}Ar$ results and analytical methods.

Sample	Lab #	Irradiation	Mineral	Age analysis	Steps/Analyses	Age	±2σ	MSWD
CAV2	65977	293	Alunite	Bulk step-heat	9	1.52	0.28	0.15

9.1.6. Discussions and Conclusions

Up to recently, the origin of Cavallone and Bove caves was believed to be epigenic, with percolating meteoric waters enlarging different discontinuities. Describing the main morphology of the passage in Cavallone Cave most authors made use of terms such as "phreatic tube" and "vadose shaft". From a morphological point of view there is either sign of vadose entrenchment, nor are there indications of the presence of fast flowing waters in the past. There are no stream sediments in the cave and the walls have no signs of scallops or erosive notches.

In addition, clear evidences of seeping waters are visible mostly close to the entrance of Cavallone Cave, in the proximity of *Galleria della Devastazione*, where stalagmites, stalactites, and flowstones copiously decorate ceilings, walls, and floors. Their occurrence is likely due the formation of extensional fractures linked to the release of stress following gorge incision.

The presence of white secondary crystalline gypsum deposits in Cavallone Cave (*Figure 71*F), the widespread occurrence of peculiar sulfates such as alunite, jarosite, natroalunite, and the abundant gibbsite in the innermost portion of the cave, are diagnostic of alteration processes involving SAS (*Figure 73* and *Figure 74*). Also, some morphologies are typical of SAS, in particular the replacement pockets and the solutional cavities (*Figure 71*C,D,E and *Figure 72*B). These diagnostic features have been found in different areas of both Cavallone and Bove caves, and always close to thick layered sulfate deposits.

The traces of the feeders in Cavallone and Bove caves are still visible under the form of rising channels and a series of upward-anastomosing cupola and megacusps (*Figure 71*A,B,C). Close to these rising channels, which are mostly impenetrable because of the presence of blocks, the concentration of secondary cave sulfates and replacement pockets is greater, further sustaining this

hypothesis.

Whereas in Cavallone Cave the walls are generally covered with sediments or speleothems, Bove Cave appear to be bare, evidently revealing the structural elements and preserving some finely sculptured walls and ceilings. In the main passage collapses have unveiled different fault planes, and the exposed ceiling is covered with replacement pockets and ceiling cupolas (*Figure 72*A,B).

The more or less horizontal development (*Figure 70*) of both caves is an indication of their origin in unconfined conditions close to the water table. This level has changed at least once, and clearly shows signatures of its standing level in several locations of the cave system (*Figure 70*). A first stationary level currently located at 1470 m, is well-visible in Cavallone Cave, and is followed by a second present-day located at 30 meters below.

Similar to what occurs in other active SAS cave systems (e.g. Frasassi), H_2S and fluids rose along the fractures reaching this level where the gases were released into the cave atmosphere. In this oxidizing environment, the sulfide (H_2S) transformed into sulfuric acid (H_2SO_4), which immediately reacted with the hosting limestone producing gypsum and carbon dioxide, the latter gas further boosting the dissolution process. This appeared to have occurred in a subterranean air-filled environment not yet well-connected to the surface, with almost no CO_2 loss (in more or less closed system conditions). Gypsum formed exclusively close to the area indicated with F (*Figure 70*) in Cavallone Cave, being the host rock, here, dominated by relatively pure limestone. On the contrary, from E towards the innermost conduits of Cavallone Cave (*Figure 70)* the host rock is composed of marly limestones, which induced the precipitation of Al-Fe-rich sulfates such as alunite, natroalunite, and jarosite deposits. These minerals are typical by-products of acid conditions (Ossaka et al., 1987; Polyak and Provencio, 2001) and are pH/Eh-dependent (Carbone et al., 2013; D'Angeli et al., 2018). Minerals belonging to the jarosite group normally form at pH <2.5, alunite precipitates at pH values of 3-4 (Kulp et al., 2009). Generally, Al-rich sulfates (i.e., alunite) precipitate separately from the Fe-rich ones (i.e., jarosite), and even if present in the same deposits, alunite and jarosite rarely belong to the same event (Rye et al., 1993; Stoffregen, 1993). Fe-rich waters tend to precipitate yellow-to red-to brown materials, whereas Al-rich fluids form milky-white precipitates (Bigham and Nordstrom, 2000). Alunite is easily attributed to hypogene processes, whilst jarosite is commonly considered a product of supergene weathering (Dill, 2001), and can replace alunite when the fluids become more acidic and oxidizing (Stoffregen et al., 2000). The studied alunite-jarosite deposits present fine-grained structures (0.7-2.5 μm), occurring as pseudo-cubic (*Figure 73*F,G,J and *Figure 74*E) rhombohedral grains (*Figure 73*I and *Figure 75*B) accumulated within bedded sediments. Fine-grained alunite deposits (Stoffregen et al., 2000) usually form at quite low temperature (<100 °C). Solid solution series as alunite-natroalunite, alunite-jarosite have been observed in the samples

collected in Cavallone and Bove caves, but more interesting are the coupled substitutions of sulfate (SO_4^{2-}) with phosphate (PO_4^{3-}) (Fig. 8A-B in the EDX spectra), which, considering their low abundance, they might exclusively be indicative of hypogene hydrothermal origin (Dill, 2001). Guano deposits might also induce phosphates and sulphates precipitation, but they would have exhibited higher abundances, in fact, we observed apatite only in two sampling sites in Cavallone Cave (CAV12 and CAV15).

Gibbsite is indicative of extreme weathering conditions (Ece and Schroeder, 2007) occurring at pH ranging between 6 and 8 (Bigham and Nordstrom, 2000). In our case, the gibbsite forms due to the progressive alteration of the Al-rich sulfates, during periods of intense leaching, which removed soluble ions and precipitated Al hydroxides. Pure samples of gibbsite have been exclusively found close to the *Pozzo senza Fine* in Cavallone Cave (site E in *Figure 70*), close to gypsum blocks (other important indicators of alteration processes). Gibbsite also occurs together with alunite and natroalunite in the lower parts of Bove Cave (site I and L in *Figure 70*). In both cases, the samples were located close to possible feeders, with clear signs of rising fluid flow. An interesting example of crystalline weathering is provided by the sample CAV9 (site B in *Figure 70*) in which solid solution of alunite and jarosite showed rounded forms, likely caused by the aggressive solutions rising from the feeder.

Ilmenite has been found exclusively in Bove Cave (site G and L in *Figure 70*), whereas rutile only occurs in the innermost zone of Cavallone Cave (site C in *Figure 70*), and both are mainly located very close to feeder structures. As described in D'Angeli et al. (2018) titanium solubility is low, and generally it occurs as a solid transported phase. Nevertheless, the acidic digestion (HNO_3 and/or H_2SO_4) might induce exothermic reactions, allowing Ti to be found in the ionic form (Westerhoff et al., 2011). Rutile mineral in CAV12 sample (site C in *Figure 70*) shows needle crystal (*Figure 75*C). Yin et al. (2004), during some experiments in laboratory, observed that acidic solutions could dissolve titanium minerals, producing mobile Ti ions, which may re-precipitate also at room temperature. They demonstrated temperature to be a limiting control for the morphology of titanium minerals. As a matter of fact, needle-like pure rutile was observed in solution with temperature ranging between 25-50°C, whereas spherical morphologies are favored at T >140°C (Yin et al., 2002, 2004). Magnetite likely reached their current locations transported as solid particles by the rising flows, especially due to its limited stability conditions. As a matter of fact, magnetite can form at pH too alkaline (10-12) for sulfuric acid environments.

Sulfur stable isotopes showed the two caves to have quite different $\delta^{34}S$ values, as a matter of fact Cavallone Cave presented homogeneous positive results ranging from +6.2 to +9.3‰, whereas in Bove we found more negative data from -8.9‰ to +4.7‰. The sources of H_2S in these two cavities

likely is not the same, and appears to be related to different degree of mixture between fluids deriving from the interaction with two main possible sources of sulfur (Triassic evaporites and bitumen).

Both caves are now high above (almost 1000 meters) the current local base level (i.e., Aventino River), and therefore the sulfuric water table. The radiogenic age of the SAS period, documented in this work, is based on the 1.52±0.28 Ma alunite $^{40}Ar/^{39}Ar$ date. This means that the cave system, and in particular the lower Cavallone Cave level at 1440 m asl., where the dated alunite sample (CAV2 in site A *Figure 70*) was taken, was at or close to the water table at that time (*Figure 77*A). Considering the height variation between the Aventino River (at 450 m asl) and the SAS cave level at 1440 m, a general uplift caused the mountain (and the cave carved within) to rise for 1 km over the last 1.5 Ma. Our precise dating allows to define a Late Pleistocene-Holocene uplift rate ranging between 0.55 and 0.80 mm y^{-1} (average 0.67 mm y^{-1}), a value in agreement with (but much more precise than) the estimates made by Pizzi (2003) (0.1-1 mm y^{-1}).

The carving of the Taranta Gorge can thus be attributed to an enhanced incision of surface waters in response to this uplift (*Figure 77*B), probably with larger downcutting taking place during the glacial to interglacial transitions, when meltwaters had a greater power of entrenchment. Thus, the incision rate of the Taranta Gorge was produced by an ephemeral river with an incision rate estimated at 0.23 mm y^{-1} (0.19-0.27 mm y^{-1}), and calculated considering the altitudal variation between the top of massif (1620 m) and the bottom of the gorge (1280) along the Cavallone-Bove cross section (it means 340 m/1.5 Ma). Such value of incision rate (0.19-0.27 mm y^{-1}) are comparable to the river incision rates of 0.1-0.3 mm/y used by Picotti et al., (2009), ~0.2-0.4 of Bartolini (2003), and 0.28-0.58 mm y^{-1} Cyr and Granger (2008).

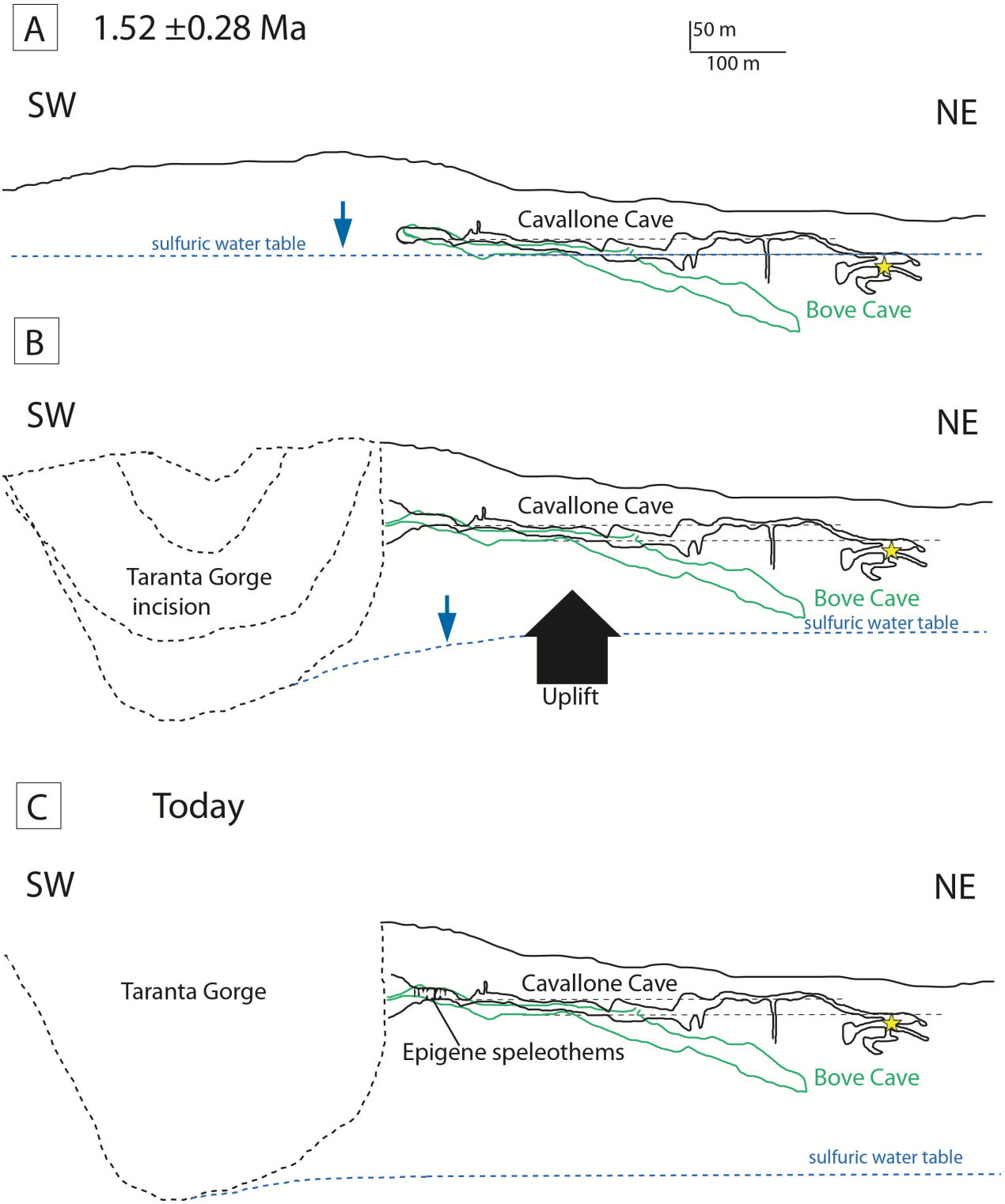

Figure 77. The sketch summarized the main stages that involved the origin of both caves and the Taranta Gorge. Cavallone Cave is black whereas Bove Cave is green. A) Sulfuric acid speleogenesis (1.52±0.28 Myr) of cave level where we collected the dated sample CAV2 (yellow star); B) The fall of base level/uplift of the massif (0.67 mm y^{-}) produced the incision of the Taranta Gorge (0.23 mm y^{-1}) and the lowering of the sulfuric water table; megacusps were likely created during and after this period; C) Only later, the gorge incision opened the cave entrances and the precipitation of local

normal epigene speleothems began. Today the sulfuric water table is located ca. 1 km below the Cavallone-Bove caves.

All of the evidence testifies to several stages of SAS forming the Cavallone-Bove system prior to the Taranta Gorge incision. The circulating rising fluids created rounded conduits (*Figure 71*F) close to and above the water table and caused the precipitation of the described mineralogical sulfate assemblages. Gypsum, on the other hand, is the most soluble mineral among all, but it survived in the highest level (1470 m) of Cavallone Cave (site F in *Figure 70*), demonstrating that no waters reached this part of the cave after it was uplifted above the water table.
Then, the fall of the base level/uplift of the massif produced the incision of the Taranta Gorge and the lowering of the sulfuric water table.

References

Aydin, A., Antonellini, M., Tondi, E., Agosta, F., 2010. Deformation along the leading edge of the Maiella thrust sheet in central Italy. Journal of Structural Geology 32: 1291-1304.

Audra, P., Hobléa, F., Bigot, J.-Y., Nobécourt, J.-C., 2007. The role of condensation-corrosion in thermal speleogenesis: study of a hypogenic sulfidic cave in Aix-les-Bains, France. Acta Carsologica 36: 185-194.

Bartolini, C., 2003. When did the Northern Apennine become a mountain chain? In: C., Bartolini, L., Piccini, N.R., Catto (Eds.), Uplift and Erosion; Driving Processes and Resulting landforms; Dynamic relations between crustal and surficial processes. Quaternary International, 101-102: 75-80.

Bigham J.M. & Nordstrom D.K., 2000. Iron and Aluminium Hydroxysulfates from acid sulfate waters. Reviews in Mineralogy and Geochemistry, 40: 351-403.

Brandano M., Lipparini L., Campagnoni V., Tomassetti L, 2012. Downslope-migrating large dunes in the Chattian carbonate rampo of the Majella Mountains (Central Apennines, Italy). Sedimentary Geology, 255-256: 29-41.

Brandano M., Cornacchia I., Raffi I., Tomassetti L., 2016. The Oligocene-Miocene stratigraphic evolution of the Majella carbonate platform (Central Apennines, Italy). Sedimentary Geology, 33: 1-14.

Carbone, C., Dinelli, E., Marescotti, P., Gasparotto, G., Lucchetti, G., 2013. The role of the AMD secondary minerals in controlling environmental pollution: indications from bulk leaching tests. Journal of Geochemical Exploration, 132: 188-200.

Cerruti, M., Segre, A. G., Patrizi, S., 1949. Notizie della grotta del Cavallone nella Majella (Abruzzo). Bollettino della Società Geologica Italiana, 2: 201-205.

Cyr, A.J., Granger, D.E., 2008. Dynamic equilibrium among erosion, river incision, and coastal uplift in the northern and central Apennines, Italy. Geology, 36(2): 103-106. Doi: 10.1130/G24003A.

D'Angeli, I.M., Vattano, M., Parise, M., De Waele, J., 2017. The coastal sulfuric acid cave system of Santa Cesarea Terme (southern Italy). In: A.B., Klimchouk, A.N., Palmer, J., De Waele, A., Auler, P. Audra (Eds.), Hypogene Karst Regions and Caves of the World, Springer: 161-168.

D'Angeli, I.M., Carbone, C., Nagostinis, M., Parise, M., Vattano, M., Madonia, G., De Waele, J., 2018. New insights on secondary minerals from Italian sulfuric acid caves. International Journal of Speleology, 47(3): 271-291.

Davis, D.G., 1980. Cave development in the Guadalupe Mountains: a critical review of recent hypotheses. National Speleological Society Bulletin, 42: 42-48.

De Waele, J., Galdenzi, S., Madonia, G., Menichetti, M., Parise, M., Piccini, L., Sanna, L., Sauro, F., Tognini, P., Vattano, M., Vigna, B., 2014. A review on hypogene caves in Italy. In: A., Klimchouk, I., Sasowsky, J., Mylroie, S.A., Engel, A.S., Engel (Eds.), Hypogene Cave Morphologies. Karst Waters Institute Special Publication 18, Leesburg, Virginia: 28-30.

De Waele, J., Audra, P., Madonia, G., Vattano, M., Plan, L., D'Angeli, I.M., Bigot, J.-Y., Nobécourt, J.-C., 2016. Sulfuric acid speleogenesis (SAS) close to the water table: Examples from southern France, Austria, and Sicily. Geomorphology, 253: 452-467.

Di Domenica A., Pizzi A., 2017. Defining a mid-Holocene earthquake through speleoseismological and independent data: implication for the outer central Apennines (Italy) seismotectonic framework. Solid Earth, 8: 161-176.

Dill H.G., 2001. The geology of aluminium phosphates and sulphates of alunite group minerals: a review. Earth-Science Reviews, 53: 35-93.

DuChene, H.R., 2000. Bedrock features of Lechuguilla Cave, Guadalupe Mountains, New Mexico. Journal of Cave and Karst Studies, 62: 109-119.

DuChene, H., Palmer, A.N., Palmer, M.V., Queen, J.M., Polyak, V.J., Decker, D.D., Hil, C.A., Spilde, M., Burger, P.A., Kirkland, D.W., Boston, P., 2017. Hypogene Speleogenesis in the Guadalupe Mountains, New Mexico and Texas, USA. In: A.B., Klimchouk, A.N., Palmer, J., De Waele, A., Auler, P., Audra (Eds.), Hypogene Karst Regions and Caves of the World, Springer, 511-530.

Ece, O.I., Schroeder, P.A., 2007. Clay mineralogy and chemistry of halloysite and alunite deposits in the Turplu area, Balikesir, Turkey. Clays and Clay Minerals, 55(1): 18-35.

Egemeier, S.J.,1971. A comparison of two types of solution caves. Unpublished report to Carlsbad Caverns National Park: 1-7.

Egemeier, S.J.,1973. Cavern development by thermal waters with a possible bearing on ore deposition. Ph.D. thesis, Stanford University: 1-88.

Egemeier, S.J.,1981. Cavern development by thermal waters. National Speleological Society Bulletin 43: 31-51.

Egemeier, S.J., 1987. A theory for the origin of Carlsbad Cavern. National Speleological Society Bulletin, 49: 73-76.

Festa, A., Accotto, C., Coscarelli, F., Malerba, E., Palazzin, G., 2014. Geology of the Aventino River Valley (eastern Majella, Central Italy). Journal of Maps, 10: 584-599.

Frank, E.D., Mylroie, J., Troester, J., Alexander Jr., E.C., Carew, J.L., 1998. Karst development and speleogenesis, Isla de Mona, Puerto Rico. Journal of Cave and Karst Studies, 60(2): 73-83.

Galdenzi S., 1997. Initial geologic observations in caves bordering the Sibari Plain (southern Italy). Journal of Cave and Karst Studies, 59(2): 81–86.

Galdenzi, S., 2004. I depositi di gesso nella Grotta di Faggeto Tondo: nuovi dati sull'evoluzione geomorfologia dell'area di Monte Cucco (Italia centrale). Studi Geologici Camerti, 2: 71-83.

Galdenzi, S., 2012. Corrosion of limestone tablets in sulfidic ground-water: measurements and speleogenetic implications. Interntinal Journal of Speleoleology, 41: 25-35

Galdenzi, S., 2017. The Thermal Hypogenic Caves of Acquasanta Terme (Central Italy). In: A.B., Klimchouk, A.N., Palmer, J., De Waele, A., Auler, P. Audra (Eds.), Hypogene Karst Regions and Caves of the World, Springer: 169-182.

Galdenzi, S., Jones, D. S., 2017. The Frasassi Caves: A "Classical" Active Hypogenic Cave. In: A.B., Klimchouk, A.N., Palmer, J., De Waele, A., Auler, P. Audra (Eds.), Hypogene Karst Regions and Caves of the World, Springer: 143-159.

Galdenzi, S., Maruoka, T., 2019. Sulfuric acid caves in Calabria (South Italy): Cave morphology and sulfate deposits. Geomorphology, 328, 211-221.

Galdenzi, S., Menichetti, M., 1995. Occurrence of hypogenic caves in a karst region: examples from central Italy. Environmental Geology, 26: 39-47.

Galdenzi, S., Menichetti, M., 2017. Hypogenic Caves in the Apennine Mountains (Italy). In: A.B., Klimchouk, A.N., Palmer, J., De Waele, A., Auler, P. Audra (Eds.), Hypogene Karst Regions and Caves of the World, Springer: 127-142.

Galdenzi, S., Cocchioni, M., Morichetti, L., Amici, V., Scuri, S., 2008. Sulfidic ground-water chemistry in the Frasassi caves, Italy. Journal of Cave and Karst Studies, 70(2): 94–107.

Galdenzi, S., Cocchioni, F., Filipponi, G., Morichetti, L., Scuri, S., Selvaggio, R., Cocchioni, M., 2010. The sulfidic thermal caves of Acquasanta Terme (central Italy). Journal of Cave Karst Studies, 72: 43-58.

Hill, C.A., 1981. Speleogenesis of Carlsbad Caverns and other caves in the Guadalupe Mountains. In: B.F., Beck (Ed.), Proceedings of 8th International Congress of Speleology, Bowling Green, Kentucky, 1: 143-144.

Hill, C.A., 1987. Geology of Carlsbad Caverns and other caves in the Guadalupe Mountains, New Mexico and Texas. New Mexico Bureau of Mines and Mineral Resources Bulletin, 117: 1-150.

Hill, C.A., 1990. Sulfuric acid speleogenesis of Carlsbad Cavern and its relationship to hydrocarbons, Delaware Basin, New Mexico and Texas. American Association of Petroleum Geologists Bulletin, 74: 1685-1694.

Hill, C.A., 2000. Sulfuric acid, hypogene karst in the Guadalupe Mountains of New Mexico and West Texas (U.S.A.). In: A.B., Klimchouk, D.C, Ford, A.N., Palmer, W., Dreybrodt (Eds.),

Speleogenesis: Evolution of karst aquifers. Huntsville, AL, National Speleological Society: 309-316.

Hose, L.D., Pisarowicz, J.A.,1999. Cueva de Villa Luz, Tabasco, Mexico: reconnaissance study of an active sulfur spring cave and ecosystem. Journal of Cave and Karst Studies, 61:13-21.

Hose, L. D., Rosales-Lagarde, L., 2017. Sulfur-Rich Caves of Southern Tabasco, Mexico. In: A.B., Klimchouk, A.N., Palmer, J., De Waele, A., Auler, P. Audra (Eds.), Hypogene Karst Regions and Caves of the World, Springer: 803-814.

Hose, L.D., Palmer, A.N., Palmer, M.V., Northup, D.E., Boston, P.J., DuChene, H.R., 2000. Microbiology and geochemistry in a hydrogen-sulphide-rich karst environment. Chemical Geology, 169: 399-423.

Jagnow, D.H., 1977. Geologic factors influencing speleogenesis in the Capitan Reef Complex, New Mexico and Texas. Unpublished MS thesis, University of New Mexico: 197 pp.

Jagnow, D.H., 1978. Geology and speleogenesis of Ogle Cave, New Mexico. National Speleological Society Bulletin, 40: 7-18.

Jagnow, D.H., 1979. Cavern development in the Guadalupe Mountains. Cave Research Foundation, Columbus, Ohio: 55 pp.

Jagnow, D.H., 1986. Current thoughts on cavern development in the Guadalupe Mountains, New Mexico. In: D.H., Jagnow, H.R., DuChene (Eds.), Proceedings National Speleological Society Convention, Tularosa, New Mexico: 85-102.

Jagnow, D.H., Hill, C.A., Davis, D.G., DuChene, H.R., Cunningham, K.I., Northup, D.E., Queen, M.J., 2000. History of the sulfuric acid theory of speleogenesis in the Guadalupe Mountains, New Mexico. Journal of Cave and Karst Studies, 62: 54-59.

Kempe, S., Al-Malabeh, A., Al-Shreideh, A., Henschel, H.V., 2006. Al-Daher Cave (Bergish), Jordan, the first extensive Jordanian limestone cave: A convective Carlsbad-type cave. Journal of Cave and Karst Studies, 68(3): 107-114.

Kirkland, D.W., 1982. Origin of gypsum deposits in Carlsbad Caverns, New Mexico. New Mexico Geology, 4: 20-21.

Kirkland, D.W., 2014. Role of hydrogen sulfide in the formation of cave and karst phenomena in the Guadalupe Mountains and western Delaware Basin, New Mexico and Texas. National Cave and Karst Research Institute, Carlsbad, Special Paper Series: 1-77.

Kuiper, K. F., Deino, A., Hilgen, F. J., Krijgsman, W., Renne, P. R., Wijbrans, J. R., 2008, Synchronizing rock clocks of earth history. Science, 320: 500-504.

Kulp E.A., Kothari H.M., Limmer S.J., Yang J., Gudavarthy R.V., Bohannan E.W., Switzer J.A., 2009. Electrodeposition of epitaxal magnetite films and ferrihydrite nanoribbons on single-crystal gold. Chemistry Materials, 21(21): 5022-5031.

Min, K., Mundil, R., Renne, P. L., Ludwig, K.R., 2000. A test for systematic errors in $^{40}Ar/^{39}Ar$ geochronology through comparison with U/Pb analysis of a 1.1-Ga rhyolite. Geochimica et Cosmochimica Acta, 64: 73-98.

Morehouse, D.F.,1968. Cave development via the sulfuric acid reaction. NSS Bull. 30,1-10.

Onac, B. P., Drăguşin, V., 2017. Hypogene Caves of Romania. In: A.B., Klimchouk, A.N., Palmer, J., De Waele, A., Auler, P. Audra (Eds.), Hypogene Karst Regions and Caves of the World, Springer: 257-265.

Onac, B.P., Sumrall, J., Tămaş, T., Povară, I., Kearns, J., Dârmiceanu, V., Veres, D., Lascu, C., 2009. The relationship between cave minerals and H_2S-rich thermal waters along Cerna Valley (SW Romania). Acta Carsologica, 38(1): 27-39.

Onac, B. P., Wynn, J. G., Sumrall, J. B., 2011. Tracing the sources of cave sulfates: a unique case from Cerna Valley, Romania. Chemical Geology, 288(3): 105-114.

Ossaka J., Otsuka N., Hirabayashi J. I, Okada K., Soga H., 1987. Synthesis of minamiite, $Ca_{0.5}Al_3(SO_4)_2(OH)_6$. Neues Jahrbuch fūr Mineralogie Monatshefte, 2: 49-63.

Palmer, M.V., Palmer A.N,. 2012. Petrographic and isotopic evidence for late-stage processes in sulfuric acid caves of the Guadalupe Mountains, New Mexico, USA. International Journal of Speleology, 41(2): 231-250.

Patacca, E., Scandone, P., 2007. Geology of the Southern Apennines. Bollettino della Società Geologica Italiana 7, 75-119.

Piccini, L., De Waele, J., Galli, E., Polyak, V.J., Bernasconi, S.M., Asmerom, Y., 2015. Sulphuric acid speleogenesis and landscape evolution: Montecchio cave, Albegna river valley (Southern Tuscany, Italy). Geomorphology, 229: 134-143.

Picotti, V., Ponza, A., Pazzaglia, F.J., 2009. Topographic expression of active faullts in the foothills of the Northern Apennines. Tectonophysics, 474: 285-294.

Pizzi A., 2003. Plio-Quaternary uplift rates in the outer zone of the central Apennines fold and thrust belt, Italy. Quaternary International, 101-102: 229-237.

Plan, L., Tschegg, C., De Waele, J., Spötl, C., 2012. Corrosion morphology and cave wall alteration in an Alpine sulfuric acid cave (Kraushöhle, Austria). Geomorphology, 169-170: 45-54.

Polyak, V.J., Güven, N., 1996. Alunite, natroalunite and hydrated halloysite in Carlsbad Caverns and Lechuguilla Cave, New Mexico. Clays and Clay Minerals, 44(6): 843-850.

Polyak V.J., Provencio P., 2001. By-product materials related to H_2S-H_2SO_4 influenced speleogenesisi of Carlsbad, Lechuguilla, and other caves of the Guadalupe Mountains, New Mexico. Journal of Cave and Karst Studies, 63(1): 23-32.

Principi, P.,1931. Fenomeni di idrologia sotteranea nei dintorni a Triponzo. Le Grotte d'Italia, 1: 45-47.

Rye R.O., Bethke P.M., Lanphere M.A. & Steven T.A., 1993. Age and stable isotope systematics of supergene alunite and jarosite from the Creede mining district, Colorado: implications for supergene processes and Neogene geomorphic evolution and climate of the southern Rocky Mountains (abs). Geological Society of America Abstract with programs 25, A-274.

Sarbu, S.M., Kane, T.C., 1995. A subterranean chemoautotrophically based ecosystem. National Speleological Society Bulletion, 57: 91-98.

Sarbu, S.M., Kane, T.C., Kinkle, B.K., 1996. A chemoautotrophically based cave ecosystem. Science, 272: 1953-1955.

Scisciani, V., Tavarnelli, E., Calamita, F., 2002. The interaction of extensional and contractional deformation in the outer zone of the central Apennines, Italy. Journal of Structural Geology, 24: 1647–1658.

Socquet, J.-M., 1801. Analyse des eaux thermales d'Aix (en Savoie), département du Mont-Blanc (Analysis of Thermal Waters at Aix, in Savoy, Mont-Blanc Department). Cleaz, Chambéry: 1-240.

Stoffregen R.E., 1993. Stability relations of jarosite and natroalunite at 100-250°C. Geochimica et Cosmochimica Acta, 58: 903-916.

Stoffregen R.E., Alpers C.N. & Jambor J.L., 2000. Alunite-jarosite crystallography, thermodynamics, and geochronology. Reviews in Mineralogy and Geochemistry, 40: 453-479.

Temovski, M., 2017. Hypogene Karst in Macedonia. In: A.B., Klimchouk, A.N., Palmer, J., De Waele, A., Auler, P. Audra (Eds.), Hypogene Karst Regions and Caves of the World, Springer: 241-256.

Temovski, M., Audra, P., Mihevc, A., Spangenberg, J.E., Polyak, V., McIntosh, W., Bigot, J.Y., 2013. Hypogenic origin of Provalata Cave, Republic of Macedonia: a distinct case of successive thermal carbonic and sulfuric acid speleogenesis. International Journal of Speleology, 42: 235-246.

Temovski, M., Futó, I., Túri, M., Palcsu, L., 2018. Sulfur and oxygen isotopes in the gypsum deposits of the Provalata sulfuric acid cave (Macedonia). Geomorphology, 315: 80-90.

Vattano, M., Madonia, G., Audra, P., D'Angeli, I. M., Galli, E., Bigot, J. Y., Nobécourt, J.C, De Waele, J., 2017. An Overview of the Hypogene Caves of Sicily. In: A.B., Klimchouk, A.N.,

Palmer, J., De Waele, A., Auler, P. Audra (Eds.), Hypogene Karst Regions and Caves of the World, Springer: 199-209.

Westerhoff P., Song G., Hristovski K. & Kiser M.A., 2011. Occurrence and removal of titanium at full scale wastewater treatment plants: implications for TiO_2 nanomaterials. Journal of Environmental Monitoring, 13: 1195-1203.

Wynn, J.G., Sumrall, J.B., Onac, B.P., 2010. Sulfur isotopic composition and the source of dissolved sulfur species in thermo-mineral springs of the Cerna Valley, Romania. Chemical Geology, 271: 31-43.

Yin, S., Li, R., He, Q., Sato, T., 2002. Low temperature sysnthesis of nanosize rutile titania crystal in liquid media. Material Chemistry and Physics, 75: 76-80.

Yin, S., Hasegawa, H., Maeda, D., Ishitsuka, M., Sato, T., 2004. Synthesis of visible-light-active nanosize rutile titania photocatalyst by low temperature dissolution-reprecipitation process. Journal of Photochemistry and Photobiology A: Chemistry, 163: 1-8.

10. CONCLUSIONS

10.1. Concluding remarks

The main conlusions of my thesis are:

Sulfuric acid speleogenetic caves form especially in carbonate rocks and are intensely influenced by rising acidic waters, interacting with deep-seated sources of H_2S such as evaporites (e.g. Triassic anhydrite and gypsum), hydrocarbons and/or organic matter layers, or volcanic and magmatic active bodies. Generally, SAS caves are considered to be hypogene systems, but peculiar cases can also occur in normal epigene conditions (e.g. Pisatela-Rana system), due to the interaction of oxidizing meteoric waters with pyrite deposits scattered in the carbonate bedrock, which indeed produces sulfuric acid able to dissolve rocks and create typical SAS signatures.

World's most famous and large SAS caves are located in the Guadalupe Mountains (e.g. Carlsbad Caverns, Lechuguilla Cave, etc.), but also Italy hosts gorgeous examples such as Frasassi and Monte Cucco cave systems.

Due to its geological and geodynamic situation, Italy hosts ~25% of the known worldwide SAS caves developed in 26 main areas, located particularly along the northern-central portion of the Apennine Chain. Nevertheless, interesting systems have been found and investigated in detail during this PhD thesis in southern Italy, such as Santa Cesarea Terme in Apulia (chapter 5 and 7.1), Cassano allo Ionio and Monte Sellaro caves in Calabria, and Acqua Fitusa and Acqua Mintina caves in Sicily (chapter 7.2). In addition, Sardinia hosts interesting mine caves located in the Sulcis-Iglesiente area.

Geomorphological and mineralogical investigations can help in recognizing inactive SAS underground environments. SAS caves can form both in confined or unconfined conditions, and therefore, show typical patterns and geomorphological features. Nevertheless, the most common geomorphic structures observed in Italian systems developed at or close to the sulfidic water table, showing peculiar subhorizontal levels that were fed by discharge channels or "feeders" (the way through which rising acidic water reaches the cave atmosphere), sulfuric notches sometimes with flat roofs, rising channels, megacusps, ceiling cupolas, blind chimneys, and replacement pockets. Generally, these caves lack features of turbulent water movements and also fluvial sediments. Some of these morphologies have been explained in detail in the articles published and accepted in Geomorphology (chapter 2 and 6).

In SAS caves, it is possible to observe a peculiar suite of mineralogical byproducts, mainly composed of secondary sulfate minerals related to the interaction of sulfuric acid (H_2SO_4) with bedrock and

insoluble deposits. The most common minerals found in SAS caves are gypsum, native sulfur, alunite, natroalunite, and jarosite, which exhibit white to yellowish or reddish colors. In several samples, EDS analyses demonstrated the presence of P-rich phases inside the crystalline structure of alunite group minerals, which may suggest a hydrothermal hypogene origin. Nevertheless, the typical minerals can also be found in association with Fe-Al-Mn oxy-hydroxides, or rarely with rutile, ilmenite and titanite minerals, likely also of authigenic origin. The results of this detailed mineralogical investigation have been documented in article published in the International Journal of Speleology (chapter 3). In addition, relatively pure gypsum and alunite deposits can be used for dating; the first can be investigated using the U/Th dating method, whereas the second using the $^{40}Ar/^{39}Ar$ methodology. Despite that, it is important to underline that gypsum is a very soluble mineral and several cycles of dissolution-reprecipitation can produce a depletion of uranium ions. On the contrary, the dating of alunite deposits, which are much more stable, may give important clues for the sulfuric acid speleogenesis (chapter 9).

Active SAS systems represent interesting environments to carry out innovative geochemical and microbiological investigations. Generally, active SAS caves are dominated by Na-Cl-SO_4 or Ca-Cl_2-SO_4 waters, commonly undersaturated with respect to gypsum and calcite. The cave atmosphere is often abundantly composed of degassing H_2S, and hypogene CO_2 and CH_4 (chapter 4.2). The study of sulfur isotopes both from mineral and water/air samples may contribute to elucidate the source of H_2S, which in Italy seems to be mainly related to bacterial sulfate reduction of deep-seated Triassic evaporites interacting with hydrocarbons and/or organic matter layers (chapter 4.1).
The special geochemical conditions of active SAS caves promote the growth of microbial biofilms, which are composed of extremophile communities of bacteria and archaea able to arrange themselves into special structures, such as white floating and/or sedimented filaments (thriving in subacqueous conditions), and also vermiculation and moonmilk deposits (chapter 5).
Active SAS environments can be used to perform in site experiments of dissolution-corrosion, and monitor the conditions of maximum weight loss/gain rate over time. Some of the active SAS systems of southern Italy have been studied from this point of view. The most interesting results have been obtained in Fetida Cave, Santa Cesarea Terme (Apulia), where different weight loss rates have been observed in subaqueous and interface conditions as a function of the vicinity to a still-active feeder (located in B1). On the contrary, weight gain rate in aerate stations was higher in the deeper section (B2), where condensation-corrosion processes are favored and gypsum can easily replace carbonate rocks. In addition, in B2 a very fast dissolution-corrosion in cave atmosphere was observed, when limestone tablets were in contact with acid (pH 0-1) moonmilk. Despite some interesting results

obtained in less than three years, a total of five years of monitoring are necessary to have a more comprehensive evaluation of dissolution-corrosion rates. In future, these data will be correlated with the ones observed in other SAS caves of the world.

Finally, in chapter 9, subhorizontal SAS cave levels of the Cavallone-Bove system and alunite dating have been used to estimate the uplift rate of the eastern portion of the Majella Massif (mean of 0.67 mm y^{-1}), and to calculate the incision/erosion rate (mean of 0.23 mm y^{-1}) of the Taranta Gorge.

11. ACKNOWLEDGEMENTS

I would like to thank my thesis supervisor Prof. Jo De Waele, for giving me the possibility to become an authonomous Ph.D. student and for supporting this complex research.
Thanks to my co-supervisor Prof. Mario Parise, which actively helped me during the numerous field campaigns in Apulia and to be part of the expedition carried out in Mt. Sellaro caves.
Thanks to Marco Vattano, Giuliana Madonia, Martina Cappelletti, Daniele Ghezzi, Cristina Carbone, Rosangela Addesso, Maria Nagostinis, Luca Pisani, Marco Antonellini, Ana Zelia Miller, Valme Jurado, Cesareo Saiz-Jimenez, Sergio Sanchez-Moral, Soledad Cuezva, Angel Fernandez-Cortès, Stefano Bernasconi, Enrico Dinelli, Stefan Leuko, Penelope Boston, Michael Spilde, Victor Polyak and Paola Provencio for your help during fieldworks and laboratory analyses, and also for the time spent together. Thanks to Bogdan Onac, Diana Northup, and Arthur Palmer which gave me interesting suggestions to improve the thesis and the overall research. I would like to thank Marco Vattano, Orlando Lacarbonara, Giuseppe Antonini, Sergio Orsini and Roberto Simonetti for the amazing pictures produced in such difficult settings: our lovely dark caves.
Thanks to the whole GSB-USB (Gruppo Speleologico Bolognese-Unione Speleologica Bolognese) which teached me the importance of being part of a team, but also to appreciate the muddy gypsum caves of Bologna.
Thanks to Giulia Barbieri and Michele Azzarrone with whom I shared most of my daily time during the last three years, I'll never forget our descent towards the last circle of the "Dante Inferno" for Ph.D. students. But, we don't know where we are, yet!
I would like to thank all the colleagues of the University of Bologna and friends, who supported and trusted in me every moment.
Thanks to the whole Lions Club Napoli Megaride district 108 YA for the finantial support; Paolo Brancaccio, I'm proud to have had the possibility to personify, with my research, your memory.
I wish all of you my best.
Finally, thanks to my family, to my loved boyfriend Fabio which always encouraged me without any hesitation, to my mother, my little brother Gabriele, to Giuseppe, to Rosa and all the relatives (uncles, aunts, cousins) and relatives in law that were with me in one of the worst moments of my life. Loredana, your support has been essential for me to overcome the hard obstacle that life recently gave me.
Dear father, this thesis is a gift to you. You told me "*La Vita è Bella"* (*Life is Beautiful*).
I'll try to do my best to follow your advices.